frontiers | Research Topics

Insights in plant symbiotic interactions: 2021

Edited by
Andrea Genre, Katharina Pawlowski, Sabine Dagmar Zimmermann and Sergio Saia

Published in
Frontiers in Plant Science

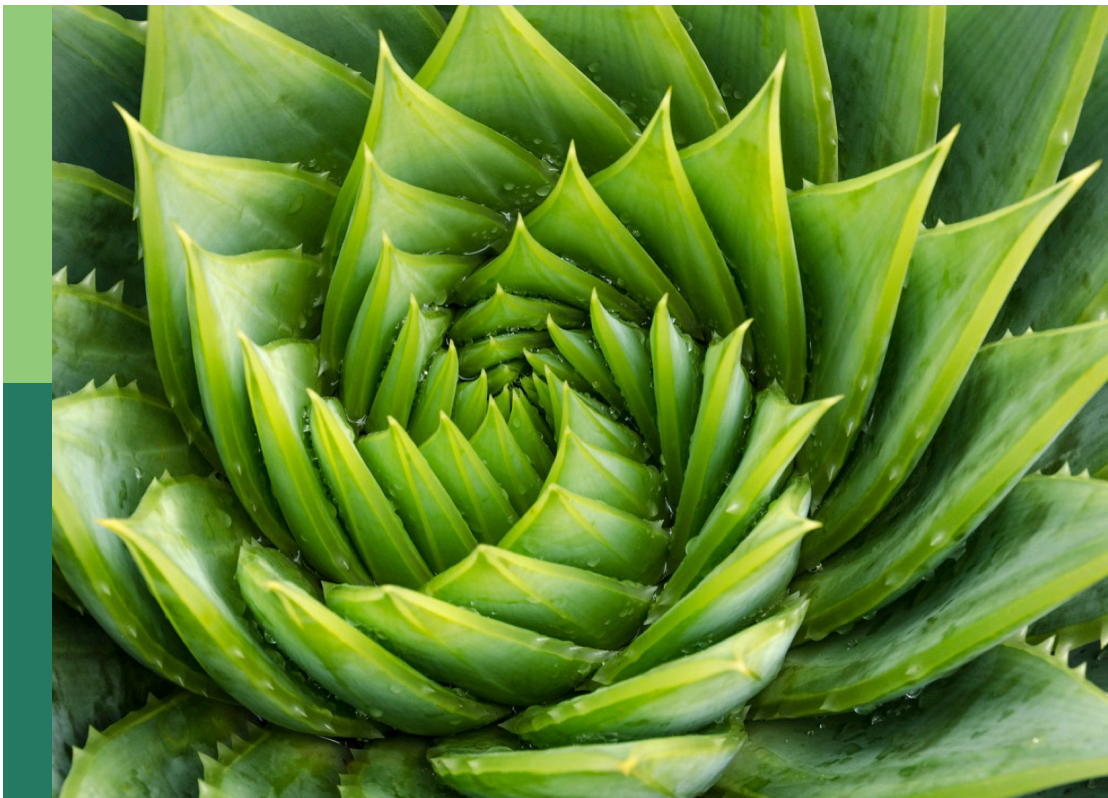

ISSN 1664-8714
ISBN 978-2-83251-749-9
DOI 10.3389/978-2-83251-749-9

About Frontiers

Frontiers is more than just an open access publisher of scholarly articles: it is a pioneering approach to the world of academia, radically improving the way scholarly research is managed. The grand vision of Frontiers is a world where all people have an equal opportunity to seek, share and generate knowledge. Frontiers provides immediate and permanent online open access to all its publications, but this alone is not enough to realize our grand goals.

Frontiers journal series

The Frontiers journal series is a multi-tier and interdisciplinary set of open-access, online journals, promising a paradigm shift from the current review, selection and dissemination processes in academic publishing. All Frontiers journals are driven by researchers for researchers; therefore, they constitute a service to the scholarly community. At the same time, the *Frontiers journal series* operates on a revolutionary invention, the tiered publishing system, initially addressing specific communities of scholars, and gradually climbing up to broader public understanding, thus serving the interests of the lay society, too.

Dedication to quality

Each Frontiers article is a landmark of the highest quality, thanks to genuinely collaborative interactions between authors and review editors, who include some of the world's best academicians. Research must be certified by peers before entering a stream of knowledge that may eventually reach the public - and shape society; therefore, Frontiers only applies the most rigorous and unbiased reviews. Frontiers revolutionizes research publishing by freely delivering the most outstanding research, evaluated with no bias from both the academic and social point of view. By applying the most advanced information technologies, Frontiers is catapulting scholarly publishing into a new generation.

What are Frontiers Research Topics?

Frontiers Research Topics are very popular trademarks of the *Frontiers journals series*: they are collections of at least ten articles, all centered on a particular subject. With their unique mix of varied contributions from Original Research to Review Articles, Frontiers Research Topics unify the most influential researchers, the latest key findings and historical advances in a hot research area.

Find out more on how to host your own Frontiers Research Topic or contribute to one as an author by contacting the Frontiers editorial office: frontiersin.org/about/contact

Insights in plant symbiotic interactions: 2021

Topic editors

Andrea Genre — University of Turin, Italy

Katharina Pawlowski — Stockholm University, Sweden

Sabine Dagmar Zimmermann — IPSiM Institute of Plant Science in Montpellier CNRS UMR5004, France

Sergio Saia — University of Pisa, Italy

Citation

Genre, A., Pawlowski, K., Zimmermann, S. D., Saia, S., eds. (2023). *Insights in plant symbiotic interactions: 2021*. Lausanne: Frontiers Media SA.

doi: 10.3389/978-2-83251-749-9

Table of contents

05 Editorial: Insights in plant symbiotic interactions: 2021
Andrea Genre, Katharina Pawlowski, Sabine Dagmar Zimmermann and Sergio Saia

08 Conservation and Diversity in Gibberellin-Mediated Transcriptional Responses Among Host Plants Forming Distinct Arbuscular Mycorrhizal Morphotypes
Takaya Tominaga, Chihiro Miura, Yuuka Sumigawa, Yukine Hirose, Katsushi Yamaguchi, Shuji Shigenobu, Akira Mine and Hironori Kaminaka

25 The Rhizobium-Legume Symbiosis: Co-opting Successful Stress Management
Justin P. Hawkins and Ivan J. Oresnik

36 The Role of Heterotrimeric G-Protein Beta Subunits During Nodulation in *Medicago truncatula* Gaertn and *Pisum sativum* L.
Andrey D. Bovin, Olga A. Pavlova, Aleksandra V. Dolgikh, Irina V. Leppyanen and Elena A. Dolgikh

48 Overexpression of the Potato Monosaccharide Transporter *StSWEET7a* Promotes Root Colonization by Symbiotic and Pathogenic Fungi by Increasing Root Sink Strength
Elisabeth Tamayo, David Figueira-Galán, Jasmin Manck-Götzenberger and Natalia Requena

66 Deciphering Genomes: Genetic Signatures of Plant-Associated *Micromonospora*
Raúl Riesco, Maite Ortúzar, José Manuel Fernández-Ábalos and Martha E. Trujillo

80 Multifarious and Interactive Roles of GRAS Transcription Factors During Arbuscular Mycorrhiza Development
Tania Ho-Plágaro and José Manuel García-Garrido

86 Varietas Delectat: Exploring Natural Variations in Nitrogen-Fixing Symbiosis Research
Ting Wang, Benedikta Balla, Szilárd Kovács and Attila Kereszt

106 Tubulin Cytoskeleton Organization in Cells of Determinate Nodules
Anna B. Kitaeva, Artemii P. Gorshkov, Pyotr G. Kusakin, Alexandra R. Sadovskaya, Anna V. Tsyganova and Viktor E. Tsyganov

121 TAIM: Tool for Analyzing Root Images to Calculate the Infection Rate of Arbuscular Mycorrhizal Fungi
Kaoru Muta, Shiho Takata, Yuzuko Utsumi, Atsushi Matsumura, Masakazu Iwamura and Koichi Kise

132 Biocontrol Potential of Endophytic *Streptomyces malaysiensis* 8ZJF-21 From Medicinal Plant Against Banana Fusarium Wilt Caused by *Fusarium oxysporum* f. sp. *cubense* Tropical Race 4
Lu Zhang, Ziyu Liu, Yong Wang, Jiaqi Zhang, Shujie Wan, Yating Huang, Tianyan Yun, Jianghui Xie and Wei Wang

148 Soil Inoculation With Beneficial Microbes Buffers Negative Drought Effects on Biomass, Nutrients, and Water Relations of Common Myrtle
Soghra Azizi, Masoud Tabari, Ali Reza Fallah Nosrat Abad, Christian Ammer, Lucia Guidi and Martin K.-F. Bader

161 Molecular Mechanisms of Intercellular Rhizobial Infection: Novel Findings of an Ancient Process
Johan Quilbé, Jesús Montiel, Jean-François Arrighi and Jens Stougaard

169 Ectomycorrhizal Networks in the Anthropocene: From Natural Ecosystems to Urban Planning
Louise Authier, Cyrille Violle and Franck Richard

184 A variable gene family encoding nodule-specific cysteine-rich peptides in pea (*Pisum sativum* L.)
Evgeny A. Zorin, Marina S. Kliukova, Alexey M. Afonin, Emma S. Gribchenko, Mikhail L. Gordon, Anton S. Sulima, Aleksandr I. Zhernakov, Olga A. Kulaeva, Daria A. Romanyuk, Pyotr G. Kusakin, Anna V. Tsyganova, Viktor E. Tsyganov, Igor A. Tikhonovich and Vladimir A. Zhukov

frontiers | Frontiers in Plant Science

TYPE Editorial
PUBLISHED 10 February 2023
DOI 10.3389/fpls.2023.1129738

OPEN ACCESS

EDITED AND REVIEWED BY
Pierre-Emmanuel Courty,
INRA Centre Dijon Bourgogne
Franche-Comté, France

*CORRESPONDENCE
Andrea Genre
andrea.genre@unito.it

SPECIALTY SECTION
This article was submitted to
Plant Symbiotic Interactions,
a section of the journal
Frontiers in Plant Science

RECEIVED 22 December 2022
ACCEPTED 31 January 2023
PUBLISHED 10 February 2023

CITATION
Genre A, Pawlowski K, Zimmermann SD
and Saia S (2023) Editorial: Insights in plant
symbiotic interactions: 2021.
Front. Plant Sci. 14:1129738.
doi: 10.3389/fpls.2023.1129738

Editorial: Insights in plant symbiotic interactions: 2021

Andrea Genre[1]*, Katharina Pawlowski[2],
Sabine Dagmar Zimmermann[3] and Sergio Saia[4,5]

[1]Department of Life Sciences and Systems Biology, University of Turin, Turin, Italy, [2]Department of Ecology, Environment and Plant Science, Stockholm University, Stockholm, Sweden, [3]IPSiM, Univ Montpellier, CNRS, INRAE, Institut Agro, Montpellier, France, [4]Department of Veterinary Sciences, University of Pisa, Pisa, Italy, [5]Centre for Climate Change Impact, University of Pisa, Pisa, Italy

KEYWORDS

plant symbioses, mycorrhiza, symbiotic nitrogen fixation (SNF), plant endophytes, plant growth promoting microbes

Editorial on the Research Topic
Insights in plant symbiotic interactions: 2021

This Research Topic was launched in late 2021 in the frame of a broad initiative covering most sections of Frontiers in Plant Science. The call for papers attracted 14 original research, method, review and mini review papers by 74 authors, largely delivering our goal to provide a transversal insight into the advances in the major symbiotic plant-microbe interactions.

The contributions embrace molecular, cellular, applicative and ecological aspects of mycorrhizas, symbiotic nitrogen fixation and plant interactions with beneficial endophytes or plant growth-promoting bacteria.

Mycorrhizal interactions

A broad interest is focused on gene regulation in mycorrhizal symbioses (Genre et al., 2020), through genomic and transcriptomic data of mycorrhizal fungi and their hosts. Moreover, novel automated image analyses now allow a breakthrough advancement in the quantification of arbuscular mycorrhizal colonization, described in a methodological article. First, Tominaga et al. analyzed and compared transcriptional changes of symbiosis-related genes in three distinct arbuscular mycorrhizal (AM) morphotypes (Arum-, Intermediate-, Paris-type) formed by distinct host plants (*Lotus japonicus*, *Daucus carota*, *Eustoma grandiflorum*), respectively. Similarities in the expression patterns for AM marker genes, such as ammonium and phosphate transporters (Boussageon et al., 2022), were found upon colonization with the AM-fungus *Rhizophagus irregularis*, but also divergent responses to the phytohormone gibberellin. These results obtained by comparative transcriptomics open further research to dissect gibberellin-mediated regulation of mycorrhiza establishment. Such transcriptional changes associated with morphological and developmental changes involved in AM formation and turnover have been shown to be linked to GRAS transcription factors, reviewed by Ho-Plágaro and Garcia-Garrido. Genome-wide expression studies in several AM models have revealed a prominent role of this GRAS gene family in AM development, nicely summarized in a scheme. However, target genes and downstream processes need further to be studied. Such a target for root colonizing fungi is proposed by Tamayo et al. at the

functional level. Indeed, overexpression of a SWEET-type monosaccharide transporter in potato favored root colonization by the AM fungus *R. irregularis* and also by the pathogenic fungus *Fusarium oxysporum*, indicating that an increase in sugar transfer from the host to the fungi is involved in the fungus-plant interaction. This study showing induction of the SWEET-type sugar transporter in AM symbiosis opens a number of questions regarding regulation under natural conditions with a multitude of interactions.

Quantification of root colonization by AM fungi is often needed for such studies and so far commonly used by manual techniques. An innovative method is proposed by Muta et al. presenting in a methodological article a software-based implementation called TAIM (Tool for Analyzing root images to calculate the Infection rate of arbuscular Mycorrhizal fungi). A similar approach was recently developed as a standalone application by Evangelisti et al. (2021) called "AMFinder" for plant root analyses using deep learning-based image processing. The novel TAIM method, described here in detail, is easily accessible from an Web-based online repository, and has the potential to revolutionize the routine in many laboratories by changing a critical activity from tedious and error-prone to rapid and reliable.

Finally, the review by Authier et al. provides a more global and ecological overview about current knowledge and research gaps concerning ectomycorrhizal (ECM) networks, found in natural but even in urban ecosystems. Mycorrhizal plants are interconnected by common mycorrhizal networks (CMNs) as described for AM plants (Wipf et al., 2019). The Authors summarize and discuss ECM-based CMNs contributing significantly to nutrient exchange, carbon trade and dynamics of plant communities, finally proposing measures for landscape and urban planning for a better use of mycorrhizal ecoservices.

Symbiotic nitrogen fixation

Four papers deal with signaling processes in symbiotic nitrogen fixation (Downie, 2014). The review by Hawkins and Oresnik focuses on the different abiotic stresses rhizobia are exposed to during the establishment of the root nodule symbiosis – acidic pH, high osmolarity, reactive oxygen species and low oxygen levels – which serve as signals; for instance, high osmolarity leads to the induction of rhizobial *nod, nif* and *fix* genes. They also discuss the effects of nodule-specific cysteine-rich peptides (NCRs and NCR-like peptides) used by some legumes, to manipulate rhizobial differentiation. Zorin et al. examine the entire NCR gene family of pea and, based on mutants and co-expression analysis, predict transcription factors involved in their regulation. Previous studies have proposed the involvement of heterotrimeric G-proteins in the symbiotic signaling in legume/rhizobia symbioses (Pingret et al., 1998). Bovin et al. examine the genes for the G beta-subunit in two legumes, providing evidence for this subunit's role in infection and nodule development, presumably *via* cross-talk between G-protein- and PLC-mediated signaling pathways. The review of Wang et al. discusses the multiple signals that can play a role in legume nodule induction, from plant flavonoids over rhizobial Nod factors, effectors and surface polysaccharides to plant peptides, and details the roles of individual factors in different stages of the interaction.

Another major focus was on cellular aspects of root symbioses, with two papers investigating rhizobial infection in legumes. The article by Kitaeva et al. presents original research comparing microtubule organization in the cells of determinate nodules from *Glycine max*, *G. soja*, *Phaseolus vulgaris* and *L. japonicus*. The major conclusions, based on a further comparison with cytoskeleton arrangement in indeterminate nodules, outlined interesting evolutionary and developmental implications impacting symbiosome accommodation and overall efficiency in nodule infection. The mini-review by Quilbé et al. presents an update on the most recent discoveries in the molecular control of intercellular rhizobial infection, a largely unexplored - but very common - alternative to the more studied intracellular infection *via* root hairs. The review provides a few intriguing starting points to stimulate future research, such as the apparent minor role of canonical Nod-factor signaling in intercellular bacterial accommodation, more strongly controlled by cytokinin signaling, or the peculiar infection strategies deployed by individual members of the legume family.

Other plant growth-promoting interactions

Riesco et al. identified potential genomic features involved in the interaction between *Micromonospora* and their host plants (Trujillo et al., 2015) exploring the relationship between several tens of *Micromonospora* genomes from contrasting environments with corresponding plant-related genes. Notably, they could cluster the bacterial genomes according to solely three groups dealing with 'plant-associated', 'soil/rhizosphere', and 'marine/mangrove' related traits and showed that representative inocula from these latter groups produced marked differences in the plant phenotypes of an inoculated *Arabidopsis thaliana* model host. These results confirm that using bacterial genomic signatures can help to select for host colonization and the plant benefit, highlighting that the common plant growth promotion markers should not be used as sole indicators to select beneficial bacteria to be used in agronomic setups or revegetation settings.

The relationship between host plants and beneficial microbes, either AM fungi or plant growth promoting bacteria (Souza et al., 2015) were explored in two elegant studies. In particular, Zhang et al. isolated several tens of actinomycetes endophytic of several medicinal plants and tested them for the antifungal activity against *F. oxysporum* f. sp. *cubense* (Foc TR4) in banana and identified a highly beneficial strain as *Streptomyces malaysiensis*. Notably, they showed that this latter *S. malaysiensis* can stimulate the banana tolerance to Foc TR4 by both stimulating the plant expression of defense-related and antioxidant enzymes, and by exuding extracellular enzymes and metabolites with plant beneficial activity. In particular, they showed that *S. malaysiensis* 8ZJF-21 extract can inhibit the germination and growth of Foc TR4 in an *in vitro* assay and identified nineteen volatile organic compounds produced by *S. malaysiensis* as potential antifungal compounds. Azizi et al. showed that inoculation of the

AM fungal species *Funneliformis mosseae* or *R. irregularis* (singly or co-inoculated) and inoculation of the bacterial species *Pseudomonas fluorescens* and *P. putida* (singly or co-inoculated) improved the tolerance of common myrtle plantlets to drought effects but not their water-use efficiency. These effects were seen mostly under the dual inoculation rather than the single inoculation, with beneficial side effects on the nutrient dynamics in both the roots and leaves.

In conclusion, this Research Topic, bringing together 14 articles dealing with different plant-microbe associations, is clearly reflecting the ongoing research linked to the important topic of such beneficial interactions. Regarding the challenge to maintain and improve further plant growth and tolerance under limiting and stressful conditions, many scientific questions remain still open and will require answers in the future.

Author contributions

All authors listed have made a substantial, direct, and intellectual contribution to the work and approved it for publication.

Acknowledgments

We are grateful to all the Authors who contributed to this Research Topic, to the Reviewers who evaluated their work and to the Frontiers editorial staff for their guidance and assistance.

Conflict of interest

The authors declare that the research was conducted in the absence of any commercial or financial relationships that could be construed as a potential conflict of interest.

Publisher's note

References

Boussageon, R., Marro, N., Janoušková, M., Brulé, D., Wipf, D., and Courty, P.-E. (2022). The fine-tuning of mycorrhizal pathway in sorghum depends on both nitrogen–phosphorus availability and the identity of the fungal partner. *Plant Cell Env.* 45, 3354–3366. doi: 10.1111/pce.14426

Downie, A. (2014). Legume nodulation. *Curr. Biol.* 24, R184–T190. doi: 10.1016/j.cub.2014.01.028

Evangelisti, E., Turner, C., McDowell, A., Shenhav, L., Yunusov, T., Gavrin, A., et al. (2021). Deep learning-based quantification of arbuscular mycorrhizal fungi in plant roots. *New Phytol.* 232, 2207–2219. doi: 10.1111/nph.17697

Genre, A., Lanfranco, L., Perotto, S., and Bonfante, P. (2020). Unique and common traits in mycorrhizal symbioses. *Nat. Rev. Microbiol.* 18, 649–660. doi: 10.1038/s41579-020-0402-3

Pingret, J. L., Journet, E. P., and Barker, D. G. (1998). *Rhizobium* nod factor signaling. evidence for a G protein-mediated transduction mechanism. *Plant Cell* 10, 659–672. doi: 10.1105/tpc.10.5.659

Souza, R.d., Ambrosini, A., and Passaglia, L. M. (2015). Plant growth-promoting bacteria as inoculants in agricultural soils. *Genet. Mol. Biol.* 38, 401–419. doi: 10.1590/S1415-475738420150053

Trujillo, M. E., Riesco, R., Benito, P., and Carro, L. (2015). Endophytic actinobacteria and the interaction of *Micromonospora* and nitrogen fixing plants. *Front. Microbiol.* 6, 1341. doi: 10.3389/fmicb.2015.01341

Wipf, D., Krajinski, F., Tuinen, D., Recorbet, G., and Courty, P. E. (2019). Trading on the arbuscular mycorrhiza market: From arbuscules to common mycorrhizal networks. *New Phytol.* 223, 1127–1142. doi: 10.1111/nph.15775

frontiers in Plant Science

ORIGINAL RESEARCH
published: 16 December 2021
doi: 10.3389/fpls.2021.795695

Conservation and Diversity in Gibberellin-Mediated Transcriptional Responses Among Host Plants Forming Distinct Arbuscular Mycorrhizal Morphotypes

Takaya Tominaga[1†], Chihiro Miura[2], Yuuka Sumigawa[2], Yukine Hirose[2], Katsushi Yamaguchi[3†], Shuji Shigenobu[3†], Akira Mine[4,5†] and Hironori Kaminaka[2†]*

[1] The United Graduate School of Agricultural Sciences, Tottori University, Tottori, Japan, [2] Faculty of Agriculture, Tottori University, Tottori, Japan, [3] Functional Genomics Facility, NIBB Core Research Facilities, National Institute for Basic Biology, Okazaki, Japan, [4] Laboratory of Plant Pathology, Graduate School of Agriculture, Kyoto University, Kyoto, Japan, [5] JST, PRESTO, Kawaguchi, Japan

Morphotypes of arbuscular mycorrhizal (AM) symbiosis, *Arum*, *Paris*, and Intermediate types, are mainly determined by host plant lineages. It was reported that the phytohormone gibberellin (GA) inhibits the establishment of *Arum*-type AM symbiosis in legume plants. In contrast, we previously reported that GA promotes the establishment of *Paris*-type AM symbiosis in *Eustoma grandiflorum*, while suppressing *Arum*-type AM symbiosis in a legume model plant, *Lotus japonicus*. This raises a hitherto unexplored possibility that GA-mediated transcriptional reprogramming during AM symbiosis is different among plant lineages as the AM morphotypes are distinct. Here, our comparative transcriptomics revealed that several symbiosis-related genes were commonly upregulated upon AM fungal colonization in *L. japonicus* (*Arum*-type), *Daucus carota* (Intermediate-type), and *E. grandiflorum* (*Paris*-type). Despite of the similarities, the fungal colonization levels and the expression of symbiosis-related genes were suppressed in *L. japonicus* and *D. carota* but were promoted in *E. grandiflorum* in the presence of GA. Moreover, exogenous GA inhibited the expression of genes involved in biosynthetic process of the pre-symbiotic signal component, strigolactone, which resulted in the reduction of its endogenous accumulation in *L. japonicus* and *E. grandiflorum*. Additionally, differential regulation of genes involved in sugar metabolism suggested that disaccharides metabolized in AM roots would be different between *L. japonicus* and *D. carota*/*E. grandiflorum*. Therefore, this study uncovered the conserved transcriptional responses during mycorrhization regardless of the distinct AM morphotype. Meanwhile, we also found diverse responses to GA among phylogenetically distant AM host plants.

Keywords: arbuscular mycorrhizal symbiosis, comparative transcriptomics, gibberellin, arbuscular mycorrhizal morphotypes, *Lotus japonicus*, *Daucus carota*, *Eustoma grandiflorum*, *Rhizophagus irregularis*

OPEN ACCESS

Edited by:
Andrea Genre,
University of Turin, Italy

Reviewed by:
Katsuharu Saito,
Shinshu University, Japan
Sergey Ivanov,
Boyce Thompson Institute,
United States

***Correspondence:**
Hironori Kaminaka
kaminaka@tottori-u.ac.jp

†ORCID:
Takaya Tominaga
orcid.org/0000-0002-1105-1693
Katsushi Yamaguchi
orcid.org/0000-0001-6871-7882
Shuji Shigenobu
orcid.org/0000-0003-4640-2323
Akira Mine
orcid.org/0000-0002-4822-4009
Hironori Kaminaka
orcid.org/0000-0002-3685-8688

Specialty section:
This article was submitted to Plant Symbiotic Interactions, a section of the journal Frontiers in Plant Science

Received: *15 October 2021*
Accepted: *12 November 2021*
Published: *16 December 2021*

Citation:
Tominaga T, Miura C, Sumigawa Y, Hirose Y, Yamaguchi K, Shigenobu S, Mine A and Kaminaka H (2021) Conservation and Diversity in Gibberellin-Mediated Transcriptional Responses Among Host Plants Forming Distinct Arbuscular Mycorrhizal Morphotypes. Front. Plant Sci. 12:795695. doi: 10.3389/fpls.2021.795695

INTRODUCTION

More than 70% of terrestrial plants associate with the symbiotic, arbuscular mycorrhizal (AM) fungi that belong to Glomeromycotina (Brundrett and Tedersoo, 2018). AM fungi supply minerals, such as inorganic phosphate and nitrogen, to their host plants, thus promoting the growth of the hosts (Ezawa and Saito, 2018; Wang et al., 2020). In return, they obtain carbohydrates, such as fatty acids, lipids, and monosaccharides, from the host plants (Bravo et al., 2017; An et al., 2019). This mutual interaction is established through several steps. Host-derived signal molecules, strigolactones (SLs), are exudates into the rhizosphere to attract AM fungi prior to the mutualism (Akiyama et al., 2005; Besserer et al., 2008; Tsuzuki et al., 2016). SLs positively regulate formation of hyphopodia on the host root epidermis (Kobae et al., 2018). After AM fungal hyphae invade the host epidermis, AM fungi form highly branched hyphal structures, the arbuscule, in the root cortical cells for nutrient exchange. Some transporters are localized on a specialized plant-derived membrane, periarbuscular membrane (PAM), to influx mineral nutrients and efflux carbohydrates such as lipids and glucose between the host and fungal symbionts (Kobae and Hata, 2010; Bravo et al., 2017; Luginbuehl and Oldroyd, 2017).

The morphology of AM fungal hyphae is known to be distinct mainly depending on the host plant species (Smith and Smith, 1997; Dickson et al., 2007). *Arum*-type AM shows that AM fungal hyphae elongate in the intercellular space of the host cortex and form arbuscules in the cortical cells. This AM morphotype is found in rice (*Oryza sativa*) and legume model plant roots such as *Medicago truncatula* and *Lotus japonicus* (Hong et al., 2012; Yu et al., 2014; Takeda et al., 2015). On the other hand, in *Paris*-type AM, the fungal hyphae invade the adjacent cortical cells and show hyphal coils on which arbuscules are formed (Smith and Smith, 1997; Dickson, 2004; Dickson et al., 2007). Moreover, an "Intermediate" type of AM showing both morphological features of *Arum*- and *Paris*-type AMs is also found in some host plants (Dickson, 2004). According to Dickson (2004), Intermediate-type AM is defined by either the existence of linear intracellular hyphae on which arbuscules are formed or hyphal coils with intercellular hyphae. The linear intercellular hyphae are sometimes found with intercellular hyphae (Dickson, 2004).

Several phytohormones have been revealed to regulate AM symbiosis. For instance, exogenous treatment of gibberellin (GA) severely reduces the number of hyphopodia and disturbs the development of arbuscule (Floss et al., 2013; Yu et al., 2014; Takeda et al., 2015; Pimprikar et al., 2016). Moreover, GA represses the expressions of some AM symbiosis-related genes (Takeda et al., 2015; Pimprikar et al., 2016; Nouri et al., 2021). Notably, it has shown that a GRAS transcription factor (TF) required for AM symbiosis, *REDUCED ARBUSCULAR MYCORRHIZA1* (*RAM1*), is transcriptionally downregulated in GA-treated *L japonicus*. This is attributable to the GA-triggered degradation of GA-signaling repressor, DELLA, which positively regulates *RAM1* expression (Silverstone et al., 2001; Achard and Genschik, 2009; Floss et al., 2013; Park et al., 2015). Notably, the *RAM1* also regulates other downstream AM marker genes: *REDUCED FOR ARBUSCULE DEVELOPMENT1 (RAD1)*–GRAS TF, *Vapyrin* (*Vpy*) (protein that regulates arbuscule development), *PHOSPHATE TRANSPORTER4* (*PT4*), *AMMONIUM TRANSPORTER2;2* (*AMT2;2*), *FatM* (acyl-acyl carrier protein thioesterase), *RAM2* (glycerol-3-phosphate acyltransferase), and *STR/STR2* (ABC transporters for lipids) (Gobbato et al., 2013; Park et al., 2015; Rich et al., 2015, 2017; Pimprikar et al., 2016; Muller et al., 2020). Thus, it has been thought that exogenous GA or the absence of functional DELLA attenuates the transcriptional promotion of downstream genes to inhibit AM fungal colonization. Interestingly, our previous study showed that GA suppresses *Arum*-type AM symbiosis in *L. japonicus* and chive, whereas promoting *Paris*-type AM symbiosis in *Eustoma grandiflorum* and *Primula malacoides* (Tominaga et al., 2020a). Another expression analysis also revealed that the expression levels of AM symbiosis-related genes in *E. grandiflorum* were increased by GA (Tominaga et al., 2020b). These findings let us hypothesize that the regulatory mechanisms underlying AM symbiosis would be diverse among host plants; however, our past studies did not simultaneously compare the GA-mediated transcriptional regulation among various host plants. To date, the effect of GA on Intermediate-type AM symbiosis has not been investigated yet.

In this study, we conducted comparative transcriptomics among three AM host plants with different AM morphotypes: *L. japonicus* (*Arum*-type AM), *E. grandiflorum* (*Paris*-type AM), and *Daucus carota* (Intermediate-type AM) (Dickson, 2004). Based on plastid genomes, Fabales, Gentianales, and Apiales, to which *L. japonicus*, *D. carota*, and *E. grandiflorum* belong, are estimated to appear *c.* 100 Ma, *c.* 80 Ma, and *c.* 90 Ma, respectively (Li et al., 2019). Our study revealed that *Rhizophagus irregularis* infection promoted shoot growth and the expression of several symbiosis-related genes conserved in all examined plants, such as *RAM1* and *STR*. However, the AM fungus-promoted expression of the conserved symbiosis-related genes was decreased in GA-treated *L. japonicus* (*Arum*-type) and *D. carota* (Intermediate-type). In contrast, the expression levels of the conserved genes were not reduced but rather increased by exogenous GA in *E. grandiflorum* (*Paris*-type). This suggests that the transcriptional reprogramming associated with AM symbiosis in *E. grandiflorum* would be tolerant to GA and unique to this plant species. Additionally, the negative effects of GA on SL biosynthetic process were commonly observed in *L. japonicus* and *E. grandiflorum*, suggesting that GA-promoted fungal colonization in *E. grandiflorum* is independent of SLs. Thus, our study uncovered the conserved responses of phylogenetically distant AM host plans regardless of AM morphotypes. Furthermore, our findings help understand the diverse effects of GA on host plant species.

MATERIALS AND METHODS

Growth Condition of Plant and Fungal Materials

The seedlings of *L. japonicus* "Miyakojima" MG-20, *D. carota* cv. Nantes, and *E. grandiflorum* cv. Pink Thumb were prepared as in our previous report (Tominaga et al., 2020a). *D. carota*

seedlings were grown in light for 7 days. Since *E. grandiflorum* exhibited relatively low colonization rates in our previous report (Tominaga et al., 2020a), high concentration of AM fungal spores, approximately 6,000 spores of *R. irregularis* DAOM197198 (Premier Tech, Quebec, Canada), were added to 50 ml 1/5 Hoagland solution containing 20 μM inorganic phosphate. GA_3 was dissolved in ethanol and treated at this procedure by diluting the stock to the 1/5 Hoagland solution at 1 μM. Ethanol was treated in the same way as the control treatment. The solution was added to approximately 300 ml autoclaved mixed soil (river sand/vermiculite, 1:1) in a plastic container combined with another one as described in Takeda et al. (2015). As a result, each tested seedling was inoculated with 1,000 spores of *R. irregularis*. Then, the prepared seedlings were transplanted into the soil and kept for 6 weeks under 14 h light/10 h dark cycles at 25°C.

Quantification and Observation of Arbuscular Mycorrhizal Symbiosis

The inoculated roots were harvested at 6 weeks post-inoculation (wpi), and fixation, staining, and quantification of AM fungal colonization rates were conducted according to previous studies (Mcgonigle et al., 1990; Tominaga et al., 2020a). To determine the AM morphotypes of root samples stained with trypan blue, single cortex layer containing AM fungal hyphae was microscopically observed by gently squashing the roots.

For fluorescence images, the fragments of fixed roots were rinsed with phosphate-buffered saline (PBS) and immersed in ClearSee (FUJIFLIM Wako Pure Chemical, Osaka, Japan) for 1 week in the dark (Kurihara et al., 2015). The instructions of the manufacturer were followed in the clearing procedure. The cleared roots were rinsed with PBS and stained with 0.01 mg/ml WGA-Alexa Fluor 488 (Thermo Fisher Scientific, Waltham, MA, United States) for 15 min. For the staining of plant cell wall, the root samples were further treated with 20 μg/ml Calcofluor White (Sigma-Aldrich, St Louis, MO, United States) for 15 min. Under a fluorescent stereomicroscope, Leica M205 FCA (Leica Microsystems, Wetzlar, Germany), the relatively bright fluorescent region, which indicates colonized area, was excised with a scalpel and embedded in 5% (w/v) agarose containing 1% (w/v) gelatin. Then, 30–50 μm cross sections were made using a Linear Slicer PRO-7 (Dosaka EM, Kyoto, Japan) and observed under a FLUOVIEW FV10i confocal laser scanning microscope (Olympus, Tokyo, Japan) with 499 nm excitation and 520 nm emission for WGA-Alexa Fluor 488 and FV10i-SW software v1.2 (Olympus, Tokyo, Japan). The images were merged using the ImageJ software v1.51k[1].

Transcriptome Analysis

RNA Extraction and RNA Sequencing

Root samples (approximately 100 mg) at 6 wpi were collected in a nuclease-free tube (INA-OPTIKA, Osaka, Japan) with two 5 mm beads, frozen by liquid nitrogen. The frozen root samples were set in ShakeMan6 (Bio-Medical Science, Tokyo, Japan) and homogenized. Then, the total RNA was extracted using the real RNA Extraction Kit Mini for Plants (RBC Bioscience, New Taipei, Taiwan) following the protocol of the manufacturer. RNase-free DNase I (Takara Bio, Shiga, Japan) was applied to remove genomic DNA from the RNA samples according to the instructions of the manufacturer. The purity and quantity of the total RNA was calculated by measuring the absorbance at 260 and 280 nm (*A*260: *A*280) with DeNovix DS-11+ (Scrum, Tokyo, Japan). RNA-seq library was constructed from the total extracted RNA and sequenced, and RNA-seq with strand-specific and paired-end reads (150 bp) was performed with DNBSEQ-G400 by Genewiz (Tokyo, Japan). Consequently, more than 20 million raw reads per sample were obtained (**Supplementary Table 1**). Low-quality reads (<QV30) and adapter sequences were removed by Fastp (Chen et al., 2018).

Data Analysis

Read mapping was conducted using STAR (Dobin et al., 2013) for the filtered single-end reads of *L. japonicus*, *D. carota*, and *R. irregularis* onto their genomes, Lotus japonicus Lj1.0v1, Daucus carota v2.0, and Rir_HGAP_ii_V2, retrieved from the Phytozome v13[2] and Ensembl Fungi[3] (Iorizzo et al., 2016; Maeda et al., 2018; Li et al., 2020). Meanwhile, Bowtie2 with default parameters except for "–loc al" was applied for *E. grandiflorum* to map the reads to *de novo* reference assembly constructed from previous RNA-seq data (Tominaga et al., 2020b) by Trinity v2.8.4 (Grabherr et al., 2011; Langmead and Salzberg, 2012; Haas et al., 2013). In this study, we mapped the reverse reads to the indicated genomes or *de novo* assembly data to perform specific alignment. The number of mapped reads to the reference genome was counted using featureCounts v1.6.4 (Liao et al., 2014) for *L. japonicus*, *D. carota*, and *R. irregularis*, whereas that of *E. grandiflorum* was quantified with eXpress v1.5.1 (Roberts and Pachter, 2013) due to using *de novo* assembled cDNA sequences as reference unlike others. For identifying differentially expressed genes (DEGs), each count data showing different library sizes were normalized by the trimmed mean of the *M*-values normalization method, and genes with $|\ \mathrm{Log_2}$ fold change (FC)$|\ > 1$ and false discovery rate (FDR) less than the indicated values (FDR < 0.01 for plants' DEGs and FDR < 0.05 for fungal DEGs) were considered DEGs using the EdgeR package (Robinson et al., 2010).

The transcripts per million (TPM) (Li et al., 2010; Wagner et al., 2012) of each sample was counted from the count data using the R software v4.0.2 (R Foundation for Statistical Computing). Genes that showed zero counts in all samples were excluded from the analysis, unless otherwise noted. Then, the mean TPM of all samples in a condition was $\mathrm{Log_2}$-transformed for each gene. The heatmaps in this study were constructed using the heatmaply package in R (Galili et al., 2018).

Gene Ontology Enrichment Analysis

Differentially expressed gene was sorted depending on their expression patterns using a Venn diagram[4]. Then, the gene

[1]http://imagej.nih.gov/ij

[2]https://phytozome-next.jgi.doe.gov

[3]https://fungi.ensembl.org/index.html

[4]http://bioinformatics.psb.ugent.be/webtools/Venn

ontology (GO) enrichment analysis was conducted using the ClueGO plugin for Cytoscape (Bindea et al., 2009, 2013). Additionally, the correlation network of enriched GO terms was created using the ClueGO. In the analysis, *p*-values were calculated using a two-sided hypergeometric test and corrected using the Benjamini–Hochberg method. The GO terms of *R. irregularis* were annotated by EnTAP v0.10.7 (Hart et al., 2020), followed by GO enrichment analysis using the topGO package in the R environment. In the topGO study, the enrichment test was performed by calculating the *p*-values using the Fisher's exact test ($p < 0.01$) and scoring with the *Elim* method (Alexa et al., 2006). The *p*-values of filtered GO terms were adjusted by the Benjamini–Hochberg method.

Ortholog Identification

Here, we identified ortholog genes in *L. japonicus*, *D. carota*, and *E. grandiflorum* to compare the influence of AM fungal colonization and GA treatment among these different host species. The proteomes of *L. japonicus* and *D. carota* were retrieved from the Phytozome v12.1 and v13, respectively. Additionally, coding sequence and amino acid sequences in the *de novo* assembly of *E. grandiflorum* were predicted using TransDecoder v5.5.0 (Haas et al., 2013). Next, the ortholog was identified using SonicParanoid with default parameters in the Python v3.8 environment (Cosentino and Iwasaki, 2019). Several known genes were used as queries for BLASTp search against *L. japonicus* proteome on the website Phytozome v13 (**Supplementary Tables 1**, **2**). The resulting top hit *L. japonicus* gene and its corresponding orthologs in *D. carota* and *E. grandiflorum* were considered orthogroups and analyzed.

Extraction of Endogenous Strigolactones and Germination Assay

To extract SLs from the host roots, we referred to the methods in a previous study with some modifications (Floková et al., 2020). The fresh 6-week-old roots (100 mg) were homogenized in ShakeMan6 (Bio-Medical Science, Tokyo, Japan) with 1 ml of 60% (v/v) acetone stored at −30°C. The suspensions were collected by centrifugation and evaporated *in vacuo* for 30 min using Savant SpeedVac DNA130 (Thermo Fisher Scientific, Waltham, MA, United States). Hydrophobic components in residual water (*c.* 500 μl) were extracted by ethyl acetate three times, and the organic layer was evaporated *in vacuo*. The samples were resolved in acetone at 400 mg FW root/ml and stored at 4°C until use. Root exudates of 4-week-old *E. grandiflorum* were collected as our previous study and rinsed with 25% acetone before elution (Tominaga et al., 2020a).

Orobanche minor seeds were incubated on two moist filter papers for 10 days at 24°C in the dark. An aliquot of acetone, 1 μM *rac*-GR24 (StrigoLab, Torino, Italy), and extracted samples (20 μl) were added to 6-mm glass fiber disks. Then, the conditioned *O. minor* seeds were placed on the disks with 20 μl distilled water. After 5 days of incubation at 24°C in the dark, the germination rate (%) was counted.

Biological Replicate and Statistical Analysis

One glass slide with 10 pieces of root fragments collected from one plant was considered a biological replicate for colonization rate quantification. One glass fiber disk with *O. minor* seeds was equivalent to one biological replicate. These experiments were reproduced three times with more than five biological replicates. In the transcriptome analysis, one library constructed from a pool of total RNA consisting of three plants was treated as one biological replicates. Statistical analyses were conducted using the R software v4.0.2.

RESULTS

Phenotypes of Arbuscular Mycorrhizal Roots in Different Host Plant Species Associated With *Rhizophagus irregularis*

In *L. japonicus*, a typical *Arum*-type AM with intercellular hyphae and highly branched arbuscules in the cortical cells were formed at 6 wpi with *R. irregularis* (**Figures 1A,D** and **Supplementary Figure 1A**). We also observed *D. carota* AM roots and found linear intraradical hyphae invading the cortical cells, but we could not confirm intercellular hyphae and clear hyphal coil (**Figures 1B,D** and **Supplementary Figures 1C,D**). AM morphotype we found in *D. carota* roots is described as Intermediate 2 (I2) of four Intermediate type AMs, and *D. carota* roots associating with another AM fungus, *Glomus mosseae*, is reported to form I2 morphotype (Dickson, 2004). Therefore, we defined the AM morphotype of *D. carota* with *R. irregularis* as Intermediate-type AM in this study. On the other hand, *E. grandiflorum* showed a classical *Paris*-type AM that forms hyphal coils elongating in a circle and invading the adjacent cortical cells and an arbuscule emerging from a hyphal coil (**Figures 1C,D** and **Supplementary Figure 1E**; Tominaga et al., 2020a). Taken together, the host plant species formed distinct AM morphologies with a single fungal species, *R. irregularis*. By contrast to the distinct AM morphotypes, the shoot growth promotion by AM fungal colonization was commonly occurred in each host plant (**Figure 1E**). However, some exceptions, such as tomato forming both *Arum*- and *Paris*-type AMs depending on the AM fungal traits, were reported (Cavagnaro et al., 2001; Dickson, 2004; Smith et al., 2004; Kubota et al., 2005; Hong et al., 2012).

Although we previously reported that exogenous GA treatment inhibits or promotes the establishment of *Arum*- and *Paris*-type AM symbiosis, respectively (Tominaga et al., 2020a), the effects of GA on Intermediate-type AM symbiosis remain to be cleared. Thus, we treated *L. japonicus*, *D. carota*, and *E. grandiflorum* with 1 μM GA_3 and observed and quantified fungal colonization. In *L. japonicus* roots, we confirmed that GA treatment significantly inhibited the AM fungal colonization and arbuscule formation compared with the control AM roots, but some intercellular hyphae were still found as described in several studies (**Figures 2A,D** and **Supplementary Figure 1B**; Floss et al., 2013; Takeda et al., 2015; Pimprikar et al., 2016;

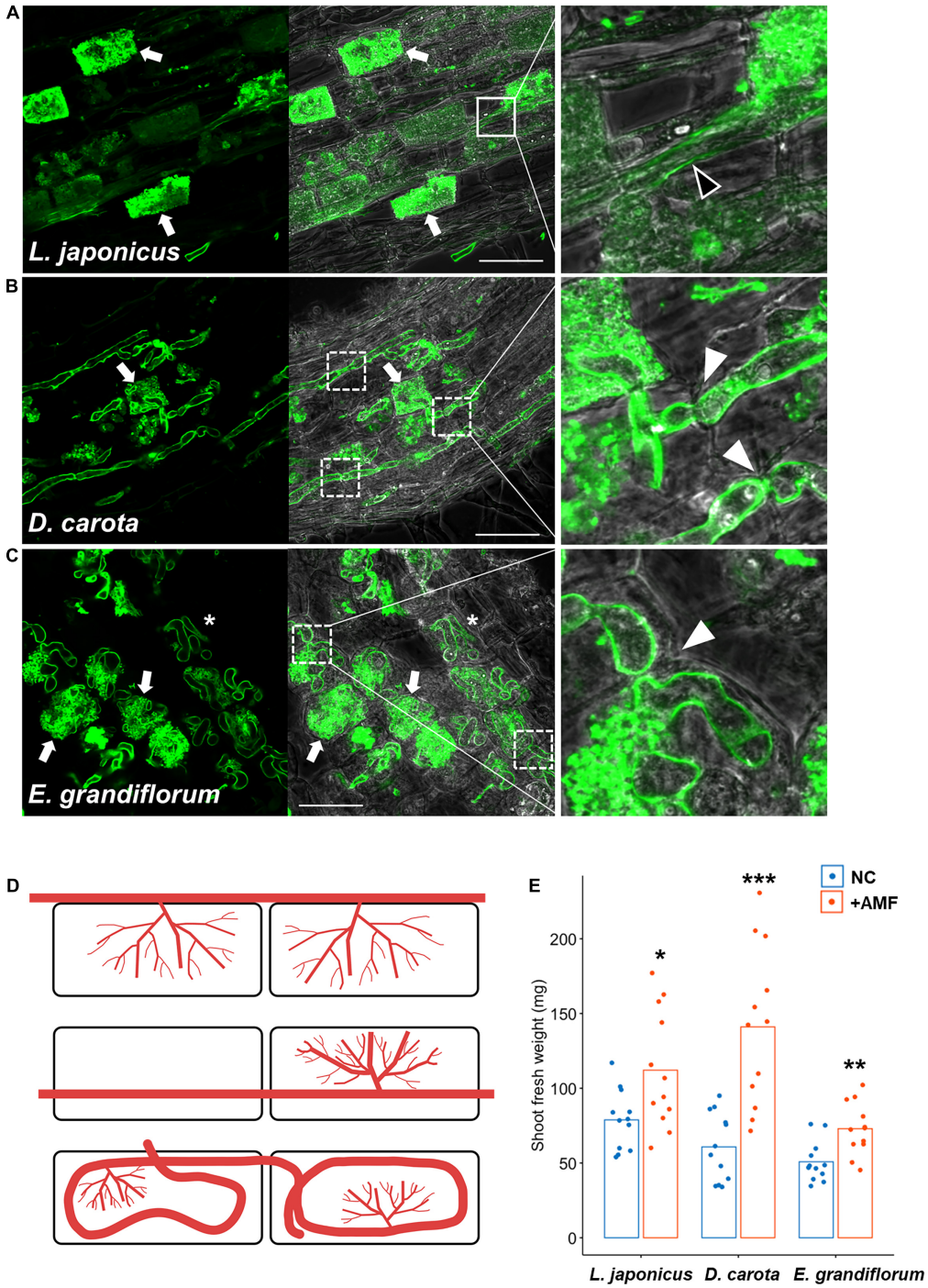

FIGURE 1 | Observation of arbuscular mycorrhizal (AM) morphotypes and quantification of plant growth promotion. AM symbiosis-related phenotypes and shoot fresh weight of *Lotus japonicus*, *Daucus carota*, and *Eustoma grandiflorum* colonized by *Rhizophagus irregularis* were observed and evaluated at 6 wpi. The collected AM roots were stained with WGA-Alexa Fluor 488 (green). **(A–C)** Confocal images of *L. japonicus* **(A)**, *D. carota* **(B)**, and *E. grandiflorum* **(C)** inoculated with *R. irregularis*. The left sides of each confocal fluorescence image are merged with their images in bright field (middle). The enlarged images showing where intraradical hyphae elongate are set on the right side of the merged pictures. Arrows, arbuscules; solid-line square, intercellular hypha (black arrowhead in the enlarged image); dotted-line squares, intracellular hyphae penetrating two adjacent cortical cells (white arrowheads in the magnified images); asterisks, hyphal coils in the root cortical cells; bars, 50 μm. **(D)** Diagrams of AM morphotypes observed in *L. japonicus* (upper), *D. carota* (middle), and *E. grandiflorum* (bottom). Red lines indicate intraradical *R. irregularis* hyphae. **(E)** The shoot fresh weight (mg) of each host plant grown in axenic conditions (NC) and colonized by *R. irregularis* (+AMF) (n = 12). The average percentage values are shown as bars. Asterisks indicate significant differences compared with the controls in the Wilcoxon rank-sum test (*$p < 0.05$, **$p < 0.01$, ***$p < 0.001$).

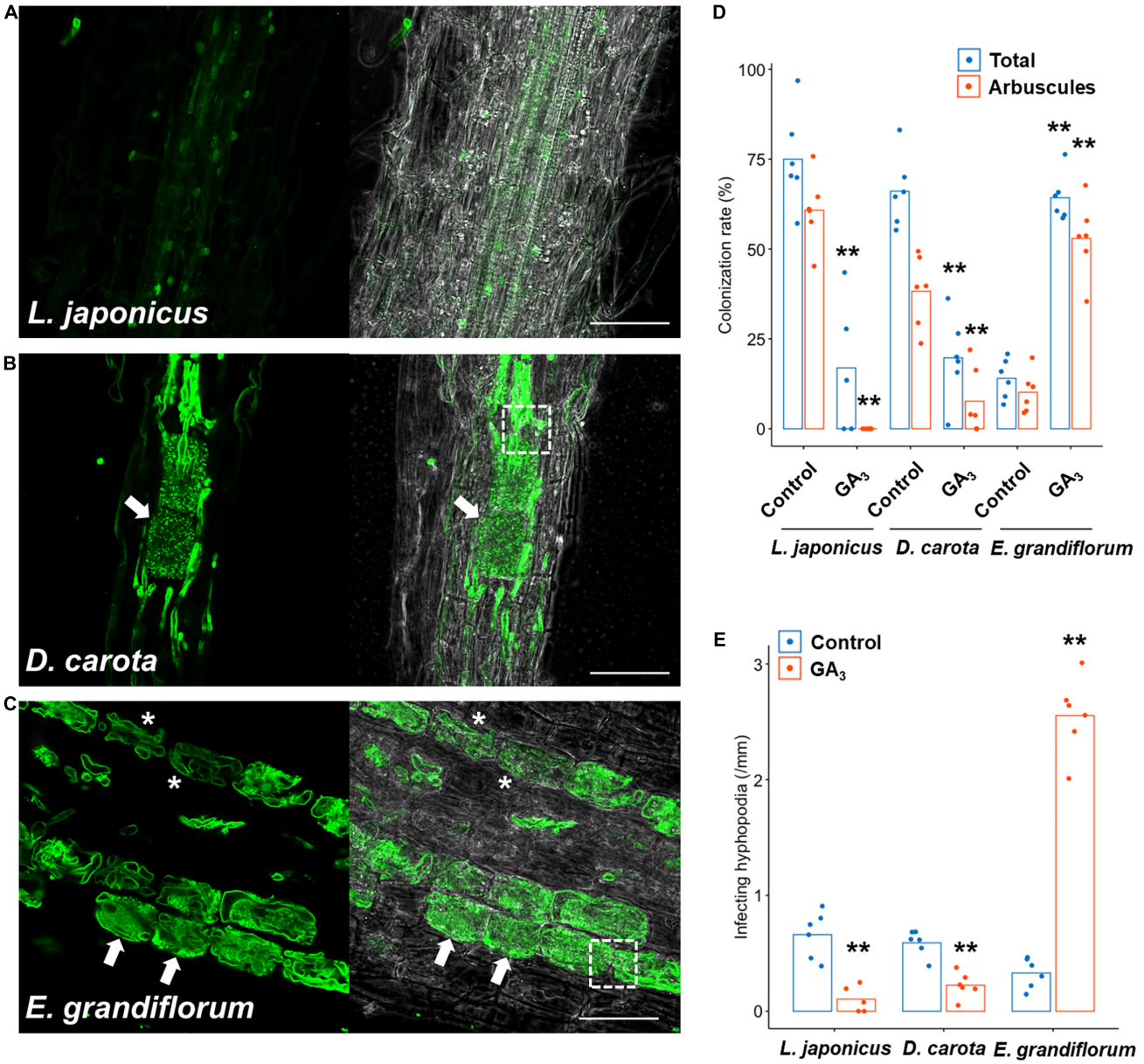

FIGURE 2 | Effects of GA on hyphal structures and AM fungal colonization in tested host plants. Each host plant was treated with 0.01% ethanol (+AMF) for the control and 1 μM GA_3 (+AMF +GA_3) for 6 weeks. The AM root samples were stained with WGA-Alexa Fluor 488 (green). **(A–C)** Confocal images of *Lotus japonicus* **(A)**, *Daucus carota* **(B)**, and *Eustoma grandiflorum* **(C)** inoculated with *Rhizophagus irregularis* in the presence of GA. Arrows, arbuscules; dotted-line squares, intracellular hyphae invading two adjacent cortical cells, asterisks, hyphal coils; bars, 200 μm in **(A)** and 50 μm in **(B,C)**. **(D)** Quantification of AM fungal colonization rates (%) of the examined plants at 6 wpi. Total, total colonization rate; arbuscules, percentage of arbuscule formation (n = 5, 6). **(E)** The number of hyphopodia penetrating the host root epidermis per root length (mm) (n = 5, 6). The average percentage values are represented as bars. Asterisks indicate statistical significance compared with the controls in the Wilcoxon rank-sum test (**$p < 0.01$). AM, arbuscular mycorrhizal; GA, gibberellin.

Nouri et al., 2021). Interestingly, the morphologies of hyphal structures in *D. carota* and *E. grandiflorum* were not influenced by GA treatment (**Figures 2B,C**). Nevertheless, GA-treated *D. carota* showed reduced AM fungal colonization compared with the control (**Figure 2D**). These results indicate that *D. carota* can form normal but less arbuscules in the presence of GA compared with the control roots, implying that AM symbiosis in *L. japonicus* was more vulnerable to 1 μM GA_3 than GA-suppressed AM symbiosis in *D. carota*. Additionally, GA-treated *E. grandiflorum* roots showed enhanced AM fungal infection with fully developed arbuscules at 6 wpi (**Figures 2C,D**) as our previous study has reported the same result at 4 wpi (Tominaga et al., 2020a). The number of AM fungal entries was consistent with the colonization rates (**Figure 2E**). Therefore,

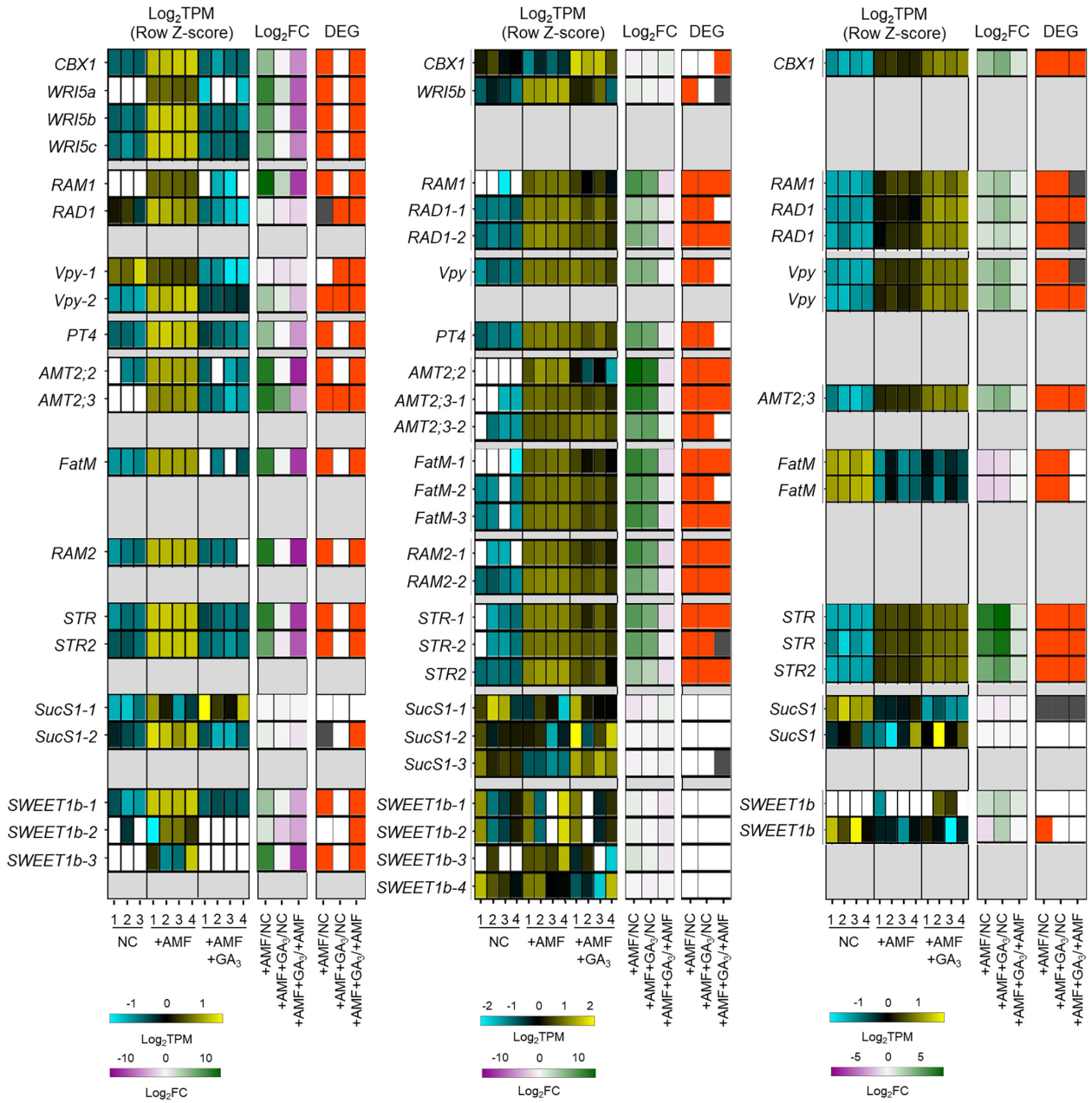

FIGURE 3 | Comparative analysis on the expression patterns of AM symbiosis-related downstream genes conserved among examined host plants. **(A–C)** Heatmaps represent the expression patterns of the selected genes in response to AM fungal colonization and GA treatment in *Lotus japonicus* **(A)**, *Daucus carota* **(B)**, and *Eustoma grandiflorum* **(C)** at 6 wpi. The left heatmaps indicate the expression levels of selected genes. The Log_2-transformed TPM in every sample is shown in blue (low expression level), black (mean), and yellow (high expression level); the expression levels are *Z*-score-normalized to turn the average value and SD to 0 and 1, respectively, across all samples. The number below the heatmaps indicates biological replicate. The middle ones show Log_2-transformed FCs in the genes compared with the controls. Magenta indicates negative values, green represents positive values, and white means 0. The right ones illustrate significance in the fold changes in gene expression levels. DEGs ($|Log_2FC| > 1$, FDR < 0.01) and genes showing significantly but slightly different expression levels compared with the controls (FDR < 0.05) are colored with red and gray, respectively. NC, non-colonized control; +AMF, *Rhizophagus irregularis* inoculation; +AMF +GA_3, simultaneous application of *R. irregularis* inoculation and 1 μM GA_3. The DEGs were identified by comparing +AMF with NC (+AMF/NC), +AMF +GA_3 against NC or +AMF (+AMF +GA_3/NC, +AMF +GA_3/+AMF). For the TPM, Log_2FC, and FDR values of the selected gene, see **Supplementary Table 4**. AM, arbuscular mycorrhizal; DEG, differentially expressed gene; FC, fold change; FDR, false discovery rate; GA, gibberellin; TPM, transcripts per million.

the association with *R. irregularis* contributed to the growth promotion in each tested plant regardless of AM morphotypes, whereas the responses to exogenous GA in *E. grandiflorum* AM roots were unique.

Comparisons of Symbiosis-Related Genes Shed Light on Conserved and Specific Transcriptional Responses Among Arbuscular Mycorrhizal Host Plants

Based on the results in **Figures 1**, **2**, the transcriptional regulation of downstream genes required for AM symbiosis would be expected to be different among the examined plants. To test this hypothesis, the expression pattern of genes conserved among the host plants was compared. First, orthogroups, including each known AM symbiosis-related gene, were identified using the SonicParanoid software (**Supplementary Figure 2A** and **Supplementary Tables 2**, **3**).

We focused on several genes involved in AM symbiosis: *RAM1*, *RAD1*, *Vpy*, *PT4*, *AMT2;2, AMT2;3*, *FatM*, *RAM2*, *STR*, and *STR2* (**Supplementary Figure 2A** and **Supplementary Table 3**). The AP2-EREBP domain TFs, *CBX1* and *WRI5a/b/c* that are involved in fatty acid biosynthesis and reciprocally regulate the expression of *RAM1*, were also included in the analysis (Luginbuehl et al., 2017; Jiang Y. et al., 2018; Xue et al., 2018; Shi et al., 2021). Additionally, we identified the sucrose synthase 1 (*SucS1*) and glucose transporter (Sugar Will Eventually be Exported Transporter 1b; *SWEET1b*) conserved in the examined plants. In arbuscule-containing cortical cells, *SucS1* and *SWEET1b* are predicted to catalyze sucrose into glucose and export the monosaccharide *via* PAM in *M. truncatula*, respectively (Hohnjec et al., 2003; Baier et al., 2010; An et al., 2019). Notably, these genes have been reported to be transcriptionally upregulated upon AM fungal colonization.

In this analysis, the examined plants were grown under several conditions as follows: non-colonized control roots (NC), AM roots (+AMF), and GA-treated AM roots (+AMF +GA_3). A common set of selected genes were transcriptionally promoted upon fungal colonization at 6 wpi in each plant (**Figure 3**). AM fungal colonization, however, did not induce the expression of *E. grandiflorum FatM* (*EgFatM*), *D. carota,* and *E. grandiflorum SucS1*s and *SWEET1b*s at 6 wpi (**Figures 3B,C**). In addition to *EgFatM*, several transcripts annotated as palmitoyl-acyl carrier protein thioesterase were transcriptionally activated upon the AM fungal colonization (**Supplementary Table 4**). In *L. japonicus*, the expression levels of several conserved genes were undetectable or mostly reduced by exogenous GA compared with NC and +AMF conditions (**Figure 3A**). In contrast, the expression levels of AM symbiosis-related genes in GA-treated *D. carota* were still increased compared with the NC but decreased compared with the +AMF (**Figure 3B**). This suggests that the sensitivity of *D. carota* to negative effect of GA on the expression of AM symbiosis genes would be relatively moderate to that in *L. japonicus* as the colonization rates showed (**Figure 2D**). In *E. grandiflorum*, the expression of the AM-induced genes was further enhanced by GA than the NC and +AMF controls (**Figure 3C**). This result further supports the positive effect of GA on AM colonization in *E. grandiflorum* (**Figure 2D**).

Eustoma grandiflorum PT4 (*EgPT4*) and *RAM2* (*EgRAM2*) were not identified by the SonicParanoid. Therefore, we conducted a BLAST search for the two genes in *E. grandiflorum* with sufficient *E*-value (<1E-5) (**Supplementary Table 3**). Consequently, one gene annotated as phosphate transporter (TRINITY_DN34977_c0_g1_i1.p1) was found to be homologs to *M. truncatula PT4* (**Supplementary Table 3**) and was transcriptionally enhanced upon the AM fungal colonization and exogenous GA (**Supplementary Table 4**; Tominaga et al., 2020b). Additionally, several *E. grandiflorum* genes were annotated as glycerol-3-phosphate acyltransferase (*RAM2*) (**Supplementary Table 4**). However, their expression levels were not promoted upon the AM fungal colonization (**Supplementary Table 4**). Alternatively, we might have missed *EgRAM2* in the *de novo* assembly after removing redundant contigs with CD-HIT (Tominaga et al., 2020b).

Genes Involved in Phytohormone Biosynthesis and Signaling Show Similar Transcriptional Responses to Exogenous Gibberellin in the Examined Host Plants

Since the number of infecting hyphopodia differed between *L. japonicus*/*D. carota* and *E. grandiflorum*, we also analyzed the expression patterns of several SL-related genes. *D27*, *CCD7*, *CCD8*, and *MAX1* are necessary for SL biosynthesis (Booker et al., 2004, 2005; Auldridge et al., 2006; Alder et al., 2012; Waters et al., 2012a; Al-Babili and Bouwmeester, 2015). *PDR1* in *Petunia hybrida* encoding a G-type ABC transporter is predicted to export SLs (Kretzschmar et al., 2012). Additionally, *D14*, *DLK2*, and *KAI2*, which belong to a D14 family, have previously been demonstrated as components in SL, karrikin (KAR), or KAI2-ligand (KL) signaling or both (Waters et al., 2012b; Kameoka and Kyozuka, 2015; Vegh et al., 2017). Based on the identification using SonicParanoid, these genes seemed to be conserved in *L. japonicus*, *D. carota,* and *E. grandiflorum* (**Supplementary Figure 2B** and **Supplementary Table 3**). For SL biosynthetic genes, *LjD27*, *LjCCD7*, and *LjCCD8* were transcriptionally downregulated by GA treatment (**Figure 4A**). Additionally, the expression of *CCD8* in *E. grandiflorum* was significantly reduced upon GA treatment, and *EgD27* and *EgCCD7* expressions were slightly inhibited by the treatment. This result suggests that GA inhibits SL biosynthesis and exudation to the rhizosphere in *E. grandiflorum* as found in *L. japonicus* and *O. sativa* (**Figure 4C**; Ito et al., 2017).

However, a statistically significant induction of *DcCCD8* at 2.46-fold was detected in GA-treated AM roots compared with that in the +AMF condition (**Figure 4B** and **Supplementary Table 4**). To confirm the effect of GA on SL production, we conducted a germination assay by using *O. minor* whose germination is induced by SLs (Ueno et al., 2014; Trabelsi et al., 2017). To prepare root extraction in the same conditions as the RNA-seq experiments, the examined plants were

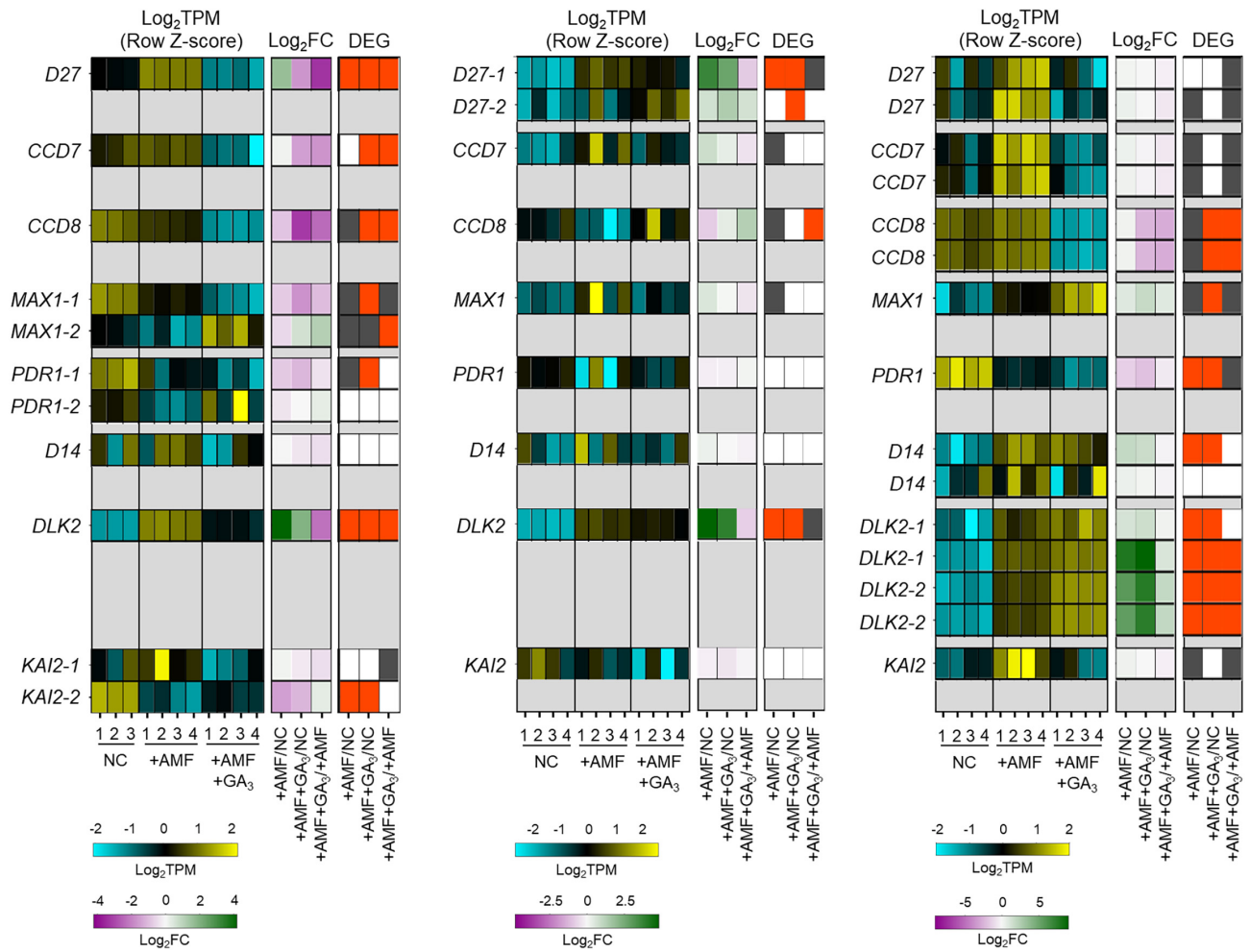

FIGURE 4 | Comparative analysis of the expression patterns of SL biosynthetic and signaling-related genes conserved among examined host plants. **(A–C)** Heatmaps represent the expression patterns of the selected SL-related genes in *Lotus japonicus* **(A)**, *Daucus carota* **(B)**, and *Eustoma grandiflorum* **(C)** at 6 wpi. The expression levels and Log_2FC compared with the controls of each gene are represented in the left heatmap (blue, low expression level; black, mean; yellow, high expression level) and the middle one (magenta, negative values; green, positive values; white, zero), respectively. The number below the heatmaps indicates a biological replicate. In the right one, the red and gray represent DEGs ($|Log_2FC| > 1$, FDR < 0.01) and genes with FDR < 0.05. NC, non-colonized control; +AMF, *Rhizophagus irregularis* inoculation; +AMF +GA_3, simultaneous application of *R. irregularis* inoculation and 1 μM GA_3. The DEGs were identified by comparing +AMF with NC (+AMF/NC), +AMF +GA_3 against NC or +AMF (+AMF +GA_3/NC, +AMF +GA_3/+AMF). The calculated values of TPM, Log_2FC, and FDR of the selected genes can be found in **Supplementary Table 4**. AM, arbuscular mycorrhizal; DEG, differentially expressed gene; FC, fold change; FDR, false discovery rate; GA, gibberellin; SL, strigolactone; TPM, transcripts per million.

grown in the soil mixture for 6 weeks. Consistent with the expression analysis, the germination activity of root extracts was significantly reduced in *L. japonicus* by GA treatment, whereas it increased in GA-treated *D. carota* (**Supplementary Figure 3**). The seed germination of *O. minor* was not promoted by *E. grandiflorum* root extracts, which might be attributed to the low quantities of SLs (Sato et al., 2003; Halouzka et al., 2020). When we hydroponically grow *E. grandiflorum*, the root exudates exhibited germination activity and negative effect of GA on SL production (**Supplementary Figure 3C**). Taken together, the enhanced AM fungal colonization in GA-treated *E. grandiflorum* would be mainly supported by unidentified components but not by SLs.

Of the SL signaling-related genes, *DLK2* was significantly induced in the examined host plants upon AM fungal colonization compared with NC control (**Figure 4**). Similarly, *DLK2* induction was reported in other host plants, *O. sativa* and *Solanum lycopersicum* (Choi et al., 2020; Ho-Plagaro et al., 2021). Moreover, compared with the +AMF control, GA treatment significantly reduced *DLK2* expression in *L. japonicus* but further increased in *E. grandiflorum* (**Figures 4A,C**; Tominaga et al., 2020b). The expression of *DLK2* in GA-treated *D. carota* was

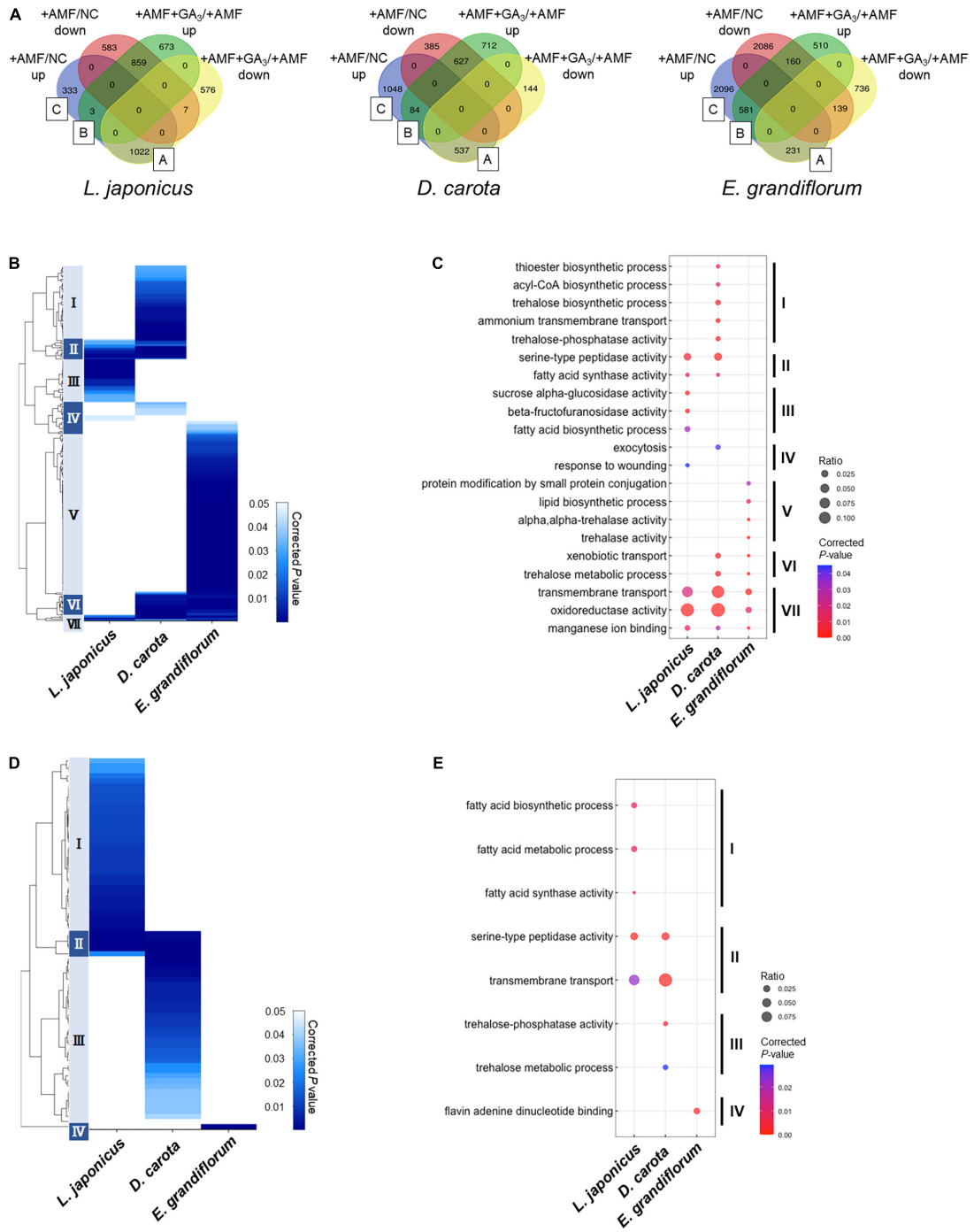

FIGURE 5 | Comparisons of enriched GO among AM roots of examined host plants. **(A)** Total DEGs ($|\text{Log}_2\text{FC}| > 1$, FDR < 0.01) in individual host plants during AM symbiosis at 6 wpi. Their expression patterns classify the DEGs. The values represent the number of DEGs. As for *Eustoma grandiflorum*, the values indicate the number of transcripts in *de novo* assembly data. Group A contains AM-upregulated but GA-downregulated DEGs, Group B represents AM- and GA-upregulated DEGs, and Group C indicates AM-upregulated DEGs. NC, non-colonized control; +AMF, *Rhizophagus irregularis* inoculation; +AMF +GA_3, simultaneous application of *R. irregularis* inoculation and 1 μM GA_3. For the determination of DEGs, transcriptomes in the host plants were compared as following: +AMF versus NC (+AMF/NC), +AMF +GA_3 versus +AMF (+AMF +GA_3/+AMF). **(B–E)** Hierarchical clustering of significantly enriched GO terms in the DEGs within Group A + B + C (upregulated upon AM fungal colonization) **(B)** and Group A **(D)** in each host plant at 6 wpi (corrected $p < 0.05$). The representative GO terms that enriched in each cluster of **(B,D)** were plotted in **(C,E)**, respectively. The size of circles represents ratio of DEGs enriched in a GO term to total number of DEGs. The color bar shows color-coded corrected *p*-value. The *p*-values were calculated using a two-sided hypergeometric test in the Cytoscape plugin, ClueGO, and corrected using the Benjamini–Hochberg method. For the detailed lists of DEGs and complete GO terms in each cluster, see **Supplementary Table 6**. AM, arbuscular mycorrhizal; DEG, differentially expressed gene; FC, fold change; FDR, false discovery rate; GA, gibberellin; GO, gene ontology.

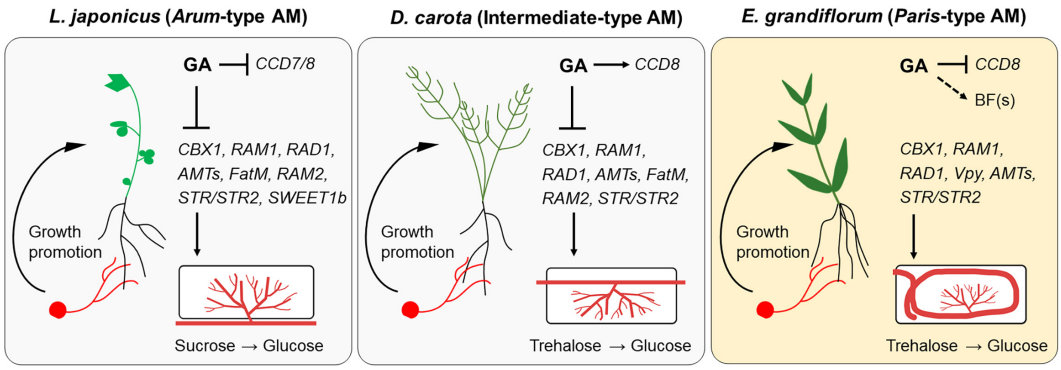

Host plant species	Responses to *R. irregularis*				Response to GA treatment				
	AM morphotype	Growth promotion	Fatty acid transport	Disaccharide metabolism	Colonization	Arbuscule formation	Hyphopodia No.	AM-responsible genes	SL biosynthesis
L. japonicus	*Arum*	+	+	Sucrose	- -	- -	-	- -	-
D. carota	*Intermediate*	+	+	Trehalose	-	-	-	-	+
E. grandiflorum	*Paris*	+	+	Trehalose	+	+	+	+	-

+: positive regulation, -: negative regulation

FIGURE 6 | Proposed model for conserved and divergent responses to AM fungi and exogenous GA in genetically distant host plants at 6 wpi. The hypothetical model and table represent common and different responses to *Rhizophagus irregularis* colonization and exogenous GA treatment in *Lotus japonicus* (*Arum*-type), *Daucus carota* (Intermediate-type), and *Eustoma grandiflorum* (*Paris*-type) AM roots. AM fungal colonization contributed to growth promotion in each tested plant forming the distinct AM morphotypes. However, GA treatment suppressed the AM fungal colonization in *L. japonicus* and *D. carota*. In contrast, GA treatment also promoted mycorrhization in *E. grandiflorum*. These alterations in colonization levels were consistent with the expression levels of the conserved downstream genes such as *RAM1*. Interestingly, our findings indicate that the upstream regulation of the symbiosis-related genes would be resistant to GA in *E. grandiflorum*, but vulnerable to GA in the others. On the other hand, GA transcriptionally inhibited SL biosynthetic genes (*CCD7* and/or *CCD8*) in *L. japonicus* and *E. grandiflorum*, implying the existence of unidentified branching factors in *E. grandiflorum*. Moreover, disaccharides mainly metabolized during AM symbiosis might be different: sucrose and trehalose in *L. japonicus* and *D. carota*/*E. grandiflorum*. Red words in the table indicate different traits and responses found among the examined host plants in this study. +, positive regulation; –, negative regulation. The figures were created with BioRender.com. AM, arbuscular mycorrhizal; GA, gibberellin; SL, strigolactone.

slightly reduced (**Figure 4B**). Thus, *DLK2* expression patterns would simply mirror the GA-mediated changes in AM fungal colonization level.

Transcriptional Responses to Exogenous Gibberellin Reflect Fungal Colonization Rates in Three Host Plant Species

To expand comparative analysis of transcriptional responses to the AM fungal colonization and GA treatment, we identified the ortholog genes with a one-to-one relationship among *L. japonicus*, *D. carota*, and *E. grandiflorum* using SonicParanoid. This resulted in 2,705 ortholog genes (**Supplementary Table 2**). The orthologs were designated as DEGs when they were differentially expressed at least in one condition of each host plant, resulting in 467 DEGs (**Supplementary Figure 4** and **Supplementary Table 5**). Hierarchical clustering showed that the transcriptional responses to GA in *L. japonicus* and *D. carota* AM roots were similar to each other (**Supplementary Figure 4**). In GA-treated *E. grandiflorum*, the transcriptional responses were found to be close to that of +AMF samples (**Supplementary Figure 4**). These data are consistent with the GA-suppressed AM symbioses in *L. japonicus* and *D. carota* and GA-resistant AM symbiosis in *E. grandiflorum* (**Figure 2**).

Since GA highlighted the different expression patterns of the conserved and orthologous genes among the examined plants so far, we next investigated GA-mediated responses shared among them. In GA-treated plants, the shoots, petioles, and leaves were significantly elongated, as other studies showed (**Supplementary Figure 5**). In addition to promoting plant growth, GA-treated host plants commonly showed significantly reduced *GA20ox* expression as previous study shows (**Supplementary Table 4**; Cheng et al., 2015). Therefore, GA appears to have common effects on plant physiological responses in *L. japonicus*, *D. carota*, and *E. grandiflorum* as expected.

Comparative Gene Ontology Enrichment Analysis Among the Examined Plant Species

To gain further insights into the similarity and difference in the regulation of AM symbiosis, we utilized our comparative transcriptome data to infer the physiological functions altered in the AM roots of each host plant by the GO enrichment analysis. To this end, DEGs were determined in each host plant, resulting in 4,056, 3,537, and 6,439 DEGs in *L. japonicus*, *D. carota*, and *E. grandiflorum*, respectively (**Figure 5A**). The relatively large number of DEGs in *E. grandiflorum* might be attributable to the redundant or alternative transcripts in *de novo* assembly (Duan et al., 2012; Ono et al., 2015), although the redundant contigs were removed from *de novo* reference data using CD-HIT (Li and Godzik, 2006; Tominaga et al., 2020b).

We classified the DEGs depending on their expression patterns (**Figure 5A**). Interestingly, we found that the ratio of DEGs in Group A representing AM fungus-induced but GA-suppressed genes was relatively low in *E. grandiflorum* (3.6%) compared to *L. japonicus* (25.2%) and *D. carota* (15.2%) (**Figure 5A**). In contrast, the percentage of DEGs in Group B representing AM fungus- and GA-induced genes was much lower in *L. japonicus* (0.074%) compared to *D. carota* (2.4%) and *E. grandiflorum* (9.0%) (**Figure 5A**).

As for DEGs upregulated by the AM fungal colonization (Group A + B + C), GO terms associated with membrane transport were enriched in all colonized plants (Cluster VII in **Figures 5B,C** and **Supplementary Table 6**). Some GO terms related to transport activity were still found in Group C of each host plant (**Supplementary Table 6**). Additionally, the analysis also detected peptidase- and fatty acid-related terms in *L. japonicus* and *D. carota* (Cluster II in **Figures 5B,C**). The enrichment of fatty acid-related GO term, fatty acid synthase activity, is consistent with the transcriptional promotions of *FatM* and *RAM2* in the two hosts colonized by *R. irregularis* (**Figures 3A,B**). On the other hand, some GO terms in Cluster II were not shared with *E. grandiflorum* (**Figures 5B,C** and **Supplementary Table 6**), which might be attributable to the fact that some homologs such as *RAM2* were not identified from the *de novo* assemble data of *E. grandiflorum* by SonicParanoid (**Supplementary Figure 1A**). However, some differences were found among different host plants. For example, the expressions of α-glucosidase and β-fructofuranosidase were promoted upon AM fungal colonization in *L. japonicus* (Cluster III in **Figures 5B,C** and **Supplementary Table 6**). Alternatively, *D. carota* and *E. grandiflorum* showed enhanced expressions of genes encoding trehalose biosynthetic enzymes and trehalase activity upon fungal inoculation, respectively (Cluster I, V, and VI in **Figures 5B,C** and **Supplementary Table 6**). These GO terms associating with trehalose also enriched in Group B, where genes were transcriptionally activated in both of AM fungal colonization and GA treatment (**Supplementary Table 6**). These results suggest that different disaccharides might be dominantly metabolized during AM symbioses: sucrose in *L. japonicus* and trehalose in the other two plants.

To compare GA-mediated change in AM-responsive genes, we next focused on Group A genes. As illustrated in the heatmap, the DEGs in the Group A of *E. grandiflorum* were significantly enriched in GO term representing flavin adenine dinucleotide binding (GO:0050660) (**Figures 5D,E** and **Supplementary Table 6**). In contrast, GO terms representing transmembrane transport and peptidase were shared in *L. japonicus* and *D. carota* (Cluster II in **Figures 5D,E** and **Supplementary Table 6**). The GO enrichment analysis again revealed that fatty acid biosynthesis was attenuated in GA-treated *L. japonicus* AM roots, corresponding to the negative effect of GA on *LjFatM* and *LjRAM2* expressions (**Figures 3A**, **5D,E** and **Supplementary Tables 4**, **6**). Moreover, trehalose-related genes were shown to be transcriptionally downregulated in GA-treated *D. carota* AM roots (Cluster III in **Figures 5D,E** and **Supplementary Table 6**). As for *E. grandiflorum* AM roots, trehalose metabolism was transcriptionally upregulated even in the presence of GA (**Supplementary Table 6**).

Comparison of Fungal Transcriptome Obtained From Three Examined Host Plants

We found that up to 13.7% of the RNA-seq reads are mapped to the genome of *R. irregularis* (**Supplementary Table 1**; Maeda et al., 2018). This allowed us to compare the transcriptomes of *R. irregularis* colonizing each of GA-treated *L. japonicus*, *D. carota*, and *E. grandiflorum* against one infecting the control plants. The number of the upregulated DEGs of *R. irregularis* was relatively smaller in GA-treated *L. japonicus* compared to other plants (**Supplementary Figure 6A**). On the other hand, the downregulated DEGs of *R. irregularis* in GA-treated *L. japonicus* were mostly shared with *D. carota* (24.7%) compared with *E. grandiflorum* (9.9%) (**Supplementary Figure 6A**).

Since *R. irregularis* seemed to differentially respond to the examined plants, we next conducted the GO enrichment analysis on the fungal DEGs. Hierarchical clustering arranged by Log_2FC revealed six clusters (**Supplementary Figure 6B**). We found several GO terms associated with a mitogen-activated protein kinase (MAPK) activity in Cluster IV, where upregulated DEGs in *R. irregularis* associating with GA-treated *E. grandiflorum* were dominant (**Supplementary Figure 6C** and **Supplementary Table 7**). Additionally, glycogen metabolism- and wax biosynthesis-related terms were found in the cluster. Interestingly, DEGs in Cluster VI, where numerous downregulated DEGs were found in GA-treated *L. japonicus*, were enriched in some GO terms corresponding to the elongation and oxidation of fatty acid (**Supplementary Figure 6D** and **Supplementary Table 7**). This may suggest that the allocation of host-derived fatty acids is attenuated by GA application in *L. japonicus*, which could be explained by the GA-suppressed the expression levels of genes for fatty acid biosynthesis in its AM roots (**Figures 3A**, **5E** and **Supplementary Tables 4**, **6**).

DISCUSSION

In this study, our comparative transcriptomics found a partially common transcriptional response during AM symbiosis among *L. japonicus*, *D. carota*, and *E. grandiflorum* roots in the absence of GA. A set of known AM symbiosis-related genes, *RAM1*, *RAD1*, *Vpy*, *PT4*, *AMT*s, *STR*, and *STR2*, conserved in the tested plants were transcriptionally promoted upon AM fungal colonization (**Figure 3**). These genes have been also shown to be transcriptionally upregulated during AM symbiosis in *L. japonicus*, *M. truncatula*, tomato, rice, and *Poncirus trifoliata* (Sugimura and Saito, 2017; An et al., 2018). Another study revealed the conservation of *RAD1*, *STR*, and *STR2* in broad AM host lineages across vascular plants and bryophytes and suggested their common functions in AM symbiosis; these AM symbiosis-related genes would comparably function in establishing AM symbiosis as well (Radhakrishnan et al., 2020). As for the function of the conserved genes, *CBX1*, *WRI5s*, *STR*, and *STR2* have been shown to be required for the full

development of arbuscule by regulating fatty acid biosynthesis and transfer to AM fungi (Bravo et al., 2017; Luginbuehl et al., 2017; Jiang Y. et al., 2018; Xue et al., 2018). Additionally, the expression levels of genes encoding phosphate and ammonium transporters were enhanced by AM fungal colonization (**Figure 3** and **Supplementary Table 4**), which would contribute to the host growth promotion regardless of the distinct AM morphotypes as shown in a previous report (**Figure 1E**; Hong et al., 2012). Taken together, nutrient exchange between the host plants and AM fungi would be commonly essential to establish AM symbiosis among the phylogenetically distant host plants. Especially, the capability of supplying fatty acids to AM fungi appears to be indispensable for the mutualism because AM fungi utilize lipids for their growth and reproduction (Kameoka et al., 2019b; Sugiura et al., 2020).

Nevertheless, GA treatment negatively and positively regulated the AM fungal colonization in *L. japonicus*/*D. carota* and *E. grandiflorum*, respectively, which were consistent with the expression patterns of the conserved genes such as *RAM1* (**Figures 2D**, **3**). Recently, CYCLOPS required for both AM symbiosis and root nodule symbiosis has been reported to bind the *cis*-element on *LjRAM1* promoter and upregulate gene expression in concert with a Ca^{+2}/calmodulin-dependent protein kinase (CCaMK) and a GA-degradable repressor of GA signaling, DELLA protein (Silverstone et al., 2001; Achard and Genschik, 2009; Jin et al., 2016; Pimprikar et al., 2016). The involvement of DELLA in the complex is thought to trigger the GA-mediated inhibition of *RAM1* expression, resulting in the severe suppression of AM fungal accommodation. The binding of DELLAs to the CCaMK-CYCLOPS complex has been also demonstrated in nodule symbiosis (Jin et al., 2016). *D. carota* and *L. japonicus* showed reduced rates of AM fungal colonization and expression levels of *RAM1*, indicating that the GA-mediated transcriptional regulation of downstream genes would be common (**Figure 6**). However, the expression levels of *RAM1* and some of the downstream genes were significantly or slightly promoted in GA-treated *E. grandiflorum* (**Figure 3C**). Although this arose an idea that GA directly modulates the expression of the downstream genes, the enhanced AM fungal colonization in GA-treated *E. grandiflorum* possibly contributed to the result since the downstream genes were responsible to AM fungal colonization levels (**Figures 2D**, **3** and **Supplementary Table 4**). On the other hand, the transcriptional regulation of the downstream genes in *E. grandiflorum* would be resistant to exogenous GA since no inhibitory effect of GA on AM symbiosis was observed in the host plant except for SL production (**Figures 1–4** and **Supplementary Figure 3C**). Therefore, DELLA might be dispensable for or inhibiting the expression of *RAM1* in *E. grandiflorum*, while this study could not uncover the DELLA function in the host plant. In fact, stabilizing DELLA proteins in *E. grandiflorum* suppresses AM fungal colonization and arbuscule formation (Tominaga et al., 2020a), whereas it did not change colonization levels or upregulate arbuscule formation (Takeda et al., 2015; Pimprikar et al., 2016). To clarify the upstream regulation of these TFs in *E. grandiflorum*, further investigation would be necessary.

Strigolactones are thought to potentiate pre-symbiotic fungal contact to the host roots because some mutants defect in SL biosynthesis and exudation showed delayed colonization and decreased the number of hyphopodia (Breuillin et al., 2010; Kretzschmar et al., 2012; Kobae et al., 2018). Additionally, SL biosynthesis and exudation are inhibited by exogenous GA (Ito et al., 2017). Indeed, we could confirm the inhibitory effects of GA on SL biosynthetic genes in *L. japonicus* and *E. grandiflorum* (**Figure 4** and **Supplementary Figure 3**). Interestingly, the number of the hyphopodia was drastically induced in GA-treated *E. grandiflorum* roots as shown in our previous study (**Figure 2E**; Tominaga et al., 2020a). This study also suggests that SLs would not be involved in the GA-promoted fungal invasion due to the negative effect of GA on SL production (**Figure 4C** and **Supplementary Figure 3C**). We could not identify the unknown signal molecule(s) yet; however, the possible existence was assumed from the GO enrichment analysis on *R. irregularis*. As shown in **Supplementary Figure 6**, some GO terms representing the activity of MAPK kinase kinase, MAPK Kinase, and MAPK were detected in *R. irregularis* colonizing GA-treated *E. grandiflorum* (**Supplementary Table 7**). In plant pathogenic fungi, such as *Ustilago maydis* and *Magnaporthe oryzae*, MAPK cascade is required for the formation of appressoria and their virulence after perceiving some signal molecules derived from the host plants (Hamel et al., 2012; Li X. et al., 2017; Jiang C. et al., 2018). Although the necessity of the MAPK cascade in *R. irregularis* hyphopodia formation remains unclear, the fungus might sense some signal molecule(s) exudates from GA-treated *E. grandiflorum* roots. Except for *L. japonicus* and *E. grandiflorum*, this study indicated that SL biosynthesis in *D. carota* might be less sensitive to GA even though exogenous GA reduced the number of invading hyphopodia (**Figures 2E**, **3B** and **Supplementary Figure 3**). A negative feedback regulation in SL biosynthesis might trigger the increase in *DcCCD8* expression upon exogenous GA at 6 wpi (Hayward et al., 2009; Proust et al., 2011). Alternatively, the reduction of SL exudation by GA might have occurred at an earlier time point than 6 wpi in *D. carota*.

Gibberellin is one of phytohormones that has versatile functions in abiotic stress responses. Light limitation makes plants accumulate GA, which results in the elongation of stem to gain efficient light for photosynthesis (Hisamatsu et al., 2005; Bou-Torrent et al., 2014; Colebrook et al., 2014; Li W. et al., 2017; Yang and Li, 2017). Interestingly, far-red treatment and *phyB* mutation have been reported to attenuate AM fungal colonization and SL production in *L. japonicus* and tomato colonized by *R. irregularis* (Nagata et al., 2015). Moreover, host plants forming *Paris*-type AM, such as Gentianaceae species, are often found in forest floor (Yamato and Iwasaki, 2002; Yamato, 2004). Thus, *Paris*-type AM symbiosis might enable the hosts to efficiently accommodate the symbionts in dark places. However, this idea should be further investigated because some plants are capable of suppressing shade-induced GA accumulation in petiole and hypocotyl elongation (Gommers et al., 2018; Paulišić et al., 2021). Recent study has also introduced that inorganic phosphate (Pi) inhibits AM symbiosis *via* GA signaling in Solanaceous model plants (Nouri et al., 2021). In contrast, *E. grandiflorum* might be capable of promoting AM fungal colonization in

high Pi concentration, although this hypothesis needs to be explored. Taken together, some plants like *E. grandiflorum* might adapt to their surroundings by exploiting the GA-resistant AM fungal colonization and unidentified signal molecule(s). The investigations of regulatory mechanisms underlying AM symbiosis with environmental cues and/or life stages of host plants would be necessary for further understanding.

The loss of genes encoding enzymes required for polysaccharide degradation in AM fungi demands host plants on glucose (Kobayashi et al., 2018). In arbuscules containing cells of *M. truncatula*, AM fungi-responsive localization and the expression of *MtSucS1* and *MtSWEET1b* are thought to produce glucose and export it toward AM fungi between the symbiotic interface (An et al., 2019). In fact, our GO enrichment analysis showed activated sucrose hydrolysis during AM symbiosis in *L. japonicus*, which was supported by AM-induced *LjSucS1* and *LjSWEET1b*s expression (**Figure 3A** and **Supplementary Table 4**). In contrast, another disaccharide, trehalose, appeared to be broken down in *D. carota* and *E. grandiflorum* during AM symbiosis, as the increases in plant trehalase (*TRE1*) gene expressions were found in the host plants upon AM fungal colonization (**Figure 5C** and **Supplementary Tables 3**, **5**). This difference might be attributable to the intracellular hyphal invasion in Intermediate- and *Paris*-type AM roots (**Figures 1B–D** and **Supplementary Figures 1C–E**). However, the increase in *TRE1* expression was also observed in *L. japonicus* AM roots at 6 wpi (**Supplementary Table 4**). Interestingly, it is known that most of the storage carbohydrates found in fungi are trehalose, and AM fungi can synthesize, metabolize, and accumulate trehalose in the spores and hyphae (Shachar-Hill et al., 1995; Bago et al., 1999; Pfeffer et al., 1999; Kameoka et al., 2019a). Additionally, the upregulation of *TRE1* expression has also been seen in *Arabidopsis thaliana* infected by a pathogenic fungus, *Plasmodiophora brassicae*, which is considered as the maintenance of sugar concentration and physiological homeostasis in the roots by removing fungal-derived trehalose (Brodmann et al., 2002). On the other hand, the suppression of the trehalose precursor trehalose-6-phosphate (T6P) production has been found in *L. japonicus* AM roots and predicted to be related to the decomposition of starch into glucose for AM fungi (Kolbe et al., 2005; Handa et al., 2015), indicating TRE1 would be involved in the regulation of symbiotic glucose metabolism. However, most of trehalose-6-phosphate synthases that catalyze T6P production were not transcriptionally suppressed at in *D. carota* and *E. grandiflorum* at 6 wpi (**Supplementary Table 4**). This suggests that the *TRE1* expression enhanced during AM symbiosis might not be involved in the starch degradation. Therefore, TRE1 might be required to reduce AM fungi-derived trehalose concentration in the host plants, for example, when arbuscules are hydrolyzed in a short period (Kobae et al., 2014; Floss et al., 2017).

In summary, a particular set of conserved AM symbiosis-related genes would commonly function to accommodate AM fungi in the phylogenetically distant AM host plants regardless of distinct AM morphotypes. However, our transcriptomics and GA treatment indicate the GA-mediated different molecular mechanisms regulating the conserved AM symbiosis-related genes between *L. japonicus*/*D. carota* and *E. grandiflorum* (**Figure 6**). These findings advance the comprehensive understanding of transcriptomic regulation and the diversity of GA-mediated effects on AM symbioses among host plants. Additionally, AM fungal traits sometimes affect AM morphotype formed in a single host species (Cavagnaro et al., 2001; Dickson, 2004; Smith et al., 2004; Kubota et al., 2005; Hong et al., 2012). Thus, the comparison of GA-mediated regulations underlying AM symbioses using a single host species would be expected to further support the causal relationship between AM-morphotyped and the different GA-mediated regulation of symbiosis in the next study.

DATA AVAILABILITY STATEMENT

The original contributions presented in the study are publicly available. The nucleotide sequence data obtained from our transcriptome analysis has been deposited into the DDBJ Sequence Read Archive under the accession number DRA012117. *De novo* assembly and annotation list of *E. grandiflorum* are available on Open Science Foundation with DOI:10.17605/OSF.IO/TQ7XJ or https://osf.io/tq7xj/?view_only=b6bec888fd80417ea636c3b6b58f07c1.

AUTHOR CONTRIBUTIONS

TT and HK conceived and designed the experiments. TT, YS, YH, and AM performed the experiments. TT, CM, KY, SS, and AM analyzed the sequencing data. TT, CM, AM, and HK wrote the manuscript. All authors approved the final manuscript.

FUNDING

This work was partially supported by the NIBB Cooperative Research Programs (Next-generation DNA Sequencing Initiative: 19-433, 20-407) and JSPS KAKENHI Grant-in-Aid for JSPS Fellows (Grant No. 20J21994 to TT).

ACKNOWLEDGMENTS

We would like to thank Gabriela Bindea (Cordeliers Research Center) for preparing the list and enabling us to conduct GO enrichment analysis on *Lotus japonicus* and *Eustoma grandiflorum*. Additionally, we appreciate the National BioResource Project (Legume Base) and Satoko Yoshida (Nara Institute of Science and Technology) for kindly providing *L. japonicus* and *Orobanche minor* seeds, respectively.

SUPPLEMENTARY MATERIAL

The Supplementary Material for this article can be found online at: https://www.frontiersin.org/articles/10.3389/fpls.2021.795695/full#supplementary-material

REFERENCES

Achard, P., and Genschik, P. (2009). Releasing the brakes of plant growth: how GAs shutdown DELLA proteins. *J. Exp. Bot.* 60, 1085–1092. doi: 10.1093/jxb/ern301

Akiyama, K., Matsuzaki, K., and Hayashi, H. (2005). Plant sesquiterpenes induce hyphal branching in arbuscular mycorrhizal fungi. *Nature* 435, 824–827. doi: 10.1038/nature03608

Al-Babili, S., and Bouwmeester, H. J. (2015). Strigolactones, a novel carotenoid-derived plant hormone. *Annu Rev Plant Biol.* 66, 161–186. doi: 10.1146/annurev-arplant-043014-114759

Alder, A., Jamil, M., Marzorati, M., Bruno, M., Vermathen, M., Bigler, P., et al. (2012). The path from β-carotene to carlactone, a strigolactone-like plant hormone. *Science* 335, 1348–1351. doi: 10.1126/science.1218094

Alexa, A., Rahnenfuhrer, J., and Lengauer, T. (2006). Improved scoring of functional groups from gene expression data by decorrelating GO graph structure. *Bioinformatics* 22, 1600–1607. doi: 10.1093/bioinformatics/btl140

An, J., Sun, M., van Velzen, R., Ji, C., Zheng, Z., Limpens, E., et al. (2018). Comparative transcriptome analysis of *Poncirus trifoliata* identifies a core set of genes involved in arbuscular mycorrhizal symbiosis. *J. Exp. Bot.* 69, 5255–5264. doi: 10.1093/jxb/ery283

An, J., Zeng, T., Ji, C., de Graaf, S., Zheng, Z., Xiao, T. T., et al. (2019). A *Medicago truncatula* SWEET transporter implicated in arbuscule maintenance during arbuscular mycorrhizal symbiosis. *New Phytol.* 224, 396–408. doi: 10.1111/nph.15975

Auldridge, M. E., Block, A., Vogel, J. T., Dabney-Smith, C., Mila, I., Bouzayen, M., et al. (2006). Characterization of three members of the Arabidopsis carotenoid cleavage dioxygenase family demonstrates the divergent roles of this multifunctional enzyme family. *Plant J.* 45, 982–993. doi: 10.1111/j.1365-313X.2006.02666.x

Bago, B., Pfeffer, P. E., Douds, D. D. Jr., Brouillette, J., Bécard, G., and Shachar-Hill, Y. (1999). Carbon metabolism in spores of the arbuscular mycorrhizal fungus *Glomus intraradices* as revealed by nuclear magnetic resonance spectroscopy. *Plant Physiol.* 121, 263–272. doi: 10.1104/pp.121.1.263

Baier, M. C., Keck, M., Godde, V., Niehaus, K., Kuster, H., and Hohnjec, N. (2010). Knockdown of the symbiotic sucrose synthase MtSucS1 affects arbuscule maturation and maintenance in mycorrhizal roots of *Medicago truncatula*. *Plant Physiol.* 152, 1000–1014. doi: 10.1104/pp.109.149898

Besserer, A., Becard, G., Jauneau, A., Roux, C., and Sejalon-Delmas, N. (2008). GR24, a synthetic analog of strigolactones, stimulates the mitosis and growth of the arbuscular mycorrhizal fungus *Gigaspora rosea* by boosting its energy metabolism. *Plant Physiol.* 148, 402–413. doi: 10.1104/pp.108.121400

Bindea, G., Galon, J., and Mlecnik, B. (2013). CluePedia Cytoscape plugin: pathway insights using integrated experimental and in silico data. *Bioinformatics* 29, 661–663. doi: 10.1093/bioinformatics/btt019

Bindea, G., Mlecnik, B., Hackl, H., Charoentong, P., Tosolini, M., Kirilovsky, A., et al. (2009). ClueGO: a Cytoscape plug-in to decipher functionally grouped gene ontology and pathway annotation networks. *Bioinformatics* 25, 1091–1093. doi: 10.1093/bioinformatics/btp101

Booker, J., Auldridge, M., Wills, S., McCarty, D., Klee, H., and Leyser, O. (2004). MAX3/CCD7 is a carotenoid cleavage dioxygenase required for the synthesis of a novel plant signaling molecule. *Curr. Biol.* 14, 1232–1238. doi: 10.1016/j.cub.2004.06.061

Booker, J., Sieberer, T., Wright, W., Williamson, L., Willett, B., Stirnberg, P., et al. (2005). *MAX1* encodes a cytochrome P450 family member that acts downstream of *MAX3/4* to produce a carotenoid-derived branch-inhibiting hormone. *Dev. Cell.* 8, 443–449. doi: 10.1016/j.devcel.2005.01.009

Bou-Torrent, J., Galstyan, A., Gallemí, M., Cifuentes-Esquivel, N., Molina-Contreras, M. J., Salla-Martret, M., et al. (2014). Plant proximity perception dynamically modulates hormone levels and sensitivity in *Arabidopsis*. *J. Exp. Bot.* 65, 2937–2947. doi: 10.1093/jxb/eru083

Bravo, A., Brands, M., Wewer, V., Dormann, P., and Harrison, M. J. (2017). Arbuscular mycorrhiza-specific enzymes FatM and RAM2 fine-tune lipid biosynthesis to promote development of arbuscular mycorrhiza. *New Phytol.* 214, 1631–1645. doi: 10.1111/nph.14533

Breuillin, F., Schramm, J., Hajirezaei, M., Ahkami, A., Favre, P., Druege, U., et al. (2010). Phosphate systemically inhibits development of arbuscular mycorrhiza in *Petunia hybrida* and represses genes involved in mycorrhizal functioning. *Plant J.* 64, 1002–1017. doi: 10.1111/j.1365-313X.2010.04385.x

Brodmann, A., Schuller, A., Ludwig-Müller, J., Aeschbacher, R. A., Wiemken, A., Boller, T., et al. (2002). Induction of trehalase in *Arabidopsis* plants infected with the trehalose-producing pathogen *Plasmodiophora brassicae*. *Mol. Plant Microbe Interact.* 15, 693–700. doi: 10.1094/mpmi.2002.15.7.693

Brundrett, M. C., and Tedersoo, L. (2018). Evolutionary history of mycorrhizal symbioses and global host plant diversity. *New Phytol.* 220, 1108–1115. doi: 10.1111/nph.14976

Cavagnaro, T. R., Gao, L. L., Smith, F. A., and Smith, S. E. (2001). Morphology of arbuscular mycorrhizas is influenced by fungal identity. *New Phytologist* 151, 469–475. doi: 10.1046/j.0028-646x.2001.00191.x

Chen, S., Zhou, Y., Chen, Y., and Gu, J. (2018). fastp: an ultra-fast all-in-one FASTQ preprocessor. *Bioinformatics* 34, i884–i890. doi: 10.1093/bioinformatics/bty560

Cheng, C., Jiao, C., Singer, S. D., Gao, M., Xu, X., Zhou, Y., et al. (2015). Gibberellin-induced changes in the transcriptome of grapevine (Vitis labrusca x V. vinifera) cv. Kyoho flowers. *BMC Genomics* 16:128. doi: 10.1186/s12864-015-1324-8

Choi, J., Lee, T., Cho, J., Servante, E. K., Pucker, B., Summers, W., et al. (2020). The negative regulator SMAX1 controls mycorrhizal symbiosis and strigolactone biosynthesis in rice. *Nat. Commun.* 11:2114. doi: 10.1038/s41467-020-16021-1

Colebrook, E. H., Thomas, S. G., Phillips, A. L., and Hedden, P. (2014). The role of gibberellin signalling in plant responses to abiotic stress. *J. Exp. Biol.* 217, 67–75. doi: 10.1242/jeb.089938

Cosentino, S., and Iwasaki, W. (2019). SonicParanoid: fast, accurate and easy orthology inference. *Bioinformatics* 35, 149–151. doi: 10.1093/bioinformatics/bty631

Dickson, S. (2004). The *Arum-Paris* continuum of mycorrhizal symbioses. *New Phytologist.* 163, 187–200. doi: 10.1111/j.1469-8137.2004.01095.x

Dickson, S., Smith, F. A., and Smith, S. E. (2007). Structural differences in arbuscular mycorrhizal symbioses: more than 100 years after Gallaud, where next? *Mycorrhiza* 17, 375–393. doi: 10.1007/s00572-007-0130-9

Dobin, A., Davis, C. A., Schlesinger, F., Drenkow, J., Zaleski, C., Jha, S., et al. (2013). STAR: ultrafast universal RNA-seq aligner. *Bioinformatics* 29, 15–21. doi: 10.1093/bioinformatics/bts635

Duan, J., Xia, C., Zhao, G., Jia, J., and Kong, X. (2012). Optimizing *de novo* common wheat transcriptome assembly using short-read RNA-Seq data. *BMC Genomics* 13:392. doi: 10.1186/1471-2164-13-392

Ezawa, T., and Saito, K. (2018). How do arbuscular mycorrhizal fungi handle phosphate? New insight into fine-tuning of phosphate metabolism. *New Phytol.* 220, 1116–1121. doi: 10.1111/nph.15187

Floková, K., Shimels, M., Andreo Jimenez, B., Bardaro, N., Strnad, M., Novák, O., et al. (2020). An improved strategy to analyse strigolactones in complex sample matrices using UHPLC-MS/MS. *Plant Methods* 16:125. doi: 10.1186/s13007-020-00669-3

Floss, D. S., Gomez, S. K., Park, H. J., MacLean, A. M., Muller, L. M., Bhattarai, K. K., et al. (2017). A Transcriptional Program for Arbuscule Degeneration during AM Symbiosis Is Regulated by MYB1. *Curr. Biol.* 27, 1206–1212. doi: 10.1016/j.cub.2017.03.003

Floss, D. S., Levy, J. G., Levesque-Tremblay, V., Pumplin, N., and Harrison, M. J. (2013). DELLA proteins regulate arbuscule formation in arbuscular mycorrhizal symbiosis. *Proc. Natl. Acad. Sci. U S A.* 110, E5025–E5034. doi: 10.1073/pnas.1308973110

Galili, T., O'Callaghan, A., Sidi, J., and Sievert, C. (2018). heatmaply: an R package for creating interactive cluster heatmaps for online publishing. *Bioinformatics* 34, 1600–1602. doi: 10.1093/bioinformatics/btx657

Gobbato, E., Wang, E., Higgins, G., Bano, S. A., Henry, C., Schultze, M., et al. (2013). *RAM1* and *RAM2* function and expression during arbuscular mycorrhizal symbiosis and *Aphanomyces euteiches* colonization. *Plant Signal. Behav.* 8:26049. doi: 10.4161/psb.26049

Gommers, C. M. M., Buti, S., Tarkowská, D., Pěnčík, A., Banda, J. P., Arricastres, V., et al. (2018). Organ-specific phytohormone synthesis in two *Geranium* species with antithetical responses to far-red light enrichment. *Plant Direct.* 2:e00066. doi: 10.1002/pld3.66

Grabherr, M. G., Haas, B. J., Yassour, M., Levin, J. Z., Thompson, D. A., Amit, I., et al. (2011). Full-length transcriptome assembly from RNA-Seq data without a reference genome. *Nat. Biotechnol.* 29, 644–652. doi: 10.1038/nbt.1883

Haas, B. J., Papanicolaou, A., Yassour, M., Grabherr, M., Blood, P. D., Bowden, J., et al. (2013). *De novo* transcript sequence reconstruction from RNA-seq using the Trinity platform for reference generation and analysis. *Nat. Protoc.* 8, 1494–1512. doi: 10.1038/nprot.2013.084

Halouzka, R., Zeljkovic, S. C., Klejdus, B., and Tarkowski, P. (2020). Analytical methods in strigolactone research. *Plant Methods* 16:76. doi: 10.1186/s13007-020-00616-2

Hamel, L. P., Nicole, M. C., Duplessis, S., and Ellis, B. E. (2012). Mitogen-activated protein kinase signaling in plant-interacting fungi: distinct messages from conserved messengers. *Plant Cell* 24, 1327–1351. doi: 10.1105/tpc.112.096156

Handa, Y., Nishide, H., Takeda, N., Suzuki, Y., Kawaguchi, M., and Saito, K. (2015). RNA-seq Transcriptional Profiling of an Arbuscular Mycorrhiza Provides Insights into Regulated and Coordinated Gene Expression in Lotus japonicus and Rhizophagus irregularis. *Plant Cell Physiol.* 56, 1490–1511.

Hart, A. J., Ginzburg, S., Xu, M. S., Fisher, C. R., Rahmatpour, N., Mitton, J. B., et al. (2020). EnTAP: Bringing faster and smarter functional annotation to non-model eukaryotic transcriptomes. *Mol. Ecol analyse strigolactones in c.Resour.* 20, 591–604. doi: 10.1111/1755-0998.13106

Hayward, A., Stirnberg, P., Beveridge, C., and Leyser, O. (2009). Interactions between auxin and strigolactone in shoot branching control. *Plant Physiol.* 151, 400–412. doi: 10.1104/pp.109.137646

Hisamatsu, T., King, R. W., Helliwell, C. A., and Koshioka, M. (2005). The involvement of gibberellin 20-oxidase genes in phytochrome-regulated petiole elongation of Arabidopsis. *Plant Physiol.* 138, 1106–1116. doi: 10.1104/pp.104.059055

Hohnjec, N., Perlick, A. M., Puhler, A., and Kuster, H. (2003). The *Medicago truncatula* sucrose synthase gene *MtSucS1* is activated both in the infected region of root nodules and in the cortex of roots colonized by arbuscular mycorrhizal fungi. *Mol. Plant Microbe Interact.* 16, 903–915. doi: 10.1094/MPMI.2003.16.10.903

Hong, J. J., Park, Y. S., Bravo, A., Bhattarai, K. K., Daniels, D. A., and Harrison, M. J. (2012). Diversity of morphology and function in arbuscular mycorrhizal symbioses in *Brachypodium distachyon*. *Planta* 236, 851–865. doi: 10.1007/s00425-012-1677-z

Ho-Plagaro, T., Morcillo, R. J. L., Tamayo-Navarrete, M. I., Huertas, R., Molinero-Rosales, N., Lopez-Raez, J. A., et al. (2021). DLK2 regulates arbuscule hyphal branching during arbuscular mycorrhizal symbiosis. *New Phytol.* 229, 548–562. doi: 10.1111/nph.16938

Iorizzo, M., Ellison, S., Senalik, D., Zeng, P., Satapoomin, P., Huang, J., et al. (2016). A high-quality carrot genome assembly provides new insights into carotenoid accumulation and asterid genome evolution. *Nat. Genet.* 48, 657–666. doi: 10.1038/ng.3565

Ito, S., Yamagami, D., Umehara, M., Hanada, A., Yoshida, S., Sasaki, Y., et al. (2017). Regulation of Strigolactone Biosynthesis by Gibberellin Signaling. *Plant Physiol.* 174, 1250–1259. doi: 10.1104/pp.17.00301

Jiang, C., Zhang, X., Liu, H., and Xu, J. R. (2018). Mitogen-activated protein kinase signaling in plant pathogenic fungi. *PLoS Pathog.* 14:e1006875. doi: 10.1371/journal.ppat.1006875

Jiang, Y., Xie, Q., Wang, W., Yang, J., Zhang, X., Yu, N., et al. (2018). *Medicago* AP2-domain transcription factor WRI5a is a master regulator of lipid biosynthesis and transfer during mycorrhizal symbiosis. *Mol. Plant.* 11, 1344–1359. doi: 10.1016/j.molp.2018.09.006

Jin, Y., Liu, H., Luo, D., Yu, N., Dong, W., Wang, C., et al. (2016). DELLA proteins are common components of symbiotic rhizobial and mycorrhizal signalling pathways. *Nat. Commun.* 7:12433. doi: 10.1038/ncomms12433

Kameoka, H., and Kyozuka, J. (2015). Downregulation of rice *DWARF 14 LIKE* suppress mesocotyl elongation via a strigolactone independent pathway in the dark. *J Genet Genomics* 42, 119–124. doi: 10.1016/j.jgg.2014.12.003

Kameoka, H., Tsutsui, I., Saito, K., Kikuchi, Y., Handa, Y., Ezawa, T., et al. (2019b). Stimulation of asymbiotic sporulation in arbuscular mycorrhizal fungi by fatty acids. *Nat. Microbiol.* 4, 1654–1660. doi: 10.1038/s41564-019-0485-7

Kameoka, H., Maeda, T., Okuma, N., and Kawaguchi, M. (2019a). Structure-specific regulation of nutrient transport and metabolism in arbuscular mycorrhizal fungi. *Plant Cell Physiol.* 60, 2272–2281. doi: 10.1093/pcp/pcz122

Kobae, Y., Gutjahr, C., Paszkowski, U., Kojima, T., Fujiwara, T., and Hata, S. (2014). Lipid droplets of arbuscular mycorrhizal fungi emerge in concert with arbuscule collapse. *Plant Cell Physiol.* 55, 1945–1953. doi: 10.1093/pcp/pcu123

Kobae, Y., and Hata, S. (2010). Dynamics of periarbuscular membranes visualized with a fluorescent phosphate transporter in arbuscular mycorrhizal roots of rice. *Plant Cell Physiol.* 51, 341–353. doi: 10.1093/pcp/pcq013

Kobae, Y., Kameoka, H., Sugimura, Y., Saito, K., Ohtomo, R., Fujiwara, T., et al. (2018). Strigolactone biosynthesis genes of rice are required for the punctual entry of arbuscular mycorrhizal fungi into the roots. *Plant Cell Physiol.* 59, 544–553. doi: 10.1093/pcp/pcy001

Kobayashi, Y., Maeda, T., Yamaguchi, K., Kameoka, H., Tanaka, S., Ezawa, T., et al. (2018). The genome of *Rhizophagus clarus* HR1 reveals a common genetic basis for auxotrophy among arbuscular mycorrhizal fungi. *BMC Genomics* 19:465. doi: 10.1186/s12864-018-4853-0

Kolbe, A., Tiessen, A., Schluepmann, H., Paul, M., Ulrich, S., and Geigenberger, P. (2005). Trehalose 6-phosphate regulates starch synthesis via posttranslational redox activation of ADP-glucose pyrophosphorylase. *Proc. Natl. Acad. Sci. U S A.* 102, 11118–11123. doi: 10.1073/pnas.0503410102

Kretzschmar, T., Kohlen, W., Sasse, J., Borghi, L., Schlegel, M., Bachelier, J. B., et al. (2012). A petunia ABC protein controls strigolactone-dependent symbiotic signalling and branching. *Nature* 483, 341–344. doi: 10.1038/nature10873

Kubota, M., McGonigle, T. P., and Hyakumachi, M. (2005). Co-occurrence of Arum- and Paris-type morphologies of arbuscular mycorrhizae in cucumber and tomato. *Mycorrhiza* 15, 73–77. doi: 10.1007/s00572-004-0299-0

Kurihara, D., Mizuta, Y., Sato, Y., and Higashiyama, T. (2015). ClearSee: a rapid optical clearing reagent for whole-plant fluorescence imaging. *Development* 142, 4168–4179. doi: 10.1242/dev.127613

Langmead, B., and Salzberg, S. L. (2012). Fast gapped-read alignment with Bowtie 2. *Nat. Methods* 9, 357–359. doi: 10.1038/nmeth.1923

Li, B., Ruotti, V., Stewart, R. M., Thomson, J. A., and Dewey, C. N. (2010). RNA-Seq gene expression estimation with read mapping uncertainty. *Bioinformatics* 26, 493–500. doi: 10.1093/bioinformatics/btp692

Li, H., Jiang, F., Wu, P., Wang, K., and Cao, Y. (2020). A high-quality genome sequence of model Legume *Lotus japonicus* (MG-20) provides insights into the evolution of root nodule Ssmbiosis. *Genes* 11:11050483. doi: 10.3390/genes11050483

Li, H. T., Yi, T. S., Gao, L. M., Ma, P. F., Zhang, T., Yang, J. B., et al. (2019). Origin of angiosperms and the puzzle of the Jurassic gap. *Nat. Plants* 5, 461–470. doi: 10.1038/s41477-019-0421-0

Li, W., and Godzik, A. (2006). Cd-hit: a fast program for clustering and comparing large sets of protein or nucleotide sequences. *Bioinformatics* 22, 1658–1659. doi: 10.1093/bioinformatics/btl158

Li, W., Katin-Grazzini, L., Gu, X., Wang, X., El-Tanbouly, R., Yer, H., et al. (2017). Transcriptome analysis reveals differential gene expression and a possible role of gibberellins in a shade-tolerant mutant of perennial ryegrass. *Front. Plant Sci.* 8:868. doi: 10.3389/fpls.2017.00868

Li, X., Gao, C., Li, L., Liu, M., Yin, Z., Zhang, H., et al. (2017). MoEnd3 regulates appressorium formation and virulence through mediating endocytosis in rice blast fungus *Magnaporthe oryzae*. *PLoS Pathog.* 13:e1006449. doi: 10.1371/journal.ppat.1006449

Liao, Y., Smyth, G. K., and Shi, W. (2014). featureCounts: an efficient general purpose program for assigning sequence reads to genomic features. *Bioinformatics* 30, 923–930. doi: 10.1093/bioinformatics/btt656

Luginbuehl, L. H., Menard, G. N., Kurup, S., Van Erp, H., Radhakrishnan, G. V., Breakspear, A., et al. (2017). Fatty acids in arbuscular mycorrhizal fungi are synthesized by the host plant. *Science* 356, 1175–1178.

Luginbuehl, L. H., and Oldroyd, G. E. D. (2017). Understanding the arbuscule at the heart of endomycorrhizal symbioses in plants. *Curr. Biol.* 27, R952–R963.

Maeda, T., Kobayashi, Y., Kameoka, H., Okuma, N., Takeda, N., Yamaguchi, K., et al. (2018). Evidence of non-tandemly repeated rDNAs and their intragenomic heterogeneity in *Rhizophagus irregularis*. *Commun. Biol.* 1:87.

Mcgonigle, T. P., Miller, M. H., Evans, D. G., Fairchild, G. L., and Swan, J. A. (1990). A new method which gives an objective-measure of colonization of roots by vesicular arbuscular mycorrhizal fungi. *New Phytologist* 115, 495–501. doi: 10.1111/j.1469-8137.1990.tb00476.x

Muller, L. M., Campos-Soriano, L., Levesque-Tremblay, V., Bravo, A., Daniels, D. A., Pathak, S., et al. (2020). Constitutive overexpression of *RAM1* leads to an increase in arbuscule density in *Brachypodium distachyon*. *Plant Physiol.* 184, 1263–1272. doi: 10.1104/pp.20.00997

Nagata, M., Yamamoto, N., Shigeyama, T., Terasawa, Y., Anai, T., Sakai, T., et al. (2015). Red/far red light controls arbuscular mycorrhizal colonization via jasmonic acid and strigolactone signaling. *Plant Cell Physiol.* 56, 2100–2109. doi: 10.1093/pcp/pcv135

Nouri, E., Surve, R., Bapaume, L., Stumpe, M., Chen, M., Zhang, Y., et al. (2021). Phosphate suppression of arbuscular mycorrhizal symbiosis involves gibberellic acid signalling. *Plant Cell Physiol.* 2021:63. doi: 10.1093/pcp/pcab063

Ono, H., Ishii, K., Kozaki, T., Ogiwara, I., Kanekatsu, M., and Yamada, T. (2015). Removal of redundant contigs from de novo RNA-Seq assemblies via homology search improves accurate detection of differentially expressed genes. *BMC Genomics* 16:1031. doi: 10.1186/s12864-015-2247-0

Park, H. J., Floss, D. S., Levesque-Tremblay, V., Bravo, A., and Harrison, M. J. (2015). Hyphal branching during arbuscule development requires *Reduced arbuscular mycorrhiza1*. *Plant Physiol.* 169, 2774–2788.

Paulišić, S., Qin, W., Arora Verasztó, H., Then, C., Alary, B., Nogue, F., et al. (2021). Adjustment of the PIF7-HFR1 transcriptional module activity controls plant shade adaptation. *Embo* J. 40:e104273. doi: 10.15252/embj.2019104273

Pfeffer, P. E., Douds, D. D. Jr., Becard, G., and Shachar-Hill, Y. (1999). Carbon uptake and the metabolism and transport of lipids in an arbuscular mycorrhiza. *Plant Physiol.* 120, 587–598. doi: 10.1104/pp.120.2.587

Pimprikar, P., Carbonnel, S., Paries, M., Katzer, K., Klingl, V., Bohmer, M. J., et al. (2016). A CCaMK-CYCLOPS-DELLA complex activates transcription of *RAM1* to regulate arbuscule branching. *Curr. Biol.* 26, 987–998. doi: 10.1016/j.cub.2016.01.069

Proust, H., Hoffmann, B., Xie, X., Yoneyama, K., Schaefer, D. G., Yoneyama, K., et al. (2011). Strigolactones regulate protonema branching and act as a quorum sensing-like signal in the moss *Physcomitrella patens*. *Development* 138, 1531–1539. doi: 10.1242/dev.058495

Radhakrishnan, G. V., Keller, J., Rich, M. K., Vernie, T., Mbadinga Mbadinga, D. L., Vigneron, N., et al. (2020). An ancestral signalling pathway is conserved in intracellular symbioses-forming plant lineages. *Nat. Plants* 6, 280–289. doi: 10.1038/s41477-020-0613-7

Rich, M. K., Courty, P. E., Roux, C., and Reinhardt, D. (2017). Role of the GRAS transcription factor ATA/RAM1 in the transcriptional reprogramming of arbuscular mycorrhiza in *Petunia hybrida*. *BMC Genomics* 18:589. doi: 10.1186/s12864-017-3988-8

Rich, M. K., Schorderet, M., Bapaume, L., Falquet, L., Morel, P., Vandenbussche, M., et al. (2015). The Petunia GRAS Transcription Factor ATA/RAM1 Regulates Symbiotic Gene Expression and Fungal Morphogenesis in Arbuscular Mycorrhiza. *Plant Physiol.* 168, 788–797. doi: 10.1104/pp.15.00310

Roberts, A., and Pachter, L. (2013). Streaming fragment assignment for real-time analysis of sequencing experiments. *Nat. Methods* 10, 71–73.

Robinson, M. D., McCarthy, D. J., and Smyth, G. K. (2010). edgeR: a Bioconductor package for differential expression analysis of digital gene expression data. *Bioinformatics* 26, 139–140. doi: 10.1093/bioinformatics/btp616

Sato, D., Awad, A. A., Chae, S. H., Yokota, T., Sugimoto, Y., Takeuchi, Y., et al. (2003). Analysis of strigolactones, germination stimulants for striga and orobanche, by high-performance liquid chromatography/tandem mass spectrometry. *J. Agric. Food Chem.* 51, 1162–1168. doi: 10.1021/jf025997z

Shachar-Hill, Y., Pfeffer, P. E., Douds, D., Osman, S. F., Doner, L. W., and Ratcliffe, R. G. (1995). Partitioning of intermediary carbon metabolism in vesicular-arbuscular mycorrhizal leek. *Plant Physiol.* 108, 7–15.

Shi, J., Zhao, B., Zheng, S., Zhang, X., Wang, X., Dong, W., et al. (2021). A phosphate starvation response-centered network regulates mycorrhizal symbiosis. *Cell* 2021:30. doi: 10.1016/j.cell.2021.09.030

Silverstone, A. L., Jung, H. S., Dill, A., Kawaide, H., Kamiya, Y., and Sun, T. P. (2001). Repressing a repressor: gibberellin-induced rapid reduction of the RGA protein in Arabidopsis. *Plant Cell* 13, 1555–1566. doi: 10.1105/tpc.010047

Smith, F. A., and Smith, S. E. (1997). Tansley Review No. 96. Structural diversity in (vesicular)-arbuscular mycorrhizal symbioses. *New Phytologist* 137, 373–388.

Smith, S. E., Smith, F. A., and Jakobsen, I. (2004). Functional diversity in arbuscular mycorrhizal (AM) symbioses: the contribution of the mycorrhizal P uptake pathway is not correlated with mycorrhizal responses in growth or total P uptake. *New Phytologist* 162, 511–524. doi: 10.1111/j.1469-8137.2004.01039.x

Sugimura, Y., and Saito, K. (2017). Comparative transcriptome analysis between *Solanum lycopersicum* L. and *Lotus japonicus* L. during arbuscular mycorrhizal development. *Soil Sci. Plant Nutrit.* 63, 127–136.

Sugiura, Y., Akiyama, R., Tanaka, S., Yano, K., Kameoka, H., Marui, S., et al. (2020). Myristate can be used as a carbon and energy source for the asymbiotic growth of arbuscular mycorrhizal fungi. *Proc. Natl. Acad. Sci. U S A.* 117, 25779–25788.

Takeda, N., Handa, Y., Tsuzuki, S., Kojima, M., Sakakibara, H., and Kawaguchi, M. (2015). Gibberellins interfere with symbiosis signaling and gene expression and alter colonization by arbuscular mycorrhizal fungi in *Lotus japonicus*. *Plant Physiol.* 167, 545–557. doi: 10.1104/pp.114.247700

Tominaga, T., Miura, C., Takeda, N., Kanno, Y., Takemura, Y., Seo, M., et al. (2020a). Gibberellin promotes fungal entry and colonization during *Paris*-type arbuscular mycorrhizal symbiosis in *Eustoma grandiflorum*. *Plant Cell Physiol.* 61, 565–575. doi: 10.1093/pcp/pcz222

Tominaga, T., Yamaguchi, K., Shigenobu, S., Yamato, M., and Kaminaka, H. (2020b). The effects of gibberellin on the expression of symbiosis-related genes in *Paris*-type arbuscular mycorrhizal symbiosis in *Eustoma grandiflorum*. *Plant Signal. Behav.* 15:1784544. doi: 10.1080/15592324.2020.1784544

Trabelsi, I., Yoneyama, K., Abbes, Z., Amri, M., Xie, X., Kisugi, T., et al. (2017). Characterization of strigolactones produced by *Orobanche foetida* and *Orobanche crenata* resistant faba bean (*Vicia faba* L.) genotypes and effects of phosphorous, nitrogen, and potassium deficiencies on strigolactone production. *South Afr. J. Bot.* 108, 15–22. doi: 10.1016/j.sajb.2016.09.009

Tsuzuki, S., Handa, Y., Takeda, N., and Kawaguchi, M. (2016). Strigolactone-induced putative secreted protein 1 Is required for the establishment of symbiosis by the arbuscular mycorrhizal fungus *Rhizophagus irregularis*. *Mol. Plant Microbe Interact.* 29, 277–286. doi: 10.1094/MPMI-10-15-0234-R

Ueno, K., Furumoto, T., Umeda, S., Mizutani, M., Takikawa, H., Batchvarova, R., et al. (2014). Heliolactone, a non-sesquiterpene lactone germination stimulant for root parasitic weeds from sunflower. *Phytochemistry* 108, 122–128.

Vegh, A., Incze, N., Fabian, A., Huo, H., Bradford, K. J., Balazs, E., et al. (2017). Comprehensive analysis of DWARF14-LIKE2 (DLK2) reveals its functional divergence from strigolactone-related paralogs. *Front. Plant Sci.* 8:1641. doi: 10.3389/fpls.2017.01641

Wagner, G. P., Kin, K., and Lynch, V. J. (2012). Measurement of mRNA abundance using RNA-seq data: RPKM measure is inconsistent among samples. *Theory Biosci.* 131, 281–285. doi: 10.1007/s12064-012-0162-3

Wang, S., Chen, A., Xie, K., Yang, X., Luo, Z., Chen, J., et al. (2020). Functional analysis of the OsNPF4.5 nitrate transporter reveals a conserved mycorrhizal pathway of nitrogen acquisition in plants. *Proc. Natl. Acad. Sci. U S A.* 117, 16649–16659. doi: 10.1073/pnas.2000926117

Waters, M. T., Brewer, P. B., Bussell, J. D., Smith, S. M., and Beveridge, C. A. (2012a). The Arabidopsis ortholog of rice DWARF27 acts upstream of MAX1 in the control of plant development by strigolactones. *Plant Physiol.* 159, 1073–1085. doi: 10.1104/pp.112.196253

Waters, M. T., Nelson, D. C., Scaffidi, A., Flematti, G. R., Sun, Y. K., Dixon, K. W., et al. (2012b). Specialisation within the DWARF14 protein family confers distinct responses to karrikins and strigolactones in *Arabidopsis*. *Development* 139, 1285–1295. doi: 10.1242/dev.074567

Xue, L., Klinnawee, L., Zhou, Y., Saridis, G., Vijayakumar, V., Brands, M., et al. (2018). AP2 transcription factor CBX1 with a specific function in symbiotic exchange of nutrients in mycorrhizal *Lotus japonicus*. *Proc. Natl. Acad. Sci. U S A.* 115, E9239–E9246. doi: 10.1073/pnas.1812275115

Yamato, M. (2004). Morphological types of arbuscular mycorrhizal fungi in roots of weeds on vacant land. *Mycorrhiza* 14, 127–131.

Yamato, M., and Iwasaki, M. (2002). Morphological types of arbuscular mycorrhizal fungi in roots of understory plants in Japanese deciduous broadleaved forests. *Mycorrhiza* 12, 291–296. doi: 10.1007/s00572-002-0187-4

Yang, C., and Li, L. (2017). Hormonal regulation in shade avoidance. *Front. Plant Sci.* 8:1527. doi: 10.3389/fpls.2017.01527

Yu, N., Luo, D., Zhang, X., Liu, J., Wang, W., Jin, Y., et al. (2014). A DELLA protein complex controls the arbuscular mycorrhizal symbiosis in plants. *Cell Res.* 24, 130–133. doi: 10.1038/cr.2013.167

Conflict of Interest: The authors declare that the research was conducted in the absence of any commercial or financial relationships that could be construed as a potential conflict of interest.

Publisher's Note: All claims expressed in this article are solely those of the authors and do not necessarily represent those of their affiliated organizations, or those of the publisher, the editors and the reviewers. Any product that may be evaluated in this article, or claim that may be made by its manufacturer, is not guaranteed or endorsed by the publisher.

frontiers in Plant Science

REVIEW
published: 03 January 2022
doi: 10.3389/fpls.2021.796045

The Rhizobium-Legume Symbiosis: Co-opting Successful Stress Management

*Justin P. Hawkins and Ivan J. Oresnik**

Department of Microbiology, University of Manitoba, Winnipeg, MB, Canada

The interaction of bacteria with plants can result in either a positive, negative, or neutral association. The rhizobium-legume interaction is a well-studied model system of a process that is considered a positive interaction. This process has evolved to require a complex signal exchange between the host and the symbiont. During this process, rhizobia are subject to several stresses, including low pH, oxidative stress, osmotic stress, as well as growth inhibiting plant peptides. A great deal of work has been carried out to characterize the bacterial response to these stresses. Many of the responses to stress are also observed to have key roles in symbiotic signaling. We propose that stress tolerance responses have been co-opted by the plant and bacterial partners to play a role in the complex signal exchange that occurs between rhizobia and legumes to establish functional symbiosis. This review will cover how rhizobia tolerate stresses, and how aspects of these tolerance mechanisms play a role in signal exchange between rhizobia and legumes.

Keywords: rhizobium, legume, symbiosis, stress, pH, osmolarity, oxygen, ROS

OPEN ACCESS

Edited by:
Sabine Dagmar Zimmermann, Délégation Languedoc Roussillon (CNRS), France

Reviewed by:
Karine Mandon, Université Côte d'Azur, France
Fabienne Cartieaux, Institut de Recherche Pour le Dévelopment (IRD), France

***Correspondence:**
Ivan J. Oresnik
Ivan.Oresnik@umanitoba.ca

Specialty section:
This article was submitted to Plant Symbiotic Interactions, a section of the journal Frontiers in Plant Science

Received: *15 October 2021*
Accepted: *02 December 2021*
Published: *03 January 2022*

Citation:
Hawkins JP and Oresnik IJ (2022) The Rhizobium-Legume Symbiosis: Co-opting Successful Stress Management. Front. Plant Sci. 12:796045. doi: 10.3389/fpls.2021.796045

INTRODUCTION

Rhizobia-legume symbiosis is a well-studied interaction which results in the formation of a plant derived organelle for the purposes of symbiotic nitrogen fixation. Establishment of this interaction occurs through a complex signal exchange which is initiated by the secretion of plant derived flavonoids that are then recognized by compatible rhizobia species (Oldroyd and Downie, 2008; Oldroyd et al., 2011). Recognition of flavonoids results in the production of a lipo-chito-oligosaccharide termed Nod factor (NF) which can be perceived by the host legume (Barnett and Fisher, 2006). This triggers calcium spiking in the inner plant cortical cells, resulting in the division of cells which will form the nodule primordia (Ehrhardt et al., 1996; Shaw and Long, 2003). Nod factor recognition also leads to root hair curling which can trap attached rhizobia and form a curled colonized root hair (Fournier et al., 2008). Infection thread formation can be observed after signals, such as exopolysaccharides or lipopolysaccharides, are recognized. This structure penetrates down toward nodule primordial cells where rhizobia become endocytosed into the cells and enclosed in a symbiotic membrane (Jones et al., 2007). Rhizobia then become bacteroids, which may or may not be terminally differentiated, that functionally serve as a plant organelle to reduce atmospheric nitrogen into ammonia which is subsequently utilized by the host legume.

While the signaling events that lead to an effective symbiosis are complex, other factors also play a major role in the establishment of an effective symbiosis. During the infection and differentiation process, rhizobia are challenged by numerous stresses, both in the rhizosphere

and *in planta* (**Figure 1**). To tolerate the stresses that are encountered, bacteria produce compounds or change their lifestyle in order to permit survival. In numerous cases, these changes are correlated with the ability to establish a functional symbiosis. Molecules involved in plant pathogen recognition may also be necessary for symbiotic establishment, and in fact may serve as a signal to the bacteria to produce symbiotic signals. The focus of this work is to review aspects of rhizobia and plant responses to stress, and how elements of these responses may have become co-opted as signals involved in establishing a functional symbiosis.

FLAVONOIDS

The symbiotic interaction between legumes and rhizobia initiates when flavonoids are recognized by bacteria. The biosynthesis of flavonoids in plants is well understood (Ferrer et al., 2008), and to date, thousands of different flavonoids have been isolated. The biochemical diversity of flavonoids is achieved through modification of a limited number of base structures. These molecules play diverse roles in plant biology ranging from affecting flower color, auxin transport, and anti-microbial defenses (Winkel-Shirley, 2001).

Flavonoids are a known anti-microbial (Hassan and Mathesius, 2012) and represent one of the first directed challenges from plant toward bacteria. The production of these molecules is known to be induced in response to pathogen invasion and has been shown to be directly involved in the plant defense response (Cramer et al., 1985). One subgroup of flavonoids called the iso-flavonoids are found exclusively in legumes (Hirsch et al., 2001). Iso-flavonoids were originally thought to be involved in the defense response against fungi and were shown to also have toxic effects on some isolated bacteria. However, it has

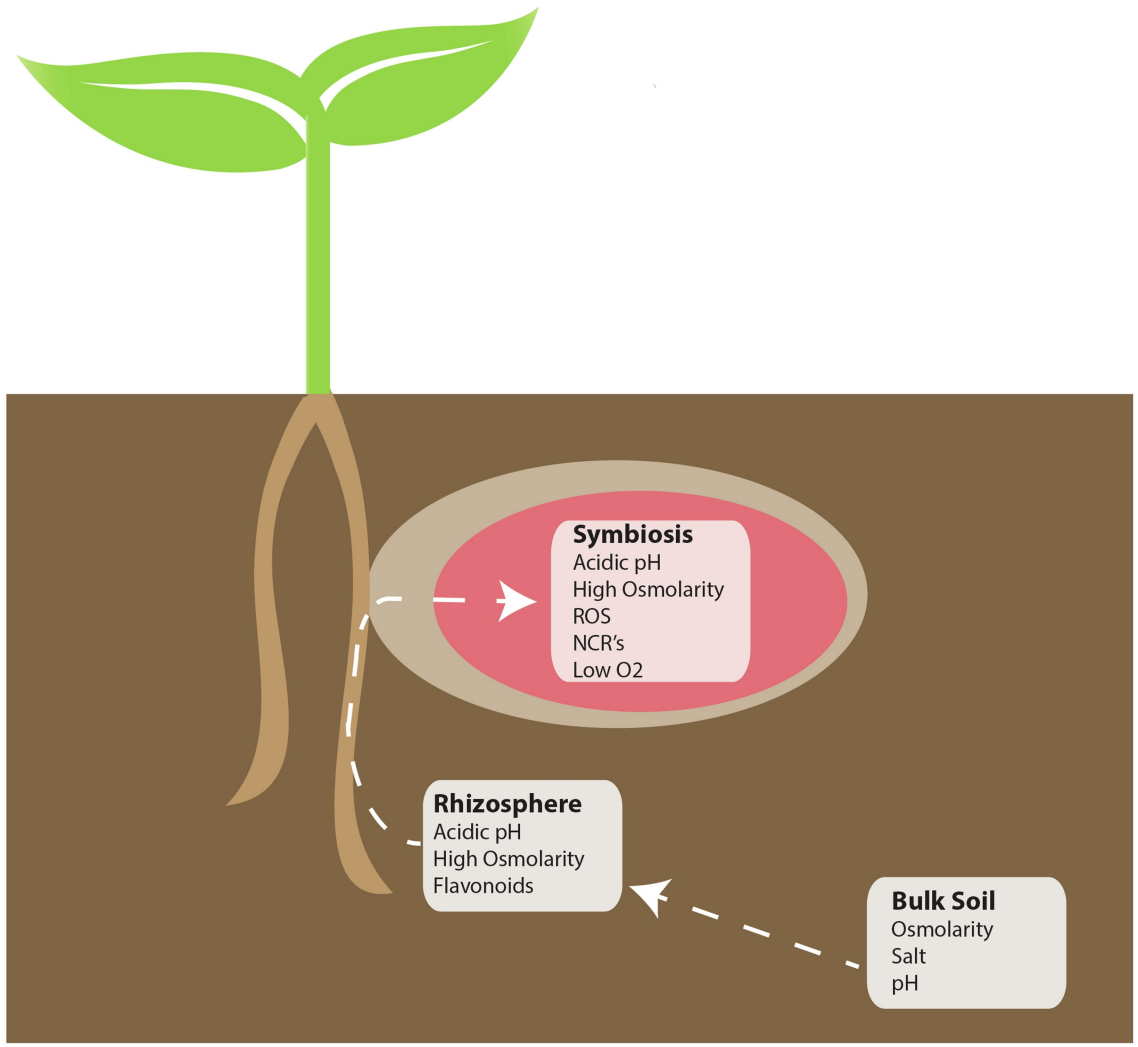

FIGURE 1 | Locations of perceived stress during the rhizobia-legume symbiosis. During symbiosis, there are three distinct environments that symbiotic bacteria must contend with: Bulk soil, the rhizosphere, and *in planta*. Each white box indicates potential "perceived" stressors that may be encountered in each of the indicated environments.

also been shown that iso-flavonoids play a role in rhizobium-legume symbiosis. Rhizobia which were exposed to purified iso-flavonoids from plant root exudates were shown to induce the transcription of *nodABC,* which encode proteins necessary for NF synthesis (Hartwig et al., 1990).

Secretion of the flavone luteolin which is produced by *Medicago sativa* has been shown to occur in distinct areas of the developing root where symbiotic interactions may occur (Ehrhardt et al., 1992). Flavones and isoflavones were also found to induce transcription of the *nod* genes in other rhizobia, and recognition of specific flavonoids was shown to play a role in plant-host specificity during symbiosis. Collectively, it seems that the initial role for flavonoids and iso-flavonoids secreted by plants was to be an anti-microbial (Cowan, 1999). However, rhizobia have been able to utilize very specific portions of flavonoids, the iso-flavonoids, as a signal indicating the presence of a compatible host and respond through the production of Nod factor to initiate symbiotic signaling.

NOD FACTOR

Signaling between host plants and symbiotic rhizobia or mycorrhizae share a common subset of genes and follow a similar pathway (Duc et al., 1989; Oldroyd, 2013). Each organism produces a lipo-chito-oligosaccharide (*myc*/*nod* factor) that is recognized by LysM type receptors on the plant (Chabaud et al., 2002; Geddes and Oresnik, 2016). Mycorrhizal symbiosis is thought to be an ancient process and able to occur with most land-based plants, with the oldest symbiotic interaction known to be with the phylum Glomeromycota (Oldroyd, 2013). The secretion of *myc* factor, which is structurally similar to nod factor, is essential to its symbiotic interaction with its host plants. Comparatively, rhizobial symbiosis is relatively new and only occurs with legumes and *Parasponia* plants through recognition of NF by LysM type receptors (Pueppke and Broughton, 1999; Madsen et al., 2003). The similarities of the signaling pathway, and insights into *Parasponia* symbiotic signaling, has led to the hypothesis that the use of Nod factor for symbiosis evolved from *myc* factor signaling in mycorrhiza (Streng et al., 2011).

The structure of NF is comprised of 3–5 β(1–4)-linked N-acetylglucosamine residues, with a fatty acid tail on the first residue, and can have various modifications to the N-acetylglucosamine residues (Mylona et al., 1995). Nod factor is structurally similar to fungal cell wall chitin, which is a known activator of the plant immune response (Pusztahelyi, 2018). In addition, both Nod factor and chitin are recognized by LysM type receptors which are thought to have evolved from an ancestral LysM receptor (Zipfel and Oldroyd, 2017). The key difference being that Nod factor contains shorter N-acetylglucosamine chain lengths. In the *S. meliloti* – *M. truncatula* model NF is recognized by the LysM receptors MtNFP and MtLYK3 (Oldroyd, 2013). This recognition induces numerous responses from *M. truncatula* which are necessary for successful symbiotic establishment. Transcriptomic studies have also revealed that Nod factor recognition regulates genes involved in the plant immune response (El-Yahyaoui et al., 2004). Studies have also shown that isolated Nod factor from rhizobia can modulate the immune response of both legumes and non-legumes. When *Arabidopsis thaliana* is exposed to the known pathogen associated molecular pattern *flg22,* the innate immune response of the plant becomes induced. Interestingly, when purified NF isolated from *B. japonicum* was applied, in addition to *flg22,* a more attenuated immune response was observed (Liang et al., 2013). This suggested that Nod factor-mediated suppression of the plants innate immune system may be necessary for successful colonization of plants.

Nod factor is also known to activate the innate defense responses from plants. Transcriptomic studies indicate that the plant immune response is initially activated due to *S. meliloti* inoculum (Lohar et al., 2006). Purified Nod factor has also been shown to induce the production of ROS in the nodulation zone of *M. truncatula* roots (Ramu et al., 2002). Further studies revealed that increased production of H_2O_2 can be observed to occur around root hair tips during Nod factor exposure (Cardenas et al., 2008). Interestingly, *S. meliloti* mutant strains over-expressing catalase also exhibited slower nodulation and malformed infection threads (Jamet et al., 2007). This suggests that while the suppression of the plant immune system is necessary for growth of rhizobia during symbiotic establishment, the initial immune response may bring about changes to both plant and bacteria that promote symbiosis. It has been suggested that the presence of H_2O_2 might be necessary for stabilizing the formation of infection threads or promoting a physiological change in rhizobia which would promote symbiosis (Jamet et al., 2007). These observations from early signaling involving the interplay of flavonoids and Nod factor production are a clear example of how a potential stress, flavonoids, induce a bacterial signal, Nod factor, that have become a key component for symbiotic interaction.

ENVIRONMENTAL CONDITIONS

The aforementioned topics on symbiotic signaling and regulation of the plant immune response provide a clear example of how tolerance of a stress has become intertwined in signaling. However, it is also important to consider how physiological conditions during symbiotic establishment may also promote symbiosis. Bacteria encounter a wide variety of conditions in both bulk soil and *in planta*. Bulk soil conditions can vary significantly around the world. In addition, the environment *in planta* can challenge bacteria with changes in osmolarity, oxygen content and oxidative stress, decreasing pH, and further plant peptide challenges. The following points investigate how these conditions can promote physiological changes necessary for stress tolerance that end up influencing symbiotic establishment or nitrogen fixation (**Table 1**).

OSMOTIC STRESS

Genes involved in adaptation to varying osmotic conditions have been shown to be critical for the establishment of a

TABLE 1 | Bacterial and plant changes due to perceived stress and their role in symbiosis.

Stress	Response	Symbiotic relevance
Bacteria/Pathogen	Flavonoid	Nod factor induction
	NCRs	Bacteroid differentiation
	Innate immune response	Oxidative burst (see ROS)
Flavonoid	Nod factor	Calcium spiking
Salt/Ion stress	Nod factor	Calcium spiking
	EPS-I	IT development
Osmotic	cyclic β(1–2) glucans	Attachment/ IT formation
	Intracellular Potassium concentration	Nitrogenase induction
Acidic pH	*actR/S*	*fixK/nifA*
	exoR/S/I	EPS-I
	Nod factor profile	Legume host range
Reactive oxygen species	EPS-I	IT development
	Membrane crosslinking	IT development
Low oxygen	Intracellular potassium	Nitrogenase induction
	Fix genes	Nitrogenase induction
	LPS modification	Legume host range

functional symbiotic relationship. Osmotic conditions before symbiosis are fully dependent on salts and exudates present in the soil. Bulk soil is generally assumed to be an area of low osmolarity (Miller and Wood, 1996). However, the area of the rhizosphere is predicted to have a higher osmolarity due to plant root exudate and water uptake from both plants and bacteria (Jungk, 2002; Miller-Williams et al., 2006). While the osmotic conditions throughout symbiosis in the rhizobia-legume interaction are unknown, current research is consistent with the hypothesis that both high and low osmolarity conditions exist throughout symbiosis (Botsford and Lewis, 1990; Dylan et al., 1990a). The area of the rhizosphere having high osmolarity is particularly interesting as these conditions have been linked with inducing genes necessary for symbiosis. The presence of high osmotic conditions has been shown to induce transcription of genes involved in nodulation and nitrogen fixation (*nod, nif,* and *fix* genes) through NodD2 in *Rhizobium tropici* CIAT 899 (Del Cerro et al., 2019). This same pattern of regulation of these genes through NodD2 is also observed when *R. tropici* is exposed to increased salt stress present in the rhizosphere (Pérez-Montaño et al., 2016). In addition, increased salt concentrations are known to regulate exopolysaccharide production in *S. meiloti* (Miller-Williams et al., 2006). These observations provide the most direct link between osmotic stress recognition and promoting symbiosis.

The major link between osmotic stress tolerance and physiological changes with importance to symbiosis is the accumulation of periplasmic glucans in the presence of hypotonic stress. The majority of the organisms in the family *Rhizobiaceae* produces a cyclic β(1–2)-linked glucan (York et al., 1980; Lelpi et al., 1990; Breedveld and Miller, 1994). Accumulation of these periplasmic glucans can be observed when grown under hypotonic conditions (Miller et al., 1986; Dylan et al., 1990a; Breedveld and Miller, 1995). Further study of cyclic β(1–2) glucans in *S. meliloti* determined that the inability to produce this polysaccharide, by mutating the gene *ndvB*, resulted in sensitivity to hypotonic conditions, and abolished nodule formation on *M. truncatula* (Dylan et al., 1990b). It was hypothesized that extracellular cyclic β(1–2) may be involved in root attachment, but addition of purified cyclic β(1–2) was unable to restore symbiosis with *M. truncatula* to a *ndvB* mutant strain (Dylan et al., 1990b). Pseudorevertants of the *ndvB* mutant strain that still did not produce the cyclic glucan have been isolated and were found to be able to establish a functional symbiosis with *M. truncatula*. However, these suppressors were still heavily impacted in infection thread formation and were sensitive to hypoosmotic stress (Dylan et al., 1990b). This suggested that while cyclic β(1–2) glucan production is important for osmotic stress tolerance and can be linked to infection thread formation, their role in symbiosis extends past stress tolerance. Suppression of the symbiotic phenotype of *ndvB* mutants was later linked to the production the symbiotically important polysaccharide succinoglycan (Nagpal et al., 1992).This lead to the suggestion that production of succinoglycan might provide just enough osmoprotectant in the form of low molecular weight succinoglycan to allow for survival in the absence of the cyclic glucans. In addition, succinoglycan may provide or mask a signal necessary for symbiosis in the absence of cyclic glucans (Abe et al., 1982; Nagpal et al., 1992). Overall, osmolarity is involved in regulating cyclic β(1–2) glucans which have a role in symbiosis that extends past stress tolerance.

Another mechanism rhizobia and other bacteria utilize to tolerate high osmolarity is the accumulation of ions, such as potassium (Yancey et al., 1982; Csonka, 1989; Botsford and Lewis, 1990; Smith et al., 1994; Miller and Wood, 1996). Interestingly, increased potassium levels lead to an increase in nitrogenase activity in *Bradyrhizobium* sp. 32H1 when grown under low oxygen conditions (Gober and Kashket, 1987). As the bacteroid is predicted to be an area of elevated osmotic stress (Miller and Wood, 1996), this provides a link showing that osmotic stress tolerance may be a signal for the regulation of nitrogenase in the bacteroid through the regulation of potassium concentration.

LOW OXYGEN CONTENT

During symbiotic establishment, rhizobia encounter areas of low oxygen concentration in the nodule. Control of oxygen concentration is important for symbiosis since oxygen inhibits the activity of nitrogenase (Hunt and Layzell, 1993). Oxygen levels are controlled through a diffusion barrier to create optimal oxygen concentrations for nitrogen fixation (Hunt et al., 1987). Tight regulation of oxygen concentration in bacteroids also leads to a number of signaling and physiological changes in bacteria, which promote symbiosis and nitrogen fixation. It has been well documented that a low oxygen concentration activates the two-component system FixJL, which in turn increases the transcription of the majority of genes involved in nitrogen fixation (David et al., 1988; Virts et al., 1988). Recent work has shown that there are 3 proteins that act oxygen sensors in *Rhizobium leguminosarum*; hFixL, FnrN, and

NifA (Dixon and Kahn, 2004; Zamorano-Sánchez and Girard, 2015; Reyes-González et al., 2016). These proteins are tightly temporally controlled, with hFixL inducing expression of FnrN in zones I and II (meristem zone and invasion zone, respectively) of indeterminate nodules. FnrN then induces expression of *fixNOQP* in zone III (nitrogen fixing zone) when oxygen concentration is near anaerobic (Rutten et al., 2021). The induction the genes necessary for production of nitrogenase in near anaerobic conditions is necessary for function of the protein and is also a clear example of how microaerobic stress acts as a signal for symbiosis.

Oxygen concentration has also been shown to regulate lipopolysaccharide (LPS) synthesis and decoration (Kannenberg and Brewin, 1989; Tang and Hollingsworth, 1998). This is thought to have a role in adaptation to the low oxygen environment. Production and modification of LPS are strain specific and are involved in determining host range for symbiosis in some rhizobia (Via et al., 2016). The ability to produce, or properly modify, LPS has been linked to defects in symbiotic establishment (Keating et al., 2002). As LPS content and decoration are dynamic based upon its environment, it is expected that LPS modification would change during symbiosis. Recent work has also shown that flavonoids can induce changes in decoration of LPS and that these changes are necessary for symbiosis (Broughton et al., 2006). It is possible that low oxygen concentration might contribute to bringing about a change in LPS production and decoration which is necessary for both symbiosis and survival in these conditions.

REACTIVE OXYGEN SPECIES

In addition to low oxygen concentration, rhizobia encounter reactive oxygen species as part of the innate immune response of the plant, and it can be found throughout symbiotic compartments ranging from the IT to mature nodules (Santos et al., 2001). Formation of ROS from the plant immune response has been shown to be beneficial for symbiotic establishment (Puppo et al., 2013). ROS are generated upon Nod factor recognition and are thought to predominantly occur from the activity of NADPH oxidase (Lohar et al., 2007). Rhizobia utilize a number of mechanisms to deal with potential damage from ROS (Boscari et al., 2013). The importance of ROS scavenging during symbiosis is highlighted by the finding that strains which carry mutations in the genes *katB/C,* which encode for catalases, are impaired in forming bacteroids (Jamet et al., 2003). However, a positive role for ROS in symbiosis has also been observed. When catalase is over-expressed in *S. meliloti*, aberrant IT formation and delayed nodule development are observed (Jamet et al., 2007). While it is unknown exactly how ROS may contribute to symbiosis, two main suggestions have been made; either ROS plays a role in IT development, or ROS induces physiological changes in rhizobium that are necessary for symbiosis (Pauly et al., 2006). Recent work has investigated this further and has shown that ROS produced by PvRbohB in *Phaseolus vulgaris* is important for symbiosis. Cultivars of *P. vulgaris* silenced in expression of PvRbohB displayed abortive infection threads when inoculated with *R. tropici* (Fonseca-García et al., 2021). RNAseq data also revealed changes in carbon metabolism and cell cycle control; both of which can be linked with symbiosis (Geddes and Oresnik, 2016; Fonseca-García et al., 2021).

Consistent with the hypothesis that ROS may act as a signal to bacteria for symbiotic establishment, it has been shown *B. japoncium* exposed to oxidative stress produces an increased amount of exopolysaccharides (Donati et al., 2011). The production of exopolysaccharides (EPS) has long been suggested to be involved in the tolerance of various stresses encountered by bacteria. In *S. meliloti* and *Pseudomonas syringae*, mutants unable to produce EPS have been observed to be sensitive to ROS (Király et al., 1997; Lehman and Long, 2013). Furthermore, it was shown that low molecular weight succinoglycan (EPS-I) is the responsible fraction which scavenges H_2O_2 from media in *S. meliloti* (Lehman and Long, 2013). Taken together, oxidative stress is seen to promote the production of exopolysaccharides which are necessary for the tolerance of ROS and critical for symbiotic establishment. Since plants are observed to produce H_2O_2 in response to symbiotic establishment, this provides a potential example of how *in planta* conditions promote production of a symbiotic signal.

pH STRESS

The ability to tolerate acidic pH conditions has largely been studied from the perspective of tolerating acidic soils in the environment. The area of the rhizosphere is predicted to be an area of increased acidic stress, as throughout their life cycle, plants can excrete acidic compounds into the surrounding soil, decreasing the pH of the soil by as much as 2 pH units (Faget et al., 2013). This occurs from the secretion of protons to maintain the net charge across the root membrane and from the secretion of organic compounds (Jones et al., 2003). During the symbiotic interaction between rhizobia and legumes, it has been hypothesized that many plant derived compartments have an acidic pH. The bacteroid and peri-bacteroid space have been predicted to be an acidic compartment, reaching a pH of 4.5 (Fedorova et al., 1999; Pierre et al., 2013). Studies have also determined that the curled colonized root hair is an area of localized acidic pH stress (Geddes et al., 2014). These findings are particularly important as *S. meliloti* is known to have poor survival when medium pH decreases below six (Hellweg et al., 2009; Hawkins et al., 2017).

Transcriptomic studies addressing the response of rhizobium to acidic pH and have revealed large networks regulating multiple genes in response to acidic pH (Hellweg et al., 2009; Guerrero-Castro et al., 2018). The response of rhizobia to acidic pH is primarily regulated though two-component systems, *actR/S* and *chvI*/*exoS*/*exoR* (Dilworth et al., 2000; Fenner et al., 2004). These systems ultimately control the regulation of cytoplasmic pH, or the production of and modification of extracellular elements for pH tolerance components (Cunningham and Munns, 1984; Chen et al., 1993). Regulation of potassium efflux proteins is important for pH tolerance. The potassium

efflux system in *R. tropici* has been shown to be regulated by glutathione, since mutants in glutathione synthesis were unable to accumulate intracellular potassium (Riccillo et al., 2000). Potassium concentrations have been shown to regulate nitrogenase activity so this accumulation of K^+ in acidic conditions may act as a symbiotic signal (Gober and Kashket, 1987). In addition, glutathione is involved in tolerating many environmental stressors, including pH and ROS stress, and has been shown to be produced in increased amounts under acidic conditions (Riccillo et al., 2000; Muglia et al., 2007). Mutations in the synthesis pathway for glutathione are known to result in either a fix$^-$ or delayed nodulation phenotype (Harrison et al., 2005).

One physiological response of *S. meliloti* to low pH is the production of the symbiotically important exopolysaccharide EPS-I (Hawkins et al., 2017). Acidic pH is known to be present throughout the symbiotic process, being present in the rhizosphere all the way to bacteroids. Mutants which are unable to produce succinoglycan are unable to establish functional symbiosis with alfalfa. Further investigation has revealed that the succinylation of EPS-I is the critical component of the symbiotic interaction (Mendis et al., 2016). Production of EPS-I is also important for tolerance of low pH and contributes to survival in nodules (Hawkins et al., 2017; Maillet et al., 2020). However, symbiotic defects observed in *exo* mutant strains are likely due to a combination of a loss of pH stress tolerance and loss of proper symbiotic signaling. *S. meliloti* strains that lack *exoK* produce a succinylated high molecular weight EPS-I still exhibit high sensitivity to acidic pH, but only display minor symbiotic defects (Maillet et al., 2020). Collectively, these data suggest that EPS-I plays a role in both stress tolerance as well as symbiotic signaling.

It has also been observed that acid tolerant strains of rhizobia produce more exopolysaccharides than acid sensitive strains under non-stress conditions (Cunningham and Munns, 1984). Interestingly, mutations that resulted in an increased production of exopolysaccharide in *R. leguminosarum* and *S. meliloti* did not result in an increased tolerance to acidic media (Howieson et al., 1988; Reeve et al., 1997). These observations suggest that in terms of stress tolerance, the production of exopolysaccharides may serve an on/off function rather than a gradient of tolerance, and that the increased production of exopolysaccharides due to pH stress may have another role.

The response to low pH is largely mediated through the ExoR/ExoS/ChvI (RSI) system, which has been shown to be upregulated due to acidic pH in *S. meliloti* (Hellweg et al., 2009; Draghi et al., 2016). The RSI system is well studied for its ability to regulate the production of EPS-I and flagella (Cheng and Walker, 1998b; Heavner et al., 2015). It is long known that the production of EPS-I is important for symbiotic interaction (González et al., 1996; York and Walker, 1997; Cheng and Walker, 1998a). The protein ExoS acts as a sensor kinase which directly phosphorylates the response regulator ChvI in response to a signal (Cheng and Walker, 1998b; Yao et al., 2004). This system is regulated through direct binding of the repressor ExoR to ExoS in the periplasm (Chen et al., 2008). Homologs of this system in *Agrobacterium tumefaciens* have been shown to be involved in gene regulation due to acidic pH, and it has been suggested that acidity is a key signal in establishing virulence with plants (Li et al., 2002). Further study of the RSI regulon in *A. tumefaciens* has revealed that at acidic pH the repressor ExoR is degraded, resulting in increased EPS-I synthesis (Heckel et al., 2014). A mechanism for degradation of ExoR in *S. meliloti* has also been shown (Lu et al., 2012). Degradation of ExoR could account for the increase in transcription of *exoR* at lower pH. Taken together, this suggests that the acidic conditions found in the curled colonized root hair leads to the production of EPS-I which is necessary for symbiotic signaling and stress tolerance, making pH a key environmental regulator for symbiosis. Overall, these works suggest that low pH induces the production of glutathione and succinoglycan which are both involved in stress tolerance and symbiosis.

NODULE-SPECIFIC CYSTEINE RICH PEPTIDES

Recently, there has been interest in a subsect of plant produced anti-microbial peptides (AMPs) called nodule-specific cysteine rich (NCR) peptides for their role in symbiotic establishment (Alunni and Gourion, 2016). AMPs are well studied for their anti-microbial activity (Maroti et al., 2011). The mechanism of action of AMPs involves the disruption of bacterial membranes through interaction with the cell surface and ribosome inactivation. In addition to their anti-microbial activity, it has been suggested that certain AMPs play a role in signaling (Schopfer, 1999).

NCRs are structurally and functionally similar to AMPs; they are predicted to be around 100 amino acids long, contain the conserved cysteine residues for disulfide bridge formation, and are predicted to be largely cationic (Mergaert et al., 2003). These peptides have also been shown to have anti-microbial activity against several organisms, including rhizobia (Haag et al., 2011). However, the presence of the protein BacA in *S. meliloti*, a transporter for AMPs, is observed to be involved in tolerating the challenge with NCRs, whereas mutants in *bacA* were observed to be hypersensitive to the anti-microbial activity *in planta* (Haag et al., 2011).

In *M. truncatula*, there are predicted to be upwards of 300 different NCRs produced by around 600 different genes (Mergaert et al., 2003; Zhou et al., 2013). Only legumes of the inverted-repeat lacking clade (IRLC) are observed to produce NCRs (Mergaert et al., 2006). In these legumes, symbiotic bacteria become terminally differentiated into bacteroids in plant nodules and cannot revert to normal functioning bacteria. Non-IRLC legumes, such as *L. japonicus,* do not produce NCRs, and symbiotic bacteria do not become terminally differentiated (Mergaert et al., 2003). This has led to the suggestion that NCRs are directly involved in the terminal differentiation of symbiotic bacteria. However, it is worth noting that examples of bacteroid differentiation outside of the IRLC legumes are starting to be found. Nodules formed in the *Aeschynomene* – *Bradyrhizobium* symbiotic relationship are found to house differentiated bacteroids with a polyploid genome (Czernic et al., 2015). While *Aeschynomene* sp. do not produce NCRs they have been shown to produce NCR-like peptides that likely play a role in differentiation of bacteroids. Silencing the homolog of

dnf1 in *Aeschynomene evenia*, which is necessary for cleavage of NCRs for transport to the symbiosome and is essential for symbiosis, results in deformed bacteroids (Czernic et al., 2015). In addition, the protein BclA was identified in *Bradyrhizobium sp.* as having weak homology to BacA. BclA was shown to be necessary for formation of bacteroids and was observed to be able to transport the peptide NCR247 from *M. truncatula* (Guefrachi et al., 2015). Taken together, there is good indirect evidence that these NCR-like peptides are used for bacteroid differentiation.

The localization of NCRs suggests much about their role in symbiosis. When NCRs are expressed in the nodule, they are targeted to the symbiotic membrane by the plant secretory system and can also be found within the cytoplasm of bacteroids (Van de Velde et al., 2010). In the same study, it was also shown that a mutation in *M. truncatula dnf-1* prevents targeting of NCRs to the bacteroid and prevented bacteroids from terminally differentiating. Also, when NCR035 from *M. truncatula* was expressed in *L. japonicum*, which is deficient in NCR production, it localized to the symbiosome of bacteroids resulting in the production of a single elongated bacteroid indicative of terminal differentiation (Alunni et al., 2007; Van de Velde et al., 2010). This highlighted the importance of NCRs for symbiotic establishment in the IRLC legumes. More recent studies on NCRs have shown that a mutation in the gene *dnf7,* which encodes for a protein involved in the production of NCR169, is unable to perform BNF in *M. truncatula* (Horváth et al., 2015). Nodules in this mutant were impaired in elongation and triggered early senescence. This was fully complemented by overexpression of NCR169. These studies show the necessity of NCRs in regulating bacteroid differentiation and symbiotic nitrogen fixation.

Microarray analysis has also revealed that NCR recognition may play a role in the bacterial stress response, as well as preventing cell division during symbiosis (Penterman et al., 2014). After exposure of *S. meliloti* to NCR247, the expression of genes involved in bacterial stress response and cellular division was found to be altered in transcription. This includes increased transcription of *rpoH1,* which is involved in regulating genes for acid and heat tolerance, and the two-component systems *exoS-chvI* and *feuP-feuQ,* which are responsible for regulating EPS and cyclic β(1–2) glucan production (Reuber et al., 1990; Griffitts et al., 2008). In line with this, NCR247 has been shown to induce transcription of the *exo* genes for EPS-I production, and high molecular weight EPS-I has been shown to aid survival when exposed to NCR247 (Arnold et al., 2017, 2018). Decreased transcription of cell cycle regulators *ctrA* and *gcrA* was also observed (Penterman et al., 2014). These observations led to the conclusion that NCR recognition may be a bacterial signal that allows for adaptation to *in planta* conditions and increase the production of polysaccharides necessary for symbiosis in addition to its role in bacteroid differentiation. This shows that NCRs may have evolved in plants from simply being an AMP produced as a response to bacterial invasion, to also being involved in symbiotic establishment as a signal which induces physiological and morphological changes in the bacteria necessary for nitrogen fixation.

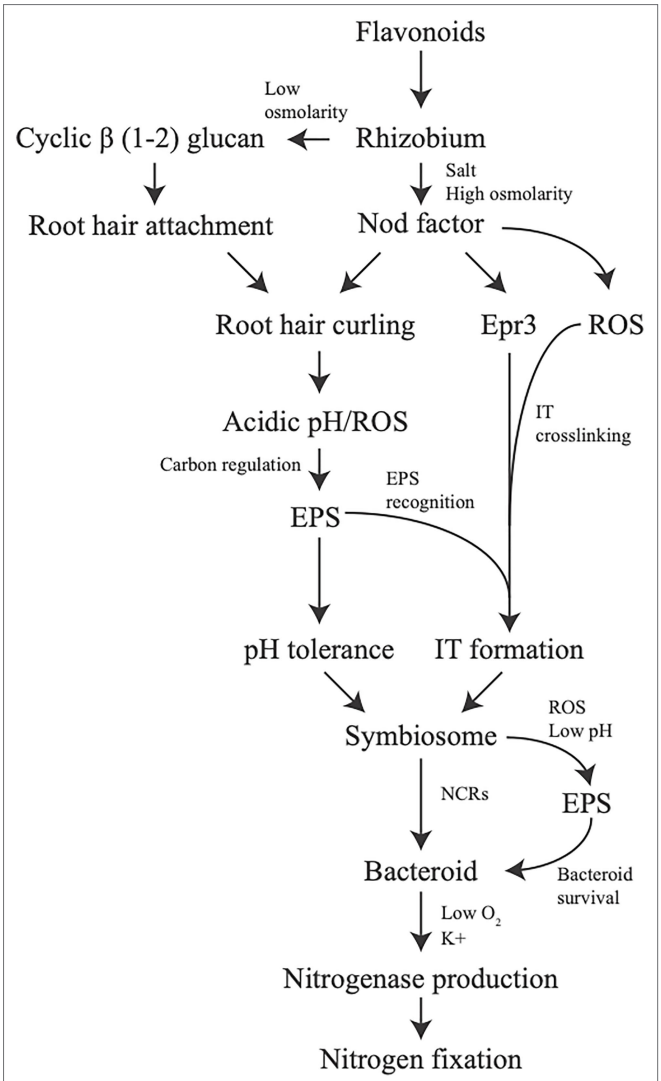

FIGURE 2 | Stress tolerance involvement in symbiotic signaling. Changes in production of molecules or overall physiology due to stress can be observed to affect symbiosis all throughout the process. Each line indicates how a potential stress, or a response from a stress, influences the next step in the symbiotic process.

DISCUSSION

The establishment of the rhizobium – legume symbiotic interaction is often described as a direct complex signal exchange between both the bacteria and the plant, with emphasis placed on how a molecule from one induces changes in the other or invokes a signaling response. However, little emphasis has been placed on how environmental conditions and stress tolerance play into the interaction. Here, we provide evidence that the tolerance of environmental conditions and challenges by the plant immune system result in alterations of bacterial physiology which promotes establishment of symbiosis between plant and bacteria. This broadens our assumptions of the signaling cross-talk between legume and rhizobia which is

largely considered from the perspective of secreted signal and direct response. In addition, we should consider overall physiological changes in bacteria due to conditions in the soil from root exudate or *in planta* as part of the signal exchange symbiosis in addition to the role in surviving the stress conditions. If molecules produced as part of the stress response by bacteria and plant are examined it can be seen that stress plays an important role from the start of symbiosis, all the way to nitrogen fixation (**Figure 2**).

Some of the examples used are already well studied for their role specifically in symbiosis. This includes iso-flavonoids, Nod factor, and NCRs. While these molecules now have roles directly in symbiotic signaling, their overall origin in this process comes from the immune response of the plant. What likely originated as a stress challenge of anti-microbials for bacteria and fungi with flavonoids and NCRs has turned into critical signals to initiate the symbiotic process or for forming terminally differentiated bacteroids. Cell wall chitin from fungi which is recognized as a PAMP has become inherited by rhizobia in the form of Nod factor, which is now the critical signaling molecule secreted by bacteria to establish symbiosis. The similarities of the responses between either plant immunity or symbiosis are significant and stretch much further past what is discussed here (Berrabah et al., 2015; Tóth and Stacey, 2015; Zipfel and Oldroyd, 2017). It is quite likely that as more detailed mechanisms of each of these responses are uncovered, it will be seen that there is significant cross-talk or similarities linking stress responses and symbiosis. In a number of cases, the difference between either killing the bacteria or establishing a functional symbiosis seems to be based upon the strength of the plant immune response to the organism. A strong response to repel an invader, or an attenuated one to induce physiological changes in a potential symbiont.

Other examples of how potential conditions bacteria may be exposed to in the soil or *in planta* are less directly tied to symbiosis, but the link is still quite clear. A large part of the stress response of symbiotic rhizobia revolves around production or modification of various polysaccharides, such as cyclic β(1–2) glucans, lipopolysaccharides, and succinoglycan. These polysaccharides are also intrinsically linked to symbiotic establishment across a number of different rhizobia-legume interactions. While the role of cyclic β(1–2) glucans in symbiosis is yet unclear, production and proper decoration of LPS and succinoglycan are suggested to be critical signaling molecules to avoid the full activation of the plant immune response (Ojeda et al., 2013; Kawaharada et al., 2015; Maillet et al., 2020). Additionally, there are around 17 different hypothetical operons for polysaccharide production in *S. meliloti* so it is plausible to think other polysaccharides that are yet unclassified may play an important role in the stress tolerance/symbiosis picture as well.

Aside from polysaccharide production, these adverse conditions encountered also changes cell physiology in terms of ion uptake, glutathione production, and shifts in carbon metabolism which can all be linked in some regards to the symbiotic process. It is not hard to imagine that symbiotic bacteria may have evolved its responses over time to stress conditions present in root exudate or *in planta* to start adjusting its physiology for a symbiotic lifecycle. In addition, it is understandable why a plant would evolve to promote certain conditions using root exudate and use an altered immune response if the eventual gain becomes a symbiotic nitrogen fixing bacteria.

One of the major overall goals of nitrogen fixation research is to eventually bring the symbiotic relationship between legumes and rhizobia to non-legume plants, such as the cereal crops. The potential impact this could have in reducing use of nitrogen fertilizers, and for overall growth of plants where fertilizers are not available, is quite significant. While research in this area is new and ongoing, it largely focuses on adjusting and tuning directly observed signaling between rhizobia and these plants. It is important to remember that aside from signaling and adjusting the plant's immune response to go from immunogenic to symbiotic, the overall environment in the rhizosphere and *in planta* may also play a key role for symbiosis and have to be accounted for. At the end of the day, it is always said that stress, unfortunately, is a great motivator in life. This also seems to be true with respect to the rhizobium-legume symbiosis.

AUTHOR CONTRIBUTIONS

JPH and IJO conceived and wrote the manuscript. All authors contributed to the article and approved the submitted version.

FUNDING

This work was supported by a Natural Sciences and Engineering Research Council of Canada Discovery grant (RGPIN-2018-04966) to IJO.

REFERENCES

Abe, M., Amemura, A., and Higashi, S. (1982). Studies on cyclic β-1,2-glucan obtained from periplasmic space of rhizobium trifolii cells. *Plant Soil* 64, 315–324. doi: 10.1007/BF02372514

Alunni, B., and Gourion, B. (2016). Terminal bacteroid differentiation in the legume - rhizobium symbiosis: nodule-specific cysteine-rich peptides and beyond. *New Phytol.* 211, 411–417. doi: 10.1111/nph.14025

Alunni, B., Kevei, Z., Redondo-Nieto, M., Kondorosi, A., Mergaert, P., and Kondorosi, E. (2007). Genomic organization and evolutionary insights on GRP and NCR genes, two large nodule-specific gene families in *Medicago truncatula*. *Mol. Plant Micro.Interact.* 20, 1138–1148. doi: 10.1094/MPMI-20-9-1138

Arnold, M. F. F., Penterman, J., Shabab, M., Chen, E. J., and Walker, C. (2018). Important late-stage symbiotic role of the Sinorhizobium meliloti exopolysaccharide Succinoglycan. *J. Bacteriol.* 200:e00665-17. doi: 10.1128/JB.00665-17

Arnold, M. F. F., Shabab, M., Penterman, J., Boehme, K. L., Griffitts, J. S., and Walker, C. (2017). Genome-wide sensitivity analysis of the Microsymbiont Sinorhizobium meliloti to symbiotically important, Defensin-Like host peptides. *MBio* 8:e01060-17. doi: 10.1128/mBio.01060-17

Barnett, M. J., and Fisher, R. F. (2006). Global gene expression in the rhizobial-legume symbiosis. *Symbiosis* 42, 1–24. doi: 10.1111/j.1574-6968.1999.tb13650.x

Berrabah, F., Ratet, P., and Gourion, B. (2015). Multiple steps control immunity during the intracellular accommodation of rhizobia. *J. Exp. Bot.* 66, 1977–1985. doi: 10.1093/jxb/eru545

Boscari, A., Meilhoc, E., Castella, C., Bruand, C., Puppo, A., and Brouquisse, R. (2013). Which role for nitric oxide in symbiotic N_2-fixing nodules: toxic by-product or useful signaling/metabolic intermediate? *Front. Plant Sci.* 4:384. doi: 10.3389/fpls.2013.00384

Botsford, J. L., and Lewis, T. A. (1990). Osmoregulation in rhizobium meliloti: production of glutamic acid in response to osmotic stress. *Appl. Environ. Microbiol.* 56, 488–494. doi: 10.1128/aem.56.2.488-494.1990

Breedveld, M. W., and Miller, K. J. (1994). Cyclic β-glucans of members of the family Rhizobiaceae. *Microbiol. Rev.* 58, 145–161. doi: 10.1128/mr.58.2.145-161.1994

Breedveld, M. W., and Miller, K. J. (1995). Synthesis of glycerophosphorylated cyclic (1,2)-β-glucans in rhizobium meliloti strain 1021 after osmotic shock. *Microbiology* 141, 583–588. doi: 10.1099/13500872-141-3-583

Broughton, W. J., Hanin, M., Relic, B., Kopcinska, J., Golinowski, W., Simsek, S., et al. (2006). Flavonoid-inducible modifications to rhamnan O antigens are necessary for rhizobium sp. strain NGR234-legume symbioses. *J. Bacteriol.* 188, 3654–3663. doi: 10.1128/JB.188.10.3654-3663.2006

Cardenas, L., Martinez, A., Sanchez, F., and Quinto, C. (2008). Fast, transient and specific intracellular ROS changes in living root hair cells responding to nod factors (NFs). *Plant J.* 56, 802–813. doi: 10.1111/j.1365-313X.2008.03644.x

Chabaud, M., Venard, C., Defaux-Petras, A., Bécard, G., and Barker, D. G. (2002). Targeted inoculation of Medicago truncatula in vitro root cultures reveals MtENOD11 expression during early stages of infection by arbuscular mycorrhizal fungi. *New Phytol.* 156, 265–273. doi: 10.1046/j.1469-8137.2002.00508.x

Chen, H., Richardson, A. E., and Rolfe, B. G. (1993). Studies of the physiological and genetic basis of acid tolerance in rhizobium leguminosarum biovar trifolii. *Appl. Environ. Microbiol.* 59, 1798–1804. doi: 10.1128/aem.59.6.1798-1804.1993

Chen, E. J., Sabio, E. A., and Long, S. R. (2008). The periplasmic regulator ExoR inhibits ExoS/ChvI two- component signaling in *Sinorhizobium meliloti*. *Mol. Microbiol.* 69, 1290–1303. doi: 10.1038/jid.2014.371

Cheng, H. P., and Walker, G. C. (1998a). Succinoglycan is required for initiation and elongation of infection threads during nodulation of alfalfa by rhizobium meliloti. *J. Bacteriol.* 180, 5183–5191. doi: 10.1128/JB.180.19.5183-5191.1998

Cheng, H. P., and Walker, G. C. (1998b). Succinoglycan production by rhizobium meliloti is regulated through the ExoS-ChvI two-component regulatory system. *J. Bacteriol.* 180, 20–26. doi: 10.1128/JB.180.1.20-26.1998

Cowan, M. M. (1999). Plant products as antimicrobial agents. *Clin. Microbiol. Rev.* 12, 564–582. doi: 10.1128/CMR.12.4.564

Cramer, C. L., Ryder, T. B., Bell, J. N., and Lamb, C. J. (1985). Rapid switching of plant gene expression induced by fungal elicitor. *Science* 227, 1240–1243. doi: 10.1126/science.227.4691.1240

Csonka, L. N. (1989). Physiological and genetic responses of bacteria to osmotic stress. *Microbiol. Rev.* 53, 121–147. doi: 10.1128/mr.53.1.121-147.1989

Cunningham, S. D., and Munns, D. N. (1984). The correlation between extracellular polysaccharide production and acid tolerance in rhizobium. *Soil Sci. Soc. Am. J.* 48, 1273–1276. doi: 10.2136/sssaj1984.03615995004800060014x

Czernic, P., Gully, D., Cartieaux, F., Moulin, L., Guefrachi, I., Patrel, D., et al. (2015). Convergent evolution of endosymbiont differentiation in Dalbergioid and inverted repeat-lacking clade legumes mediated by nodule-specific cysteine-rich peptides. *Plant Physiol.* 169, 1254–1265. doi: 10.1104/pp.15.00584

David, M., Daveran, M. L., Batut, J., Dedieu, A., Domergue, O., Ghai, J., et al. (1988). Cascade regulation of Nif gene-expression in rhizobium meliloti. *Cell* 54, 671–683. doi: 10.1016/S0092-8674(88)80012-6

Del Cerro, P., Megías, M., López-Baena, F. J., Gil-Serrano, A., Pérez-Montaño, F., and Ollero, F. J. (2019). Osmotic stress activates nif and fix genes and induces the rhizobium tropici CIAT 899 nod factor production via $NodD_2$ by up-regulation of the nodA2 operon and the nodA3 gene. *PLoS One* 14:e0213298. doi: 10.1371/journal.pone.0213298

Dilworth, M. J., Tiwari, R. P., Reeve, W. G., and Glenn, A. R. (2000). Legume root nodule bacteria and acid pH. *Sci. Prog.* 83, 357–389.

Dixon, R., and Kahn, D. (2004). Genetic regulation of biological nitrogen fixation. *Nat. Rev. Microbiol.* 2, 621–631. doi: 10.1038/nrmicro954

Donati, A. J., Jeon, J. M., Sangurdekar, D., So, J. S., and Chang, W. S. (2011). Genome-wide transcriptional and physiological responses of Bradyrhizobium japonicum to paraquat-mediated oxidative stress. *Appl. Environ. Microbiol.* 77, 3633–3643. doi: 10.1128/AEM.00047-11

Draghi, W. O., Del Papa, M. F., Hellweg, C., Watt, S. A., Watt, T. F., Barsch, A., et al. (2016). A consolidated analysis of the physiologic and molecular responses induced under acid stress in the legume-symbiont model-soil bacterium Sinorhizobium meliloti. *Sci. Rep.* 6:e29278. doi: 10.1038/srep29278

Duc, G., Trouvelot, A., Gianinazzi-Pearson, V., and Gianinazzi, S. (1989). First report of non-mycorrhizal plant mutants (Myc-) obtained in pea (Pisum sativum L.) and fababean (Vicia faba L.). *Plant Sci.* 60, 215–222. doi: 10.1016/0168-9452(89)90169-6

Dylan, T., Helinski, D. R., and Ditta, G. S. (1990a). Hypoosmotic adaptation in rhizobium meliloti requires beta-(1-2)-glucan. *J. Bacteriol.* 172, 1400–1408. doi: 10.1128/jb.172.3.1400-1408.1990

Dylan, T., Nagpal, P., Helinski, D. R., and Ditta, G. S. (1990b). Symbiotic pseudorevertants of rhizobium meliloti ndv mutants. *J. Bacteriol.* 172, 1409–1417. doi: 10.1128/jb.172.3.1409-1417.1990

Ehrhardt, D. W., Atkinson, E. M., and Long, S. R. (1992). Depolarization of alfalfa root hair membrane potential by rhizobium meliloti nod factors. *Science* 256, 998–1000. doi: 10.1126/science.10744524

Ehrhardt, D. W., Wais, R., and Long, S. R. (1996). Calcium spiking in plant root hairs responding to rhizobium nodulation signals. *Cell* 85, 673–681. doi: 10.1016/S0092-8674(00)81234-9

El-Yahyaoui, F., Kuster, H., Amor, B. B., Hohnjec, N., Pu, A., Becker, A., et al. (2004). Expression profiling in Medicago truncatula pdentifies more than 750 genes differentially expressed during nodulation, including many potential regulators of the symbiotic program. *Plant Physiol.* 136, 3159–3176. doi: 10.1104/pp.104.043612.the

Faget, M., Blossfeld, S., von Gillhaussen, P., Schurr, U., and Temperton, V. M. (2013). Disentangling who is who during rhizosphere acidification in root interactions: combining fluorescence with optode techniques. *Front. Plant Sci.* 4:392. doi: 10.3389/fpls.2013.00392

Fedorova, E., Thomson, R., Whitehead, L. F., Maudoux, O., Udvardi, M. K., and Day, D. A. (1999). Localization of H^+-ATPase in soybean root nodules. *Planta* 209, 25–32. doi: 10.1007/s004250050603

Fenner, B. J., Tiwari, R. P., Reeve, W. G., Dilworth, M. J., and Glenn, A. R. (2004). Sinorhizobium medicae genes whose regulation involves the ActS and/or ActR signal transduction proteins. *FEMS Microbiol. Lett.* 236, 21–31. doi: 10.1016/j.femsle.2004.05.016

Ferrer, J. L., Austin, M. B., Stewart, C., and Noel, J. P. (2008). Structure and function of enzymes involved in the biosynthesis of phenylpropanoids. *Plant Physiol. Biochem.* 46, 356–370. doi: 10.1016/j.plaphy.2007.12.009

Fonseca-García, C., Nava, N., Lara, M., and Quinto, C. (2021). An NADPH oxidase regulates carbon metabolism and the cell cycle during root nodule symbiosis in common bean (Phaseolus vulgaris). *BMC Plant Biol.* 21, 274–290. doi: 10.1186/s12870-021-03060-z

Fournier, J., Timmers, A. C. J., Sieberer, B. J., Jauneau, A., Chabaud, M., and Barker, D. G. (2008). Mechanism of infection thread elongation in root hairs of *Medicago truncatula* and dynamic interplay with associated rhizobial colonization. *Plant Physiol.* 148, 1985–1995. doi: 10.1104/pp.108.125674

Geddes, B. A., González, J. E., and Oresnik, I. J. (2014). Exopolysaccharide production in response to medium acidification is correlated with an increase in competition for nodule occupancy. *Mol. Plant-Microbe Interact.* 27, 1307–1317. doi: 10.1094/MPMI-06-14-0168-R

Geddes, B. A., and Oresnik, I. J. (2016). "The mechanism of symbiotic nitrogen fixation," in *The Mechanistic Benefits of Microbial Symbionts. Advances in Environmental Microbiology. Vol. 2*. C. J. Hurst (Ed.) (Switzerland: Springer International Publishing), 69–97.

Gober, J. W., and Kashket, E. R. (1987). K^+ regulates bacteroid-associated functions of Bradyrhizobium. *Proc. Natl. Acad. Sci. U. S. A.* 84, 4650–4654. doi: 10.1073/pnas.84.13.4650

González, J. E., Reuhs, B. L., and Walker, G. C. (1996). Low molecular weight EPS II of rhizobium meliloti allows nodule invasion in Medicago sativa. *Proc. Natl. Acad. Sci. U. S. A.* 93, 8636–8641. doi: 10.1073/pnas.93.16.8636

Griffitts, J. S., Carlyon, R. E., Erickson, J. H., Moulton, J. L., Barnett, M. J., Toman, C. J., et al. (2008). A Sinorhizobium meliloti osmosensory two-component system required for cyclic glucan export and symbiosis. *Mol. Microbiol.* 69, 479–490. doi: 10.1111/j.1365-2958.2008.06304.x

Guefrachi, I., Pierre, O., Timchenko, T., Alunni, B., Barrière, Q., Czernic, P., et al. (2015). Bradyrhizobium BclA is a peptide transporter required for bacterial differentiation in Symbiosis with Aeschynomene legumes. *Mol. Plant-Microbe Interact.* 28, 1155–1166. doi: 10.1094/MPMI-04-15-0094-R

Guerrero-Castro, J., Lozano, L., and Sohlenkamp, C. (2018). Dissecting the acid stress response of rhizobium tropici CIAT 899. *Front. Microbiol.* 9:846. doi: 10.3389/fmicb.2018.00846

Haag, A. F., Baloban, M., Sani, M., Kerscher, B., Pierre, O., Farkas, A., et al. (2011). Protection of Sinorhizobium against host cysteine-rich antimicrobial peptides is critical for symbiosis. *PLoS Biol.* 9:e1001169. doi: 10.1371/journal.pbio.1001169

Harrison, J., Jamet, A., Muglia, C. I., Sype, G.Van, De Aguilar, O. M., Puppo, A., et al. (2005). Glutathione plays a fundamental role in growth and symbiotic capacity of Sinorhizobium meliloti. *J. Bacteriol.* 187, 168–174. doi:10.1128/JB.187.1.168.

Hartwig, U. A., Maxwell, C. A., Joseph, C. M., and Phillips, D. A. (1990). Effects of alfalfa nod gene-inducing flavonoids on nodABC transcription in rhizobium meliloti strains containing different nodD genes. *J. Bacteriol.* 172, 2769–2773. doi: 10.1128/jb.172.5.2769-2773.1990

Hassan, S., and Mathesius, U. (2012). The role of flavonoids in root-rhizosphere signalling: opportunities and challenges for improving plant-microbe interactions. *J. Exp. Bot.* 63, 3429–3444. doi: 10.1093/jxb/err430

Hawkins, J. P., Geddes, B. A., and Oresnik, I. J. (2017). Succinoglycan directly contributes to pH tolerance in Sinorhizboium meliloti Rm1021. *Mol. Plant-Microbe Interact.* 30, 1009–1019. doi: 10.1094/MPMI-07-17-0176-R

Heavner, M. E., Qiu, W. G., and Cheng, H. (2015). Phylogenetic co-occurrence of ExoR, ExoS, and ChvI, components of the RSI bacterial invasion switch, suggests a key adaptive mechanism regulating the transition between free-living and host-invading phases in Rhizobiales. *PLoS One* 10:e0135655. doi: 10.1371/journal.pone.0135655

Heckel, B. C., Tomlinson, A. D., Morton, E. R., Choi, J. H., and Fuqua, C. (2014). Agrobacterium tumefaciens ExoR controls acid response genes and impacts exopolysaccharide synthesis, horizontal gene transfer, and virulence gene expression. *J. Bacteriol.* 196, 3221–3233. doi: 10.1128/JB.01751-14

Hellweg, C., Pühler, A., and Weidner, S. (2009). The time course of the transcriptomic response of Sinorhizobium meliloti 1021 following a shift to acidic pH. *BMC Microbiol.* 9, 37–53. doi: 10.1186/1471-2180-9-37

Hirsch, A. M., Lum, M. R., and Downie, J. A. (2001). What makes the rhizobia-legume symbiosis so special? *Plant Physiol.* 127, 1484–1492. doi: 10.1104/pp.010866

Horváth, B., Domonkos, Á., Kereszt, A., Szűcs, A., Ábrahám, E., Ayaydin, F., et al. (2015). Loss of the nodule-specific cysteine rich peptide, NCR169, abolishes symbiotic nitrogen fixation in the Medicago truncatula dnf7 mutant. *Proc. Natl. Acad. Sci. U. S. A.* 112, 15232–15237. doi: 10.1073/pnas.1500777112

Howieson, J. G., Ewing, M. A., and D'Antuono, M. F. (1988). Selection for acid tolerance in rhizobium meliloti. *Plant Soil* 105, 179–188. doi: 10.1007/BF02376781

Hunt, S., King, B. J., Canvin, D. T., and Layzell, D. B. (1987). Steady and nonsteady state gas exchange characteristics of soybean nodules in relation to the oxygen diffusion barrier. *Plant Physiol.* 84, 164–172. doi: 10.1104/pp.84.1.164

Hunt, S., and Layzell, D. B. (1993). Gas exchange of legume nodules and the regulation of nitrogenase activity. *Annu. Rev. Plant Physiol. Plant Mol. Biol.* 44, 483–511. doi: 10.1146/annurev.pp.44.060193.002411

Jamet, A., Mandon, K., Puppo, A., and Hérouart, D. (2007). H_2O_2 is required for optimal establishment of the Medicago sativa/Sinorhizobium meliloti symbiosis. *J. Bacteriol.* 189, 8741–8745. doi: 10.1128/JB.01130-07

Jamet, A., Sigaud, S., Van de Sype, G., Puppo, A., and Herouart, D. (2003). Expression of the bacterial catalase genes during Sinorhizobium meliloti-Medicago sativa symbiosis and their crucial role during the infection process. *Mol. Plant-Microbe Interact.* 16, 217–225. doi: 10.1094/MPMI.2003.16.3.217

Jones, D. L., Dennis, P. G., Owen, A. G., and Van Hees, P. A. W. (2003). Organic acid behavior in soils - misconceptions and knowledge gaps. *Plant Soil* 248, 31–41. doi: 10.1023/A:1022304332313

Jones, K. M., Kobayashi, H., Davies, B. W., Taga, M. E., and Walker, G. C. (2007). How rhizobial symbionts invade plants: the Sinorhizobium-Medicago model. *Nat. Rev. Microbiol.* 5, 619–633. doi: 10.1038/nrmicro1705

Jungk, A. O. (2002). "Dynamics of nutrient movement at the soil root interface," in *Plant Roots. The Hidden Half*. U. Kafkafi, Y. Waisel and A. Eshel (Eds.) (United States: CRC Press), 587–616.

Kannenberg, E. L., and Brewin, N. J. (1989). Expression of a cell surface antigen from rhizobium leguminosarum 3841 is regulated by oxygen and pH. *J. Bacteriol.* 171, 4543–4548. doi: 10.1128/jb.171.9.4543-4548.1989

Kawaharada, Y., Kelly, S., Nielsen, M. W., Hjuler, C. T., Gysel, K., Muszyński, A., et al. (2015). Receptor-mediated exopolysaccharide perception controls bacterial infection. *Nature* 523, 308–312. doi: 10.1038/nature14611

Keating, D. H., Willits, M. G., and Long, S. R. (2002). A Sinorhizobium meliloti lipopolysaccharide mutant altered in cell surface sulfation. *J. Bacteriol.* 184, 6681–6689. doi: 10.1128/JB.184.23.6681

Király, Z., El-Zahaby, H. M., and Klement, Z. (1997). Role of extracellular polysaccharide (EPS) slime of plant pathogenic bacteria in protecting cells to reactive oxygen species. *J. Phytopathol.* 145, 59–68. doi: 10.1111/j.1439-0434.1997.tb00365.x

Lehman, A. P., and Long, S. R. (2013). Exopolysaccharides from Sinorhizobium meliloti can protect against H_2O_2-dependent damage. *J. Bacteriol.* 195, 5362–5369. doi: 10.1128/JB.00681-13

Lelpi, L., Dylan, T., Ditta, G. S., Helinski, D. R., and Stanfield, S. W. (1990). The ndvB locus of rhizobium meliloti encodes a 319-kDa involved in the production of β-(1-2)-glucan. *J. Biol. Chem.* 265, 2643–2651.

Li, L., Jia, Y., Hou, Q., Charles, T. C., Nester, E. W., and Pan, S. Q. (2002). A global pH sensor: agrobacterium sensor protein ChvG regulates acid-inducible genes on its two chromosomes and Ti plasmid. *Proc. Natl. Acad. Sci. U. S. A.* 99, 12369–12374. doi: 10.1073/pnas.192439499

Liang, Y., Cao, Y., Tanaka, K., Thibivilliers, S., Wan, J., Choi, J., et al. (2013). Nonlegumes respond to Rhizobial nod factors by suppressing the innate immune response. *Science* 341, 1384–1387. doi: 10.1126/science.1242736

Lohar, D. P., Haridas, S., Gantt, J. S., and VandenBosch, K. A. (2007). A transient decrease in reactive oxygen species in roots leads to root hair deformation in the legume-rhizobia symbiosis. *New Phytol.* 173, 39–49. doi: 10.1111/j.1469-8137.2006.01901.x

Lohar, D. P., Sharopova, N., Endre, G., Peñuela, S., Samac, D., Town, C., et al. (2006). Transcript analysis of early nodulation events in Medicago truncatula. *Plant Physiol.* 140, 221–234. doi: 10.1104/pp.105.070326.1

Lu, H. Y., Luo, L., Yang, M. H., and Cheng, H.-P. (2012). Sinorhizobium meliloti ExoR is the target of periplasmic proteolysis. *J. Bacteriol.* 194, 4029–4040. doi: 10.1128/JB.00313-12

Madsen, E. B., Madsen, L. H., Radutoiu, S., Olbryt, M., Rakwalska, M., Szczyglowski, K., et al. (2003). A receptor kinase gene of the LysM type is involved in legume perception of rhizobial signals. *Nature* 425, 637–640. doi: 10.1038/nature02045

Maillet, F., Fournier, J., Mendis, H. C., Tadege, M., Wen, J., Ratet, P., et al. (2020). Sinorhizobium meliloti succinylated high-molecular-weight succinoglycan and the Medicago truncatula LysM receptor-like kinase MtLYK10 participate independently in symbiotic infection. *Plant J.* 102, 311–326. doi: 10.1111/tpj.14625

Maroti, G. G., Kereszt, A., Kondorosi, E., and Mergaert, P. (2011). Natural roles of antimicrobial peptides in microbes, plants and animals. *Res. Microbiol.* 162, 363–374. doi: 10.1016/j.resmic.2011.02.005

Mendis, H. C., Madzima, T. F., Queiroux, C., and Jones, K. M. (2016). Function of succinoglycan polysaccharide in Sinorhizobium meliloti host plant invasion depends on succinylation, not molecular weight. *MBio* 7:e00606-16. doi: 10.1128/mBio.00606-16

Mergaert, P., Nikovics, K., Kelemen, Z., Maunoury, N., Vaubert, D., Kondorosi, A., et al. (2003). A novel family in Medicago truncatula consisting of more than 300 nodule-specific genes coding for small, secreted polypeptides with conserved cysteine motifs. *Plant Physiol.* 132, 161–173. doi: 10.1104/pp.102.018192

Mergaert, P., Uchiumi, T., Alunni, B., Evanno, G., Cheron, A., Catrice, O., et al. (2006). Eukaryotic control on bacterial cell cycle and differentiation in the rhizobium-legume symbiosis. *Proc. Natl. Acad. Sci. U. S. A.* 103, 5230–5235. doi: 10.1073/pnas.0600912103

Miller, K. J., Kennedy, E. P., and Reinhold, V. N. (1986). Osmotic adaptation by gram-negative bacteria: possible role for periplasmic oligosaccharides. *Science* 231, 48–51. doi: 10.1126/science.3941890

Miller, K. J., and Wood, J. M. (1996). Osmoadatptation by rhizosphere bacteria. *Annu. Rev. Microbiol.* 6:e23307. doi: 10.1371/journal.pone.0023307

Miller-Williams, M., Loewen, P. C., and Oresnik, I. J. (2006). Isolation of salt-sensitive mutants of Sinorhizobium meliloti strain Rm1021. *Microbiology* 152, 2049–2059. doi: 10.1099/mic.0.28937-0

Muglia, C. I., Grasso, D. H., and Aguilar, O. M. (2007). Rhizobium tropici response to acidity involves activation of glutathione synthesis. *Microbiology* 153, 1286–1296. doi: 10.1099/mic.0.2006/003483-0

Mylona, P., Pawlowski, K., and Bisseling, T. (1995). Symbiotic nitrogen fixation. *Plant Cell* 7, 869–885. doi: 10.1097/00010694-199511000-00009

Nagpal, P., Khanuja, S. P., and Stanfield, S. W. (1992). Suppression of the ndv mutant phenotype of rhizobium meliloti by cloned exo genes. *Mol. Microbiol.* 6, 479–488. doi: 10.1111/j.1365-2958.1992.tb01492.x

Ojeda, K. J., Simonds, L., and Noel, K. D. (2013). Roles of predicted glycosyltransferases in the biosynthesis of the rhizobium etli CE3 O antigen. *J. Bacteriol.* 195, 1949–1958. doi: 10.1128/JB.02080-12

Oldroyd, G. E. D. (2013). Speak, friend, and enter: signalling systems that promote beneficial symbiotic associations in plants. *Nat. Rev. Microbiol.* 11, 252–263. doi: 10.1038/nrmicro2990

Oldroyd, G. E. D., and Downie, J. A. (2008). Coordinating nodule morphogenesis with rhizobial infection in legumes. *Annu. Rev. Plant Biol.* 59, 519–546. doi: 10.1146/annurev.arplant.59.032607.092839

Oldroyd, G. E. D., Murray, J. D., Poole, P. S., and Downie, J. A. (2011). The rules of engagement in the legume-rhizobial symbiosis. *Annu. Rev. Genet.* 45, 119–144. doi: 10.1146/annurev-genet-110410-132549

Pauly, N., Pucciariello, C., Mandon, K., Innocenti, G., Jamet, A., Baudouin, E., et al. (2006). Reactive oxygen and nitrogen species and glutathione: key players in the legume-rhizobium symbiosis. *J. Exp. Bot.* 57, 1769–1776. doi: 10.1093/jxb/erj184

Penterman, J., Abo, R. P., De Nisco, N. J., Arnold, M. F. F., Longhi, R., Zanda, M., et al. (2014). Host plant peptides elicit a transcriptional response to control the Sinorhizobium meliloti cell cycle during symbiosis. *Proc. Natl. Acad. Sci. U. S. A.* 111, 3561–3566. doi: 10.1073/pnas.1400450111

Pérez-Montaño, F., del Cerro, P., Jiménez-Guerrero, I., López-Baena, F. J., Cubo, M. T., Hungria, M., et al. (2016). RNA-seq analysis of the rhizobium tropici CIAT 899 transcriptome shows similarities in the activation patterns of symbiotic genes in the presence of apigenin and salt. *BMC Genomics* 17, 198–111. doi: 10.1186/s12864-016-2543-3

Pierre, O., Engler, G., Hopkins, J., Brau, F., Boncompagni, E., and Hérouart, D. (2013). Peribacteroid space acidification: A marker of mature bacteroid functioning in Medicago truncatula nodules. *Plant Cell Environ.* 36, 2059–2070. doi: 10.1111/pce.12116

Pueppke, S. G., and Broughton, W. J. (1999). Rhizobium sp. strain NGR234 and R. fredii USDA257 share exceptionally broad, nested host ranges. *Mol. Plant-Microbe Interact.* 12, 293–318. doi: 10.1094/MPMI.1999.12.4.293

Puppo, A., Pauly, N., Boscari, A., Mandon, K., and Brouquisse, R. (2013). Hydrogen peroxide and nitric oxide: key regulators of the legume-rhizobium and mycorrhizal symbioses. *Antioxid. Redox Signal.* 18, 2202–2219. doi: 10.1089/ars.2012.5136

Pusztahelyi, T. (2018). Chitin and chitin-related compounds in plant–fungal interactions. *Mycology* 9, 189–201. doi: 10.1080/21501203.2018.1473299

Ramu, S. K., Peng, H. M., and Cook, D. R. (2002). Nod factor induction of reactive oxygen species production is correlated with expression of the early nodulin gene rip1 in Medicago truncatula. *Mol. Plant-Microbe Interact.* 15, 522–528. doi: 10.1094/MPMI.2002.15.6.522

Reeve, W. G., Dilworth, M. J., Tiwari, R. P., and Glenn, A. R. (1997). Regulation of exopolysaccharide production in rhizobium leguminosarum biovar viciae WSM710 involves exoR. *Microbiology* 143, 1951–1958. doi: 10.1099/00221287-143-6-1951

Reuber, T. L., Urzainqui, A., Glazebrook, J., Reed, J. W., and Walker, G. C. (1990). Genetic analyses and manipulations of rhizobium meliloti exopolysaccharides. *Nov. Biodegrad. Microb. Polym.* 12, 285–294. doi: 10.1007/978-94-009-2129-0_24

Reyes-González, A., Talbi, C., Rodríguez, S., Rivera, P., Zamorano-Sánchez, D., and Girard, L. (2016). Expanding the regulatory network that controls nitrogen fixation in Sinorhizobium meliloti: elucidating the role of the two-component system hFixL-FxkR. *Microbiology* 162, 979–988. doi: 10.1099/mic.0.000284

Riccillo, P. M., Muglia, C. I., De Bruijn, F. J., Roe, A. J., Booth, I. R., and Aguilar, O. M. (2000). Glutathione is involved in environmental stress responses in rhizobium tropici, including acid tolerance. *J. Bacteriol.* 182, 1748–1753. doi: 10.1128/JB.182.6.1748-1753.2000

Rutten, P. J., Steel, H., Hood, G. A., Ramachandran, V. K., McMurtry, L., Geddes, B., et al. (2021). Multiple sensors provide spatiotemporal oxygen regulation of gene expression in a rhizobium-legume symbiosis. *PLoS Genet.* 17:e1009099. doi: 10.1371/journal.pgen.1009099

Santos, R., Hérouart, D., Sigaud, S., Touati, D., and Puppo, A. (2001). Oxidative burst in alfalfa- Sinorhizobium meliloti symbiotic interaction. *Mol. Plant-Microbe Interact.* 14, 86–89. doi: 10.1094/MPMI.2001.14.1.86

Schopfer, C. R. (1999). The male determinant of self-incompatibility in brassica. *Science* 286, 1697–1700. doi: 10.1126/science.286.5445.1697

Shaw, S. L., and Long, S. R. (2003). Nod factor inhibition of reactive oxygen efflux in a host legume. *Plant Physiol.* 132, 2196–2204. doi: 10.1104/pp.103.021113

Smith, L. T., Allaith, A. A., and Smith, G. M. (1994). Mechanism of osmotically regulated N-acetylglutaminylglutamine amide production in rhizobium meliloti. *Plant Soil* 161, 103–108. doi: 10.1007/BF02183090

Streng, A., Op Den Camp, R., Bisseling, T., Geurts, R., Camp, R.Den, Bisseling, T., et al. (2011). Evolutionary origin of rhizobium nod factor signaling. *Plant Signal. Behav.* 6, 1510–1514. doi:10.4161/psb.6.10.17444.

Tang, Y., and Hollingsworth, R. I. (1998). Regulation of lipid synthesis in Bradyrhizobium japonicum: low oxygen concentrations trigger phosphatidylinositol biosynthesis. *Appl. Environ. Microbiol.* 64, 1963–1966. doi: 10.1128/AEM.64.5.1963-1966.1998

Tóth, K., and Stacey, G. (2015). Does plant immunity play a critical role during initiation of the legume-rhizobium symbiosis? *Front. Plant Sci.* 06, 401–408. doi: 10.3389/fpls.2015.00401

Van de Velde, W., Zehirov, G., Szatmari, A., Debreczeny, M., Ishihara, H., Kevei, Z., et al. (2010). Plant peptides govern terminal differentiation of bacteria in symbiosis. *Science* 327, 1122–1126. doi: 10.1126/science.1184057

Via, V. D., Zanetti, M. E., and Blanco, F. (2016). How legumes recognize rhizobia. *Plant Signal. Behav.* 11:e1120396. doi: 10.1080/15592324.2015.1120396

Virts, E. L., Stanfield, S. W., Helinski, D. R., and Ditta, G. S. (1988). Common regulatory elements control symbiotic and microaerobic induction of nifA in rhizobium meliloti. *Proc. Natl. Acad. Sci. U. S. A.* 85, 3062–3065. doi: 10.1073/pnas.85.9.3062

Winkel-Shirley, B. (2001). Flavonoid biosynthesis. A colorful model for genetics, biochemistry, cell biology, and biotechnology. *Plant Physiol.* 126, 485–493. doi: 10.1104/pp.126.2.485

Yancey, P. H., Clark, M. E., Hand, S. C., Bowlus, R. D., and Somero, G. N. (1982). Living with water stress: evolution of osmolyte systems. *Science* 217, 1214–1222. doi: 10.1126/science.7112124

Yao, S. Y., Luo, L., Har, K. J., Becker, A., Rüberg, S., Yu, G. Q., et al. (2004). Sinorhizobium meliloti ExoR and ExoS proteins regulate both succinoglycan and flagellum production. *J. Bacteriol.* 186, 6042–6049. doi: 10.1128/JB.186.18.6042-6049.2004

York, W. S., McNeil, M., Darvill, A. G., and Albersheim, P. (1980). Beta-2-linked glucans secreted by fast-growing species of rhizobium. *J. Bacteriol.* 142, 243–248. doi: 10.1128/jb.142.1.243-248.1980

York, G. M., and Walker, G. C. (1997). The rhizobium meliloti exoK gene and prsD/prsE/exsH genes are components of independent degradative pathways which contribute to production of low-molecular-weight succinoglycan. *Mol. Microbiol.* 25, 117–134. doi: 10.1046/j.1365-2958.1997.4481804.x

Zamorano-Sánchez, D., and Girard, L. (2015). "FNR-like proteins in rhizobia: past and future," in *Biology Nitrogen Fixation*. F. J. Brujin (Ed.) (United States: John Wiley & Sons), 155–166.

Zhou, P., Silverstein, K. A., Gao, L., Walton, J. D., Nallu, S., Guhlin, J., et al. (2013). Detecting small plant peptides using SPADA (small peptide alignment discovery application). *BMC Bioinfo.* 14, 335–351. doi: 10.1186/1471-2105-14-335

Zipfel, C., and Oldroyd, G. E. D. (2017). Plant signalling in symbiosis and immunity. *Nature* 543, 328–336. doi: 10.1038/nature22009

Conflict of Interest: The authors declare that the research was conducted in the absence of any commercial or financial relationships that could be construed as a potential conflict of interest.

Publisher's Note: All claims expressed in this article are solely those of the authors and do not necessarily represent those of their affiliated organizations, or those of the publisher, the editors and the reviewers. Any product that may be evaluated in this article, or claim that may be made by its manufacturer, is not guaranteed or endorsed by the publisher.

frontiers in Plant Science

ORIGINAL RESEARCH
published: 12 January 2022
doi: 10.3389/fpls.2021.808573

The Role of Heterotrimeric G-Protein Beta Subunits During Nodulation in *Medicago truncatula* Gaertn and *Pisum sativum* L.

*Andrey D. Bovin[1], Olga A. Pavlova[1], Aleksandra V. Dolgikh[1,2], Irina V. Leppyanen[1] and Elena A. Dolgikh[1]**

[1] All-Russia Research Institute for Agricultural Microbiology, Saint Petersburg, Russia, [2] Department of Genetics and Biotechnology, Saint Petersburg State University, Saint Petersburg, Russia

Heterotrimeric G-proteins regulate plant growth and development as master regulators of signaling pathways. In legumes with indeterminate nodules (e.g., *Medicago truncatula* and *Pisum sativum*), the role of heterotrimeric G-proteins in symbiosis development has not been investigated extensively. Here, the involvement of heterotrimeric G-proteins in *M. truncatula* and *P. sativum* nodulation was evaluated. A genome-based search for G-protein subunit-coding genes revealed that *M. truncatula* and *P. sativum* harbored only one gene each for encoding the canonical heterotrimeric G-protein beta subunits, MtG beta 1 and PsG beta 1, respectively. RNAi-based suppression of *MtGbeta1* and *PsGbeta1* significantly decreased the number of nodules formed, suggesting the involvement of G-protein beta subunits in symbiosis in both legumes. Analysis of composite *M. truncatula* plants carrying the *pMtGbeta1:GUS* construct showed β-glucuronidase (GUS) staining in developing nodule primordia and young nodules, consistent with data on the role of G-proteins in controlling organ development and cell proliferation. In mature nodules, GUS staining was the most intense in the meristem and invasion zone (II), while it was less prominent in the apical part of the nitrogen-fixing zone (III). Thus, MtG beta 1 may be involved in the maintenance of meristem development and regulation of the infection process during symbiosis. Protein–protein interaction studies using co-immunoprecipitation revealed the possible composition of G-protein complexes and interaction of G-protein subunits with phospholipase C (PLC), suggesting a cross-talk between G-protein- and PLC-mediated signaling pathways in these legumes. Our findings provide direct evidence regarding the role of MtG beta 1 and PsG beta 1 in symbiosis development regulation.

Keywords: legume-rhizobial symbiosis, heterotrimeric G-protein, beta subunits, RNAi based suppression, promoter-GUS fusion localization, *Medicago truncatula* Gaertn, pea *Pisum sativum* L., co-immunoprecipitation

OPEN ACCESS

Edited by:
Katharina Pawlowski, Stockholm University, Sweden

Reviewed by:
Maurizio Chiurazzi, National Research Council (CNR), Italy
Swarup Roy Choudhury, Indian Institute of Science Education and Research Tirupati, India

****Correspondence:***
Elena A. Dolgikh
dol2helen@yahoo.com

Specialty section:
This article was submitted to Plant Symbiotic Interactions, a section of the journal Frontiers in Plant Science

Received: *03 November 2021*
Accepted: *16 December 2021*
Published: *12 January 2022*

Citation:
Bovin AD, Pavlova OA, Dolgikh AV, Leppyanen IV and Dolgikh EA (2022) The Role of Heterotrimeric G-Protein Beta Subunits During Nodulation in Medicago truncatula Gaertn and Pisum sativum L.. Front. Plant Sci. 12:808573. doi: 10.3389/fpls.2021.808573

INTRODUCTION

Heterotrimeric G-proteins are known to respond to a wide variety of external stimuli and interact with different cytosolic and membrane-associated effectors, therefore they may play an essential role in regulating plant growth and development as master regulators of signal transduction pathways (Urano and Jones, 2014; Pandey and Vijayakumar, 2018). Analysis of mutants showed

that the heterotrimeric G-proteins in plants are involved in such processes as the control of organ development (Lease et al., 2001; Ullah et al., 2003; Ding et al., 2008; Mudgil et al., 2009), response to biotic and abiotic stress (Joo et al., 2005; Llorente et al., 2005; Delgado-Cerezo et al., 2012), hormonal regulation and signaling, and cell proliferation (Ullah, 2001).

Heterotrimeric G-proteins consist of G alpha, G beta, and G gamma subunits and are associated with the cell membrane in the inactive state. In animals and fungi, G alpha subunits are activated by several G-protein-coupled receptors (GPCRs); however, although single GPCRs were found in plants, their functional association with G-proteins was not shown (Urano and Jones, 2014; Roy Choudhury and Pandey, 2016). Recent studies have demonstrated that G-proteins in plants are activated by single-pass transmembrane receptor-like kinases (RLKs) or through the interaction between RLKs and seven-transmembrane domain regulators of G-protein signaling (RGSs) (Bommert et al., 2013; Choudhury and Pandey, 2013; Ishida et al., 2014; Tunc-Ozdemir et al., 2016). During signal perception, a conformational change stimulates the exchange of GTP for GDP on the G alpha subunit, promoting dissociation of the G beta-gamma complex. This event is required for signal transduction in plants and animals. In contrast to animals, the genomes of plants encode significantly less G-protein subunits. For example, *Arabidopsis* and rice contain only one G alpha, three extra-large G alpha (XLG), one G beta, and three G gamma subunits (Perfus-Barbeoch et al., 2004; Trusov and Botella, 2016).

Using a pharmacological approach, previous studies proposed the involvement of G-proteins in legume-rhizobial symbiosis regulation in legumes (Pingret, 1998); however, the exact mechanisms underlying this regulation and specific components of the G-protein network remain poorly characterized. Some effectors of G-protein signaling, such as phospholipase C (PLC) and D (PLD), are involved in mastoparan-induced root hair deformations during nodulation (Pingret, 1998; den Hartog et al., 2001, 2003; Charron et al., 2004; De Los Santos-Briones et al., 2009). Mastoparan is a well-known heterotrimeric G-protein agonist. Using a pharmacological approach, the relationships among G-protein activation, production of phospholipid metabolites by PLC and PLD, generation of calcium spiking, expression of specific *ENOD* genes, and root hair deformations were revealed in *Vicia sativa*, *Medicago sativa*, and *Medicago truncatula* (den Hartog et al., 2001, 2003; Charron et al., 2004; Sun et al., 2007).

In legumes with determinate types of nodules, such as soybean, a set of G alpha, G beta, and G gamma subunits were found using a genome-wide approach (Bisht et al., 2011) and some of them shown to be required for symbiosis development with rhizobia (Choudhury et al., 2011; Choudhury and Pandey, 2013, 2015). Moreover, the interaction between the G alpha subunits of soybean with lysin motif (LysM)-RLKs NFR1α and NFR1β (involved in Nod factor perception) was shown using the yeast split-ubiquitin system and bimolecular fluorescence complementation (Choudhury and Pandey, 2013). These findings were in line with previous hypotheses regarding the possible participation of G-proteins in signal transduction pathways activated upon perception of Nod factors.

In contrast, in legumes with indeterminate nodules, such as *M. truncatula* and *Pisum sativum*, in which nodule primordia develop in inner cortex and mature nodules retain a persistent meristem, the role of heterotrimeric G-proteins in symbiosis development has not been investigated in detail. However, several isoforms of G-protein subunits have been described in *P. sativum* and have been shown to be involved in the regulation of salinity and heat stress (Misra et al., 2007). Although heterotrimeric G-proteins are promising downstream components of the Nod factor perception pathway, their specific role in symbiosis development remains unclear. Advances in our understanding of G-protein networks will allow precise manipulation of legume plants to improve agronomically important traits. Here, RNAi-based suppression, promoter-β-glucuronidase (GUS) fusion, and co-immunoprecipitation were used to evaluate the involvement of the G-protein complex in the nodulation process in the model legume, *M. truncatula*, and the crop legume pea *P. sativum* (pea).

MATERIALS AND METHODS

Bacterial Strains and Inoculation

Inoculation of *M. truncatula* plants was performed with the *Sinorhizobium meliloti* strain 2011. Pea plants *P. sativum* L. were inoculated with *Rhizobium leguminosarum* biovar *viciae* wild type strain CIAM1026. Bacterial liquid culture was grown in B^- medium (Van Brussel et al., 1977), diluted up to the optical density at 600 nm (OD_{600}) 1.0 and applied to plants at the next day after planting.

Plant Material and Growth Conditions

Seeds of *Medicago truncatula* cv Jemalong A17 were sterilized in concentrated sulfuric acid for 10 min followed by washing with sterile water six times at room temperature. After that the seeds were incubated in bleach for 2 min with subsequent rinsing with excess of sterile distilled water three times. Seeds were germinated on 0.8% water agar in Petri dishes and incubated at 4°C in 24 h for imbibition. After that the dishes were placed in inverted position in the dark at 23°C for germination and incubated for overnight.

Pea seeds of cultivar Finale were sterilized in concentrated sulfuric acid for 5 min followed by washing at least 4 times with excess of sterile distilled water. Seeds were germinated on sterile 1% water agar in Petri dishes for 5 – 7 days in the dark at 23°C.

Constructs for RNAi Based Suppression of *G beta* Genes

Fragments of coding sequences of *MtGbeta1* or *PsGbeta1* genes (226 bp each, from 150 to 375 bp in both *MtGbeta1* and *PsGbeta1*) were amplified with specific primers flanked with *attB1* and *attB2r* sequences using Phusion Plus DNA Polymerase (Thermo Fisher Scientific, United States). Amplified fragments were separated by agarose gel electrophoresis and then purified from the gel using Cleanup standard kit (Evrogen, Russia) according to the user manual. Purified fragments were cloned into gateway pDONR221 vector using BP clonase (Thermo Fisher Scientific, United States). Chemically competent *E. coli* TOP10

cells were used for transformation, selection was performed on LB medium containing kanamycin 100 μg/ml. After checking by sequencing, the pDONR221 vectors with cloned fragments were used for recombination in pK7GWIWG2II destination vector (Ghent University, Belgium) using LR clonase (Thermo Fisher Scientific, United States). Transformants were grown on selective LB medium containing spectinomycin 75 μg/ml and chloramphenicol 25 μg/ml. Final constructs were checked by sequencing.

Protein Synthesis in *Escherichia coli* and Co-immunoprecipitation Assay

Full-length coding sequences of *MtGbeta1, PsGbeta1, MtGalpha1, MtGalpha2, PsGalpha1, PsGalpha2* as well as *MtPLC1, PsPLC1*, *MtPLD1, PsPLD1* genes were amplified with specific primers flanked with the sequences of restriction sites (**Supplementary Table 1**) using Phusion Plus DNA Polymerase (Thermo Fisher Scientific, United States). After purification from the gel, the full-length coding sequences were cloned in the frames into pRSETa-6xHIS or/and pRSETa-3xFLAG vectors using T4 ligase. Transformants were grown on selective LB medium containing ampicillin 100 μg/ml. Constructs were checked by sequencing. Electrocompetent *E. coli* C41 were transformed with constructs in pRSETa-6xHIS or pRSETa-3xFLAG vectors using Gene Pulser XCell electroporation system (Bio-Rad Laboratories, United States). Transformants were grown on selective solid LB medium containing ampicillin 100 μg/ml for overnight, then a few fresh colonies were transferred into a big flask containing 200 ml LB with ampicillin 100 μg/ml. Suspension was grown up to OD_{600} = 0.6 at 37°C in shaker and then synthesis was induced by addition 0.5 mM IPTG. After 2 h of cultivation at 28°C with intensive shaking, the cells were pelleted by centrifugation at 3000 g for 15 min in 50 ml Falcon tubes. Supernatant was removed thoroughly and cell pellets in tubes were stored at −80°C.

Frozen bacterial cells containing synthesized proteins were thawed and resuspended in lysis buffer (2 ml per pellet from 50 ml of culture) with protease inhibitor cocktail INHIB1-1KT (Merck, Germany) (0.1 mM AEBSF and 1 μg/ml of each leupeptin, aprotinin, antipain, pepstatin and chymostatin). Samples were aliquoted in two 1.5 ml tubes (1 ml) and sonicated 3 times for 30 s with 30 s pauses on ice. After sonication the lysates were centrifugated at 20000 g for 25 min. Soluble protein fractions were collected and used for co-immunoprecipitation. Co-immunoprecipitation was carried out using a μMACS kit (Miltenyi Biotec, Germany) containing MicroBeads with immobilized anti-HIS or anti-FLAG antibodies. Pairs of proteins with appropriate tags were placed in tubes with 50 μl of μMACS MicroBeads and incubates with slow shaking at 4°C for 1.5 h. Protein mixture and lysis buffer (used for column washing) were degassed by vacuum for 5 min on ice and then applied to μMACS columns according to the user manual. Washing was performed using lysis buffer in total volume of 1 ml. Elution performed according to the user manual. Eluted proteins were separated in 12% polyacrylamide gels and then transferred to nitrocellulose membrane for subsequent Western blot analysis.

Promoter Fusion Analysis

2700 bp fragment upstream of start codon of the *MtGbeta1* gene was amplified with specific primers containing *attB1* and *attB2r* sequences using two-step protocol (98°C 0:30, 60°C 2:30, 30 cycles) with Phusion Plus DNA Polymerase (Thermo Fisher Scientific, United States). After purification from the gel, the promoter was cloned into pDONR221 vector by BP clonase (Thermo Fisher Scientific, United States). Finally, the promoter was subcloned into pBGWFS7.0 destination vector using LR clonase (Thermo Fisher Scientific, United States). *E. coli* TOP10 cells were used for chemical transformation and selection was done on LB medium containing spectinomycin 50 μ g/ml.

Agrobacterium rhizogenes Mediated Plant Transformation

5 – 7 days-old pea seedlings of cv. Finale were transferred to light into sterile dark plastic boxes with liquid Jensen's medium (1 g/l $CaHPO_4$, 0.2 g/l K_2HPO_4, 0.2 g/l $MgSO_4$, 0.2 g/l NaCl, 7.34 mg/l Na-Fe-EDTA, 87.5 mg/l $CuSO_4 \times 5H_2O$, 1.16 mg/l $MnSO_4 \times 7H_2O$, 2.4 mg/l $ZnSO_4 \times 7H_2O$, 3.17 mg/l H_3BO_3, 1 mg/l $Na_2MoO_4 \times 2H_2O$), which were placed in a big plastic vessel (Sac O2, Belgium). Seedlings were cultivated in the growth chamber for 5 – 7 days (+ 21°C, humidity 60%, 16 h/8 h light/darkness) until the stage of two internodes. Seedlings were cut at the hypocotyl region and transformed with freshly grown *Agrobacterium rhizogenes* strain ARqua 1 carrying an appropriate construct. After transformation plants were placed on solid Jensen's medium (3 – 4 plants per box) in round plastic boxes with green filter (E1674, Duchefa, The Netherlands). Lower parts of plants were covered with wet cotton wool and aluminum foil and cultivated for 10 – 14 days until callus is appeared (Leppyanen et al., 2019). After that seedlings were transferred to Emergence medium (3 mM MES pH 5.8, 2.5 g/l KNO_3, 0.4 g/l, $MgSO_4 \times 7H_2O$, 0.3 g/l $NH_4H_2PO_4$, 0.2 g/l $CaCl_2 \times 2H_2O$, 10 mg/l $MnSO_4 \times 4H_2O$, 5 mg/l, H_3BO_3, 1 mg/l $ZnSO_4 \times 7H_2O$, 1 mg/l KI, 0.2 mg/l $CuSO_4 \times 5H_2O$, 0.1 mg/l, $NaMoO_4 \times 2H_2O$, 0.1 mg/l $CoCl_2 \times 6H_2O$, 15 mg/l $FeSO_4 \times 7H_2O$, 20 mg/l Na_2EDTA, 100 mg/l myoinositol, 5 mg/l nicotinic acid, 10 mg/l pyridoxine HCl, 10 mg/l thiamine HCl, 2 mg/l glycine, 1% sucrose, 1% Gelrite agar) containing 150 μg/ml cefotaxime and incubated for additional 3 – 4 days. Transgenic roots were selected by visualization of DsRED or GFP (green fluorescent protein) expression. Plants were transferred into pots with vermiculite saturated with Jensen's medium containing 1.5 mM NH_4NO_3.

1 days – old *M. truncatula* cv. Jemalong A17 seedlings were transferred on Fahreus agar plates [60 mg/l $MgSO_4 \times 7H_2O$, 50 mg/l KH_2PO_4, 78 mg/l Na_2HPO_4, 7.34 mg/l Na-Fe-EDTA, 83 mg/l $Ca(NO_3)_2$, 66 mg/l $CaCl_2$, 87.5 mg/l $CuSO_4 \times 5H_2O$, 1.16 mg/l $MnSO_4 \times 7H_2O$, 2.4 mg/l $ZnSO_4 \times 7H_2O$, 3.17 mg/l H_3BO_3, 1 mg/l $Na_2MoO_4 \times 2H_2O$], roots were covered with wet filter paper and incubated in the growth chamber (+ 21°C, humidity 60%, 16 h/8 h day/night) for 48 h. Plants were cut off at the hypocotyl region and transformed with *A. rhizogenes* Arqua1 strain carrying a necessary construct. Plants were incubated on Fahreus medium with roots positioned between two wet

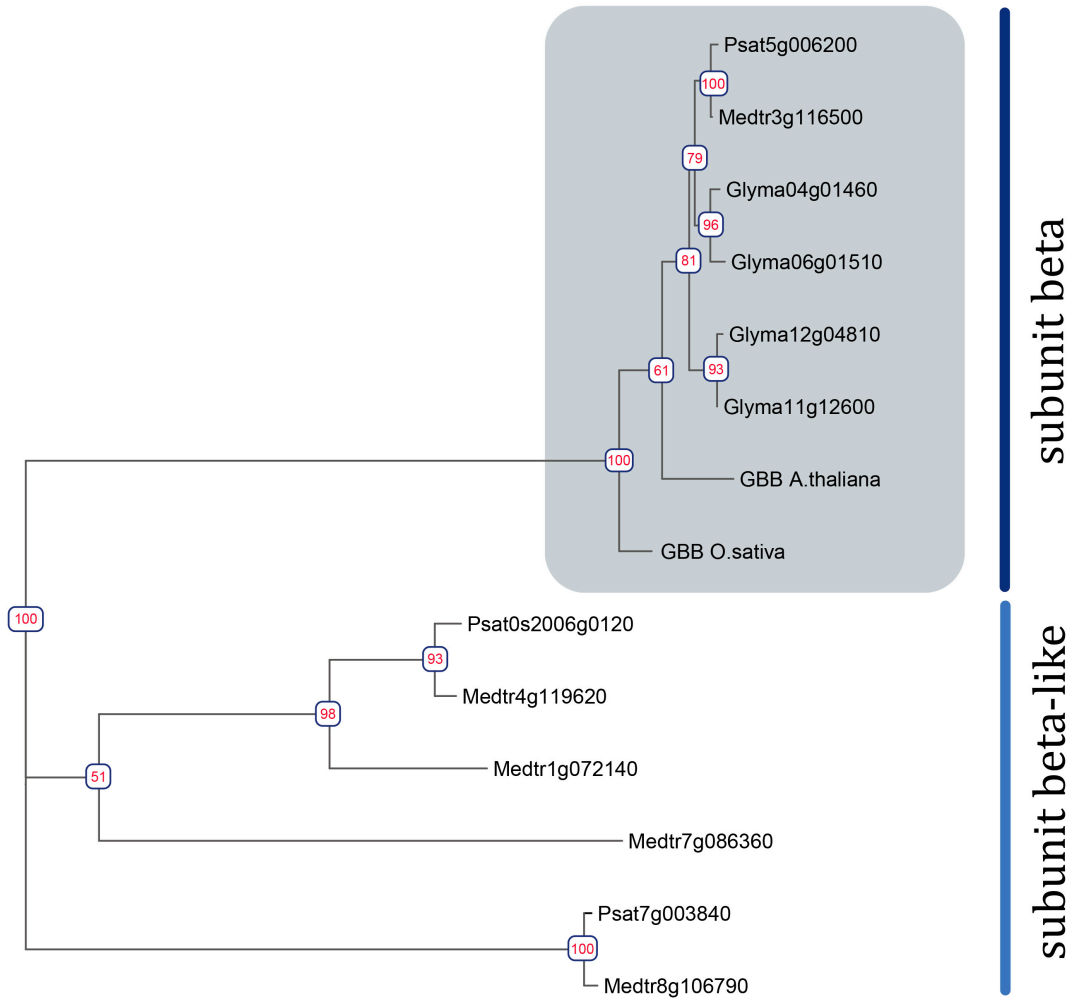

FIGURE 1 | Phylogenetic tree constructed using the Maximum-Likelihood method based on amino acid sequences of *G. max* and *A. thaliana Gbeta* genes and their homologous identified in *P. sativum* and *M. truncatula* genomes. Numeric values indicate branch support based on 1000 UltraFast bootstrap replicates.

filter papers for 7 days until calli are appeared. After that they were transferred to plates with Emergence medium containing 150 μg/ml cefotaxime and incubated for additional 7 days or more. Plants with transgenic roots were transferred to vermiculite saturated with Farheus medium.

The fragments of roots without nodules (about 100 mg) or nodules (10 – 15 nodules per probe) were harvested from the plants and used for subsequent gene expression analysis. In experiments on RNAi based suppression and promoter fusion analysis two or three biological replicates were analyzed with 15 – 20 plants in each group.

Quantitative Reverse Transcription–Polymerase Chain Reaction (qRT-PCR) Analysis

Total RNA was isolated from frozen roots. Material was ground with a mortar and pestle to a fine powder in liquid nitrogen and extracted with Trizol reagent (Bio-Rad Laboratories, United States). 1 μg of total RNA was used to synthesize cDNA with the RevertAid Reverse Transcriptase (Thermo Fisher Scientific, United States). cDNA samples were diluted to a total volume of 100 μl. Quantitative real-time PCR was performed using Bio-Rad iQ Sybr master mix (Bio-Rad Laboratories, United States) following the manufacturer's recommendations and run on a CFX-96 real-time PCR detection system with C1000 thermal cycler (Bio-Rad Laboratories, United States). The threshold cycle (Ct) values were calculated using the Bio-Rad CFX Manager 1.6 program and analyzed using the 2-ΔΔCt method. List of primers was presented in **Supplementary Table 1**.

Glucuronidase Staining of Material

Roots with nodules were thoroughly washed in tap water. Parts of roots with primordia or nodules were degassed under a vacuum (-0.8 bar; ME 1C vacuum pump, Vacuubrand) for 5 min in 100 mM sodium phosphate buffer (pH 7.0). For GUS staining the samples were incubated in 100 mM sodium phosphate buffer (pH 7.0), containing 1% Triton-X-100, 1 mM X-Gluc, 1 mM EDTA

(pH 8.0), 0.5 mM potassium ferricyanide, 0.5 mM potassium ferrocyanide for 4 – 24 h until staining development. For fixation plant material was placed in phosphate saline buffer (5 mM KH_2PO_4, 140 mM NaCl, 2.7 mM KCl, Na_2HPO_4 6.5 mM).

Phylogenetic Reconstruction

For identification of homologous of previously detected *Galpha*, *Gbeta* and *Ggamma A. thaliana* and *G. max* genes in *P. sativum* and *M. truncatula* genomes BLASTP analysis (v 2.6.0, word_size = 3, evalue < 10e-20) was performed. Sequences selected during such analysis were investigated for the presence of specific G-protein conserved domains (Urano et al., 2013) using InterProScan web server (Jones et al., 2014).

First of all, for phylogenetic reconstruction amino acid sequences of selected genes were aligned using MAFFT tool v7.453 (Katoh and Standley, 2013). Based on these alignments, a phylogenetic tree was constructed using the Maximum-Likelihood method with help of the IQ-TREE web server (Trifinopoulos et al., 2016). The bootstrap values were obtained from 1000 bootstrap replicates of Ultrafast Bootstrap (Minh et al., 2013). For visualization of resulted trees R package ggtree was used (Yu, 2020).

Assessment of *Galpha, Gbeta* and *Ggamma* Gene Expression in *Medicago truncatula*

Raw reads from RNA-Seq project PRJNA552042 (Schiessl et al., 2019) including data for 24, 48, 72, 96,120, and 168 h after inoculation or mock treatment for WT plants were used for analysis. The *M. truncatula* genome version 4.0 was used as a reference. The reads were mapped to the genome using HISAT2 (Kim et al., 2019) tool v 2.1.0 with default parameters, and raw counts were obtained by FeatureCounts from Subreasd package (Liao et al., 2014). The edgeR package was used to calculate CPM values. Expression data for nodules was obtained from Pecrix et al. (2018). For data visualization ggplot2 (Wickham, 2016) package was used and Adobe Illustrator was implemented for final figures assemblies.

Statistical Methods and Computer Software

One-way ANOVA and Tukey's test were used to compare gene expression levels.

RESULTS

Medicago truncatula and *Pisum sativum* Genomes Encode a Set of G-Protein Alpha, Beta, and Gamma Subunits

A genome-based search for genes encoding G-protein subunits in the model legume *M. truncatula* and the crop legume *P. sativum* was performed. Briefly, amino acid sequences of *Arabidopsis thaliana* and *Glycine max* orthologs were used for BLASTP analysis (Camacho et al., 2009), after which, specific domains were identified using InterProScan (Jones et al., 2014).

The search revealed two *Galpha*, three *extra-large Galpha (XLG),* one *Gbeta*, and five *Ggamma* genes in the *M. truncatula* genome (sequence v4) (Tang et al., 2014), and two *Galpha*, three *XLGs*, one *Gbeta*, and six *G gamma* genes in the *P. sativum* genome (sequence v1) (**Figure 1** and **Supplementary Figures 1**, **2**) (Pecrix et al., 2018). Structurally, canonical G beta subunits contain an N-terminal Coil domain and at least seven WD40 domains, which form a beta-propeller structure (Urano et al., 2013). Only one gene encoding a G beta subunit with the latter structure was found in the genomes of *M. truncatula* and *P. sativum* genomes. However, at least four *MtGbeta*-like and two *PsGbeta*-like genes exist in the genomes of these legumes and may be of interest for future research. These proteins lack an N-terminal coil domain as well as family specific domains; however, they do contain at least seven WD40 domains.

To assess the homology between the identified G beta subunits and those of well-studied model plants (*A. thaliana*, *Oryza sativa, G. max*), a phylogenetic tree was constructed (**Figure 1**). Phylogenetic trees were also constructed for *G alpha, G gamma*, and *XLG* genes (**Supplementary Figures 1**, **2**).

To evaluate the expression levels of *G alpha*, *G beta*, and *G gamma* in *M. truncatula* roots after inoculation, a publicly available RNAseq dataset was analyzed (GSE133612) (Schiessl et al., 2019). This particular dataset encompasses expression data across early stages of symbiosis development. In addition, an RNAseq dataset for nodules was also analyzed (Roux et al., 2014; Pecrix et al., 2018). *In silico* analyses revealed that *MtGbeta1* (Medtr3g116500) expression was relatively high in inoculated roots and nodules and non-inoculated roots. Moreover, a significant upregulation in the expression of *MtGalpha1* (Medtr1g015750) was detected in inoculated roots at the early stages of symbiosis development and in nodules, when compared to control roots (**Supplementary Figure 3**). However, *MtGalpha2* (Medtr3g105240) was not expressed in roots or nodules (**Supplementary Figure 3**).

The Heterotrimeric G-Protein Beta 1 Subunit Positively Regulates Nodulation in *Medicago truncatula* and *Pisum sativum*

Since the complex of G beta/gamma subunits may play an important role in signal transduction following signal perception, the remainder of the study focused on the *G beta* genes. Since only one typical G beta 1 subunit was found in both *M. truncatula* (*MtGbeta1*) and *P. sativum* (*PsGbeta1*), the role thereof was evaluated on symbiosis. To silence the *Gbeta1* genes in *M. truncatula* and *P. sativum*, an RNAi approach was employed. Composite plants were obtained with approximately 50% suppression of the *Gbeta1* gene in the transgenic roots and nodules of both legumes (**Figure 2**). As controls, plants expressing beta-galactosidase under the p35S promoter (GUS-OE) were used. Comparative analyses showed a statistically significant decrease in nodule number in the transgenic fluorescent roots in RNAi lines of both legumes, while other parameters such as number of lateral roots did not change (**Figures 2A-E** and **Supplementary Figure 4**). It correlated with

decreasing the expression of early symbiotic markers such as *MtEnod11* and *MtRR4* in the transgenic hairy roots of *Gbeta1* - RNAi plants (**Figure 2C**). The results suggested that *MtGbeta1* in *M. truncatula* (**Figures 2A,B** and **Supplementary Figure 4**) and *PsGbeta1* in *P. sativum* (**Figures 2D,E**) were required for symbiosis development in legumes with indeterminate type of nodules.

The *MtGbeta1* Promoter Is Active at the Various Stages of Symbiosis Development

Next, the promoter activity of the *MtGbeta1* gene was analyzed in the roots of composite plants expressing *pMtGbeta:GUS* at different stages following *Sinorhizobium meliloti* 2011. At the early stages of symbiosis development, GUS staining was detected in the root hairs; however, the intensity of the signal was comparable to that of non-inoculated plants (**Figures 3A,B**). In the developing primordia of nodules and in young nodules appearing above the surface of roots, strong GUS staining was observed (**Figures 3C,D**). Staining was also observed in the primordia of lateral roots (data not shown). In mature nodules [2 weeks after inoculation (wai)] (**Figures 3E–G**), GUS staining was most intense in the meristem and invasion zone (II), while the signal was significantly weaker in interzone II-III, and in the apical part of the nitrogen-fixing zone (III) (**Figures 3E,F**). Although a signal was observed in the central part of nodules, it had a variable pattern, having a less or more pronounced intensity in the nitrogen-fixing zone (III) depending on the length of staining time and the level of transgene expression (**Figure 3G**). Finally, *pMtGbeta:GUS* expression was also observed in the vascular bundles.

G Beta 1 and G Alpha Subunits Interact in Both *Medicago truncatula* and *Pisum sativum*

Although the G beta subunits of the complex are predominantly connected to signal transduction in the cell, the activation of the complex is achieved by G alpha subunits due to their association with GDP or GTP and their release from the complex. A BLASTP search revealed two G alpha subunits in *M. truncatula*, MtG alpha 1 (Medtr1g015750) and MtG alpha 2 (Medtr3g105240), which showed a high level of homology to two PsG alpha subunits, PsG alpha 1 (AF537218) and PsG alpha 2 (AF533438) previously identified in *P. sativum* (Misra et al., 2007). However, expression analysis showed that *MtGalpha2* was not expressed in roots and nodules (**Supplementary Figure 3**), and therefore, MtG alpha 2 was omitted from co-immunoprecipitation experiments.

To verify the interactions between the G beta 1 and G alpha subunits, *in vitro* co-immunoprecipitations were performed. A heterologous protein expression was carried out in *Escherichia coli* C41, allowing high levels of expression of all subunits of interest (MtG beta1, PsG beta 1, MtG alpha 1, PsG alpha 1, and PsG alpha 2) fused to either a 6xHIS or a 3xFLAG tag (**Figures 4**, **5**). Subunits were co-incubated and complexes purified using a μMACS column with antibodies. When MtG beta 1 and MtG alpha1 were co-incubated, both proteins were identified in the eluate. Moreover, PsG beta 1 co-eluted with both PsG alpha 1 and PsG alpha 2, as revealed by western blot analysis (**Figure 5**). However, the interaction was much stronger between PsG beta 1 and PsG alpha 2. Therefore, both pea PsG alpha 1 and PsG alpha 2 subunits may co-precipitate with PsG beta 1 protein and can be potential participants in heterotrimeric G-protein complex, while in *M. truncatula* the formation of one complex between MtG beta 1 and MtG alpha1 was shown.

Phospholipase C Interacts With G Alpha and G Beta Subunits in Both *Medicago truncatula* and *Pisum sativum*

The involvement of PLC and PLD in the regulation of nodulation was previously described using a pharmacological approach (Charron et al., 2004). In the same study, PLC and PLD were suggested to be connected with heterotrimeric G-protein activation. The genome of *M. truncatula* encodes nine *PLC* and fifteen *PLD* genes (**Supplementary Table 2**), but we searched for significantly activated genes at the early stages of symbiosis.

Analysis of transcriptomic datasets for *M. truncatula* roots inoculated with rhizobia, or treated with Nod factors (van Zeijl et al., 2015; Damiani et al., 2016; Schiessl et al., 2019), revealed that the expression of *MtPLC1* (Medtr3g070560, MtrunA17_Chr3g0113471) (Damiani et al., 2016; Schiessl et al., 2019) and *MtPLD1* (Medtr4g010650, MtrunA17_Chr4g0003411) increased at the early stages of symbiosis development (**Supplementary Figures 5**, **6** and **Supplementary Table 2**). Genes in *P. sativum* were selected based on homology to the orthologs of *M. truncatula* and included one *PsPLC1* (Psat5g128400) gene and one *PsPLD1* (Psat7g255400) gene (**Supplementary Table 2**).

The respective coding sequences of *MtPLC, MtPLD* and *PsPLC, PsPLD* were cloned into pRSETa-6xHIS and pRSETa-3xFLAG, and proteins were expressed as before for co-immunoprecipitation assays. The assays revealed interactions between MtG beta 1 and MtPLC, and MtG alpha 1 and MtPLC (**Figures 4**, **5**). Moreover, PsG beta 1 was able to interact with PsPLC, while only PsG alpha 2 could interact with PsPLC (**Figures 4**, **5**). No interactions were detected between any of the G-protein subunits and MtPLD. It seems like either MtPLD do not interact with components of G-protein complex or more complicated regulation through additional regulators may be take place. At the same time, we could not exclude an incorrect folding of such big proteins (91.5 kDa) as MtPLD in heterologous system. Finally, PsPLD expression in the bacterial system failed; hence, its interaction with G-protein subunits could not be examined.

Kinase Domain of LysM-Containing Receptor-Like Kinase K1 May Interact With G alpha Subunit *in vitro*

G-protein activation is mainly maintained by single-pass transmembrane RLKs. In *P. sativum*, at least two RLK complexes may be involved in the perception of Nod factors, which are activated at different stages of symbiosis development, PsSYM10/PsK1 and PsSYM10/PsSYM37 (Zhukov et al., 2008; Kirienko et al., 2018). In the complex PsSYM10/PsK1, the RLK

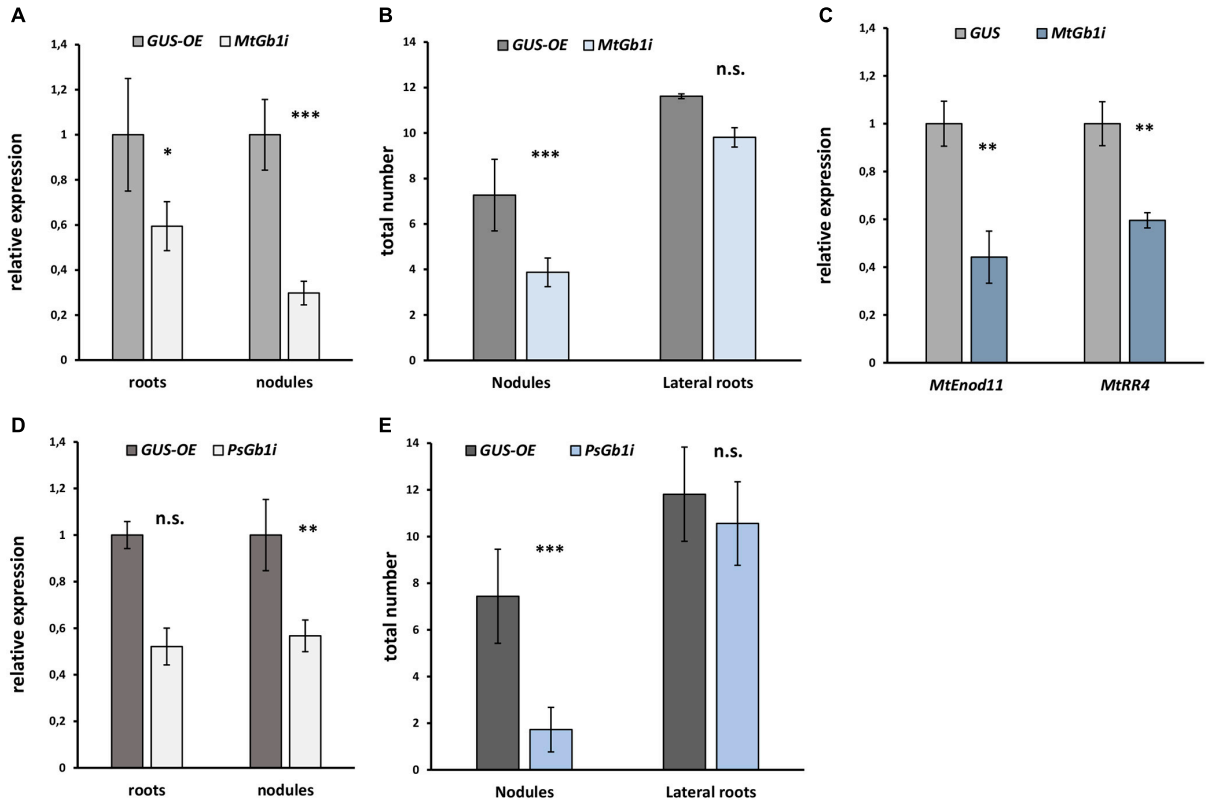

FIGURE 2 | The effect of *Gbeta1* gene suppression on root development and nodulation in *M. truncatula* A17 **(A,B)** and *P. sativum* cv. Finale **(D,E)** plants. Composite plants with the *Gbeta1* gene suppression in transgenic roots (*Gbeta*-RNAi) were compared with control plants with β-glucuronidase gene overexpression (*GUS*-OE). Analysis was performed two weeks after inoculation (2 wai) (*M. truncatula*) and 3 weeks after inoculation (3 wai) (*P. sativum*). Approximately 50% suppression of the *Gbeta1* gene in the transgenic roots and nodules of both legumes was revealed **(A,D)**. The number of nodules in transgenic fluorescent roots of *Gbeta*-RNAi plants was significantly reduced **(B,E)**, whereas the total number of transgenic fluorescent lateral roots did not change in both cases. Expression of early symbiotic markers, the *MtEnod11* and *MtRR4,* in the transgenic hairy roots of *MtGbeta1*-RNAi plants **(C)**. Two biological replicates were analyzed for *M. truncatula* and *P. sativum*, each contained 15 – 20 plants per variant. In case of *M. truncatula* totally 47 and 26 transgenic fluorescent roots of *MtGbeta*-RNAi and *GUS*-OE plants, correspondently, were included in the analysis, while 29 and 16 transgenic fluorescent roots of *PsGbeta*-RNAi and *GUS*-OE plants were used in *P. sativum*. The number of nodules were scored only in transgenic fluorescent roots. Values are means ± SEM. *, Significant difference at $P \leq 0.05$; **, Significant difference at $P \leq 0.01$; ***, Significant difference at $P \leq 0.01$; ns, non-significant difference.

PsK1 possesses an active kinase domain and seems to be required for signal transduction during early stages of pea-rhizobial symbiosis development (Zhukov et al., 2008; Kirienko et al., 2018). Here it was demonstrated using a co-immunoprecipitation assay that the kinase domain of PsK1 RLK interacts with PsG alpha 2, but not PsG alpha 1 (**Figure 6**). It may suggest the involvement of G-protein in the control of early stages of symbiosis development.

DISCUSSION

The main goal of this study was to analyze the role of the heterotrimeric G-protein beta subunits as the most important subunits for signal transduction in the cell during symbiosis development in *M. truncatula* and *P. sativum*. A genome-based search for genes encoding G-protein subunits revealed that the *M. truncatula* and *P. sativum* genomes encode one gene each for the canonical G beta subunit, MtG beta 1 and PsG beta 1, respectively. These subunits contain seven WD40 motifs and a coiled-coil motif at their N-terminal ends. These findings are in line with previous data for *P. sativum* (Misra et al., 2007). Moreover, additional *Gbeta*-like genes were found in the genomes of *M. truncatula* and *P. sativum*.

RNAi-based suppression of the *MtGbeta1* and *PsGbeta1* resulted in a significant decrease in the number of nodules formed. This suggests that these G beta 1 subunits of heterotrimeric G-proteins have a positive effect on the development of symbiosis in both legume plants, which belong to the same group. Moreover, the results of our experiments based on RNA interference were in line with those obtained in *G. max* for *GmGbeta1-4* genes, all having a high level of homology with *MtGbeta1/PsGbeta1* (Choudhury and Pandey, 2013). These results indicate that *MtGbeta1* and *PsGbeta1* are required for symbiosis development in legumes with indeterminate types of nodules. Further research, however, is necessary regarding their influence at specific stages of this symbiosis development.

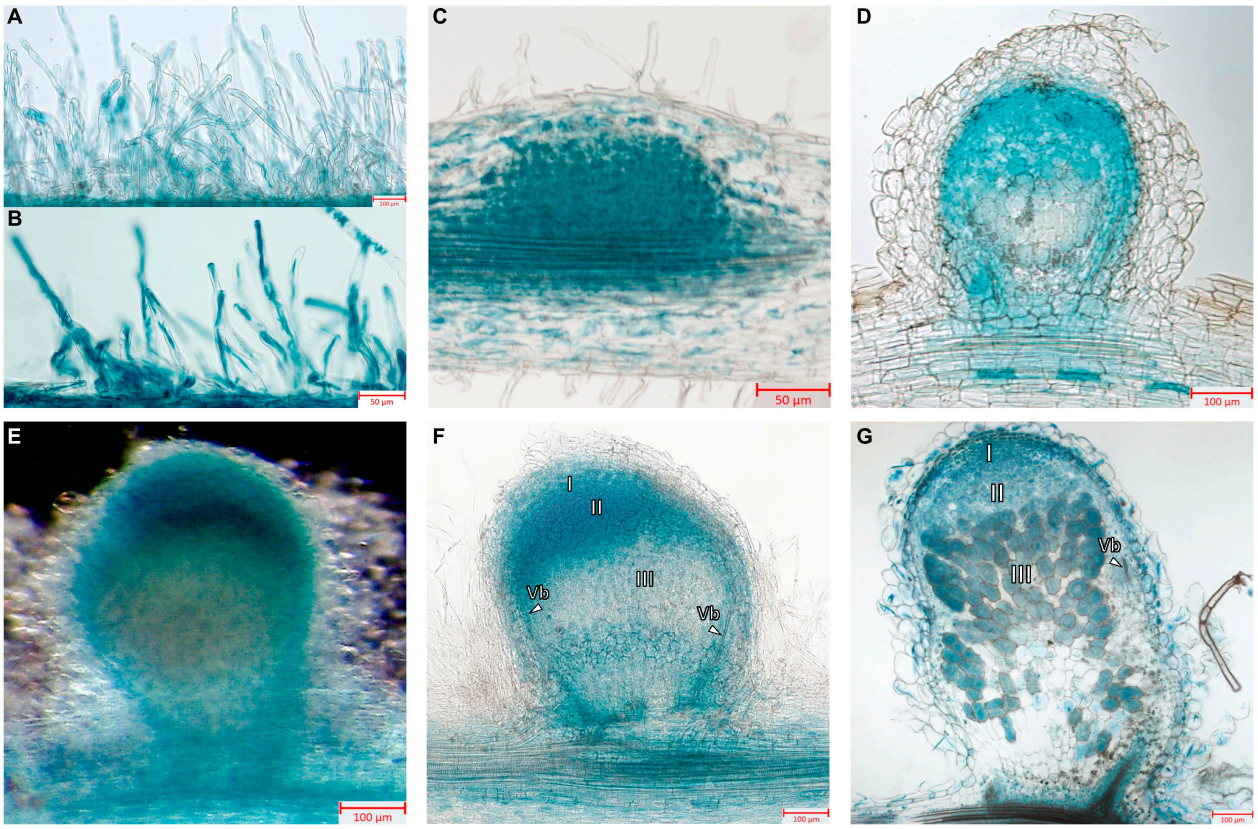

FIGURE 3 | Localization of *MtGbeta1* expression in *M. truncatula* non-inoculated and inoculated roots, nodule primordia and 2-week-old nodules carrying a *pMtGbeta1:GUS* genetic construct. **(A)** Non-inoculated roots. **(B)** Inoculated roots. **(C)** Nodule primordia (50 µm section). **(D)** Young nodule (50 µm section). **(E)** A general view of the nodule. Image was done using dark field like illumination **(E–G)** Two-week-old nodules (50 µm section). I, meristem zone; II, infection zone; III, nitrogen fixation zone; arrows indicate vascular bundles (Vb). Scale bars are 50 µm **(B,C)** and 100 µm **(A,D–G)**.

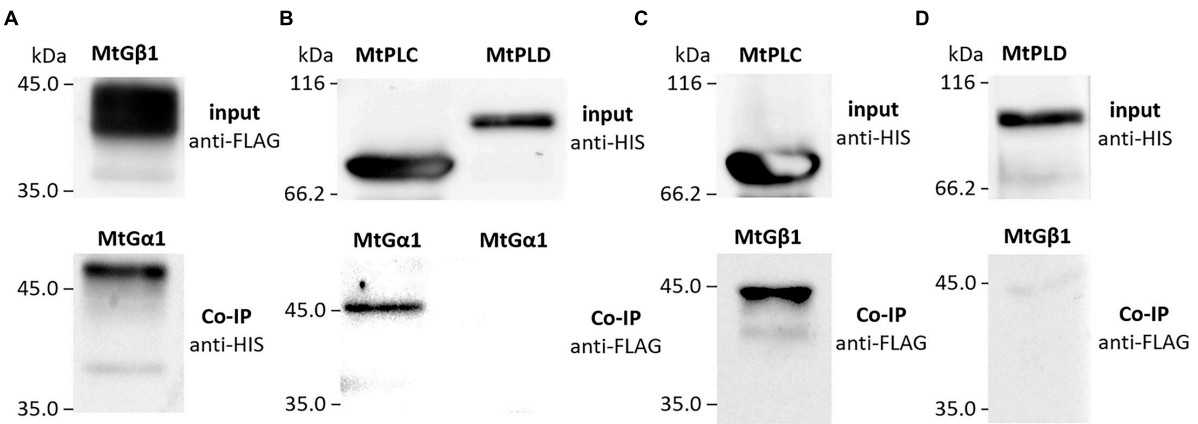

FIGURE 4 | The result of co-immunoprecipitation of heterotrimeric G-protein subunits and phospholipases C (MtPLC) and D (MtPLD) from *M. truncatula*. A heterologous protein expression was carried out in *Escherichia coli* C41, allowing high levels of expression of all subunits of interest (MtG beta1, MtG alpha 1, MtPLC, MtPLD) fused to either a 6xHIS or a 3xFLAG tag. The assays revealed interactions between MtG beta 1 and MtG alpha 1 **(A)** as well as MtG alpha 1 and MtPLC **(B)**, MtG beta 1 and MtPLC **(C)**. No interactions were detected between any of the G-protein subunits and MtPLD **(B,D)**.

Composite plants expressing *GUS* under the *MtGbeta1* promoter allowed insight into the activity of the *MtGbeta1* promoter. During the early stages of symbiosis development, intensive GUS staining was observed in the developing nodule primordia and young nodules. Staining was also observed in the primordia of lateral roots. *Gbeta1* promoter activity

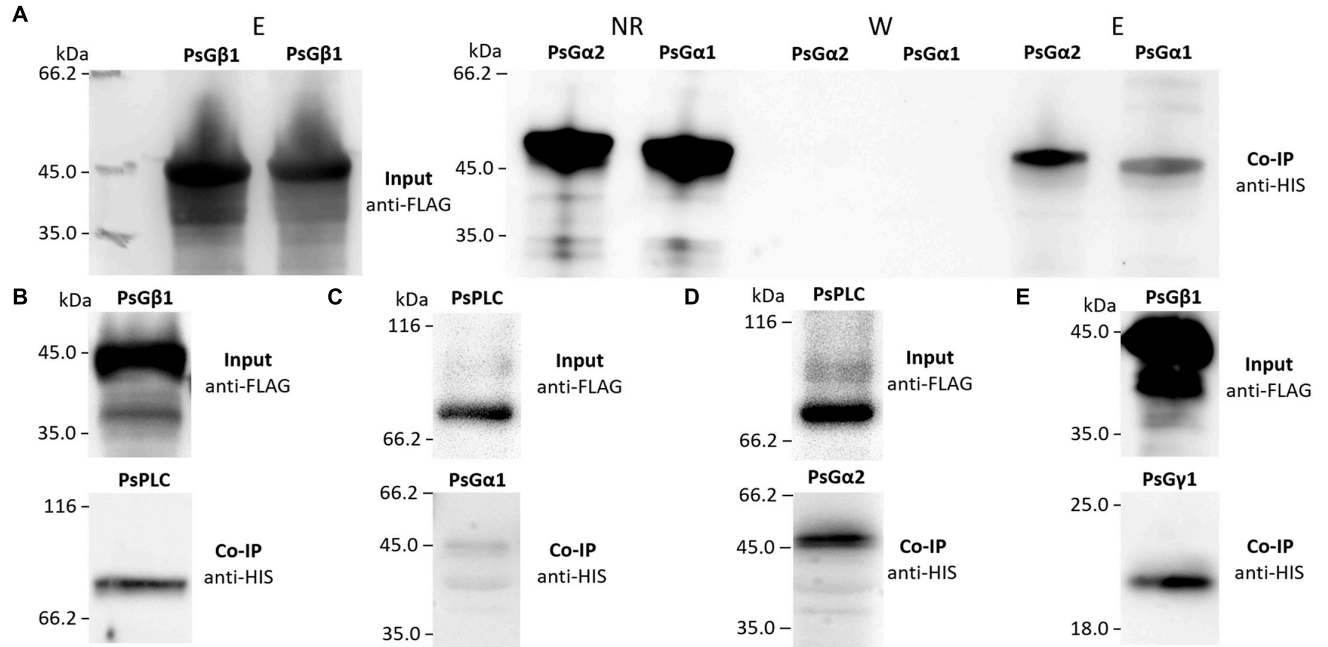

FIGURE 5 | The result of co-immunoprecipitation of heterotrimeric G-protein subunits and phospholipases C (PsPLC) and D (PsPLD) from *P. sativum*. A heterologous protein expression was carried out in *E. coli* C41. Co-immunoprecipitation of PsG beta 1 with PsG alpha 1 and PsG alpha 2 **(A)** as well as PsG beta 1 with PsPLC **(B)**. PsPLC interacts with PsG alpha 2, but does not interact with PsG alpha 1 **(C,D)**. The interaction was detected between PsG beta 1 and PsG gamma 1 **(E)**. Eluted proteins were separated in 12% polyacrylamide gels and then transferred to nitrocellulose membrane for subsequent Western blot analysis. E – elution, NR – non-retained fraction, W – washing.

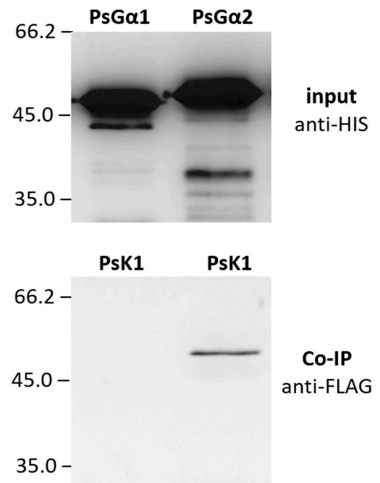

FIGURE 6 | The result of co-immunoprecipitation between LysM-RLK PsK1 kinase domain and PsG alpha 1 and PsG alpha 2 subunits. LysM-RLK PsK1 interacts with PsG alpha 2, but does not interact with PsG alpha 1.

fits well with the data on the participation of G-proteins in the control of organ development and cell proliferation. As shown previously in *Arabidopsis,* G-proteins may influence cell cycle regulation through modulation of auxin transport (Lease et al., 2001; Chen et al., 2006; Mudgil et al., 2009). In mature nodules, the localization of GUS staining was the most intense in the meristem and invasion zone (II), while the signal was less prominent in interzones II-III and in the apical part of the nitrogen-fixing zone (III). These results suggest that MtG beta 1 may be involved in the maintenance of meristem development and regulation of the infection process. The exact mechanisms behind this still needs further research. The localization in vascular bundles may be related to regulation of the nutrients translocating via the vasculature.

To elucidate the composition of the heterotrimeric G-protein complex in *M. truncatula* and *P. sativum*, the corresponding G-proteins were expressed in *E. coli*, and their interactions analyzed using *in vitro* co-immunoprecipitations. The interaction between MtG beta 1 and MtG alpha 1, as well as MtG beta 1 and MtG gamma 1, was shown in our experiments. These results suggest the existence of a heterotrimeric G-protein complex comprising the MtG alpha 1/MtG beta 1 subunits in *M. truncatula*. Concurrently, two putative complexes consisting of PsG beta 1 and PsG alpha 1, and PsG beta 1 and PsG alpha 2 may exist in *P. sativum*. Hence, both *P. sativum* PsG alpha 1 and PsG alpha 2 subunits interact with PsG beta 1, serving as potential participants in the heterotrimeric G-protein complex, while in *M. truncatula*, the formation of a single complex between MtG beta 1 and MtG alpha1 takes place.

Signal transduction pathway activation depends on Nod factor perception by a few receptor complexes in *M. truncatula* and *P. sativum* (Ardourel et al., 1994; Geurts et al., 2005;

Kirienko et al., 2018). Since G beta subunits usually do not bind to receptors themselves, the interaction between receptors to Nod factors and G alpha subunits were analyzed. In *P. sativum*, the interaction between LysM-RLK K1 – the Nod factor receptor, which controls the earliest reactions after signal perception (Kirienko et al., 2018) – and the PsG alpha 2 subunit was demonstrated. In accordance with these results, it was previously shown that the LysM-RLKs in soybean, GmNFR1a and GmNFRb, were able to interact with GmG alpha subunits. This suggests that heterotrimeric G-proteins may play an important role in plant response to Nod factor perception in legume plants during the early stages of symbiosis development.

Subsequent signal transduction in legume-rhizobial symbiosis may be connected to the activation of PLC and PLD by heterotrimeric G-protein subunits, as shown by previous studies using inhibitors (Pingret, 1998; den Hartog et al., 2003). Analysis of *M. truncatula* transcriptomic datasets of roots inoculated with rhizobia or treated with Nod factors (van Zeijl et al., 2015; Damiani et al., 2016; Schiessl et al., 2019) allowed the identification of *PLC* and *PLD* genes induced at the early stages of symbiosis. *In vitro* co-immunoprecipitation assays showed that MtG beta 1 and MtG alpha 1 interacted with MtPLC. Similarly, PsG beta 1 interacted with homologous PsPLC, while among the two alpha subunits, only PsG alpha 2 formed a complex with PsPLC and not PsG alpha 1. These results demonstrate possible cross-talk between G-protein- and PLC-mediated signaling pathways in legumes with indeterminate nodule types. It is also important to note that during heat and salinity stress in *P. sativum*, G-protein subunits interact with other forms of PsPLC (Y15253) (Misra et al., 2007), suggesting the specificity of signal transduction pathways in the activation in different processes.

Although the involvement of PLD in the regulation of root hair deformations was shown in *M. truncatula,* no interactions between PLD and G subunits were detected in both legumes. However, it could not be excluded that the interaction may be indirect through the stimulation of PLD by intracellular signals such as calcium.

In legume plants, two types of calcium reactions take place in response to the perception of Nod factors. These include calcium influx into the cells and calcium spiking in the nucleus and perinuclear space at the early stages of symbiosis (Shaw and Long, 2003). It was previously shown that different signaling pathways may be involved in the activation of calcium influx and calcium spiking. Perception of Nod factors activates the signaling pathway, including a receptor kinase with leucine reach repeats in its extracellular domain, DOES NOT MAKE INFECTIONS 2 (DMI2), and the putative cation channel DOES NOT MAKE INFECTIONS 1 (DMI1), which are important for the activation of calcium spiking in the perinuclear zone and nucleus. In contrast, calcium influx and subsequent deformations of root hairs are not dependent on DMI2 and DMI1 (Esseling et al., 2004). Similarly, in the *symrk* (orthologous to DMI2), *castor, pollux* (orthologous to DMI1) (Ané et al., 2004; Imaizumi-Anraku et al., 2005) *Lotus japonicus* mutants with disturbed calcium spiking, nevertheless, the calcium influx and deformation of root hairs were observed (Miwa et al., 2006). Finally, both pathways result in the phosphorylation of calcium and calmodulin-dependent kinase, DOES NOT MAKE INFECTIONS 3 (DMI3), which stimulates a complex of transcription factors required for infection thread development and nodule organogenesis.

Activation of differing signaling pathways may be related to the involvement of two receptor complexes in legume plants that regulate calcium influx and calcium spiking (Geurts et al., 2005). It is interesting to note that the responses induced by the G-protein complex agonist mastoparan also occurred in *dmi2* and *dmi1 M. truncatula* mutants, but these responses were not observed in the *dmi3* mutant (den Hartog et al., 2003). The lack of dependence on DMI2 and DMI1 suggests that the heterotrimeric G-protein complex may be involved in the activation of calcium influx, followed by root hair deformation. This hypothesis will need to be tested in future studies and requires more precise analysis of G-protein subunits interaction with kinase domains of receptors to Nod factors. In our experiments the interaction between PsG alpha and kinase domain of LysM-RLK K1 was shown. Since LysM-RLK K1 controls the earliest reactions like deformations after signal perception in pea plants, further analysis of *k1* mutants should be performed to obtain evidences of G-protein involvement in signal transduction.

DATA AVAILABILITY STATEMENT

The datasets presented in this study can be found in online repositories. The names of the repository/repositories and accession number(s) can be found in the article/ **Supplementary Material**.

AUTHOR CONTRIBUTIONS

AB: investigation, writing original draft preparation, and methodology. OP: investigation, heterologous protein synthesis, and co-immunoprecipitation. AD: genome-based searching and analysis and graphic output of phylogenetic tree. IL: methodology, cloning, and plant transformation. ED: conceptualization, writing and editing, and supervision. All authors have read and agreed to the manuscript.

FUNDING

This article was made with support of the Russian Science Foundation RSF 21-16-00106.

SUPPLEMENTARY MATERIAL

The Supplementary Material for this article can be found online at: https://www.frontiersin.org/articles/10.3389/fpls.2021.808573/full#supplementary-material

Supplementary Figure 1 | Phylogenetic tree constructed using the Maximum-Likelihood method based on amino acid sequences of *G. max G alpha* and *A. thaliana G alpha* and *XLG* genes and their homologous identified in *P. sativum* and *M. truncatula* genomes. Previously identified and exposed in NCBI *PsGalpha1* (AF537218) and *PsGalpha2* (AF533438) were also included in this tree. Numeric values indicate branch support based on 1000 UltraFast bootstrap replicates.

Supplementary Figure 2 | Phylogenetic tree constructed using the Maximum-Likelihood method based on amino acid sequences of *G. max* and *A. thaliana Ggamma* genes and their homologous identified in *P. sativum* and *M. truncatula* genome. Numeric values indicate branch support based on 1000 UltraFast bootstrap replicates.

Supplementary Figure 3 | (A) Heatmap shows log-tranformed CPM values of *Gbeta*, *Galpha*, *XLG* and *Ggamma* genes expression in *M. truncatula* during early stages of symbiosis development based on Gene expression data from GSE133612 project (Schiessl et al., 2019). **(B)** Bar plots represent CPM values of *Gbeta, Galpha, XLG* and *Ggamma* gene expression in *M. truncatula* nodules and non-inoculated roots (Roux et al., 2014).

Supplementary Figure 4 | Composite plants of *M. truncatula* A17 **(A,B)** and *P. sativum* cv. Finale **(C,D)** plants with the *Gbeta1* gene suppression in transgenic roots (*Gbeta*-RNAi) **(B,D)** and control plants with β-glucuronidase gene overexpression (*GUS*-OE) **(A,C)**. The number of nodules were scored only in transgenic fluorescent roots.

Supplementary Figure 5 | Bar plots represent CPM values of *MtPLC* genes expression in *M. truncatula* during early stages of symbiosis development based on Gene expression data from GSE133612 project (Schiessl et al., 2019).

Supplementary Figure 6 | Bar plots represent CPM values of *MtPLD* genes expression in *M. truncatula* during early stages of symbiosis development based on Gene expression data from GSE133612 project (Schiessl et al., 2019).

Supplementary Table 1 | List of primers used in this study.

Supplementary Table 2 | The genome of M. truncatula encodes nine PLC and fifteen PLD genes. Analysis of transcriptomic datasets for M. truncatula roots inoculated with rhizobia, or treated with Nod factors factors (van Zeijl et al., 2015; Damiani et al., 2016; Schiessl et al., 2019), revealed that the expression of MtPLC1 (Medtr3g070560) (Damiani et al., 2016; Schiessl et al., 2019) and MtPLD1 (Medtr4g010650) increased at the early stages of symbiosis development (**Supplementary Figures 4**, **5**). Genes in P. sativum were selected based on homology to the orthologs of M. truncatula and included one PsPLC1 (Psat5g128400) gene and one PsPLD1 (Psat7g255400) gene.

REFERENCES

Ané, J.-M., Kiss, G. B., Riely, B. K., Penmetsa, R. V., Oldroyd, G. E. D., Ayax, C., et al. (2004). Medicago truncatula DMI1 required for bacterial and fungal symbioses in legumes. *Science* 303, 1364–1367. doi: 10.1126/science.1092986

Ardourel, M., Demont, N., Debellé, F., Maillet, F., de Billy, F., Promé, J. C., et al. (1994). Rhizobium meliloti lipooligosaccharide nodulation factors: different structural requirements for bacterial entry into target root hair cells and induction of plant symbiotic developmental responses. *Plant Cell* 6, 1357–1374. doi: 10.1105/tpc.6.10.1357

Bisht, N. C., Jez, J. M., and Pandey, S. (2011). An elaborate heterotrimeric G-protein family from soybean expands the diversity of plant G-protein networks. *New Phytol.* 190, 35–48. doi: 10.1111/j.1469-8137.2010.03581.x

Bommert, P., Je, B., Goldshmidt, A., and Jackson, D. (2013). The maize Gα gene COMPACT PLANT2 functions in CLAVATA signalling to control shoot meristem size. *Nature* 502, 555–558. doi: 10.1038/nature12583

Camacho, C., Coulouris, G., Avagyan, V., Ma, N., Papadopoulos, J., Bealer, K., et al. (2009). BLAST+: architecture and applications. *BMC Bioinform.* 10:421. doi: 10.1186/1471-2105-10-421

Charron, D., Pingret, J.-L., Chabaud, M., Journet, E.-P., and Barker, D. G. (2004). Pharmacological Evidence That Multiple Phospholipid Signaling Pathways Link Rhizobium Nodulation Factor Perception in Medicago truncatula Root Hairs to Intracellular Responses, Including Ca2+ Spiking and Specific ENOD Gene Expression. *Plant Physiol.* 136, 3582–3593. doi: 10.1104/pp.104.051110

Chen, J.-G., Gao, Y., and Jones, A. M. (2006). Differential roles of Arabidopsis heterotrimeric G-protein subunits in modulating cell division in roots. *Plant Physiol.* 141, 887–897. doi: 10.1104/pp.106.079202

Choudhury, S. R., Bisht, N. C., Thompson, R., Todorov, O., and Pandey, S. (2011). Conventional and novel gγ protein families constitute the heterotrimeric g-protein signaling network in soybean. *PLoS One* 6:23361. doi: 10.1371/journal.pone.0023361

Choudhury, S. R., and Pandey, S. (2013). Specific Subunits of Heterotrimeric G Proteins Play Important Roles during Nodulation in Soybean. *Plant Physiol.* 162, 522–533. doi: 10.1104/pp.113.215400

Choudhury, S. R., and Pandey, S. (2015). Phosphorylation-Dependent Regulation of G-Protein Cycle during Nodule Formation in Soybean. *Plant Cell* 27, 3260–3276. doi: 10.1105/tpc.15.00517

Damiani, I., Drain, A., Guichard, M., Balzergue, S., Boscari, A., Boyer, J.-C., et al. (2016). Nod Factor Effects on Root Hair-Specific Transcriptome of Medicago truncatula: Focus on Plasma Membrane Transport Systems and Reactive Oxygen Species Networks. *Front. Plant Sci.* 7:1–22. doi: 10.3389/fpls.2016.00794

De Los Santos-Briones, C., Cárdenas, L., Estrada-Navarrete, G., Santana, O., Minero-García, Y., Quinto, C., et al. (2009). GTPγS antagonizes the mastoparan-induced in vitro activity of PIP2-phospholipase C from symbiotic root nodules of Phaseolus vulgaris. *Physiol. Plant.* 135, 237–245. doi: 10.1111/j.1399-3054.2008.01184.x

Delgado-Cerezo, M., Sánchez-Rodríguez, C., Escudero, V., Miedes, E., Fernández, P. V., Jordá, L., et al. (2012). Arabidopsis heterotrimeric G-protein regulates cell wall defense and resistance to necrotrophic fungi. *Mol. Plant* 5, 98–114. doi: 10.1093/mp/ssr082

den Hartog, M., Musgrave, A., and Munnik, T. (2001). Nod factor-induced phosphatidic acid and diacylglycerol pyrophosphate formation: a role for phospholipase C and D in root hair deformation. *Plant J.* 25, 55–65. doi: 10.1046/j.1365-313x.2001.00931.x

den Hartog, M., Verhoef, N., and Munnik, T. (2003). Nod factor and elicitors activate different phospholipid signaling pathways in suspension-cultured alfalfa cells. *Plant Physiol.* 132, 311–317. doi: 10.1104/pp.102.017954

Ding, L., Pandey, S., and Assmann, S. M. (2008). Arabidopsis extra-large G proteins (XLGs) regulate root morphogenesis. *Plant J.* 53, 248–263. doi: 10.1111/j.1365-313X.2007.03335.x

Esseling, J. J., Lhuissier, F. G. P., and Emons, A. M. C. (2004). A nonsymbiotic root hair tip growth phenotype in NORK-mutated legumes: implications for nodulation factor-induced signaling and formation of a multifaceted root hair pocket for bacteria. *Plant Cell* 16, 933–944. doi: 10.1105/tpc.019653

Geurts, R., Fedorova, E., and Bisseling, T. (2005). Nod factor signaling genes and their function in the early stages of Rhizobium infection. *Curr. Opin. Plant Biol.* 8, 346–352. doi: 10.1016/j.pbi.2005.05.013

Imaizumi-Anraku, H., Takeda, N., Charpentier, M., Perry, J., Miwa, H., Umehara, Y., et al. (2005). Plastid proteins crucial for symbiotic fungal and bacterial entry into plant roots. *Nature* 433, 527–531. doi: 10.1038/nature03237

Ishida, T., Tabata, R., Yamada, M., Aida, M., Mitsumasu, K., Fujiwara, M., et al. (2014). Heterotrimeric G proteins control stem cell proliferation through CLAVATA signaling in Arabidopsis. *EMBO Rep.* 15, 1202–1209. doi: 10.15252/embr.201438660

Jones, P., Binns, D., Chang, H. Y., Fraser, M., Li, W., McAnulla, C., et al. (2014). InterProScan 5: Genome-scale protein function classification. *Bioinformatics* 30, 1236–1240. doi: 10.1093/bioinformatics/btu031

Joo, J. H., Wang, S., Chen, J. G., Jones, A. M., and Fedoroff, N. V. (2005). Different Signaling and Cell Death Roles of Heterotrimeric G Protein {alpha} and {beta} Subunits in the Arabidopsis Oxidative Stress Response to Ozone\r10.1105/tpc.104.029603. *Plant Cell* 17, 957–970. doi: 10.1105/tpc.104.029603.1

Katoh, K., and Standley, D. M. (2013). MAFFT multiple sequence alignment software version 7: Improvements in performance and usability. *Mol. Biol. Evol.* 30, 772–780. doi: 10.1093/molbev/mst010

Kim, D., Paggi, J. M., Park, C., Bennett, C., and Salzberg, S. L. (2019). Graph-based genome alignment and genotyping with HISAT2 and HISAT-genotype. *Nat. Biotechnol.* 37, 907–915. doi: 10.1038/s41587-019-0201-4

Kirienko, A. N., Porozov, Y. B., Malkov, N. V., Akhtemova, G. A., Le Signor, C., Thompson, R., et al. (2018). Role of a receptor-like kinase K1 in pea Rhizobium symbiosis development. *Planta* 248, 1101–1120. doi: 10.1007/s00425-018-2944-4

Lease, K. A., Wen, J., Li, J., Doke, J. T., Liscum, E., and Walker, J. C. (2001). A mutant Arabidopsis heterotrimeric G-protein beta subunit affects leaf, flower, and fruit development. *Plant Cell* 13, 2631–2641. doi: 10.1105/tpc.010315

Leppyanen, I. V., Kirienko, A. N., and Dolgikh, E. A. (2019). Agrobacterium rhizogenes-mediated transformation of Pisum sativum L. Roots as a tool for studying the mycorrhizal and root nodule symbioses. *PeerJ* 2019:6552. doi: 10.7717/peerj.6552

Liao, Y., Smyth, G. K., and Shi, W. (2014). FeatureCounts: An efficient general purpose program for assigning sequence reads to genomic features. *Bioinformatics* 30, 923–930. doi: 10.1093/bioinformatics/btt656

Llorente, F., Alonso-Blanco, C., Sánchez-Rodriguez, C., Jorda, L., and Molina, A. (2005). ERECTA receptor-like kinase and heterotrimeric G protein from Arabidopsis are required for resistance to the necrotrophic fungus Plectosphaerella cucumerina. *Plant J.* 43, 165–180. doi: 10.1111/j.1365-313X.2005.02440.x

Minh, B. Q., Nguyen, M. A. T., and Von Haeseler, A. (2013). Ultrafast approximation for phylogenetic bootstrap. *Mol. Biol. Evol.* 30, 1188–1195. doi: 10.1093/molbev/mst024

Misra, S., Wu, Y., Venkataraman, G., Sopory, S. K., and Tuteja, N. (2007). Heterotrimeric G-protein complex and G-protein-coupled receptor from a legume (Pisum sativum): Role in salinity and heat stress and cross-talk with phospholipase C. *Plant J.* 51, 656–669. doi: 10.1111/j.1365-313X.2007.03169.x

Miwa, H., Sun, J., Oldroyd, G. E. D., and Downie, J. A. (2006). Analysis of Nod-Factor-Induced Calcium Signaling in Root Hairs of Symbiotically Defective Mutants of Lotus japonicus. *Mol. Plant-Microbe Interact.* 19, 914–923. doi: 10.1094/MPMI-19-0914

Mudgil, Y., Uhrig, J. F., Zhou, J., Temple, B., Jiang, K., and Jones, A. M. (2009). Arabidopsis N-MYC DOWNREGULATED-LIKE1, a positive regulator of auxin transport in a G protein-mediated pathway. *Plant Cell* 21, 3591–3609. doi: 10.1105/tpc.109.065557

Pandey, S., and Vijayakumar, A. (2018). Emerging themes in heterotrimeric G-protein signaling in plants. *Plant Sci.* 270, 292–300. doi: 10.1016/j.plantsci.2018.03.001

Pecrix, Y., Staton, S. E., Sallet, E., Lelandais-Brière, C., Moreau, S., Carrère, S., et al. (2018). Whole-genome landscape of Medicago truncatula symbiotic genes. *Nat. Plants* 4, 1017–1025. doi: 10.1038/s41477-018-0286-7

Perfus-Barbeoch, L., Jones, A. M., and Assmann, S. M. (2004). Plant heterotrimeric G protein function: insights from Arabidopsis and rice mutants. *Curr. Opin. Plant Biol.* 7, 719–731. doi: 10.1016/j.pbi.2004.09.013

Pingret, J.-L. (1998). Rhizobium Nod Factor Signaling: Evidence for a G ProteinMediated Transduction Mechanism. *Plant Cell Online* 10, 659–672. doi: 10.1105/tpc.10.5.659

Roux, B., Rodde, N., Jardinaud, M. F., Timmers, T., Sauviac, L., Cottret, L., et al. (2014). An integrated analysis of plant and bacterial gene expression in symbiotic root nodules using laser-capture microdissection coupled to RNA sequencing. *Plant J.* 77, 817–837. doi: 10.1111/tpj.12442

Roy Choudhury, S., and Pandey, S. (2016). The role of PLDα1 in providing specificity to signal-response coupling by heterotrimeric G-protein components in Arabidopsis. *Plant J.* 86, 50–61. doi: 10.1111/tpj.13151

Schiessl, K., Lilley, J. L. S., Lee, T., Tamvakis, I., Kohlen, W., Bailey, P. C., et al. (2019). NODULE INCEPTION Recruits the Lateral Root Developmental Program for Symbiotic Nodule Organogenesis in Medicago truncatula. *Curr. Biol.* 29, 3657.e–3668.e. doi: 10.1016/j.cub.2019.09.005

Shaw, S. L., and Long, S. R. (2003). Nod factor elicits two separable calcium responses in Medicago truncatula root hair cells. *Plant Physiol.* 131, 976–984. doi: 10.1104/pp.005546

Sun, J., Miwa, H., Downie, J. A., and Oldroyd, G. E. D. (2007). Mastoparan Activates Calcium Spiking Analogous to Nod Factor-Induced Responses in Medicago truncatula Root Hair Cells. *Plant Physiol.* 144, 695–702. doi: 10.1104/pp.106.093294

Tang, H., Krishnakumar, V., Bidwell, S., Rosen, B., Chan, A., Zhou, S., et al. (2014). An improved genome release (version Mt4.0) for the model legume Medicago truncatula. *BMC Genomics* 15:312. doi: 10.1186/1471-2164-15-312

Trifinopoulos, J., Nguyen, L. T., von Haeseler, A., and Minh, B. Q. (2016). W-IQ-TREE: a fast online phylogenetic tool for maximum likelihood analysis. *Nucleic Acids Res.* 44, W232–W235. doi: 10.1093/nar/gkw256

Trusov, Y., and Botella, J. R. (2016). Plant G-Proteins Come of Age: Breaking the Bond with Animal Models. *Front. Chem.* 4, 1–9. doi: 10.3389/fchem.2016.00024

Tunc-Ozdemir, M., Urano, D., Jaiswal, D. K., Clouse, S. D., and Jones, A. M. (2016). Direct Modulation of Heterotrimeric G Protein-coupled Signaling by a Receptor Kinase Complex. *J. Biol. Chem.* 291, 13918–13925. doi: 10.1074/jbc.C116.736702

Ullah, H. (2001). Modulation of Cell Proliferation by Heterotrimeric G Protein in Arabidopsis. *Science* 292, 2066–2069. doi: 10.1126/science.1059040

Ullah, H., Chen, J. G., Temple, B., Boyes, D. C., Alonso, J. M., Davis, K. R., et al. (2003). The beta-subunit of the Arabidopsis G protein negatively regulates auxin-induced cell division and affects multiple developmental processes. *Plant Cell* 15, 393–409. doi: 10.1105/tpc.006148

Urano, D., Chen, J.-G., Botella, J. R., and Jones, A. M. (2013). Heterotrimeric G protein signalling in the plant kingdom. *Open Biol.* 3, 120186–120186. doi: 10.1098/rsob.120186

Urano, D., and Jones, A. M. (2014). Heterotrimeric G Protein–Coupled Signaling in Plants. *Annu. Rev. Plant Biol.* 65, 365–384. doi: 10.1146/annurev-arplant-050213-040133

Van Brussel, A. A. N., Planque, K., and Quispel, A. (1977). The Wall of Rhizobium leguminosarum in Bacteroid and Free-living Forms. *J. Gen. Microbiol.* 101, 51–56. doi: 10.1099/00221287-101-1-51

van Zeijl, A., Op, den Camp, R. H. M., Deinum, E. E., Charnikhova, T., Franssen, H., et al. (2015). Rhizobium Lipo-chitooligosaccharide Signaling Triggers Accumulation of Cytokinins in Medicago truncatula Roots. *Mol. Plant* 8, 1213–1226. doi: 10.1016/j.molp.2015.03.010

Wickham, H. (2016). *ggplot2 Elegant Graphics for Data Analysis (Use R!)*. New York, NY: Springer.

Yu, G. (2020). Using ggtree to Visualize Data on Tree-Like Structures. *Curr. Protoc. Bioinforma.* 69:e96. doi: 10.1002/cpbi.96

Zhukov, V., Radutoiu, S., Madsen, L. H., Rychagova, T., Ovchinnikova, E., Borisov, A., et al. (2008). The Pea *Sym37* Receptor Kinase Gene Controls Infection-Thread Initiation and Nodule Development. *Mol. Plant-Microbe Interact.* 21, 1600–1608. doi: 10.1094/MPMI-21-12-1600

Conflict of Interest: The authors declare that the research was conducted in the absence of any commercial or financial relationships that could be construed as a potential conflict of interest.

Publisher's Note: All claims expressed in this article are solely those of the authors and do not necessarily represent those of their affiliated organizations, or those of the publisher, the editors and the reviewers. Any product that may be evaluated in this article, or claim that may be made by its manufacturer, is not guaranteed or endorsed by the publisher.

frontiers in Plant Science

ORIGINAL RESEARCH
published: 24 March 2022
doi: 10.3389/fpls.2022.837231

Overexpression of the Potato Monosaccharide Transporter *StSWEET7a* Promotes Root Colonization by Symbiotic and Pathogenic Fungi by Increasing Root Sink Strength

*Elisabeth Tamayo, David Figueira-Galán, Jasmin Manck-Götzenberger and Natalia Requena**

Molecular Phytopathology, Botanical Institute, Karlsruhe Institute of Technology (KIT), Karlsruhe, Germany

OPEN ACCESS

Edited by:
Andrea Genre, University of Turin, Italy

Reviewed by:
Woei-Jiun Guo, National Cheng Kung University, Taiwan
Philipp Franken, Friedrich Schiller University Jena, Germany

***Correspondence:**
Natalia Requena
natalia.requena@kit.edu

Specialty section:
This article was submitted to Plant Symbiotic Interactions, a section of the journal Frontiers in Plant Science

Received: *16 December 2021*
Accepted: *11 February 2022*
Published: *24 March 2022*

Citation:
Tamayo E, Figueira-Galán D, Manck-Götzenberger J and Requena N (2022) Overexpression of the Potato Monosaccharide Transporter StSWEET7a Promotes Root Colonization by Symbiotic and Pathogenic Fungi by Increasing Root Sink Strength. Front. Plant Sci. 13:837231. doi: 10.3389/fpls.2022.837231

Root colonization by filamentous fungi modifies sugar partitioning in plants by increasing the sink strength. As a result, a transcriptional reprogramming of sugar transporters takes place. Here we have further advanced in the characterization of the potato SWEET sugar transporters and their regulation in response to the colonization by symbiotic and pathogenic fungi. We previously showed that root colonization by the AM fungus *Rhizophagus irregularis* induces a major transcriptional reprogramming of the 35 potato SWEETs, with 12 genes induced and 10 repressed. In contrast, here we show that during the early colonization phase, the necrotrophic fungus *Fusarium solani* only induces one SWEET transporter, *StSWEET7a*, while represses most of the others (25). StSWEET7a was also induced during root colonization by the hemi-biotrophic fungus *Fusarium oxysporum* f. sp. *tuberosi*. StSWEET7a which belongs to the clade II of SWEET transporters localized to the plasma membrane and transports glucose, fructose and mannose. Overexpression of *StSWEET7a* in potato roots increased the strength of this sink as evidenced by an increase in the expression of the cell wall-bound invertase. Concomitantly, plants expressing *StSWEET7a* were faster colonized by *R. irregularis* and by *F. oxysporum* f. sp. *tuberosi*. The increase in sink strength induced by ectopic expression of *StSWEET7a* in roots could be abolished by shoot excision which reverted also the increased colonization levels by the symbiotic fungus. Altogether, these results suggest that AM fungi and *Fusarium* spp. might induce *StSWEET7a* to increase the sink strength and thus this gene might represent a common susceptibility target for root colonizing fungi.

Keywords: potato, SWEET transporters, arbuscular mycorrhizal symbiosis, *Rhizophagus irregularis*, *Fusarium oxysporum*

INTRODUCTION

Sugar transport proteins play a crucial role in the long-distance distribution of carbohydrates throughout the plant. Photosynthates from source tissues have to be transported to net importer organs such as young leaves, reproductive structures, roots or tubers, in general known as sinks (Williams et al., 2000). And thus, a complex regulation of importers and exporters is required to guarantee the coordinated sugar partitioning that meets each organ demands. However, plant colonization by microbes creates new sinks, significantly altering sugar partitioning and sugar related metabolic activities (Doidy et al., 2012). Depending on the trophic mechanism exerted by microbes they might exert extensive tissue maceration leading to the release of the cell content including sugars (necrotrophs) or develop sophisticated mechanisms to divert nutrients toward the colonization interface (biotrophs). However, carbohydrates play a dual role in plant microbial interactions because they are necessary to cover the energetic costs of the defense responses and to sustain microbial growth. Therefore, carbohydrate reprogramming is intrinsic to plant-microbial compatibility.

There is accumulating evidence that sugar allocation might be tightly linked to the control of plant defenses and susceptibility (Moore et al., 2015; Hacquard et al., 2016; Yamada et al., 2016; Gebauer et al., 2017). For instance, Moore et al. (2015) showed that the partial resistance of wheat toward multiple pathogens in the locus Lr67 was due to mutations in a high affinity glucose transporter from the STP13 cluster. Furthermore, Yamada et al. (2016) showed that in *Arabidopsis* the regulation of the STP13 transporter activity is key for the resistance to bacterial pathogens. Another example showing how sugar availability modifies plant defense responses has been reported for the double mutant *SWEET11*/*SWEET12* in *Arabidopsis* (Gebauer et al., 2017). This mutant, impaired in sugar loading into the phloem, exhibits reduced susceptibility toward the infection by the fungus *Colletotrichum higginsianum*. Increased resistance was mediated by activation of the salicylic acid-mediated defense response (Gebauer et al., 2017). Although there are several other examples of sugar transporter activation by microbes that potentially implicate changes in susceptibility toward those microbes, perhaps the most prominent example is the activation of rice SWEET transporters by bacteria of the genus *Xanthomonas* by transcriptional activator like (TAL) effectors (reviewed in Eom et al., 2015; Kim et al., 2021). Because even before knowing which genes were involved, mutations in SWEET genes were shown to be susceptibility targets toward those bacteria (Yang et al., 2006; Antony et al., 2010; Liu et al., 2011).

AM fungi are obligate biotrophs, requiring the plant for their carbon nutrition, provided in form of monosaccharides and lipids (Shachar-Hill et al., 1995; Helber et al., 2011; Bravo et al., 2017; Keymer et al., 2017; Luginbuehl et al., 2017). Consequently, and similar to other microbes colonizing plants, AM fungi impose a major reorganization in the carbon partitioning, and an increase in the sink strength of the colonized tissue (Wright et al., 1998; Graham, 2000; Boldt et al., 2011; Bitterlich et al., 2014). Furthermore, AM colonization affects the subsequent or parallel colonization by other microorganisms, and the defense capacities of the plant. For instance, AM fungi have been associated with reduction of incidence of several root rot and wilting phenotypes caused by several fungal species including *Fusarium*, as well as by several oomycetes (summarized in Whipps, 2004).

However, the protection they offer is not universal, and the magnitude depends on the AM species employed and on the environmental conditions (Pozo and Azcon-Aguilar, 2007). Liu and coworkers (Liu et al., 2007) using an Affymetrix microarray approach demonstrated that mycorrhizal colonization significantly alters gene expression in a local and systemic manner and demonstrated the induction of a functional defense response in shoots toward a pathogenic *Xanthomonas* spp. Moreover, a study in rice showed that the transcriptomic responses imposed by arbuscular mycorrhizal and pathogenic fungi on plants are partially overlapping, suggesting that root infecting fungi might have similar plant targets required for root infection (Guimil et al., 2005). However, the mechanisms behind are still elusive, and more studies are required involving complex interactions of AM fungi and pathogens on the same plant to investigate if modification of sugar partitioning could be involved in the altered defense responses of mycorrhizal plants.

Two models have been proposed to explain how sugars can modulate plant defense responses toward microbial pathogens (Bezrutczyk et al., 2018). In the first model, and given that the goal of every colonizing microbe is to obtain fixed carbon from its host, plants starve the pathogen for sugar thereby increasing resistance. The second model, which is not incompatible with the first one, proposes that specific sugar ratios at infection sites elicit defense responses that keep microbes at bay (Bezrutczyk et al., 2018). There is supporting evidence for both models in the literature, and likely it depends on many other factors such as the type of pathogen, the infected organ and the pathogenicity tools (i.e., effector secretion) of the given microbe. In any case, it is thus expected that reorganization of plant sugar transporter expressions will accompany each plant-microbial interaction.

In this context, it is thus conceivable that changes in susceptibility to pathogens observed in plants colonized by mycorrhizal fungi might be at least in part due to the changes in the carbon partitioning imposed by the symbiosis. We decided to start investigating this hypothesis by further characterizing the function of several SWEET transporters that were found induced during symbiosis between potato plants and the AM fungus *Rhizophagus irregularis* (Manck-Gotzenberger and Requena, 2016) and in particular by analyzing their involvement in the colonization by pathogenic fungi. SWEET transporters are bidirectional sugar facilitators (Chen L. Q. et al., 2015; Eom et al., 2015; Breia et al., 2021). They can be located either at the plasma membrane, at the tonoplast or in the Golgi membrane. Although their primary role in plants is to serve functions such as pollen nutrition, seed filling, flower and fruit development or phloem loading (Chen et al., 2010, 2012; Sosso et al., 2015; Yang et al., 2018), they are a paradigm of how microbes can modify the plant carbohydrate program toward their own benefit as shown above. Thus, SWEET transcriptional activation in response to TAL effectors from pathogenic bacteria such as *Xanthomonas* spp. allows those bacteria to access sugars particularly in tissues where sugar movement is symplastic (Yang et al., 2006; Chen et al., 2010;

Yu et al., 2011; Cohn et al., 2014; Hu et al., 2014). Furthermore, disease resistance can be achieved if transcriptional activation is prevented for instance by mutations in the binding site of TAL effectors in the promoter of SWEET genes (Chen et al., 2010; Yu et al., 2011; Streubel et al., 2013).

Here we have analyzed the spatial induction of four mycorrhiza-induced SWEET genes in potato, their transport activity and their subcellular localization. The expression of all potato SWEETs in response to root colonization of the necrotrophic fungus *Fusarium solani* was also analyzed, and the results showed that only one SWEET gene, *StSWEET7a*, is induced, while the majority are downregulated. Furthermore, we present data about the functional role of *StSWEET7a,* commonly induced by both symbiotic and pathogenic fungi, using overexpression composite plants. Our results point toward a role of StSWEET7a at increasing the sink strength of colonized roots thereby facilitating the colonization by both types of microbes.

MATERIALS AND METHODS

Biological Material and Growth Conditions

Solanum tuberosum cv. Desiree was propagated as cuttings axenically in plastic containers with Murashige and Skoog medium containing vitamins and 30 g/L sucrose (Murashige and Skoog, 1962) solidified with 3 g/L Phytagel (P8169, Sigma-Aldrich, Germany) at 21°C and 16 /8 h day/night rhythm.

For mycorrhizal colonization experiments, 2-week-old cuttings or transgenic composite plants were transferred to 80 ml falcons with a sand:gravel (1:4) mixture. Plants were inoculated by mixing the substrate with 2-month-old *Daucus carota* root cultures grown monoaxenically in association with *R. irregularis* DAOM 197198 (Schenck and Smith, 1982; Kruger et al., 2012) on M-medium with sucrose at 27°C in darkness (Bécard and Fortin, 1988). One Petri dish of carrot roots was used to inoculate two 80 ml falcons. Plants were grown at 25°C and 16/8 h light/darkness photoperiod and fertilized twice a week with 5 ml Murashige and Skoog nutrient solution with low phosphate content (50 μM). Non-mycorrhizal controls were treated the same. After 6 weeks (6 weeks post inoculation), a fraction of the roots was separated and stored in 1X PBS for further analysis and quantification of mycorrhizal colonization, while the rest of the roots and shoots were harvested separately, immediately frozen in liquid nitrogen and stored at −80°C until used.

Nicotiana benthamiana was used for transient expression of GFP fusion proteins in localization analyses. Plants were grown in soil at 28°C in a growth chamber (CLF Plant Climatics, Germany), with a 16/8 h of light/darkness photoperiod and watered on demand.

Fusarium solani strain BBA72084 (Malonek et al., 2005), was cultivated on CM at 28°C for 6 days to obtain microconidia (Talbot et al., 1993). *S. tuberosum* plants (3 weeks old) were inoculated with a spore suspension containing 5×10^6 microconidia/ml, according to Di Pietro et al. (2001). Roots were harvested 48 h post inoculation.

Fusarium oxysporum f. sp. *tuberosi* (CABI culture collection, strain 141127[1]), was propagated on CM at 28°C. For the infection assays, roots of *S. tuberosum* cv. Desiree cuttings were immersed in a sterile 0.2% gelatine solution containing 5×10^6 microconidia/ml for 30 min under gentle agitation. Plants were then transferred to falcons containing the above-mentioned sand:gravel mixture and grown at 25°C as described above, but fertilized with Murashige and Skoog nutrient solution with full phosphate concentration (1.25 mM). Plants were harvested at 9 days or 7 weeks post inoculation and immersed in 1X PBS to visualize infection using WGA-FITC as described in Rech et al. (2013).

Gene Isolation and Constructs

For growth assays in *Saccharomyces cerevisiae*, the full-length cDNAs of *StSWEET1b*, *2c*, *7a*, and*12a* were amplified from cDNA with *Pst*I and *Xho*I restriction sites and subcloned into pCR8/GW/TOPO (Invitrogen by Thermo Fisher Scientific, Germany), to afterward clone them into pDR196, which contains a fragment of the plasma membrane ATPase promoter (Rentsch et al., 1995). The full-length cDNA of *Htx2* yeast gene was also cloned into pDR196 and used as positive control in the complementation analyses of the EBY.VW4000 mutant strain (Wieczorke et al., 1999).

For localization analyses in *N. benthamiana*, the ORFs of *StSWEET1b*, *2b*, *2c*, *7a*, and *12a* without stop codon were amplified from cDNA and subcloned into pENTR/D-TOPO (Invitrogen by Thermo Fisher Scientific, Germany). Afterward, the constructs were cloned into the destination vector pCGFP-RR for a C-terminal GFP-tagging (Kuhn et al., 2010).

For overexpression analyses in *S. tuberosum* roots, the open reading frame of *StSWEET7a* was amplified from gDNA, subcloned into pENTR/D-TOPO (Invitrogen by Thermo Fisher Scientific, Germany) and cloned into the destination vector 2xP35S-pKGW-RedRoot (Heck et al., 2016).

All primers used for cloning of the constructs are listed in **Supplementary Table 1**.

Promoter Analysis

For promoter-reporter assays, 2 kb fragments of the *StSWEET1b*, *2c*, *7a*, and *12a* promoters were cloned into the Gateway binary vector pPGFPGUS-RR as described in Manck-Gotzenberger and Requena (2016). *Agrobacterium rhizogenes*-mediated transformation of *S. tuberosum* and mycorrhizal inoculation with *R. irregularis* was carried out.

Yeast Growth Assays

Yeasts were transformed with the corresponding constructs using a lithium acetate-based method (Gietz and Woods, 2002), and transformants were selected in SD medium by autotrophy to uracil. For the complementation assay, the yeast strain EBY.VW4000 (Wieczorke et al., 1999) and SD media supplemented with fructose, galactose, glucose, and mannose were used.

[1]https://www.cabi.org/products-and-services/bioscience-services/microorganism-supply-services/

For the complementation assay, the medium contained 1.5% gold agar (Affymetrix). Yeast cultures were grown in SD liquid medium without uracil and supplemented with 2% maltose were diluted to an optical density at 600 nm of 0.4 and then grown to exponential phase (OD_{600} 0.8–1). Cultures were washed twice with distilled water and brought to an optical density at 600 nm of 1. Serial 1:10 dilutions were spotted (5 μl) onto plates containing the different sugars to determine transport as compared with strains transformed with the empty vector (EV).

Transient Expression of Proteins in *Nicotiana benthamiana*

The plasmids constructed for localization analyses were transformed into *Agrobacterium tumefaciens* GV3101 strain. A bacterial suspension was infiltrated into leaves of 3-week-old *N. benthamiana* plants using a needleless syringe and the p19 protein of tomato bushy stunt virus was used to suppress gene silencing in co-transformation, after the protocol of Voinnet et al. (2003). Cells were kept overnight in the dark in infiltration media [2% sucrose solution 10 mM $MgCl_2$, 10 mM MES-KOH, 150 μM acetosyringone in dimethyl sulfoxide (DMSO)], with an OD_{600} of 0.8–1 at room temperature before co-infiltration with a ratio of 1:1. After infiltration of the cultures into the underside of two-three leaves per plant, plants were incubated at 21°C in a low illuminated place and confocal microscopy was performed 2–3 days after infiltration.

Agrobacterium rhizogenes-Mediated Transformation

Agrobacterium rhizogenes ARquaI containing the appropriate vector was used for the root transformation of *S. tuberosum* cv. Desiree. *S. tuberosum* composite plants were generated by stab inoculation after (Horn et al., 2014). For this purpose, 2-week-old cuttings were transferred to fresh potato medium slants without sucrose in 15 cm Petri dishes. The plants were stabbed into the second or third internode from the roots with an inoculation needle dipped into the agrobacteria. Two weeks after transformation, the wild-type roots were cut and the *S. tuberosum* cuttings were washed two times in water supplemented with 600 mg/L Augmentin (AmoxiClav, Hikma Farmaceutical, Portugal) and 200 mg/L Cefotaxime (Actavis GmbH & Co. KG, Langenfeld, Germany) and transferred to fresh potato medium slants without sucrose supplemented with 400 mg/L Augmentin and 200 mg/L Cefotaxime. Transformed roots were visualized using the DsRed marker under the fluorescence binocular. Transformed plants were transferred to 80 ml pots 4 weeks after transformation.

Microscopy and Image Processing

Confocal microscopy images were taken using a Leica TCS SP5 (DM5000) confocal microscope with conventional PMT detectors and the color camera Leica DFC295, using the LASAF v2.6 software. The fluorescent proteins eGFP (488 nm) and WGA-FITC (488 nm) were excited with an argon laser while DsRed (561 nm) was excited with a DPSS laser. Emission of eGFP was detected from 493 to 530 nm and DsRed from 566 to 670 nm. Emission of WGA-FITC was collected from 505 to 525 nm after excitation at 494 nm (argon laser). Pictures were processed using ImageJ 1.51n.[2]

Morphometric Analysis of Composite Plants

For morphometric analysis of leaf surface and shoot branching, images of plants were taken and analyzed using AutoCAD 2010 (Autodesk, Inc., San Rafael, CA, United States). For this purpose, pictures of five plants from each treatment were scaled taking into account the length of the plate (15 cm). Five leaves of each plant were used for further calculations.

Quantification of Mycorrhizal Colonization

Fungal structures were immunostained with WGA-FITC as described in Rech et al. (2013) for phenotypical analysis and quantification of mycorrhizal colonization. Quantification of mycorrhizal structures was carried out according to Trouvelot et al. (1986). F% represents the frequency of mycorrhization, M% the intensity of colonization, A% the abundance of arbuscules, and I% the abundance of hyphae in the root system. Vesicle quantification was carried out counting the number of vesicles present along at least 68 fields of vision per biological replicate observed with the 10× magnification at the confocal microscope (Leica TCS SP5, DM5000) and expressed as percentage of vesicles per root segment. Roots of four biological replicates per treatment (EV mycorrhizal and *StSWEET7a* OE mycorrhizal) were analyzed after immunostaining of *R. irregularis* with WGA-FITC.

Quantification of Pathogen Colonization

To quantify the *F. oxysporum* f. sp. *tuberosi* colonization at 7 weeks post inoculation (wpi) in EV and *StSWEET7a* overexpressing roots, the fungus was stained with WGA-FITC and confocal microscopy pictures from different root regions for each treatment (four biological replicates each) were taken, with $n \geq 17$ (n, number of root sections analyzed for each treatment). Using Fiji, the root surface areas were outlined manually and the fungal area was determined by applying a Minimum threshold to the FITC fluorescence channel (Schindelin et al., 2012). The extent of colonization was calculated as the fraction of root surface area covered by fungus.

Gene Expression Analyses

Total RNA was extracted using the innuPREP RNA Kit (Analytik Jena AG). cDNA was synthesized as described in Kuhn et al. (2010) with the reverse transcriptase SuperScript II (Invitrogen, United States). Control PCRs were carried out using the *StActin* gene (XM_006345899) to check for the absence of genomic DNA contamination in the cDNA samples. Real time expression analyses were carried out using an iCycler MyIQ (Bio-Rad, United States) and MESA Green 231qPCR Master Mix Plus (Eurogentec, Germany) with 3–5 independent biological

[2]http://fiji.sc/Fiji

replicates depending on the experiment. Expression of *StActin* gene was used for normalization of the expression of plant genes as well as of *RiTEF* (DQ282611). Fugal genes' expression was normalized to *RiTEF* transcript levels. *StPT4* (AY793559), *StInvCD141* (Z22645), *RiTEF*, *RiMST2* (HM143864), and *StFatM* (PGSC0003DMP400059797) were used as indicators of symbiosis status. The PCR program consisted in a 1 min incubation at 95°C, followed by 40 cycles of 30 s at 95°C, 30 s at 56°C and 30 s at 72°C, where the fluorescence signal was measured. The specificity of the PCR amplification procedure was checked with a heat-dissociation protocol (from 57 to 95°C) after the final cycle of the PCR. Oligonucleotides used can be found in **Supplementary Table 1**.

Determination of Phosphate Concentration

Potato shoot phosphate concentration was determined with the *Malachite Green Phosphate Assay Kit* from Sigma. Frozen tissue was first homogenized using a mixer mill (three rounds of 1 min each with a frequency of 25 oscillations per second). A known amount of frozen tissue powder was collected in a separate tube to extract the phosphate from and later relativize the phosphate amount to the corresponding collected weight. Phosphate isolation was achieved through the incubation of the samples with 250 mM NaOH (sodium hydroxide) for 1 min at 95°C and later with an added equivalent volume of 250 mM HCl (hydrochloric acid, for pH neutralization) for 2 min at 95°C. Samples were then centrifuged to precipitate cell debris and supernatants containing the isolated phosphate were collected into new tubes. The determination of the phosphate concentration was conducted according to manufacturer instructions. Absorbances (λ = 620 nm) were measured using a plate reader (Tecan Infinite M Nano, Männerdorf, Switzerland) in two replicates. A calibration curve was prepared according to the manufacturer specifications and samples were diluted with Milli-Q water to produce absorbances within the range of the calibration curve.

Statistical Analyses

Data shown in **Figure 5A** represent the mean of five biological replicates and error bars correspond to the standard deviation. For the rest of the figures showing graphs, boxplots were used to represent the data. In those, the mean is shown by an "x" and the median by a horizontal line while each dot represents the individual value for each biological replicate. For each parameter analyzed, each treatment was first subjected to the Shapiro–Wilk test for normality. If treatments were normally distributed, a two-tailed Student's *T*-test was applied. In case one of the treatments (or both) were not normally distributed, a Mann–Whitney U test was applied. Significance is indicated by asterisks ($^*p < 0.05$; $^{**}p < 0.01$) or "ns" (non-significant, $p \geq 0.05$). The number of biological replicates (n) is indicated in each of the corresponding figure legend. Additional statistical analyses were carried out for data in **Figures 4**, **6** and **Supplementary Figure 1** that are shown in **Supplementary Tables 2, 3**. For data comparing more than two groups and showing no normal distribution, the Kruskal–Wallis test was carried out and the significance calculated according to the Mann–Whitney U test.[3] If data were showing a normal distribution an ANOVA and a Tuckey *post hoc* test were carried out. Significant differences with $p < 0.05$ are shown with different letters.

RESULTS AND DISCUSSION

SWEET Promoter Activity Is Induced in Potato Roots in Arbuscule-Containing Regions

We had previously shown that root colonization by arbuscular mycorrhizal fungi induces a major transcriptional reprogramming affecting the expression of 22 of the 35 *SWEET* genes from potato, including the genes *StSWEET1b*, *2b, 2c*, *7a*, and *12a*. Furthermore, promoter-reporter analyses of three of these genes in the heterologous host *Medicago truncatula* showed promoter activity in arbuscule-enriched regions (Manck-Gotzenberger and Requena, 2016), suggesting they could be involved in carbohydrate regulation during symbiosis. Here, we analyzed the promoter activity of these genes in potato using the promoter-reporter GUS. Unfortunately, the promoter of *StSWEET2b* could not be amplified and was therefore not included in the assay. All these genes had basal expression levels in the cortex, sometimes also in root tips (*StSWEET2c*) under non-mycorrhizal conditions (**Figure 1**). However, transcript accumulation of *StSWEET1b*, *2c*, *7a*, and *12a* occurred in roots

[3]https://www.Statskingdom.com

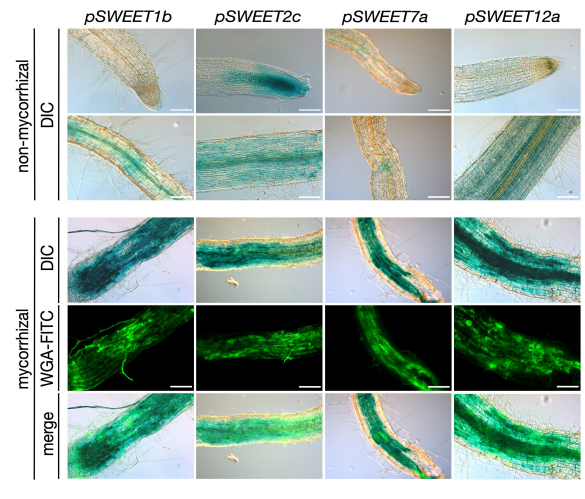

FIGURE 1 | Promoter-reporter assay of *S. tuberosum SWEET* genes during AM symbiosis. A 2 kb fragment upstream of the ATG of the *S. tuberosum SWEET* genes *1b*, *2c*, *7a*, or *12a* was cloned in front of the GUS (β-*glucuronidase*) reporter gene and transformed in *S. tuberosum*. Composite plants were inoculated with *R. irregularis* and harvested 4 wpi (weeks post inoculation). β-Glucuronidase staining was carried out in non-mycorrhizal control roots and mycorrhizal roots. Fungal colonization was visualized by WGA-FITC (wheat germ agglutinin-fluorescein isothiocyanate) counterstaining labeling the fungal cell wall. Scale bars represent 200 μm. DIC, differential interference contrast; WGA-FITC signal is shown in green.

colonized by the AM fungus *R. irregularis* in areas enriched in arbuscules, and thus consistent with the localization data previously observed in *M. truncatula*. This result supports the hypothesis that these SWEETs could play a role in the mycorrhizal symbiosis by regulating the carbon partitioning in colonized roots and eventually increasing their sink capacity. Interestingly, putative orthologs of several of these genes in other plants have been shown to be also transcriptionally regulated during microbial interactions. Thus, for instance, the ortholog of potato *StSWEET1b* in *M. truncatula* was recently functionally characterized and also found to be strongly expressed in arbuscule-containing cells and to play a role in arbuscule maintenance (An et al., 2019). Furthermore, *MtSWEET1b* is also induced by nodulation (Kryvoruchko et al., 2016), supporting a symbiotic role for this transporter. *AtSWEET2* is induced in roots colonized by the pathogenic oomycete *Pythium* and its mutation reduces the resistance of plants to this pathogen (Chen H. Y. et al., 2015). The authors proposed this to be linked to a mechanism to prevent excess of glucose leakage out of roots. Three putative orthologs of potato *StSWEET7a*, the *M. truncatula MtSWEET6*, *Vitis vinifera VvSWEET7*, and the tomato ortholog *SlSWEET7b* have been also shown to be transcriptionally induced by microbes. *MtSWEET6* was induced in roots colonized either by AM fungi or by rhizobia (Kafle et al., 2019), further supporting our findings in potato (Manck-Gotzenberger and Requena, 2016). *VvSWEET7* transcription was increased in grapes in response to *Botrytis cinerea* infection (Breia et al., 2019), while *SlSWEET7b* was induced in roots of tomato upon infection with the root knot nematode *Meloidogyne incognita* (Zhao et al., 2018). *AtSWEET11* and *AtSWEET12* have been shown to be induced at infection sites during clubroot disease in order to deliver carbohydrate to the developing plasmodia and coincident with increases in apoplastic invertase and sucrose synthase gene expression (Walerowski et al., 2018). Collectively, these findings suggest that microbial colonization of plants imposes changes in carbon distribution that are facilitated by SWEET transporters.

StSWEET1b and StSWEET7a Are Monosaccharide Transporters

Eom et al. (2015) had proposed that the phylogenetic classification of SWEETs in clades did not correlate with their physiological function (seed filling, pollen nutrition, etc.) but rather with their substrate preference. Thus, it was proposed that proteins from clade I and II (like StSWEET1b, 2b, 2c and 7a) would be monosaccharide transporters, while SWEETs in clade III (like StSWEET12a) would be more likely sucrose transporters. However, the specificity of SWEET transporters for mono- or disaccharides is sometimes controversial in the literature. Thus, while most SWEET transporters are specific for only one type of sugar, for some others it is not totally clear, and some have been shown to transport both, mono- and disaccharides (Kim et al., 2021). Furthermore, some SWEETs have been demonstrated to transport even sugar unrelated substrates, such as GA (Kanno et al., 2016; Morii et al., 2020).

In order to investigate the sugar transport activity of the mycorrhiza-induced potato SWEETs, complementation analyses in yeast were carried out. To that end, the hexose transport-deficient strain EBY.VW4000, that can only grow on monosaccharides if complemented with a functional plasma membrane-localized hexose transporter was used. The ability of the selected potato SWEET proteins to restore growth of this strain was then analyzed using different monosaccharides as single carbon sources. The full-length cDNAs of the *StSWEETs 1b*, *2b, 2c*, *7a*, and *12a* were expressed under the control of the constitutive promoter *PMA1* (coding for the yeast proton ATPase). As a positive control the yeast high affinity monosaccharide transporter ScHXT2, cloned in the same vector, was used. Growth of the transformed strains containing either one of the transporters or the EV was scored on minimal medium containing 2% of D-glucose, D-fructose, or D-mannose as single carbon sources. The results showed that the yeast strain expressing the potato *StSWEET1b* is able to grow on 2% D-glucose but it is not able to restore growth on any of the other monosaccharides analyzed (**Figure 2**). This is consistent with the results obtained for the *Arabidopsis thaliana* and *M. truncatula* orthologs, AtSWEET1 and MtSWEET1b, that have been shown to be specific glucose transporters (Chen et al., 2010; An et al., 2019).

In contrast to StSWEET1b, StSWEET2b and StSWEET2c, which also belong to clade I, were not able to complement the yeast growth on monosaccharides, although some residual growth was observed for StSWEET2b at pH 5, indicating that they might transport another substrate or that they are not localized at the plasma membrane (**Figure 2**). In fact, both SWEETs are in the same phylogenetic branch as AtSWEET2, a vacuolar transporter that likely transports glucose in and out of the vacuole to buffer the cytoplasmic content, and it is regulated in response to pathogens (Chen H. Y. et al., 2015). Similarly, *VvSWEET2a,* another transporter from this group from *V. vinifera,* is also induced by microbial colonization, suggesting that vacuolar control of sugar might be a critical issue for plants hosting microbes (Chong et al., 2014). Thus, we hypothesize that the regulation of StSWEET2b and 2c in potato by AM fungi might have an impact in the carbon partitioning of sugars among the cortical cells and allow arbuscule-containing cells to accumulate sugars in the vacuole to support the increased metabolic demands of these cells.

Similar to StSWEET1b, StSWEET7a was also able to transport glucose but in addition fructose and mannose (**Figure 2**). In all cases, the transport of these sugars was better at pH 5, while the glucose transport of StSWEET1b was equally good at both pHs. *V. vinifera* SWEET7, a putative ortholog of StSWEET7a, that is induced during infection with *B. cinerea*, was shown using radioactive sugar uptake measurements to also transport glucose and fructose, as well as polyols (Breia et al., 2019). Surprisingly, it also showed sucrose transport activity. However, the yeast strain used for these assays was also the EBYVW.4000 which contains the *SUC2* gene, coding for secreted and intracellular invertase (Carlson and Botstein, 1982). Therefore, the possibility that sucrose might be cleaved and taken up exists, and thus another strain with a deletion in *SUC2* could help to rule out that possibility (Helber et al., 2011). Potato StSWEET12a was unable to transport monosaccharides in the yeast assay and thus it might indicate that it is a sucrose transporter, similar to other SWEETs

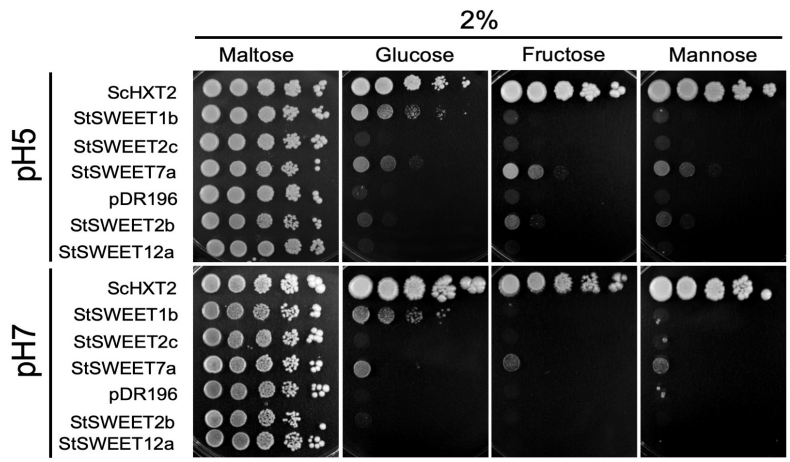

FIGURE 2 | Analysis of the monosaccharide transport ability of five *S. tuberosum* SWEETs in yeast at pH 5 and pH 7. The EBY.VW4000 yeast strain was transformed with an empty vector (pDR196) or with the positive control *ScHXT2* or with the potato transporters *StSWEET1b*, *StSWEET2b*, *StSWEET2c*, *StSWEET7a*, or *StSWEET12a*, all cloned in pDR196. Strains were plated on SD medium without uracil supplemented with 2% maltose (growth control) or with 2% D-fructose, D-glucose, or D-mannose. Plates were incubated at 28°C for 5 days (pH 5) or for 12 days (pH 7).

from clade III. We tested several other yeast strains to analyze the putative sucrose transport ability of StSWEET12a but results were not conclusive. Hence, other methods, such as the esculin uptake assay in yeast that was used to show the sucrose transport ability of StSWEET11 (Abelenda et al., 2019), are necessary.

As mentioned above, some SWEET transporters have shown to transport more than one substrate (including mono- and disaccharides) and for a few of them somewhat contradictory results have been shown. One example is the AtSWEET9, a sucrose transporter required for nectar production that was shown to be unable to transport glucose using the same yeast complementation assay employed here. However, this transporter exhibited a weak glucose transport activity when analyzed using FRET sensors (Lin et al., 2014). Also, the vacuolar transporter AtSWEET16 was shown to be able to take up mono- and disaccharides when expressed in *Xenopus* oocytes (Klemens et al., 2013). However, this is slightly contradictory to the experiments carried out by Guo et al. (2014). Using isolated *A. thaliana* vacuoles they could show that AtSWEET16 and the closely related AtSWEET17 exhibited similar phenotypes and sugar accumulation patterns in plants, but transport activity could be shown only for AtSWEET17 (Guo et al., 2014).

These results show the difficulty of these type of studies to ascertain the substrate and direction of transport for SWEET proteins and the need to establish further complementing methodologies.

Subcellular Localization of Potato SWEETs

In silico analyses using WoLF Psort[4] and the results above indicated that SWEETs 1b, 7a and 12a are likely plasma membrane transporters, while SWEET2b and 2c might be tonoplast transporters. In order to obtain more information about their subcellular localization, the corresponding proteins were tagged with GFP at their carboxy-terminus and expressed in *N. benthamiana* leaves. As positive control free eGFP, which localizes in the cytoplasm and in the nucleus, was also analyzed. In all cases, the DsRed fluorescent protein was used as transformation control, also showing localization in the cytoplasm and in the nucleus. Confocal microscopy analyses confirmed that, as predicted, StSWEETs 1b, 7a and 12a have plasma membrane localization (**Figure 3**). In contrast, StSWEETs 2b and 2c exhibited tonoplast localization, with visible accumulation of DsRed in the cytoplasm between tonoplast and plasma membrane (indicated with white arrows). These results could explain the inability of StSWEETs 2b and 2c to complement the mutant yeast strain, because they likely also localize at the tonoplast in the heterologous host.

Overexpression of *StSWEET7a* in Roots Alters Sink Strength, Plant Architecture, and Mycorrhizal Colonization

In order to investigate the role of StSWEET7a during symbiosis, we deregulated its expression in roots by ectopically expressing the gene under the control of a constitutive promoter (*CMV 35S*) and carried out mycorrhizal colonization assays. Shoots of potato plant ectopically expressing *StSWEET7a* in roots had larger leaves, were less etiolated and survived better than control plants the adaptation to the substrate after transformation (**Supplementary Figure 1**). Furthermore, overexpressing plants developed less shoot branches than plants transformed with an EV (**Figures 4A,B** and **Supplementary Figure 1**). These differences in shoot development were, however, no longer visible at the end of the experiment, Exp1 (**Figure 4C**). However, under mycorrhizal conditions, *StSWEET7a* overexpressing plants developed significantly smaller roots (**Figures 4C,D**). In order to test whether these differences in growth at the end of the

[4]https://wolfpsort.hgc.jp

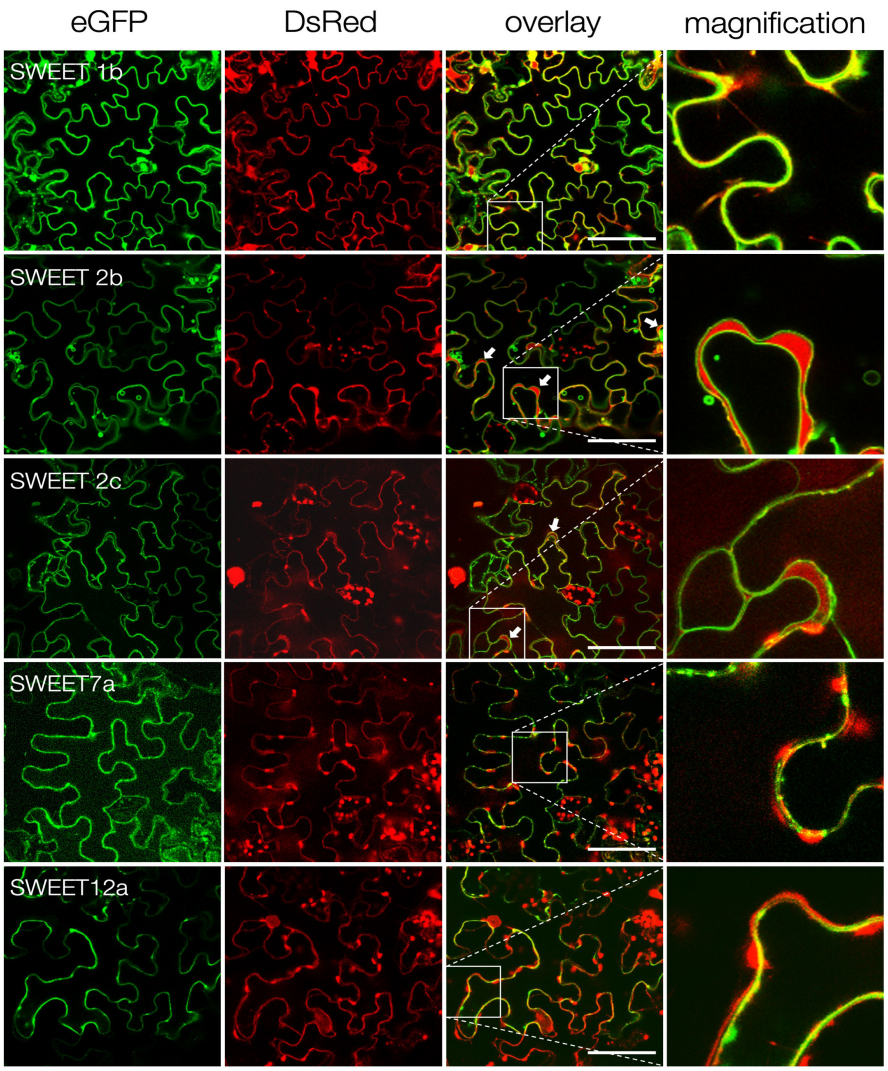

FIGURE 3 | Subcellular localization of *S. tuberosum* SWEET proteins. Confocal imaging of ectopically expressed potato SWEET proteins fused to eGFP in *N. benthamiana* epidermal cells. Free DsRed was co-expressed as control for transformation and labels the cytoplasm and the plant nucleus. White arrows indicate cytoplasmic DsRed accumulations between the tonoplast and the plasma membrane. Zoom images of inlets are shown in the last column. Scale bars are 50 μm.

experiment were due to the larger size of the potato leaves and the reduced branching caused by the ectopic expression of *StSWEET7a*, a parallel experiment (Exp2) was carried out in which shoots from transformed plants were cropped before transplanting to the pots (**Figure 4B**). As expected, shoots from plants in Exp2 were smaller than those of Exp1, while root sizes were similar. Interestingly, the differences in root size observed in Exp1 between overexpressing plants and control plants (EV) were no longer visible when plants were colonized by *R. irregularis* (**Figure 4D**). This is similar of the conserved response of plants to decapitation that react with an increase in shoot branching mediated by sugars (Mason et al., 2014; Salam et al., 2021). This phenomenon has been recently explained as a competition for sucrose between the apical meristem and the axillary buds. The apical meristem acts as a strong sink depriving of sucrose the outgrowing buds and thus preventing branching (Barbier et al., 2015a,b). Taken together these results suggest that ectopic expression in roots of *StSWEET7a* alters the sugar partitioning in potato producing an increase in the root sink capacity as indicated by the change in shoot architecture, with a decrease in shoot branching and an increase in leaf size. In support of that, decapitation of all plants prior transplanting in Exp2 abolished the differences in plant architecture observed between control and *StSWEET7a* expressing plants in Exp1.

Plants ectopically expressing *StSWEET7a* in roots in Exp1 were faster colonized by *R. irregularis* than control plants (**Figures 5A,B**). Together with the decrease in root growth of those plants, this is reminiscent of the phenotype observed in the experiments of Bitterlich and coworkers, in which silencing of the *SlSUT2*, coding for a sucrose importer, increased mycorrhizal colonization but led to a shift in biomass from the plant to the fungus, thus abolishing the positive growth response of the

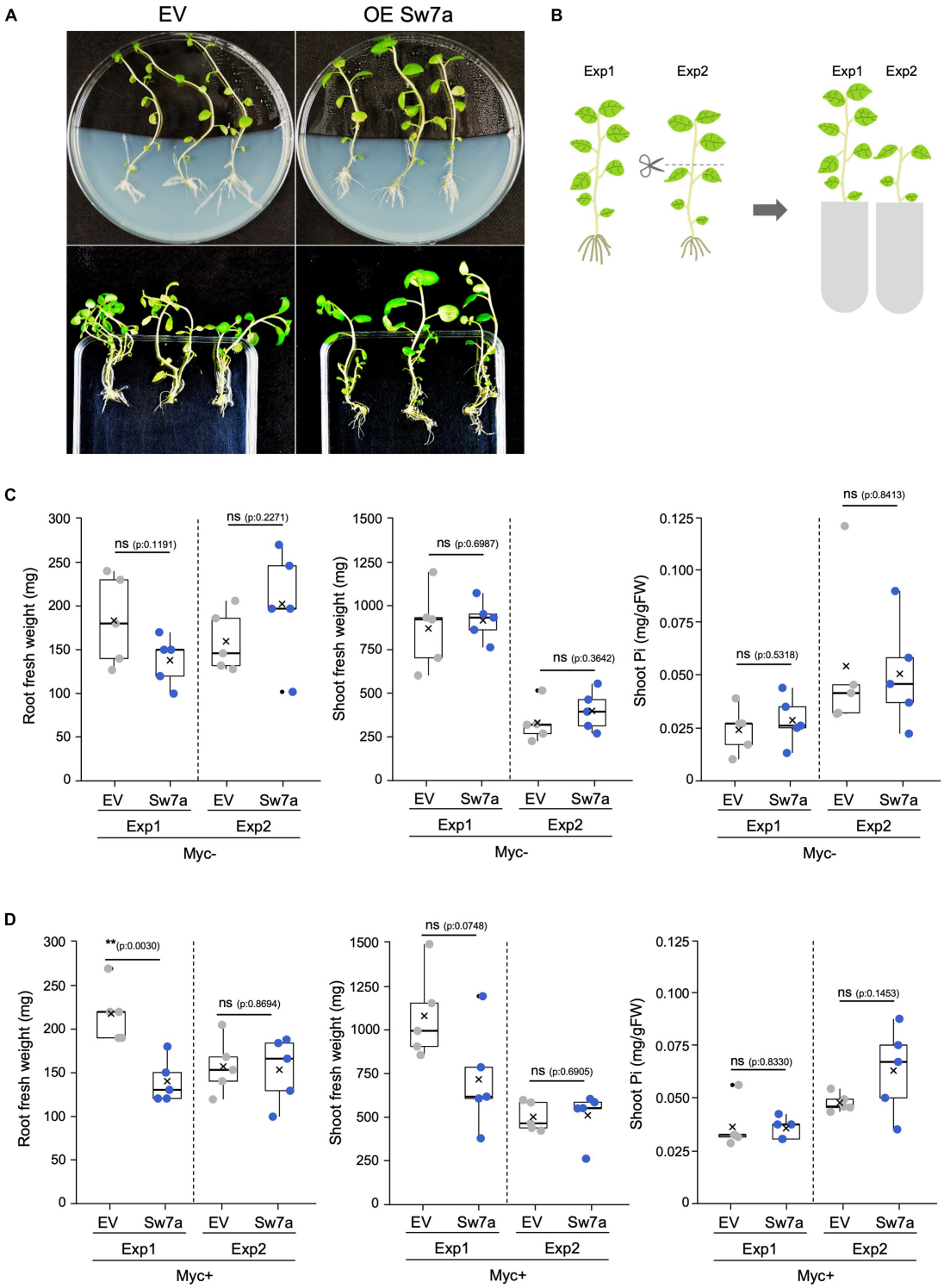

FIGURE 4 | Effect in plants of the ectopic expression of *StSWEET7a*. **(A)** Ectopic expression of *StSWEET7a* in roots of composite potato plants modified shoot development as compared with plants transformed with an empty vector (EV). *StSWEET7a* expressing plants had larger leaves and less branches than EV plants before transplanting to pots. **(B)** Graphic representation of how Exp1 and Exp2 were carried out. Plants in both experiments were transplanted 4 weeks after transformation. In Exp1 plants were directly transplanted to pots, while in Exp2 plant shoots were excised right before transplanting. Plant growth parameters at the end of each experiment under non-mycorrhizal (Myc–) **(C)** and mycorrhizal (Myc+) conditions **(D)**. Five biological replicates ($n = 5$) were used for each treatment. Statistical significance (calculated as explained in section "Materials and Methods") is shown with exact p-values and with asterisks, ns, non-significant, $p > 0.05$; $^{*}p < 0.05$; $^{**}p < 0.01$.

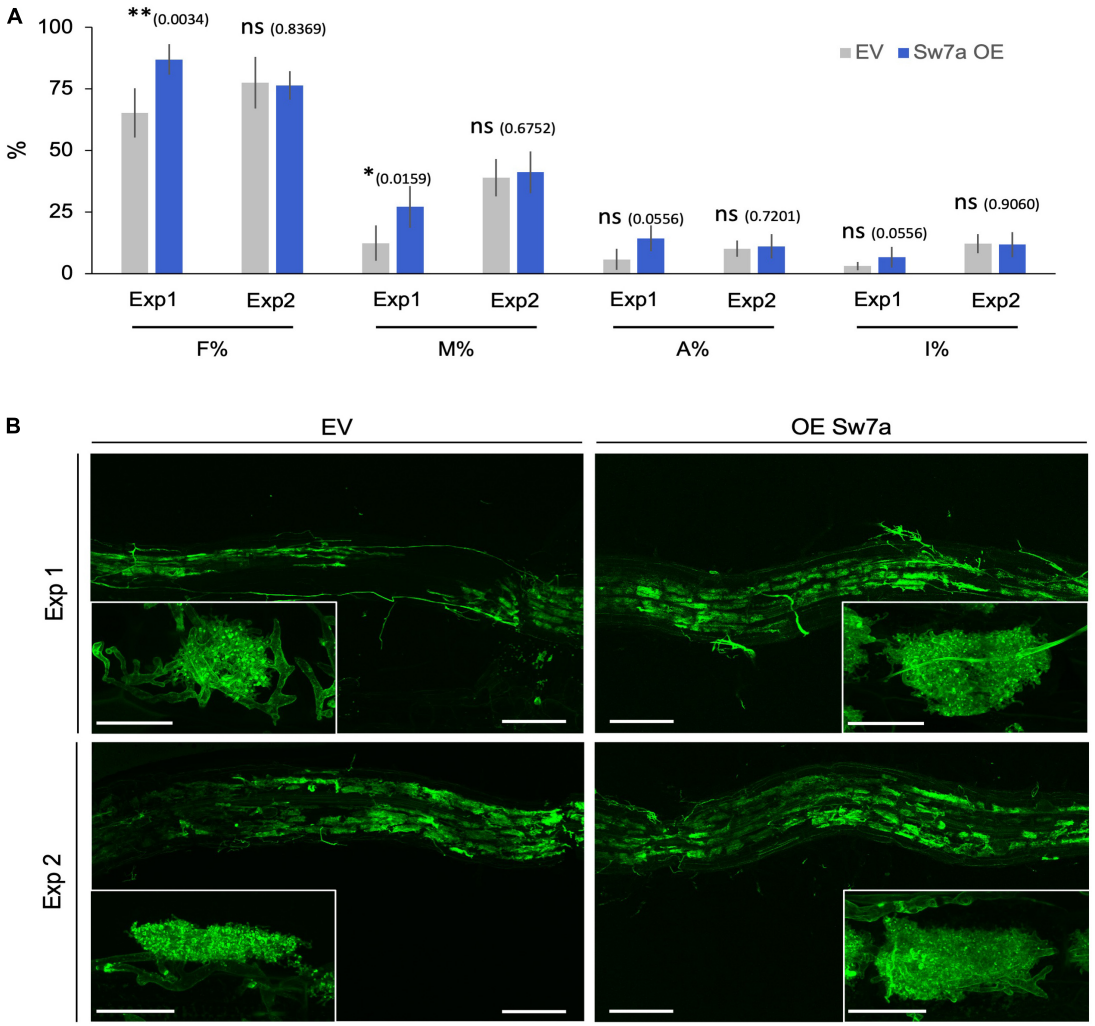

FIGURE 5 | Ectopic expression of *StSWEET7a* modifies root colonization when shoot is intact. **(A)** Quantification of *R. irregularis* colonization was carried according to Trouvelot et al. (1986). F% represents the frequency of mycorrhization, M% the intensity of colonization, A% the abundance of arbuscules, and I% the abundance of hyphae in the root system. Five biological replicates ($n = 5$) were used for each treatment. Statistical significance (calculated as explained in section "Materials and Methods") is shown with exact p-values and with asterisks, ns, non-significant, $p > 0.05$; *$p < 0.05$; **$p < 0.01$. **(B)** Representative pictures of the observed colonization in potato roots stained with WGA-FITC (green signal). Scale bars are 200 μm for overview pictures and 30 μm for pictures in inlets depicting single arbuscules.

mycorrhizal colonization (Bitterlich et al., 2014). In support of that hypothesis, the number of vesicles, fungal carbon storage structures, in roots expressing *StSWEET7a* was significantly higher than in EV plants (**Supplementary Figure 1**).

The higher mycorrhizal colonization of *StSWEET7a* plants in Exp1 paralleled to a higher expression of the symbiotic plant phosphate transporter *StPT4* but surprisingly not of the fungal translation elongation factor *RiTEF* (**Figure 6A**). This is interesting because an overexpression of *MtSWEET1b*, also a glucose transporter, led also to an increase in the mycorrhization levels in *M. truncatula* when inoculated by *R. irregularis* (An et al., 2019). However, this increase was also reflected in a higher *RiTEF* expression but not on a higher *MtPT4* expression (An et al., 2019), suggesting that MtSWEET1b and StSWEET7a despite transporting the same substrate are not fully redundant to each other. An and coworkers hypothesized that a higher MtSWEET1b activity could fuel monosaccharides toward the apoplast increasing fungal growth (An et al., 2019). Our results for StSWEET7a rather suggest that its role could be to support arbuscule functioning. However, we could not observe any significant change in the amount of phosphate accumulated in shoots between *StSWEET7a* overexpressing and control plants (**Figure 4D**). Another interesting observation of An et al. (2019) was that while impairment of the transport activity of MtSWEET1b did not alter mycorrhizal colonization, the expression of a dominant negative form accelerated arbuscule turn over and decreased *MtPT4* expression. This suggests that MtSWEET1b is able to oligomerize with itself or with other SWEETs, as it has been demonstrated for AtSWEET1 (Xuan et al., 2013). Therefore, it is tempting to speculate that StSWEET1b and

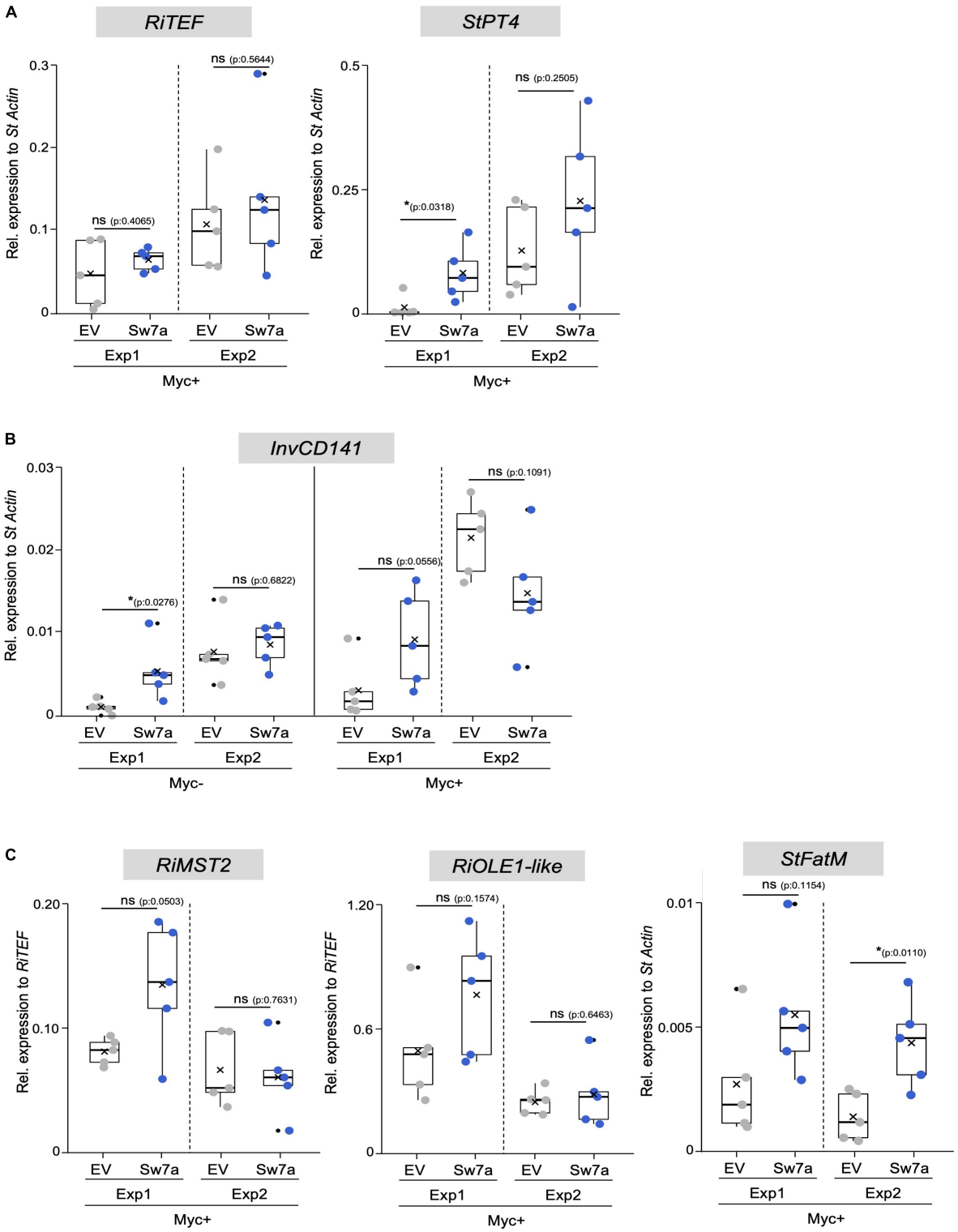

FIGURE 6 | Gene expression analysis in potato roots ectopically expressing *StSWEET7a*. The impact of *StSWEET7a* overexpression on the colonization by *R. irregularis* was analyzed by qRT-PCR in roots of composite plants under the two experimental conditions (Exp1 and Exp2) using several symbiotic markers. **(A)** *RiTEF* and *StPT4* expression, **(B)** *StInvCD141*, **(C)** *RiMST2*, *RiOLE1*-like, *StFatM*. Transcript levels were normalized to *StActin* in the case of plant genes and *RiTEF* and to *RiTEF* in the case of fungal genes. Statistical significance was calculated either using a two-tailed Student's *T*-test or the Mann–Whitney U test, depending on the normality, as explained in section "Materials and Methods." Significance is given by *p*. Exact *p*-values are shown, ns, non-significant, $p > 0.05$; $^{*}p < 0.05$; $^{**}p < 0.01$.

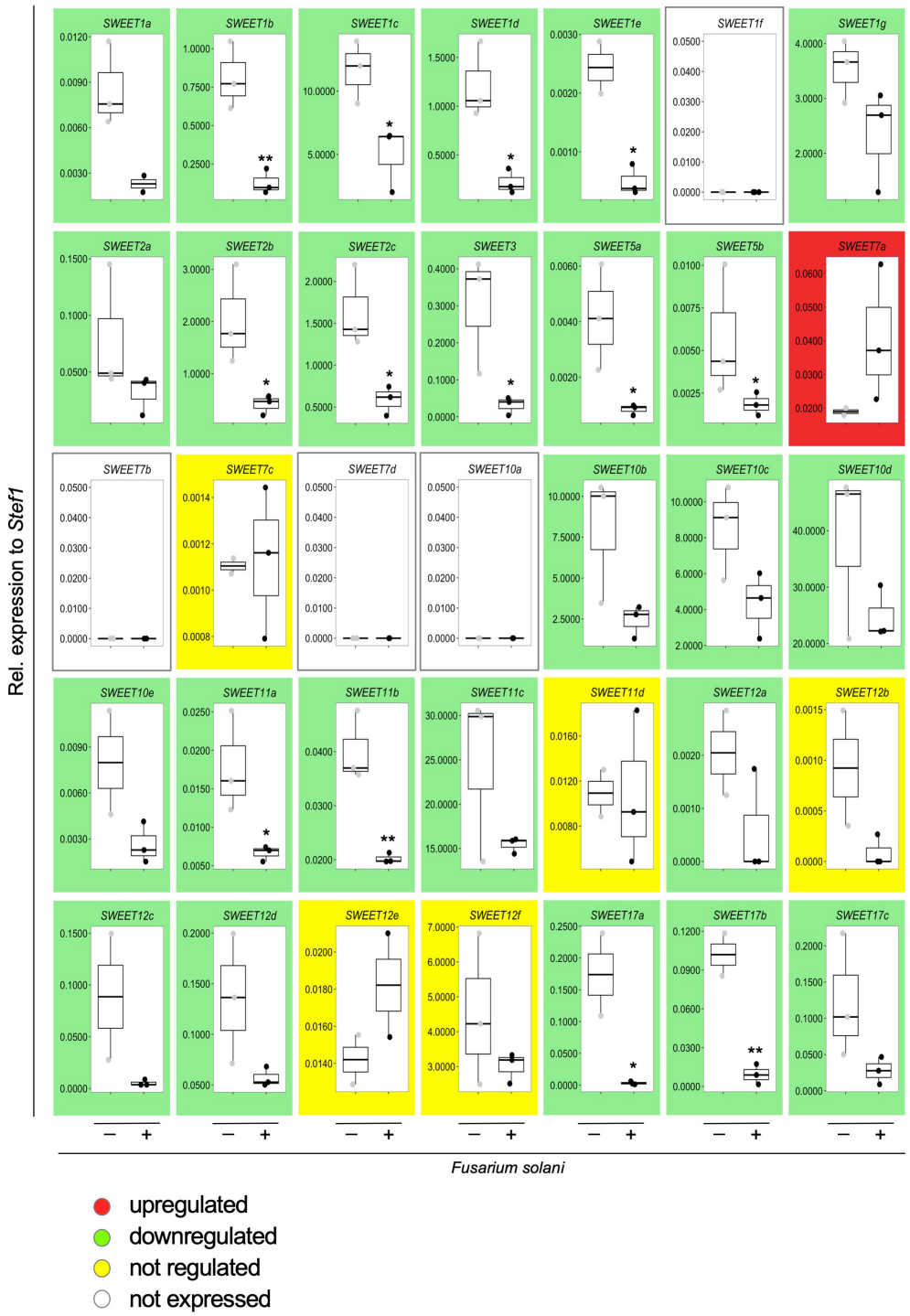

FIGURE 7 | Effect of the infection by the necrotrophic fungus *Fusarium solani* on the expression of potato *SWEET* genes. Transcript levels of all potato *SWEET* genes in response to infection by *F. solani* were analyzed by qRT-PCR and normalized to *StTEF1*. Background color indicates whether the gene at issue is upregulated (red), downregulated (green), not regulated (yellow), or not expressed (white) in response to infection with *F. solani*. Pairwise comparisons were done with a two-tailed Student's *T*-test. Significance is indicated with asterisks, $^{*}p < 0.05$ or $^{**}p < 0.01$.

StSWEET7a, which are both induced in arbuscule-containing cells in potato, could be acting as a dimer controlling glucose transport during symbiosis.

Interestingly, shoot decapitation prior transplanting in Exp2 accelerated mycorrhizal colonization as compared to Exp1, but eliminated the advantage given by the ectopic expression

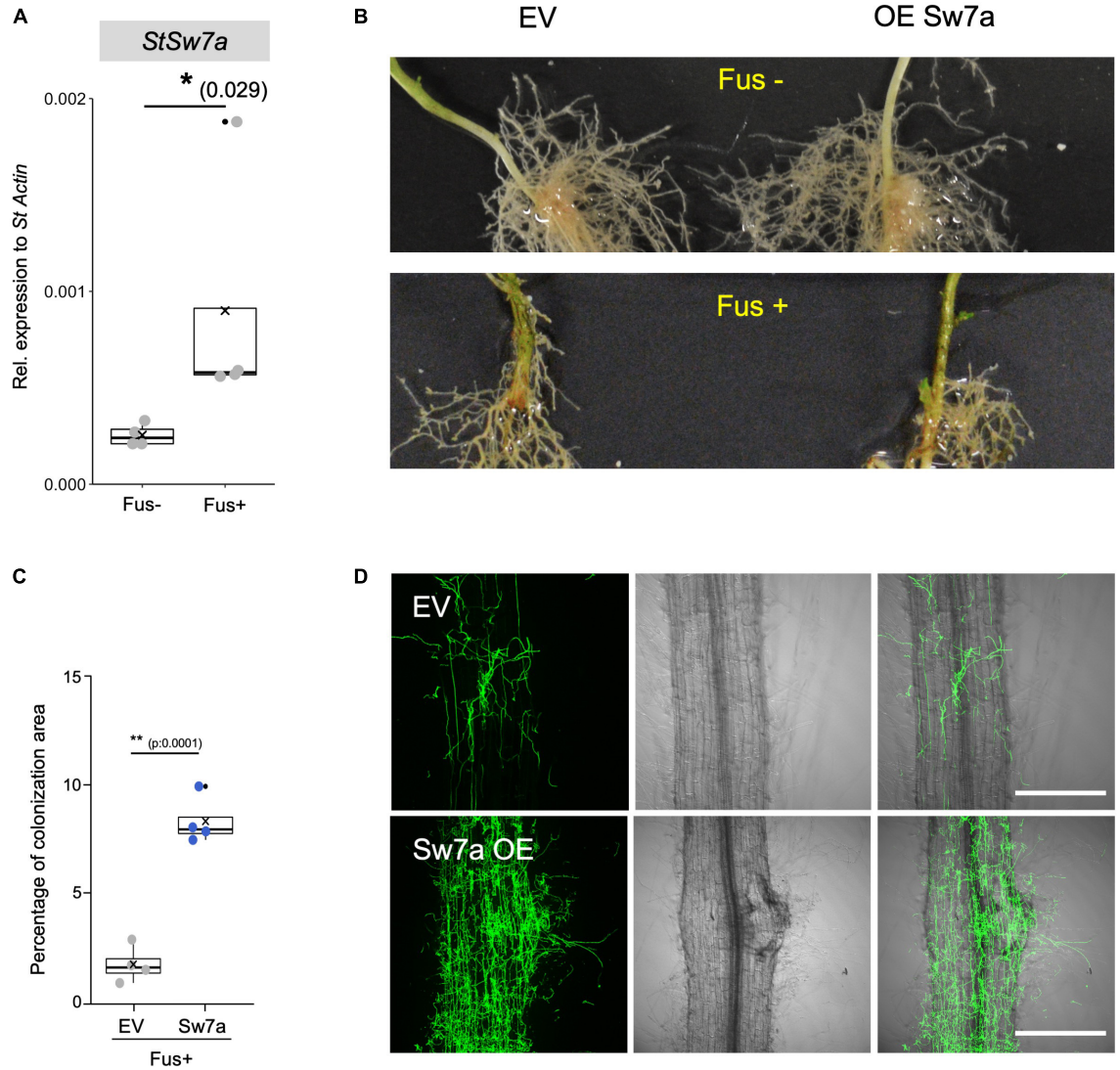

FIGURE 8 | Ectopic expression of *StSWEET7a* accelerates potato root colonization by *Fusarium oxysporum* f. sp. *tuberosi*. **(A)** Colonization of potato roots by *F. oxysporum* f. sp. *tuberosi* significantly induces expression of *StSWEET7a* as shown by qRT-PCR normalized to *StActin*. Four biological replicates were analyzed ($n = 4$). Significance was calculated with a Mann–Whitney U test and represented by an asterisk, $^*p < 0.05$. **(B)** Symptoms caused by *F. oxysporum* f. sp. *tuberosi* (Fus+) at the base of the shoot in both EV and *StSWEET7a* composite plants are shown as compared to non-infected plants (Fus–). **(C)** The extent of colonization by *Fusarium* was calculated as the fraction of root surface area covered by fungus using the Fiji software after staining the fungus with WGA-FITC. Confocal microscopy pictures from different root regions for each treatment (four biological replicates each) were taken, with $n > 17$, (*n*, number of root sections analyzed for each treatment). **(D)** Representative confocal microscopy pictures showing the colonization of EV and *StSWEET7a* overexpressing roots by *F. oxysporum* f. sp. *tuberosi*. The fungus was stained using WGA-FITC (left, green channel; center, bright field; right, overlay). Scale bar corresponds to 200 μm.

of *StSWEET7a,* and all plants were equally well colonized (**Figures 5A,B**). In agreement, *StPT4* levels were in general higher in Exp2 but there were no significant differences between treatments (**Figure 6A**).

In order to investigate whether the increased colonization in roots observed in Exp1 in response to the expression of *StSWEET7a* was related to changes in the carbon partitioning, the expression of the cell wall-bound invertase, that cleaves sucrose into glucose and fructose in the apoplast of sink organs, was analyzed in roots. Cell wall-bound invertases are essential enzymes for apoplastic phloem unloading and sink induction (Proels and Huckelhoven, 2014) and their expression and activity are known to be induced during symbiosis with arbuscular mycorrhizal fungi (Schaarschmidt et al., 2006). This induction takes place in and around arbuscule-containing cells, indicating that colonized cells act as a new sink organ. In potato, induction of *StInvCD141* gene expression paralleled to the expression of the mycorrhiza-induced SWEETs, including *StSWEET7a* (Manck-Gotzenberger and Requena, 2016). Here we could show that ectopic expression of *StSWEET7a* in roots significantly induces *StInvCD141* transcript accumulation under non-mycorrhizal conditions (**Figure 6B**), consistent with the hypothesized higher

sink strength in those roots. In mycorrhizal plants, which already have a higher level of invertase expression, *StSWEET7a* also promoted transcript accumulation of *StInvCD141*, albeit not significantly. As we have shown above, StSWEE7a is able to transport glucose and fructose, and thus, we speculated that its constitutive expression in roots depletes the apoplast of those sugars inducing the cell wall-bound invertase what in turn boosts the unloading of sucrose from the phloem. A similar situation has been observed in tomato sink leaves, where SlSWEET1a fuels the unloading of sucrose from the phloem by taking up hexoses into phloem parenchyma (Ho et al., 2019). In agreement with our hypothesis that shoot decapitation prior transplanting increased sink strength in roots, invertase expression was higher in Exp2 than in Exp1 in all treatments, but differences between control and *StSWEET7a* overexpressing plants were no longer visible (**Figure 6B**).

We next investigated how these changes affected the expression of other symbiotic markers and, in particular, how the transport of fixed carbon toward the fungus could be affected. AM fungi are known to take up sugars, in the form of monosaccharides, and lipids from cortical cells (Choi et al., 2018). Thus, *RiMST2*, a fungal monosaccharide transporter only expressed during symbiosis was shown to import glucose and be critical for arbuscule integrity (Helber et al., 2011). Furthermore, AM fungi are fatty acid auxotrophs (Wewer et al., 2014), and arbuscules have been also shown to be nourished by monoacyl fatty acids synthesized in arbuscule-containing cells with the concomitant participation of several mycorrhiza-specific enzymes (Pimprikar et al., 2016; Bravo et al., 2017; Luginbuehl et al., 2017). We therefore analyzed the expression of two fungal markers, *RiMST2*, and *RiOLE1-like*, an acyl-CoA desaturase responsible for the synthesis of the unusual fatty acid, palmitvaccenic acid ($16{:}1^{\Delta 11 cis}$) which is characteristic of AM fungi (Olsson et al., 1995; Graham, 2000; Brands et al., 2020; Cheeld et al., 2020). In addition, and the expression of the plant marker *StFatM*, the ortholog of *MtFatM*, the plastidial acyl-ACP thioesterase mycorrhiza specific and required for lipid accumulation in the fungus was also investigated (Bravo et al., 2017; Brands et al., 2018). All three markers were transcriptionally more elevated in plants expressing *StSWEET7a* in Exp1, although none of them significantly, suggesting a higher metabolic activity in those roots (**Figure 6C**). Surprisingly, while both fungal genes were no longer regulated in Exp2, expression of *StFatM* was significantly induced in plants expressing *StSWEET7a*, although colonization in those plants was identical to control plants (**Figure 5B**). Taken together, these results suggest that the increase of the sink capacity mediated by the overexpression of *StSWEET7a* leads to an increased transport of fixed carbon toward the fungus boosting arbuscule development in the root.

The Pathogen *Fusarium solani* Represses Most Potato *SWEET* Genes in Roots but Induces *StSWEET7a*

That overexpression of *StSWEET7a* in mycorrhizal potato roots led to an increase in the colonization of roots prompted us to investigate how the colonization by a pathogenic fungus would be affected in those plants. Sugars in the apoplast might play a dual role (Bezrutczyk et al., 2018). On one hand they serve as food for pathogens, and thus plants will try to downregulate sugar export while pathogens will seek the opposite. And on the other hand, apoplastic sugars have been shown to act as signals inducing defense reactions (Herbers et al., 1996; Herbers and Sonnewald, 1998). And hence both, the plant and the pathogen, might try to regulate sugar export/import to induce or prevent the elicitation of defense reactions. It is therefore not surprising that in addition to SWEET transporters, pathogens also induce monosaccharide transporters that likely try to compensate leakage of sugars to the microbial side (Fotopoulos et al., 2003; Lemonnier et al., 2014; Moore et al., 2015).

Therefore, we first analyzed the expression of all potato *SWEETs* in response to *F. solani*. This necrotrophic fungus is the cause of potato tuber rot and can rapidly colonize the root system of *S. tuberosum*. We inoculated potato roots with *F. solani* spores and collected samples after 48 h when the fungus was extensively developing in the apoplastic spaces of the root cortex, but necrosis has not yet set on, and analyzed *SWEET* expression (**Figure 7**). Surprisingly, and in contrast to the reprogramming of SWEET genes observed during mycorrhizal colonization that included many upregulated genes (Manck-Gotzenberger and Requena, 2016), inoculation with *F. solani* repressed the expression of the majority of *SWEET* genes, including *StSWEET1b, 2b, 2c and 12a* (**Figure 7**). This is reminiscent of the situation observed when tomato cotyledons were infected with the necrotrophic fungus *B. cinerea* (Asai et al., 2016). In that experiment, most of the *SWEET* transporters were donwregulated in the pre-necrotic stage and only one transporter *SlSWEET15* was induced in response to *B. cinerea*. The authors suggested that *B. cinerea* uses SlSWEET15 to obtain glucose and sucrose from living tomato cells prior inducing the necrotrophic stage (Asai et al., 2016). In contrast, the reason why so many other transporters were downregulated, as it is also the case in our experiment is not clear. It is possible that either plants try to limit the amount of sugar released to the apoplastic space to limit pathogen development, or to change the hexose/sucrose ratio to elicit defense reactions as mentioned above. But alternatively, this repression might be mediated by the pathogen in order to prevent such defense reactions.

Interestingly, the only potato *SWEET* gene that showed an upregulation in response to *F. solani* (albeit not significant) was *StSWEET7a* (**Figure 7**), suggesting that colonization by the pathogen might activate the expression of this transporter to provide the fungus with monosaccharides and/or to increase the sink strength of the root, as in the case of *B. cinerea* in tomato (*SlSWEET15*) or in *V. vinifera* (*VvSWEET7*) (Asai et al., 2016; Breia et al., 2019). We then went on to analyze the expression of *StSWEET7a* in potato plants colonized by *F. oxysporum* f. sp. *tuberosi*, a less aggressive pathogen than *F. solani* (Manici and Cerato, 1994), that rather behaves like a hemi-biotrophic fungus and takes longer to colonize the root and produces a variety of symptoms such as wilting, stem end rot, chlorosis, necrosis or damping-off (Majeed et al., 2018). Results showed that this species also induces the expression of *StSWEET7a* in roots

(**Figure 8A**), suggesting that perhaps a common mechanism of induction might take place in all cases.

Overexpression of *StSWEET7a* Accelerates Root Colonization by *Fusarium oxysporum* f. sp. *tuberosi*

To investigate the role of StSWEET7a in the *F. oxysporum* f. sp. *tuberosi* infection we inoculated plants ectopically expressing *StSWEET7a* in roots or control plants. Although all plants were colonized, there were no wilting symptoms at the end of the experiment. Only minor stem end rot symptoms occurred, but there were no differences between the two treatments (**Figure 8B**). This lack of wilting symptoms by some *F. oxysporum* f. sp. *tuberosi* strains causing dry rot is not unusual, and it has been previously reported (Tivoli et al., 1988; Manici and Cerato, 1994). However, the microscopic observation of roots, clearly showed their colonization by the fungus. Furthermore, it could be observed that increasing the expression of *StSWEET7a* in roots led to a faster colonization (**Figures 8C,D** and **Supplementary Figure 2**). Overall, these results support the hypothesis that induction of *StSWEET7a* by *Fusarium* serves the feeding of the fungus by increasing unloading of sucrose from the apoplast and thus mirroring the effect of root colonization by the symbiotic fungus *R. irregularis* as described above. In addition, we cannot exclude that StSWEET7a might directly feed root colonizing fungi by exporting monosaccharides at the places of colonization.

Similar results in other plants have been observed in response to ectopic expression of other *SWEET* genes. Thus, in rice, colonization by the necrotrophic *Rhizoctonia solani* induces the expression of *OsSWEET11*, and plants overexpressing this transporter were faster colonized than control plants (Gao et al., 2018). Also, *A. thaliana* plants in which *AtSWEET4* was deleted were more resistant to *B. cinerea* (Chong et al., 2014). However, this is not always the case, and in some cases, overexpression of several *SWEET* genes led to increased resistance toward certain pathogens. Thus, overexpression of *VvSWEET4* in *V. vinifera* led to a decreased susceptibility toward *Pythium irregulare* (Meteier et al., 2019). The authors explain this effect, which is contrary to the observations made by Chong et al. (2014) in the same group, by explaining that the rise in sugars in roots expressing *VvSWEET4* was responsible for the observed increase in flavonoid compounds that ultimately acted as antifungal agents (Meteier et al., 2019). Also, in sweet potato, resistance to *F. oxysporum* was induced in transgenic plants overexpressing *IbSWEET10* (Li et al., 2017). Here the authors suggested that reduction in sugar content (sucrose, glucose, and fructose) observed in leaves of the transgenic plants contributed to restrict the growth of the pathogen (Li et al., 2017).

CONCLUSION

Sugar transport is the hub where plants and their colonizing microbes converge to regulate it in their own benefit and SWEET transporters are emerging as important players in this market. However, because plants are in nature not colonized by just one type of microorganism, it seems currently difficult to predict how induction or deletion of a specific SWEET gene might impact on the colonization of this plant by this or by other pathogenic/symbiotic microbes. This makes it difficult to use these transporters as targets to improve plant growth or resistance. Therefore, attention should be paid to different aspects such as the root organ in which SWEET transporters are induced by microbes, whether deregulation takes place systemically or in one specific organ, as well as the type of microbial interaction (biotrophic or necrotrophic). All these are key factors that need to be taken into account in a more systematic manner. An outstanding question is also how microbes regulate expression of *SWEET* genes by mechanisms other than those involving TAL effectors. Are there other effectors? Why are some transporters like StSWEET7a induced by pathogenic and symbiotic fungi? Do they use the same activation mechanisms? And in case plants are colonized by both microbes simultaneously, how will plant susceptibility be affected by the deregulation of StSWEET7a? Can we learn of these mechanisms to produce improved plants? These and many other questions remain yet unsolved and will require further research efforts.

DATA AVAILABILITY STATEMENT

The datasets presented in this study can be found either in the NCBI database or in the Solgenomics database.

AUTHOR CONTRIBUTIONS

NR, ET, and JM-G conceptualized the work. ET, JM-G, and DF-G carried out the experiments. NR wrote the manuscript with contributions from ET and DF-G. All authors contributed to the article and approved the submitted version.

FUNDING

ET was supported by a postdoctoral fellowship from the Alfonso Martin Escudero Foundation, Spain.

ACKNOWLEDGMENTS

We are grateful to E. Boles (Frankfurt University) for providing the EBY.VW400 yeast strain and to R. Fischer (KIT) for reading and comments on the manuscript. We are thankful to L. Hilbert (KIT) for his help with the fluorescence quantification of fungal root colonization. We also thank S. Heupel and W. Gubaidulin for excellent technical assistance.

SUPPLEMENTARY MATERIAL

The Supplementary Material for this article can be found online at: https://www.frontiersin.org/articles/10.3389/fpls.2022.837231/full#supplementary-material

Supplementary Figure 1 | Ectopic expression of *StSWEET7a* in roots modifies plant architecture and survival after transplanting. **(A)** Relative expression of *StSWEET7a* (*StSw7a*) normalized to *StActin* was measured by qRT-PCR in roots of composite plants grown under two mycorrhizal conditions (Myc−, Myc+) and under two different experimental conditions (Exp1 and Exp2). Statistical significance was calculated using the Mann–Whitney U test. Significance is given by *p*-values. Exact *p*-values are given, ns, non-significant, $p > 0.05$; $^{*}p < 0.05$; $^{**}p < 0.01$. **(B)** Leaf surface and shoot branching were analyzed in plants ectopically expressing *StSWEET7a* as compared to EV plants. The number of biological replicates for each treatment for leaf surface analyses was five ($n = 5$) with five leaves analyzed per biological replicate. Six biological replicates per treatment were analyzed for root branching ($n = 6$). Statistical significance was calculated either using a two-tailed Student's *T*-test (leaf surface) or the Mann–Whitney U test (shoot branching), depending on the normality, as explained in section "Materials and Methods." Significance is given by *p*-values. Exact *p*-values are given, ns, non-significant, $p > 0.05$; $^{*}p < 0.05$; $^{**}p < 0.01$. **(C)** Survival percentage of transformed plants after transplanting to pots comparing plants expressing StSWEET7a in roots vs. EV plants. Significance was calculated according to the Kruskal–Wallis and each pair of groups was compared using the Mann–Whitney U test. Different letters indicate significance with *p*-value < 0.05. **(D)** Percentage of vesicles (as number of vesicles per root segment) of transformed plants expressing *StSWEET7a* in roots compared to EV plants. Statistical significance was calculated using a two-tailed Student's *T*-test. $^{*}p < 0.05$.

Supplementary Figure 2 | Representative pictures of plant roots infected with *Fusarium oxysporum* f. sp. *tuberosi* in plants expressing *StSWEET7a* or an empty vector (EV). Confocal microscopy pictures showing *F. oxysporum* f. sp. *tuberosi* colonization 7 weeks post inoculation in four different transgenic lines for each treatment. The fungus was stained with WGA-FITC (left, bright field; center, green channel; right, overlay). Scale bar corresponds to 200 μm.

REFERENCES

Abelenda, J. A., Bergonzi, S., Oortwijn, M., Sonnewald, S., Du, M., Visser, R. G. F., et al. (2019). Source-Sink Regulation Is Mediated by Interaction of an FT Homolog with a SWEET Protein in Potato. *Curr. Biol.* 29, 1178–1186e1176. doi: 10.1016/j.cub.2019.02.018

An, J., Zeng, T., Ji, C., de Graaf, S., Zheng, Z., Xiao, T. T., et al. (2019). A *Medicago truncatula* SWEET transporter implicated in arbuscule maintenance during arbuscular mycorrhizal symbiosis. *New Phytol.* 224, 396–408. doi: 10.1111/nph.15975

Antony, G., Zhou, J., Huang, S., Li, T., Liu, B., White, F., et al. (2010). Rice *xa13* recessive resistance to bacterial blight is defeated by induction of the disease susceptibility gene *Os-11N3*. *Plant Cell* 22, 3864–3876. doi: 10.1105/tpc.110.078964

Asai, Y., Kobayashi, Y., and Kobayashi, I. (2016). Increased expression of the tomato *SlSWEET15* gene during grey mold infection and the possible involvement of the sugar efflux to apoplasm in the disease susceptibility. *J. Plant Pathol. Microbiol.* 7:329.

Barbier, F. F., Peron, T., Lecerf, M., Perez-Garcia, M. D., Barriere, Q., Rolcik, J., et al. (2015a). Sucrose is an early modulator of the key hormonal mechanisms controlling bud outgrowth in *Rosa hybrida*. *J. Exp. Bot.* 66, 2569–2582. doi: 10.1093/jxb/erv047

Barbier, F. F., Lunn, J. E., and Beveridge, C. A. (2015b). Ready, steady, go! A sugar hit starts the race to shoot branching. *Curr. Opin. Plant Biol.* 25, 39–45. doi: 10.1016/j.pbi.2015.04.004

Bécard, G., and Fortin, J. A. (1988). Early events of vesicular–arbuscular mycorrhiza formation on Ri T-DNA transformed roots. *New Phytol.* 108, 211–218. doi: 10.1111/j.1469-8137.1988.tb03698.x

Bezrutczyk, M., Yang, J., Eom, J. S., Prior, M., Sosso, D., Hartwig, T., et al. (2018). Sugar flux and signaling in plant-microbe interactions. *Plant J.* 93, 675–685. doi: 10.1111/tpj.13775

Bitterlich, M., Krugel, U., Boldt-Burisch, K., Franken, P., and Kuhn, C. (2014). The sucrose transporter SlSUT2 from tomato interacts with brassinosteroid functioning and affects arbuscular mycorrhiza formation. *Plant J.* 78, 877–889. doi: 10.1111/tpj.12515

Boldt, K., Pors, Y., Haupt, B., Bitterlich, M., Kuhn, C., Grimm, B., et al. (2011). Photochemical processes, carbon assimilation and RNA accumulation of sucrose transporter genes in tomato arbuscular mycorrhiza. *J. Plant Physiol.* 168, 1256–1263. doi: 10.1016/j.jplph.2011.01.026

Brands, M., Cahoon, E. B., and Dormann, P. (2020). Palmitvaccenic Acid (Delta11-cis-hexadecenoic acid) Is Synthesized by an OLE1-like Desaturase in the Arbuscular Mycorrhiza Fungus *Rhizophagus irregularis*. *Biochemistry* 59, 1163–1172. doi: 10.1021/acs.biochem.0c00051

Brands, M., Wewer, V., Keymer, A., Gutjahr, C., and Dormann, P. (2018). The Lotus japonicus acyl-acyl carrier protein thioesterase FatM is required for mycorrhiza formation and lipid accumulation of *Rhizophagus irregularis*. *Plant J.* 95, 219–232. doi: 10.1111/tpj.13943

Bravo, A., Brands, M., Wewer, V., Dormann, P., and Harrison, M. J. (2017). Arbuscular mycorrhiza-specific enzymes FatM and RAM2 fine-tune lipid biosynthesis to promote development of arbuscular mycorrhiza. *New Phytol.* 214, 1631–1645. doi: 10.1111/nph.14533

Breia, R., Conde, A., Badim, H., Fortes, A. M., Geros, H., and Granell, A. (2021). Plant SWEETs: from sugar transport to plant-pathogen interaction and more unexpected physiological roles. *Plant Physiol.* 186, 836–852. doi: 10.1093/plphys/kiab127

Breia, R., Conde, A., Pimentel, D., Conde, C., Fortes, A. M., Granell, A., et al. (2019). VvSWEET7 Is a Mono- and Disaccharide Transporter Up-Regulated in Response to *Botrytis cinerea* Infection in Grape Berries. *Front. Plant Sci.* 10:1753. doi: 10.3389/fpls.2019.01753

Carlson, M., and Botstein, D. (1982). Two differentially regulated mRNAs with different 5' ends encode secreted with intracellular forms of yeast invertase. *Cell* 28, 145–154. doi: 10.1016/0092-8674(82)90384-1

Cheeld, H., Bhutada, G., Beaudoin, F., and Eastmond, P. J. (2020). DES2 is a fatty acid Delta11 desaturase capable of synthesizing palmitvaccenic acid in the arbuscular mycorrhizal fungus *Rhizophagus irregularis*. *FEBS Lett.* 594, 1770–1777. doi: 10.1002/1873-3468.13762

Chen, H. Y., Huh, J. H., Yu, Y. C., Ho, L. H., Chen, L. Q., Tholl, D., et al. (2015). The *Arabidopsis* vacuolar sugar transporter SWEET2 limits carbon sequestration from roots and restricts Pythium infection. *Plant J.* 83, 1046–1058. doi: 10.1111/tpj.12948

Chen, L. Q., Cheung, L. S., Feng, L., Tanner, W., and Frommer, W. B. (2015). Transport of sugars. *Annu. Rev. Biochem.* 84, 865–894. doi: 10.1146/annurev-biochem-060614-033904

Chen, L. Q., Hou, B. H., Lalonde, S., Takanaga, H., Hartung, M. L., Qu, X. Q., et al. (2010). Sugar transporters for intercellular exchange and nutrition of pathogens. *Nature* 468, 527–532. doi: 10.1038/nature09606

Chen, L. Q., Qu, X. Q., Hou, B. H., Sosso, D., Osorio, S., Fernie, A. R., et al. (2012). Sucrose efflux mediated by SWEET proteins as a key step for phloem transport. *Science* 335, 207–211. doi: 10.1126/science.1213351

Choi, J., Summers, W., and Paszkowski, U. (2018). Mechanisms Underlying Establishment of Arbuscular Mycorrhizal Symbioses. *Annu. Rev. Phytopathol.* 56, 135–160. doi: 10.1146/annurev-phyto-080516-035521

Chong, J., Piron, M. C., Meyer, S., Merdinoglu, D., Bertsch, C., and Mestre, P. (2014). The SWEET family of sugar transporters in grapevine: VvSWEET4 is involved in the interaction with *Botrytis cinerea*. *J. Exp. Bot.* 65, 6589–6601. doi: 10.1093/jxb/eru375

Cohn, M., Bart, R. S., Shybut, M., Dahlbeck, D., Gomez, M., Morbitzer, R., et al. (2014). *Xanthomonas axonopodis* virulence is promoted by a transcription activator-like effector-mediated induction of a SWEET sugar transporter in cassava. *Mol. Plant Microbe Interact.* 27, 1186–1198. doi: 10.1094/MPMI-06-14-0161-R

Di Pietro, A., Garcia-MacEira, F. I., Meglecz, E., and Roncero, M. I. (2001). A MAP kinase of the vascular wilt fungus *Fusarium oxysporum* is essential for root penetration and pathogenesis. *Mol. Microbiol.* 39, 1140–1152.

Doidy, J., Grace, E., Kuhn, C., Simon-Plas, F., Casieri, L., and Wipf, D. (2012). Sugar transporters in plants and in their interactions with fungi. *Trends Plant Sci.* 17, 413–422. doi: 10.1016/j.tplants.2012.03.009

Eom, J. S., Chen, L. Q., Sosso, D., Julius, B. T., Lin, I. W., Qu, X. Q., et al. (2015). SWEETs, transporters for intracellular and intercellular sugar translocation. *Curr. Opin. Plant Biol.* 25, 53–62. doi: 10.1016/j.pbi.2015.04.005

Fotopoulos, V., Gilbert, M. J., Pittman, J. K., Marvier, A. C., Buchanan, A. J., Sauer, N., et al. (2003). The monosaccharide transporter gene, AtSTP4, and the cell-wall invertase, Atbetafruct1, are induced in *Arabidopsis* during infection with the fungal biotroph *Erysiphe cichoracearum*. *Plant Physiol.* 132, 821–829. doi: 10.1104/pp.103.021428

Gao, Y., Zhang, C., Han, X., Wang, Z. Y., Ma, L., Yuan, P., et al. (2018). Inhibition of OsSWEET11 function in mesophyll cells improves resistance of rice to sheath blight disease. *Mol. Plant Pathol.* 19, 2149–2161. doi: 10.1111/mpp.12689

Gebauer, P., Korn, M., Engelsdorf, T., Sonnewald, U., Koch, C., and Voll, L. M. (2017). Sugar Accumulation in Leaves of *Arabidopsis sweet11/sweet12* Double Mutants Enhances Priming of the Salicylic Acid-Mediated Defense Response. *Front. Plant Sci.* 8:1378. doi: 10.3389/fpls.2017.01378

Gietz, R. D., and Woods, R. A. (2002). Transformation of yeast by lithium acetate/single-stranded carrier DNA/polyethylene glycol method. *Methods Enzymol.* 350, 87–96. doi: 10.1016/s0076-6879(02)50957-5

Graham, J. H. (2000). *Assessing costs of arbuscular mycorrhizal symbiosis in agroecosystems*. Eagan, MN: APS Press.

Guimil, S., Chang, H. S., Zhu, T., Sesma, A., Osbourn, A., Roux, C., et al. (2005). Comparative transcriptomics of rice reveals an ancient pattern of response to microbial colonization. *Proc. Natl. Acad. Sci. U S A* 102, 8066–8070. doi: 10.1073/pnas.0502999102

Guo, W. J., Nagy, R., Chen, H. Y., Pfrunder, S., Yu, Y. C., Santelia, D., et al. (2014). SWEET17, a facilitative transporter, mediates fructose transport across the tonoplast of Arabidopsis roots and leaves. *Plant Physiol.* 164, 777–789. doi: 10.1104/pp.113.232751

Hacquard, S., Kracher, B., Hiruma, K., Munch, P. C., Garrido-Oter, R., Thon, M. R., et al. (2016). Survival trade-offs in plant roots during colonization by closely related beneficial and pathogenic fungi. *Nat. Commun.* 7:11362. doi: 10.1038/ncomms11362

Heck, C., Kuhn, H., Heidt, S., Walter, S., Rieger, N., and Requena, N. (2016). Symbiotic Fungi Control Plant Root Cortex Development through the Novel GRAS Transcription Factor MIG1. *Curr. Biol.* 26, 2770–2778. doi: 10.1016/j.cub.2016.07.059

Helber, N., Wippel, K., Sauer, N., Schaarschmidt, S., Hause, B., and Requena, N. (2011). A versatile monosaccharide transporter that operates in the arbuscular mycorrhizal fungus *Glomus* sp is crucial for the symbiotic relationship with plants. *Plant Cell* 23, 3812–3823. doi: 10.1105/tpc.111.089813

Herbers, K., Meuwly, P., Frommer, W. B., Metraux, J. P., and Sonnewald, U. (1996). Systemic Acquired Resistance Mediated by the Ectopic Expression of Invertase: Possible Hexose Sensing in the Secretory Pathway. *Plant Cell* 8, 793–803. doi: 10.1105/tpc.8.5.793

Herbers, K., and Sonnewald, U. (1998). Molecular determinants of sink strength. *Curr. Opin. Plant Biol.* 1, 207–216. doi: 10.1016/s1369-5266(98)80106-4

Ho, L. H., Klemens, P. A. W., Neuhaus, H. E., Ko, H. Y., Hsieh, S. Y., and Guo, W. J. (2019). SlSWEET1a is involved in glucose import to young leaves in tomato plants. *J. Exp. Bot.* 70, 3241–3254. doi: 10.1093/jxb/erz154

Horn, P., Santala, J., Nielsen, S. L., Huhns, M., Broer, I., and Valkonen, J. P. (2014). Composite potato plants with transgenic roots on non-transgenic shoots: a model system for studying gene silencing in roots. *Plant Cell Rep.* 33, 1977–1992. doi: 10.1007/s00299-014-1672-x

Hu, Y., Zhang, J., Jia, H., Sosso, D., Li, T., Frommer, W. B., et al. (2014). Lateral organ boundaries 1 is a disease susceptibility gene for citrus bacterial canker disease. *Proc. Natl. Acad. Sci. U S A* 111, E521–E529. doi: 10.1073/pnas.1313271111

Kafle, A., Garcia, K., Wang, X., Pfeffer, P. E., Strahan, G. D., and Bucking, H. (2019). Nutrient demand and fungal access to resources control the carbon allocation to the symbiotic partners in tripartite interactions of *Medicago truncatula*. *Plant Cell Environ.* 42, 270–284. doi: 10.1111/pce.13359

Kanno, Y., Oikawa, T., Chiba, Y., Ishimaru, Y., Shimizu, T., Sano, N., et al. (2016). AtSWEET13 and AtSWEET14 regulate gibberellin-mediated physiological processes. *Nat. Commun.* 7:13245. doi: 10.1038/ncomms13245

Keymer, A., Pimprikar, P., Wewer, V., Huber, C., Brands, M., Bucerius, S. L., et al. (2017). Lipid transfer from plants to arbuscular mycorrhiza fungi. *Elife* 6:29107. doi: 10.7554/eLife.29107

Kim, J. Y., Loo, E. P., Pang, T. Y., Lercher, M., Frommer, W. B., and Wudick, M. M. (2021). Cellular export of sugars and amino acids: role in feeding other cells and organisms. *Plant Physiol.* 2021:228. doi: 10.1093/plphys/kiab228

Klemens, P. A., Patzke, K., Deitmer, J., Spinner, L., Le Hir, R., Bellini, C., et al. (2013). Overexpression of the vacuolar sugar carrier AtSWEET16 modifies germination, growth, and stress tolerance in *Arabidopsis*. *Plant Physiol.* 163, 1338–1352. doi: 10.1104/pp.113.224972

Kruger, M., Kruger, C., Walker, C., Stockinger, H., and Schussler, A. (2012). Phylogenetic reference data for systematics and phylotaxonomy of arbuscular mycorrhizal fungi from phylum to species level. *New Phytol.* 193, 970–984. doi: 10.1111/j.1469-8137.2011.03962.x.

Kryvoruchko, I. S., Sinharoy, S., Torres-Jerez, I., Sosso, D., Pislariu, C. I., Guan, D., et al. (2016). MtSWEET11, a Nodule-Specific Sucrose Transporter of *Medicago truncatula*. *Plant Physiol.* 171, 554–565. doi: 10.1104/pp.15.01910

Kuhn, H., Kuster, H., and Requena, N. (2010). Membrane steroid-binding protein 1 induced by a diffusible fungal signal is critical for mycorrhization in *Medicago truncatula*. *New Phytol.* 185, 716–733. doi: 10.1111/j.1469-8137.2009.03116.x

Lemonnier, P., Gaillard, C., Veillet, F., Verbeke, J., Lemoine, R., Coutos-Thevenot, P., et al. (2014). Expression of *Arabidopsis* sugar transport protein STP13 differentially affects glucose transport activity and basal resistance to *Botrytis cinerea*. *Plant Mol. Biol.* 85, 473–484. doi: 10.1007/s11103-014-0198-5

Li, Y., Wang, Y., Zhang, H., Zhang, Q., Zhai, H., Liu, Q., et al. (2017). The Plasma Membrane-Localized Sucrose Transporter IbSWEET10 Contributes to the Resistance of Sweet Potato to *Fusarium oxysporum*. *Front. Plant Sci.* 8:197. doi: 10.3389/fpls.2017.00197

Lin, I. W., Sosso, D., Chen, L. Q., Gase, K., Kim, S. G., Kessler, D., et al. (2014). Nectar secretion requires sucrose phosphate synthases and the sugar transporter SWEET9. *Nature* 508, 546–549. doi: 10.1038/nature13082

Liu, J., Maldonado-Mendoza, I., Lopez-Meyer, M., Cheung, F., Town, C. D., and Harrison, M. J. (2007). Arbuscular mycorrhizal symbiosis is accompanied by local and systemic alterations in gene expression and an increase in disease resistance in the shoots. *Plant J.* 50, 529–544. doi: 10.1111/j.1365-313X.2007.03069.x

Liu, Q., Yuan, M., Zhou, Y., Li, X., Xiao, J., and Wang, S. (2011). A paralog of the MtN3/saliva family recessively confers race-specific resistance to *Xanthomonas oryzae* in rice. *Plant Cell Environ.* 34, 1958–1969. doi: 10.1111/j.1365-3040.2011.02391.x

Luginbuehl, L. H., Menard, G. N., Kurup, S., Van Erp, H., Radhakrishnan, G. V., Breakspear, A., et al. (2017). Fatty acids in arbuscular mycorrhizal fungi are synthesized by the host plant. *Science* 356, 1175–1178. doi: 10.1126/science.aan0081

Majeed, N., Javaid, B., Deeba, F., Naqvi, S. M. S., and Douches, D. S. (2018). Enhanced *Fusarium oxysporum* f.sp. *tuberosi* resistance in transgenic potato expressing a rice GLP superoxide dismutase gene. *Am. J. Potato Res.* 95, 383–394. doi: 10.1007/s12230-018-9639-z

Malonek, S., Bomke, C., Bornberg-Bauer, E., Rojas, M. C., Hedden, P., Hopkins, P., et al. (2005). Distribution of gibberellin biosynthetic genes and gibberellin production in the *Gibberella fujikuroi* species complex. *Phytochemistry* 66, 1296–1311. doi: 10.1016/j.phytochem.2005.04.012

Manck-Gotzenberger, J., and Requena, N. (2016). Arbuscular mycorrhiza Symbiosis Induces a Major Transcriptional Reprogramming of the Potato SWEET Sugar Transporter Family. *Front. Plant Sci.* 7:487. doi: 10.3389/fpls.2016.00487

Manici, L. M., and Cerato, C. (1994). Pathogenicity of *Fusarium oxysporum* f.sp. *tuberosi* isolates from tubers and potato plants. *Potato Res.* 37, 129–134. doi: 10.1007/Bf02358713

Mason, M. G., Ross, J. J., Babst, B. A., Wienclaw, B. N., and Beveridge, C. A. (2014). Sugar demand, not auxin, is the initial regulator of apical dominance. *Proc. Natl. Acad. Sci. U S A* 111, 6092–6097. doi: 10.1073/pnas.1322045111

Meteier, E., La Camera, S., Goddard, M. L., Laloue, H., Mestre, P., and Chong, J. (2019). Overexpression of the *VvSWEET4* Transporter in Grapevine Hairy Roots Increases Sugar Transport and Contents and Enhances Resistance to *Pythium irregulare*, a Soilborne Pathogen. *Front. Plant Sci.* 10:884. doi: 10.3389/fpls.2019.00884

Moore, J. W., Herrera-Foessel, S., Lan, C., Schnippenkoetter, W., Ayliffe, M., Huerta-Espino, J., et al. (2015). A recently evolved hexose transporter variant confers resistance to multiple pathogens in wheat. *Nat. Genet.* 47, 1494–1498. doi: 10.1038/ng.3439

Morii, M., Sugihara, A., Takehara, S., Kanno, Y., Kawai, K., Hobo, T., et al. (2020). The Dual Function of OsSWEET3a as a Gibberellin and Glucose Transporter Is Important for Young Shoot Development in Rice. *Plant Cell Physiol.* 61, 1935–1945. doi: 10.1093/pcp/pcaa130

Murashige, T., and Skoog, F. (1962). A Revised Medium for Rapid Growth and Bio Assays with Tobacco Tissue Cultures. *Physiologia Plantarum* 15, 473–497. doi: 10.1111/j.1399-3054.1962.tb08052.x

Olsson, P. A., Baath, E., Jakobsen, I., and Söderström, B. (1995). The use of phopholipid and neutral lipid fatty acids to estimate biomass of arbuscular mycorrhizal fungi in soil. *Mycol. Res.* 99, 623–629. doi: 10.1016/s0953-7562(09)80723-5

Pimprikar, P., Carbonnel, S., Paries, M., Katzer, K., Klingl, V., Bohmer, M. J., et al. (2016). A CCaMK-CYCLOPS-DELLA Complex Activates Transcription of RAM1 to Regulate Arbuscule Branching. *Curr. Biol.* 26, 987–998. doi: 10.1016/j.cub.2016.01.069

Pozo, M. J., and Azcon-Aguilar, C. (2007). Unraveling mycorrhiza-induced resistance. *Curr. Opin. Plant Biol.* 10, 393–398. doi: 10.1016/j.pbi.2007.05.004

Proels, R. K., and Huckelhoven, R. (2014). Cell-wall invertases, key enzymes in the modulation of plant metabolism during defence responses. *Mol. Plant Pathol.* 15, 858–864. doi: 10.1111/mpp.12139

Rech, S. S., Heidt, S., and Requena, N. (2013). A tandem Kunitz protease inhibitor (KPI106)-serine carboxypeptidase (SCP1) controls mycorrhiza establishment and arbuscule development in *Medicago truncatula*. *Plant J.* 75, 711–725. doi: 10.1111/tpj.12242

Rentsch, D., Laloi, M., Rouhara, I., Schmelzer, E., Delrot, S., and Frommer, W. B. (1995). Ntr1 Encodes a High-Affinity Oligopeptide Transporter in *Arabidopsis*. *Febs Lett.* 370, 264–268. doi: 10.1016/0014-5793(95)00853-2

Salam, B. B., Barbier, F., Danieli, R., Teper-Bamnolker, P., Ziv, C., Spichal, L., et al. (2021). Sucrose promotes stem branching through cytokinin. *Plant Physiol.* 185, 1708–1721. doi: 10.1093/plphys/kiab003

Schaarschmidt, S., Roitsch, T., and Hause, B. (2006). Arbuscular mycorrhiza induces gene expression of the apoplastic invertase LIN6 in tomato (*Lycopersicon esculentum*) roots. *J. Exp. Bot.* 57, 4015–4023. doi: 10.1093/jxb/erl172

Schenck, N., and Smith, G. (1982). Additional new and unreported species of mycorrhizal fungi (Endogonaceae) from Florida. *Mycologia* 74, 77–92. doi: 10.2307/3792631

Schindelin, J., Arganda-Carreras, I., Frise, E., Kaynig, V., Longair, M., Pietzsch, T., et al. (2012). Fiji: an open-source platform for biological-image analysis. *Nat. Methods* 9, 676–682. doi: 10.1038/nmeth.2019

Shachar-Hill, Y., Pfeffer, P. E., Douds, D., Osman, S. F., Doner, L. W., and Ratcliffe, R. G. (1995). Partitioning of Intermediary Carbon Metabolism in Vesicular-Arbuscular Mycorrhizal Leek. *Plant Physiol.* 108, 7–15. doi: 10.1104/pp.108.1.7

Sosso, D., Luo, D., Li, Q. B., Sasse, J., Yang, J., Gendrot, G., et al. (2015). Seed filling in domesticated maize and rice depends on SWEET-mediated hexose transport. *Nat. Genet.* 47, 1489–1493. doi: 10.1038/ng.3422

Streubel, J., Pesce, C., Hutin, M., Koebnik, R., Boch, J., and Szurek, B. (2013). Five phylogenetically close rice SWEET genes confer TAL effector-mediated susceptibility to *Xanthomonas oryzae* pv. *oryzae*. *New Phytol.* 200, 808–819. doi: 10.1111/nph.12411

Talbot, N. J., Ebbole, D. J., and Hamer, J. E. (1993). Identification and characterization of MPG1, a gene involved in pathogenicity from the rice blast fungus *Magnaporthe grisea*. *Plant Cell* 5, 1575–1590. doi: 10.1105/tpc.5.11.1575

Tivoli, B., Torres, H., and French, E. R. (1988). Inventory, Distribution and Aggressivity of Species or Varieties of *Fusarium* Present on Potato or in Its Environment in Different Agroecological Zones in Peru. *Potato Res.* 31, 681–690. doi: 10.1007/Bf02361861

Trouvelot, A., Kough, J., and Gianinazzi-Pearson, V. (1986). *Estimation of VA mycorrhizal infection levels. Research for methods having a functional significance. Physiological and Genetical Aspects of Mycorrhizae*. Paris: INRA Presse, 223–232.

Voinnet, O., Rivas, S., Mestre, P., and Baulcombe, D. (2003). An enhanced transient expression system in plants based on suppression of gene silencing by the p19 protein of tomato bushy stunt virus. *Plant J.* 33, 949–956.

Walerowski, P., Gundel, A., Yahaya, N., Truman, W., Sobczak, M., Olszak, M., et al. (2018). Clubroot Disease Stimulates Early Steps of Phloem Differentiation and Recruits SWEET Sucrose Transporters within Developing Galls. *Plant Cell* 30, 3058–3073. doi: 10.1105/tpc.18.00283

Wewer, V., Brands, M., and Dormann, P. (2014). Fatty acid synthesis and lipid metabolism in the obligate biotrophic fungus *Rhizophagus irregularis* during mycorrhization of *Lotus japonicus*. *Plant J.* 79, 398–412. doi: 10.1111/tpj.12566

Whipps, J. M. (2004). Prospects and limitations for mycorrhizas in biocontrol of root pathogens. *Can. J. Bot. Rev.Canadienne De Botanique* 82, 1198–1227. doi: 10.1139/B04-082

Wieczorke, R., Krampe, S., Weierstall, T., Freidel, K., Hollenberg, C. P., and Boles, E. (1999). Concurrent knock-out of at least 20 transporter genes is required to block uptake of hexoses in *Saccharomyces cerevisiae*. *FEBS Lett.* 464, 123–128. doi: 10.1016/s0014-5793(99)01698-1

Williams, L. E., Lemoine, R., and Sauer, N. (2000). Sugar transporters in higher plants–a diversity of roles and complex regulation. *Trends Plant Sci.* 5, 283–290. doi: 10.1016/s1360-1385(00)01681-2

Wright, D. P., Read, D. J., and Scholes, J. D. (1998). Mycorrhizal sink strength influences whole plant carbon balance of *Trifolium repens* L. *Plant Cell Environ.* 21, 881–891.

Xuan, Y. H., Hu, Y. B., Chen, L. Q., Sosso, D., Ducat, D. C., Hou, B. H., et al. (2013). Functional role of oligomerization for bacterial and plant SWEET sugar transporter family. *Proc. Natl. Acad. Sci. U S A* 110, E3685–E3694. doi: 10.1073/pnas.1311244110

Yamada, K., Saijo, Y., Nakagami, H., and Takano, Y. (2016). Regulation of sugar transporter activity for antibacterial defense in *Arabidopsis*. *Science* 354, 1427–1430. doi: 10.1126/science.aah5692

Yang, B., Sugio, A., and White, F. F. (2006). Os8N3 is a host disease-susceptibility gene for bacterial blight of rice. *Proc. Natl. Acad. Sci. U S A* 103, 10503–10508. doi: 10.1073/pnas.0604088103

Yang, J., Luo, D., Yang, B., Frommer, W. B., and Eom, J. S. (2018). SWEET11 and 15 as key players in seed filling in rice. *New Phytol.* 218, 604–615. doi: 10.1111/nph.15004

Yu, Y., Streubel, J., Balzergue, S., Champion, A., Boch, J., Koebnik, R., et al. (2011). Colonization of rice leaf blades by an African strain of *Xanthomonas oryzae* pv. *oryzae* depends on a new TAL effector that induces the rice nodulin-3 Os11N3 gene. *Mol. Plant Microbe Interact.* 24, 1102–1113. doi: 10.1094/MPMI-11-10-0254

Zhao, D., You, Y., Fan, H., Zhu, X., Wang, Y., Duan, Y., et al. (2018). The Role of Sugar Transporter Genes during Early Infection by Root-Knot Nematodes. *Int. J. Mol. Sci.* 19:1. doi: 10.3390/ijms19010302

Conflict of Interest: The authors declare that the research was conducted in the absence of any commercial or financial relationships that could be construed as a potential conflict of interest.

Publisher's Note: All claims expressed in this article are solely those of the authors and do not necessarily represent those of their affiliated organizations, or those of the publisher, the editors and the reviewers. Any product that may be evaluated in this article, or claim that may be made by its manufacturer, is not guaranteed or endorsed by the publisher.

frontiers in Plant Science

ORIGINAL RESEARCH
published: 25 March 2022
doi: 10.3389/fpls.2022.872356

Deciphering Genomes: Genetic Signatures of Plant-Associated *Micromonospora*

*Raúl Riesco, Maite Ortúzar, José Manuel Fernández-Ábalos and Martha E. Trujillo**

Department of Microbiology and Genetics, University of Salamanca, Salamanca, Spain

Understanding plant-microbe interactions with the possibility to modulate the plant's microbiome is essential to design new strategies for a more productive and sustainable agriculture and to maintain natural ecosystems. Therefore, a key question is how to design bacterial consortia that will yield the desired host phenotype. This work was designed to identify the potential genomic features involved in the interaction between *Micromonospora* and known host plants. Seventy-four *Micromonospora* genomes representing diverse environments were used to generate a database of all potentially plant-related genes using a novel bioinformatic pipeline that combined screening for microbial-plant related features and comparison with available plant host proteomes. The strains were recovered in three clusters, highly correlated with several environments: plant-associated, soil/rhizosphere, and marine/mangrove. Irrespective of their isolation source, most strains shared genes coding for commonly screened plant growth promotion features, while differences in plant colonization related traits were observed. When *Arabidopsis thaliana* plants were inoculated with representative *Micromonospora* strains selected from the three environments, significant differences were in found in the corresponding plant phenotypes. Our results indicate that the identified genomic signatures help select those strains with the highest probability to successfully colonize the plant and contribute to its wellbeing. These results also suggest that plant growth promotion markers alone are not good indicators for the selection of beneficial bacteria to improve crop production and the recovery of ecosystems.

Keywords: genome, *Micromonospora*, microbe-plant interaction, endophyte, actinobacteria, PGP

OPEN ACCESS

Edited by:
Katharina Pawlowski, Stockholm University, Sweden

Reviewed by:
Christopher Milton Mathew Franco, Flinders University, Australia
Dongliang Huang, Guangxi Academy of Agricultural Sciences, China

****Correspondence:***
Martha E. Trujillo
mett@usal.es

Specialty section:
This article was submitted to Plant Symbiotic Interactions, a section of the journal Frontiers in Plant Science

Received: *09 February 2022*
Accepted: *28 February 2022*
Published: *25 March 2022*

Citation:
Riesco R, Ortúzar M, Fernández-Ábalos JM and Trujillo ME (2022) Deciphering Genomes: Genetic Signatures of Plant-Associated Micromonospora. Front. Plant Sci. 13:872356. doi: 10.3389/fpls.2022.872356

INTRODUCTION

The relationship between plants and microbial communities present in the soil is highly complex. These communities and especially those associated with the rhizosphere fluctuate in response to the surrounding environment which is affected by biotic and abiotic parameters (Sun et al., 2021; Yukun et al., 2021; Zhang et al., 2021). The collective communities of plant-associated microorganisms are known as the plant microbiome (Mendes et al., 2013) and play a major role in plant health and adaptation to environmental factors (Yukun et al., 2021).

In shaping the plant microbiome, plants select for those microbial partners that will contribute to improve its growth and resilience. In return, the microbiota associated will be provided with nutrients, mainly secreted as root exudates (Zhang et al., 2021). All together, they establish complex

microbial-plant and microbe-microbe interactions (microbial networks) to produce a particular plant phenotype (Reid and Greene, 2012; Toju et al., 2018).

Hitherto, only a few individual effects that plants and microbes have on each other have been well-characterized (e.g., nitrogen fixation of rhizobia). However, it is essential to understand how different interactions combine to produce a particular function (chemical, genetic, and/or physical) in a highly dynamic environment (Reid and Greene, 2012). Levy and colleagues recently reported that plant- and root-associated bacteria contained enriched genomes with significant overlap of the same function (e.g., carbohydrate metabolism) indicating an evolutionary adaptation to a specific niche (Levy et al., 2018) and suggesting a common strategy across diverse bacterial taxa to adapt to a plant environment.

Understanding plant-microbe interactions with the possibility to modulate the plant's microbiome is essential to design new strategies for a more productive and sustainable agriculture (Finkel et al., 2017; Benito et al., 2022). Most bacterial inoculants currently used to improve crops are composed of a single strain randomly isolated and equipped with a set of traits known as plant growth promotion (PGP) (Bulgarelli et al., 2013; Finkel et al., 2017; de Souza et al., 2019). In addition, many of the PGP features have been determined by *in vitro* screening assays or inoculation experiments under controlled conditions, rarely tested in the field (de Souza et al., 2020). Despite being broadly adopted, these strategies fail to capture important aspects of plant–microbe interactions (de Souza et al., 2019). To improve the use of bioinoculants, synthetic microbial communities are gaining a lot of interest as they can be custom built based on information derived from their ecology and genetics and translated into predictable traits. Thus, a key question is how to design bacterial consortia that will yield the desired host phenotypic outputs (Herrera Paredes et al., 2018). Together with the need to understand how microbial communities interact and shape the plant microbiome, it is also necessary to learn about the function and contribution of individual microorganisms, at the organismal/molecular level, to design manageable and traceable consortia containing all needed functions for a successful interaction (Vorholt et al., 2017).

Bacterial plant colonization is also a crucial step. In a recent study, a set of genomic features for bacteria with high capacity for plant colonization was identified (de Souza et al., 2019). The combination of colonization features and specific functions that confer benefits to the plant growth are, therefore, essential to design bacterial consortia to apply to crops.

It is logical to assume that bacteria closely related to plant/rhizosphere habitats would present a higher potential to interact with a plant and contribute to the host phenotype. It is likely that bacterial communities from a specific niche evolved and present characteristic traits (metabolism, biofilm formation, etc.) not found in individuals from other habitats (e.g., soil, sediments, marine, etc.) (Vorholt et al., 2017; Levy et al., 2018).

Micromonospora is a cosmopolitan actinobacterium widely found in diverse environments, especially soil, marine, and freshwater habitats (de Menezes et al., 2012; Genilloud, 2015). In the last decade, many micromonosporae have been reported from diverse plant tissues, specially from nitrogen fixing nodules (Trujillo et al., 2010; Carro et al., 2013; Benito et al., 2022) and this bacterium has been shown to closely interact with plants acting as a helper bacterium (Trujillo et al., 2014; Martínez-Hidalgo et al., 2015). This work was designed to identify the potential genomic features involved in the interaction between *Micromonospora* and known host plants. Seventy-four *Micromonospora* genomes representing diverse environments were used to generate a database of all potentially plant-related genes using a novel bioinformatic pipeline that combined screening for microbial-plant related features and comparison with available plant host proteomes. After this, a comparative genomic analysis based on the newly generated database was performed. Our results indicate that the identified genomic signatures help select those strains with the highest probability to successfully colonize and contribute to the wellbeing of the host plant. This strategy could be useful for the selection of other taxa using appropriate databases. The use of genome sequence data to define genomic signatures would be an excellent alternative to the limiting information obtained from defining PGP features.

MATERIALS AND METHODS

Isolation of Strains, Genome Sequencing, and Phylogenomics

Seventeen *Micromonospora* strains isolated from nodules and leaves of six different legumes, as described before (Trujillo et al., 2010) were selected for whole genome sequencing (**Table 1**) with Illumina MiSeq. DNA preparation and sequencing followed methods described previously (Riesco et al., 2018). Reads were assembled with SPAdes v. 3.10.1 (Bankevich et al., 2012) and protein coding sequences (CDSs) were predicted using Prodigal v. 2.6.2 (Hyatt et al., 2010). Up to date Bacterial Core Gene (UBCG) tool[1] was used for phylogenomic tree reconstruction, using codon-based alignment and filtering all gap-containing positions. Visualization of the phylogenomic tree was made using iTOL online viewer (Letunic and Bork, 2021), with the aid of table2itol R script.[2]

Data Compilation and Proteome Annotation

Fifty-four available *Micromonospora* genomes were retrieved from GenBank and IMG depositories (Markowitz et al., 2012; Clark et al., 2016). Additionally, three *Salinispora* genomes were included given their close phylogenetic relationship with *Micromonospora* and their unique marine obligate lifestyle (Millán-Aguinãga et al., 2017; Carro et al., 2018; Riesco et al., 2018). All genomes were checked for contamination using CheckM in KBase environment (Parks et al., 2015; Arkin et al., 2018).

For data normalization, the 74 bacterial proteomes were re-annotated. HMMER v. 3.1b2 (hmmer.org) was used to annotate all proteomes against Pfam v. 31.0, TIGRFAM v. 15.0 and the

[1]https://www.ezbiocloud.net/tools/ubcg

[2]https://github.com/mgoeker/table2itol

TABLE 1 | Source of strains used in this study and identification according to the 16S rRNA gene sequence.

Strain	Host plant	Isolation	Plant collection site	Geographical coordinates	Identification (16S rRNA)	References
GAR05	*Cicer arietinum*	Nodule	Cabrerizos	40° 58′ 40′′ N; 5° 35′ 56′′ W	*M. saelicesensis* (99.9%)	Riesco et al., 2018
GAR06	*C. arietinum*	Nodule	Cabrerizos	40° 58′ 40′′ N; 5° 35′ 56′′ W	*M. saelicesensis* (100%)	Riesco et al., 2018
LAH08	*Lupinus angustifolius*	Leaf	Cabrerizos	40° 58′ 39′′ N; 5° 35′ 48′′ W	*M. noduli* (99.9%)	Riesco et al., 2018
LAH09	*L. angustifolius*	Leaf	Cabrerizos	40° 58′ 39′′ N; 5° 35′ 48′′ W	*M. zamorensis* (100%)	This study
Lupac 06	*L. angustifolius*	Nodule	Saelices	40° 40′ 06′′ N; 6° 38′ 02′′ W	*M. saelicesensis* (99.9%)	Trujillo et al., 2007
Lupac 07	*L. angustifolius*	Nodule	Saelices	40° 40′ 06′′ N; 6° 38′ 02′′ W	*M. saelicesensis* (99.9%)	Trujillo et al., 2007
MED01	*Medicago* sp.	Nodule	Salamanca	40° 57′ 26′′ N; 5° 39′ 37′′ W	*M. arida* (99.9%)	This study
MED15	*Medicago* sp.	Nodule	Salamanca	40° 57′ 26′′ N; 5° 39′ 37′′ W	*M. noduli* (100%)	Riesco et al., 2018
ONO23	*Ononis* sp.	Nodule	Cabrerizos	40° 58′ 40′′ N; 5° 35′ 56′′ W	*M. noduli* (100%)	Riesco et al., 2018
ONO86	*Ononis* sp.	Nodule	Cabrerizos	40° 58′ 40′′ N; 5° 35′ 56′′ W	*M. noduli* (99.9%)	Riesco et al., 2018
GUI43^T	*Pisum sativum*	Nodule	Cañizal	41° 10′ 04′′ N; 5° 22′ 08′′ W	*M. noduli* (100%)	Carro et al., 2016
PSH03	*P. sativum*	Leaf	Salamanca	40° 57′ 24′′ N; 5° 39′ 31′′ W	*M. arida* (99.7%)	This study
PSH25	*P. sativum*	Leaf	Salamanca	40° 57′ 24′′ N; 5° 39′ 31′′ W	*M. zamorensis* (99.7%)	This study
PSN01	*P. sativum*	Nodule	Salamanca	40° 57′ 24′′ N; 5° 39′ 31′′ W	*M. saelicesensis* (99.9%)	Riesco et al., 2018
PSN13	*P. sativum*	Nodule	Salamanca	40° 57′ 24′′ N; 5° 39′ 31′′ W	*M. saelicesensis* (99.9%)	Riesco et al., 2018
NIE111	*Trifolium* sp.	Nodule	Villamanta	40° 17′ 45′′ N; 4° 6′ 48′′ W	*M. saelicesensis* (99.9%)	This study
NIE79	*Trifolium* sp.	Nodule	Villamanta	40° 17′ 52′′ N; 5° 6′ 56′′ W	*M. saelicesensis* (99.9%)	This study

Genomic Features of Bacterial Adaptation to Plants (GFOBAP) HMM protein profiles (Haft, 2001; Finn et al., 2016; The UniProt Consortium, 2017; Levy et al., 2018). EggNOG-mapper online tool (Huerta-Cepas et al., 2017) was used to annotate all proteomes against the EggNOG v. 4.5.1 bacterial database (Huerta-Cepas et al., 2016).

Construction of the *Micromonospora* Database

A cut-off BLAST value was calculated using a pre-established bacterial core-gene set comprising 92 bacterial genes described in the UBCG method (Na et al., 2018). All genomes were screened for these markers and aligned using UBCG 3.0 (Na et al., 2018). Identity matrices were calculated for all alignments, and the mean maximum, and minimum percentages were determined. Roary v. 3.11.2 (Page et al., 2015) was used to define the core and pan-genomes, using the previously calculated BLAST identity cut-off for the clustering of proteins.

The selection of plant-related bacterial genes (PR) was based on a pre-defined dataset of plant-associated annotation features included in the GFOBAP database (Levy et al., 2018). Considering the phylogenetic position of *Micromonospora* (Nouioui et al., 2018), the dataset was restricted to the first group of the *Actinobacteria* (*Actinobacteria*1 database). Orthofinder groups, COGs, KEGG Orthologs (KO), Pfam and TIGRFAM within *Actinobacteria*1, "Reproducible Plant Associated Domains" and "Plant-Resembling Plant-Associated and Root-Associated Domains" (PREPARADOs) were used. Annotations of the bacterial genomes were screened against GFOBAP database using *data.table* v. 1.13.6 and *tidyr* v. 1.1.2 packages (Finn et al., 2016; Wickham and Henry, 2018) in R v. 3.6.2 (R Development Core Team and R Core Team, 2011), and only those supported by two or more statistical approaches as described in the original database were considered (Levy et al., 2018).

Proteomes of known *Micromonospora* host plants were screened in UniprotKB database (release 2018_6) (The UniProt Consortium, 2017). Eighteen proteomes, comprising different species of *Cicer, Glycine*, *Lupinus*, *Medicago*, *Oryza*, *Phaseolus*, and *Trifolium* were used to create a BLAST database, comprising 731,325 proteins.

Proteomes of the 74 bacterial strains were blasted against the plant proteome database, using BLASTp included in BLAST + executables v. 2.7.1 (Camacho et al., 2009), with a threshold of $1e^{-30}$ for the E-value, 70% coverage and 30% identity. All identified coding genes found in the analysis were labeled as "plant-resembling bacterial genes" (PRB).

Arabidopsis Plant Assays

Nine strains randomly selected from clusters 1 (MED15, PSN01, and PSH03), 2 (*M. aurantiaca* DSM 43813^T, *M. chaiyaphumensis* DSM 45246^T, and *M. chalcea* DSM 43026^T), and 3 (*M. pattaloongensis* JCM 12833^T, *M. palomenae* DSM 102131^T, and *M. olivasterospora* DSM 43868^T) were used to inoculate *Arabidopsis thaliana* Col0 seedlings in axenic conditions. Forty plants per strain were prepared and inoculated as described previously (Ortúzar et al., 2020). After 4 weeks, root length, rosette leaves diameter, number of flowers, and fruits were registered. Data were standardized using Z-scores and analyzed by Kruskal-Wallis test. Principal component analysis (PCA) was used to associate the parameters measured with the strains.

Statistical Analyses and Phylogenomic Reconstruction

Kruskal-Wallis test ($p < 0.05$) was used to determine the relationships between habitat and *Micromonospora* genome lengths; number of potential plant-related genes, and habitat

(IBM® SPSS® Statistics v.25). Bar-plots for COG analyses were made using *ggplot2* v. 3.3.3 and *ggfortify* v. 0.4.11 packages (Tang et al., 2016; Wickham, 2016). *FactoMineR* v. 2.4, *factoextra v. 1.0.7*, *FactoInvestigate* v. 1.7, and *cluster* v. 2.1.1 packages (Lê et al., 2008; Kassambara and Mundt, 2017; Maechler et al., 2018; Thuleau and Husson, 2018) were used for PCA and cluster analysis of the COGs and plant-related functional KEGG characterization. KEGG annotations were compared using *factoextra* package for PCA and hierarchical clustering. Unique strain KEGG elements were deleted from the analysis.

P-values (hereafter, *q* value) generated in KEGG abundance analysis were corrected using *p.adjust* tool, included in *stats* R native package, with Bonferroni adjustment method (R Development Core Team and R Core Team, 2011; Jafari and Ansari-Pour, 2019) and $q < 0.05$ was used for KEGG elements abundance in each calculated cluster, unless stated otherwise. A Pearson's chi-square test and a contingency table analysis using multiple regression were used to study the clusters generated in the KEGG analysis and the habitat distribution of the strains in each cluster (Beasley and Schumacker, 1995) (IBM® SPSS® Statistics v.25). *ComplexHeatmap* v. 2.2.0 package (Gu et al., 2016) was used for heatmap constructions. A flowchart explaining how the database was constructed is provided in **Figure 1**.

RESULTS

Genomic Features and Habitat Distribution

Genome size ranged from 6.8 to 7.6 Mb (mean 7.1), with isolates PSH25 and MED01 having the smallest and largest genomes, respectively. Other genome characteristics including number of coding DNA, tRNAs, rRNAs, and regularly interspaced short palindromic repeat sequences (CRISPR) are summarized in **Supplementary Table 1**. The 74 bacterial genomes represented soil/rhizosphere (39%), plant-associated (34%), mangrove/marine sediments (19%), and other environments (8%) (**Supplementary Table 2**). No correlation was found between the *Micromonospora* genome sizes and their specific habitats ($p < 0.05$) (**Supplementary Figure 1**). The plant-associated (PA) strains showed similar genome lengths with a mean of 7.1 ± 0.4 Mb. The genomes of the remaining habitats presented higher dispersion values, but their sizes were very similar to the PA strains (soil/rhizosphere, 7.1 Mb ± 0.4; marine/mangrove sediments 6.7 ± 0.7; others 6.8 ± 0.4). PCA of the COG distributions and their relation to the strain habitats were highly influenced by transcription (K, ∼30%), replication and repair (L, ∼26%), carbohydrate metabolism and transport (G, ∼16%), and secondary metabolism (Q, ∼12%) gene categories, accounting for 84% of the variance (**Supplementary Figure 2**). The PA strains were recovered as a well-recognized cluster highly influenced by the K and G categories, as reported for other plant-related bacteria (Levy et al., 2018; Pinski et al., 2019). On the contrary, the strains representing the remaining habitats were highly dispersed with no apparent correlation. The complete COG distribution of each strain is given in **Supplementary Table 3**.

Genomic Features and Functional Diversity of Plant-Related *Micromonospora*

The *Micromonospora* core genome based on an identity threshold of 70% protein homology contained 992 genes (15.5% for an average genome of 6,407 genes). This data was labeled as not differential and removed. In addition, 307 ± 38 genes (per genome) labeled as "plant-resembling genes" in the BLASTp query against the host plant proteomes were included in the gene pool (**Supplementary Table 4**). The above data, together with the plant-related annotation features supported by two or more statistical analyses derived from the GFOBAP database (517 Pfam, 368 KEGG Orthology (KO), 158 TIGRFAM, and 395 Orthofinder-generated orthologs) were combined for a final database of 69,046 putative plant-related genes (PPR) (**Supplementary Table 4**).

The distribution of putative plant-related genes varied among strains, with *M. pisi* DSM 45175^T showing the highest number (1,137), followed by *M. cremea* DSM 45599^T (1,121). As expected, the *Salinispora* strains had the lowest number of PPR genes (570-629). The plant-associated strains showed the highest number of PPR genes as compared to those from other environments ($q < 0.01$) with a mean of 1036 ± 58 (**Supplementary Figure 3**).

Principal component analysis of the putative plant-related gene COGSs represented in the curated database (69,046) revealed a distribution highly dependent on four categories: carbohydrate metabolism and transport (G, ∼60%), transcription (K, ∼20%), secondary metabolism (Q, ∼10%), and inorganic ion transport and metabolism (P, ∼5%) (**Figure 2**). Based on the COG annotations, the *Micromonospora* strains formed three groups: the first one (G1), comprised 29 strains of which 22 were plant-associated (76%), six soil/rhizosphere-related (21%), and a single mangrove/marine sediment isolate (3%). This group was highly influenced by K, G, and P categories, showing a compact distribution (**Figure 2**). Thirty-five strains made up a highly heterogeneous group, G2, 18 from soil/rhizosphere (51%), eight from mangrove/marine sediments (23%), nine plant-associated (3%), and six from other environments (17%); highly impacted by secondary metabolism. Group 3 (G3) contained 10 isolates, five from soil/rhizosphere and 5 from mangrove/marine sediments which included the three *Salinispora* strains. Unlike G1, groups 2 and 3, appeared more scattered, showing the diverse origin of the strains (**Figure 2**).

KEGG annotations of the putative plant-related genes were also compared to determine any differential traits that selected the plant-associated micromonosporae from other environments (**Supplementary Figure 4**). PCA analysis also yielded three groups (referred to as *clusters*) with similar strain distribution to the COGs. The first cluster (C1) contained 30 members, with plant-associated strains representing 77%, soil/rhizosphere 16.6%, and marine/mangrove

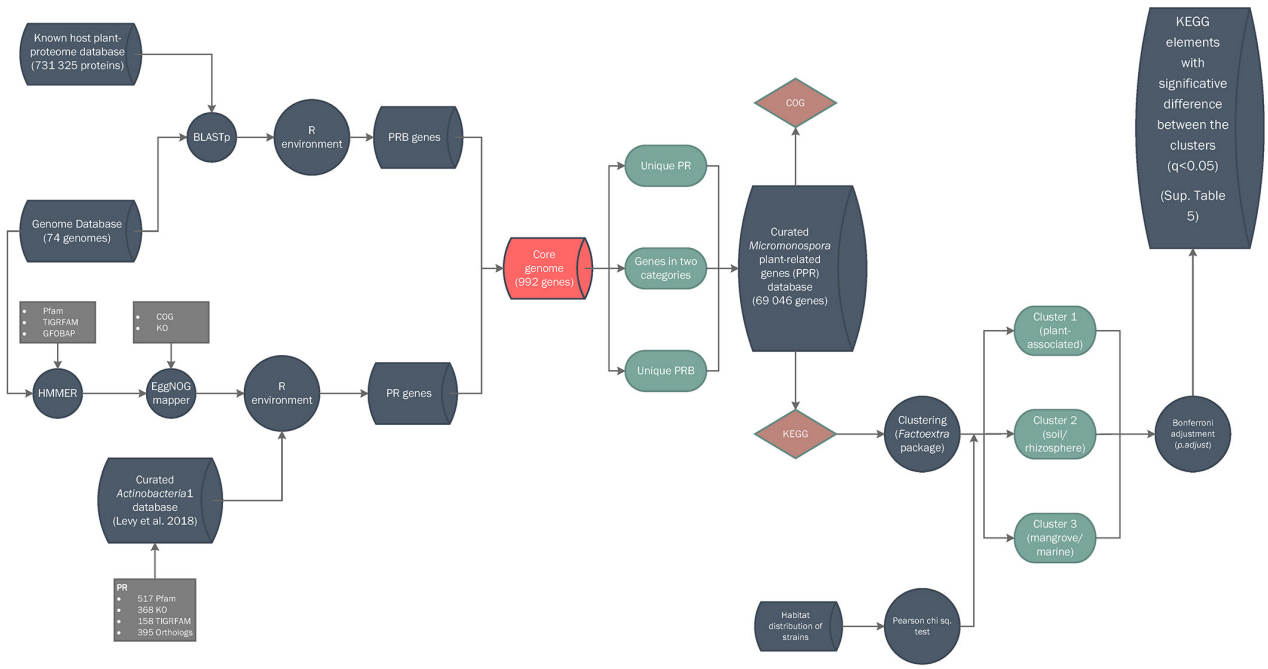

FIGURE 1 | Bioinformatic workflow for database construction. Symbols: cylinders, databases; circles, pipeline processes; rhomboids, annotations; squares, input data; balloons, partial results.

sediments accounting for 6.4%. The second cluster (C2) had 32 strains: soil/rhizosphere, 65.6%; mangrove/marine sediments, 12.5%; plant-related 6.3%; and other environments 15.6%. Cluster 3 (C3) was composed of twelve strains isolated from soil/rhizosphere (25%); mangrove/marine sediments (66.7%) and other environments, including the *Salinispora* strains (8.3%). Pearson chi-square test revealed a strong correlation between the strain clusters and their isolation source. A phylogenomic tree of the study strains, their habitat, and cluster assignment based on KEGG orthology is provided in **Figure 3**.

KEGG orthology (KO) revealed significant differences in the distribution of enriched gene functions within the three clusters. Cluster 1 (plant-associated) contained the highest number of overrepresented KEGG annotations with 105, followed by clusters 2 and 3 with 22 and 2 functions, respectively (**Figure 4**). Underrepresented functions were 20 (C1), 24 (C2), and 16 (C3). The full KEGG annotation list is found in **Supplementary Table 5**.

Predictive Functional Signatures of Plant Associated *Micromonospora* Strains

Eighteen differential KO categories were identified as genomic signatures of *Micromonospora* plant-associated strains when compared to soil/rhizosphere and marine/mangrove habitats. Of these, the major categories were carbohydrate metabolism, membrane transport, amino acid metabolism and transport, signal transduction, metabolism of cofactors and vitamins, and nucleotide metabolism (**Figure 4** and **Supplementary Table 5**).

Plant associated strains (C1) showed an important enrichment of genes related to carbohydrate metabolism, which decreased for the rhizosphere/soil related strains (C2) and were depleted in the mangrove/marine sediment isolates (C3) (except for glucose-6-phosphate isomerase). B*eta*-glucosidases that hydrolyze cellobiose released during the initial hydrolysis of cellulose (Medie et al., 2012), were found in as many as six copies in C1 strains. Also, genes coding for *L*-arabonate dehydratase (*ara*C) and arabinoxylan arabinofuranohydrolase (*xyn*D) were over-represented, with more than a two-fold difference with respect to the overall mean. In addition, *mal*Z, *sac*A, and *gal*A genes, coding for several sugar interconversions (e.g., raffinose, sucrose, and melibiose to glucose, galactose, and fructose) were found over-represented in the C1 isolates. These results are in line with previous results showing that the endophytic model strain *Micromonospora lupini* Lupac 08 contained a significant number of functional carbohydrate related genes, especially for degradation of plant-polysaccharides (Trujillo et al., 2014). Similar results were reported when plant-associated bacterial genomes were compared against those of non-plant environments, but phylogenetically related (Levy et al., 2018).

Transport systems are highly correlated to lifestyles and are essential for an organism to survive in a given environment (Ren and Paulsen, 2007). Several oligosaccharide transporters were found to be over-represented in C1 isolates (plant associated). ABC transporter genes for various sugars (e.g., *msm*X, K, E, F, and G) such as raffinose and melibiose were found highly over-enriched by more than two-fold change with respect to the overall mean. Part of the ribose ABC

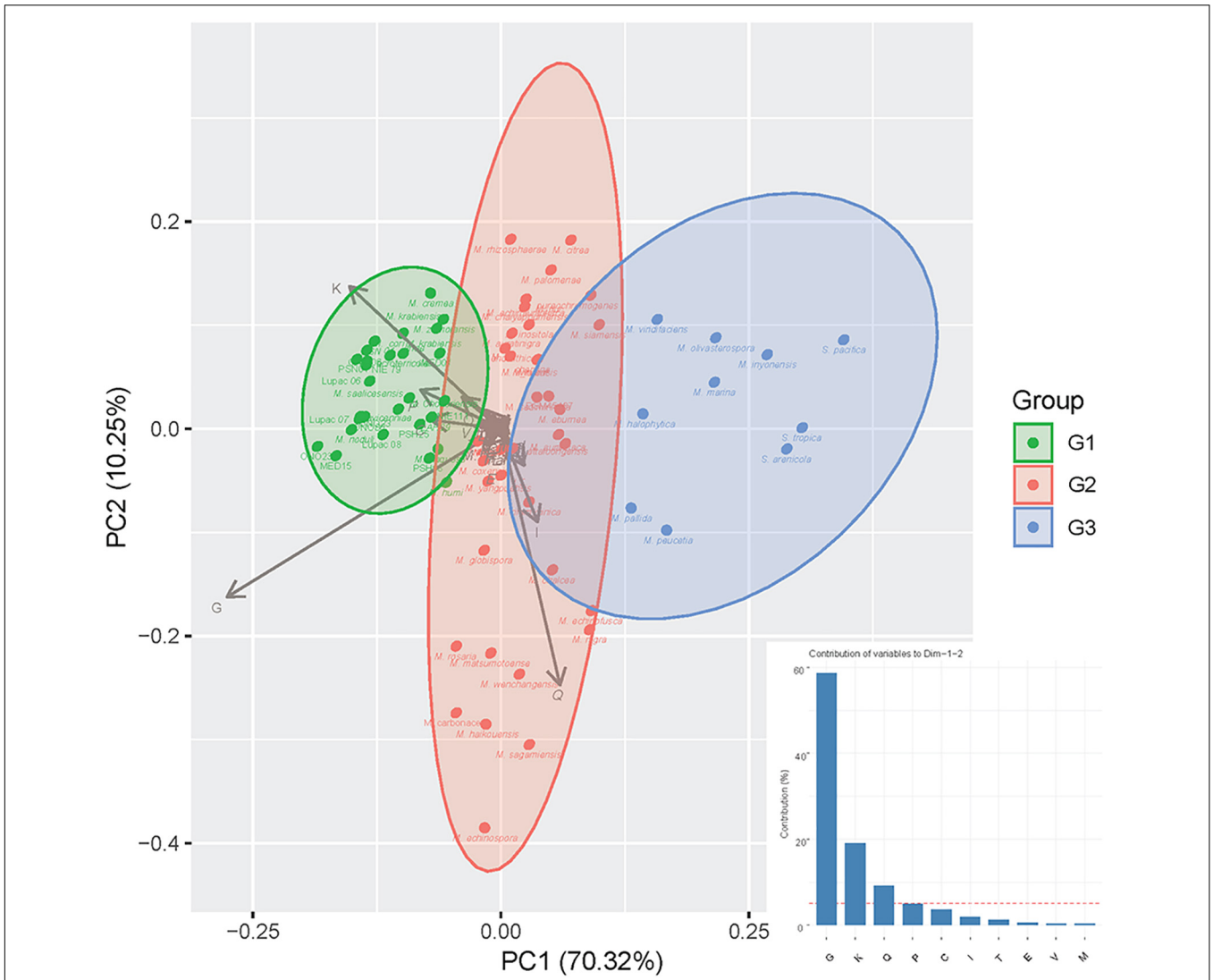

FIGURE 2 | Principal component analysis (PCA) of putative plant-related genes according to COG categories with strains recovered in groups G1, G2, and G3, respectively (for Group composition, see Section "Results"). The bar graph represents the contribution (%) of each COG category to dimensions 1 and 2 of the PCA.

transport system coding genes (*rbs*A, B, and C) were also found with four to five gene copies per strain. These results correlate well with the carbohydrate metabolism category as many of the sugars released by the plant in the form of root exudates need to be introduced into the bacterial cell to serve as carbon sources. It was recently shown how several *Pseudomonas* strains responded to root exudates by inducing several transport systems that encoded a Major Facilitator Superfamily (MFS) transporter and an L-arabonate dehydratase, an important enzyme for the catabolism of arabinose (Mavrodi et al., 2021).

Amino acids secreted by the host plant can serve as carbon and nitrogen sources for plant-associated bacteria. In this category, genes related to the degradation of leucine, isoleucine, and valine were especially enriched. Interestingly, genes coding for branched-chain amino-acid transporters (*liv*) were also overrepresented in all strains in cluster 1 (plant-associated), with a mean of 10 genes per genome (*liv*G and *liv*F). Other enriched genes related to the metabolism of cysteine and methionine, tryptophan and lysine were found. A large proportion of genes encoding for proteins involved in amino acid transport and metabolism has been proposed as a key function in plant colonization (Cole et al., 2017). Similar results were also observed for good plant colonizers related to the sugarcane microbiome (de Souza et al., 2019).

Transduction systems are especially important for bacteria to respond to abrupt environmental changes. Seven KO categories related to signal transduction mechanisms were also identified as signatures of C1 strains. Five of these were related to two-component systems of the OmpR families. Several sensor histidine kinases were enriched by two-fold, including one representing an osmolarity sensor (EnvZ). In addition, a

FIGURE 3 | Up-to-date bacterial core gene phylogenomic tree reconstructed with 92 bacterial core genes. Gene support indices are given at nodes as filled purple circles.

C4-dicarboxylate transport protein was found. The important role played by a new regulator from the OmpR family in the symbiosis of *Rhizobium etli* and *Phaseolus vulgaris* was recently reported (Rodríguez et al., 2020). Similarly, transcription regulators, related to biofilm formation, biosynthesis of antibiotics, response to osmotic stress and toxic chemicals, and pathogenicity were found enriched for bacteria colonizing plants (de Souza et al., 2019).

It is reported that vitamins can act as elicitors or priming agents to stimulate the plant defense mechanisms (Westman et al., 2019). Vitamins have also been reported to play an important role in root colonization (Lugtenberg et al., 2001; Babalola, 2010). Complete metabolic pathways for production of thiamine (B1), riboflavin (B2), niacin (B3), pantothenate (B5), pyridoxine (B6), biotin (B7), and folate (B9) were found in almost all *Micromonospora* genomes analyzed. The genes *thi*D, *ilv*D, and one coding for a pyridoxine 4-dehydrogenase (involved in B1, B6, and B5 biogenesis) were found significantly over-represented in the plant-associated cluster.

Urate is one of the main end products of rhizobial infected cells in legumes. It is transported to uninfected nodular cells where it is transformed into ureides that are transported in the xylem to the rest of the plant (Baral et al., 2016; Izaguirre-Mayoral et al., 2018). In this category, genes coding for xanthine dehydrogenases (*xdh*G and *yag*T), involved in the metabolization of urates, were over-represented in cluster 1 (>two-fold difference).

Genomic Features of Clusters 2 and 3

Cluster 2 (soil/rhizosphere) shared an equal number of over and underrepresented functions and could be considered a transition cluster between 1 and 3. Cluster 3 (mangrove/marine sediments) was characterized by the low number of plant-related features, presenting only 18 differential features, 16 of them under-represented (**Supplementary Table 5**). Most of the under-represented features (fold < 0.5) were involved in carbon source metabolism and transport (*ara*A, *msm*FG, and several multiple

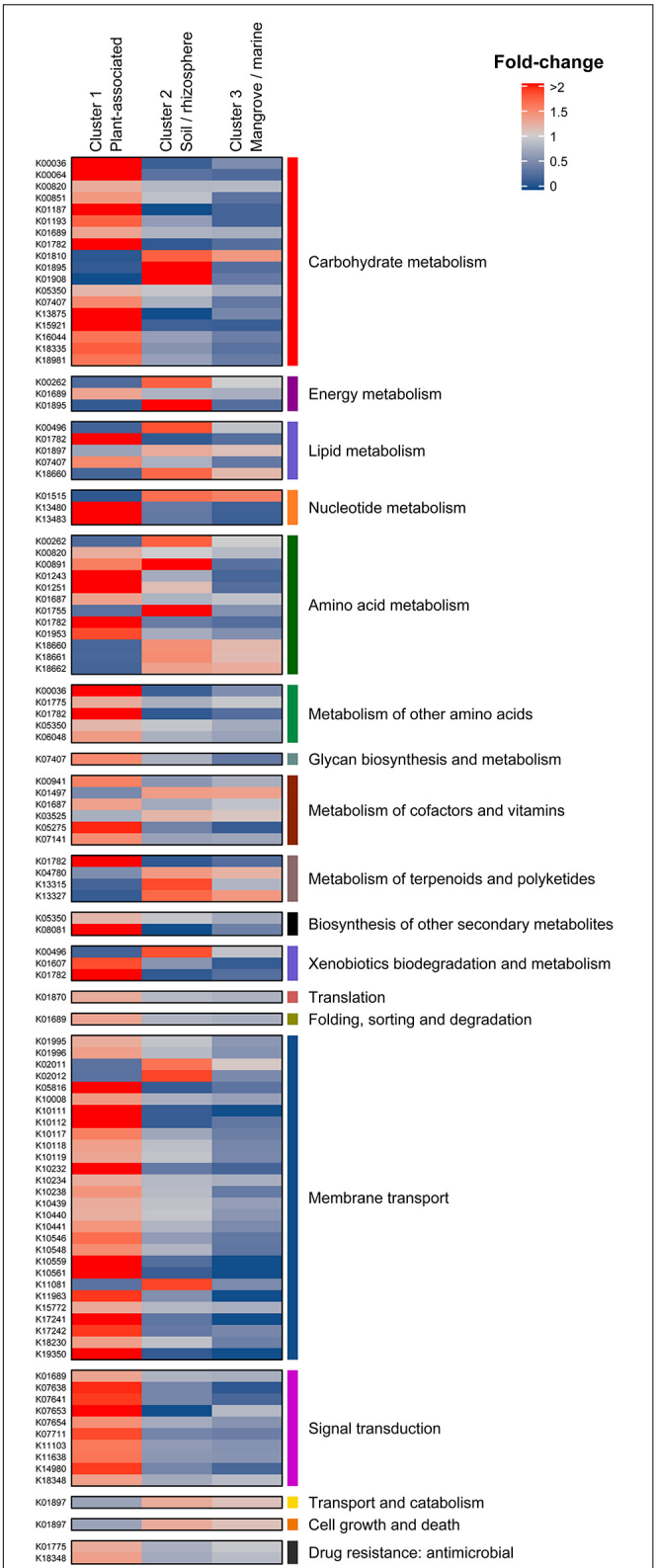

FIGURE 4 | Differential KEGG annotations between Cluster 1 (Plant associated), Cluster 2 (Soil/rhizosphere), and Cluster 3 (Mangrove/marine). Annotations are grouped in their corresponding KEGG categories (first and last columns).

sugar transport permease coding genes). Clearly, these results highly correlate with the origin of the strains.

Effect of *Micromonospora* on *Arabidopsis*

After 4 weeks, important growth differences were observed between the plants inoculated with selected strains from the three different environments. Those treated with the plant-associated isolates (cluster 1) showed the best growth and development, followed by the plants inoculated with strains from soil/rhizosphere (cluster 2). The least growth was obtained for the plants inoculated with the strains from mangrove/sediment (cluster 3) where growth was similar to the control plants, except for the ones treated with *M. pattaloongensis* JCM 12833^T (**Figure 5**). Overall Z-scores of the 360 plants inoculated with the different isolates showed that strains PSH03, PSN01, and MED15 (plant-associated) had the highest effect on the *Arabidopsis* plants (**Figure 6A**). The number of flowers and fruits, root length, and rosette leaf diameter values highly correlated in the PCA analysis with these strains (**Figure 6B**). Interestingly, all strains used for plant inoculations shared common markers identified as plant growth promotion characteristics.

DISCUSSION

Micromonospora, a common bacterium in soils and aquatic habitats was reported more than 10 years ago, as part of the legume nitrogen fixing nodule microbiome (Trujillo et al., 2010; Carro et al., 2012). This actinobacterium has gained interest, given its potential use in combination with rhizobia to enhance legume growth and nitrogen fixation (Martínez-Hidalgo and Hirsch, 2017).

The number of *Micromonospora* genomes sequenced has increased in recent years facilitating comparative genomic analyses in search for plant-growth promotion traits (Trujillo et al., 2014; Carro et al., 2018). Despite this increase, representative genomes of strains isolated from plant tissues (e.g., nodules, roots, etc.) is still low when compared to the soil environment. In this work we sequenced 17 new genomes from *Micromonospora* strains that were previously isolated from several legumes (Riesco et al., 2018; Benito et al., 2022). A working database containing 74 *Micromonospora* genomes with an almost equal number of soil- and plant-related representatives was used as the basis of this work. Using a novel comparative genomic approach that combined a bacterial plant-related database (Levy et al., 2018) and the proteome of *Micromonospora* host plants, we determined a set of genomic features that suggest a strong relation to plants.

It was recently suggested that bacterial association to plants is partially reflected in the size of the bacterial genome (larger) as compared to those which are not associated (smaller) (Levy et al., 2018). In this study, no significant correlation between genome size and environment was found. Furthermore, genome size in the two main isolation habitats (soil and plants) was very similar (7.1 ± 0.4 Mbp). As expected, the genome sizes of the *Micromonospora* and *Salinispora* strains varied greatly, with a

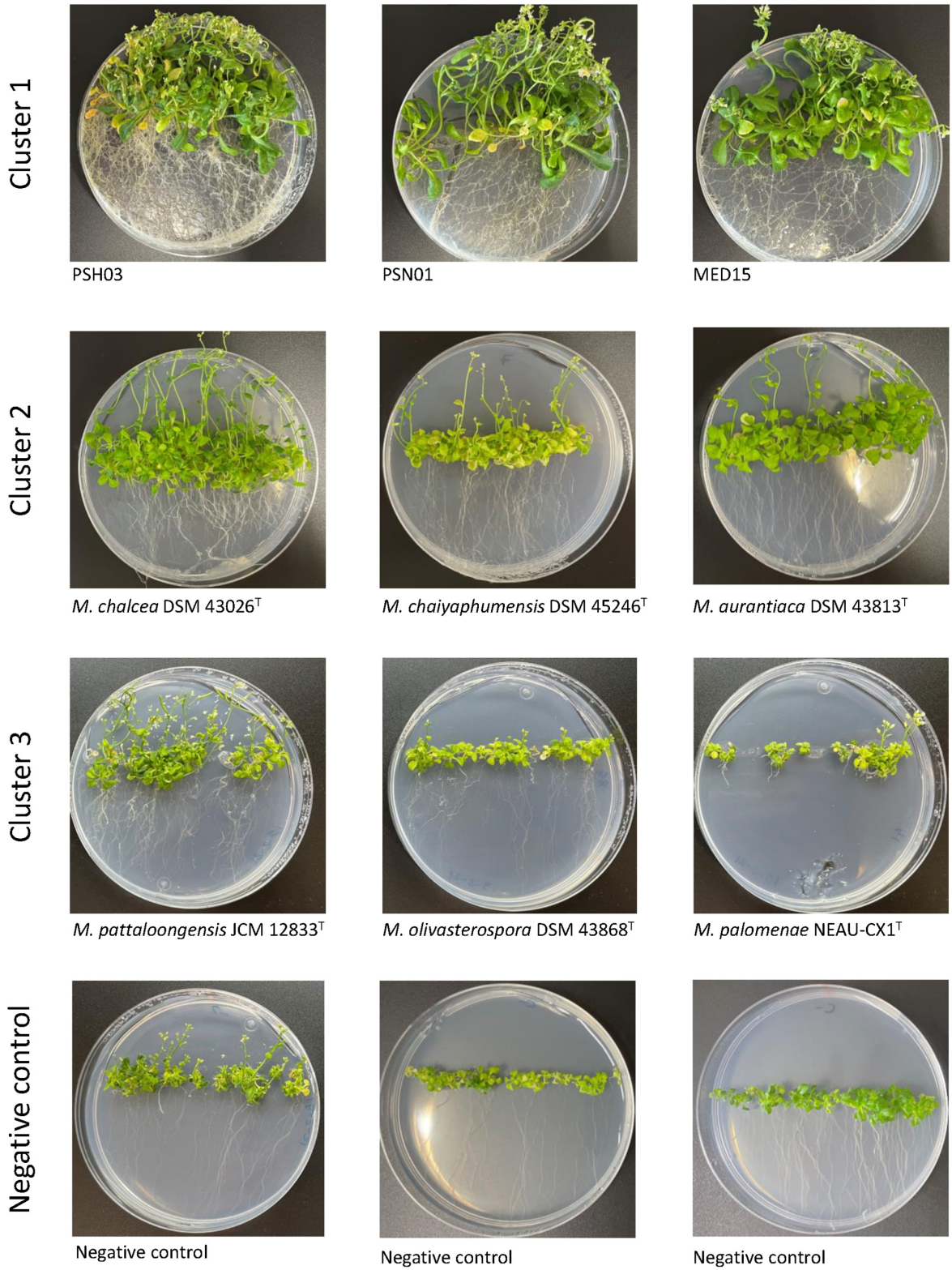

FIGURE 5 | *Arabidopsis thaliana* plants after 4 weeks of growth and inoculated with strains from Cluster 1 (MED15, PSN01, and PSH03), Cluster 2 (*M. aurantiaca* DSM 43813^{T}, *M. chaiyaphumensis* DSM 45246^{T}, and *M. chalcea* DSM 43026^{T}), and Cluster 3 (*M. pattaloongensis* JCM 12833^{T}, *M. palomenae* DSM 102131^{T}, and *M. olivasterospora* DSM 43868^{T}).

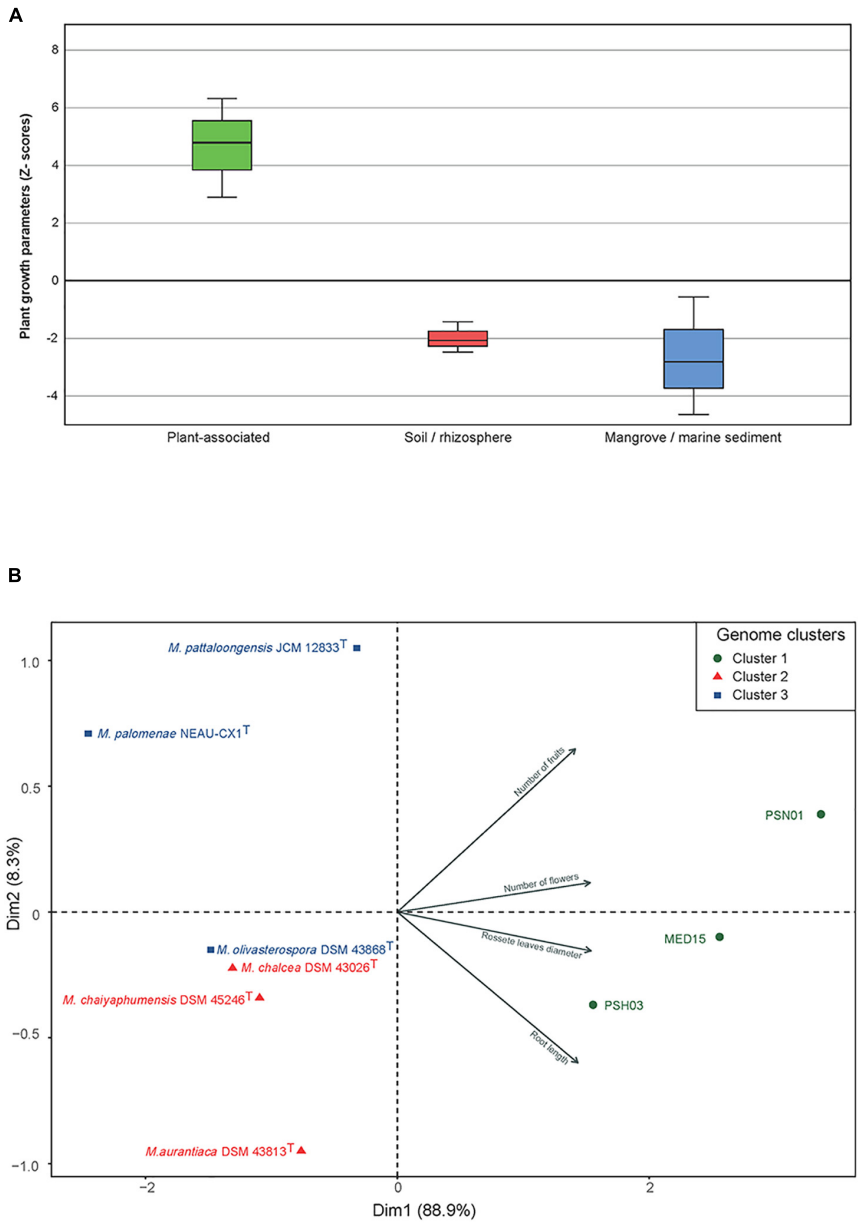

FIGURE 6 | (A) Accumulated Z-scores of the growth parameters measured in *A. thaliana* after 4 weeks of growth and inoculated with *Micromonospora* strains selected from clusters C1, C2, and C3. **(B)** PCA distribution of the strains based on the plant growth parameters measured. Symbols: green circles, C1 (plant-associated); red triangles, C22 (soil/rhizosphere); blue squares, C3 (mangrove/marine sediments).

mean difference of 1.5 Mb. While these two microorganisms are phylogenetically closely related, important differences can be found at the genomic level. *Salinispora* is a marine obligate bacterium, and its reduced genome strongly suggests an adaptation to this environment. *Micromonospora* on the other hand, appears to have evolved to adapt to multiple niches which could be translated in larger genomes to accommodate different life styles (Trujillo et al., 2014).

To select for plant-associated bacteria and especially those that provide a benefit to the host, PGP traits are commonly used as selective markers. In the present study, several genomic characteristics commonly related to plant growth promoting bacteria were initially included in the pool of 69,046 genes and tagged as plant-related genes (e.g., siderophores, phytohormones, etc.), however, most of these traits were not part of the final list of genomic signatures that differentiated between the strains and their environments. In fact, many strains included in this work were previously screened for common PGP traits and most yielded positive activities for production of siderophores, indol-acetic acid, and ACC deaminase, irrespective of their origin

(Ortúzar, 2017). Thus, the presence of PGP traits does not appear to be reliable for the selection of strains that will successfully colonize a plant and interact with it (Finkel et al., 2017; Cai et al., 2018; de Souza et al., 2019).

Root exudates play a key role in the selection of bacterial communities that colonize a plant and serve as mediators in the establishment of both positive and negative interactions in the rhizosphere (Badri and Vivanco, 2009; Chaparro et al., 2014). Exudates include sugars, amino acids, fatty acids, sterols, phenolics, and organic acids that serve as carbon and energy sources for the surrounding bacteria, initiating a cross-talk which may result in successful root colonization of the host (Nguyen et al., 2003; Badri and Vivanco, 2009; Mavrodi et al., 2021). The genomic signatures defined for the plant-associated micromonosporae were especially rich in genes coding for carbohydrate metabolism, membrane transport, amino acid metabolism, and signal transduction, strongly suggesting that these features are especially important in establishing communication and successful root colonization. Transcriptomic analysis of several *Micromonospora* strains in contact with lupin root exudates demonstrated that the *msm* and *rsb* systems found enriched in this work, were up regulated (Benito, 2020). Similarly, a recent study showed how the genomes of a bacterial community of "robust colonizers" in maize were enriched in similar metabolic functions (de Souza et al., 2019). Interestingly, these authors also reported that PGP features were not determinant for a successful colonization (de Souza et al., 2019). Both results are in line with those obtained in the present work.

In vitro production of plant cell wall hydrolytic enzymes (e.g., cellulases, xylanases, amylases, etc.) was previously demonstrated in *Micromonospora* strains isolated from nitrogen fixing nodules (Trujillo et al., 2014; Benito et al., 2022). When some of these strains were exposed to the lupin root exudates, several α- and β-glucosidases were found overexpressed (four to ten-fold) (Benito, 2020). These enzymes are known to play a key role in bacterial root colonization and tissue penetration (Reinhold-Hurek et al., 2006; Liu et al., 2017; Compant et al., 2021). In addition, cellulases are not restricted to cellulose hydrolysis but could be involved in other biological functions (Medie et al., 2012); they have also been shown to be essential for root infection in rhizobia (Robledo et al., 2012). Furthermore, plant hydrolytic enzymes were also found highly represented in metagenomic samples of endophytic bacterial communities residing inside rice roots (Sessitsch et al., 2012). Overall, carbohydrate metabolism and its corresponding transports are clearly a main feature of plant-associated bacteria.

Amino acids are exudated by many plants and can be used as carbon and nitrogen sources by bacteria surrounding the rhizosphere (Badri and Vivanco, 2009). Within these molecules, branched-chain amino acids (LIV) are recognized as important factors in the bacteroid-legume relationship as they serve as nitrogen sources for the bacteroid (Prell et al., 2009a,b). LIV transporters are essential to help LIVs move across the symbiosome membrane to make nitrogen available to the bacteroids inside (Prell et al., 2009b). In this study, LIV transporters were found overrepresented with an average of 10 copies in the genomes of strains associated with an endophytic lifestyle (cluster 1). It was previously reported that *Micromonospora* increases nutrition efficiency in *Medicago* (Trujillo et al., 2014; Martínez-Hidalgo et al., 2015). *Micromonospora* could act as a backup system for the provision of LIV transporters to secure good bacteroid development and subsequently efficient nitrogen fixation. LIV transporters were also enriched in the bacterial community of root colonizers in maize, strongly suggesting that amino acid metabolism and transport play a key role in plant-microbe interactions and is not restricted to the rhizobium-legume symbiosis (de Souza et al., 2019).

Glutamine and arginine together with ureides are end products in nitrogen fixing nodules. These molecules are transported through the xylem to other plant organs (e.g., leaves) and serve as sources of N (Baral et al., 2016; Izaguirre-Mayoral et al., 2018). In the case of ureides these are the final products in determinate nodules, while amino acids are found in plant species with indeterminate ones (e.g., lupin). Interestingly, plant-associated micromonosporae (cluster 1) have been found in both types of nodules (Trujillo et al., 2010; Carro et al., 2012). Purine metabolism involving plants and their associated bacteria is very complex and includes various metabolic pathways (Izaguirre-Mayoral et al., 2018). Apart from rhizobia and nitrogen fixation in legumes, it is not clear how other bacteria (e.g., *Micromonospora*) participate.

Recent studies have demonstrated that vitamins can be used to prime plant defenses against pathogens and abiotic stress (Boubakri et al., 2016; Westman et al., 2019). Specifically, thiamine has been shown to activate systemic acquired resistance (SAR) in plants against pathogens (Ahn et al., 2005). B-complex vitamins which act as coenzymes in several metabolic processes such as glycolysis, Krebs cycle, and nucleic acid synthesis among others, are produced by plants and microbes, including bacteria that are present in the microbiome of a plant and could, in turn, supply vitamins to enhance plant resistance.

The bacterial transcripts of three strains from C1 (*M. cremea* CR30^T, *M. lupini* Lupac 08, and *M. saelicesensis* Lupac 09^T) were obtained when grown in contact with lupin root exudates. Various genes involved in the transport of sugars and aminoacids (*rbs* and *liv*), multiple sugar transporters (*msm* and ABC-MS), synthesis of vitamins (*ilv*D, *coa*X and *moc*A), and carbohydrate hydrolysis (e.g., *gal*A, *bgl*B, and *ara*C) were found overexpressed (Benito, 2020). These results are interesting as they coincide with some of the metabolic functions found in this work. However, it is necessary to fully validate the genomic signatures with additional plant assays that include gene expression analyses upon exposure of the bacterium to the host plant, not only to the root exudates. In this line, *in-planta* assays in combination with transcriptomic analyses are underway.

Important differences in plant phenotype were found when *Arabidopsis* plants were inoculated with *Micromonospora* strains selected from the three different environment clusters defined by the genomic traits identified. All strains had previously been screened for PGP characteristics that included among others, siderophore, IAA, and AC deaminase production, yielding a positive reaction. These findings strongly suggest that PGP markers alone, are not good indicators for the selection of

bacterial strains to develop a desired phenotype, especially to increase crop production or the recovery of ecosystems.

CONCLUSION

The genomic features defined in this work, using a new bioinformatic pipeline confirm and expand those previously identified in the bacterial adaptation process to plants. Other studies have shown that several of these genomic markers are also present in phylogenetically diverse bacterial taxa that interact with non-leguminous plants. Highly related genomes of *Micromonospora* strains isolated from diverse habitats, were separated in three clusters and their genomic differences (genomic signatures) could be used to select for strains with the highest probability to successfully colonize and interact with a host plant. Many of the genes commonly identified as PGP did not have any weight as differential characteristics in the new database, therefore their presence is not necessarily a good indication to establish a successful interaction with the host plant. These genetic markers could be considered in microbiome engineering when *Micromonospora* strains are included as part of a consortium aiming to create predictable plant phenotypes.

DATA AVAILABILITY STATEMENT

The datasets presented in this study can be found in online repositories. The names of the repository/repositories and accession number(s) can be found in the article/ **Supplementary Material**.

AUTHOR CONTRIBUTIONS

RR: investigation, methodology, software development, data analysis, and writing. MO: investigation, data analysis, and writing. JF-Á: conceptualization, supervision, funding resources, and writing. MT: conceptualization, methodology, funding resources, project supervision, and writing. All authors contributed to the article and approved the submitted version.

FUNDING

This work was funded by the Spanish Ministry of Sciences, Innovation and Universities (MICINN) under project PGC2018-096185-B-I00 to MT and JF-Á. RR received a postdoctoral fellowship from the University of Salamanca and the Bank of Santander. MO acknowledges the *Junta de Castilla y León* (Spain) for a Ph.D. grant.

SUPPLEMENTARY MATERIAL

The Supplementary Material for this article can be found online at: https://www.frontiersin.org/articles/10.3389/fpls.2022.872356/full#supplementary-material

REFERENCES

Ahn, I. P., Kim, S., and Lee, Y. H. (2005). Vitamin B1 functions as an activator of plant disease resistance. *Plant Physiol.* 138, 1505–1515. doi: 10.1104/pp.104.058693

Arkin, A. P., Cottingham, R. W., Henry, C. S., Harris, N. L., Stevens, R. L., Maslov, S., et al. (2018). KBase: The United States Department of Energy Systems Biology Knowledgebase. *Nat. Biotechnol.* 36, 566–569. doi: 10.1038/nbt.4163

Babalola, O. O. (2010). Beneficial bacteria of agricultural importance. *Biotechnol. Lett.* 32, 1559–1570. doi: 10.1007/s10529-010-0347-0

Badri, D. V., and Vivanco, J. M. (2009). Regulation and function of root exudates. *Plant Cell Environ.* 32, 666–681. doi: 10.1111/j.1365-3040.2009.01926.x

Bankevich, A., Nurk, S., Antipov, D., Gurevich, A. A., Dvorkin, M., Kulikov, A. S., et al. (2012). SPAdes: a New Genome Assembly Algorithm and Its Applications to Single-Cell Sequencing. *J. Comput. Biol.* 19, 455–477. doi: 10.1089/cmb.2012.0021

Baral, B., Teixeira da Silva, J. A., and Izaguirre-Mayoral, M. L. (2016). Early signaling, synthesis, transport and metabolism of ureides. *J. Plant Physiol.* 193, 97–109. doi: 10.1016/j.jplph.2016.01.013

Beasley, T. M., and Schumacker, R. E. (1995). Multiple Regression Approach to Analyzing Contingency Tables: post Hoc and Planned Comparison Procedures. *J. Exp. Educ.* 64, 79–93. doi: 10.1080/00220973.1995.9943797

Benito, P. (2020). *Comparative Proteomic and Transcriptomic Profiling of Micromonospora Strains Associated with Legumes*. [PhD Thesis]. Salamanca: University of Salamanca, doi: 10.14201/gredos.143687.

Benito, P., Carro, L., Bacigalupe, R., Ortuzar, M., and Trujillo, M. E. (2022). From roots to leaves: the capacity of Micromonospora to colonize different legume tissues. *Phytobiom. J.* 6, 35–44. doi: 10.1094/PBIOMES-02-21-0015-R

Boubakri, H., Gargouri, M., Mliki, A., Brini, F., Chong, J., and Jbara, M. (2016). Vitamins for enhancing plant resistance. *Planta* 244, 529–543. doi: 10.1007/s00425-016-2552-0

Bulgarelli, D., Schlaeppi, K., Spaepen, S., van Themaat, E. V. L., and Schulze-Lefert, P. (2013). Structure and Functions of the Bacterial Microbiota of Plants. *Annu. Rev. Plant Biol.* 64, 807–838. doi: 10.1146/annurev-arplant-050312-120106

Cai, H., Bai, Y., and Guo, C. (2018). Comparative genomics of 151 plant-associated bacteria reveal putative mechanisms underlying specific interactions between bacteria and plant hosts. *Genes Genom.* 40, 857–864. doi: 10.1007/s13258-018-0693-1

Camacho, C., Coulouris, G., Avagyan, V., Ma, N., Papadopoulos, J., Bealer, K., et al. (2009). BLAST+: architecture and applications. *BMC Bioinform.* 10:421. doi: 10.1186/1471-2105-10-421

Carro, L., Nouioui, I., Sangal, V., Meier-Kolthoff, J. P., Trujillo, M. E., Montero-Calasanz, M., et al. (2018). Genome-based classification of micromonosporae with a focus on their biotechnological and ecological potential. *Sci. Rep.* 8:525. doi: 10.1038/s41598-017-17392-0

Carro, L., Pujic, P., Trujillo, M. E., and Normand, P. (2013). Micromonospora is a normal occupant of actinorhizal nodules. *J. Biosci.* 38, 685–693. doi: 10.1007/s12038-013-9359-y

Carro, L., Riesco, R., Spröer, C., and Trujillo, M. E. (2016). *Micromonospora ureilytica* sp. nov., *Micromonospora noduli* sp. nov. and *Micromonospora vinacea* sp. nov., isolated from *Pisum sativum* nodules. *Int. J. Syst. Evol. Microbiol.* 66, 3509–3514. doi: 10.1099/ijsem.0.001231

Carro, L., Spröer, C., Alonso, P., and Trujillo, M. E. (2012). Diversity of *Micromonospora* strains isolated from nitrogen fixing nodules and rhizosphere of Pisum sativum analyzed by multilocus sequence analysis. *Syst. Appl. Microbiol.* 35, 73–80. doi: 10.1016/j.syapm.2011.11.003

Chaparro, J. M., Badri, D. V., and Vivanco, J. M. (2014). Rhizosphere microbiome assemblage is affected by plant development. *ISME J.* 8, 790–803. doi: 10.1038/ismej.2013.196

Clark, K., Karsch-Mizrachi, I., Lipman, D. J., Ostell, J., and Sayers, E. W. (2016). GenBank. *Nucleic Acids Res.* 44, D67–D72. doi: 10.1093/nar/gkv1276

Cole, B. J., Feltcher, M. E., Waters, R. J., Wetmore, K. M., Mucyn, T. S., Ryan, E. M., et al. (2017). Genome-wide identification of bacterial plant colonization genes. *PLoS Biol.* 15, 1–24. doi: 10.1371/journal.pbio.2002860

Compant, S., Cambon, M. C., Vacher, C., Mitter, B., Samad, A., and Sessitsch, A. (2021). The plant endosphere world – bacterial life within plants. *Environ. Microbiol.* 23, 1812–1829. doi: 10.1111/1462-2920.15240

de Menezes, A. B., McDonald, J. E., Allison, H. E., and McCarthy, A. J. (2012). Importance of Micromonospora spp. as colonizers of cellulose in freshwater lakes as demonstrated by quantitative reverse transcriptase PCR of 16s rRNA. *Appl. Environ. Microbiol.* 78, 3495–3499. doi: 10.1128/AEM.07314-11

de Souza, R. S. C., Armanhi, J. S. L., and Arruda, P. (2020). From Microbiome to Traits: designing Synthetic Microbial Communities for Improved Crop Resiliency. *Front. Plant Sci.* 11:1179. doi: 10.3389/fpls.2020.01179

de Souza, R. S. C., Armanhi, J. S. L., Damasceno, N., de, B., Imperial, J., and Arruda, P. (2019). Genome Sequences of a Plant Beneficial Synthetic Bacterial Community Reveal Genetic Features for Successful Plant Colonization. *Front. Microbiol.* 10:1779. doi: 10.3389/fmicb.2019.01779

Finkel, O. M., Castrillo, G., Herrera Paredes, S., Salas González, I., and Dangl, J. L. (2017). Understanding and exploiting plant beneficial microbes. *Curr. Opin. Plant Biol.* 38, 155–163. doi: 10.1016/j.pbi.2017.04.018

Finn, R. D., Coggill, P., Eberhardt, R. Y., Eddy, S. R., Mistry, J., Mitchell, A. L., et al. (2016). The Pfam protein families database: towards a more sustainable future. *Nucleic Acids Res.* 44, D279–D285. doi: 10.1093/nar/gkv1344

Genilloud, O. (2015). "Micromonospora" in *Bergey's Manual of Systematics of Archaea and Bacteria*, eds M. E. Trujillo, S. Dedysh, P. DeVos, B. Hedlund, P. Kämpfer, F. A. Rainey, et al. (New Jersey: John Wiley & Sons, Inc.), 1–6. doi: 10.1002/9781118960608.gbm00148

Gu, Z., Eils, R., and Schlesner, M. (2016). Complex heatmaps reveal patterns and correlations in multidimensional genomic data. *Bioinformatics* 32, 2847–2849. doi: 10.1093/bioinformatics/btw313

Haft, D. H. (2001). TIGRFAMs: a protein family resource for the functional identification of proteins. *Nucleic Acids Res.* 29, 41–43. doi: 10.1093/nar/29.1.41

Herrera Paredes, S., Gao, T., Law, T. F., Finkel, O. M., Mucyn, T., Teixeira, P. J. P. L., et al. (2018). Design of synthetic bacterial communities for predictable plant phenotypes. *PLoS Biol.* 16:e2003962. doi: 10.1371/journal.pbio.2003962

Huerta-Cepas, J., Forslund, K., Coelho, L. P., Szklarczyk, D., Jensen, L. J., von Mering, C., et al. (2017). Fast Genome-Wide Functional Annotation through Orthology Assignment by eggNOG-Mapper. *Mol. Biol. Evol.* 34, 2115–2122. doi: 10.1093/molbev/msx148

Huerta-Cepas, J., Szklarczyk, D., Forslund, K., Cook, H., Heller, D., Walter, M. C., et al. (2016). eggNOG 4.5: a hierarchical orthology framework with improved functional annotations for eukaryotic, prokaryotic and viral sequences. *Nucleic Acids Res.* 44, D286–D293. doi: 10.1093/nar/gkv1248

Hyatt, D., Chen, G. L., LoCascio, P. F., Land, M. L., Larimer, F. W., and Hauser, L. J. (2010). Prodigal: prokaryotic gene recognition and translation initiation site identification. *BMC Bioinform.* 11:119. doi: 10.1186/1471-2105-11-119

Izaguirre-Mayoral, M. L., Lazarovits, G., and Baral, B. (2018). Ureide metabolism in plant-associated bacteria: purine plant-bacteria interactive scenarios under nitrogen deficiency. *Plant Soil* 428, 1–34. doi: 10.1007/s11104-018-3674-x

Jafari, M., and Ansari-Pour, N. (2019). Why, when and how to adjust your P values? *Cell J.* 20, 604–607. doi: 10.22074/cellj.2019.5992

Kassambara, A., and Mundt, F. (2017). *factoextra: Extract and Visualize the Results of Multivariate Data Analyses*. Available online at: https://cran.r-project.org/package=factoextra (accessed January 2022).

Lê, S., Josse, J., and Husson, F. (2008). {FactoMineR}: a Package for Multivariate Analysis. *J. Stat. Softw.* 25, 1–18. doi: 10.18637/jss.v025.i01

Letunic, I., and Bork, P. (2021). Interactive tree of life (iTOL) v5: an online tool for phylogenetic tree display and annotation. *Nucleic Acids Res.* 49, W293–W296. doi: 10.1093/nar/gkab301

Levy, A., Salas Gonzalez, I., Mittelviefhaus, M., Clingenpeel, S., Herrera Paredes, S., Miao, J., et al. (2018). Genomic features of bacterial adaptation to plants. *Nat. Genet.* 50, 138–150. doi: 10.1038/s41588-017-0012-9

Liu, C., Jiang, Y., Wang, X., Chen, D., Chen, X., Wang, L., et al. (2017). Diversity, Antimicrobial Activity, and Biosynthetic Potential of Cultivable Actinomycetes Associated with Lichen Symbiosis. *Microb. Ecol.* 74, 570–584. doi: 10.1007/s00248-017-0972-4

Lugtenberg, B. J. J., Dekkers, L., and Bloemberg, G. V. (2001). Molecular determinants of rhizosphere colonization by *Pseudomonas*. *Annu. Rev. Phytopathol.* 39, 461–490. doi: 10.1146/annurev.phyto.39.1.461

Maechler, M., Rousseeuw, P., Struyf, A., Hubert, M., and Hornik, K. (2018). *cluster: Cluster Analysis Basics and Extensions*. Available online at: https://CRAN.R-project.org/package=cluster (accessed January 2022).

Markowitz, V. M., Chen, I. M. A., Palaniappan, K., Chu, K., Szeto, E., Grechkin, Y., et al. (2012). IMG: the integrated microbial genomes database and comparative analysis system. *Nucleic Acids Res.* 40, D115–D122. doi: 10.1093/nar/gkr1044

Martínez-Hidalgo, P., Galindo-Villardón, P., Trujillo, M. E., Igual, J. M., and Martínez-Molina, E. (2015). Micromonospora from nitrogen fixing nodules of alfalfa (Medicago sativa L.). A new promising Plant Probiotic Bacteria. *Sci. Rep.* 4:6389. doi: 10.1038/srep06389

Martínez-Hidalgo, P., and Hirsch, A. M. (2017). The nodule microbiome: N2 fixing rhizobia do not live alone. *Phytobiomes J.* 1, 70–82. doi: 10.1094/PBIOMES-12-16-0019-RVW

Mavrodi, O. V., McWilliams, J. R., Peter, J. O., Berim, A., Hassan, K. A., Elbourne, L. D. H., et al. (2021). Root Exudates Alter the Expression of Diverse Metabolic, Transport, Regulatory, and Stress Response Genes in Rhizosphere *Pseudomonas*. *Front. Microbiol.* 12:651282. doi: 10.3389/fmicb.2021.651282

Medie, F. M., Davies, G. J., Drancourt, M., and Henrissat, B. (2012). Genome analyses highlight the different biological roles of cellulases. *Nat. Rev. Microbiol.* 10, 227–234. doi: 10.1038/nrmicro2729

Mendes, R., Garbeva, P., and Raaijmakers, J. M. (2013). The rhizosphere microbiome: significance of plant beneficial, plant pathogenic, and human pathogenic microorganisms. *FEMS Microbiol. Rev.* 37, 634–663. doi: 10.1111/1574-6976.12028

Millán-Aguinãga, N., Chavarria, K. L., Ugalde, J. A., Letzel, A. C., Rouse, G. W., and Jensen, P. R. (2017). Phylogenomic Insight into Salinispora (Bacteria, Actinobacteria) Species Designations. *Sci. Rep.* 7:3564. doi: 10.1038/s41598-017-02845-3

Na, S. I. I, Kim, Y. O., Yoon, S. H. H., Ha, S., Baek, I., and Chun, J. (2018). UBCG: up-to-date bacterial core gene set and pipeline for phylogenomic tree reconstruction. *J. Microbiol.* 56, 280–285. doi: 10.1007/s12275-018-8014-6

Nguyen, N. T., Nakabayashi, K., Thompson, J., and Fujita, K. (2003). Role of exudation of organic acids and phosphate in aluminum tolerance of four tropical woody species. *Tree Physiol.* 23, 1041–1050. doi: 10.1093/treephys/23.15.1041

Nouioui, I., Carro, L., García-López, M., Meier-Kolthoff, J. P., Woyke, T., Kyrpides, N. C., et al. (2018). Genome-Based Taxonomic Classification of the Phylum Actinobacteria. *Front. Microbiol.* 9:2007. doi: 10.3389/fmicb.2018.02007

Ortúzar, M. (2017). *Estudio del Potencial PGPB de Micromonospora saelicesensis*. Salamanca: University of Salamanca.

Ortúzar, M., Trujillo, M. E., Román-Ponce, B., and Carro, L. (2020). *Micromonospora* metallophores: a plant growth promotion trait useful for phytobioremediation? *Sci. Total Environ.* 739:139850. doi: 10.1016/j.scitotenv.2020.139850

Page, A. J., Cummins, C. A., Hunt, M., Wong, V. K., Reuter, S., Holden, M. T. G., et al. (2015). Roary: rapid large-scale prokaryote pan genome analysis. *Bioinformatics* 31, 3691–3693. doi: 10.1093/bioinformatics/btv421

Parks, D. H., Imelfort, M., Skennerton, C. T., Hugenholtz, P., and Tyson, G. W. (2015). CheckM: assessing the quality of microbial genomes recovered from isolates, single cells, and metagenomes. *Genome Res.* 25, 1043–1055. doi: 10.1101/gr.186072.114

Pinski, A., Betekhtin, A., Hupert-Kocurek, K., Mur, A. J. L., and Hasterok, R. (2019). Defining the Genetic Basis of Plant–Endophytic Bacteria Interactions. *Int. J. Mol. Sci.* 20:1947. doi: 10.3390/ijms20081947

Prell, J., Bourdès, A., Karunakaran, R., Lopez-Gomez, M., and Poole, P. (2009a). Pathway of gamma-aminobutyrate metabolism in *Rhizobium leguminosarum* 3841 and its role in symbiosis. *J. Bacteriol.* 191, 2177–2186. doi: 10.1128/JB.01714-08

Prell, J., White, J. P., Bourdes, A., Bunnewell, S., Bongaerts, R. J., and Poole, P. S. (2009b). Legumes regulate Rhizobium bacteroid development and persistence by the supply of branched-chain amino acids. *Proc. Natl. Acad. Sci. U.S.A.* 106, 12477–12482. doi: 10.1073/pnas.0903653106

R Development Core Team, R., and R Core Team (2011). *R: A Language and Environment for Statistical Computing*. Vienna: R Core Team. doi: 10.1007/978-3-540-74686-7

Reid, A., and Greene, S. E. (2012). *How Microbes Can Help Feed the World*. Washington DC: American society for Microbiology. doi: 10.1128/AAMCol.Dec.2012

Reinhold-Hurek, B., Maes, T., Gemmer, S., Van Montagu, M., and Hurek, T. (2006). An endoglucanase is involved in infection of rice roots by the not-cellulose-metabolizing endophyte *Azoarcus* sp. strain BH72. *Mol. Plant Microbe Interact.* 19, 181–188. doi: 10.1094/MPMI-19-0181

Ren, Q., and Paulsen, I. T. (2007). Large-scale comparative genomic analyses of cytoplasmic membrane transport systems in prokaryotes. *J. Mol. Microbiol. Biotechnol.* 12, 165–179. doi: 10.1159/000099639

Riesco, R., Carro, L., Román-Ponce, B., Prieto, C., Blom, J., Klenk, H. P., et al. (2018). Defining the species *Micromonospora saelicesensis* and *Micromonospora noduli* under the framework of genomics. *Front. Microbiol.* 9:1360. doi: 10.3389/fmicb.2018.01360

Robledo, M., Rivera, L., Jiménez-Zurdo, J. I., Rivas, R., Dazzo, F., Velázquez, E., et al. (2012). Role of *Rhizobium* endoglucanase CelC2 in cellulose biosynthesis and biofilm formation on plant roots and abiotic surfaces. *Microb. Cell Fact.* 11:125. doi: 10.1186/1475-2859-11-125

Rodríguez, S., Correa-Galeote, D., Sánchez-Pérez, M., Ramírez, M., Isidra-Arellano, M. C., Reyero-Saavedra, M., et al. (2020). A Novel OmpR-Type Response Regulator Controls Multiple Stages of the *Rhizobium etli – Phaseolus vulgaris* N2-Fixing Symbiosis. *Front. Microbiol.* 11:615775. doi: 10.3389/fmicb.2020.615775

Sessitsch, A., Hardoim, P., Döring, J., Weilharter, A., Krause, A., Woyke, T., et al. (2012). Functional Characteristics of an Endophyte Community Colonizing Rice Roots as Revealed by Metagenomic Analysis. *Mol. Plant Microbe Interact.* 25, 28–36. doi: 10.1094/MPMI-08-11-0204

Sun, H., Jiang, S., Jiang, C., Wu, C., Gao, M., and Wang, Q. (2021). A review of root exudates and rhizosphere microbiome for crop production. *Environ. Sci. Pollut. Res.* 28, 54497–54510. doi: 10.1007/s11356-021-15838-7

Tang, Y., Horikoshi, M., and Li, W. (2016). ggfortify: unified Interface to Visualize Statistical Results of Popular R Packages. *R J.* 8:474. doi: 10.32614/RJ-2016-060

The UniProt Consortium (2017). UniProt: the universal protein knowledgebase. *Nucleic Acids Res.* 45, D158–D169. doi: 10.1093/nar/gkw1099

Thuleau, S., and Husson, F. (2018). *FactoInvestigate: Automatic Description of Factorial Analysis*. Available online at: https://cran.r-project.org/package=FactoInvestigate (accessed January 2022).

Toju, H., Peay, K. G., Yamamichi, M., Narisawa, K., Hiruma, K., Naito, K., et al. (2018). Core microbiomes for sustainable agroecosystems. *Nat. Plants* 4, 247–257. doi: 10.1038/s41477-018-0139-4

Trujillo, M. E., Alonso-Vega, P., Rodríguez, R., Carro, L., Cerda, E., Alonso, P., et al. (2010). The genus *Micromonospora* is widespread in legume root nodules: the example of Lupinus angustifolius. *ISME J.* 4, 1265–1281. doi: 10.1038/ismej.2010.55

Trujillo, M. E., Bacigalupe, R., Pujic, P., Igarashi, Y., Benito, P., Riesco, R., et al. (2014). Genome Features of the Endophytic Actinobacterium *Micromonospora lupini* Strain Lupac 08: on the Process of Adaptation to an Endophytic Life Style? *PLoS One* 9:e108522. doi: 10.1371/journal.pone.0108522

Trujillo, M. E., Kroppenstedt, R. M., Fernández-Molinero, C., Schumann, P., and Martínez-Molina, E. (2007). *Micromonospora lupini* sp. nov. and *Micromonospora saelicesensis* sp. nov., isolated from root nodules of *Lupinus angustifolius*. *Int. J. Syst. Evol. Microbiol.* 57, 2799–2804. doi: 10.1099/ijs.0.65192-0

Vorholt, J. A., Vogel, C., Carlström, C. I., and Müller, D. B. (2017). Establishing Causality: opportunities of Synthetic Communities for Plant Microbiome Research. *Cell Host Microbe* 22, 142–155. doi: 10.1016/j.chom.2017.07.004

Westman, S. M., Kloth, K. J., Hanson, J., Ohlsson, A. B., and Albrectsen, B. R. (2019). Defence priming in Arabidopsis – a Meta-Analysis. *Sci. Rep.* 9:13309. doi: 10.1038/s41598-019-49811-9

Wickham, H. (2016). *ggplot2. Elegant Graphics for Data Analysis*. Cham: Springer International Publishing, doi: 10.1007/978-3-319-24277-4

Wickham, H., and Henry, L. (2018). *tidyr: Easily Tidy Data with "spread()" and "gather()" Functions*. Available online at: https://cran.r-project.org/package=tidyr (accessed January 2022).

Yukun, G., Jianghui, C., Genzeng, R., Shilin, W., Puyuan, Y., Congpei, Y., et al. (2021). Changes in the root-associated bacteria of sorghum are driven by the combined effects of salt and sorghum development. *Environ. Microbiomes* 16, 1–15. doi: 10.1186/s40793-021-00383-0

Zhang, J., Cook, J., Nearing, J. T., Zhang, J., Raudonis, R., Glick, B. R., et al. (2021). Harnessing the plant microbiome to promote the growth of agricultural crops. *Microbiol. Res.* 245:126690. doi: 10.1016/j.micres.2020.126690

Conflict of Interest: The authors declare that the research was conducted in the absence of any commercial or financial relationships that could be construed as a potential conflict of interest.

Publisher's Note: All claims expressed in this article are solely those of the authors and do not necessarily represent those of their affiliated organizations, or those of the publisher, the editors and the reviewers. Any product that may be evaluated in this article, or claim that may be made by its manufacturer, is not guaranteed or endorsed by the publisher.

frontiers in Plant Science

MINI REVIEW
published: 28 March 2022
doi: 10.3389/fpls.2022.836213

Multifarious and Interactive Roles of GRAS Transcription Factors During Arbuscular Mycorrhiza Development

*Tania Ho-Plágaro and José Manuel García-Garrido**

Department of Soil Microbiology and Symbiotic Systems, Zaidín Experimental Station (EEZ), CSIC, Granada, Spain

Arbuscular mycorrhiza (AM) is a mutualistic symbiotic interaction between plant roots and AM fungi (AMF). This interaction is highly beneficial for plant growth, development and fitness, which has made AM symbiosis the focus of basic and applied research aimed at increasing plant productivity through sustainable agricultural practices. The creation of AM requires host root cells to undergo significant structural and functional modifications. Numerous studies of mycorrhizal plants have shown that extensive transcriptional changes are induced in the host during all stages of colonization. Advances have recently been made in identifying several plant transcription factors (TFs) that play a pivotal role in the transcriptional regulation of AM development, particularly those belonging to the GRAS TF family. There is now sufficient experimental evidence to suggest that GRAS TFs are capable to establish intra and interspecific interactions, forming a transcriptional regulatory complex that controls essential processes in the AM symbiosis. In this minireview, we discuss the integrative role of GRAS TFs in the regulation of the complex genetic re-programming determining AM symbiotic interactions. Particularly, research being done shows the relevance of GRAS TFs in the morphological and developmental changes required for the formation and turnover of arbuscules, the fungal structures where the bidirectional nutrient translocation occurs.

Keywords: arbuscular mycorrhiza, GRAS transcription factors, transcriptional regulatory network, transcriptional complexes, symbiotic plant genes

OPEN ACCESS

Edited by:
Andrea Genre,
University of Turin, Italy

Reviewed by:
Alessandra Salvioli di Fossalunga,
University of Turin, Italy
Didier Reinhardt,
Université de Fribourg, Switzerland

****Correspondence:***
José Manuel García-Garrido
josemanuel.garcia@eez.csic.es

Specialty section:
This article was submitted to Plant Symbiotic Interactions, a section of the journal Frontiers in Plant Science

Received: *15 December 2021*
Accepted: *10 March 2022*
Published: *28 March 2022*

Citation:
Ho-Plágaro T and García-Garrido JM (2022) Multifarious and Interactive Roles of GRAS Transcription Factors During Arbuscular Mycorrhiza Development. Front. Plant Sci. 13:836213. doi: 10.3389/fpls.2022.836213

INTRODUCTION

Arbuscular mycorrhiza (AM) is a mutual symbiosis between soil-borne fungi from the phylum Glomeromycotina and the majority of higher plants. This highly beneficial symbiotic interaction substantially boosts plant growth, development and fitness by facilitating growth and reproduction under mineral-stress conditions (Clark and Zeto, 2000). In exchange, AM fungi obtain their carbon from the host plant in the form of plant photosynthates and lipids (Bago et al., 2003; Luginbuehl et al., 2017). This whole process of bidirectional nutrient exchange between plant and fungus is closely linked to and highly dependent on environmental and biological variables (Smith and Read, 2008).

The formation of AM requires the host root cells to undergo significant structural and functional modifications, leading eventually to reciprocal beneficial effects. A combination of genetic, molecular and cellular studies has shown that functional symbiosis appears to occur

following a series of plant-controlled checkpoints. During the establishment of the symbiosis, host plant root cells regulate the development and functioning of arbuscules, which are specialized intraradical and highly branched fungal structures, through complex stage-specific transcriptional reprogramming (Pimprikar and Gutjahr, 2018).

Genes involved in signaling, protein metabolism, nutrient transport, secondary metabolite biosynthesis, cell wall modification and lipid metabolism are activated during symbiosis, suggesting that complex transcriptional regulation is required for AM development and functioning. Consequently, a growing number of accumulating transcripts encoding putative transcriptional regulators as well as certain cis-regulatory elements essential for AM-specific gene expression in arbuscule-containing cells have been described (Rubio et al., 2001; Karandashov et al., 2004; Chen et al., 2011; Pimprikar and Gutjahr, 2018).

Genome-wide characterization and expression studies of TF genes activated during AM in *Petunia* (Rich et al., 2017), *Lotus* (Xue et al., 2015), *Medicago* (Hartmann et al., 2019) and tomato (Ho-Plágaro et al., 2019), have revealed that the GRAS gene family is prominent among the AM-inducible TF genes in plants. Moreover, most of these AM-induced GRAS genes belong to the scarecrow-like (A and B), RAD1, and RAM1 subfamilies, which are absent in the whole non-AM host Brassicaceae family (Cenci and Rouard, 2017), suggesting that these GRAS genes play a specific role during mycorrhization. In this minireview, we discuss the integrative roles of GRAS TFs in the regulation of transcriptional changes associated with AM development.

A BRIEF DESCRIPTION OF GRAS TFs FUNCTIONS AND INTERACTIONS

The acronym GRAS is based on the first three members identified in this family: gibberellin-acid insensitive (GAI), repressor of GA1 (RGA), and scarecrow-like (SCL) proteins (Pysh et al., 1999). GRAS TFs play a crucial regulatory role in a diverse range of fundamental plant biology processes such as plant development, gibberellin signaling, stress responses, and symbiotic processes (Tian et al., 2004; Gutjahr et al., 2015). All GRAS proteins are between 360 and 850 amino acids length and share a common conserved GRAS domain in their C-terminal region, consisting of two leucine heptad repeats (LHRs), as well as the motifs VHIID, SAW, and PFYRE (Pysh et al., 1999). These five motifs constitute the GRAS domain (Hirsch et al., 2009). In contrast, the amino (N-) terminal part of GRAS proteins is variable as well as intrinsically disordered (Sun et al., 2011) and can also include other motifs such as the DELLA motif, which is known to modulate DELLA protein interactions with many structurally diverse TFs (Marín-de la Rosa et al., 2014).

Although several genome-wide analyses have been carried out on the GRAS family, and GRAS genes have been characterized in a number of plant species, their classification has not been fully resolved. Based on a panel of eight representative angiosperm species, Cenci and Rouard (2017) identified 29 orthologous groups for the GRAS gene family and they regrouped them into 17 subfamilies whose names were homogenized based on a review of the literature. Interestingly, having found that certain members were missing from some taxonomic groups, they created five new subfamilies which include the RAD1 and RAM1 subfamilies, reported to be involved in mycorrhizal signaling (Park et al., 2015; Xue et al., 2015) and missing from all Brassicales.

Some of the most representative GRAS protein subfamilies act as regulators of GA signaling and root development, which are important processes that occur during AM formation. DELLA proteins, which share the amino acid sequence DELLA in their N-terminal region, repress gibberellin responses (Silverstone et al., 1998). The SCARECROW (SCR) and SHORT-ROOT (SHR) transcription factors are both involved in radial root organization (Cui et al., 2014), while the SCARECROW-LIKE3 (SCL3) transcription factor, which mediates GA-promoted cell elongation during root development, acts as a coordinator of GA/DELLA and SCR/SHR pathways in *Arabidopsis* (Heo et al., 2011; Zhang et al., 2011). Nodulation Signaling Pathway 1 (NSP1) and Nodulation Signaling Pathway 2 (NSP2) GRAS TFs regulate the Nod factor–induced transcriptional responses in legume species (Smit et al., 2005). However, members of these groups also play a role in mycorrhization, acting as positive regulators of strigolactone (SL) biosynthesis in *Medicago truncatula* and *Oryza sativa* (Liu et al., 2011).

In a simple biological model of transcriptional regulation, gene expression regulation is mediated by the action of transcription factors (TFs) which directly bind promoter cis-elements. However, the functioning of TFs is often mediated by their synergistic and combinatorial capacity to interact with other transcription factors and other transcriptional regulators (TRs) to form regulatory complexes (Gutjahr et al., 2015). Many GRAS proteins have been found to be associated with promoter regions. Surprisingly, in some cases, the targeted promoters also correspond to other GRAS genes, or even to the same GRAS genes (reviewed by Bolle, 2016). However, in most of the experiments performed, it is not possible to discern whether a protein is directly bound to DNA or whether it is part of a complex bound to the chromatin. To date, the direct binding of GRAS TFs to DNA has been confirmed for only very few GRAS proteins (Hirsch et al., 2009; Ma et al., 2014; Li et al., 2016). This, together with the involvement of GRAS proteins in so many diverse processes, suggests that most GRAS proteins do not bind directly to DNA and thus act as TRs rather than TFs (Bolle, 2016). Specific interactions of GRAS proteins with many other interactor proteins have been described. In addition, GRAS proteins, even from different subfamilies, have been shown to be able to interact to form heterodimers, which are often necessary for GRAS protein functionality (Bolle, 2016).

GRAS INTERACTIONS AND AM SYMBIOSIS REGULATION

Initial evidence of the action of GRAS factors in mycorrhization processes emerged from a comparative study between the processes of nodulation in legumes, as well as mycorrhization

in most plant species (Hirsch et al., 2009; Liu et al., 2011). The discovery and characterization of the GRAS TF RAM1 (Required for Arbuscular Mycorrhization 1; Park et al., 2015; Rich et al., 2015; Xue et al., 2015; Pimprikar et al., 2016; Müller et al., 2020) and subsequent identification of many other GRAS transcription factors as central regulators of arbuscule development in plants forming arbuscular mycorrhiza (Floss et al., 2013; Yu et al., 2014; Xue et al., 2015; Heck et al., 2016; Hartmann et al., 2019; Ho-Plágaro et al., 2019) point out the relevance of the GRAS family for mycorrhiza development.

Little is known about how combinations of different GRAS protein TFs and TRs control AM formation and functionality. Several studies have identified direct interactions between GRAS proteins during AM, suggesting that networks of GRAS TFs are necessary to regulate mycorrhization and that AM-related GRAS proteins act synergistically and in a combined manner. Interactions between GRAS proteins appear to play a particular role in regulating arbuscule development and here we focus on the integrative role of these GRAS TFs in the regulation of morphological and developmental changes associated to the accommodation and arbuscule functionality in inner cortical cells.

Functional arbuscule development needs host cells to be increased in size to accommodate the AM fungal structures. Some reports showed that fungal colonization induced cellular changes that affected root morphometric parameters (Russo et al., 2019). The accommodation of AM fungal structures in inner cortical cells impacts cortical root cell development although the molecular mechanisms behind these changes were unknown. Root development is positively regulated by GA in *Arabidopsis* where SCL3 proteins have been shown to interact with GA and DELLA signaling through interactions with plant-specific INDETERMINATE DOMAIN (IDD) family proteins which physically bind to both DELLA and the promoter sequence of the *SCL3* gene (Yoshida et al., 2014). Conversely, GA negatively regulate root system development in *M. truncatula* (Fonouni-Farde et al., 2019) and the SHR–SCR module in cortical cells in this legume showed a distinct expression pattern than in *Arabidopsis* (Dong et al., 2021). Interestingly, the SHR–SCR module in *Medicago* is enable to couple cell division with rhizobial infection (Dong et al., 2021).

Curiously, the differential regulation of root developmental processes in *Arabidopsis,* a non-host plant unable to form AM, and legume plants is accompanied by the absence in *Arabidopsis* of several GRAS TFs specific for mycorrhizal development. Then, it is tempting to speculate that GRAS factors from SCL, SHR, and SCR subfamilies, which are implicated in radial root organization and that mediate GA-promoted cell elongation during root development, are also part of the complex system regulating AM development in roots.

In this sense, Ho-Plágaro et al., revealed that, in addition to some classic GRAS transcription factors involved in AM symbiosis, members of the GRAS subfamilies SHR, SCL3, SCR, and SCL32, which form a regulatory module for the root elongation process (Heo et al., 2011; Zhang et al., 2011), are also involved in regulating mycorrhizal processes in tomato and showed specific expression in cells containing arbuscules (Ho-Plágaro et al., 2019). Previous evidence demonstrated that MIG1 (Mycorrhiza Induced GRAS1) is induced in colonized cortical cells and, together with DELLA, promotes cell expansion to accommodate the developing arbuscule (Heck et al., 2016). Recently, Seeman and co-workers characterized two new MIG (MIG2 and MIG3) and one SCL3 GRAS transcription factors that are induced in arbuscule-containing cells and act as positive or negative regulators of cortical cell size. MIG3 interacts with SCL3 in a transcriptional complex to modulate the activity of the central regulator DELLA and antagonizes the positive action of MIG1 and DELLA in cortical cell size (Seeman et al., 2022). It seems clear that the regulation of cell size to accommodate arbuscules in root cortical cells is controlled by a fine-tuned regulated network of interactive GRAS transcription factors from the DELLA, SCL, SHR, and SCR subfamilies. Thus, it is expected that research addressed to this issue will provide new and interesting results in deciphering the complex regulatory circuits coordinating arbuscule formation and root cell morphology.

In addition to its role in rearranging cell morphology to house arbuscules, the action of DELLA is essential for arbuscule development. In a complex containing CYCLOPS and other proteins, DELLA activates *RAM1* transcription (Pimprikar et al., 2016), and consequently the expression of genes involved in arbuscule development. RAM1 target genes include plant carbohydrate and lipid metabolism genes such as RAM2 (encoding a glycerol-3-phosphate acyltransferase), as well as genes encoding membrane proteins which are essential for the formation and functioning of the arbuscules, such as AM-induced phosphate transporter genes (Park et al., 2015; Bravo et al., 2017; Luginbuehl et al., 2017). Furthermore, RAM1 interacts with RAD1 (Xue et al., 2015) and two other *M. truncatula* AM-related GRAS TFs, TF80, and TF124 (Park et al., 2015), supporting the idea that all these regulators interact to control arbuscule development. RAD1 (Required for Arbuscule Development 1) is a GRAS TF closely related to RAM1, and the relative importance of RAM1 and RAD1 in supporting arbuscule development appears to differ between plant species (Park et al., 2015; Xue et al., 2015), pointing to a putative diversification of AM regulatory networks among mycorrhizal host species. Accordingly, transcriptomic analyses of *ram1* mutants from *L. japonicus*, *M. truncatula*, and *P. hybrida*, suggest differences in the RAM1-induced target genes depending on the plant species (Park et al., 2015; Pimprikar et al., 2016; Luginbuehl et al., 2017; Rich et al., 2017).

DELLA has also been shown to be involved in adverse roles during the arbuscule life-cycle. In particular, a transcriptional regulatory complex composed of the GRAS proteins DELLA and NSP1, together with the transcription factor MYB1, a member of the MYB family, forms a regulatory module required for arbuscular degeneration (Floss et al., 2017). While the specific mechanisms of action and regulation remain to be determined, the involvement of DELLA in the modulation of both arbuscule formation and degeneration, seems to depend on the regulatory complexes formed by the differential combination and association of DELLA with specific additional GRAS and other TFs.

Interestingly, downstream targets of RAM1 include genes encoding AP2-domain TFs such as the WRI (WRINKLED) family (MtWRI5a, MtWRI5b, and MtWRI5c) in *M. truncatula* (Jiang et al., 2018) and CBX1 (CTTC-BINDING TRANSCRIPTION FACTOR1; LjWRI1) in *L. japonicus* (Xue et al., 2018). These are members of the APETALA2 TF family that have also been described as differentially regulated upon mycorrhization (Xue et al., 2015; Ho-Plágaro et al., 2019). During AM formation, these AP2/ERF domain transcription factors regulate host genes involved in phosphate uptake and fatty acid biosynthesis. *L. japonicus* CBX1 and *M. truncatula* WRI5 directly bind to CTTC and AW motifs in the promoter sequences of genes involved in phosphate transport and fatty acid biosynthesis (Jiang et al., 2018; Xue et al., 2018). In a genome-wide analysis with several AM-competent plant species and some non-AM plants it was shown that CTTC motifs are very common in AM-related genes (Favre et al., 2014), hence indicating that RAM1 GRAS TF regulate reprogramming of mycorrhizal roots through these downstream target TFs that bind CTTC motifs. Curiously, overexpression of WRI5a in *M. truncatula* activates expression of RAM1 and *MtRam1* and *MtWri5a* gene expression has been shown to be interdependent, while WRI5a and RAM1 regulate each other at the transcriptional level, thus supporting a model in which both TFs form a positive feedback loop to regulate AM symbiosis (Jiang et al., 2018).

Further research is needed to determine whether WRINKLED transcription factor proteins are involved in mycorrhizal gene expression independently, cooperatively, or downstream of RAM1 during AM development. The lack of an AWbox-related cis element in the promoter of RAM1 suggests that WRI5a-mediated regulation of this gene might be indirect. The possibility of GRAS/AP2-ERF heterocomplex formation also needs to be explored.

CONCLUDING REMARKS AND PERSPECTIVES

In this mini review, we discuss the key regulatory role played by GRAS proteins in AM formation, as well as AM symbiotic competence, mainly in arbuscule formation (**Figure 1**). While their functional significance for symbiosis remains to be further determined, the data suggest the existence of interconnected transcriptional modules that are regulated by multiple GRAS transcription factors. Although the role of GRAS TFs in AM symbiosis appears to be conserved in plants, functional diversification in the GRAS protein repertoire is a basis for variations in AM traits among plant species. Genome-wide characterization and expression studies need to be complemented by protein–protein and protein-DNA interaction studies. Also, further research into the specific inter-GRAS TF interactions and crosstalk, as well as with other TFs and TRs, in addition to identification of regulatory transcriptional modules, would provide a better understanding of how plants are prepared for the establishment of AM symbiosis. AM-forming fungi, whose optimal use would improve plant production in a more sustainable

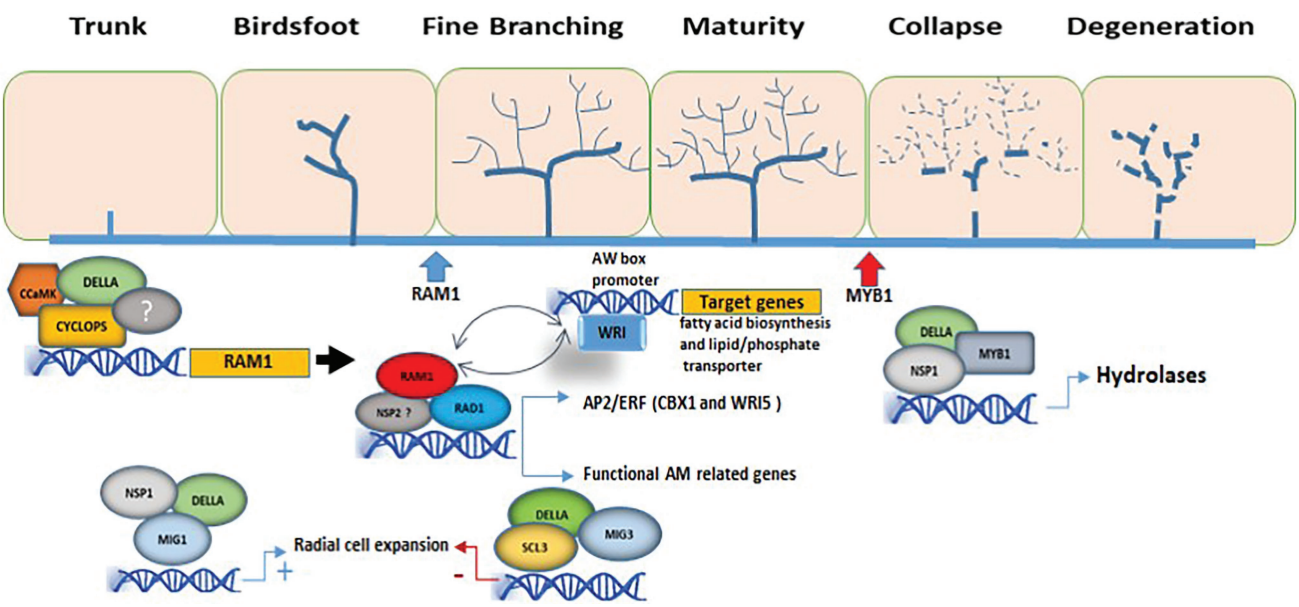

FIGURE 1 | Involvement of GRAS TFs in the regulation of arbuscule formation. The DELLA/CYCLOPS complex regulates the expression of RAM1. In this manner, RAM1 is able to interact with several other GRAS-domain proteins such as RAD1, regulating the expression of genes involved in arbuscule development and functionality, as well as with TFs from the WRI family, activating genes involved in lipid biosynthesis and in nutrient exchanges at the periarbuscular membrane. In this model, WRI and RAM1 regulate each other at the transcriptional level. The interaction of the GRAS-domain protein MIG1 with DELLA and NSP1 is necessary to regulate genes involved in the radial expansion of cortical cells for AM fungal accommodation, while SCL3, together with MIG3 and DELLA, counteracts the positive effect of MIG1 on cell expansion. MYB1 is required for the transcriptional regulation of genes involved in arbuscule degeneration (hydrolytic activity) and interacts with both DELLA proteins and the GRAS-domain protein NSP1. The different stages of arbuscule development are shown. The blue and red arrows mark the beginning of RAM1 activity and MYB1 activity, respectively. Only GRAS TFs with known function during AM are shown.

way, are a natural resource that has great potential in agro-biotechnological procedures. Thus, the identification of essential target genes, regulatory modules and downstream processes during AM formation and functioning would be invaluable in order to make AM symbiosis more effective.

AUTHOR CONTRIBUTIONS

All authors listed have made a substantial, direct, and intellectual contribution to the work and approved it for publication.

FUNDING

This study was supported by grant (PID2020-115336GB-I00) funded by Spanish MCIN/AEI/10.13039/501100011033 and by "ERDF A way of making Europe," by the "European Union".

ACKNOWLEDGMENTS

The authors wish to thank Michael O'Shea for proofreading the document.

REFERENCES

Bago, B., Pfeffer, P. E., Abubaker, J., Jun, J., Allen, J. W., Brouillette, J., et al. (2003). Carbon export from arbuscular mycorrhizal roots involves the translocation of carbohydrate as well as lipid. *Plant Physiol.* 131, 1496–1507. doi: 10.1104/pp.102.007765

Bolle, C. (2016). "Functional aspects of GRAS family proteins," in *Plant Transcription Factors, Evolutionary, Structural, and Functional Aspects.* ed. D. H. Gonzalez (Cambridge: Elsevier), 295–311.

Bravo, A., Brands, M., Wewer, V., Dörmann, P., and Harrison, M. J. (2017). Arbuscular mycorrhiza-specific enzymes FatM and RAM2 fine-tune lipid biosynthesis to promote development of arbuscular mycorrhiza. *New Phytol.* 214, 1631–1645. doi: 10.1111/nph.14533

Cenci, A., and Rouard, M. (2017). Evolutionary analyses of GRAS transcription factors in angiosperms. *Front. Plant Sci.* 8:273. doi: 10.3389/fpls.2017.00273

Chen, A., Gu, M., Sun, S., Zhu, L., Hong, S., and Xu, G. (2011). Identification of two conserved cis-acting elements, MYCS and P1BS, involved in the regulation of mycorrhiza-activated phosphate transporters in eudicot species. *New Phytol.* 189, 1157–1169. doi: 10.1111/j.1469-8137.2010.03556.x

Clark, R. Á., and Zeto, S. (2000). Mineral acquisition by arbuscular mycorrhizal plants. *J. Plant Nutr.* 23, 867–902. doi: 10.1080/01904160009382068

Cui, H., Kong, D., Liu, X., and Hao, Y. (2014). SCARECROW, SCR-LIKE 23 and SHORT-ROOT control bundle sheath cell fate and function in *Arabidopsis thaliana*. *Plant J.* 78, 319–327. doi: 10.1111/tpj.12470

Dong, W., Zhu, Y., Chang, H., Wang, C., Yang, J., Shi, J., et al. (2021). An SHR-SCR module specifies legume cortical cell fate to enable nodulation. *Nature* 589, 586–590. doi: 10.1038/s41586-020-3016-z

Favre, P., Bapaume, L., Bossolini, E., Delorenzi, M., Falquet, L., and Reinhardt, D. (2014). A novel bioinformatics pipeline to discover genes related to arbuscular mycorrhizal symbiosis based on their evolutionary conservation pattern among higher plants. *BMC Plant Biol.* 14:333. doi: 10.1186/s12870-014-0333-0

Floss, D. S., Gomez, S. K., Park, H.-J., Maclean, A. M., Müller, L. M., Bhattarai, K. K., et al. (2017). A transcriptional program for arbuscule degeneration during AM symbiosis is regulated by MYB1. *Curr. Biol.* 27, 1206–1212. doi: 10.1016/j.cub.2017.03.003

Floss, D. S., Levy, J. G., Lévesque-Tremblay, V., Pumplin, N., and Harrison, M. J. (2013). DELLA proteins regulate arbuscule formation in arbuscular mycorrhizal symbiosis. *Proc. Natl. Acad. Sci.* 110, E5025–E5034. doi: 10.1073/pnas.1308973110

Fonouni-Farde, C., Miassod, A., Laffont, C., Morin, H., Bendahmane, A., Diet, A., et al. (2019). Gibberellins negatively regulate the development of *Medicago truncatula* root system. *Sci. Rep.* 9:2335. doi: 10.1038/s41598-019-38876-1

Gutjahr, C., Sawers, R. J., Marti, G., Andrés-Hernández, L., Yang, S.-Y., Casieri, L., et al. (2015). Transcriptome diversity among rice root types during asymbiosis and interaction with arbuscular mycorrhizal fungi. *Proc. Natl. Acad. Sci.* 112, 6754–6759. doi: 10.1073/pnas.1504142112

Hartmann, R. M., Schaepe, S., Nübel, D., Petersen, A. C., Bertolini, M., Vasilev, J., et al. (2019). Insights into the complex role of GRAS transcription factors in the arbuscular mycorrhiza symbiosis. *Sci. Rep.* 9, 1–15. doi: 10.1038/s41598-019-40214-4

Heck, C., Kuhn, H., Heidt, S., Walter, S., Rieger, N., and Requena, N. (2016). Symbiotic fungi control plant root cortex development through the novel GRAS transcription factor MIG1. *Curr. Biol.* 26, 2770–2778. doi: 10.1016/j.cub.2016.07.059

Heo, J. O., Chang, K. S., Kim, I. A., Lee, M. H., Lee, S. A., Song, S. K., et al. (2011). Funneling of gibberellin signaling by the GRAS transcription regulator scarecrow-like 3 in the Arabidopsis root. *Proc. Natl. Acad. Sci. U. S. A.* 108, 2166–2171. doi: 10.1073/pnas.1012215108

Hirsch, S., Kim, J., Munoz, A., Heckmann, A. B., Downie, J. A., and Oldroyd, G. E. (2009). GRAS proteins form a DNA binding complex to induce gene expression during nodulation signaling in Medicago truncatula. *Plant Cell* 21, 545–557. doi: 10.1105/tpc.108.064501

Ho-Plágaro, T., Molinero-Rosales, N., Flores, D. F., Díaz, M. V., and García-Garrido, J. M. (2019). Identification and expression analysis of GRAS transcription factor genes involved in the control of arbuscular mycorrhizal development in tomato. *Front. Plant Sci.* 10:268. doi: 10.3389/fpls.2019.00268

Jiang, Y., Xie, Q., Wang, W., Yang, J., Zhang, X., Yu, N., et al. (2018). Medicago AP2-domain transcription factor WRI5a is a master regulator of lipid biosynthesis and transfer during mycorrhizal symbiosis. *Mol. Plant* 11, 1344–1359. doi: 10.1016/j.molp.2018.09.006

Karandashov, V., Nagy, R., Wegmüller, S., Amrhein, N., and Bucher, M. (2004). Evolutionary conservation of a phosphate transporter in the arbuscular mycorrhizal symbiosis. *Proc. Natl. Acad. Sci. U. S. A.* 101, 6285–6290. doi: 10.1073/pnas.0306074101

Li, S., Zhao, Y., Zhao, Z., Wu, X., Sun, L., Liu, Q., et al. (2016). Crystal structure of the GRAS domain of SCARECROW-LIKE7 in *Oryza sativa*. *Plant Cell* 28, 1025–1034. doi: 10.1105/tpc.16.00018

Liu, W., Kohlen, W., Lillo, A., Op Den Camp, R., Ivanov, S., Hartog, M., et al. (2011). Strigolactone biosynthesis in *Medicago truncatula* and rice requires the symbiotic GRAS-type transcription factors *NSP1* and *NSP2*. *Plant Cell* 23, 3853–3865. doi: 10.1105/tpc.111.089771

Luginbuehl, L. H., Menard, G. N., Kurup, S., Van Erp, H., Radhakrishnan, G. V., Breakspear, A., et al. (2017). Fatty acids in arbuscular mycorrhizal fungi are synthesized by the host plant. *Science* 356, 1175–1178. doi: 10.1126/science.aan0081

Ma, Z., Hu, X., Cai, W., Huang, W., Zhou, X., Luo, Q., et al. (2014). Arabidopsis miR171-targeted scarecrow-like proteins bind to GT cis-elements and mediate gibberellin-regulated chlorophyll biosynthesis under light conditions. *PLoS Genet.* 10:e1004519. doi: 10.1371/journal.pgen.1004519

Marín-de la Rosa, N., Sotillo, B., Miskolczi, P., Gibbs, D. J., Vicente, J., Carbonero, P., et al. (2014). Large-Scale Identification of Gibberellin-Related Transcription Factors Defines Group VII ETHYLENE RESPONSE FACTORS as Functional DELLA Partners. *Plant Physiol.* 166, 1022–1032. doi: 10.1104/pp.114.244723

Müller, L. M., Campos-Soriano, L., Levesque-Tremblay, V., Bravo, A., Daniels, D. A., Pathak, S., et al. (2020). Constitutive overexpression of RAM1 leads to an increase in arbuscule density in Brachypodium distachyon. *Plant Physiol.* 184, 1263–1272. doi: 10.1104/pp.20.00997

Park, H.-J., Floss, D. S., Levesque-Tremblay, V., Bravo, A., and Harrison, M. J. (2015). Hyphal Branching during Arbuscule Development Requires RAM1. *Plant Physiol* 169, 2774–2788. doi: 10.1104/pp.15.01155

Pimprikar, P., Carbonnel, S., Paries, M., Katzer, K., Klingl, V., Bohmer, M. J., et al. (2016). A CCaMK-CYCLOPS-DELLA complex activates transcription of *RAM1* to regulate arbuscule branching. *Curr. Biol.* 26, 987–998. doi: 10.1016/j.cub.2016.01.069

Pimprikar, P., and Gutjahr, C. (2018). Transcriptional regulation of arbuscular mycorrhiza development. *Plant Cell Physiol.* 59, 673–690. doi: 10.1093/pcp/pcy024

Pysh, L. D., Wysocka-Diller, J. W., Camilleri, C., Bouchez, D., and Benfey, P. N. (1999). The GRAS gene family in Arabidopsis: sequence characterization and basic expression analysis of the SCARECROW-LIKE genes. *Plant J.* 18, 111–119. doi: 10.1046/j.1365-313X.1999.00431.x

Rich, M. K., Courty, P. E., Roux, C., and Reinhardt, D. (2017). Role of the GRAS transcription factor *ATA/RAM1* in the transcriptional reprogramming of arbuscular mycorrhiza in *Petunia hybrida*. *BMC Genomics* 18:589. doi: 10.1186/s12864-017-3988-8

Rich, M. K., Schorderet, M., Bapaume, L., Falquet, L., Morel, P., Vandenbussche, M., et al. (2015). The petunia GRAS transcription factor *ATA/RAM1* regulates symbiotic gene expression and fungal morphogenesis in arbuscular mycorrhiza. *Plant Physiol.* 168, 788–797. doi: 10.1104/pp.15.00310

Rubio, V., Linhares, F., Solano, R., Martín, A. C., Iglesias, J., Leyva, A., et al. (2001). A conserved MYB transcription factor involved in phosphate starvation signaling both in vascular plants and in unicellular algae. *Genes Dev.* 15, 2122–2133. doi: 10.1101/gad.204401

Russo, G., Carotenuto, G., Fiorilli, V., Volpe, V., Chiapello, M., Van Damme, D., et al. (2019). Ectopic activation of cortical cell division during the accommodation of arbuscular mycorrhizal fungi. *New Phytol.* 221, 1036–1048. doi: 10.1111/nph.15398

Seemann, C., Heck, C., Voß, S., Schmoll, J., Enderle, E., Schwarz, D., et al. (2022). Root cortex development is fine-tuned by the interplay of MIGs, SCL3 and DELLA during arbuscular mycorrhizal symbiosis. *New Phytol.* 233, 948–965. doi: 10.1111/nph.17823

Silverstone, A. L., Ciampaglio, C. N., and Sun, T.-P. (1998). The Arabidopsis RGA gene encodes a transcriptional regulator repressing the gibberellin signal transduction pathway. *Plant Cell* 10, 155–169. doi: 10.1105/tpc.10.2.155

Smit, P., Raedts, J., Portyanko, V., Debellé, F., Gough, C., Bisseling, T., et al. (2005). NSP1 of the GRAS protein family is essential for rhizobial nod factor-induced transcription. *Science* 308, 1789–1791. doi: 10.1126/science.1111025

Smith, S., and Read, D. (2008). "*Mycorrhizal Symbiosis. 3*". (Academic Press. London).

Sun, X., Xue, B., Jones, W. T., Rikkerink, E., Dunker, A. K., and Uversky, V. N. (2011). A functionally required unfoldome from the plant kingdom: intrinsically disordered N-terminal domains of GRAS proteins are involved in molecular recognition during plant development. *Plant Mol. Biol.* 77, 205–223. doi: 10.1007/s11103-011-9803-z

Tian, C., Wan, P., Sun, S., Li, J., and Chen, M. (2004). Genome-wide analysis of the GRAS gene family in rice and *Arabidopsis*. *Plant Mol. Biol.* 54, 519–532. doi: 10.1023/B:PLAN.0000038256.89809.57

Xue, L., Cui, H., Buer, B., Vijayakumar, V., Delaux, P.-M., Junkermann, S., et al. (2015). Network of GRAS transcription factors involved in the control of arbuscule development in *Lotus japonicus*. *Plant Physiol.* 167, 854–871. doi: 10.1104/pp.114.255430

Xue, L., Klinnawee, L., Zhou, Y., Saridis, G., Vijayakumar, V., Brands, M., et al. (2018). AP2 transcription factor CBX1 with a specific function in symbiotic exchange of nutrients in mycorrhizal Lotus japonicus. *Proc. Natl. Acad. Sci.* 115, E9239–E9246. doi: 10.1073/pnas.1812275115

Yoshida, H., Hirano, K., Sato, T., Mitsuda, N., Nomoto, M., Maeo, K., et al. (2014). DELLA protein functions as a transcriptional activator through the DNA binding of the indeterminate domain family proteins. *Proc. Natl. Acad. Sci.* 111, 7861–7866. doi: 10.1073/pnas.1321669111

Yu, N., Luo, D., Zhang, X., Liu, J., Wang, W., Jin, Y., et al. (2014). A DELLA protein complex controls the arbuscular mycorrhizal symbiosis in plants. *Cell Res.* 24, 130–133. doi: 10.1038/cr.2013.167

Zhang, Z. L., Ogawa, M., Fleet, C. M., Zentella, R., Hu, J., Heo, J. O., et al. (2011). Scarecrow-like 3 promotes gibberellin signaling by antagonizing master growth repressor DELLA in Arabidopsis. *Proc. Natl. Acad. Sci. U. S. A.* 108, 2160–2165. doi: 10.1073/pnas.1012232108

Conflict of Interest: The authors declare that the research was conducted in the absence of any commercial or financial relationships that could be construed as a potential conflict of interest.

Publisher's Note: All claims expressed in this article are solely those of the authors and do not necessarily represent those of their affiliated organizations, or those of the publisher, the editors and the reviewers. Any product that may be evaluated in this article, or claim that may be made by its manufacturer, is not guaranteed or endorsed by the publisher.

frontiers | Frontiers in Plant Science

REVIEW
published: 11 April 2022
doi: 10.3389/fpls.2022.856187

Varietas Delectat: Exploring Natural Variations in Nitrogen-Fixing Symbiosis Research

*Ting Wang[1,2], Benedikta Balla[1,2], Szilárd Kovács[1] and Attila Kereszt[1]**

[1] Eötvös Loránd Research Network, Biological Research Centre, Institute of Plant Biology, Szeged, Hungary, [2] Doctoral School in Biology, University of Szeged, Szeged, Hungary

The nitrogen-fixing symbiosis between leguminous plants and soil bacteria collectively called rhizobia plays an important role in the global nitrogen cycle and is an essential component of sustainable agriculture. Genetic determinants directing the development and functioning of the interaction have been identified with the help of a very limited number of model plants and bacterial strains. Most of the information obtained from the study of model systems could be validated on crop plants and their partners. The investigation of soybean cultivars and different rhizobia, however, has revealed the existence of ineffective interactions between otherwise effective partners that resemble gene-for-gene interactions described for pathogenic systems. Since then, incompatible interactions between natural isolates of model plants, called ecotypes, and different bacterial partner strains have been reported. Moreover, diverse phenotypes of both bacterial mutants on different host plants and plant mutants with different bacterial strains have been described. Identification of the genetic factors behind the phenotypic differences did already and will reveal novel functions of known genes/proteins, the role of certain proteins in some interactions, and the fine regulation of the steps during nodule development.

Keywords: symbiotic nitrogen fixation, rhizobium strains, legume ecotypes/cultivars, symbiotic incompatibility, partner dependent mutation manifestation

OPEN ACCESS

Edited by:
Katharina Pawlowski, Stockholm University, Sweden

Reviewed by:
Ulrike Mathesius, Australian National University, Australia
Michael Göttfert, Technical University Dresden, Germany

****Correspondence:***
Attila Kereszt
kereszta@gmail.com

Specialty section:
This article was submitted to Plant Symbiotic Interactions, a section of the journal Frontiers in Plant Science

Received: *16 January 2022*
Accepted: *08 March 2022*
Published: *11 April 2022*

Citation:
Wang T, Balla B, Kovács S and Kereszt A (2022) Varietas Delectat: Exploring Natural Variations in Nitrogen-Fixing Symbiosis Research. Front. Plant Sci. 13:856187. doi: 10.3389/fpls.2022.856187

INTRODUCTION

Nitrogen is an essential macronutrient for plants and is required for the synthesis of nucleic acids, amino acids, and many other important metabolites. It is one of the most limiting elements for plant growth despite dinitrogen gas (N_2) accounting for a large proportion (around 78%) of Earth's atmosphere. Its strong chemical stability, however, makes it inaccessible for most organisms including plants, only certain prokaryotic microorganisms can fix nitrogen, i.e., to break the triple covalent bonds between the nitrogen atoms and produce ammonium (Vance, 2001).

Leguminous plants have the unique ability to grow in nitrogen-poor soils because they establish symbiosis (Suzaki et al., 2015) with a wide range of nitrogen-fixing Gram-negative α- and β-Proteobacteria collectively referred to as rhizobia (Masson-Boivin et al., 2009; Lindström and Mousavi, 2020). This interaction provides advantages for the participating partners. Legumes have access to reduced nitrogen, which they can metabolize, at the cost of energy and organic materials originating from photosynthesis. At the same time, bacteria are provided by a nutrient-rich environment in the symbiotic nodules formed on the roots or occasionally on the stems of the host plant (see later), where a much larger population of descendants than in soil can be established.

As crop and pasture legumes can fix as much as 200–300 kg of nitrogen per hectare per year (Peoples et al., 1995), they have been an important element of crop rotation systems for a very long time and provide multiple benefits for agriculture sustainability (Stagnari et al., 2017). The ability of legumes to convert N_2 into ammonia, as well as the first isolation and the morphological changes of rhizobia from and in nodules, were demonstrated in the 1880s, which was quickly followed by the market introduction of the first commercial *Rhizobium* inoculant (Nitragen) in 1895, almost 20 years earlier than performing industrial-scale ammonia synthesis by Carl Bosch (for a historical review, see Soumare et al., 2020). Since then, many inocula containing rhizobia for different legumes have been developed and commercialized to improve the yield of leguminous crops through symbiotic nitrogen fixation.

The development of the symbiosis between leguminous plants and rhizobia is a complex program including several interconnected developmental processes (bacterial infection and nodule organogenesis), multiple exchanges of signals (Gibson et al., 2008), and the activity and coordinated regulation of the expression of numerous genes (Mergaert et al., 2020; Roy et al., 2020). Legumes perceive the lack of nitrogen in soils and secrete flavonoids into the rhizosphere that are recognized as signals by rhizobia (Peters et al., 1986; Redmond et al., 1986) and—through their putative interaction with the NodD transcription factor (TF) proteins (Györgypál and Kondorosi, 1991; Györgypál et al., 1991; Peck et al., 2006), inducing the expression of nodulation (*nod*) genes. The proteins encoded by *nod* genes are essential for the synthesis and export of lipo-chitooligosaccharides called nodulation or Nod Factors (NFs) that have a core structure with 4-5 N-acetyl-glucosamine residues and an acyl chain conserved in all different species of rhizobia. Length and saturation level of the acyl chain, as well as the decoration of the backbone with several chemical modifications, such as methyl, acetyl, carbamoyl, or fucosyl groups are determined and mediated by enzymes encoded by the strain-specific *nod* genes and contribute to the specificity of the symbiosis between the partners (Dénarié et al., 1996; Long, 1996). Even in the absence of rhizobia (Truchet et al., 1991), the NFs induce quick ion fluxes through the membrane of root hairs (Felle et al., 1988), oscillations in calcium concentrations (calcium spiking) in the nuclei of epidermal cells (Ehrhardt et al., 1996), swelling and deformation of the root hairs as well as division of cortical cells (Catoira et al., 2000). The NFs are recognized by a membrane-anchored receptor complex and the perceived signal is transmitted through the so-called common symbiosis signaling (CSS) pathway, shared by another beneficial symbiosis that is established with arbuscular mycorrhizal fungi (Suzaki et al., 2015; Kronauer and Radutoiu, 2021) and, then, translated into gene expression changes by a network of transcription factors (Diedhiou and Diouf, 2018).

In the presence of NF-producing rhizobia and after the original electrophysiological changes, bacteria enter the root and then, invade the cells of the developing nodules (**Figure 1**). Depending on the interaction, there are two main ways for rhizobia to enter root tissues (Ibáñez et al., 2017): (i) For intercellular invasion, bacteria cross the epidermal layer between neighboring root hair cells or root hair and epidermal cells or through cracks/fissures, and spread through the cortex between cell walls or intercellular air spaces or by a progressive collapse of the invaded cells; (ii) In the model legume plants (*Medicago truncatula* and *Lotus japonicus*), as well as in most crop plants (such as soybean, bean, and pea), rhizobia invade roots through the transcellular infection threads (ITs), tubular structures that guide bacteria into the inner tissues of the nodule. In this latter mode, NF production by attached rhizobia induces continuous re-orientation of the root hair growth resulting in a shepherd's crook-like curled root hair, which forms a so-called infection pocket and surrounds bacteria that establish a microcolony (Gage, 2004). In the infection pocket, the IT is initiated by cell wall degradation and invagination of the root hair membrane (Murray, 2011), and then, it extends by polar growth toward the base of the root hair cell, enters the cortical cell layers until it reaches the new cells produced by the nodule primordium. The IT polar growth requires the coordinated and dynamic action of several proteins that determine membrane domains, polarity, or involvement in the rearrangement of the cytoskeleton or the regulation of NF levels (Tsyganova et al., 2021). On the rhizobial side, the initiation and growth of ITs required from the rhizobia, which are topologically in the extracellular space and multiply in the growing ITs, the adaptation to the specific osmotic, pH, and ionic environment of ITs (Dylan et al., 1990; Putnoky et al., 1998), the regulation of NF levels (Malolepszy et al., 2018) and correct production of surface polysaccharides (López-Baena et al., 2016), such as extracellular polysaccharide (EPS), K-antigen capsular polysaccharide (KPS), or lipopolysaccharide (LPS). In *L. japonicus*, a receptor structurally similar to the NF receptors monitors, whether the EPS of the symbiotic bacteria has the correct structure, i.e., it prevents bacterial entry if *Mesorhizobium loti* produces truncated EPS, but it allows infection of bacteria that produce wild-type or no EPS (Kawaharada et al., 2015). In contrast, the *Sinorhizobium meliloti* strains that are defective in the production of the succinoglycan EPS are not able to infect *Medicago* roots (Leigh et al., 1985), unless they produce a second exopolysaccharide (galactoglycan EPS II) or KPS (Glazebrook and Walker, 1989; Putnoky et al., 1990; Pellock et al., 2000). In other legumes, such as *Glycine* or *Phaseolus* species, the correct structure of LPS is required for the successful infection program (Carlson et al., 1987; Stacey et al., 1991; Margaret et al., 2013).

In the newly formed differentiating nodule cells, individual bacteria are released from the ITs through an endocytosis-like process (**Figure 2**) and become surrounded by a membrane of host origin called peribacteroid or symbiosome membrane (Roth and Stacey, 1989). These organelle-like structures, called symbiosomes, divide to fill the cytoplasm of the nodule cells and the rhizobia, thus, differentiating into their nitrogen-fixing form called bacteroids (Vasse et al., 1990). The parallel differentiation of bacteria and plant cells is accompanied by drastic physiological, metabolic, and gene expression changes. The new cells formed by the nodule meristem and being infected by rhizobia complete multiple cycles of endoreduplication resulting in enlargement of nuclear and cell volumes (Foucher and Kondorosi, 2000), change their expression profile in multiple waves (Maunoury et al., 2010) and adjust their metabolism and the cellular environment for nitrogen fixation (Udvardi and Poole, 2013). To protect the oxygen-sensitive nitrogenase enzyme

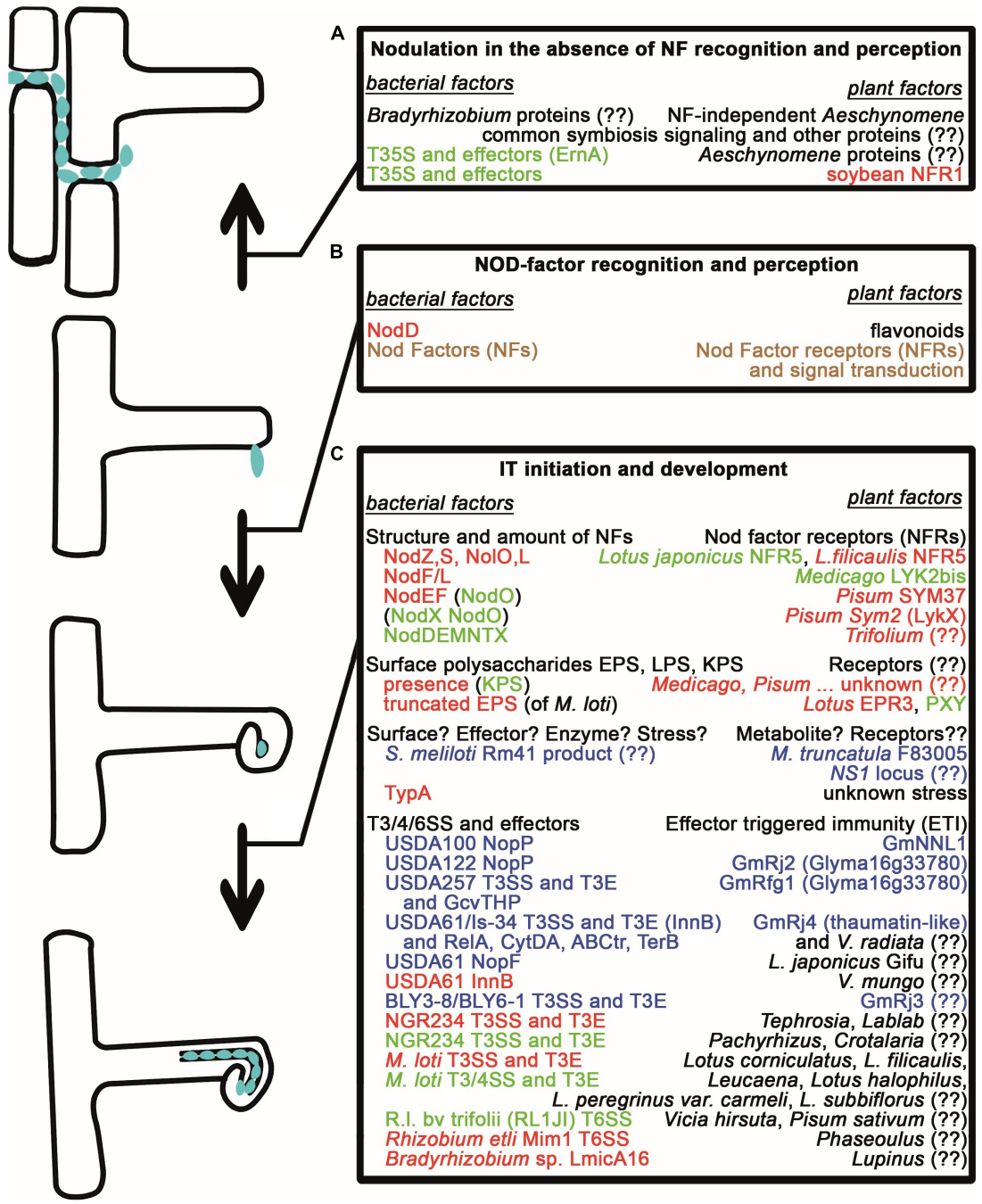

FIGURE 1 | Natural variations affecting early nodule development and infection. **(A)** Nodule formation and intercellular infection in the absence of Nod factors and NF recognition/perception requires either an unknown mechanism or the activity of Type III secretion systems for the translocation of effector proteins in bradyrhizobia as well as the common symbiosis signaling pathway and other unknown proteins in *Aeschynomene* species and in soybean plants. **(B)** Nod Factor production of rhizobia and NF recognition/perception are required for the early symbiotic events such as root hair curling. **(C)** Initiation and progression of bacterial invasion through ITs are strictly controlled. The structure and amount of NFs determine whether NF receptors allow the initiation of IT development. Similarly, the presence of surface polysaccharides with correct structure is checked by the plants with help of receptors and unknown mechanisms. Unknown mechanisms and stress from the plants also might inhibit infection unless bacteria can deal with them, for example, by expressing the TypA stress protein. Bacterial effector molecules (Nops) resembling pathogen virulence factors transported into the plant cells and Effector Triggered Immunity often led to the restriction of infection, however, there are cases, when they have a positive effect on nodulation. Those bacterial macromolecules, whose lack or incorrect structure led to the arrest of the interaction with certain partners, and those plant proteins, which restrict the bacterial mutants or whose lack can be overturned, are shown in red. Plant molecules, as well as bacterial proteins/molecules, whose lack or presence (in parenthesis), that are able to overturn these defects, are shown in green. Those bacterial and corresponding plant proteins, that are responsible for incompatibility and a defect in either of them leads to compatibility, are shown in blue. If the compatibility needs both the plant and bacterial factors, the proteins are shown in brown. (??) denotes that the given factor has not been identified yet.

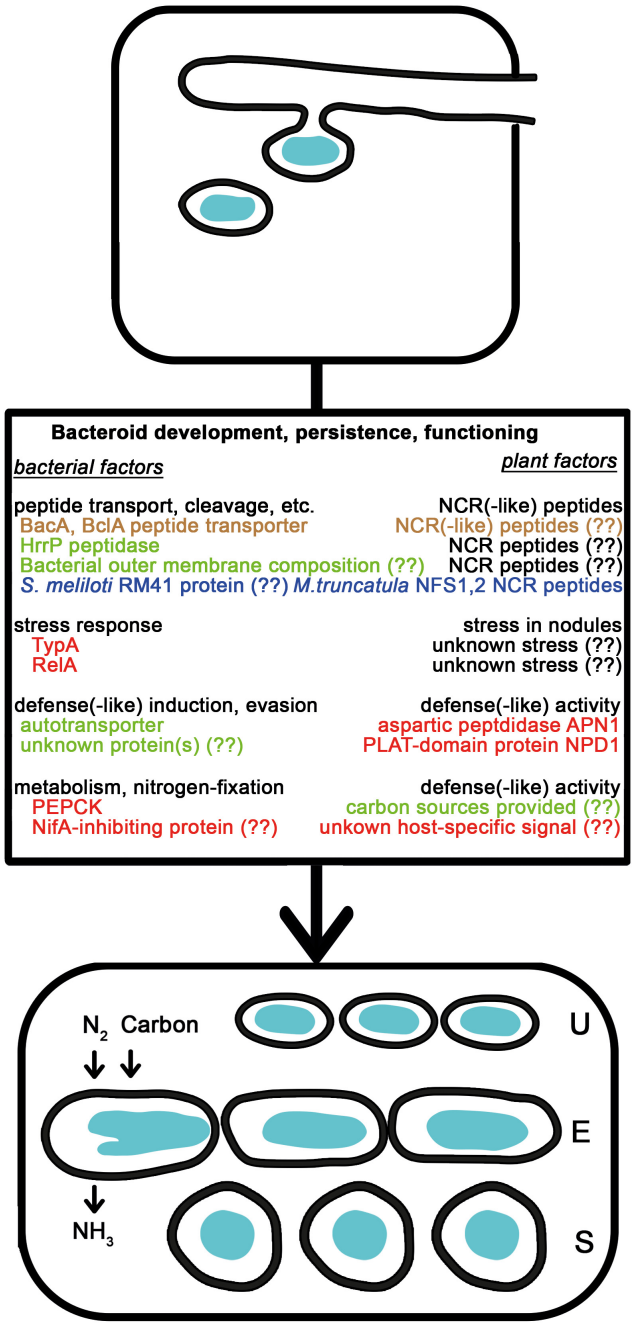

FIGURE 2 | Natural variations affecting bacteroid development, persistence, and functioning. After the release of rhizobia from the ITs, bacteria differentiate into nitrogen-fixing bacteroids of unmodified (U), elongated (E), or spherical (S) morphotypes. The NCR peptides affecting bacterial membrane and intracellular functions are delivered into bacteria by peptide transporters and contribute to the terminal differentiation of E and U morphotype bacteroids. Bacterial outer membrane composition, peptidases and independently evolved transporters affect the success of bacteroid development. The NCR peptides are also involved in strain discrimination. The level of stress and the available carbon sources in the plants affect how bacteria with mutations in stress related genes or carbon metabolism perform. Bacteria also might induce and endure plant defense reactions and sense signals from certain plants that affect gene expression. Colors are the same as in **Figure 1**.

and at the same time, to support bacterial respiration energizing nitrogen fixation, the free oxygen concentration is kept at a very low but constant level within the infected nodule cells. The low free oxygen concentration is achieved by a physical barrier in the outer cortical layer of the nodule and massive production of the oxygen-binding leghemoglobin protein (Rutten and Poole, 2019). This low oxygen concentration regulates the production of bacterial proteins that are involved in the reduction of nitrogen,

in the metabolism and transport of the fixed nitrogen, as well as in the exchange of metabolites between the bacterial and plant cells (Terpolilli et al., 2012; Udvardi and Poole, 2013).

After reaching its peak, the nitrogen fixation in the nodule cells declines, and this is accompanied by the decrease of leghemoglobin concentration and nitrogenase activity by morphological changes of the cells, or lifestyle of the rhizobial population present. This complex and programmed process called nodule senescence is a normal stage of the symbiosis, however, it can also be induced by the transition from vegetative to the reproductive stage of plant development or by adverse environmental and physiological conditions (Zhou et al., 2021).

Based on their development and morphology that is determined by the plant, both the nodules and the bacteroids can be divided into two major types (Ferguson et al., 2010; Alunni and Gourion, 2016). Indeterminate nodules on the roots of, for example, the *Medicago*, *Pisum*, *Coronilla*, *Leucaena*, and *Amorpha* species have a cylindrical shape resulting from the activity of a persistent meristem, which continuously produces new cells. These new cells become infected with bacteria and develop into nitrogen fixation tissue. As a consequence, indeterminate nodules keep increasing in size and have a gradient of developmental stages recognized as meristematic (Zone I), infection (Zone II), differentiation (Interzone II-III), nitrogen fixation (Zone III), and in older nodules, the senescence (Zone IV) zones. In contrast, determinate nodules that form on legume species from, for example, the *Lotus*, *Glycine*, *Phaseolus*, *Aeschynomene,* or *Arachys* genera are spherical and the cell population in the inner tissues is relatively homogenous and does not form a developmental gradient. During the formation of determinate nodules, the meristem is not persistent, it ceases to divide at an early stage, and further nodule development takes place more-or-less synchronously.

Independently from the nodule morphology, the differentiation and the fate of bacteria also depend on the plant host (Mergaert et al., 2006): Bacteroids in the nodules of *Lotus*, *Glycine*, *Phaseolus* or *Leucaena* are similar to the free-living cells in shape, size, DNA content and retain their cell division capacity. In contrast, bacteroids in the nodule cells of *Medicago*, *Pisum*, *Aeschynomene* or *Arachys* species have increased size, membrane permeability and DNA content, different—spherical or elongated-(branched)—shape compared to their free-living siblings. These nodule bacteria also lost their cell division capacity, thus, they are considered terminally differentiated bacteroids (Alunni and Gourion, 2016). The ability to impose terminal bacteroid differentiation on the bacterial partner appeared at least five times during the evolution of the *Papilionoideae* legumes indicating a possible fitness benefit for the plant (Oono et al., 2010). Using bacteria, which can establish symbiosis with plant's hosts governing different bacteroid fates, it was shown that terminally differentiated bacteroids have increased symbiotic efficiency as compared to unmodified bacteroids (Oono and Denison, 2010). Moreover, even the level of terminal differentiation correlates with nitrogen fixation efficiency, as in nodules of different *Aeschynomene* species, highly polyploid spherical bacteroids are more efficient than the elongated ones with lower ploidy level (Lamouche et al., 2018, 2019). Terminal bacteroid differentiation is induced by plant-derived molecules, termed as nodule-specific cysteine-rich (NCR and NCR-like) peptides (Mergaert et al., 2003; Van de Velde et al., 2010; Czernic et al., 2015), which are produced almost exclusively in the infected cells of nodules (Guefrachi et al., 2014) solely by those plants, which impose terminal bacteroid differentiation on their symbiont. The number and type of NCR peptides in the Inverted Repeat Lacking Clade (IRLC) of *Papilionoideae* legumes are highly variable and correlate with the morphotype of the bacteroids in the nodules of these species (Montiel et al., 2016, 2017). The NCR peptides were shown to interact with several bacterial proteins in *M. truncatula*, thus, affecting, for example, the transcription, translation, and cell cycle regulation (Tiricz et al., 2013; Farkas et al., 2014; Penterman et al., 2014). Despite their high number (over 700 genes in *Medicago*) and putatively redundant functions, individual NCR peptides were proven to be required for bacteroid development and persistence (Horváth et al., 2015; Kim et al., 2015).

NATURAL VARIATIONS SUPERIMPOSED ON GENERAL NODULE DEVELOPMENTAL PATHWAYS

In general, if the symbionts possess the above-reviewed tool kits, they can establish symbiosis with the partners in their cross-inoculation group to reduce atmospheric nitrogen and to support plant growth. However, it was recognized by early investigations performed mainly on crop plants that there exist symbiotic incompatibilities (i.e., no nodule formation or no nitrogen fixation) among symbionts that form effective interactions with other cultivars, or strains of the partner species (Bergersen and Nutman, 1957; Caldwell, 1966; Melino et al., 2012). It was also shown that when compatible interactions lead to nitrogen fixation, their efficiency, i.e., the plant benefit derived from the symbiosis is highly variable (Snyman and Srijdom, 1980; Terpolilli et al., 2008; Kazmierczak et al., 2017). To further complicate the picture, mutations may have different effects on the interaction depending on the partners investigated [for example (Wilson et al., 1987; Osteras et al., 1991; Rodpothong et al., 2009)].

Natural Variation in the Stringency Requirements of Nodulation Factor Induced Processes

Nodulation Factor Recognition in *Medicago*

It was recognized early after the discovery of NFs that the induction of root hair deformation and cortical cell division does not require the full and proper decoration of these signal molecules in contrast to root hair curling, as well as the initiation and growth of ITs (Ardourel et al., 1994). IT development in alfalfa root hairs was strongly inhibited by the *nodL* and *nodEF* mutants of *Sinorhizobium meliloti* lacking the O-acetylation and N-acylation with specific fatty acids, respectively, at the non-reducing end of NFs that was more pronounced with the double

mutant. These observations led to the hypothesis that different receptor forms, i.e., less stringent signaling receptors for the initiation of root hair deformation and cortical cell division, and the entry receptors with more rigorous requirements for bacterial infection regulate the nodulation process.

Similar to *M. sativa*, most *M. truncatula* accessions form no nodule with the *nodF*/*nod*L double mutant *S. meliloti* strains, but *M. truncatula* ssp. *tricycla* R108 establishes an effective nitrogen-fixing symbiosis with the mutant as with the wild-type strain (Luu et al., Under review[1]). As the NF receptor proteins NFP and LYK3 (Arrighi et al., 2006; Smit et al., 2007) in ecotype Jemalong, and the NFP protein in R108 (Feng et al., 2019) were shown to be essential for NF perception and nodulation, the genomic sequence of R108 around the *LYK3* gene was analyzed in more detail. Between *LYK2* and *LYK3*, an additional gene designated as *LYK2bis*, which is a chimera of the two neighboring genes, was identified in R108 that could not be found in any other *M. truncatula* accessions with a sequenced genome. Using loss-of-function (*lyk2bis* mutant in R108) and gain-of-function (transforming *LYK2bis* into Jemalong) approaches, it was proven that the LYK2bis protein enables R108 to be nodulated and infected by the *nodF*/*nodL* mutant.

Variations in the *Rhizobium leguminosarum* Nodulation Factor Structure Requirements

The *nodE* gene of *Rhizobium leguminosarum* was also shown to be a determinant of host specificity of the biovars and mutations in this gene's generally decreased nodulation on pea (Surin and Downie, 1989). Interestingly, the *nodE* mutation in *R. leguminosarum* bv. *viciae* almost blocked the nodulation on certain pea lines but affected less severely the other accessions. Genetic analysis revealed that *nodE*-dependent nodulation is associated with a haplotype (Li et al., 2011) of the *PsSym37* gene coding for a LysM-type receptor kinase, which is closely related to the LjNFR1/MtLYK3 Nod Factor receptors, and is essential for infection-thread initiation in pea (Zhukov et al., 2008). Wild isolates—commonly referred to as Afghan peas—from the Middle East (Afghanistan, Iran, Turkey, Israel, Uzbekistan, and Tajikistan) and known as the center of origin for peas, cannot be nodulated by rhizobia collected in Europe, but only by strains isolated from soils from the same region (Lie, 1984). In Afghan peas, cortical cell divisions are initiated upon induction by European *R. leguminosarum* bv. *viciae* strains but IT formation and bacterial invasion are blocked. This inhibition can be overcame either by growing the plants at elevated temperature (Kozik et al., 1995) or by the production of the NodX protein in rhizobia that adds an O-acetyl group to the C6 carbon of N-acetylglucosamine residue at the reducing end of the pentameric NF (Götz et al., 1985; Firmin et al., 1993). Genetic analysis of the locus called *sym2,* which is responsible for the incompatibility of Afghan peas, added a level of complexity. The $sym2^A$ allele of Afghan peas is dominant over the $sym2^C$ alleles of cultivated peas when *R. leguminosarum* bv. *viciae* strain PRE is used as inoculum, however, the dominance is changed when strains 248 or PF2, producing higher amount of Nfs, are applied (Kozik et al., 1995). Despite the long history of research on the specificity of Afghan peas, no direct evidence, such as changing the specificity of a cultivated line by transformation, about responsible for the strict partner selection has emerged. However, several genetic and bioinformatics data indicates that another LysM-type receptor kinase, termed PsLykX (for *P. sativum* LysM kinase eXclusive), probably interacting with the pea NFR1 (PsSym10) receptor may determine the trait (Sulima et al., 2017, 2019; Solovev et al., 2021). Interestingly, the *nodO* gene coding for a secreted protein, which was shown to form ion channels in membranes (Sutton et al., 1994), can compensate both for the *nodE* mutation (Walker and Downie, 2000) and partially or fully for the absence of the *nodX* gene in strain 248 on plants carrying the $sym2^A$ allele in homozygous or heterozygous forms, respectively (Geurts et al., 1997). The non-nodulating phenotype of the *nodO* mutant of strain 248 on the heterozygous plants, as compared to nodule formation by wild-type bacteria, might explain the strain-specific differences regarding the dominance of the *sym2* alleles. It is possible that the genome of strain PRE does not code for a functional NodO protein for compensation. It is hypothesized that NodO might function either to bypass the NF receptor activity or to amplify a weak signal originating from the interaction of the not fully compatible NFs and receptors.

Similar variability in NF recognition and sensitivity might exist in *Trifolium* species. *R. leguminosarum* bv. *trifolii* strain TA is not able to nodulate *T. subterraneum* cv. Woogenellup at 22°C because of the arrest of IT development but forms an effective symbiosis with this cultivar at 28°C (Lewis-Henderson and Djordjevic, 1991a). This trait is determined by the recessive alleles of a gene named *rwtl* (resistance of Woogenellup to strain TA1). The nodulation deficiency of strain TA1 is overcome by mutations in genes that affect the structure (*nodE* and *nodX*), the amount (*nodD*, *nodM*, *nodN,* and probably, the negatively acting *csn-1* (for *cultivar-specific nodulation*) of unknown identity and function), or transport (*nodT*) of Nod Factors (Lewis-Henderson and Djordjevic, 1991b).

Nodulation Factor Recognition in *Lotus* Species

The most numerous and most detailed investigations of NF recognition and perception have been performed in *Lotus* species, mostly in *L. japonicus*, serving as a model for determinate nodule development, in symbiosis with *Mesorhizobium loti*. This rhizobium produces mainly pentameric NFs with an acetylated fucosyl residue at the C6 carbon of the reducing sugar, a carbamoyl group, and a N-methylated 18:1 acyl chain at the C4 and C2 carbons, respectively, of the non-reducing sugar (López-Lara et al., 1995). The symbiotic capability of *M. loti* R7A mutants that fail to synthetize acetyl-fucosylated NFs depends on the *Lotus* species serving as partner (Rodpothong et al., 2009). Nodule formation by a *nolL* mutants failing to add the acetyl modification to the fucosyl moiety is delayed on all four *Lotus* species (*L. japonicus*, *L. corniculatus*, *L. filicaulis*, and *L. burttii*) tested. Moreover, IT formation in *L. filicaulis* is also arrested. Defects in the synthesis (in the *nolK* and *noeL* mutants) and transfer to the NF backbone (in the *nodZ* mutant) of the fucosyl residue prevent infection not only in *L. filicaulis* but also in

[1] Luu, T., Ourt, A., Pouzet, C., Pauly, N., and Cullimore, J. (2022). *A Newly-Evolved Chimeric Lysin Motif Receptor-Like Kinase in Medicago truncatula spp. Tricycla R108 Extends Its Rhizobia Symbiotic Partnership*.

L. corniculatus, revealing different stringency requirements in the *Lotus-Mesorhizobium* cross-inoculation group. An engineered symbiont of *Lotus* called strain DZL and was created by expressing an inducer-independent NodD protein, as well as the NodZ fucosyl-transferase and the NolL acetyltransferase in *R. leguminosarum* bv. *viciae* (Pacios Bras et al., 2000), produces NFs that only differ from those of *M. loti* in the decorations of the non-reducing sugar, i.e., the acyl chain on the C2 carbon is not methylated, the C6 carbon is not carbamoylated but the C5 carbon is acetylated. This strain effectively nodulated *L. japonicus* but failed to infect *L. filicaulis*. It was shown by domain and amino acid swaps between the Nfr receptors of the two species that a single amino acid difference in the M2 domain of Nfr5 is responsible for the differential recognition of NFs (Radutoiu et al., 2007).

Summary

Legumes rigorously choose their rhizobial partners by recognizing the chemical structure of the first signal molecules, the Nod Factors, via the activity of the NF receptors. Structural variations and extension of the NF receptor repertoire might both strengthen (NodX requirement by SYM2) or weaken (LYS2bis) the stringency of the identification process, which is also affected by the amount of NFs and temperature.

Natural Variation in Surface Polysaccharide Requirements for Infection

In the indeterminate nodule forming rhizobia, an efficient infection (thread development) requires the production of exopolysaccharides (EPSs), the lack of EPS resulting in no IT formation or in ITs aborted in the root hairs (Skorupska et al., 2006). In *S. meliloti* strain Rm41, however, EPS-deficient (*exoB* mutant) bacteria induce the formation of infected, nitrogen-fixing nodules on alfalfa and this phenotype is associated with its ability to produce a strain-specific K-antigen (KPS), a polymer of a disaccharide repeating units composed of glucuronic acid and N5-β-hydroxybutyryl-N7-acetyl-5,7-diamino-3,5,7,9-tetradeoxynonulosonic acid (pseudaminic acid) on the surface (Putnoky et al., 1990; Kereszt et al., 1998; Reuhs et al., 1998). Interestingly, if the *lpsZ* (*rkpZ*) gene, found in the Rm41 strain-specific *rkp-3* gene cluster (Kiss et al., 2001), responsible for the synthesis of the pseudaminic acid precursor, as well as for the export of the KPS, is introduced into an EPS-deficient mutant of strain 1,021 producing a structurally different KPS, the transconjugant forms effective symbiosis with alfalfa (Williams et al., 1990). The LpsZ protein determines (decreases) the polymerization level of the KPS in both strains and enables the formation of the symbiotically efficient molecular weight form (Reuhs et al., 1995). The KPS of strain Rm41 can complement for the absence of EPS, not only on alfalfa (*M. sativa*), but also on other *Medicago* (*M. media* and *M. varia*) and *Melilotus* (*M. albus* and *M. officinalis*) species tested (Putnoky et al., 1990), however, not on *M. truncatula* (Hozbor et al., 2004; Liu et al., 2014). In *S. meliloti* strain 1,021, a third polysaccharide, the galactoglucan EPS II with a disaccharide repeating unit of a β-(1-3)-linked acetylated glucose and succinylated galactose can contribute to the infection process by replacing the succinoglycan EPS I during nodulation of *M. sativa* (Glazebrook and Walker, 1989). However, EPS II cannot function in place of EPS I on other investigated hosts such as *M. coerulea*, *M. truncatula*, *Melilotus albus,* and *Trigonella foenum-graecum*.

Determinate nodule formation and infection require the correct structure of LPS on the bacterial surface, while the production of exopolysaccharides by rhizobia infecting these nodules seems to be not important. In *Lotus corniculatus* and *L. japonicus* Gifu, however, bacteria, which do not produce EPS, can establish as effective symbiosis as the wild-type strain, whereas mutants affected in mid or late biosynthetic steps (e.g., *exoU*) and produce truncated form of the polysaccharide induced uninfected nodule primordia (Kelly et al., 2013). In contrast, *L. japonicus* MG20 is less stringent in its selection because it forms nitrogen-fixing nodules with mesorhizobia that are both producing no or truncated EPS. The incompatibility in *L. japonicus* Gifu is mediated by the LysM-type receptor EPR3 (Kawaharada et al., 2015), recognizing the diffusible octasaccharide monomer of EPS, not only from *M. loti*, but also from *R. leguminosarum* and *S. meliloti* (Wong et al., 2020). The PXY leucine-rich repeat receptor-like kinase in *L. japonicus* MG20, which also regulates stem vascular development, was identified by quantitative trait locus sequencing (QTL-seq) as a casual component of the differential and less stringent *exoU* response (Kawaharada et al., 2021).

The *S. fredii* strain HH103 establishes symbiosis with a wide variety of legumes forming indeterminate and determinate nodules (Margaret et al., 2011). Infection of the determinate nodules of soybean and pigeon pea (*Cajanus cajan*) by this bacterium necessitates the production of the 5-acetamido-3,5,7,9-tetradeoxy-7-(3-hydroxybutyramido)-L-glycero-L-manno-nonulosonic acid homopolymer K-antigen, however, KPS-deficient mutants of HH103 induce infected and nitrogen-fixing determinate nodules on cowpea (Parada et al., 2006; Hidalgo et al., 2010).

Summary

The presence of certain polysaccharides on the bacterial surface is essential for the infection process monitored by a currently unknown mechanism in the plants. Certain bacteria are able to produce alternative polysaccharides to compensate for the absence of the generally used ones, however, this compensation might not be effective on all hosts. Moreover, not only the presence, but the correct structure, for example, of the EPS is checked by another mechanism.

Other Natural Variations Affecting Bacterial Infection

Large collections of legume hosts and bacteria isolated from nodules developed on plants in natural habitats have allowed the establishment of cross-inoculation groups and investigation of natural variations within cross-inoculation groups and species. Investigations, for example, with the model legumes *L. japonicus* and *M. truncatula* and/or species closely related to them, revealed large variations in symbiotic compatibility and efficiency

(Snyman and Srijdom, 1980; Crook et al., 2012; Gossmann et al., 2012; Granada et al., 2014; Liu et al., 2014; Lorite et al., 2018). For example, experiments using a number of *Medicago* species and *M. truncatula* accessions in combination with different *S. meliloti* isolates revealed tremendous variation in nodulation capacity and nitrogen fixation specificity between different genotype-rhizobial combinations, 40–50% of all host-strain pairs resulted in an ineffective symbiosis (Crook et al., 2012; Liu et al., 2014). Detailed characterization accompanied with the identification of the genes and alleles determining these symbiotic variations beyond soybeans' incompatibility (see later) has been very rare.

Liu et al. (2014) reported that *S. meliloti* strain Rm41 induced root hair curling and nodule primordium formation but failed to infect the roots of *M. truncatula* ecotype F83005.5, although both partners have the genetic capacity for nitrogen fixation. The infection process is arrested at the microcolony stage, either no or occasionally, aberrant ITs not entering the cortex can be observed on the roots. This phenotype is similar to the ones induced by EPS-deficient mutants of *S. meliloti* or by *M. loti* producing truncated EPS or by rhizobia incompatible with certain genotypes of soybean. This dominant trait in *M. truncatula*, however, must be independent of these bacterial effectors. EPS recognition can be ruled out because the strain produces wild-type EPS and its EPS-deficient derivatives cannot establish effective symbiosis with other ecotypes of the plant either. The possibility of effector-triggered immunity (ETI) responsible for the soybean incompatibilities (see later) can also be excluded because the genome of strain Rm41 does not code for any Type III, Type IV, and Type VI secretion systems implicated in ETI.

An *R. leguminosarum* strain (termed Norway) isolated from *L. corniculatus* nodules shows host-genotype specific differences when inoculated on wild-type plants of *Lotus* species and pea cultivars. It induced no nodules on *L. japonicus* Gifu and *L. filicaulis*, *L. japonicus* MG20 formed bumps and occasionally, very small and infected nodules, while *L. japonicus* Nepal showed broadened elongated infection zones. On *L. glaber*, the strains provoked the development of swellings and tumor-like structures, while *L. burtii* developed normal-sized and infected but inefficient nodules. The strain-induced ITs on *Pisum sativum* cv. Sparkle without the formation of nodule(-like) structures, whereas pea cultivar Little Marvel and *Latyrus sativus* plants had ineffective nodules (Gossmann et al., 2012; Liang et al., 2019). In *Lotus* species, the strain induced early and strong induction of a symbiosis-specific gene but no ITs, and rather intercellular accumulation of the bacteria through epidermal cracks could be observed. The strain could invade intact nodule cells where it formed symbiosomes, however, these infected cells exhibited the signs of early senescence (Liang et al., 2019). As the strain seems to possess all the genetic repertoire required for and still fails in the establishment of an effective sysmbiosis (Liang et al., 2018), it will be interesting to find one or more compatible hosts and determine which factors in the bacteria and plants cause the incompatibilities.

Summary

The incompatible interactions arrested at the infection stage indicate the presence of additional checkpoints beyond NF and polysaccharide recognition.

Bacterial Effector Molecules and Plant Immunity Affecting Compatibility

Bacteria secrete proteins and other (macro)molecules to modulate their interactions with the environments, especially when they are interacting with eukaryotic host organisms. In the case of Gram-negative bacteria, secretion requires translocation across both the inner and the outer membranes, and several different molecular machines have been elaborated for this purpose. Many proteins secreted by pathogens and symbionts are aimed to enter the host cells to modify the physiology of the partner, and, thus, several secretion systems include an apparatus to translocate proteins across the plasma membrane of the host also (Tseng et al., 2009). In this context, it is not surprising that rhizobia are also equipped with certain or all types of effector delivery machinery that may have special roles in their interactions with different legume partners.

Microbe-Associated Molecular Patterns and Effector-Triggered Immunity, Type III Secretion System Effectors, and Symbiotic Compatibility

Plants developed a multilayered defense system against microbes that acts both locally and systematically (Ngou et al., 2021) and its elements are also important during the interaction of legumes and rhizobia (Cao et al., 2017). The first line of defense detects the presence of microorganisms *via* the activity of receptors recognizing microbe/pathogen-associated molecular patterns (MAMPs/PAMPs), which are conserved motifs present on essential components of a microbe/pathogen. The binding of MAMPs by these pattern recognition receptors (PRRs) induces rapid changes in the cell—as can be observed upon the recognition of NFs—and leads to MAMP/PAMP-triggered immunity (MTI/PTI). Interestingly, rhizobial MAMPs investigated, so far, such as flagellin or LPS, differ from, for example, those of plant pathogenic or enteric bacteria and do not induce MTI (Tellström et al., 2007; Lopez-Gomez et al., 2012). The legume hosts also evolved recognition mechanisms to distinguish beneficial and harmful microorganisms. *L. japonicus* and *M. truncatula* have LysM pattern-recognition receptors that are related to the NF receptors to separate the perception of chitin oligomeric microbe-associated molecular patterns from the perception of NFs by the NFR1/NFR5 receptor complex (Bozsóki et al., 2017). Another LysM receptor in *L. japonicus*, EPR3 distinguishes *M. loti* cells producing no or normal EPS from those that produce a truncated one with a pentasaccharide repeat instead of an octasaccharide repeat (Kawaharada et al., 2015). Although MTI/PTI at the cell surface is very effective, microbes evolved virulence factors and apparatus for their delivery to the host cells to modify or attenuate the original immune responses. The type III secretion system (T3SS) of Gram-negative bacteria including pathogens and symbionts is a complex multiprotein secretion apparatus that actively exports effector proteins (T3 effectors) with diverse biochemical activities (Schreiber et al., 2021) through the lumen of these tubular structures and directly into the eukaryotic host cells. In rhizobia, proteins that are either extracellular components of or secreted by the T3SS apparatus are termed as Nops, nodulation outer proteins, and are produced upon NF induction (Staehelin and Krishnan, 2015).

The T3 effector proteins can be detected by intracellular receptors of the plant immune system that are usually highly specific in the effectors they recognize, an observation that led to the gene-for-gene hypothesis (Flor, 1971). The recognition of the effector results in a very robust immune response called Effector Triggered Immunity (ETI), which is often culminated in programmed cell death called hypersensitive response to halt the spread of the pathogen.

Classical Resistance and Defense Proteins Determine Symbiotic Incompatibility in Soybeans

The incompatibilities between soybean cultivars and specific rhizobium strains that have been studied and described as gene-for-gene interactions for a long time (Hayashi et al., 2012) seem true to be determined by ETI. Four dominant genes of soybean, *Rj2* (Caldwell, 1966), *Rj3* (Vest, 1970), *Rj4* (Vest and Caldwell, 1972), and *Rfg1* (Trese, 1985) were described to prevent nodulation with certain soybean-nodulating strains belonging to the *Bradyrhizobium* and *Sinorhizobium* genera. The block of these interactions takes place just after the first initial steps. Root hair deformation and/or curling and cortical cell division can be observed although in a lower number than in compatible interactions, but ITs and nodule meristems are not formed (Sadowsky et al., 1995; Yasuda et al., 2016). Analyses of rhizobial mutants have revealed the important role of T3 effectors in the determination of incompatibility with all the *Rj2*, *Rj3*, *Rj4,* and *Rfg1* soybeans because mutants defective in the T3SS, or the production of certain effectors, could form functional nodules on the roots of their incompatible hosts (Meinhardt et al., 1993; Tsukui et al., 2013; Faruque et al., 2015; Tsurumaru et al., 2015; Shobudani et al., 2020; Ratu et al., 2021a).

The *Rj2*, *Rj4,* and *Rfg1* genes of soybean were identified by map-based cloning with surprising results. The *Rj4* gene codes for a thaumatin-like protein (TLP), which belongs to the PR-5 family of pathogenesis-related proteins (Tang et al., 2016), considered as effectors to biotic (for example, fungal attack) and abiotic (for example, osmotic shock) stresses. It was most probably evolved by recent local gene duplication and diversification because both *Rj4* and *rj4* plants harbor a gene coding for another thaumatin-like protein, which is highly similar to Rj4 (only 13 amino acid differences between the two proteins of 296 residues) but does not cause incompatibility with *B. elkanii* strain USDA61, while the second gene causing the incompatibility is present only in the *Rj4* plants. The fact that the Rj4 protein is not a classical receptor protein is surprising and it will be intriguing to understand how this thaumatin-like protein is involved in ETI to regulate bacterial infection.

Another surprising and interesting result was that the allelic variants of the same gene, *Glyma16g33780* coding for a toll-interleukin receptor/nucleotide-binding site/leucine-rich repeat (TIR-NBS-LRR) resistance (R) protein are responsible for the *Rj2* and *Rfg1* incompatibilities (Yang et al., 2010). It was shown that a single amino acid difference, isoleucine versus arginine at amino acid position 490 after the NBS domain in the *Rj2* and *rj2* alleles, respectively, determines symbiotic (in)compatibility (Sugawara et al., 2019). Polymorphism at five amino acids in and after the sixth LRR domain of this R protein differentiates the *Rfg1* and *rfg1* alleles (Yang et al., 2010), however, systematic investigation of these differences to reveal the role of the individual residues has not been conducted yet. All four possible alleles (*rj2*/*rfg1*, *Rj2*/*rfg1*, *rj2*/*Rfg1*, and *Rj2*/*Rfg1*) of the gene were constructed and shown to determine the expected compatibility profile when transformed into a non-restrictive (*rj2*/*rfg1*) soybean (Fan et al., 2017). A genome-wide association study (GWAS) to identify natural variants in key loci that regulate the compatibility between soybean and rhizobia, using Chinese landraces and improved cultivars and *B. diazoefficiens* strain USDA110 as inoculant, pinpointed and confirmed the *Glyma.02G076900* gene termed *G. max Nodule Number Locus 1* (*GmNNL1*) coding for another TIR–NBS–LRR receptor protein and carrying a SINE transposon in the compatible plants as the determinant of the incompatibility (Zhang et al., 2021).

Role of the Type III Secretion System and Nodulation Outer Proteins in Symbiotic Incompatibility With Soybeans

As for the bacterial side, the T3 effector NopP protein of strains USDA122 and USDA110 were shown to be responsible for the incompatibility with *Rj2* and *GmNNL1*-positive soybeans, respectively. Interestingly, if only three amino acids of USDA122 NopP are replaced by those of the compatible strain USDA110, the compatibility with *Rj2* cultivars is restored (Sugawara et al., 2018). Such specificity has not been identified between the *Rfg1* allele-encoded protein and any of the T3 effectors in strain USDA257. Lack of synthesis and/or secretion of the T3 effectors leads to compatibility with soybeans carrying the *Rfg1* allele (Meinhardt et al., 1993) indicating that classical ETI affects compatibility. Moreover, mutations disrupting the *gcvTHP* operon coding for the elements of the glycine cleavage system enables strain USDA257 to form nitrogen-fixing nodules on *Rfg1* soybeans (Lorio et al., 2010). The glycine cleavage system is involved in the generation of C1 units in the form of N^5, N^{10}-methylene tetrahydrofolate, that is used in a variety of biochemical reactions, including the synthesis of purines, histidine, thymine, and methionine as well as the formylation of $tRNA^{fMet}$ already loaded with methionine. The *gcvTHP* mutations do not affect the synthesis and secretion of the Nop proteins in general, thus, further studies are required to elucidate whether a putative decrease in the C1 pool has a direct or indirect role. This putative decrease might affect, for example, the T3SS/T3 effectors or decrease the amount of the innate immune system activating formyl-methionine containing oligopeptides released by damaged bacteria as described in mammalian systems (Zhang et al., 2010).

The incompatibilities of *B. elkanii* strain USDA61 and *B. japonicum* strain Is-34 with *Rj4* soybeans are also dependent on the T3SS because these hosts form an effective symbiosis with the strains if their T3SS systems are non-functional (Faruque et al., 2015; Tsurumaru et al., 2015). Moreover, mutations in four genes coding for proteins (the RelA ppGpp synthetase; a cytosine deaminase; a TerB family tellurite resistance protein; a substrate-binding protein of an ABC transporter) that are not T3E effectors but might affect T3SS synthesis and/or function also restored compatibility (Nguyen et al., 2017). Indeed, it was recently shown

that ppGpp synthetase deficient bradyrhizobia are not able to activate the T3SS (Pérez-Giménez et al., 2021).

Type III Secretion System and Nodulation Outer Proteins Can Both Restrict and Extend the Host-Range

The Nop proteins are indeed "double-edged swords" of rhizobia (Staehelin and Krishnan, 2015) because they can restrict nodulation on one host, while promoting interaction with another plant. At present, it is not known why bacteria are equipped with these effectors that can restrict their symbiotic interactions. One possible explanation, which would be worth investigating, is that these molecules facilitate the interactions of the given strain with legumes of the natural flora where the strain evolved, and their incompatibilities can be observed with plants with different spatial origin. The *B. elkanii* strain USDA61 is incompatible not only with *Rj4* soybeans but also with *Vigna radiata* cultivar KPS1 and different *Lotus* accessions. As with *Rj4* soybean plants, these hosts form effective symbiosis with USDA61 if its T3SS system and the above-mentioned four genes are non-functional. This similarity suggests that the proteins participate in a common mechanism contributing to nodulation restriction in these legumes. Intriguingly, the lack of another T3E Nop effector identified in the same screen as the four non-Nops, a protein of unknown function termed InnB restored the compatibility of the strain with *Vigna radiata* cultivar KPS1 but not with *Rj4* soybean, meaning that different effector proteins might be recognized by the R proteins of the two plant species. To further complicate the picture, the InnB deficient strain proved to be less efficient than the wild-type bacterium when the host was *V. mungo* (Nguyen et al., 2018). Similarly, the T3SS had a positive impact on the symbiotic efficiency of the *B. vignae* strain ORS3257 in *V. unguiculata* and *V. mungo*, but it blocked symbiosis with *V. radiata* (Songwattana et al., 2021). In line with the observations on the host-dependent effect of InnB effector, T3SS-based incompatibility of strain USDA61, with the diverse *Lotus* accessions, arrests the interaction at different developmental stages. The *L. japonicus* Gifu inhibited infection while *L. burttii* inhibited nodule maturation at the post-infection stage, whereas both in *L. burttii* and *L. japonicus* MG-20, a nodule early senescence-like response can be observed (Kusakabe et al., 2020). It was shown that NopF and NopM were the effector proteins that triggered the inhibition of infection and the nodule early senescence–like response, respectively.

In general, the T3SS of a rhizobium strain may play both positive and negative role or can be indifferent during nodulation depending on the plant partner and, thus, may determine (in)compatibility and host-range (Marie et al., 2001; Nelson and Sadowsky, 2015; Songwattana et al., 2017). For example, in the case of *S. fredii* strain NGR234 with extreme broad host range (Pueppke and Broughton, 1999), abolition of the T3SS has no effect on nodulation of *V. unguiculata,* but increased nodule number on *Pachyrhizus tuberosus* and allowed to form effective symbiosis instead of empty pseudo-nodules on *Crotalaria juncea*, while the mutant strains formed fewer nodules on *Tephrosia vogeli*, *Lablab purpureus,* and *Flemingia congesta* roots (Viprey et al., 1998; Marie et al., 2003). Similarly, it was shown that the NopC effector protein of *S. fredii* strain HH103 is beneficial for the symbiosis with *Glycine max* and *V. unguiculata* (Jiménez-Guerrero et al., 2015), but blocks nodulation with *L. japonicus* (Jiménez-Guerrero et al., 2020). The T3SS of *Mesorhizobium loti* strain MAFF303099 inhibits the interaction with *Leucaena leucocephala* (Sánchez et al., 2009) and three *Lotus* species (*L. peregrinus var. carmeli, L. subbiflorus*, and *L. halophilus*), while having positive effect on the nodulation of *L. corniculatus* subsp. *frondosus* and *L. filicaulis* (Okazaki et al., 2010). In addition, the competitiveness of the T3SS mutants against the wild-type strain also depends on the host. *L. tenuis* cultivars INTA Pampa and Esmeralda have contrasting, while *L. japonicus* MG20 has no strain preference (Sánchez et al., 2012).

Influence of Other Translocation Systems (T4SS and T6SS) on Symbiotic Performance

Besides T3SS, only Type IV (T4SS) and Type VI (T6SS) Secretion Systems have the ability to deliver effector proteins from bacteria into the cytosol of eukaryotic cells and, thus, to affect their interactions. Compared to T3SS, a relatively very low information is available about the potential influence of T4SS and T6SS of rhizobia on symbiotic performance and compatibility.

Most *M. loti* strains including R7A lack the genes coding for the elements and effectors of T3SS, but contain genes coding for a type 4 secretion system (T4SS) that can also deliver effectors into target cells. Interestingly, as reported on the T3SS mutants of *M. loti* strain MAFF303099, strain R7A T4SS mutants formed large and bacteroid-containing effective nodules on *Leucaena leucocephala* in contrast to the wild-type strain that could not infect the plant, were delayed in nodulation, and less competitive than the wild-type bacteria on *L. corniculatus* (Hubber et al., 2004). Based on this similarity in the phenotypes, the authors concluded that the type IV and type III system are interchangeable and over the course of evolution, rhizobia can adopt either type. Among sinorhizobia nodulating, only *Medicago, Trigonella and Melilotus* species, the presence of T4SS is quite widespread, while T3SS have been detected in a small number of *S. meliloti* strains and no T6SS coding genes have been shown to be present in the *S. meliloti* and *S. medicae* genomes (Sugawara et al., 2013). Abolition of T4SS function in one strain of both species revealed no, as well as positive and negative, effects on the symbiosis depending on host inoculated.

The pRL1JI (pRle248a) symbiotic plasmid carries the nodulation and nitrogen fixation genes of *R. leguminosarum bv. viciae* strain 248, a symbiotic partner of *Pisum*, *Vicia,* and *Lens* species. Introduction of pRL1JI into *R. leguminosarum bv. trifolii* strain RCR5, from which its symbiotic plasmid had been cured, resulted in a strain, which could form effective symbiosis with *Vicia sativa* but failed to infect *V. hirsuta* and pea (Roest et al., 1997). A transposon insertion mutant that is able to establish nitrogen-fixing symbiosis with the two incompatible hosts led to the identification of a gene cluster that later turned out to code for the T6SS of *R. leguminosarum bv. trifolii* strain RCR5 (Bladergroen et al., 2003). In contrast to pea, the Type VI Secretion Systems of *Rhizobium etli* Mim1 (Salinero-Lanzarote et al., 2019) and *Bradyrhizobium* sp. LmicA16 (Tighilt et al., 2021) have a positive and essential role in developing effective symbiosis with *Phaseolus* and *Lupinus* species, respectively.

Effectors to Promote Symbiosis in the Absence of Nodulation Factors and Nodulation Factors Perception

In the majority of cases, nodule development in legume plants is initiated by the bacterial NFs that are recognized by plasma membrane receptors of the plant. It was, however, shown that certain photosynthetic bradyrhizobia, such as *Bradyrhizobium* sp. BTAi1 and ORS278, do not produce NFs because they have no *nodABC* genes, but they are able to still form nodules on the stem of certain *Aeschynomene* species, such as *A. indica, A. evenia,* and *A. sensitive,* which are exclusively nodulated by photosynthetic bradyrhizobia (Giraud et al., 2007). This surprising discovery was conformed when a *nodB* mutant of *Bradyrhizobium* sp. ORS285 could form nodules on these plants, while it could not establish symbiosis with other host species (for example, *A. afraspera*) that are stem-nodulated by both non-photosynthetic and photosynthetic strains. Searching for the genetic determinants required to induce nodule formation in the absence of NFs by transposon insertion mutagenesis has not revealed any essential genes indicating the likely redundancy of currently unknown functions involved in nodule induction (Bonaldi et al., 2010). Despite the NF independent nodule formation, nodulation of *A. evenia* requires the activity of the common symbiosis signaling pathway because if the genes coding for the Symbiosis Receptor Kinase (SYMRK), the Ca^{2+}/calmodulin-dependent kinase (DMI3) or the cytokinin receptor histidine kinase (LH1/CRE1) were silenced, nodule formation was inhibited (Fabre et al., 2015).

Even NF-dependent hosts can be nodulated in the absence of NFs and NF perception. NFR1-deficient mutants of soybean varieties Enrei and Clark formed nodules when inoculated with *B. elkanii* strain USDA61 even if its NF production was abolished by a mutation in the *nodC* gene, providing the T3SS was functional (Okazaki et al., 2013). Root-hair curling and ITs were not observed in the roots and nodules formed on the NF receptor mutants, indicating that T3SS is involved in crack entry or intercellular infection. Similarly, USDA61 could form (though ineffective) nodules on NF-independent *Aeschynomene* species in a T3SS-dependent manner, however, not all the species or all ecotypes of *A. evenia* were nodulated by USDA61. These results prompted an investigation to determine whether other non-photosynthetic bradyrhizobia are able to induce nodules on these *Aeschynomene* plants, and whether such nodulation depends on the T3SS (Okazaki et al., 2016). The authors observed a whole spectrum of responses from no nodule formation through uninfected and infected ineffective nodules to nitrogen-fixing interactions. while the invasion of nodules happened through both intercellular and root hair infection.

The efficiency of the more intimate interaction between strain ORS3257 and NF-independent *Aeschynomene* accessions showed plant-determined natural variations (such as disturbed bacteroid differentiation and nitrogen fixation) and the nodule formation also depended on T3SS activity. In contrast, the genome of most photosynthetic bradyrhizobia does not contain genes coding for the T3SS and T3Es, and if it contains, as the case with strain ORS285, this translocation system is not required for NF-independent symbiosis, meaning that two mechanisms to induce nodules exists; one depends on T3SS, while the other uses a so far unknown activity. The T3SS of ORS285, however, contributes to the NF-dependent nodulation although it affects the efficiency, but not equally in all plants. The T3SS mutation had no consequences on certain NF-dependent hosts, but had positive (more nodules) or negative (less nodules) effect on others. To determine which T3Es of strains ORS3257 and USDA61 are responsible for the induction of NF-independent nodule formation on *Aeschynomene* species and the *nfr1* mutant soybean, respectively, mutants deficient in genes coding for the T3Es were inoculated on the corresponding partners. The ORS3257 mutants showed a wide variety of phenotypes (Teulet et al., 2019). One mutation increased both nodulation and nitrogen fixation, two mutations led to reduced number of nodules, some of which displayed large necrotic zones, and the nodules induced by two other mutants contained no bacteria. A strain with mutation in an effector gene termed *ernA* for "effector required for nodulation-A" and widely conserved among bradyrhizobia lost the capacity for nodule formation, not only in ORS3257 but also in strain USDA61. Introduction of the *ernA* gene into a *Bradyrhizobium* strain, which does not have an *ernA* gene and is unable to nodulate *Aeschynomene* species in an NF-independent manner, despite the presence of a functional T3SS, enabled the transconjugant to form nodules. Moreover, the nucleus targeted ErnA protein, if ectopically produced in *A. indica* roots, activated organogenesis of root- and nodule-like structures.

The Bel2-5 effector of strain USDA61 that resembles the XopD effector of the plant pathogen *Xanthomonas campestris* was shown by both loss-of-function and gain-of-function approaches to enable the *nfr1* mutant of soybean cultivar Enrei to form nodules (Ratu et al., 2021b). The same effector causes restriction of nodulation on soybeans carrying the *Rj4* allele, and it was shown by mutational analysis that most of its predicted domains were essential for both NF-independent nodulation and nodulation restriction (Ratu et al., 2021a).

Summary

As pathogenic bacteria, some rhizobia equipped themselves with effector molecules that can modify the functioning of plant cells and with the delivery machinery to translocate these effectors into the partners' cells. These effector molecules sometimes facilitate more efficient interaction with certain plants and, thus, extend host-range or overcome the lack of NFs/NF recognition, but in other interactions, they trigger plant defenses, which arrest the interaction.

Natural Variations Affecting Bacteroid Development, Persistence, and Function

Does Outer Membrane Composition Affect Nodule-Specific Cysteine-Rich Peptide-Induced Terminal Bacteroid Differentiation?

Legumes in the dalbergioid and inverted repeat-lacking clades of the *Papilionoideae* subfamily produce NCR and NCR-like peptides to impose terminal bacteroid differentiation on their bacterial partners (**Figure 2**). In the IRLC species, there was a

positive correlation between the degree of bacteroid elongation and the number of the expressed NCRs, but the process can be affected by the inoculant. When the basal IRLC legume *Glycyrrhiza uralensis* producing seven NCR peptides is inoculated with *Mesorhizobium tianshanense* HAMBI3372, bacteroids show the signs of terminal bacteroid differentiation, such as increased cell size and decreased cell division capacity (Montiel et al., 2016), but the bacteroids of *S. fredi*i strain HH103 are not terminally differentiated in the nodules of this plant (Crespo-Rivas et al., 2016). Interestingly, the electrophoretic profile of the LPSs, especially in the O-antigen containing S(mooth)-LPS region, was markedly different from that of cultured cells when the bacteroids were isolated from *G. uralensis* nodules, whereas it was indistinguishable when bacteroids were isolated from soybean or pigeon pea. Whether this LPS modification or/and the observed decreased sensitivity toward the antimicrobial activity of cationic NCR peptides are responsible for the lack of terminal bacteroid differentiation remains to be elucidated (Crespo-Rivas et al., 2016).

Co-evolution of the BacA Peptide Transporters With Host Peptides

The *bacA* gene coding for a peptide transporter plays an essential role in bacteroid development and survival in those rhizobia that form nodules on NCR peptide producing IRLC legumes, such as pea and alfalfa. In contrast, the orthologous sequence is dispensable when plants such as *Lotus* not having NCRs are infected (Kereszt et al., 2011). Although the BacA proteins of different rhizobia play the same role during the terminal differentiation of bacteroids, it turned out that *bacA* genes from *S. fredii* or *R. leguminosarum bv. Viciae 3841* failed to restore the Fix^+ phenotype of an *S. meliloti bacA* mutant on *M. sativa*, however, they allowed for further developmental progression before a loss of viability (diCenzo et al., 2017). Interestingly, the same genes could complement the mutant when *Melilotus albus* was the host and the *S. meliloti bacA* gene could complement the symbiotic defect of the *R. leguminosarum* bv. *Viciae* mutants during nodule development on pea roots. The authors showed that the *S. meliloti* BacA has rapidly diverged from the other rhizobial proteins and suggested that it most probably has evolved toward a specific interaction with *Medicago* (NCR peptides). This suggestion is in agreement with the observation that, although NCR peptides have a single origin, their evolution has followed different routes in individual IRLC legume lineages (Montiel et al., 2017).

Differential Role of the BclA Peptide Transporter of Bradyrhizobia

As described in a previous chapter, the Dalbergoid clade contains *Aeschynomene* species with either NF-dependent or NF-independent nodulation ability. A comparative study using the *Bradyrhizobium* strain ORS285, which can nodulate both types of plants, revealed that bacteria enter plant tissues *via* intercellular infection mechanism, and the division and development of infected founder cells give rise to the nodule tissues, where bacteria go through a terminal differentiation program (Bonaldi et al., 2011). Later it was shown that NCR-like peptides govern the terminal bacteroid differentiation in these species too, which is completed as spherical morphotype in the NF-independent species and as elongated bacteroids in NF-dependent species (Czernic et al., 2015). The differentiation of both S and E morphotype bacteroids requires the activity of the peptide transporter BclA, a homolog of *S. meliloti* BacA, both implicated in the transport of the NCR(-like) peptides, although it is required for the survival of bacteria only in the NF-independent plants (Guefrachi et al., 2015). Interestingly, *B. diazoefficiens* strain USDA110, the soybean model symbiont can nodulate the NF-dependent *Aeschynomene* species, however, the nodulation is associated with atypical bacteroid differentiation showing the signs of both the terminal and non-terminal developments and with suboptimal symbiotic efficiency (Barrière et al., 2017; Nicoud et al., 2021). The size and DNA content of the bacteroids in the *Aeschynomene* nodules and the requirement, more precisely, the indifference of the BclA protein during bacteroid differentiation were the same as in the soybean nodules, while the membrane permeability of the bacteroids is more similar to that of the ORS285 bacteroids.

Strain Discrimination With Nodule-Specific Cysteine-Rich Peptides

The *S. meliloti* strains A145 and Rm41 form ineffective symbiosis with *M. truncatula* cv. Jemalong (Tirichine et al., 2000; Liu et al., 2014), while their interactions with other ecotypes, such as DZA315.16 or A20, is normal. Jemalong nodules are invaded by these strains, even bacteroid differentiation and *nif* gene induction takes place at 7 days post-inoculation (dpi), but the elongated bacteroids are eliminated (14 dpi), and only saprophytic bacteria remain in the older nodules at 21 dpi (Wang et al., 2017). Surprisingly, dominant allelic variants of two genes termed *NFS1* and *NFS2* (nitrogen fixation specificity) coding for NCR peptides function as a negative regulator of symbiotic persistence (Wang et al., 2017, 2018; Yang et al., 2017). The NCRs were shown not only to be positive regulators of bacteroid development and persistence (Van de Velde et al., 2010; Horváth et al., 2015; Kim et al., 2015), but the cationic peptides also have antimicrobial activity (Van de Velde et al., 2010; Tiricz et al., 2013). Although the NCR variants from the incompatible host possess stronger antimicrobial activity than those from the compatible plants, the differences in the bactericidal activity do not correlate with and are not responsible for the *in planta* function because the responses of a compatible strain are similar. The bacterial targets of the peptides and the genetic determinants of the incompatibility in the bacteria, however, remain to be identified.

A Peptidase, Which Can Cleave Nodule-Specific Cysteine-Rich Peptides, Causes Incompatibility

Crook et al. (2012) described several accessory plasmids that restrict nodule development, cause impaired symbiotic nitrogen fixation, and enhance host invasion. One of these plasmids was reported to encode the HrrP metallopeptidase that is responsible for the symbiotic incompatibility with some host plants (Price et al., 2015). This enzyme was shown to cleave NCR peptides *in vitro*, although with different efficiency, suggesting some

level of NCR peptide substrate selectivity. Bacteroids in the nodules—that are much smaller than normal, most probably because of the loss of meristem persistence—on the incompatible host plant develop normally and express the *nif* genes but in older cells, they appear to fragment and to degenerate. In addition, the saprophytic rhizobial population in both compatible and incompatible nodules is significantly larger. One possible explanation for these phenotypes is that the peptidase cleaves NCR peptides/peptide variants, both those that are required for bacteroid persistence and those that have antibacterial activity. This cleavage activity might be more efficient on the peptides of the incompatible ecotypes leading to bacteroid senescence. On the other hand, cleaving the cationic peptides that would restrict the cheaters might increase the saprophytic population.

Host-Specific Regulation of Nitrogen Fixation Genes in Clovers

Strains of *R. leguminosarum* bv. *trifolii* (such as ICC105), able to form effective nodules on *Trifolium ambiguum* (Caucasian clover), form bacteroid containing but ineffective nodules on *T. repens* (white clover), whereas strains (for example, NZP514) that form effective nodules on white clover usually do not nodulate Caucasian clover. It was shown (Miller et al., 2007) that the *nifHDKEN*, *fixABCX,* and, probably, the *NifBfdxNfixU* operons of strain ICC105 are not induced in the white clover nodules that were not caused by the lack of *nifA* expression or NifA function. Rather, it is supposed that the intergenic region between the *nifH* and *fixA* genes might be bound not only by the canonical transcription factors NifA and RpoN, but also by additional host-specific regulatory elements. This proposed protein might bind upstream of the NifA binding sites either in response to or in the absence of a host-specific signal and interacts with NifA to prevent it from activating the expression of the *nif/fix* operons.

Summary

Certain host plants impose terminal bacteroid differentiation on their rhizobial partners with the help of NCR(-like) peptides produced in the infected nodule cells. The NCRs are required not only for bacteroid differentiation, persistence, and functioning, but are also used for strain discrimination and elimination. Bacteria might counteract the effects of NCRs by producing a modified outer membrane or a peptidase cleaving the peptides. Some of these peptides possess antibacterial activity, which is attenuated by the BacA/BclA peptide transporters to a different extent in different hosts that show only limited interchangeability between bacteria infecting legumes with diverse peptide profiles. It is not known whether NCRs or other factors are responsible for the host-specific activation of the nitrogen-fixation genes in nodules of clovers.

PARTNER-DEPENDENT MANIFESTATION OF MUTATIONS

The majority of the genes required for the development and function of nitrogen-fixing nodules were identified by forward genetics studies when the failure of the mutants in establishing effective symbiosis indicated their essentiality in the interaction. Intriguingly, there are cases, apart from bacterial T3SS effectors and ETI elements, when a mutation manifested in the arrest of the interaction at a certain developmental stage with one partner, whereas in no disturbance or halt in another stage with another partner(s).

Host Plants Put Different Levels of Stress on Their Partners

The production of NFs and exopolysaccharides are controlled by complex regulatory networks including the stringent response, which induces a physiological change in response to adverse growth conditions/stress and can also control bacterial development, virulence using guanosine tetra- and penta-phosphate (ppGpp) as effector molecules (Wells and Long, 2002). The *relA*-deletion mutant of *S. meliloti* incapable of ppGpp synthesis fails to nodulate *M. sativa* because of the early arrest in IT development and meristem formation, but successfully infects *M. truncatula* although bacteroids have disorganized positioning within nodule cells and reduced nitrogen-fixation capacity in this host (Wippel and Long, 2019). The mutant seems to produce NFs and EPS in a higher amount than the wild-type cells and these elevated levels might be inhibitory for alfalfa and neutral or even stimulant in barrel medic. Transcriptomic changes in the mutant upon luteolin induction also pointed to other stress regulatory processes, such as osmoregulation, that might also affect the infection process. In the nodules of *M. truncatula*, the number of differentially expressed bacterial genes are rather low, however, the upregulation of numerous transcripts related to metabolism and transcriptional regulation depends on RelA, indicating that full metabolic adaptation to the nodule environment and, as a direct or indirect consequence, the normal bacteroid organization and nitrogen fixation might require RelA function.

Mutation in another stress-related gene of *S. meliloti*, *typA*, coding for a ribosome-binding GTPase acting at the level of protein synthesis, was shown to be involved not only in stress adaptation, but to be required for the establishment of nitrogen-fixing symbiosis on certain *Medicago* hosts (Kiss et al., 2004). The mutant formed efficient nodules on different *M. sativa* cultivars, with only ∼20% decrease in shoot dry weight of some lines and with *M. truncatula* ecotype DZA315.16. In contrast, it formed Fix^- nodules on ecotypes Jemalong and F83005, however, the nodules on the former were small and devoid of bacteroids, while no obvious differences in nodule occupancy between the wild-type and mutant bacteria-induced F83005 nodules could be observed. The TypA and related proteins in other bacteria are required for the adaptation to several stresses under different conditions. Rhizobia must adapt to ever-changing physiological conditions such as pH, ion composition, osmotic concentration, oxidative stress, or plant defense reactions during nodule invasion and bacteroid differentiation. These conditions, which are most probably different in each host plant, may explain why TypA is not required equally on the investigated hosts.

The Severity of a Carbon Metabolism Defect Depends on the Host Plant

Energy and carbon sources for bacteria in the nodule cells are provided in the forms of the TCA-cycle intermediary C4-dicarboxylates, succinate, fumarate, and malate that necessitate the activity of gluconeogenesis to generate intermediates for growth and metabolism. The first step of gluconeogenesis, the decarboxylation and phosphorylation of the TCA-cycle intermediate oxaloacetate is catalyzed by the phosphoenolpyruvate carboxykinase (PEPCK) enzyme. The effect of a mutation in the *pck* gene coding for PEPCK in *S. fredii* strain NGR234 on nodule development and nitrogen fixation was shown to depend on the host inoculated with the mutant (Osteras et al., 1991). The determinate nodule-forming plants, *Macroptilium atropurpureum* and *V. unguiculata* formed fewer nodules when inoculated with the mutant as compared to the wild-type that provided very low or no gain in plant biomass attributable to the symbiosis. On *Leucaena leucocephala* forming indeterminate nodules, the mutant induced an excess number of nodules that had 60% of wild-type efficiency of symbiotic nitrogen fixation. In all nodules harboring the mutant, the number of infected cells was lower compared to that observed in NGR234 induced nodules. One possible explanation for the variability of symbiotic efficiency is that different carbon source availability might be provided by a given plant during the invasion, bacteroid development, and nitrogen-fixation that would determine the relative importance of the bacterial gluconeogenesis pathway.

Plant Mutations Cause Bacteroid Senescence Only for Certain Strains

The forward genetic screen of *M. truncatula* Tnt1 insertion mutants using *S. meliloti* strain 1021, as inoculant identified the *npd1-1* mutant (line NF4608), which formed Fix$^-$ nodules, arrested at an early developmental phase, just after bacteria are released from the ITs (Pislariu et al., 2019). The released rhizobia start to elongate but fail to differentiate into functional, nitrogen-fixing bacteroids, rather, they go through a degradative senescence process most probably caused by the activation of plant defense responses. Interestingly, strain Rm41 induces functional, nitrogen-fixing nodules that can support plant growth as in wild-type plants. The mutation abolishes the function of a symbiotically expressed gene termed *NPD1* (Nodule-specific PLAT Domain) coding for a small protein localized in the endoplasmatic reticulum (ER) and symbiosomes, but not co-localized with Golgi. It is supposed that NPD1 with other ER-localized proteins suppresses rhizobium induced plant defense reactions. How and why the hosts discriminate against bacterial strains remains to be elucidated.

The *L. japonicus apn1* (*sym104*) mutants, when inoculated with *Mesorhiozobium loti* strain TONO, display severe nitrogen deficiency symptoms and form small white nodules, in which the early senescence of nodule cells and the bacteroids therein can be observed (Yamaya-Ito et al., 2018). This senescence was manifested in a decrease in bacteroid density, abnormal enlargement, and irregular shapes of symbiosomes, the presence of lytic vacuoles, and disintegration of infected cells. Interestingly, not all the *M. loti* strains induce Fix$^-$ nodules on the mutant plants; out of the nine strains tested five bacteria, including strain MAFF303099, formed effective pink nodules. The mutations in *Lotus* disrupt a symbiosis-specific late nodulin gene coding for a secreted aspartic peptidase enzyme termed ASPARTIC PEPTIDASE NODULE-INDUCED 1 (APN1). Random mutagenesis of strain TONO identified the causal gene termed *DCA1* (Determinant of nitrogen fixation Compatibility of APN1) causing the incompatibility that encodes an active autotransporter, one of the proteins also known as the Type V protein secretion system found in Gram-negative bacteria (Shimoda et al., 2020). The protein contains an N-terminal secretion signal peptide, a C-terminal autotransporter β-domain, and 43 divergent glycine-rich repeats of 44–53 amino acids. Autotransporters cleave a part of their protein known as the passenger domain and transport it through the outer membrane to the outside of the cell and the whole length of this passenger domain with all glycine-rich repeats is required for its activity. It was shown that the APN1 protein can degrade the DCA1 protein under the acidic conditions required for the activity of aspartic peptidases. The phenotypic dissimilarity caused by the different strains producing orthologous, basically identical autotransporter is determined by the expression differences of the gene in the bacteria, i.e., *DCA1* promoter-GUS activity in wild-type and *apn1* mutant nodules was negligible in strain MAFF303099 and high in strain TONO. It is proposed that strain TONO produces a higher amount of the effector protein than MAFF303099 that is degraded by the APN1 aspartic peptidase in the wild-type plant. In the mutant plants, however, the effector is not degraded and is able to induce the expression of cysteine protease genes leading to suppression of nodule maturation and initiation of senescence, while the amount of DCA1 from MAFF303099 is not enough for the induction.

Summary

Bacteria face diverse levels of stresses and defense responses, as well as metabolite availability and composition, in different wild-type and mutant plants. The ability of wild-type and mutant bacteria to respond and adapt to those conditions is not the same in different strains, and that is manifested in phenotypic variations. These phenotypic variations will allow us to reveal what causes the differences.

CONCLUSION AND PERSPECTIVES

Exploring natural variations has already facilitated the recognition of important determinants of symbiotic nodule initiation, development, and function, such as the identification of the LysM2 domain of NFR5 as a potential binding site for the bacterial NFs or recognition of the role of T3SS, Type3 effectors, and ETI in partner selection or revealing that NCR peptides, not only direct the terminal differentiation and persistence

of bacteroids, but also participate in partner discrimination and selection. These examples as well as the results with mutants showing multiple phenotypes depending on the hosts suggest that it is worth to reinvestigate the already existing mutants with other symbiotic partners and identify the genetic determinants behind the phenotypic differences in both wild-type and mutant interactions. The agricultural productivity of legume crops depends on their interaction, i.e., (in)compatibility with the rhizobia resident or introduced as inoculum in the soils that is also affected by the competition of the different strains. Similarly, engineering nitrogen-fixing non-legume crops in the future, as well as their cultivation on the field, requires the knowledge of the details and fine-regulation of the symbiotic process. The results of studies on natural variations will identify the determinants of symbiotic (in)compatibility and reveal the fine details that exist in the regulation of the interaction, thus, may contribute to the implementation and realization of the plans aiming at the development of novel crops for sustainable agriculture.

AUTHOR CONTRIBUTIONS

TW, BB, and SK collected, collated, organized the reviewed publications, and participated in the writing of the manuscript. AK conceived the topic of the review, supervised the co-authors' work, and wrote the manuscript. All authors contributed to the article and approved the submitted version.

FUNDING

Work in the lab of AK was supported by the Hungarian National Office for Research, Development, and Innovation (NKFIH Grant Nos. K120122, K128486, and K134841), with contribution from the NKFIH Frontline Research project KKP129924 and the Balzan Research Grant to É. Kondorosi. SK has been a recipient of the Young Researcher Fellowship previously from the Hungarian Academy of Sciences, and currently from the Eötvös Loránd Research Network (ELKH).

REFERENCES

Alunni, B., and Gourion, B. (2016). Terminal bacteroid differentiation in the legume-rhizobium symbiosis: nodule-specific cysteine-rich peptides and beyond. *New Phytol.* 211, 411–417. doi: 10.1111/nph.14025

Ardourel, M., Demont, N., Debellé, F., Maillet, F., De Billy, F., Prome, J. C., et al. (1994). Rhizobium meliloti lipooligosaccharide nodulation factors: different structural requirements for bacterial entry into target root hair cells and induction of plant symbiotic developmental responses. *Plant Cell* 6, 1357–1374. doi: 10.1105/tpc.6.10.1357

Arrighi, J. F., Barre, A., Ben Amor, B., Bersoult, A., Soriano, L. C., Mirabella, R., et al. (2006). The medicago truncatula lysin [corrected] motif-receptor-like kinase gene family includes NFP and new nodule-expressed genes. *Plant Physiol.* 142, 265–279. doi: 10.1104/pp.106.084657

Barrière, Q., Guefrachi, I., Gully, D., Lamouche, F., Pierre, O., Fardoux, J., et al. (2017). Integrated roles of BclA and DD-carboxypeptidase 1 in bradyrhizobium differentiation within NCR-producing and NCR-lacking root nodules. *Sci. Rep.* 7:9063. doi: 10.1038/s41598-017-08830-0

Bergersen, F. J., and Nutman, P. S. (1957). Symbiotic effectiveness in nodulated red clover. IV. the influence of the host factors i1 and ie upon nodule structure and cytology. *Heredity* 11, 175–184. doi: 10.1038/hdy.1957.15

Bladergroen, M. R., Badelt, K., and Spaink, H. P. (2003). Infection-blocking genes of a symbiotic rhizobium leguminosarum strain that are involved in temperature-dependent protein secretion. *Mol. Plant Microbe Int.* 16, 53–64. doi: 10.1094/MPMI.2003.16.1.53

Bonaldi, K., Gargani, D., Prin, Y., Fardoux, J., Gully, D., Nouwen, N., et al. (2011). Nodulation of *Aeschynomene afraspera* and a. indica by photosynthetic bradyrhizobium sp. strain ORS285: the nod-dependent versus the nod-independent symbiotic interaction. *Mol. Plant Microbe Int.* 24, 1359–1371. doi: 10.1094/MPMI-04-11-0093

Bonaldi, K., Gourion, B., Fardoux, J., Hannibal, L., Cartieaux, F., Boursot, M., et al. (2010). Large-scale transposon mutagenesis of photosynthetic bradyrhizobium sp. strain ORS278 reveals new genetic loci putatively important for nod-independent symbiosis with aeschynomene indica. *Mol. Plant Microbe Int.* 23, 760–770. doi: 10.1094/MPMI-23-6-0760

Bozsóki, Z., Cheng, J., Feng, F., Gysel, K., Vinther, M., Andersen, K. R., et al. (2017). Receptor-mediated chitin perception in legume roots is functionally separable from nod factor perception. *Proc. Natl. Acad. Sci. U.S.A.* 114, E8118–E8127. doi: 10.1073/pnas.1706795114

Caldwell, B. E. (1966). Inheritance of a strain-specific ineffective nodulation in soybeans. *Crop Sci.* 6, 427–428. doi: 10.2135/cropsci1966.0011183x000600050010x

Cao, Y., Halane, M. K., Gassmann, W., and Stacey, G. (2017). The role of plant innate imunity in the legume-rizobium smbiosis. *Ann. Rev. Plant Biol.* 68, 535–561. doi: 10.1146/annurev-arplant-042916-041030

Carlson, R. W., Kalembasa, S., Turowski, D., Pachori, P., and Noel, K. D. (1987). Characterization of the lipopolysaccharide from a rhizobium phaseoli mutant that is defective in infection thread development. *J. Bacteriol.* 169, 4923–4928. doi: 10.1128/jb.169.11.4923-4928.1987

Catoira, R., Galera, C., De Billy, F., Penmetsa, R. V., Journet, E. P., Maillet, F., et al. (2000). Four genes of medicago truncatula controlling components of a nod factor transduction pathway. *Plant Cell* 12, 1647–1666. doi: 10.1105/tpc.12.9.1647

Crespo-Rivas, J. C., Guefrachi, I., Mok, K. C., Villaécija-Aguilar, J. A., Acosta-Jurado, S., Pierre, O., et al. (2016). *Sinorhizobium fredii* HH103 bacteroids are not terminally differentiated and show altered O-antigen in nodules of the inverted repeat-lacking clade legume glycyrrhiza uralensis. *Environ. Microbiol.* 18, 2392–2404. doi: 10.1111/1462-2920.13101

Crook, M. B., Lindsay, D. P., Biggs, M. B., Bentley, J. S., Price, J. C., Clement, S. C., et al. (2012). Rhizobial plasmids that cause impaired symbiotic nitrogen fixation and enhanced host invasion. *Mol. Plant Microbe Int.* 25, 1026–1033. doi: 10.1094/MPMI-02-12-0052-R

Czernic, P., Gully, D., Cartieaux, F., Moulin, L., Guefrachi, I., Patrel, D., et al. (2015). Convergent evolution of endosymbiont differentiation in dalbergioid and inverted repeat-lacking clade legumes mediated by nodule-specific cysteine-rich peptides. *Plant Physiol.* 169, 1254–1265. doi: 10.1104/pp.15.00584

Dénarié, J., Debellé, F., and Promé, J. C. (1996). Rhizobium lipo-chitooligosaccharide nodulation factors: signaling molecules mediating recognition and morphogenesis. *Ann. Rev. Biochem.* 65, 503–535. doi: 10.1146/annurev.bi.65.070196.002443

diCenzo, G. C., Zamani, M., Ludwig, H. N., and Finan, T. M. (2017). Heterologous complementation reveals a specialized activity for BacA in the medicago-sinorhizobium meliloti symbiosis. *Mol. Plant Microbe Int.* 30, 312–324. doi: 10.1094/MPMI-02-17-0030-R

Diedhiou, I., and Diouf, D. (2018). Transcription factors network in root endosymbiosis establishment and development. *World J. Microbiol. Biotechnol.* 34:37. doi: 10.1007/s11274-018-2418-7

Dylan, T., Nagpal, P., Helinski, D. R., and Ditta, G. S. (1990). Symbiotic pseudorevertants of *Rhizobium meliloti* ndv mutants. *J. Bacteriol.* 172, 1409–1417. doi: 10.1128/jb.172.3.1409-1417.1990

Ehrhardt, D. W., Wais, R., and Long, S. R. (1996). Calcium spiking in plant root hairs responding to rhizobium nodulation signals. *Cell* 85, 673–681. doi: 10.1016/s0092-8674(00)81234-9

Fabre, S., Gully, D., Poitout, A., Patrel, D., Arrighi, J. F., Giraud, E., et al. (2015). Nod factor-independent nodulation in aeschynomene evenia required

the common plant-microbe symbiotic toolkit. *Plant Physiol.* 169, 2654–2664. doi: 10.1104/pp.15.01134

Fan, Y., Liu, J., Lyu, S., Wang, Q., Yang, S., and Zhu, H. (2017). The soybean Rfg1 gene restricts nodulation by *Sinorhizobium fredii* USDA193. *Front. Plant Sci.* 8:1548. doi: 10.3389/fpls.2017.01548

Farkas, A., Maróti, G., Dürgõ, H., Györgypál, Z., Lima, R. M., Medzihradszky, K. F., et al. (2014). Medicago truncatula symbiotic peptide NCR247 contributes to bacteroid differentiation through multiple mechanisms. *Proc. Natl. Acad. Sci. U.S.A.* 111, 5183–5188. doi: 10.1073/pnas.1404169111

Faruque, O. M., Miwa, H., Yasuda, M., Fujii, Y., Kaneko, T., Sato, S., et al. (2015). Identification of *Bradyrhizobium elkanii* genes involved in incompatibility with soybean plants carrying the Rj4 allele. *Appl. Environ. Microbiol.* 81, 6710–6717. doi: 10.1128/AEM.01942-15

Felle, H. H., Kondorosi, É, Kondorosi, Á, and Schultze, M. (1988). The role of ion fluxes in nod factor signalling in *Medicago sativa*. *Plant J.* 13, 455–463. doi: 10.1046/j.1365-313X.1998.00041.x

Feng, F., Sun, J., Radhakrishnan, G. V., Lee, T., Bozsoki, Z., Fort, S., et al. (2019). A combination of chitooligosaccharide and lipochitooligosaccharide recognition promotes arbuscular mycorrhizal associations in medicago truncatula. *Nat. Commun.* 10:5047. doi: 10.1038/s41467-019-12999-5

Ferguson, B. J., Indrasumunar, A., Hayashi, S., Lin, M. H., Lin, Y. H., Reid, D. E., et al. (2010). Molecular analysis of legume nodule development and autoregulation. *J. Integr. Plant Biol.* 52, 61–76. doi: 10.1111/j.1744-7909.2010.00899.x

Firmin, J. L., Wilson, K. E., Carlson, R. W., Davies, A. E., and Downie, J. A. (1993). Resistance to nodulation of cv. afghanistan peas is overcome by nodX, which mediates an O-acetylation of the rhizobium leguminosarum lipo-oligosaccharide nodulation factor. *Mol. Microbiol.* 10, 351–360. doi: 10.1111/j.1365-2958.1993.tb01961.x

Flor, H. H. (1971). Current status of the gene-for-gene concept. *Ann. Rev. Phytopathol.* 9, 275–296. doi: 10.1146/annurev-phyto-072910-095339

Foucher, F., and Kondorosi, É (2000). Cell cycle regulation in the course of nodule organogenesis in medicago. *Plant Mol. Biol.* 43, 773–786. doi: 10.1023/a:1006405029600

Gage, D. J. (2004). Infection and invasion of roots by symbiotic, nitrogen-fixing rhizobia during nodulation of temperate legumes. *Microbiol. Mol. Biol. Rev.* 68, 280–300. doi: 10.1128/MMBR.68.2.280-300.2004

Geurts, R., Heidstra, R., Hadri, A. E., Downie, J. A., Franssen, H., Van Kammen, A., et al. (1997). Sym2 of pea is involved in a nodulation factor-perception mechanism that controls the infection process in the epidermis. *Plant Physiol.* 115, 351–359. doi: 10.1104/pp.115.2.351

Gibson, K. E., Kobayashi, H., and Walker, G. C. (2008). Molecular determinants of a symbiotic chronic infection. *Ann. Rev. Gene.t* 42, 413–441. doi: 10.1146/annurev.genet.42.110807.091427

Giraud, E., Moulin, L., Vallenet, D., Barbe, V., Cytryn, E., Avarre, J. C., et al. (2007). Legumes symbioses: absence of nod genes in photosynthetic bradyrhizobia. *Science* 316, 1307–1312. doi: 10.1126/science.1139548

Glazebrook, J., and Walker, G. C. (1989). A novel exopolysaccharide can function in place of the calcofluor-binding exopolysaccharide in nodulation of alfalfa by *Rhizobium meliloti*. *Cell* 56, 661–672. doi: 10.1016/0092-8674(89)90588-6

Gossmann, J. A., Markmann, K., Brachmann, A., Rose, L. E., and Parniske, M. (2012). Polymorphic infection and organogenesis patterns induced by a *Rhizobium leguminosarum* isolate from lotus root nodules are determined by the host genotype. *New Phytol.* 196, 561–573. doi: 10.1111/j.1469-8137.2012.04281.x

Götz, R., Evans, I. J., Downie, J. A., and Johnston, A. W. B. (1985). Identification of the host-range DNA which allows *Rhizobium leguminosarum* strain TOM to nodulate cv. afghanistan peas. *Mol. General Genet. MGG* 201, 296–300. doi: 10.1007/BF00425674

Granada, C. E., Strochein, M., Vargas, L. K., Bruxel, M., De Sa, E. L., and Passaglia, L. M. (2014). Genetic diversity and symbiotic compatibility among rhizobial strains and desmodium incanum and lotus spp. plants. *Genet. Mol. Biol.* 37, 396–405. doi: 10.1590/s1415-47572014000300012

Guefrachi, I., Nagymihály, M., Pislariu, C. I., Van De Velde, W., Ratet, P., Mars, M., et al. (2014). Extreme specificity of NCR gene expression in medicago truncatula. *BMC Genom.* 15:712. doi: 10.1186/1471-2164-15-712

Guefrachi, I., Pierre, O., Timchenko, T., Alunni, B., Barrière, Q., Czernic, P., et al. (2015). Bradyrhizobium BclA is a peptide transporter required for bacterial differentiation in symbiosis with aeschynomene legumes. *Mol. Plant Microbe Int.* 28, 1155–1166. doi: 10.1094/MPMI-04-15-0094-R

Györgypál, Z., Kiss, G. B., and Kondorosi, Á (1991). Transduction of plant signal molecules by the rhizobium NodD proteins. *Bioessays* 13, 575–581. doi: 10.1002/bies.950131106

Györgypál, Z., and Kondorosi, Á (1991). Homology of the ligand-binding regions of *Rhizobium symbiotic* regulatory protein NodD and vertebrate nuclear receptors. *Mol. Gen. Genet.* 226, 337–340. doi: 10.1007/BF00273624

Hayashi, M., Saeki, Y., Haga, M., Harada, K., Kouchi, H., and Umehara, Y. (2012). Rj (rj) genes involved in nitrogen-fixing root nodule formation in soybean. *Breed Sci.* 61, 544–553. doi: 10.1270/jsbbs.61.544

Hidalgo, A., Margaret, I., Crespo-Rivas, J. C., Parada, M., Murdoch, P. D. S., López, A., et al. (2010). The rkpU gene of *Sinorhizobium fredii* HH103 is required for bacterial K-antigen polysaccharide production and for efficient nodulation with soybean but not with cowpea. *Microbiology* 156, 3398–3411. doi: 10.1099/mic.0.042499-0

Horváth, B., Domonkos, Á, Kereszt, A., Szücs, A., Ábrahám, E., Ayaydin, F., et al. (2015). Loss of the nodule-specific cysteine rich peptide, NCR169, abolishes symbiotic nitrogen fixation in the *Medicago truncatula* dnf7 mutant. *Proc. Natl. Acad. Sci. U.S.A.* 112, 15232–15237. doi: 10.1073/pnas.1500777112

Hozbor, D. F., Pich Otero, A. J., Lodeiro, A. R., Del Papa, M. F., Pistorio, M., and Lagares, A. (2004). The symbiotic defect in a *Sinorhizobium meliloti* lipopolysaccharide mutant can be overcome by expression of other surface polysaccharides. *Res. Microbiol.* 155, 855–860. doi: 10.1016/j.resmic.2004.06.012

Hubber, A., Vergunst, A. C., Sullivan, J. T., Hooykaas, P. J., and Ronson, C. W. (2004). Symbiotic phenotypes and translocated effector proteins of the mesorhizobium loti strain R7A VirB/D4 type IV secretion system. *Mol. Microbiol.* 54, 561–574. doi: 10.1111/j.1365-2958.2004.04292.x

Ibáñez, F., Wall, L., and Fabra, A. (2017). Starting points in plant-bacteria nitrogen-fixing symbioses: intercellular invasion of the roots. *J. Exp. Bot.* 68, 1905–1918. doi: 10.1093/jxb/erw387

Jiménez-Guerrero, I., Acosta-Jurado, S., Medina, C., Ollero, F. J., Alias-Villegas, C., Vinardell, J. M., et al. (2020). The *Sinorhizobium fredii* HH103 type III secretion system effector NopC blocks nodulation with Lotus japonicus gifu. *J. Exp. Bot.* 71, 6043–6056. doi: 10.1093/jxb/eraa297

Jiménez-Guerrero, I., Pérez-Montano, F., Medina, C., Ollero, F. J., and López-Baena, F. J. (2015). NopC is a rhizobium-specific type 3 secretion system effector secreted by sinorhizobium (ensifer) fredii HH103. *PLoS One* 10:e0142866. doi: 10.1371/journal.pone.0142866

Kawaharada, Y., Kelly, S., Nielsen, M. W., Hjuler, C. T., Gysel, K., Muszynski, A., et al. (2015). Receptor-mediated exopolysaccharide perception controls bacterial infection. *Nature* 523, 308–312. doi: 10.1038/nature14611

Kawaharada, Y., Sandal, N., Gupta, V., Jin, H., Kawaharada, M., Taniuchi, M., et al. (2021). Natural variation identifies a pxy gene controlling vascular organisation and formation of nodules and lateral roots in lotus japonicus. *New Phytol.* 230, 2459–2473. doi: 10.1111/nph.17356

Kazmierczak, T., Nagymihály, M., Lamouche, F., Barrière, Q., Guefrachi, I., Alunni, B., et al. (2017). Specific host-responsive associations between medicago truncatula accessions and sinorhizobium strains. *Mol. Plant Microbe Int.* 30, 399–409. doi: 10.1094/MPMI-01-17-0009-R

Kelly, S. J., Muszynski, A., Kawaharada, Y., Hubber, A. M., Sullivan, J. T., Sandal, N., et al. (2013). Conditional requirement for exopolysaccharide in the mesorhizobium-lotus symbiosis. *Mol. Plant Microbe Int.* 26, 319–329. doi: 10.1094/MPMI-09-12-0227-R

Kereszt, A., Kiss, E., Reuhs, B. L., Carlson, R. W., Kondorosi, Á, and Putnoky, P. (1998). Novel rkp gene clusters of *Sinorhizobium meliloti* involved in capsular polysaccharide production and invasion of the symbiotic nodule: the rkpK gene encodes a UDP-glucose dehydrogenase. *J. Bacteriol.* 180, 5426–5431. doi: 10.1128/JB.180.20.5426-5431.1998

Kereszt, A., Mergaert, P., Maróti, G., and Kondorosi, É (2011). Innate immunity effectors and virulence factors in symbiosis. *Curr. Opin. Microbiol.* 14, 76–81. doi: 10.1016/j.mib.2010.12.002

Kim, M., Chen, Y., Xi, J., Waters, C., Chen, R., and Wang, D. (2015). An antimicrobial peptide essential for bacterial survival in the nitrogen-fixing symbiosis. *Proc. Natl. Acad. Sci. U.S.A.* 112, 15238–15243. doi: 10.1073/pnas.1500123112

Kiss, E., Huguet, T., Poinsot, V., and Batut, J. (2004). The typA gene is required for stress adaptation as well as for symbiosis of *Sinorhizobium meliloti* 1021 with certain *Medicago truncatula* lines. *Mol. Plant Microbe Int.* 17, 235–244. doi: 10.1094/MPMI.2004.17.3.235

Kiss, E., Kereszt, A., Barta, F., Stephens, S., Reuhs, B. L., Kondorosi, Á, et al. (2001). The rkp-3 gene region of *Sinorhizobium meliloti* Rm41 contains strain-specific genes that determine K antigen structure. *Mol. Plant Microbe Int.* 14, 1395–1403. doi: 10.1094/MPMI.2001.14.12.1395

Kozik, A., Heidstra, R., Horváth, B., Kulikova, O., Tikhonovich, I., Ellis, T. H. N., et al. (1995). Pea lines carrying Sym1 or Sym2 can be nodulated by rhizobium strains containing nodX - syml and sym2 are allelic. *Plant Sci.* 108, 41–49. doi: 10.1016/0168-9452(95)04123-C

Kronauer, C., and Radutoiu, S. (2021). Understanding nod factor signalling paves the way for targeted engineering in legumes and non-legumes. *Curr. Opin. Plant Biol.* 62:102026. doi: 10.1016/j.pbi.2021.102026

Kusakabe, S., Higasitani, N., Kaneko, T., Yasuda, M., Miwa, H., Okazaki, S., et al. (2020). Lotus accessions possess multiple checkpoints triggered by different type III secretion system effectors of the wide-host-range symbiont bradyrhizobium elkanii USDA61. *Microbes Environ.* 35:141. doi: 10.1264/jsme2.ME19141

Lamouche, F., Bonadé-Bottino, N., Mergaert, P., and Alunni, B. (2019). Symbiotic efficiency of spherical and elongated eacteroids in the aeschynomene-bradyrhizobium symbiosis. *Front. Plant Sci.* 10:377. doi: 10.3389/fpls.2019.00377

Lamouche, F., Gully, D., Chaumeret, A., Nouwen, N., Verly, C., Pierre, O., et al. (2018). Transcriptomic dissection of *Bradyrhizobium* sp. strain ORS285 in symbiosis with *Aeschynomene* spp. inducing different bacteroid morphotypes with contrasted symbiotic efficiency. *Environ. Microbiol.* 21, 3244–3258. doi: 10.1111/1462-2920.14292

Leigh, J. A., Signer, E. R., and Walker, G. C. (1985). Exopolysaccharide-deficient mutants of Rhizobium meliloti that form ineffective nodules. *Proc. Natl. Acad. Sci. U.S.A.* 82, 6231–6235. doi: 10.1073/pnas.82.18.6231

Lewis-Henderson, W. R., and Djordjevic, M. A. (1991a). A cultivar-specific interaction between *Rhizobium leguminosarum* bv. trifolii and subterranean clover is controlled by nodM, other bacterial cultivar specificity genes, and a single recessive host gene. *J. Bacteriol.* 173, 2791–2799. doi: 10.1128/jb.173.9.2791-2799.1991

Lewis-Henderson, W. R., and Djordjevic, M. A. (1991b). nodT, a positively-acting cultivar specificity determinant controlling nodulation of *Trifolium subterraneum* by *Rhizobium leguminosarum* biovar trifolii. *Plant Mol. Biol.* 16, 515–526. doi: 10.1007/BF00023418

Li, R., Knox, M. R., Edwards, A., Hogg, B., Ellis, T. H., Wei, G., et al. (2011). Natural variation in host-specific nodulation of pea is associated with a haplotype of the SYM37 LysM-type receptor-like kinase. *Mol. Plant Microbe Int.* 24, 1396–1403. doi: 10.1094/MPMI-01-11-0004

Liang, J., Hoffrichter, A., Brachmann, A., and Marin, M. (2018). Complete genome of *Rhizobium leguminosarum* norway, an ineffective lotus micro-symbiont. *Stand Gen. Sci.* 13:36. doi: 10.1186/s40793-018-0336-9

Liang, J., Klingl, A., Lin, Y. Y., Boul, E., Thomas-Oates, J., and Marin, M. (2019). A subcompatible rhizobium strain reveals infection duality in lotus. *J. Exp. Bot.* 70, 1903–1913. doi: 10.1093/jxb/erz057

Lie, T. A. (1984). Host genes in *Pisum sativum* L. conferring resistance to european rhizobium leguminosarum strains. *Plant Soil* 82, 415–425. doi: 10.1007/bf02184279

Lindström, K., and Mousavi, S. A. (2020). Effectiveness of nitrogen fixation in rhizobia. *Microb Biotechnol.* 13, 1314–1335. doi: 10.1111/1751-7915.13517

Liu, J., Yang, S., Zheng, Q., and Zhu, H. (2014). Identification of a dominant gene in *Medicago truncatula* that restricts nodulation by *Sinorhizobium meliloti* strain Rm41. *BMC Plant Biol.* 14:167. doi: 10.1186/1471-2229-14-167

Long, S. R. (1996). Rhizobium symbiosis: nod factors in perspective. *Plant Cell* 8, 1885–1898. doi: 10.1105/tpc.8.10.1885

López-Baena, F. J., Ruiz-Sainz, J. E., Rodríguez-Carvajal, M. A., and Vinardell, J. M. (2016). Bacterial molecular signals in the sinorhizobium fredii-soybean symbiosis. *Int. J. Mol. Sci.* 17:755. doi: 10.3390/ijms17050755

Lopez-Gomez, M., Sandal, N., Stougaard, J., and Boller, T. (2012). Interplay of flg22-induced defence responses and nodulation in lotus japonicus. *J. Exp. Bot.* 63, 393–401. doi: 10.1093/jxb/err291

López-Lara, I. M., Van Den Berg, J. D., Thomas-Oates, J. E., Glushka, J., Lugtenberg, B. J., and Spaink, H. P. (1995). Structural identification of the lipo-chitin oligosaccharide nodulation signals of rhizobium loti. *Mol. Microbiol.* 15, 627–638. doi: 10.1111/j.1365-2958.1995.tb02372.x

Lorio, J. C., Kim, W. S., Krishnan, A. H., and Krishnan, H. B. (2010). Disruption of the glycine cleavage system enables *Sinorhizobium fredii* USDA257 to form nitrogen-fixing nodules on agronomically improved north american soybean cultivars. *Appl. Environ. Microbiol.* 76, 4185–4193. doi: 10.1128/AEM.00437-10

Lorite, M. J., Estrella, M. J., Escaray, F. J., Sannazzaro, A., Videira, E. C. I. M., Monza, J., et al. (2018). The rhizobia-lotus symbioses: deeply specific and widely diverse. *Front. Microbiol.* 9:2055. doi: 10.3389/fmicb.2018.02055

Malolepszy, A., Kelly, S., Sørensen, K. K., James, E. K., Kalisch, C., Bozsoki, Z., et al. (2018). A plant chitinase controls cortical infection thread progression and nitrogen-fixing symbiosis. *Elife* 7, e38874. doi: 10.7554/eLife.38874

Margaret, I., Becker, A., Blom, J., Bonilla, I., Goesmann, A., Göttfert, M., et al. (2011). Symbiotic properties and first analyses of the genomic sequence of the fast growing model strain *Sinorhizobium fredii* HH103 nodulating soybean. *J. Biotechnol.* 155, 11–19. doi: 10.1016/j.jbiotec.2011.03.016

Margaret, I., Lucas, M. M., Acosta-Jurado, S., Buendía-Clavería, A. M., Fedorova, E., Hidalgo, A., et al. (2013). The *Sinorhizobium fredii* HH103 lipopolysaccharide is not only relevant at early soybean nodulation stages but also for symbiosome stability in mature nodules. *PLoS One* 8:e74717. doi: 10.1371/journal.pone.0074717

Marie, C., Broughton, W. J., and Deakin, W. J. (2001). Rhizobium type III secretion systems: legume charmers or alarmers? *Curr. Opin. Plant Biol.* 4, 336–342. doi: 10.1016/s1369-5266(00)00182-5

Marie, C., Deakin, W. J., Viprey, V., Kopciñska, J., Golinowski, W., Krishnan, H. B., et al. (2003). Characterization of Nops, nodulation outer proteins, secreted via the type III secretion system of NGR234. *Mol. Plant Microbe Int.* 16, 743–751. doi: 10.1094/MPMI.2003.16.9.743

Masson-Boivin, C., Giraud, E., Perret, X., and Batut, J. (2009). Establishing nitrogen-fixing symbiosis with legumes: how many rhizobium recipes? *Trends Microbiol.* 17, 458–466. doi: 10.1016/j.tim.2009.07.004

Maunoury, N., Redondo-Nieto, M., Bourcy, M., Van De Velde, W., Alunni, B., Laporte, P., et al. (2010). Differentiation of symbiotic cells and endosymbionts in *Medicago truncatula* nodulation are coupled to two transcriptome-switches. *PLoS One* 5:e9519. doi: 10.1371/journal.pone.0009519

Meinhardt, L. W., Krishnan, H. B., Balatti, P. A., and Pueppke, S. G. (1993). Molecular cloning and characterization of a sym plasmid locus that regulates cultivar-specific nodulation of soybean by *Rhizobium fredii* USDA257. *Mol. Microbiol.* 9, 17–29. doi: 10.1111/j.1365-2958.1993.tb01665.x

Melino, V. J., Drew, E. A., Ballard, R. A., Reeve, W. G., Thomson, G., White, R. G., et al. (2012). Identifying abnormalities in symbiotic development between *Trifolium* spp. and *Rhizobium leguminosarum* bv. trifolii leading to sub-optimal and ineffective nodule phenotypes. *Ann. Bot.* 110, 1559–1572. doi: 10.1093/aob/mcs206

Mergaert, P., Kereszt, A., and Kondorosi, É (2020). Gene expression in nitrogen-fixing symbiotic nodule cells in *Medicago truncatula* and other nodulating plants. *Plant Cell* 32, 42–68. doi: 10.1105/tpc.19.00494

Mergaert, P., Nikovics, K., Kelemen, Z., Maunoury, N., Vaubert, D., Kondorosi, Á, et al. (2003). A novel family in *Medicago truncatula* consisting of more than 300 nodule-specific genes coding for small, secreted polypeptides with conserved cysteine motifs. *Plant Physiol.* 132, 161–173. doi: 10.1104/pp.102.018192

Mergaert, P., Uchiumi, T., Alunni, B., Evanno, G., Cheron, A., Catrice, O., et al. (2006). Eukaryotic control on bacterial cell cycle and differentiation in the rhizobium-legume symbiosis. *Proc. Natl. Acad. Sci. U.S.A.* 103, 5230–5235. doi: 10.1073/pnas.0600912103

Miller, S. H., Elliot, R. M., Sullivan, J. T., and Ronson, C. W. (2007). Host-specific regulation of symbiotic nitrogen fixation in *Rhizobium leguminosarum* biovar trifolii. *Microbiology* 153, 3184–3195. doi: 10.1099/mic.0.2007/006924-0

Montiel, J., Downie, J. A., Farkas, A., Bihari, P., Herczeg, R., Bálint, B., et al. (2017). Morphotype of bacteroids in different legumes correlates with the number and type of symbiotic NCR peptides. *Proc. Natl. Acad. Sci. U.S.A.* 114, 5041–5046. doi: 10.1073/pnas.1704217114

Montiel, J., Szücs, A., Boboescu, I. Z., Gherman, V. D., Kondorosi, É, and Kereszt, A. (2016). Terminal bacteroid differentiation is associated with variable

morphological changes in legume species belonging to the inverted repeat-lacking clade. *Mol. Plant Microbe Int.* 29, 210–219. doi: 10.1094/MPMI-09-15-0213-R

Murray, J. D. (2011). Invasion by invitation: rhizobial infection in legumes. *Mol. Plant Microbe Int.* 24, 631–639. doi: 10.1094/MPMI-08-10-0181

Nelson, M. S., and Sadowsky, M. J. (2015). Secretion systems and signal exchange between nitrogen-fixing rhizobia and legumes. *Front. Plant Sci.* 6:491. doi: 10.3389/fpls.2015.00491

Ngou, B. P. M., Jones, J. D. G., and Ding, P. (2021). Plant immune networks. *Trends Plant Sci.* 2021:12. doi: 10.1016/j.tplants.2021.08.012

Nguyen, H. P., Miwa, H., Kaneko, T., Sato, S., and Okazaki, S. (2017). Identification of *Bradyrhizobium elkanii* genes involved in incompatibility with vigna radiata. *Genes (Basel)* 8:374. doi: 10.3390/genes8120374

Nguyen, H. P., Ratu, S. T. N., Yasuda, M., Göttfert, M., and Okazaki, S. (2018). InnB, a novel type III effector of *Bradyrhizobium elkanii* USDA61, controls symbiosis with vigna species. *Front. Microbiol.* 9:3155. doi: 10.3389/fmicb.2018.03155

Nicoud, Q., Lamouche, F., Chaumeret, A., Balliau, T., Le Bars, R., Bourge, M., et al. (2021). Bradyrhizobium diazoefficiens USDA110 nodulation of *Aeschynomene afraspera* is associated with atypical terminal bacteroid differentiation and suboptimal symbiotic efficiency. *mSystems* 6, e01237-20. doi: 10.1128/mSystems.01237-20

Okazaki, S., Kaneko, T., Sato, S., and Saeki, K. (2013). Hijacking of leguminous nodulation signaling by the rhizobial type III secretion system. *Proc. Natl. Acad. Sci. U.S.A.* 110, 17131–17136. doi: 10.1073/pnas.1302360110

Okazaki, S., Okabe, S., Higashi, M., Shimoda, Y., Sato, S., Tabata, S., et al. (2010). Identification and functional analysis of type III effector proteins in mesorhizobium loti. *Mol. Plant Microbe Int.* 23, 223–234. doi: 10.1094/MPMI-23-2-0223

Okazaki, S., Tittabutr, P., Teulet, A., Thouin, J., Fardoux, J., Chaintreuil, C., et al. (2016). Rhizobium-legume symbiosis in the absence of nod factors: two possible scenarios with or without the T3SS. *ISME J.* 10, 64–74. doi: 10.1038/ismej.2015.103

Oono, R., and Denison, R. F. (2010). Comparing symbiotic efficiency between swollen versus nonswollen rhizobial bacteroids. *Plant Physiol.* 154, 1541–1548. doi: 10.1104/pp.110.163436

Oono, R., Schmitt, I., Sprent, J. I., and Denison, R. F. (2010). Multiple evolutionary origins of legume traits leading to extreme rhizobial differentiation. *New Phytol* 187, 508–520. doi: 10.1111/j.1469-8137.2010.03261.x

Osteras, M., Finan, T. M., and Stanley, J. (1991). Site-directed mutagenesis and DNA sequence of pckA of rhizobium NGR234, encoding phosphoenolpyruvate carboxykinase: gluconeogenesis and host-dependent symbiotic phenotype. *Mol. Gen. Genet.* 230, 257–269. doi: 10.1007/BF00290676

Pacios Bras, C., Jorda, M. A., Wijfjes, A. H., Harteveld, M., Stuurman, N., Thomas-Oates, J. E., et al. (2000). A lotus japonicus nodulation system based on heterologous expression of the fucosyl transferase NodZ and the acetyl transferase NoIL in *Rhizobium leguminosarum*. *Mol. Plant Microbe Int.* 13, 475–479. doi: 10.1094/MPMI.2000.13.4.475

Parada, M., Vinardell, J. M., Ollero, F. J., Hidalgo, A., Gutiérrez, R., Buendía-Clavería, A. M., et al. (2006). Sinorhizobium fredii HH103 mutants affected in capsular polysaccharide (KPS) are impaired for nodulation with soybean and cajanus cajan. *Mol. Plant Microbe Int.* 19, 43–52. doi: 10.1094/MPMI-19-0043

Peck, M. C., Fisher, R. F., and Long, S. R. (2006). Diverse flavonoids stimulate NodD1 binding to nod gene promoters in *Sinorhizobium meliloti*. *J. Bacteriol.* 188, 5417–5427. doi: 10.1128/JB.00376-06

Pellock, B. J., Cheng, H. P., and Walker, G. C. (2000). Alfalfa root nodule invasion efficiency is dependent on *Sinorhizobium meliloti* polysaccharides. *J. Bacteriol.* 182, 4310–4318. doi: 10.1128/JB.182.15.4310-4318.2000

Penterman, J., Abo, R. P., De Nisco, N. J., Arnold, M. F., Longhi, R., Zanda, M., et al. (2014). Host plant peptides elicit a transcriptional response to control the *Sinorhizobium meliloti* cell cycle during symbiosis. *Proc. Natl. Acad. Sci. U.S.A.* 111, 3561–3566. doi: 10.1073/pnas.1400450111

Peoples, M. B., Herridge, D. F., and Ladha, J. K. (1995). Biological nitrogen fixation: an efficient source of nitrogen for sustainable agricultural production? *Plant Soil* 174, 3–28. doi: 10.1007/BF00032239

Pérez-Giménez, J., Iturralde, E. T., Torres Tejerizo, G., Quelas, J. I., Krol, E., Borassi, C., et al. (2021). A stringent-response-defective *Bradyrhizobium diazoefficiens* strain does not activate the type 3 secretion system, elicits an early plant defense response, and circumvents NH4NO3-induced inhibition of nodulation. *Appl. Environ. Microbiol.* 87:e02989-20. doi: 10.1128/AEM.02989-20

Peters, N. K., Frost, J. W., and Long, S. R. (1986). A plant flavone, luteolin, induces expression of Rhizobium meliloti nodulation genes. *Science* 233, 977–980. doi: 10.1126/science.3738520

Pislariu, C. I., Sinharoy, S., Torres-Jerez, I., Nakashima, J., Blancaflor, E. B., and Udvardi, M. K. (2019). The nodule-specific PLAT domain protein NPD1 is equired for nitrogen-fixing symbiosis. *Plant Physiol.* 180, 1480–1497. doi: 10.1104/pp.18.01613

Price, P. A., Tanner, H. R., Dillon, B. A., Shabab, M., Walker, G. C., and Griffitts, J. S. (2015). Rhizobial peptidase HrrP cleaves host-encoded signaling peptides and mediates symbiotic compatibility. *Proc. Natl. Acad. Sci. U.S.A.* 112, 15244–15249. doi: 10.1073/pnas.1417797112

Pueppke, S. G., and Broughton, W. J. (1999). Rhizobium sp. strain NGR234 and R. fredii USDA257 share exceptionally broad, nested host ranges. *Mol. Plant Microbe Int.* 12, 293–318. doi: 10.1094/MPMI.1999.12.4.293

Putnoky, P., Kereszt, A., Nakamura, T., Endre, G., Grosskopf, E., Kiss, P., et al. (1998). The pha gene cluster of rhizobium meliloti involved in pH adaptation and symbiosis encodes a novel type of K+ efflux system. *Mol. Microbiol.* 28, 1091–1101. doi: 10.1046/j.1365-2958.1998.00868.x

Putnoky, P., Petrovics, G., Kereszt, A., Grosskopf, E., Ha, D. T., Bánfalvi, Z., et al. (1990). Rhizobium meliloti lipopolysaccharide and exopolysaccharide can have the same function in the plant-bacterium interaction. *J. Bacteriol.* 172, 5450–5458. doi: 10.1128/jb.172.9.5450-5458.1990

Radutoiu, S., Madsen, L. H., Madsen, E. B., Jurkiewicz, A., Fukai, E., Quistgaard, E. M., et al. (2007). LysM domains mediate lipochitin-oligosaccharide recognition and Nfr genes extend the symbiotic host range. *EMBO J.* 26, 3923–3935. doi: 10.1038/sj.emboj.7601826

Ratu, S. T. N., Hirata, A., Kalaw, C. O., Yasuda, M., Tabuchi, M., and Okazaki, S. (2021a). Multiple domains in the rhizobial type III effector Bel2-5 determine symbiotic efficiency with soybean. *Front. Plant Sci.* 12:689064. doi: 10.3389/fpls.2021.689064

Ratu, S. T. N., Teulet, A., Miwa, H., Masuda, S., Nguyen, H. P., Yasuda, M., et al. (2021b). Rhizobia use a pathogenic-like effector to hijack leguminous nodulation signalling. *Sci. Rep.* 11:2034. doi: 10.1038/s41598-021-81598-6

Redmond, J., Batley, M., Djordjevic, M. A., Innes, R. W., Kuempel, P. L., and Rolfe, B. G. (1986). Flavones induce expression of nodulation genes in rhizobium. *Nature* 323, 632–635. doi: 10.1038/323632a0

Reuhs, B. L., Geller, D. P., Kim, J. S., Fox, J. E., Kolli, V. S., and Pueppke, S. G. (1998). *Sinorhizobium fredii* and *Sinorhizobium meliloti* produce structurally conserved lipopolysaccharides and strain-specific K antigens. *Appl. Environ. Microbiol.* 64, 4930–4938. doi: 10.1128/AEM.64.12.4930-4938.1998

Reuhs, B. L., Williams, M. N., Kim, J. S., Carlson, R. W., and Côté, F. (1995). Suppression of the Fix- phenotype of rhizobium meliloti exoB mutants by lpsZ is correlated to a modified expression of the K polysaccharide. *J. Bacteriol.* 177, 4289–4296. doi: 10.1128/jb.177.15.4289-4296.1995

Rodpothong, P., Sullivan, J. T., Songsrirote, K., Sumpton, D., Cheung, K. W., Thomas-Oates, J., et al. (2009). Nodulation gene mutants of mesorhizobium loti R7A-nodZ and nolL mutants have host-specific phenotypes on lotus spp. *Mol. Plant Microbe Int.* 22, 1546–1554. doi: 10.1094/MPMI-22-12-1546

Roest, H. P., Mulders, I. H., Spaink, H. P., Wijffelman, C. A., and Lugtenberg, B. J. (1997). A rhizobium leguminosarum biovar trifolii locus not localized on the sym plasmid hinders effective nodulation on plants of the pea cross-inoculation group. *Mol. Plant Microbe Int.* 10, 938–941. doi: 10.1094/MPMI.1997.10.7.938

Roth, L. E., and Stacey, G. (1989). Bacterium release into host cells of nitrogen-fixing soybean nodules: the symbiosome membrane comes from three sources. *Eur. J Cell Biol* 49, 13–23.

Roy, S., Liu, W., Nandety, R. S., Crook, A., Mysore, K. S., Pislariu, C. I., et al. (2020). Celebrating 20 years of genetic discoveries in legume nodulation and symbiotic nitrogen fixation. *Plant Cell* 32, 15–41. doi: 10.1105/tpc.19.00279

Rutten, P. J., and Poole, P. S. (2019). Oxygen regulatory mechanisms of nitrogen fixation in rhizobia. *Adv. Microb Physiol.* 75, 325–389. doi: 10.1016/bs.ampbs.2019.08.001

Sadowsky, M. J., Kosslak, R. M., Madrzak, C. J., Golinska, B., and Cregan, P. B. (1995). Restriction of nodulation by *Bradyrhizobium japonicum* is mediated by factors present in the roots of glycine max. *Appl. Environ. Microbiol.* 61, 832–836. doi: 10.1128/aem.61.2.832-836.1995

Salinero-Lanzarote, A., Pacheco-Moreno, A., Domingo-Serrano, L., Durán, D., Ormeño-Orrillo, E., Martinez-Romero, E., et al. (2019). The type VI secretion system of *Rhizobium etli* mim1 has a positive effect in symbiosis. *FEMS Microbiol. Ecol.* 95:54. doi: 10.1093/femsec/fiz054

Sánchez, C., Iannino, F., Deakin, W. J., Ugalde, R. A., and Lepek, V. C. (2009). Characterization of the mesorhizobium loti MAFF303099 type-three protein secretion system. *Mol. Plant Microbe Int.* 22, 519–528. doi: 10.1094/MPMI-22-5-0519

Sánchez, C., Mercante, V., Babuin, M. F., and Lepek, V. C. (2012). Dual effect of *Mesorhizobium loti* T3SS functionality on the symbiotic process. *FEMS Microbiol. Lett.* 330, 148–156. doi: 10.1111/j.1574-6968.2012.02545.x

Schreiber, K. J., Chau-Ly, I. J., and Lewis, J. D. (2021). What the wild things do: mechanisms of plant host manipulation by bacterial type III-secreted effector proteins. *Microorganisms* 9:1029. doi: 10.3390/microorganisms9051029

Shimoda, Y., Nishigaya, Y., Yamaya-Ito, H., Inagaki, N., Umehara, Y., Hirakawa, H., et al. (2020). The rhizobial autotransporter determines the symbiotic nitrogen fixation activity of *Lotus japonicus* in a host-specific manner. *Proc. Natl. Acad. Sci. U.S.A.* 117, 1806–1815. doi: 10.1073/pnas.1913349117

Shobudani, M., Htwe, A. Z., Yamakawa, T., Ishibashi, M., and Tsurumaru, H. (2020). Mutants disrupted in the type III secretion system of *Bradyrhizobium elkanii* BLY3-8 overcame nodulation restriction by Rj3-genotype soybean. *Microbes Environ.* 35:151. doi: 10.1264/jsme2.ME19151

Skorupska, A., Janczarek, M., Marczak, M., Mazur, A., and Król, J. (2006). Rhizobial exopolysaccharides: genetic control and symbiotic functions. *Microb Cell Fact.* 5:7. doi: 10.1186/1475-2859-5-7

Smit, P., Limpens, E., Geurts, R., Fedorova, E., Dolgikh, E., Gough, C., et al. (2007). Medicago LYK3, an entry receptor in rhizobial nodulation factor signaling. *Plant Physiol.* 145, 183–191. doi: 10.1104/pp.107.100495

Snyman, C. P., and Srijdom, B. W. (1980). Symbiotic characteristics of lines and cultivars of *Medicago truncatula* inoculated with strains of *Rhizobium meliloti*. *Phytophylatica* 12, 173–176.

Solovev, Y. V., Igolkina, A. A., Kuliaev, P. O., Sulima, A. S., Zhukov, V. A., Porozov, Y. B., et al. (2021). Towards understanding afghanistan pea symbiotic phenotype through the molecular modeling of the interaction between LykX-Sym10 receptor heterodimer and nod factors. *Front. Plant Sci.* 12:642591. doi: 10.3389/fpls.2021.642591

Songwattana, P., Chaintreuil, C., Wongdee, J., Teulet, A., Mbaye, M., Piromyou, P., et al. (2021). Identification of type III effectors modulating the symbiotic properties of *Bradyrhizobium vignae* strain ORS3257 with various vigna species. *Sci. Rep.* 11:4874. doi: 10.1038/s41598-021-84205-w

Songwattana, P., Noisangiam, R., Teamtisong, K., Prakamhang, J., Teulet, A., Tittabutr, P., et al. (2017). Type 3 secretion system (T3SS) of *Bradyrhizobium* sp. DOA9 and its roles in legume symbiosis and rice endophytic association. *Front. Microbiol.* 8:1810. doi: 10.3389/fmicb.2017.01810

Soumare, A., Diedhiou, A. G., Thuita, M., Hafidi, M., Ouhdouch, Y., Gopalakrishnan, S., et al. (2020). Exploiting biological nitrogen fixation: a route towards a sustainable agriculture. *Plants* 9:1011. doi: 10.3390/plants9081011

Stacey, G., So, J. S., Roth, L. E., Lakshmi, S. B., and Carlson, R. W. (1991). A lipopolysaccharide mutant of *Bradyrhizobium japonicum* that uncouples plant from bacterial differentiation. *Mol. Plant Microbe Int.* 4, 332–340. doi: 10.1094/mpmi-4-332

Staehelin, C., and Krishnan, H. B. (2015). Nodulation outer proteins: double-edged swords of symbiotic rhizobia. *Biochem J.* 470, 263–274. doi: 10.1042/BJ20150518

Stagnari, F., Maggio, A., Galieni, A., and Pisante, M. (2017). Multiple benefits of legumes for agriculture sustainability: an overview. *Chem. Biol. Technol. Agric.* 4. doi: 10.1186/s40538-016-0085-1

Sugawara, M., Epstein, B., Badgley, B. D., Unno, T., Xu, L., Reese, J., et al. (2013). Comparative genomics of the core and accessory genomes of 48 sinorhizobium strains comprising five genospecies. *Genome Biol.* 14:R17. doi: 10.1186/gb-2013-14-2-r17

Sugawara, M., Takahashi, S., Umehara, Y., Iwano, H., Tsurumaru, H., Odake, H., et al. (2018). Variation in bradyrhizobial NopP effector determines symbiotic incompatibility with Rj2-soybeans via effector-triggered immunity. *Nat. Commun.* 9:3139. doi: 10.1038/s41467-018-05663-x

Sugawara, M., Umehara, Y., Kaga, A., Hayashi, M., Ishimoto, M., Sato, S., et al. (2019). Symbiotic incompatibility between soybean and bradyrhizobium arises from one amino acid determinant in soybean Rj2 protein. *PLoS One* 14:e0222469. doi: 10.1371/journal.pone.0222469

Sulima, A. S., Zhukov, V. A., Afonin, A. A., Zhernakov, A. I., Tikhonovich, I. A., and Lutova, L. A. (2017). Selection signatures in the first exon of paralogous receptor kinase genes from the Sym2 region of the *Pisum sativum* L. genome. *Front. Plant Sci.* 8:1957. doi: 10.3389/fpls.2017.01957

Sulima, A. S., Zhukov, V. A., Kulaeva, O. A., Vasileva, E. N., Borisov, A. Y., and Tikhonovich, I. A. (2019). New sources of Sym2(A) allele in the pea (*Pisum sativum* L.) carry the unique variant of candidate LysM-RLK gene LykX. *PeerJ* 7:e8070. doi: 10.7717/peerj.8070

Surin, B. P., and Downie, J. A. (1989). *Rhizobium leguminosarum* genes required for expression and transfer of host specific nodulation. *Plant Mol. Biol.* 12, 19–29. doi: 10.1007/BF00017444

Sutton, J. M., Lea, E. J., and Downie, J. A. (1994). The nodulation-signaling protein NodO from *Rhizobium leguminosarum* biovar viciae forms ion channels in membranes. *Proc. Natl. Acad. Sci. U.S.A.* 91, 9990–9994. doi: 10.1073/pnas.91.21.9990

Suzaki, T., Yoro, E., and Kawaguchi, M. (2015). Leguminous plants: inventors of root nodules to accommodate symbiotic bacteria. *Int. Rev. Cell. Mol. Biol.* 316, 111–158. doi: 10.1016/bs.ircmb.2015.01.004

Tang, F., Yang, S., Liu, J., and Zhu, H. (2016). Rj4, a gene controlling nodulation specificity in soybeans, encodes a thaumatin-like protein but not the one previously reported. *Plant Physiol.* 170, 26–32. doi: 10.1104/pp.15.01661

Tellström, V., Usadel, B., Thimm, O., Stitt, M., Küster, H., and Niehaus, K. (2007). The lipopolysaccharide of *Sinorhizobium meliloti* suppresses defense-associated gene expression in cell cultures of the host plant *Medicago truncatula*. *Plant Physiol.* 143, 825–837. doi: 10.1104/pp.106.090985

Terpolilli, J. J., Hood, G. A., and Poole, P. S. (2012). What determines the efficiency of N(2)-fixing rhizobium-legume symbioses? *Adv. Microb Physiol.* 60, 325–389. doi: 10.1016/B978-0-12-398264-3.00005-X

Terpolilli, J. J., O'hara, G. W., Tiwari, R. P., Dilworth, M. J., and Howieson, J. G. (2008). The model legume medicago truncatula A17 is poorly matched for N2 fixation with the sequenced microsymbiont sinorhizobium meliloti 1021. *New Phytol.* 179, 62–66. doi: 10.1111/j.1469-8137.2008.02464.x

Teulet, A., Busset, N., Fardoux, J., Gully, D., Chaintreuil, C., Cartieaux, F., et al. (2019). The rhizobial type III effector ErnA confers the ability to form nodules in legumes. *Proc. Natl. Acad. Sci. U.S.A.* 116, 21758–21768. doi: 10.1073/pnas.1904456116

Tighilt, L., Boulila, F., De Sousa, B. F. S., Giraud, E., Ruiz-Argüeso, T., Palacios, J. M., et al. (2021). The bradyrhizobium sp. LmicA16 type VI secretion system is required for efficient nodulation of *Lupinus* spp. *Microb Ecol.* doi: 10.1007/s00248-021-01892-8 [Epub ahead of print].

Tirichine, L., De Billy, F., and Huguet, T. (2000). Mtsym6, a gene conditioning sinorhizobium strain-specific nitrogen fixation in medicago truncatula. *Plant Physiol.* 123, 845–851. doi: 10.1104/pp.123.3.845

Tiricz, H., Szücs, A., Farkas, A., Pap, B., Lima, R. M., Maróti, G., et al. (2013). Antimicrobial nodule-specific cysteine-rich peptides induce membrane depolarization-associated changes in the transcriptome of sinorhizobium meliloti. *Appl. Environ. Microbiol.* 79, 6737–6746. doi: 10.1128/AEM.01791-13

Trese, A. T. (1985). A single dominant gene in McCall soybean prevents effective nodulation with rhizobium fredii USDA257. *Euphytica* 81, 279–282. doi: 10.1007/bf00025618

Truchet, G., Roche, P., Lerouge, P., Vasse, J., Camut, S., De Billy, F., et al. (1991). Sulphated lipo-oligosaccharide signals of rhizobium meliloti elicit root nodule organogenesis in alfalfa. *Nature* 351, 670–673. doi: 10.1038/351670a0

Tseng, T. T., Tyler, B. M., and Setubal, J. C. (2009). Protein secretion systems in bacterial-host associations, and their description in the gene ontology. *BMC Microbiol* 9:S2. doi: 10.1186/1471-2180-9-S1-S2

Tsukui, T., Eda, S., Kaneko, T., Sato, S., Okazaki, S., Kakizaki-Chiba, K., et al. (2013). The type III secretion system of *Bradyrhizobium japonicum* USDA122 mediates symbiotic incompatibility with Rj2 soybean plants. *Appl. Environ. Microbiol.* 79, 1048–1051. doi: 10.1128/AEM.03297-12

Tsurumaru, H., Hashimoto, S., Okizaki, K., Kanesaki, Y., Yoshikawa, H., and Yamakawa, T. (2015). A putative type III secretion system effector encoded by the MA20_12780 gene in *Bradyrhizobium japonicum* is-34 causes incompatibility with Rj4 genotype soybeans. *Appl. Environ. Microbiol.* 81, 5812–5819. doi: 10.1128/AEM.00823-15

Tsyganova, A. V., Brewin, N. J., and Tsyganov, V. E. (2021). Structure and development of the legume-rhizobial symbiotic interface in infection threads. *Cells* 10:1050. doi: 10.3390/cells10051050

Udvardi, M., and Poole, P. S. (2013). Transport and metabolism in legume-rhizobia symbioses. *Ann. Rev. Plant Biol.* 64, 781–805. doi: 10.1146/annurev-arplant-050312-120235

Van de Velde, W., Zehirov, G., Szatmári, A., Debreczeny, M., Ishihara, H., Kevei, Z., et al. (2010). Plant peptides govern terminal differentiation of bacteria in symbiosis. *Science* 327, 1122–1126. doi: 10.1126/science.1184057

Vance, C. P. (2001). Symbiotic nitrogen fixation and phosphorus acquisition. plant nutrition in a world of declining renewable resources. *Plant Physiol.* 127, 390–397. doi: 10.1104/pp.010331

Vasse, J., De Billy, F., Camut, S., and Truchet, G. (1990). Correlation between ultrastructural differentiation of bacteroids and nitrogen fixation in alfalfa nodules. *J. Bacteriol.* 172, 4295–4306. doi: 10.1128/jb.172.8.4295-4306.1990

Vest, G. (1970). Rj3 - a gene conditioning ineffective nodulation in soybean. *Crop Sci.* 10, 34–35. doi: 10.2135/cropsci1970.0011183X001000010013x

Vest, G., and Caldwell, B. E. (1972). Rj4 - a gene conditioning ineffective nodulation in soybean. *Crop Sci.* 12, 692–693. doi: 10.1104/pp.94.3.899

Viprey, V., Del Greco, A., Golinowski, W., Broughton, W. J., and Perret, X. (1998). Symbiotic implications of type III protein secretion machinery in rhizobium. *Mol. Microbiol.* 28, 1381–1389. doi: 10.1046/j.1365-2958.1998.00920.x

Walker, S. A., and Downie, J. A. (2000). Entry of *Rhizobium leguminosarum* bv.viciae into root hairs requires minimal nod factor specificity, but subsequent infection thread growth requires nodO or nodE. *Mol. Plant Microbe Int.* 13, 754–762. doi: 10.1094/MPMI.2000.13.7.754

Wang, Q., Liu, J., Li, H., Yang, S., Körmöczi, P., Kereszt, A., et al. (2018). Nodule-specific cysteine-rich peptides negatively regulate nitrogen-fixing symbiosis in a strain-specific manner in *Medicago truncatula*. *Mol. Plant Microbe Int.* 31, 240–248. doi: 10.1094/MPMI-08-17-0207-R

Wang, Q., Yang, S., Liu, J., Terecskei, K., Ábrahám, E., Gombár, A., et al. (2017). Host-secreted antimicrobial peptide enforces symbiotic selectivity in *Medicago truncatula*. *Proc. Natl. Acad. Sci. U.S.A.* 114, 6854–6859. doi: 10.1073/pnas.1700715114

Wells, D. H., and Long, S. R. (2002). The *Sinorhizobium meliloti* stringent response affects multiple aspects of symbiosis. *Mol. Microbiol.* 43, 1115–1127. doi: 10.1046/j.1365-2958.2002.02826.x

Williams, M. N., Hollingsworth, R. I., Klein, S., and Signer, E. R. (1990). The symbiotic defect of rhizobium meliloti exopolysaccharide mutants is suppressed by lpsZ+, a gene involved in lipopolysaccharide biosynthesis. *J. Bacteriol.* 172, 2622–2632. doi: 10.1128/jb.172.5.2622-2632.1990

Wilson, K. J., Anjaiah, V., Nambiar, P. T., and Ausubel, F. M. (1987). Isolation and characterization of symbiotic mutants of *Bradyrhizobium* sp. (Arachis) strain NC92: mutants with host-specific defects in nodulation and nitrogen fixation. *J. Bacteriol.* 169, 2177–2186. doi: 10.1128/jb.169.5.2177-2186.1987

Wippel, K., and Long, S. R. (2019). Symbiotic performance of *Sinorhizobium meliloti* lacking ppGpp depends on the medicago host species. *Mol. Plant Microbe Int.* 32, 717–728. doi: 10.1094/MPMI-11-18-0306-R

Wong, J., Gysel, K., Birkefeldt, T. G., Vinther, M., Muszynski, A., Azadi, P., et al. (2020). Structural signatures in EPR3 define a unique class of plant carbohydrate receptors. *Nat. Commun.* 11:3797. doi: 10.1038/s41467-020-17568-9

Yamaya-Ito, H., Shimoda, Y., Hakoyama, T., Sato, S., Kaneko, T., Hossain, M. S., et al. (2018). Loss-of-function of ASPARTIC PEPTIDASE NODULE-INDUCED 1 (APN1) in lotus japonicus restricts efficient nitrogen-fixing symbiosis with specific mesorhizobium loti strains. *Plant J.* 93, 5–16. doi: 10.1111/tpj.13759

Yang, S., Tang, F., Gao, M., Krishnan, H. B., and Zhu, H. (2010). R gene-controlled host specificity in the legume-rhizobia symbiosis. *Proc. Natl. Acad. Sci. U.S.A.* 107, 18735–18740. doi: 10.1073/pnas.1011957107

Yang, S., Wang, Q., Fedorova, E., Liu, J., Qin, Q., Zheng, Q., et al. (2017). Microsymbiont discrimination mediated by a host-secreted peptide in medicago truncatula. *Proc. Natl. Acad. Sci. U.S.A.* 114, 6848–6853. doi: 10.1073/pnas.1700460114

Yasuda, M., Miwa, H., Masuda, S., Takebayashi, Y., Sakakibara, H., and Okazaki, S. (2016). Effector-triggered immunity determines host genotype-specific incompatibility in legume-rhizobium symbiosis. *Plant Cell Physiol.* 57, 1791–1800. doi: 10.1093/pcp/pcw104

Zhang, B., Wang, M., Sun, Y., Zhao, P., Liu, C., Qing, K., et al. (2021). Glycine max NNL1 restricts symbiotic compatibility with widely distributed bradyrhizobia via root hair infection. *Nat. Plants* 7, 73–86. doi: 10.1038/s41477-020-00832-7

Zhang, Q., Raoof, M., Chen, Y., Sumi, Y., Sursal, T., Junger, W., et al. (2010). Circulating mitochondrial DAMPs cause inflammatory responses to injury. *Nature* 464, 104–107. doi: 10.1038/nature08780

Zhou, S., Zhang, C., Huang, Y., Chen, H., Yuan, S., and Zhou, X. (2021). Characteristics and research progress of legume nodule senescence. *Plants* 10:1103. doi: 10.3390/plants10061103

Zhukov, V., Radutoiu, S., Madsen, L. H., Rychagova, T., Ovchinnikova, E., Borisov, A., et al. (2008). The pea Sym37 receptor kinase gene controls infection-thread initiation and nodule development. *Mol. Plant Microbe Int.* 21, 1600–1608. doi: 10.1094/MPMI-21-12-1600

Conflict of Interest: The authors declare that the research was conducted in the absence of any commercial or financial relationships that could be construed as a potential conflict of interest.

Publisher's Note: All claims expressed in this article are solely those of the authors and do not necessarily represent those of their affiliated organizations, or those of the publisher, the editors and the reviewers. Any product that may be evaluated in this article, or claim that may be made by its manufacturer, is not guaranteed or endorsed by the publisher.

frontiers | Frontiers in Plant Science

ORIGINAL RESEARCH
published: 26 April 2022
doi: 10.3389/fpls.2022.823183

Tubulin Cytoskeleton Organization in Cells of Determinate Nodules

*Anna B. Kitaeva[1], Artemii P. Gorshkov[1], Pyotr G. Kusakin[1], Alexandra R. Sadovskaya[2], Anna V. Tsyganova[1] and Viktor E. Tsyganov[1,3]**

[1] Laboratory of Molecular and Cellular Biology, All-Russia Research Institute for Agricultural Microbiology, Saint Petersburg, Russia, [2] Faculty of Biology, Saint Petersburg State University, Saint Petersburg, Russia, [3] Saint Petersburg Scientific Center RAS, Saint Petersburg, Russia

Plant cell differentiation is based on rearrangements of the tubulin cytoskeleton; this is also true for symbiotic nodules. Nevertheless, although for indeterminate nodules (with a long-lasting meristem) the organization of microtubules during nodule development has been studied for various species, for determinate ones (with limited meristem activity) such studies are rare. Here, we investigated bacteroid morphology and dynamics of the tubulin cytoskeleton in determinate nodules of four legume species: *Glycine max*, *Glycine soja*, *Phaseolus vulgaris*, and *Lotus japonicus*. The most pronounced differentiation of bacteroids was observed in *G. soja* nodules. In meristematic cells in incipient nodules of all analyzed species, the organization of both cortical and endoplasmic microtubules was similar to that described for meristematic cells of indeterminate nodules. In young infected cells in developing nodules of all four species, cortical microtubules formed irregular patterns (microtubules were criss-crossed) and endoplasmic ones were associated with infection threads and infection droplets. Surprisingly, in uninfected cells the patterns of cortical microtubules differed in nodules of *G. max* and *G. soja* on the one hand, and *P. vulgaris* and *L. japonicus* on the other. The first two species exhibited irregular patterns, while the remaining two exhibited regular ones (microtubules were oriented transversely to the longitudinal axis of cell) that are typical for uninfected cells of indeterminate nodules. In contrast to indeterminate nodules, in mature determinate nodules of all four studied species, cortical microtubules formed a regular pattern in infected cells. Thus, our analysis revealed common patterns of tubulin cytoskeleton in the determinate nodules of four legume species, and species-specific differences were associated with the organization of cortical microtubules in uninfected cells. When compared with indeterminate nodules, the most pronounced differences were associated with the organization of cortical microtubules in nitrogen-fixing infected cells. The revealed differences indicated a possible transition during evolution of infected cells from anisotropic growth in determinate nodules to isodiametric growth in indeterminate nodules. It can be assumed that this transition provided an evolutionary advantage to those legume species with indeterminate nodules, enabling them to host symbiosomes in their infected cells more efficiently.

Keywords: legume–rhizobial symbiosis, microtubules, symbiosome, bacteroid, determinate nodules, *Glycine* spp., *Phaseolus vulgaris*, *Lotus japonicus*

OPEN ACCESS

Edited by:
Andrea Genre,
University of Turin, Italy

Reviewed by:
Elena Erika Fedorova,
Timiryazev Institute of Plant Physiology (RAS), Russia
Sabine Dagmar Zimmermann,
Délégation Languedoc Roussillon (CNRS), France

***Correspondence:**
Viktor E. Tsyganov
vetsyganov@arriam.ru

Specialty section:
This article was submitted to Plant Symbiotic Interactions, a section of the journal Frontiers in Plant Science

Received: *26 November 2021*
Accepted: *23 March 2022*
Published: *26 April 2022*

Citation:
Kitaeva AB, Gorshkov AP, Kusakin PG, Sadovskaya AR, Tsyganova AV and Tsyganov VE (2022) Tubulin Cytoskeleton Organization in Cells of Determinate Nodules. Front. Plant Sci. 13:823183. doi: 10.3389/fpls.2022.823183

INTRODUCTION

Legumes have a symbiotic relationship with rhizobia through the formation of nitrogen-fixing nodules. Nodule formation involves different molecular-genetic and cellular mechanisms, one of which is cytoskeleton reorganization. In plants, the tubulin cytoskeleton is involved in various processes of cell development and function (Kost et al., 1999). Endoplasmic microtubules are involved in cell division (Li et al., 2015), organelle movement, and intracellular transport (Peña and Heinlein, 2013). At the same time, cortical microtubules (underlying the plasma membrane) are involved in cell wall formation and determine the shape of the cell (Wasteneys, 2004; Paradez et al., 2006; Bashline et al., 2014).

It has been clearly demonstrated that active cytoskeleton rearrangements are required at different stages of nodule development (Timmers, 2008; Genre and Timmers, 2019; Tsyganov et al., 2019). Symbiotic nodules can be subdivided into two main types: indeterminate and determinate (Hirsch, 1992). The nodules of the first type are characterized by a prolonged functioning of the meristem, while in nodules of the second type, the meristem activity is transient. Differences in the activity of meristems lead to differences in the structure of nodules. Histological zonation is characteristic of indeterminate nodules, while it is absent in determinate ones (Guinel, 2009). As a result, indeterminate nodules are characterized by an elongated shape, while determinate nodules are spherical.

The mechanisms of organogenesis of determinate and indeterminate nodules also differ. Thus, in indeterminate nodules, the infection thread reaches the cells of the nodule primordium, which is formed as a result of the induction of cell division in the pericycle and inner cortex (Timmers et al., 1999). In determinate nodules, the infection thread reaches the outer (in *Glycine max* nodules) or middle (in *Lotus japonicus* nodules) cortex, which is located in the vicinity of the infected root hairs (van Spronsen et al., 2001). Involvement of the tubulin cytoskeleton during the early stages of infection thread growth has been demonstrated for nodules of both types (Timmers et al., 1999, 2007; Sieberer et al., 2005; Vassileva et al., 2005; Perrine-Walker et al., 2014). For *Medicago sativa* and *M. truncatula* nodules, reorientation of microtubules in cells of the inner cortex during nodule primordium formation has been described (Timmers et al., 1999). In mature indeterminate nodules, the important role of tubulin (Kitaeva et al., 2016) and actin cytoskeletons (Zhang et al., 2019) in infection thread and infection droplet development has been clearly demonstrated.

After being released from infection droplets into the cytoplasm of the plant cell, bacteria differentiate into bacteroids, while they are separated from the cytoplasm by the symbiosome membrane, forming organelle-like symbiosomes (Coba de la Peña et al., 2018; Tsyganova et al., 2018). In many legume species indeterminate nodules are characterized by strong morphological differentiation of bacteroids, which may even be terminal (Mergaert, 2020). At the same time, differentiation of bacteroids in determinate nodules is less morphologically pronounced. For example, bacteroids of *L. japonicus* strongly resemble free-living bacteria (Szczyglowski et al., 1998). A striking feature of bacteroids in determinate nodules is their ability to divide, which leads to the formation of symbiosomes containing several bacteroids. It has been shown for *G. max* that the juvenile symbiosome contains one bacteroid, while the mature symbiosome contains 2–4 bacteroids (Fedorova et al., 1999). Symbiosomes containing several bacteroids are also described for *Phaseolus vulgaris* (Cermola et al., 2000), *L. japonicus* (Szczyglowski et al., 1998), and *G. soja* (Temprano-Vera et al., 2018).

In both types of nodules, the number of symbiosomes in infected cells is crucially increased. The hosting of symbiosomes in infected cells recruits both tubulin (Kitaeva et al., 2016, 2021; Tsyganova et al., 2021) and actin cytoskeletons (Gavrin et al., 2015; Zhang et al., 2019). The detailed analysis of tubulin organization in the nodules of six different legume species forming indeterminate nodules revealed that endoplasmic microtubules are spread between symbiosomes and are organized in two main patterns: regular and irregular ones, corresponding to ordered or disordered distribution of symbiosomes (Kitaeva et al., 2016, 2021; Tsyganova et al., 2021). The regular pattern is common for infected cells in *M. truncatula* and *Galega orientalis* nodules, whereas the irregular one is a prerequisite for *Cicer arietinum* and *Pisum sativum* infected cells; finally, an intermediate pattern is characteristic of *Vicia sativa* and *Glycyrrhiza uralensis* infected cells. It has been suggested that the pattern of endoplasmic microtubules correlates with bacteroid size and shape (Kitaeva et al., 2021).

The accommodation of thousands of symbiosomes in the infected cell requires plant cell differentiation that is accompanied by a significant increase in cell volume in both determinate and indeterminate nodules (Tsyganova et al., 2018). It is known that the cortical tubulin cytoskeleton is involved in the determination of type of cell growth. Cortical microtubules that are oriented transverse to the cell growth axis determine anisotropic cell growth, whereas irregular orientation of cortical microtubules leads to isodiametric cell growth (Crowell et al., 2010; Hamada, 2014). In indeterminate nodules of six legume species the transverse orientation of cortical microtubules is a prerequisite for anisotropic growth of uninfected cells and colonized cells (with infection threads and droplets but without bacterial release). However, bacterial release leads to irregular orientation of cortical microtubules, which provides a possibility for isodiametric cell growth that allows a notable increase in cell size for the hosting of numerous symbiosomes (Kitaeva et al., 2016, 2021; Tsyganova et al., 2021).

It is necessary to note that involvement of the cytoskeleton, specifically microtubules, is poorly studied in determinate nodules; there is just one description of microtubular organization in *G. max* nodules (Whitehead et al., 1998). The aim of this study was to compare the organization of the tubulin cytoskeleton in four legume species that form determinate nodules, in order to compare the identified patterns with those in indeterminate nodules. Such an analysis should make it possible to reveal both general patterns and typical differences in the development of nodules of the two types.

MATERIALS AND METHODS

Plant Material and Bacterial Strains

Seeds of *Glycine max* (L.) Merrill accession K-5892 Fiskeby V and *Glycine soja* Siebold & Zucc. accession K-11570 from the collection of the Federal Research Center N. I. Vavilov All-Russian Institute of Plant Genetic Resources (VIR) were kindly provided by Dr. Margarita Vishnyakova. Seeds of *Lotus japonicus* (Regel) K. Larsen accession B-129 "Gifu" (Jiang and Gresshoff, 1997) were kindly provided by Prof. Jens Stougaard, Aarhus University, Denmark. For *Phaseolus vulgaris* L. cv "Supernano" commercial seeds were used.

Seeds were sterilized in concentrated sulfuric acid for 5 min (*G. max*, *G. soja*, *P. vulgaris*) or 1 min (*L. japonicus*). After sterilization, the seeds were washed with sterile water 10 times and germinated at 28°C. Seeds of *G. soja* were scarified with a scalpel (Pueppke, 1983), prior to leaving for germination. Seeds of *L. japonicus* were germinated under full-light conditions. For inoculation, the following strains from the Russian Collection of Agricultural Microorganisms (All-Russia Research Institute for Agricultural Microbiology) were used: *Bradyrhizobium liaoningense* RCAM04656 (*G. max* and *G. soja*), *Rhizobium leguminosarum* bv. *phaseoli* RCAM2624 (*P. vulgaris*), and *Mesorhizobium loti* RCAM1804 (*L. japonicus*). Seedlings were inoculated with the corresponding rhizobia strain, using 1 ml of an aqueous suspension containing 10^7–10^8 cells per seed.

Plants were grown in sterile vermiculite wetted with nitrogen-free nutrient solution (Fåhraeus, 1957), in an MLR-352H growth chamber (Sanyo Electric Co., Ltd., Moriguchi, Japan) under controlled conditions: day/night, 16/8 h; temperature 21°C; humidity 75%; and illumination 280 μmol photons m^{-2} s^{-1}). The nodules were harvested at days 10, 14, and 21 after inoculation.

Microscopy

Electron Microscopy

The nodules for electron microscopy were harvested at day 21 after inoculation. The electron microscopy protocol was as previously described (Serova et al., 2018). Samples were embedded in Epon (Honeywell Fluka™, Fisher Scientific, Loughborough, United Kingdom). For transmission electron microscopy, ultrathin sections were cut on a Leica EM UC7 ultramicrotome (Leica Microsystems, Vienne, Austria). The nodule tissues were examined and photographed under a JEM-1400 transmission electron microscope (JEOL Corporation, Tokyo, Japan) at 80 kV.

For scanning electron microscopy, nodules were prepared as previously described (Tsyganova et al., 2021). The samples were observed in a Tescan MIRA3 LMU scanning electron microscope (Tescan, Brno, Czech Republic) at 9 kV.

Immunolocalization and Laser Scanning Confocal Microscopy

Visualization of microtubules was performed as previously described (Kitaeva et al., 2016). Some modifications that are necessary according to the specificity of every species (Kitaeva et al., 2018) were made. For each species, an optimally composed fixing solution was selected and used. Nodules of *G. max*, *G. soja,* and *P. vulgaris* were fixed in 1/5 microtubule stabilizing buffer (MTSB) (50 mM PIPES, 5 mM $MgSO_4 \cdot 7H_2O$, 5 mM EGTA, pH 6.9) containing 3% formaldehyde, 0.25% glutaraldehyde, 0.3% Tween-20, 0.3% Triton X-100; *L. japonicus* nodules were fixed in 1/10 MTSB containing 3% formaldehyde, 0.25% glutaraldehyde, 0.3% Tween-20, 0.3% Triton X-100, 10% dimethyl sulfoxide. Nodule longitudinal sections were made using a microtome with a vibrating blade HM650V (Microm, Walldorf, Germany). Immunolocalization of the tubulin cytoskeleton, infection droplets, infection threads, and staining of nuclei and bacteria were performed as previously described (Kitaeva et al., 2021). Prior to staining with propidium iodide, sections of *G. soja* and *P. vulgaris* were incubated in RNAse A solution (Thermo Fisher Scientific, Waltham, MA, United States) at a dilution of 1:10 for 30 min at 28°C. Microtubule pattern analysis in nodule cells was performed using an LSM 780 laser scanning confocal microscope and ZEN 2012 software (Zeiss, Oberkochen, Germany). AlexaFluor 488 was excited at 488 nm, and fluorescence emitted between 499 to 543 nm was collected; Alexa Fluor 546 was excited at 561 nm, and emitted fluorescence between 568 and 572 nm was collected; propidium iodide was excited at 561, and emitted fluorescence between 606 and 677 nm was collected.

Bacteroid Isolation

Bacteroids were isolated as previously described (Tsyganova et al., 2021). Briefly, 3-week-old nodules (five nodules for each species) were cut into pieces, digested by cellulase, and stained with propidium iodide. The length of 50 bacteroids of each species (165 bacteroids for *G. soja* due to the high variation in bacteroid length) was determined. Pairwise comparisons were conducted using Tukey's range test.

Free-Living Bacteria Visualization

Bacteria were visualized according to Tsyganova et al. (2021). Bacteria were heat-treated at 70°C and stained with propidium iodide. The length of 25 bacteria was determined. Pairwise comparisons were conducted using Tukey's range test.

Quantitative Analysis

For determining microtubule orientations in nodule cells of studied species a previously described method was used (Tsyganova et al., 2021). This involved converting confocal images to maximum intensity projections, their thresholding, and the use of MicroFilament Analyzer software (Jacques et al., 2013). Obtained frequencies of microtubule angles were classified relative to the longitudinal axis of the cell as axial (0–30, 150–180), oblique (30–60, 120–150), or transverse (60–120). Isolation and analysis of endoplasmic microtubules from z-stack confocal images were performed as described previously (Kitaeva et al., 2021; Tsyganova et al., 2021). Statistically significant differences in angle frequencies between the cell types were determined using Kruskal–Wallis test and Dunn's *post hoc* test.

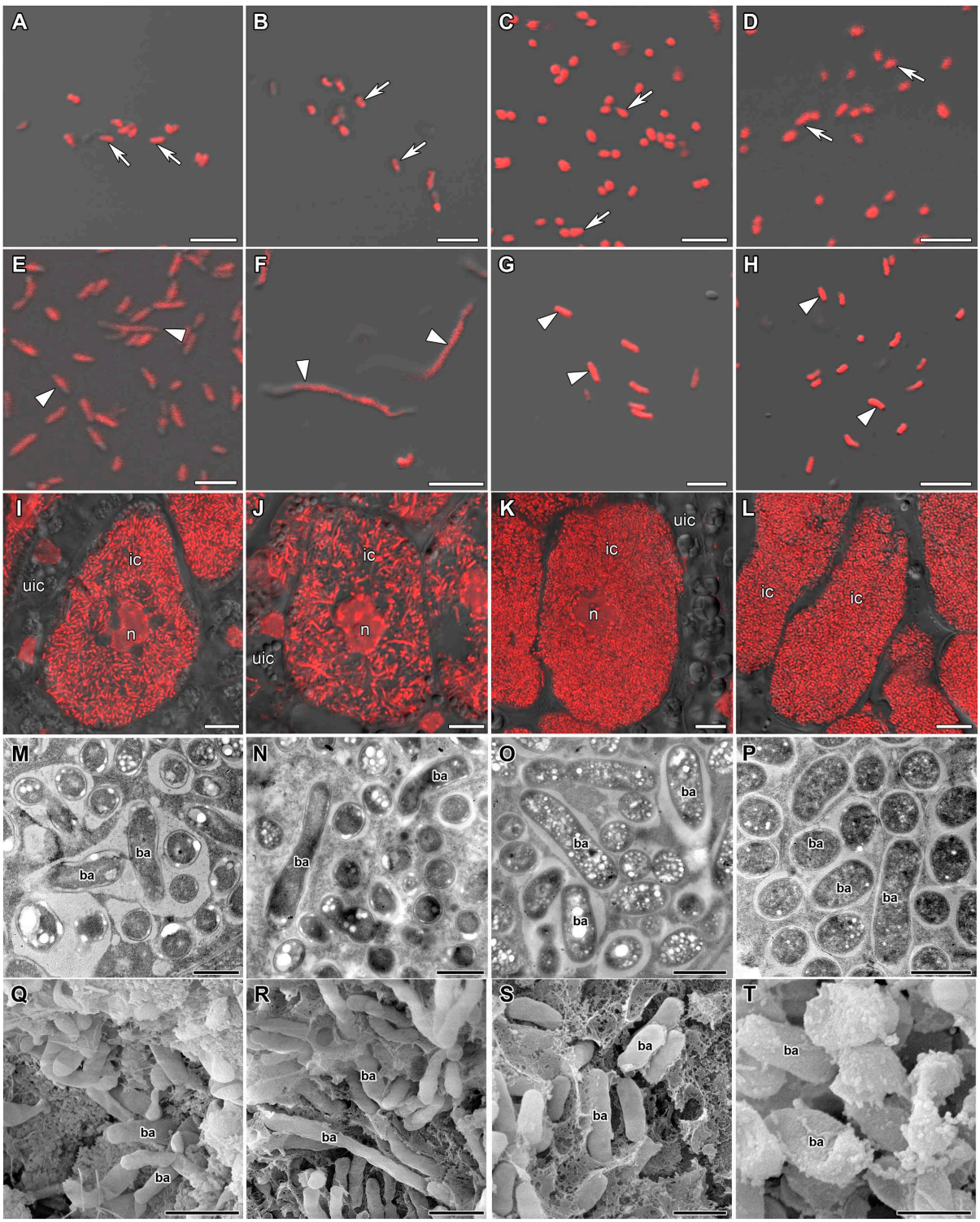

FIGURE 1 | Morphology of bacteria, bacteroids, and infected cells in *G. max* **(A,E,I,M,Q)**, *G. soja* **(B,F,J,N,R)**, *P. vulgaris* **(C,G,K,O,S)**, and *L. japonicus* **(D,H,L,P,T)** nodules. ic, infected cell; uic, uninfected cell; n, nucleus; ba, bacteroid; arrows indicate bacteria, triangles indicate bacteroids. **(A–D)** Bacteria. **(E–H)** Bacteroids. **(I–L)** Symbiosome arrangement in infected cells of the nitrogen fixation zone. **(M–P)** Ultrastructure of an infected cell. **(Q–T)** Scanning electron microscopy of infected cells. **(A–L)** Merged images of differential interference contrast and red channel (DNA staining with propidium iodide (nuclei and bacteria)). Scale bar **(A–H)** = 5 μm, **(I–L)** = 10 μm, **(M–P)** = 1 μm, **(Q–T)** = 2 μm.

RESULTS

Bacteroid and Symbiosome Morphology

Free-living bacteria of *B. liaoningense* RCAM04656, *R. leguminosarum* bv. *phaseoli* RCAM2624, and *M. loti* RCAM1804 were characterized by a similar shape (**Figures 1A–D**) and length of around 1 μm (**Figure 2**). At the same time, bacteroids in nodules of studied species had a different shape (**Figures 1E–H, M–T**) and size (**Figure 2**). In *L. japonicus* nodules, bacteroids were rod-shaped (**Figures 1H,P,T**), and were double the size of free-living bacteria (**Figure 2**). Bacteroids in nodules of *P. vulgaris* and *G. max* were bigger than the bacteroids of *L. japonicus* (**Figure 2**). In both *P. vulgaris* (**Figures 1G,O,S**) and *G. max* nodules (**Figures 1E,M,Q**), bacteroids exhibited a rod-shape. However, some bacteroids in *G. max* nodules were elongated (**Supplementary Figure 1A**) or elongated-branched (**Supplementary Figures 1B,C**). The most striking increase in bacteroid size was observed in *G. soja* nodules, which were about 5-fold longer than bacteria (some of them reached about 17 μm) (**Figure 2**) and had an elongated or elongated-branched shape (**Figures 1F,N,R** and **Supplementary Figure 1F**).

In the nodules of all studied species, both symbiosomes containing a single bacteroid and symbiosomes containing several bacteroids (multibacteroid symbiosomes) were found in infected cells (**Figures 1M,O,P** and **Supplementary Figure 1E**). The multibacteroid symbiosomes were formed as a result of the division of bacteroids (**Supplementary Figure 1D**).

The symbiosomes in infected cells in nodules of the studied species were randomly distributed. Symbiosomes in infected cells of *P. vulgaris* and *L. japonicus* nodules were more densely packed (**Figures 1K,L**) compared with symbiosomes of the infected cells of *G. max* (**Figure 1I**) and *G. soja* nodules (**Figure 1J** and **Supplementary Video 1**).

Microtubule Organization in Meristematic Cells

Determinate nodules are characterized by the absence of persistent meristems. In all analyzed species meristematic cells were visible in incipient 10-day-old nodules only (**Figure 3**). The infection threads reached these cells. Endoplasmic microtubules in meristematic cells were involved in the formation of mitotic spindles (**Figure 3**) and preprophase bands (**Figures 3G,H**). A dense network of randomly organized cortical microtubules formed irregular patterns (**Figure 3**). Perinuclear microtubules were randomly arranged around the nucleus and formed a dense network (**Supplementary Video 2**).

In developing 14-day-old nodules, some cells continued to divide among infected cells. In *G. max* nodules, cell division occurred in the center (**Supplementary Figures 2A,B**) as well as at the periphery of the nodule among maturating infected cells and parenchymal cells (**Supplementary Figure 2C**). In nodules of *G. soja,* mitoses were spread throughout the nodule, likely among uninfected cells (**Supplementary Figures 3A,B**). In nodules of *P. vulgaris*, mitoses were observed at the periphery of the nodule (**Supplementary Figures 3C,D**). In nodules of *L. japonicus*, dividing cells were observed only in incipient nodules.

Microtubule Organization in Young Infected Cells

In incipient nodules after active cell division, cells began to be infected with released bacteria. In these infected cells

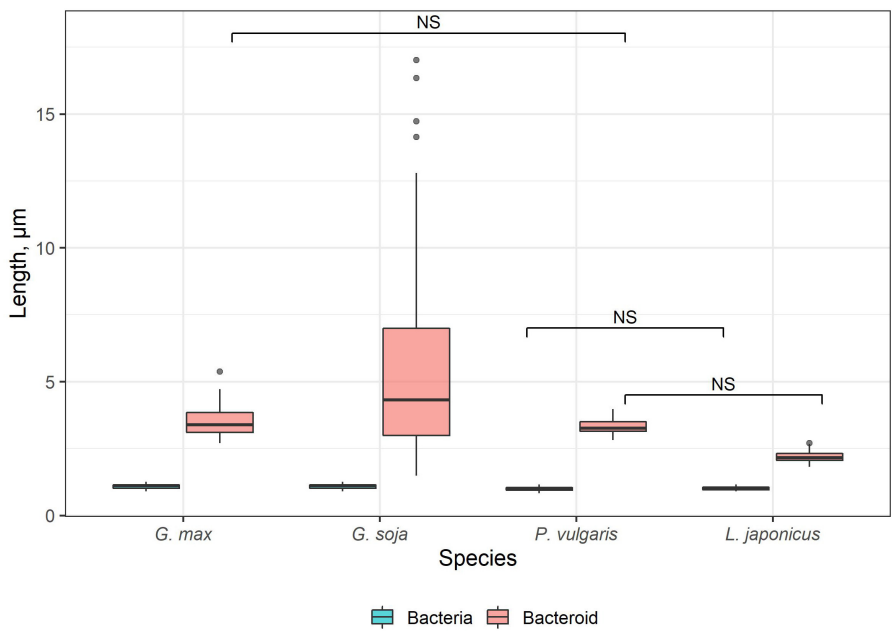

FIGURE 2 | Length of free-living bacteria and bacteroids in nitrogen-fixing cells of *G. max*, *G. soja*, *P. vulgaris,* and *L. japonicus* nodules. Pairwise comparisons were conducted using Tukey's range test. NS indicates not significant differences ($p > 0.05$); $n = 50$ (for *G. soja* n = 165 due to the high variation of bacteroid length).

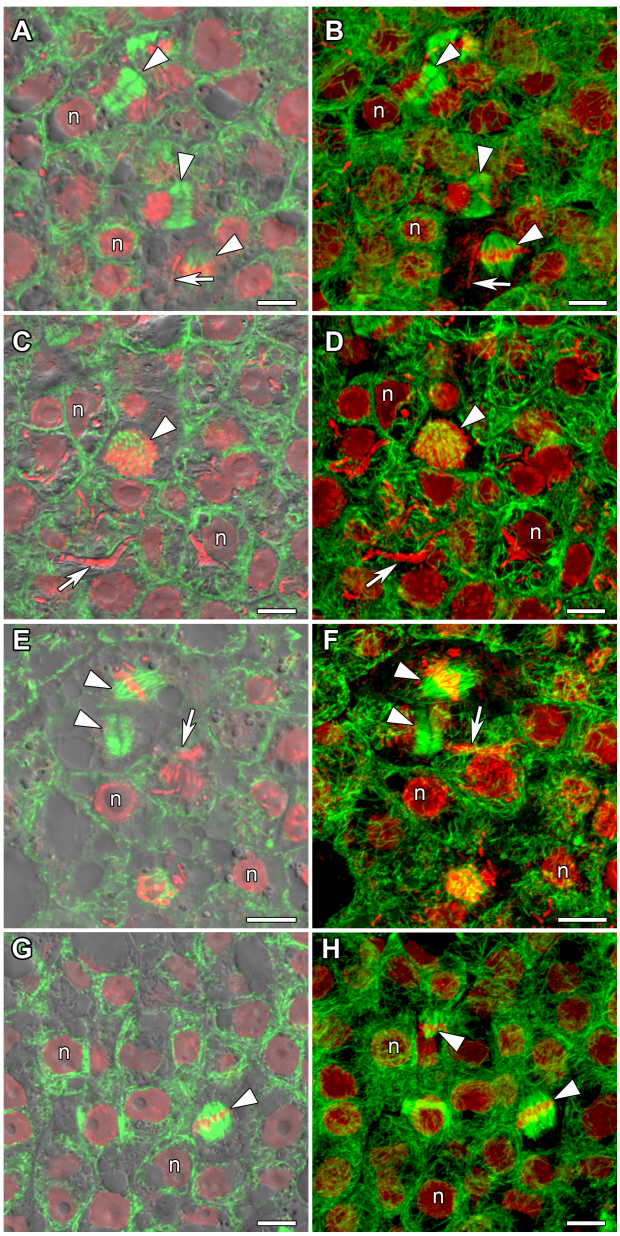

FIGURE 3 | Microtubule organization in meristematic cells of *G. max* **(A,B)**, *G. soja* **(C,D)**, *P. vulgaris* **(E,F)**, and *L. japonicus* **(G,H)** nodules. n, nucleus; triangles indicate mitotic figures, arrows indicate infection threads. Confocal laser scanning microscopy of **(A–F)** 50 μm and **(G,H)** 35 μm longitudinal vibratome sections. Immunolocalization of tubulin (microtubules), green channel; DNA staining with propidium iodide (nuclei and bacteria), red channel. **(A,C,E,G)** Merged images of a single optical section of differential interference contrast and green and red channels. **(B,D,F,H)** Maximum intensity projections of 30 optical sections in green and red channels. Scale bar = 10 μm.

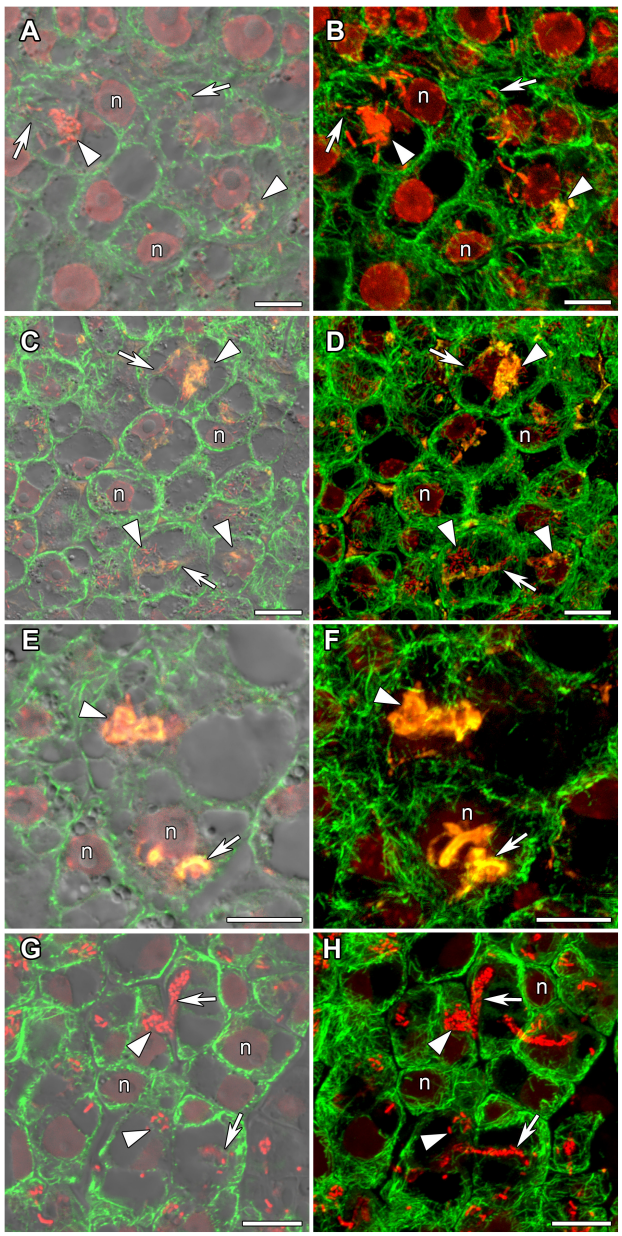

FIGURE 4 | Cortical and endoplasmic microtubule organization in infected cells of infection zone in *G. max* **(A,B)**, *G. soja* **(C,D)**, *P. vulgaris* **(E,F)**, and *L. japonicus* **(G,H)** nodules. n, nucleus; triangles indicate infection droplets; arrows indicate infection threads. Confocal laser scanning microscopy of **(A–F)** 50 μm and **(G,H)** 35 μm longitudinal vibratome sections. Immunolocalization of tubulin (microtubules), green channel; DNA staining with propidium iodide (nuclei and bacteria), red channel and **(A–F)** immunolocalization of MAC265 (infection droplets), yellow channel. **(A,C,E)** Merged images of a single optical section of differential interference contrast and green, red, and yellow channels. **(G)** Merged images of a single optical section of differential interference contrast and green, and red channels. **(B,D,F)** Maximum intensity projections of **(B,D)** 40 and **(F)** 30 optical sections in green, red, and yellow channels. **(H)** Maximum intensity projections of 40 optical sections in green and red channels. Scale bar = 10 μm.

the organization of cortical and endoplasmic microtubules was similar in nodules of all studied species (**Figure 4**). Cortical microtubules were oriented at different angles and formed an irregular pattern. Endoplasmic microtubules passed along infection threads and formed a dense network around infection droplets.

Microtubule Organization in Uninfected Cells

In developing and mature (21-day-old) nodules of all four species, uninfected cells formed clusters (data not shown). In *G. max* nodules, uninfected cells were spherical (**Figures 5A,B**) and in *G. soja* nodules they were more or less spherical (**Figures 5C,D**), whereas in *L. japonicus* and *P. vulgaris* nodules, uninfected cells were elongated (**Figures 5E–H**). In uninfected cells only cortical microtubules were observed (**Figure 5**). In nodules of *G. max* and *G. soja,* cortical microtubules were organized at different angles and formed an irregular pattern (**Figures 5A–D**). Quantitative analysis revealed a roughly equal distribution of axial, oblique, and transverse microtubules in uninfected cells of *G. max* (**Figure 6A** and **Supplementary Figure 4A**). Uninfected cells of *G. soja* had fewer axial microtubules compared with *G. max* cells (**Figure 6B** and **Supplementary Figure 4A**). In uninfected cells of *L. japonicus* and *P. vulgaris* nodules, cortical microtubules formed a regular pattern (**Figures 5E–H**). The portions of axial and oblique microtubules in these nodules were lower than in *G. max* and *G. soja* nodules (**Figures 6C,D** and **Supplementary Figure 4A**); on the contrary, the portion of transverse microtubules was greater than 50% (**Supplementary Figure 4A**).

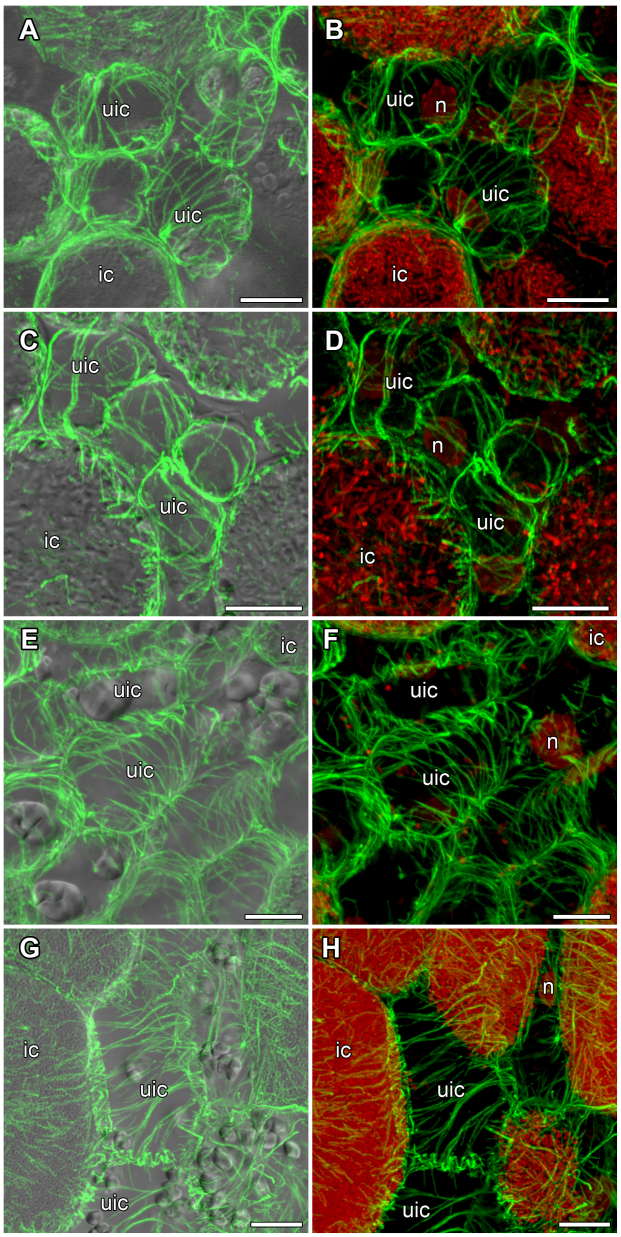

FIGURE 5 | Cortical microtubule organization in uninfected cells of *G. max* **(A,B)**, *G. soja* **(C,D)**, *P. vulgaris* **(E,F)**, and *L. japonicus* **(G,H)** nodules. ic, infected cell; uic, uninfected cell; n, nucleus. Confocal laser scanning microscopy of **(A–F)** 50 μm and **(G,H)** 35 μm longitudinal vibratome sections. Immunolocalization of tubulin (microtubules), green channel; DNA staining with propidium iodide (nuclei and bacteria), red channel. **(A,C,E,G)** Merged images of a single optical section of differential interference contrast and maximum intensity projection of optical sections in the green channel. **(B,D,F,H)** Maximum intensity projections of **(B)** 45, **(D)** 55, and **(F,H)** 50 optical sections in green and red channels. Scale bar = 10 μm.

Microtubule Organization in Nitrogen-Fixing Cells

In mature nodules of all studied species, nitrogen-fixing cells were elongated (**Figure 7**). Both cortical and endoplasmic microtubules were distinguished. Cortical microtubules were arranged parallel to each other and perpendicular to the longitudinal axis, forming a regular pattern in all studied species (**Figure 7**). However quantitative analysis showed that the studied species varied in the number of different types of microtubules. The smallest number of transverse microtubules (and the largest axial) was in *G. max* (**Figure 8A** and **Supplementary Figure 4B**), and the largest number of transverse microtubules (and the smallest axial) was in *L. japonicus* (**Figure 8D** and **Supplementary Figure 4B**). In *G. soja* and *P. vulgaris*, the number of transverse and axial microtubules occupied an intermediate value (**Figures 8B,C** and **Supplementary Figure 4B**).

In nodules of all four legume species, endoplasmic microtubules formed networks located among symbiosomes in infected cells (**Figure 9**). Thick long bundles were barely branched and passed from the center part of the cell to the periphery (**Supplementary Video 3**). The density of endoplasmic microtubules in nitrogen-fixing cells of nodules *G. max* (**Figures 9A,B**) and *P. vulgaris* (**Figures 9E,F**) and in cells of nodules *G. soja* (**Figures 9C,D**) and *L. japonicus* (**Figures 9G,H**) looked similar.

Quantitative Analysis of Endoplasmic Microtubules in Nitrogen-Fixing Cells

Quantitative analysis revealed similarities in the mean number of branches per cell (**Figure 10A**), and total length of branches (**Figure 10B**) between endoplasmic microtubules in nitrogen-fixing cells of *G. max* and *P. vulgaris* nodules. The nitrogen-fixing cells of *G. soja* and *L. japonicus* nodules had a similar number of junctions per cell (**Figure 10D**) and mean number of junctions per skeleton (**Figure 10F**). The degree of branching

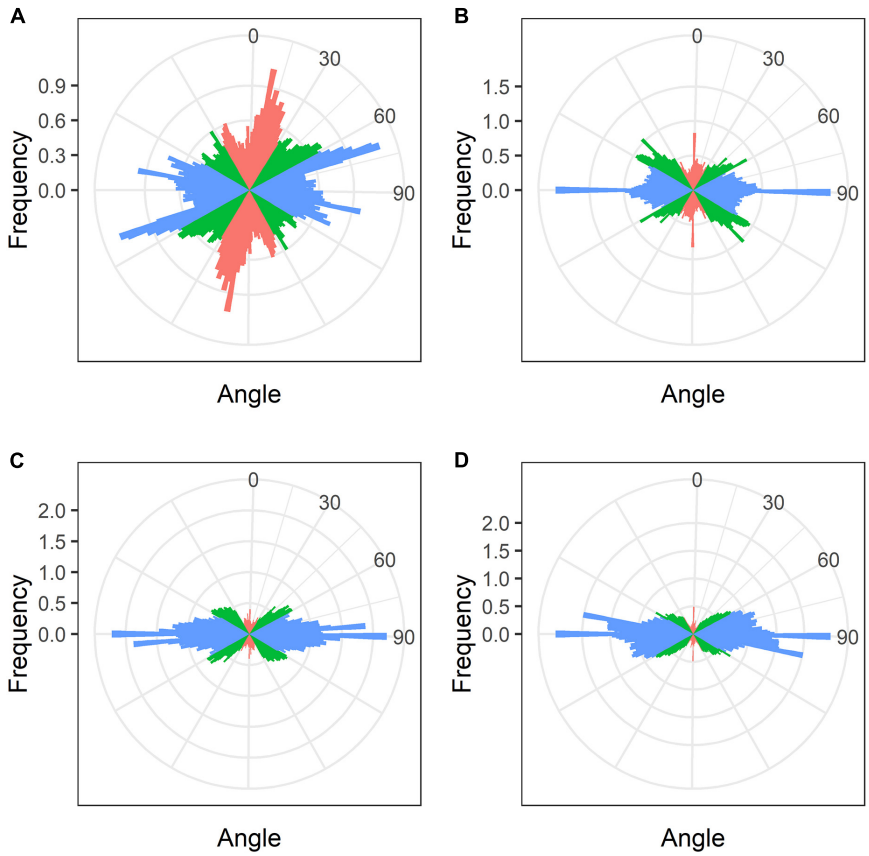

FIGURE 6 | Quantitative analysis of cortical microtubule orientation in uninfected cells of *G. max* **(A)**, *G. soja* **(B)**, *P. vulgaris* **(C)**, and *L. japonicus* **(D)** nodules. Color indicates the class of angles of the microtubules relative to the longitudinal axis of the cell: red, axial (0–30°, 150–180°); green, oblique (30–60°, 120–150°); blue, transverse (60–120°).

was similar for all four species. However, there were statistical differences between *G. max* and *G. soja* and between *P. vulgaris* and *G. soja* (**Figure 10E**). These results demonstrated that the density of endoplasmic microtubules in nitrogen-fixing cells of nodules of *G. max* and *P. vulgaris* and in cells of nodules of *G. soja* and *L. japonicus* were similar. Endoplasmic microtubules in nitrogen-fixing cells of *G. max* were characterized by the highest mean straightness compared with the other three species (**Figure 10C**). At the same time cells of *G. soja* and *L. japonicus* were characterized by a similar mean number of junctions per skeleton (**Figure 10F**).

DISCUSSION

Bacteroid Morphology

The shape and size of bacteroids are controlled by the host plant (Terpolilli et al., 2012). Generally, elongated and branched bacteroids are characteristic of indeterminate nodules, and rod-shaped ones of determinate nodules (Oono et al., 2010; Montiel et al., 2017). However, in *C. arietinum* and *Glycyrrhiza uralensis* indeterminate nodules, bacteroids are spherical and swollen, respectively (Montiel et al., 2016; Kitaeva et al., 2021; Tsyganova et al., 2021). In the current study in *L. japonicus* nodules, bacteroids were similar to free-living bacteria by shape, but their size showed a twofold increase (**Figures 1D,H,P,T**, **2**). It is important to note, that originally only a 20% increase in size in comparison with free-living bacteria was described for bacteroids in *L. japonicus* nodules (Szczyglowski et al., 1998). However, more latterly, a significant increase in bacteroid size in *L. japonicus* nodules has been shown (Suganuma et al., 2003). The rod-shaped form of bacteroids in infected cells of *L. japonucus* nodules has been previously described (Pankhurst et al., 1979; Imaizumi-Anraku et al., 1997; Szczyglowski et al., 1998; Suganuma et al., 2003; Regus et al., 2017). However, upon inoculation of *L. angustissimus* L., *L. pedunculatus* Car., and *L. tenuis* Waldst. Et Kit. with different rhizobia species, bacteria differentiated into spherical, swollen, or rod-shaped bacteroids (Craig and Williamson, 1972; Craig et al., 1973). Moreover, when *L. japonicus* was inoculated with the *R. etli* strain CE3, a significant part of symbiosomes contained a single bacteroid with an elongated and even branching shape (Banba et al., 2001).

On the contrary, upon inoculation of *P. vulgaris* and *G. max* plants with various species and strains of rhizobia, differentiated bacteroids were uniformly rod-shaped (Werner and Mörschel, 1978; Studer et al., 1992; Cermola et al., 1994; Moris et al., 2005; Arthikala et al., 2014), which has been confirmed by studies using scanning electron microscopy (Tu, 1975, 1977).

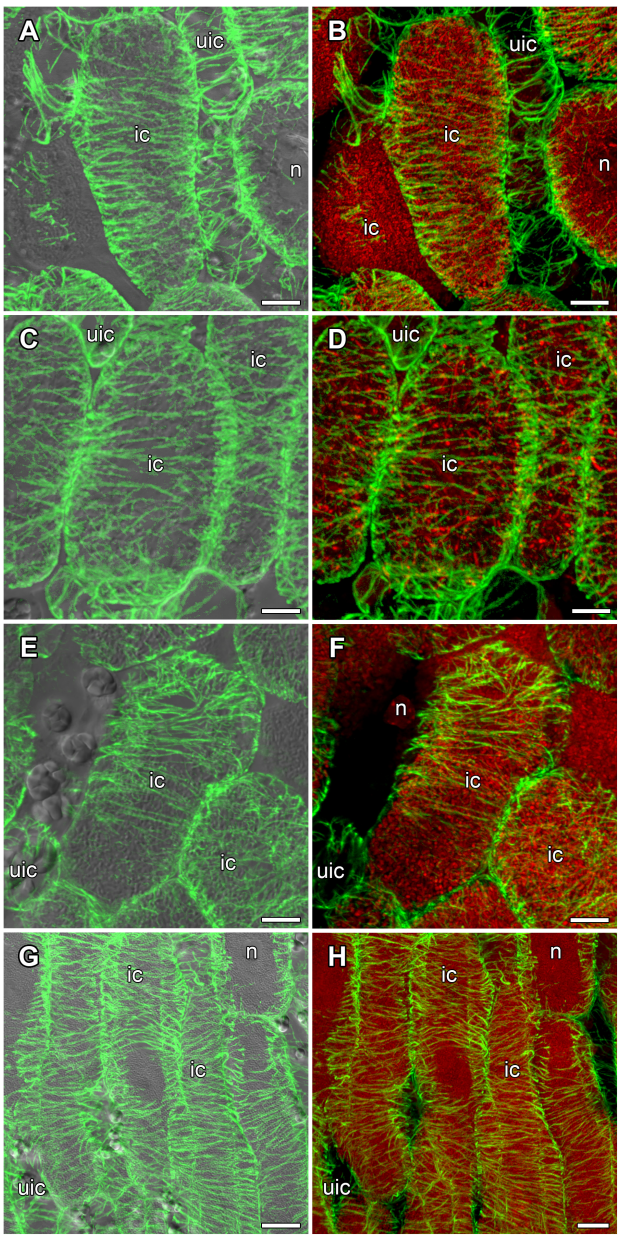

FIGURE 7 | Cortical microtubule organization within infected cells of the nitrogen fixation zone in *G. max* **(A,B)**, *G. soja* **(C,D)**, *P. vulgaris* **(E,F)**, and *L. japonicus* **(G,H)** nodules. ic, infected cell; uic, uninfected cell; n, nucleus. Confocal laser scanning microscopy of **(A–F)** 50 μm and **(G,H)** 35 μm longitudinal vibratome sections. Immunolocalization of tubulin (microtubules), green channel; DNA staining with propidium iodide (nuclei and bacteria), red channel. **(A,C,E,G)** Merged images of a single optical section of differential interference contrast and maximum intensity projection of optical sections in the green channel. **(B,D,F,H)** Maximum intensity projections of **(B,D)** 50, **(F)** 20 and **(H)** 55 optical sections in green and red channels. Scale bar = 10 μm.

According to our data, the bacteroids in nodules of these species were morphologically similar upon inoculation of *P. vulgaris* with the *R. leguminosarum* bv. *phaseoli* RCAM2624 and *G. max* with *B. liaoningense* RCAM04656 (**Figures 1E,G,M,O,Q,S**). Measurements of the length of the bacteroids in nodules of these species showed them to be similar and equal to approximately 3.3 μm and 3.5 μm (**Figure 2**) for nodules of *P. vulgaris* and *G. max*, respectively. In previous studies, the length of bacteroids in *P. vulgaris* nodules upon inoculation with *R. etli* was 1.79 μm (Moris et al., 2005), while the length of bacteroids in *G. max* nodules upon inoculation with *B. japonicum* was different in various studies: 3–5 μm (Bergersen and Briggs, 1958) and about 2.5 μm (Montiel et al., 2016). The observed variation of bacteroid length can be explained by the difference in the rhizobia species infecting the nodules.

It was especially striking that bacteroids in the symbiosis between *G. soja* and *B. liaoningense* RCAM04656 significantly increased in size, reaching 5.5 μm (some of them reached about 17 μm) (**Figures 1F,N,R**, **2**). Unfortunately, studies of *G. soja* bacteroid morphology are limited. For example, in *G. soja* nodules infected with *S. fredii*, bacteroids were spherical, swollen, and rod-shaped (Temprano-Vera et al., 2018), while upon inoculation with *B. diazoefficiens* sp. nov. USDA110 they were rod-shaped or elongated (Muñoz et al., 2016). These differences can be explained by the fact that different species of rhizobia were used for plant inoculation.

Symbiosomes

In this study, in the nodules of all studied species, both symbiosomes with a single bacteroid and multibacteroid symbiosomes were presented in infected cells (**Figures 1M–P** and **Supplementary Figure 1E**). Previously it was shown that in mature determinate nodules, symbiosomes usually contain two or more bacteroids (Lodwig et al., 2005; Oono et al., 2010) and their number depends on the conditional stage of development (early, intermediate, or late), and all three stages can be present simultaneously in nodules. For example, in young infected cells of *P. vulgaris* (Bal et al., 1982; Cermola et al., 2000) and *G. max* (Bergersen and Briggs, 1958; Werner and Mörschel, 1978; Reagan et al., 2017) nodules, symbiosomes contain a single bacteroid, which was confirmed by focused ion beam-scanning electron microscopy and 3D reconstruction (Reagan et al., 2017). With age, after several rounds of division of bacteroids, their number can be increased up to 20 (Muñoz et al., 2016). The increase in bacteroid number in mature symbiosomes can be also caused by the fusion of symbiosomes containing a single bacteroid (Fedorova et al., 1999; Cermola et al., 2000). In 2–3-week-old nodules (nodules of this age were analyzed in this study) both single and multibacteroid symbiosomes can be observed (Studer et al., 1992; Imaizumi-Anraku et al., 1997; Cermola et al., 2000; Ott et al., 2009; Arthikala et al., 2014; Temprano-Vera et al., 2018).

Microtubular Organization

In the current study, we performed a comparative analysis of the organization of the tubulin cytoskeleton in determinate nodules of four legume species (**Table 1**), which should complement our previous studies of the organization of microtubules in indeterminate nodules of six legume species (Kitaeva et al., 2016, 2021; Tsyganova et al., 2021). The study included nodules of various ages, which made it possible to observe the dynamics of changes in the organization of the tubulin cytoskeleton. At the same time, both the patterns of cortical microtubules and

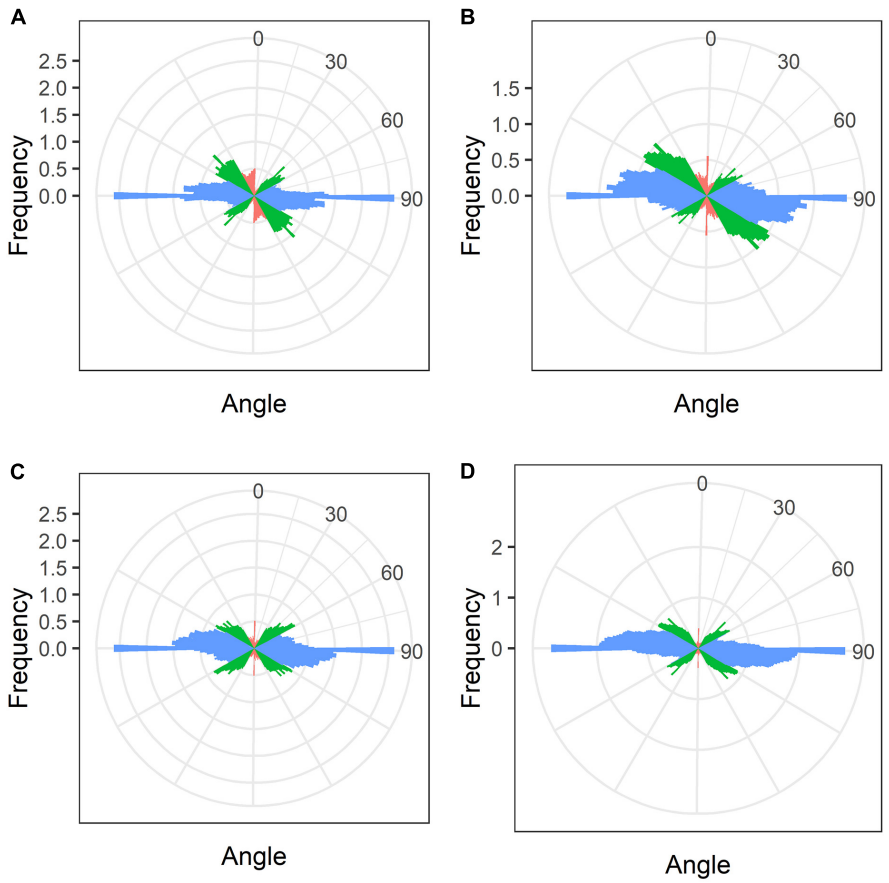

FIGURE 8 | Quantitative analysis of cortical microtubule orientation in infected cells of the nitrogen fixation zone of *G. max* **(A)**, *G. soja* **(B)**, *P. vulgaris* **(C)**, and *L. japonicus* **(D)** nodules. Color indicates the class of angles of the microtubules relative to the longitudinal axis of the cell: red, axial (0–30°, 150–180°); green, oblique (30–60°, 120–150°); blue, transverse (60–120°).

endoplasmic ones were analyzed. When analyzing endoplasmic microtubules, special attention was paid to their interaction with infection structures in the cell.

Despite the transient character of meristem functioning in determinate nodules, in incipient (10-day-old) nodules of all analyzed legume species, numerous meristematic cells were observed (**Figure 3**). Endoplasmic microtubules were involved in the formation of mitotic spindles and preprophase bands whereas cortical microtubules formed irregular patterns (**Table 1** and **Supplementary Video 2**). The organization of both cortical and endoplasmic microtubules was similar to that described for meristematic cells of indeterminate nodules (Kitaeva et al., 2016, 2021; Tsyganova et al., 2021) and root meristem cells (Baluška et al., 1992; Adamakis et al., 2010). In developing nodules, in *G. max*, *G. soja*, and *P. vulgaris,* some mitoses were still visible (**Supplementary Figures 2, 3**). In *G. soja* mitotic activity was observed among uninfected cells that likely led to the formation of clusters of uninfected cells (see below).

In young, infected cells of all studied legume species, cortical microtubules formed irregular patterns and endoplasmic ones were associated with infection threads and infection droplets (**Figure 4** and **Table 1**). These patterns were similar to those observed in indeterminate nodules (Kitaeva et al., 2016, 2021; Tsyganova et al., 2021). This indicates that the development of infection in nodules shares common mechanisms in both determinate and indeterminate nodules.

Analysis of the orientation of cortical microtubules in uninfected cells revealed striking differences between *G. max* and *G. soja* nodules on the one hand, and *P. vulgaris* and *L. japonicus* nodules, on the other. Uninfected cells in *G. max* (**Figures 5A,B** and **Table 1**) and *G. soja* (**Figures 5C,D** and **Table 1**) nodules were characterized by an irregular pattern, while uninfected cells in *P. vulgaris* (**Figures 5E,F** and **Table 1**) and *L. japonicus* (**Figures 5G,H** and **Table 1**) nodules were characterized by a regular pattern. The observed differences were confirmed by quantitative analysis that revealed predominant transverse orientation of microtubules in uninfected cells of *P. vulgaris* and *L. japonicus* (**Figures 6C,D**). The observed differences in the patterns of cortical microtubules suggest that they lead to various types of growth (isodiametric and anisotropic), which is reflected in the form of uninfected cells. In *G. max* and *G. soja*, they are spherical, and in *P. vulgaris* and *L. japonicus*, they are elongated. Early investigation revealed similar irregular patterns of cortical microtubules in uninfected cells in nodules of different age in *G. max* (Whitehead et al., 1998). In indeterminate nodules, it was previously demonstrated that the cortical microtubules

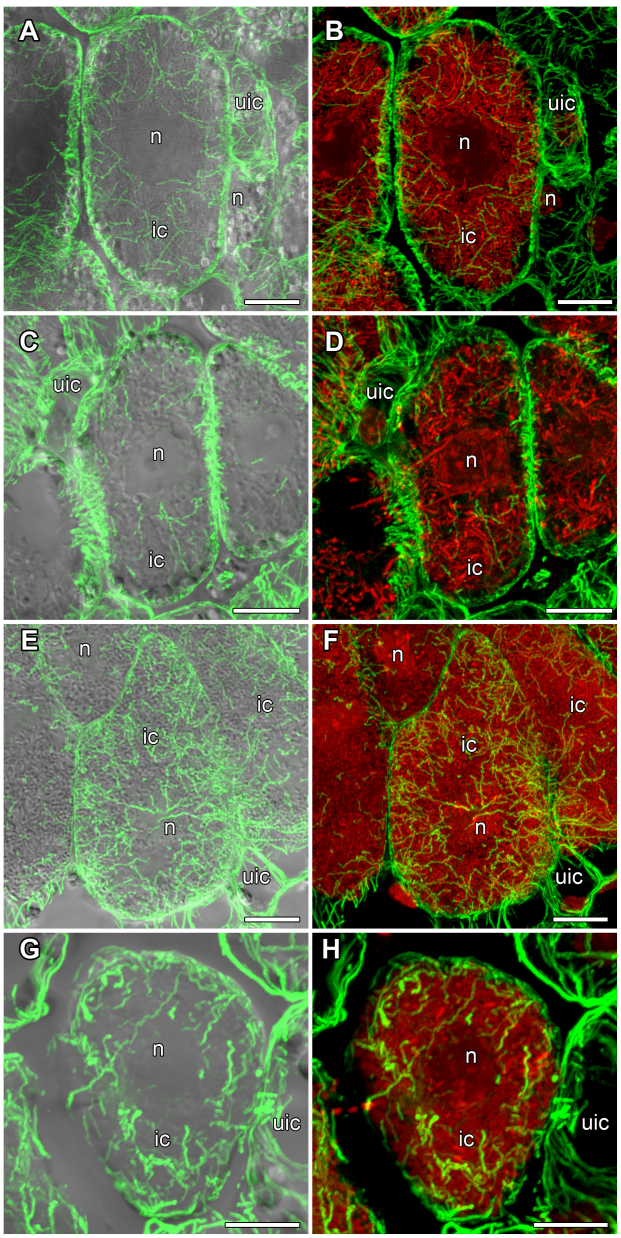

FIGURE 9 | Endoplasmic microtubule organization in infected cells of the nitrogen fixation zone in *G. max* **(A,B)**, *G. soja* **(C,D)**, *P. vulgaris* **(E,F)**, and *L. japonicus* **(G,H)** nodules. ic, infected cell; uic, uninfected cell; n, nucleus. Confocal laser scanning microscopy of **(A–F)** 50 μm and **(G,H)** 35 μm longitudinal vibratome sections. Immunolocalization of tubulin (microtubules), green channel; DNA staining with propidium iodide (nuclei and bacteria), red channel. **(A,C,E,G)** Merged images of a single optical section of differential interference contrast and maximum intensity projection of optical sections in the green channel. **(B,D,F,H)** Maximum intensity projections of **(B,D)** 30, **(F)** 40, and **(H)** 30 optical sections in green and red channels. Scale bar = 10 μm.

of uninfected cells changed from an irregular pattern in the infection zone to a regular one in the nitrogen fixation zone (Kitaeva et al., 2016, 2021; Tsyganova et al., 2021). Thus, the pattern of uninfected cells formed by cortical microtubules in nodules of *G. max* and *G. soja* seems to be unique for the *Glycine* genus and is not linked to nodule type.

It should be noted that, in all four species, uninfected cells were grouped into clusters. The formation of uninfected cells in groups and rows was previously described for *G. max* nodules (Selker and Newcomb, 1985). It is likely that such an arrangement will ensure contact of small, uninfected cells with large, infected cells and facilitate the transfer of ammonia into them. On the other hand, it is possible that the formation of clusters of uninfected cells is associated with the production and transport of ureids, which are the product of nitrogen assimilation in determinate nodules (Pate et al., 1980; Newcomb and Tandon, 1981; Newcomb et al., 1985).

In mature nodules of all four legume species, the cortical microtubules in infected cells formed well pronounced regular patterns (**Figure 7** and **Table 1**) that were confirmed by quantitative analysis (**Figure 8**). Nevertheless, some variation in the number of microtubules of different orientations was observed between species (**Supplementary Figure 4B**). A regular pattern has been previously observed in developing (15-day-old) *G. max* nodules; in mature nodules (42–49-day-old), which were significantly older than the mature nodules analyzed in this study (21-day-old); the regular pattern was retained only in certain regions of the cell (Whitehead et al., 1998). The observed regular pattern of cortical microtubules in infected cells in determinate nodules is strikingly different from the irregular pattern characteristic of indeterminate nodules (Kitaeva et al., 2016, 2021; Tsyganova et al., 2021). The revealed differences mean that infected cells in determinate nodules use anisotropic growth to increase the cell volume and accommodate symbiosomes, while isodiametric growth is used for these purposes in indeterminate nodules. The reason for the identified differences is fascinating, but is currently unclear. It is unlikely to be associated with the morphology of bacteroids, since although in *G. max*, *P. vulgaris*, and *L. japonicus* bacteroids are less differentiated than bacteroids in indeterminate nodules, in *G. soja* there was a significant increase in the size of bacteroids compared to bacteria, while infected cells of *G. soja* were also characterized by anisotropic growth. Taking into consideration the fact that determinate nodules within the Papilionoideae subfamily appeared at an earlier stage of evolution than indeterminate nodules (Ren, 2018), it can be assumed that the transition of infected cells to isodiametric growth was an adaptation providing an evolutionary advantage of indeterminate nodules. It is possible that, topologically, the distribution of symbiosomes in an infected cell in the form of a sphere, which is created by isodiametric growth, is facilitated in comparison with cylindrical infected cells resulting from anisotropic growth. It is also important to note that, in infected cells, the central vacuole is absent in determinate nodules, while in indeterminate nodules a large vacuole occupies a central position in the cell (Newcomb, 1976). Nevertheless, in order to confirm the universality of the identified patterns of cortical microtubules for infected cells in determinate and indeterminate nodules, it is necessary to analyze the organization of the tubulin cytoskeleton in a greater number of legume species. To date, of the six legume species forming indeterminate nodules, for which the analysis of the organization of the tubulin cytoskeleton was carried out, five belong to the same Vicioid clade

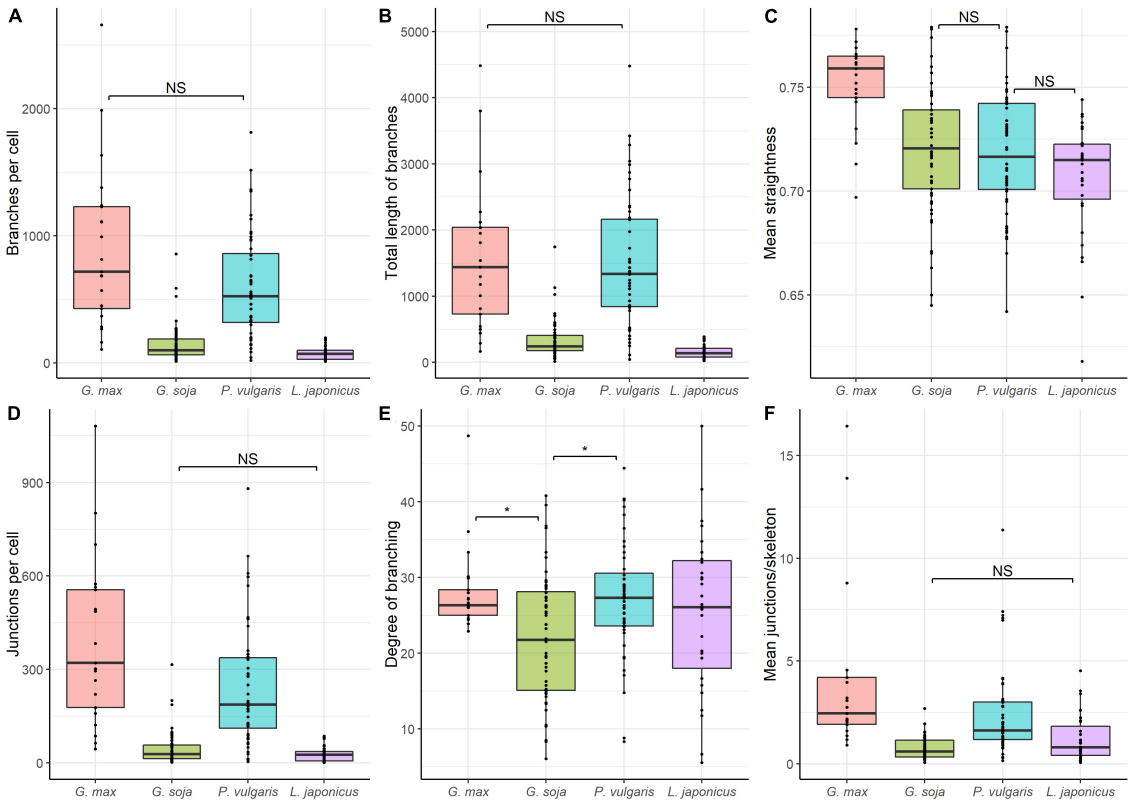

FIGURE 10 | Quantitative analysis of tubulin microtubule organization in nitrogen-fixing cells of *G. max* (n = 21), *G. soja* (n = 56), *P. vulgaris* (n = 48), and *L. japonicus* (n = 31) nodules. **(A)** Total number of branches per cell, number of all detected microtubules. **(B)** Total length of branches per cell, the total length of all detected microtubules per cell. **(C)** Mean straightness index of detected microtubules per cell, the Euclidian distance between the starting and ending point of each branch divided by its full length. **(D)** Total number of junctions per cell. **(E)** Degree of branching per cell, number of skeletons (sets of branches, connected together) with more than one branch divided by the total number of skeletons in the image. **(F)** Mean number of junctions per skeleton, average number of branching points across all skeletons in the cell. Dots indicate analyzed images of individual cells. Pairwise comparisons were conducted using Tukey's range test, NS indicates not significant differences ($p > 0.05$), otherwise differences are significant ($p < 0.05$).

TABLE 1 | Comparative analysis of microtubular patterns in determinate nodules of *G. max*, *G. soja*, *P. vulgaris*, *L. japonicus*, and indeterminate nodules.

Cell type	Type of microtubules	*Glycine max*	*Glycine soja*	*Phaseolus vulgaris*	*Lotus japonicus**	Indeterminate nodules**
Meristematic	*Cortical*	Irregular				Irregular
	Endoplasmic	Mitotic spindles, preprophase bands, perinuclear				Mitotic spindles, preprophase bands, perinuclear
Young infected	*Cortical*	Irregular				Irregular
	Endoplasmic	A network around infection threads and droplets				A network around infection threads and droplets
Uninfected	*Cortical*	**Irregular*** **		Regular		**Regular**
	Endoplasmic	Unidentified				Unidentified
Nitrogen-fixing	*Cortical*	**Regular**				**Irregular**
	Endoplasmic	A network among symbiosomes; **irregular**				A network among symbiosomes; irregular, **regular**, and intermediate

**The current study.*
***Based on Kitaeva et al., 2016, 2021; Tsyganova et al., 2021.*
****Differences observed between microtubular patterns in determinate and indeterminate nodules are shown in bold.*

(Wojciechowski et al., 2004). Future analyses should include species representing different clades of legumes.

In the infected cells in the nodules of all four studied species, a well-developed network of endoplasmic microtubules, forming an irregular pattern and located between chaotically distributed symbiosomes, was observed (**Figure 9** and **Table 1**). However, surprisingly, the visual network of endoplasmic microtubules was observed to be denser in *G. max* and *P. vulgaris* infected cells than in *G. soja* and *L. japonicus* cells. The observed differences were confirmed by quantitative analysis (**Figure 10**). Previously, we observed an irregular and regular pattern of endoplasmic microtubules in infected cells of various legume species, which coincided with an ordered or disordered arrangement of symbiosomes, respectively (Kitaeva et al., 2016, 2021; Tsyganova et al., 2021). Nevertheless, in mature determinate nodules, symbiosomes containing several bacteroids are present and, accordingly, their size is significantly larger than the size of the bacteroids themselves, as assessed in this study (**Figure 2**). It would be interesting to evaluate the size and shape of symbiosomes in determinate nodules and relate them to the pattern of endoplasmic microtubules.

CONCLUSION

Thus, the similarity of the organization of endoplasmic microtubules involved in the development of infection threads and infection droplets in the cells of indeterminate and determinate nodules revealed the commonality of the role of tubulin cytoskeleton in the development of infection structures in nodules of both types. Notable differences were revealed in the organization of cortical microtubules in infected cells between indeterminate and mature determinate nodules, which were manifested in the isodiametric growth of infected cells in an indeterminate nodule and anisotropic growth in a determinate nodule. The fact that within the Papilionoideae subfamily determinate nodules appeared in evolution earlier than indeterminate ones raises an intriguing question regarding the possible advantage of isodiametric growth of infected cells over anisotropic for their accommodation of numerous symbiosomes. Further research should address this question. However, it is necessary to analyze the organization of the tubulin cytoskeleton in a larger number of legume species in order to confirm the revealed patterns of cortical microtubule organization in infected cells of determinate and indeterminate nodules.

DATA AVAILABILITY STATEMENT

The raw data supporting the conclusions of this article will be made available by the authors, without undue reservation.

AUTHOR CONTRIBUTIONS

VT: conceptualization and writing—review and editing. AG and AT: electron microscopy studies. AK: immunolocalization of tubulin cytoskeleton and laser scanning confocal microscopy. PK and AS: quantitative analysis of tubulin cytoskeleton. AK and AT: writing—original draft preparation. All authors have read and agreed to the published version of the manuscript.

FUNDING

This research was funded by the Russian Foundation for Basic Research grant number 20-316-70004.

ACKNOWLEDGMENTS

This work was carried out using the equipment of the Core Centrum "Genomic Technologies, Proteomics and Cell Biology" at the All-Russia Research Institute for Agricultural Microbiology (St. Petersburg, Russia), the Core Facilities Center "Cell and Molecular Technologies in Plant Science" at the Komarov Botanical Institute RAS (St. Petersburg, Russia), and the Molecular and Cell Technologies Research Resource Centre at Saint Petersburg State University (St. Petersburg, Russia).

SUPPLEMENTARY MATERIAL

The Supplementary Material for this article can be found online at: https://www.frontiersin.org/articles/10.3389/fpls.2022.823183/full#supplementary-material

Supplementary Video 1 | Organization of bacteroids in infected cells of mature *G. soja* nodules.

Supplementary Video 2 | Organization of microtubules in meristematic cells of *G. max* nodules.

Supplementary Video 3 | Organization of microtubules in infected cells of mature *P. vulgaris* nodules.

REFERENCES

Adamakis, I. D. S., Panteris, E., and Eleftheriou, E. P. (2010). Tungsten affects the cortical microtubules of *Pisum sativum* root cells: experiments on tungsten-molybdenum antagonism. *Plant Biol.* 12, 114–124. doi: 10.1111/j.1438-8677.2009.00197.x

Arthikala, M.-K., Sánchez-López, R., Nava, N., Santana, O., Cárdenas, L., and Quinto, C. (2014). *RbohB*, a *Phaseolus vulgaris* NADPH oxidase gene, enhances symbiosome number, bacteroid size, and nitrogen fixation in nodules and impairs mycorrhizal colonization. *New Phytol.* 202, 886–900. doi: 10.1111/nph.12714

Bal, A. K., Shantharam, S., and Wong, P. P. (1982). Nodulation of pole bean (*Phaseolus vulgaris* L.) by *Rhizobium* species of two cross-inoculation groups. *Appl. Environ. Microbiol.* 44, 965–971. doi: 10.1128/aem.44.4.965-971.1982

Baluška, F., Parker, J. S., and Barlow, P. W. (1992). Specific patterns of cortical and endoplasmic microtubules associated with cell growth and tissue differentiation in roots of maize (*Zea mays* L.). *J. Cell Sci.* 103, 191–200.

Banba, M., Siddique, A.-B. M., Kouchi, H., Izui, K., and Hata, S. (2001). *Lotus japonicus* forms early senescent root nodules with *Rhizobium etli*. *Mol. Plant Microbe Interact.* 14, 173–180. doi: 10.1094/MPMI.2001.14.2.173

Bashline, L., Lei, L., Li, S., and Gu, Y. (2014). Cell wall, cytoskeleton, and cell expansion in higher plants. *Mol. Plant* 7, 586–600. doi: 10.1093/mp/ssu018

Bergersen, F. J., and Briggs, M. J. (1958). Studies on the bacterial component of soybean root nodules: cytology and organization in the host tissue. *Microbiology* 19, 482–490. doi: 10.1099/00221287-19-3-482

Cermola, M., Fedorova, E., Taté, R., Riccio, A., Favre, R., and Patriarca, E. J. (2000). Nodule invasion and symbiosome differentiation during *Rhizobium etli–Phaseolus vulgaris* symbiosis. *Mol. Plant Microbe Interact.* 13, 733–741.

Cermola, M., Hermann, R., Müller, M., Taté, R., and Favre, R. (1994). Ultrastructural analysis of *Rhizobium leguminosarum phaseoli* in high-pressure cryofixed bean root nodules. *J. Struct. Biol.* 113, 142–147. doi: 10.1006/jsbi.1994.1045

Coba de la Peña, T., Fedorova, E., Pueyo, J. J., and Lucas, M. M. (2018). The symbiosome: legume and rhizobia co-evolution toward a nitrogen-fixing organelle? *Front. Plant Sci.* 8:2229. doi: 10.3389/fpls.2017.02229

Craig, A. S., Greenwood, R. M., and Williamson, K. I. (1973). Ultrastructural inclusions of rhizobial bacteroids of Lotus nodules and their taxonomic significance. *Arch. Mikrobiol.* 89, 23–32. doi: 10.1007/BF00409396

Craig, A. S., and Williamson, K. I. (1972). Three inclusions of rhizobial bacteroids and their cytochemical character. *Arch. Mikrobiol.* 87, 165–171. doi: 10.1007/BF00424997

Crowell, E. F., Gonneau, M., Vernhettes, S., and Höfte, H. (2010). Regulation of anisotropic cell expansion in higher plants. *Comptes Rendus Biol.* 333, 320–324. doi: 10.1016/j.crvi.2010.01.007

Fåhraeus, G. (1957). The infection of clover root hairs by nodule bacteria studied by a simple glass slide technique. *J. Gen. Microbiol.* 16, 374–381. doi: 10.1099/00221287-16-2-374

Fedorova, E., Thomson, R., Whitehead, L. F., Maudoux, O., Udvardi, M. K., and Day, D. A. (1999). Localization of H^+-ATPases in soybean root nodules. *Planta* 209, 25–32. doi: 10.1007/s004250050603

Gavrin, A., Jansen, V., Ivanov, S., Bisseling, T., and Fedorova, E. (2015). ARP2/3-mediated actin nucleation associated with symbiosome membrane is essential for the development of symbiosomes in infected cells of *Medicago truncatula* root nodules. *Mol. Plant Microbe Interact.* 28, 605–614. doi: 10.1094/MPMI-12-14-0402-R

Genre, A., and Timmers, T. (2019). The symbiotic role of the actin filament cytoskeleton. *New Phytol.* 221, 611–613. doi: 10.1111/nph.15506

Guinel, F. C. (2009). Getting around the legume nodule: I. The structure of the peripheral zone in four nodule types. *Botany* 87, 1117–1138. doi: 10.1139/B09-074

Hamada, T. (2014). "Microtubule organization and microtubule-associated proteins in plant cells," in *International Review of Cell and Molecular Biology*, ed. K. W. Jeon (Boston, MA: Academic Press). 1–52.

Hirsch, A. M. (1992). Developmental biology of legume nodulation. *New Phytol.* 122, 211–237. doi: 10.1111/j.1469-8137.1992.tb04227.x

Imaizumi-Anraku, H., Kawaguchi, M., Koiwa, H., Akao, S., and Syōno, K. (1997). Two ineffective-nodulating mutants of *Lotus japonicus*—different phenotypes caused by the blockage of endocytotic bacterial release and nodule maturation. *Plant Cell Physiol.* 38, 871–881. doi: 10.1093/oxfordjournals.pcp.a029246

Jacques, E., Buytaert, J., Wells, D. M., Lewandowski, M., Bennett, M. J., Dirckx, J., et al. (2013). MicroFilament Analyzer, an image analysis tool for quantifying fibrillar orientation, reveals changes in microtubule organization during gravitropism. *Plant J.* 74, 1045–1058. doi: 10.1111/tpj.12174

Jiang, Q., and Gresshoff, P. M. (1997). Classical and molecular genetics of the model legume *Lotus japonicus*. *Mol. Plant Microbe Interact.* 10, 59–68. doi: 10.1094/mpmi.1997.10.1.59

Kitaeva, A. B., Demchenko, K. N., Tikhonovich, I. A., Timmers, A. C. J., and Tsyganov, V. E. (2016). Comparative analysis of the tubulin cytoskeleton organization in nodules of *Medicago truncatula* and *Pisum sativum*: bacterial release and bacteroid positioning correlate with characteristic microtubule rearrangements. *New Phytol.* 210, 168–183. doi: 10.1111/nph.13792

Kitaeva, A. B., Gorshkov, A. P., Kirichek, E. A., Kusakin, P. G., Tsyganova, A. V., and Tsyganov, V. E. (2021). General patterns and species-specific differences in the organization of the tubulin cytoskeleton in indeterminate nodules of three legumes. *Cells* 10:1012. doi: 10.3390/cells10051012

Kitaeva, A. B., Kusakin, P. G., Demchenko, K. N., and Tsyganov, V. E. (2018). Key methodological features of tubulin cytoskeleton studies in nodules of legume plants. *Agric. Biol.* 53, 634–644. doi: 10.15389/agrobiology.2018.3.634eng

Kost, B., Mathur, J., and Chua, N.-H. (1999). Cytoskeleton in plant development. *Curr. Opin. Plant Biol.* 2, 462–470. doi: 10.1016/S1369-5266(99)00024-2

Li, S., Sun, T., and Ren, H. (2015). The functions of the cytoskeleton and associated proteins during mitosis and cytokinesis in plant cells. *Front. Plant Sci.* 6:282. doi: 10.3389/fpls.2015.00282

Lodwig, E. M., Leonard, M., Marroqui, S., Wheeler, T. R., Findlay, K., Downie, J. A., et al. (2005). Role of polyhydroxybutyrate and glycogen as carbon storage compounds in pea and bean bacteroids. *Mol. Plant Microbe Interact.* 18, 67–74. doi: 10.1094/mpmi-18-0067

Mergaert, P. (2020). "Chapter Six - Differentiation of symbiotic nodule cells and their rhizobium endosymbionts," in *Advances in Botanical Research*, eds P. Frendo, F. Frugier, and C. Masson-Boivin (Cambridge, MA: Academic Press). 149–180.

Montiel, J., Downie, J. A., Farkas, A., Bihari, P., Herczeg, R., Bálint, B., et al. (2017). Morphotype of bacteroids in different legumes correlates with the number and type of symbiotic NCR peptides. *Proc. Natl. Acad. Sci. U.S.A* 114, 5041–5046. doi: 10.1073/pnas.1704217114

Montiel, J., Szűcs, A., Boboescu, I. Z., Gherman, V. D., Kondorosi, É, and Kereszt, A. (2016). Terminal bacteroid differentiation is associated with variable morphological changes in legume species belonging to the inverted repeat-lacking clade. *Mol. Plant Microbe Interact.* 29, 210–219. doi: 10.1094/MPMI-09-15-0213-R

Moris, M., Braeken, K., Schoeters, E., Verreth, C., Beullens, S., Vanderleyden, J., et al. (2005). Effective symbiosis between *Rhizobium etli* and *Phaseolus vulgaris* requires the alarmone ppGpp. *J. Bacteriol.* 187, 5460–5469. doi: 10.1128/JB.187.15.5460-5469.2005

Muñoz, N., Qi, X., Li, M. W., Xie, M., Gao, Y., Cheung, M. Y., et al. (2016). Improvement in nitrogen fixation capacity could be part of the domestication process in soybean. *Heredity* 117, 84–93. doi: 10.1038/hdy.2016.27

Newcomb, E. H., and Tandon, S. R. (1981). Uninfected cells of soybean root nodules: ultrastructure suggests key role in ureide production. *Science* 212, 1394–1396. doi: 10.1126/science.212.4501.1394

Newcomb, E. H., Tandon, S. R., and Kowal, R. R. (1985). Ultrastructural specialization for ureide production in uninfected cells of soybean root nodules. *Protoplasma* 125, 1–12. doi: 10.1007/BF01297345

Newcomb, W. (1976). A correlated light and electron microscopic study of symbiotic growth and differentiation in *Pisum sativum* root nodules. *Can. J. Bot.* 54, 2163–2186. doi: 10.1139/b76-233

Oono, R., Schmitt, I., Sprent, J. I., and Denison, R. F. (2010). Multiple evolutionary origins of legume traits leading to extreme rhizobial differentiation. *New Phytol.* 187, 508–520. doi: 10.1111/j.1469-8137.2010.03261.x

Ott, T., Sullivan, J., James, E. K., Flemetakis, E., Günther, C., Gibon, Y., et al. (2009). Absence of symbiotic leghemoglobins alters bacteroid and plant cell differentiation during development of *Lotus japonicus* root nodules. *Mol. Plant Microbe Interact.* 22, 800–808. doi: 10.1094/mpmi-22-7-0800

Pankhurst, C. E., Craig, A. S., and Jones, W. T. (1979). Effectiveness of *Lotus* root nodules: I. Morphology and flavolan content of nodules formed on *Lotus pedunculatus* by fast-growing *Lotus* rhizobia. *J. Exp. Bot.* 30, 1085–1093. doi: 10.1093/jxb/30.6.1085

Paradez, A., Wright, A., and Ehrhardt, D. W. (2006). Microtubule cortical array organization and plant cell morphogenesis. *Curr. Opin. Plant Biol.* 9, 571–578. doi: 10.1016/j.pbi.2006.09.005

Pate, J. S., Atkins, C. A., White, S. T., Rainbird, R. M., and Woo, K. C. (1980). Nitrogen nutrition and xylem transport of nitrogen in ureide-producing grain legumes. *Plant Physiol.* 65, 961–965. doi: 10.1104/pp.65.5.961

Peña, E. J., and Heinlein, M. (2013). Cortical microtubule-associated ER sites: organization centers of cell polarity and communication. *Curr. Opin. Plant Biol.* 16, 764–773. doi: 10.1016/j.pbi.2013.10.002

Perrine-Walker, F. M., Lartaud, M., Kouchi, H., and Ridge, R. W. (2014). Microtubule array formation during root hair infection thread initiation and elongation in the *Mesorhizobium-Lotus* symbiosis. *Protoplasma* 251, 1099–1111. doi: 10.1007/s00709-014-0618-z

Pueppke, S. G. (1983). *Rhizobium* infection threads in root hairs of *Glycine max* (L.) Merr., *Glycine soja* Sieb. & Zucc, and *Vigna unguiculata* (L.) Walp. *Can. J. Microbiol.* 29, 69–76. doi: 10.1139/m83-011

Reagan, B. C., Kim, P. J.-Y., Perry, P. D., Dunlap, J. R., and Burch-Smith, T. M. (2017). Spatial distribution of organelles in leaf cells and soybean root nodules revealed by focused ion beam-scanning electron microscopy. *Funct. Plant Biol.* 45, 180–191. doi: 10.1071/FP16347

Regus, J. U., Quides, K. W., O'Neill, M. R., Suzuki, R., Savory, E. A., Chang, J. H., et al. (2017). Cell autonomous sanctions in legumes target ineffective rhizobia in nodules with mixed infections. *Am. J. Bot.* 104, 1299–1312. doi: 10.3732/ajb.1700165

Ren, G. (2018). *The Evolution of Determinate and Indeterminate Nodules Within the Papilionoideae Subfamily*. Ph.D. Wageningen: Wageningen University.

Selker, J. M. L., and Newcomb, E. H. (1985). Spatial relationships between uninfected and infected cells in root nodules of soybean. *Planta* 165, 446–454. doi: 10.1007/BF00398089

Serova, T. A., Tsyganova, A. V., and Tsyganov, V. E. (2018). Early nodule senescence is activated in symbiotic mutants of pea (*Pisum sativum* L.) forming ineffective nodules blocked at different nodule developmental stages. *Protoplasma* 255, 1443–1459. doi: 10.1007/s00709-018-1246-9

Sieberer, B. J., Timmers, A. C., and Emons, A. M. C. (2005). Nod factors alter the microtubule cytoskeleton in *Medicago truncatula* root hairs to allow root hair reorientation. *Mol. Plant Microbe Interact.* 18, 1195–1204. doi: 10.1094/MPMI-18-1195

Studer, D., Hennecke, H., and Müller, M. (1992). High-pressure freezing of soybean nodules leads to an improved preservation of ultrastructure. *Planta* 188, 155–163. doi: 10.1007/BF00216809

Suganuma, N., Nakamura, Y., Yamamoto, M., Ohta, T., Koiwa, H., Akao, S., et al. (2003). The *Lotus japonicus Sen1* gene controls rhizobial differentiation into nitrogen-fixing bacteroids in nodules. *Mol. Genet. Genom.* 269, 312–320. doi: 10.1007/s00438-003-0840-4

Szczyglowski, K., Shaw, R. S., Wopereis, J., Copeland, S., Hamburger, D., Kasiborski, B., et al. (1998). Nodule organogenesis and symbiotic mutants of the model legume *Lotus japonicus*. *Mol. Plant Microbe Interact.* 11, 684–697. doi: 10.1094/MPMI.1998.11.7.684

Temprano-Vera, F., Rodríguez-Navarro, D. N., Acosta-Jurado, S., Perret, X., Fossou, R. K., Navarro-Gómez, P., et al. (2018). *Sinorhizobium fredii* strains HH103 and NGR234 form nitrogen fixing nodules with diverse wild soybeans (*Glycine soja*) from Central China but are ineffective on Northern China accessions. *Front. Microbiol.* 9:2843. doi: 10.3389/fmicb.2018.02843

Terpolilli, J. J., Hood, G. A., and Poole, P. S. (2012). "Chapter 5 - What determines the efficiency of N_2-fixing *Rhizobium*-legume symbioses?," in *Advances in Microbial Physiology*. ed. R. K. Poole (Cambridge, MA: Academic Press). 325–389.

Timmers, A. C., Auriac, M. C., and Truchet, G. (1999). Refined analysis of early symbiotic steps of the *Rhizobium-Medicago* interaction in relationship with microtubular cytoskeleton rearrangements. *Development* 126, 3617–3628.

Timmers, A. C., Vallotton, P., Heym, C., and Menzel, D. (2007). Microtubule dynamics in root hairs of *Medicago truncatula*. *Eur. J. Cell Biol.* 86, 69–83. doi: 10.1016/j.ejcb.2006.11.001

Timmers, A. C. J. (2008). The role of the plant cytoskeleton in the interaction between legumes and rhizobia. *J. Microsc.* 231, 247–256. doi: 10.1111/j.1365-2818.2008.02040.x

Tsyganov, V. E., Kitaeva, A. B., and Demchenko, K. N. (2019). "Comparative analysis of tubulin cytoskeleton rearrangements in nodules of *Medicago truncatula* and *Pisum sativum*," in *The Model Legume Medicago truncatula*, ed. F. J. de Bruijn (Hoboken, NJ: JohnWiley & Sons, Inc.). 543–547.

Tsyganova, A. V., Kitaeva, A. B., Gorshkov, A. P., Kusakin, P. G., Sadovskaya, A. R., Borisov, Y. G., et al. (2021). *Glycyrrhiza uralensis* nodules: histological and ultrastructural organization and tubulin cytoskeleton dynamics. *Agronomy* 11:2508. doi: 10.3390/agronomy11122508

Tsyganova, A. V., Kitaeva, A. B., and Tsyganov, V. E. (2018). Cell differentiation in nitrogen-fixing nodules hosting symbiosomes. *Funct. Plant Biol.* 45, 47–57. doi: 10.1071/Fp16377

Tu, J. (1975). Rhizobial root nodules of soybean as revealed by scanning and transmission electron microscopy. *Phytopathology* 65, 447–454.

Tu, J. (1977). Effects of soybean mosaic virus infection on ultrastructure of bacteroidal cells in soybean root nodules. *Phytopathology* 67, 199–205.

van Spronsen, P. C., Grønlund, M., Bras, C. P., Spaink, H. P., and Kijne, J. W. (2001). Cell biological changes of outer cortical root cells in early determinate nodulation. *Mol. Plant Microbe Interact.* 14, 839–847. doi: 10.1094/mpmi.2001.14.7.839

Vassileva, V. N., Kouchi, H., and Ridge, R. W. (2005). Microtubule dynamics in living root hairs: transient slowing by lipochitin oligosaccharide nodulation signals. *Plant Cell* 17, 1777–1787. doi: 10.1105/tpc.105.031641

Wasteneys, G. O. (2004). Progress in understanding the role of microtubules in plant cells. *Curr. Opin. Plant Biol.* 7, 651–660. doi: 10.1016/j.pbi.2004.09.008

Werner, D., and Mörschel, E. (1978). Differentiation of nodules of *Glycine max*. *Planta* 141, 169–177. doi: 10.1007/BF00387885

Whitehead, L. F., Day, D. A., and Hardham, A. R. (1998). Cytoskeletal arrays in the cells of soybean root nodules: the role of actin microfilaments in the organisation of symbiosomes. *Protoplasma* 203, 194–205. doi: 10.1007/bf01279476

Wojciechowski, M. F., Lavin, M., and Sanderson, M. J. (2004). A phylogeny of legumes (*Leguminosae*) based on analysis of the plastid *matK* gene resolves many well-supported subclades within the family. *Am. J. Bot.* 91, 1846–1862. doi: 10.3732/ajb.91.11.1846

Zhang, X., Han, L., Wang, Q., Zhang, C., Yu, Y., Tian, J., et al. (2019). The host actin cytoskeleton channels rhizobia release and facilitates symbiosome accommodation during nodulation in *Medicago truncatula*. *New Phytol.* 221, 1049–1059. doi: 10.1111/nph.15423

Conflict of Interest: The authors declare that the research was conducted in the absence of any commercial or financial relationships that could be construed as a potential conflict of interest.

Publisher's Note: All claims expressed in this article are solely those of the authors and do not necessarily represent those of their affiliated organizations, or those of the publisher, the editors and the reviewers. Any product that may be evaluated in this article, or claim that may be made by its manufacturer, is not guaranteed or endorsed by the publisher.

frontiers | Frontiers in Plant Science

METHODS
published: 03 May 2022
doi: 10.3389/fpls.2022.881382

TAIM: Tool for Analyzing Root Images to Calculate the Infection Rate of Arbuscular Mycorrhizal Fungi

Kaoru Muta[1], *Shiho Takata*[2], *Yuzuko Utsumi*[1]*, *Atsushi Matsumura*[2], *Masakazu Iwamura*[1] *and Koichi Kise*[1]

[1] Graduate School of Engineering, Osaka Prefecture University, Osaka, Japan, [2] Graduate School of Life and Environmental Sciences, Osaka Prefecture University, Osaka, Japan

Arbuscular mycorrhizal fungi (AMF) infect plant roots and are hypothesized to improve plant growth. Recently, AMF is now available for axenic culture. Therefore, AMF is expected to be used as a microbial fertilizer. To evaluate the usefulness of AMF as a microbial fertilizer, we need to investigate the relationship between the degree of root colonization of AMF and plant growth. The method popularly used for calculation of the degree of root colonization, termed the magnified intersections method, is performed manually and is too labor-intensive to enable an extensive survey to be undertaken. Therefore, we automated the magnified intersections method by developing an application named "Tool for Analyzing root images to calculate the Infection rate of arbuscular Mycorrhizal fungi: TAIM." TAIM is a web-based application that calculates the degree of AMF colonization from images using automated computer vision and pattern recognition techniques. Experimental results showed that TAIM correctly detected sampling areas for calculation of the degree of infection and classified the sampling areas with 87.4% accuracy. TAIM is publicly accessible at http://taim.imlab.jp/.

Keywords: arbuscular mycorrhizal fungi, magnified intersections method, computer vision, pattern recognition, deep convolutional neural networks, system development

OPEN ACCESS

Edited by:
Sabine Dagmar Zimmermann, Délégation Languedoc Roussillon (CNRS), France

Reviewed by:
Natacha Bodenhausen, Research Institute of Organic Agriculture (FiBL), Switzerland
Eva Nouri, Université de Fribourg, Switzerland
Andrea Genre, University of Turin, Italy
Daniel Leitner, University of Vienna, Austria

***Correspondence:**
Yuzuko Utsumi
yuzuko@omu.ac.jp

Specialty section:
This article was submitted to Frontiers in Plant Science, a section of the journal Frontiers in Plant Science

Received: *22 February 2022*
Accepted: *31 March 2022*
Published: *03 May 2022*

Citation:
Muta K, Takata S, Utsumi Y, Matsumura A, Iwamura M and Kise K (2022) TAIM: Tool for Analyzing Root Images to Calculate the Infection Rate of Arbuscular Mycorrhizal Fungi. Front. Plant Sci. 13:881382. doi: 10.3389/fpls.2022.881382

1. INTRODUCTION

Arbuscular mycorrhizal fungi (AMF) infect plant roots and are considered to improve plant growth (Treseder, 2013). Recent research (Kameoka et al., 2019) has succeeded in the axenic culture of AMF. Therefore, AMF may be mass-produced in the future and are predicted to be used as a microbial fertilizer. To evaluate the usefulness of AMF as a microbial fertilizer, we need to investigate the relationship between the degree of root colonization of AMF and plant growth.

The most commonly studied effect of AMF infections on plant roots is the absorption of phosphorus. However, some studies have shown that injecting mycorrhizal fungi was one of the causes of promoting phosphorus absorption (Van Der Heijden et al., 1998; Smith and Read, 2010; Richardson et al., 2011; Yang et al., 2012), while others have ruled it out (Smith et al., 2004). Therefore, as the results are still controversial, further research on the relationship between phosphorus and AMF is needed. To promote the research, objective evaluation of experiments conducted by different observers under different conditions is indispensable. Therefore, calculating a reliable AMF colonization degree is essential for the research.

In general, the degree of AMF colonization is calculated using the magnified intersections (MI) method (McGonigle et al., 1990). All steps of the MI method are performed manually and thus the method is extremely labor-intensive. Moreover, given that the colonization degree is assessed manually, the decision criterion and results will vary among observers. For these reasons, conducting a comprehensive survey with this method is difficult, and the relationship between AMF colonization and plant growth remains unclear. Clarification of this relationship requires a fixed criterion for estimation of AMF colonization and automation of estimation of colonization degree.

In this article we propose a method for automation of the MI method for estimation of AMF infection degree. Based on the proposed method, we developed an application system named "Tool for Analyzing root images to calculate the Infection rate of arbuscular Mycorrhizal fungi" (TAIM) (Muta et al., 2020). TAIM is a web-based application that automatically calculates the AMF colonization degree from microscopic images with 40x magnification prepared for an AMF infection rate measurement method. Using a machine-learning-based classifier, TAIM calculates the AMF infection rate objectively, unlike manual calculation. Moreover, TAIM has two functions that allow the user to be incorporated to boost its estimation accuracy. One is to upload their own data, which increases training data for TAIM. The other is to correct wrong estimation results, which improves the quality of training data. By retraining TAIM using the updated training data, the estimation accuracy of TAIM can be boosted. Experiments to evaluate the performance of the proposed method demonstrated that the sampling areas for calculation of the infection rate were detected correctly and the degree of infection was determined with 87.7% accuracy.

2. RELATED WORK

As microscopic images are captured under stable lighting, the images are especially suitable for image processing. Therefore, many processing methods have been proposed.

The most popular target for processing of microscopic images is a cell. In many cases, images include too many cells for manual observation. Therefore, image processing methods for cell image analysis have been proposed as an alternative to human observation. To date, procedures for detection (Al-Kofahi et al., 2010; Buggenthin et al., 2013; Schmidt et al., 2018; Weigert et al., 2020), tracking (Debeir et al., 2005; Chen et al., 2006; Dzyubachyk et al., 2010), and cell counting (Lempitsky and Zisserman, 2010) have been proposed. Given the stable lighting used for observation of microscopic images, many methods previously proved to be relatively accurate even before the emergence of deep neural networks (DNNs). Subsequent to the advent of DNNs, the accuracy of detection and tracking has drastically improved (Xie et al., 2018; Korfhage et al., 2020; Kushwaha et al., 2020; Nishimura et al., 2020; Liu et al., 2021). In addition, methods for performing more challenging tasks, such as detection of mitosis (Su et al., 2017), three-dimensional cell segmentation (Weigert et al., 2020), nuclei (Xing et al., 2019), and chromosomes (Sharma et al., 2017) have been published.

Image processing is also used for microscopic medical images. It is practical to use microscopic images to diagnose a disease caused by abnormal cell growth, such as cancer. Many methods have been developed to detect cancer (Yu et al., 2016; Vu et al., 2019) and diagnose cancer from microscopic images (Song et al., 2017; Huttunen et al., 2018; Kurmi et al., 2020). Microscopic images are also helpful to detect infectious diseases. Malaria is an infectious disease for which image processing is the most widely used detection method, and various methods have been proposed for its detection and diagnosis (Ave et al., 2017; Muthu and Angeline Kirubha, 2020). In addition, virus detection methods (Devan et al., 2019; Xiao et al., 2021) have been proposed. For medical applications other than disease diagnosis, methods such as blood cell identification have been developed (Razzak and Naz, 2017).

A typical example of microscopic image analysis in plants is the analysis of pollen. As pollen grains are small, microscopic observation is essential. For example, pollen detection and recognition methods from air samples have been proposed (Rodrìuez-Damián et al., 2006; Landsmeer et al., 2009). Recently, a method applying DNNs has been developed (Gallardo-Caballero et al., 2019). Pollen is also an object of study in paleontology as well as in botany. Pollen analysis, or palynology, involves the study of pollen grains in fossil-bearing matrices or sediments for consideration of the history of plants and climatic changes, for example. As pollen classification requires a broad range of knowledge and is labor-intensive, methods for automated pollen classification (Battiato et al., 2020; Bourel et al., 2020; Romero et al., 2020) have been proposed to replace manual observation.

Recently, Evangelisti et al. (2021) developed AMFinder to analyze plant roots using deep learning-based image processing. This tool can detect AMF and visualize the degree of AMF colonization. These authors' motivation and methodology were similar to our own. The main differences between AMFinder and TAIM are as follows. TAIM is based on the MI method (McGonigle et al., 1990), which uses the intersections of grid lines to quantify AMF colonization of roots, whereas AMFinder divides an image into squares of a user-defined size. TAIM is designed to be a web-based application accessible to all users who can use a web browser, whereas AMFinder is a standalone application consisting of a command-line tool and a graphical interface that requires installation on a computer equipped with graphics processing units (GPUs) and users must set up the environment themselves.

3. MATERIALS AND METHODS

3.1. Materials

The roots used for the dataset were from soybean. The soybean plants were grown in a glasshouse under an average temperature of 30.9°C in the experimental field of Osaka Prefecture University. Each plant was grown in a pot in sterilized soil and was subsequently inoculated with AMF (*Rhizophagus irregularis* MAFF520059). Therefore, AMF were the only fungi present in the soil of the pots. **Table 1** lists the cultivar, place of origin, and number of days growth for the soybeans.

TABLE 1 | Details of the soybean root dataset used in the experiment.

Genotypes	Place of origin	Growing days
M 581	India	48
OUDU	Korea	36
JAVA 7	Indonesia	52
U 1290-1	Nepal	54
KARASUMAME	Taiwan	44
KADI BHATTO	Nepal	59

The plants were removed from the pots and the roots were washed with water. The roots were softened using 10% potassium hydroxide to aid decolorization. We used 0.5% hydrogen peroxide aqueous solution to clear the softened roots and hydrochloric acid to neutralize. The roots were stained using 0.05% trypan blue to stain the AMF blue. The stained root sample is placed on a glass microscope slide with 0.25-mm-wide grid lines at 1.00 mm intervals. We use the glass microscope slide to make observation more efficient.

The prepared slides were observed under a 40x objective with an optical microscope (OLYMPUS BH-2) and images were captured with a digital camera (OLYMPUS PEN E-PLI). The resolution of the images was 4,032 × 3,024 pixels.

3.2. AMF Infection Rate Measurement Method

We automate a method to measure the infection rate of AMF based on the MI method (McGonigle et al., 1990), which is a popular and accurate method for estimation of AMF colonization degree (Sun and Tang, 2012). The MI method is an improved version of the grid-line intersect (GLI) method (Giovannetti and Mosse, 1980). The GLI method uses a dissecting microscope and measures the colonization degree as the ratio of colonized sampling areas. The MI method uses a light microscope, which provides higher resolution and therefore MI can measure the colonization degree more accurately.

The method we automated uses roots prepared as described in Section 3.1. An observer categorizes the roots at the intersections of the grid lines into four categories. In the MI method categorizes the sampling areas into four categories: negative, arbuscules, vesicles, and hyphae only. While the proposed method and MI method essentially perform the same procedure, there is one difference in the categorization of sampling areas between the methods: the MI method excludes the sampling areas that do not include roots in advance, whereas the proposed method does not. Therefore, we added a new class, "no root," for the intersections that do not include roots, to enable the proposed method to classify the root-less sampling areas.

In addition, in our experiments, we integrated the "hyphae only" class into the "arbuscules" class to reflect the experimental environment. In our experiments, we sterilized the soil and then inoculated it with AMF. To avoid mixing the other microorganisms with the unsterilized soils in the pots, the plants were placed in a separate area from the unsterilized potted plants and treated to prevent soil contamination by watering. Hence, all the hyphae in the soil originate from AMF. In summary, we added a new class named "no root" and treated "hyphae only" as "arbuscules." Therefore, in our experiments, we classified the sampling area into four categories: "vesicles," "arbuscules," "no root," and "negative." The original MI method uses a magnification of 200x, but this paper uses a 40x image. The reason for this is that 40x was sufficient for classifying in this study. **Figure 1** shows a sample of each class.

After classifying the intersections, the proportions of arbuscular colonization (AC), vesicular colonization (VC) are calculated as

$$\mathrm{AC} = \frac{N_a}{N_s - N_{\mathrm{nr}}}, \quad \mathrm{VC} = \frac{N_v}{N_s - N_{\mathrm{nr}}}, \tag{1}$$

where N_a, N_v, N_n, and N_{nr} are the numbers of intersections categorized into arbuscules, vesicles, and no root, respectively, and N_s is the total number of intersections.

3.3. Software Design

We propose TAIM, a web-based application system to automate calculation of the degree of AMF colonization. In this section, we explain the system architecture of TAIM in Section 3.3.1, the method by which TAIM automatically calculates the infection rate of AMF in Section 3.3.2. We also explain a dataset we used for constructing TAIM in Section 3.3.3, and functions of TAIM in Section 3.3.4.

3.3.1. Overview of TAIM

Figure 2 presents an overview of TAIM. TAIM consists of client and server systems. The client system runs on a web platform, receives images from users, and shows the calculation results. We use a web platform because it is independent of an OS environment and thus users can use TAIM on any device that can run a web browser. The server receives images from the client, calculates the AMF colonization degree, and transmits the results to the user. The server calculates the AMF colonization degree by detecting the sampling area using computer vision techniques and categorizing the sampling areas as colonized or not using machine-learning techniques. We use HTML5, CSS3, and JavaScript for client development and Django, which is a web application framework implemented by Python, for server development.

3.3.2. Calculation of the AMF Colonization Degree

In this section, we explain the method for calculating the AMF colonization degree in detail. TAIM automates the method described in Section 3.2. Server part of **Figure 2** shows an overview of the procedure for calculating the AMF colonization degree. The inputs are images captured from a microscope slide prepared for the MI method (**Figure 2A**). TAIM detects intersections of the grid lines as sampling areas for calculating the colonization degree. Examples of the intersections are shown as green rectangles in **Figure 2B**. TAIM then categorizes the sampling areas into four categories (**Figure 1**). Finally, TAIM calculates the AMF colonization degrees using Equation (1).

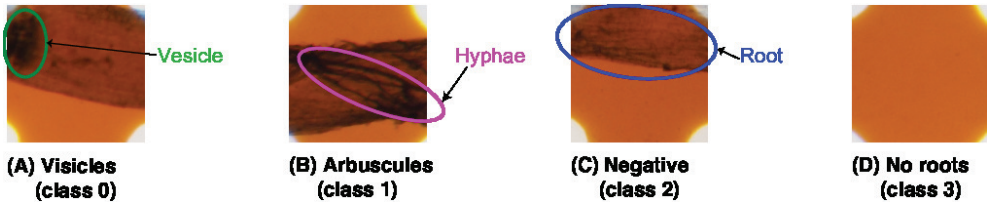

FIGURE 1 | Target classes for the categorization. TAIM categorizes the sampling areas into four classes: **(A)** vesicles (class 0), **(B)** arbuscules (class 1), **(C)** negative (class 2), and **(D)** no root (class 3). Note that the four classes are not identical to those used in the MI method and the magnification of the slide images was 40x.

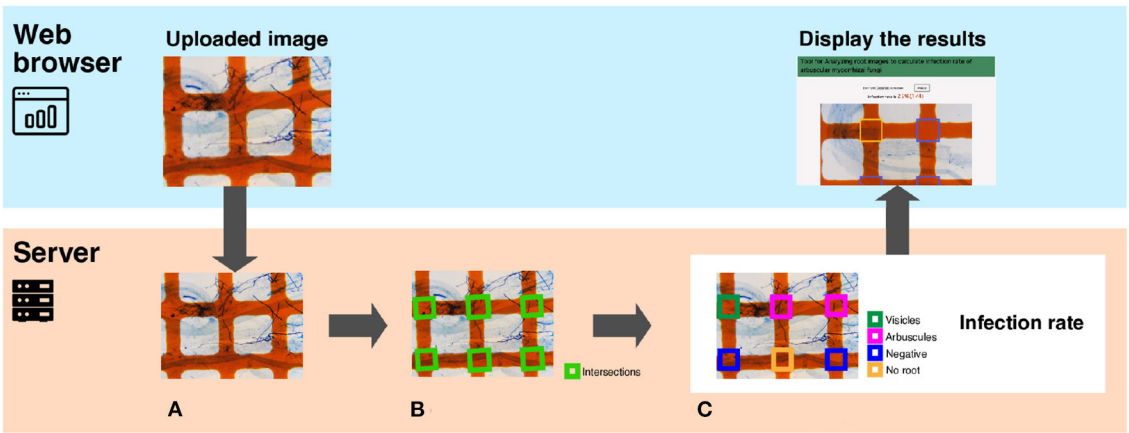

FIGURE 2 | A system overview of TAIM. The system consists of a client and a server. The client, implemented on a web browser, receives the microscope slide images with the grid filter from users and shows the calculation results of the AMF colonization degree. The server receives images, calculates the AMF colonization degree, and returns the calculation results to the web client. The process for calculating the AMF colonization degree by the server are following; **(A)** The input image is a microscope slide image with a grid filter for calculating AMF colonization. **(B)** The intersections denoted by green rectangles are detected. They are used as sampling areas for calculating the AMF colonization degree. **(C)** Categorization results are visualized with different colors. The magnification of the slide images was 40x.

Note that these four categories recognized by TAIM differ from the four categories of the MI method. Details are provided in Section 3.3.2.2.

3.3.2.1. Intersection Detection

For intersection detection, we use a simple computer vision technique, namely edge detection using projection profile. The overall intersection detection process is shown in **Figure 4A**. The orange grid lines in the image are almost orthogonal (**Figure 4A**) If the lines are oriented in the horizontal or vertical direction of the image, the horizontal and vertical lines are expressed as the horizontal and vertical lines and are easily detected. Therefore, before intersection detection, we rotate the image so that the orange lines are oriented in the horizontal and vertical directions of the image. We term this process image rotation normalization.

Figure 3 shows the process of image rotation normalization. To execute image normalization, we estimate the angle of rotation. We use a histogram of the gradient directions of an input image to determine the angles. First, we apply a derivative filter, i.e., Sobel filter, horizontally and vertically to the input image to calculate the image gradients. We then calculate the gradient direction in each pixel and make a histogram of the gradient directions. As the orange lines are orthogonal, the histogram ideally has four peaks in every 90°. Therefore, the image should be rotated around the image center by the minimum angle that ensures the peaks are oriented in the horizontal and vertical directions. The image rotation normalization is applied to all input images.

As shown in **Figure 4**, the intersections of the grid lines are detected on the normalized images in the following manner. We begin by applying the Sobel filter horizontally and vertically to the normalized image to calculate the gradient of each pixel (**Figure 4B**). We then detect the edges of the grid lines by detecting the peaks of the projection profiles of the gradients shown in **Figure 4C**. A projection profile is a sum of pixel values along an axis. Given that the grid lines in the normalized image are oriented in the horizontal and vertical directions, the edges of the lines appear as peaks of the horizontal and vertical projection profiles. As a result of the projection profile, we detect the edges of the grid lines, denoted in green in **Figure 4D**. The width of the grid lines is narrower than the distance between the lines (**Figure 4A**). Therefore, we regard a pair of green lines as a grid line if two green lines are at a close distance. Finally, we detect the intersections; the crossings of the grid lines are detected as intersections (**Figure 4E**).

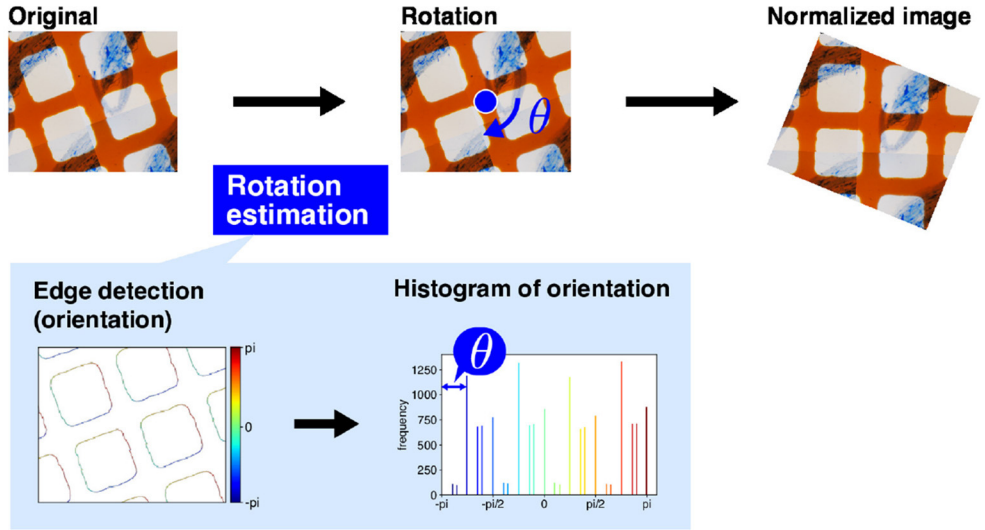

FIGURE 3 | Image rotation normalization. First, the dominant angles in the original image are calculated to estimate the directions of the grid lines. The input image is then rotated. The magnification of the slide images was 40x. The blue arrow mark and blue circle dot are rotation direction of image normalization and image center, respectively.

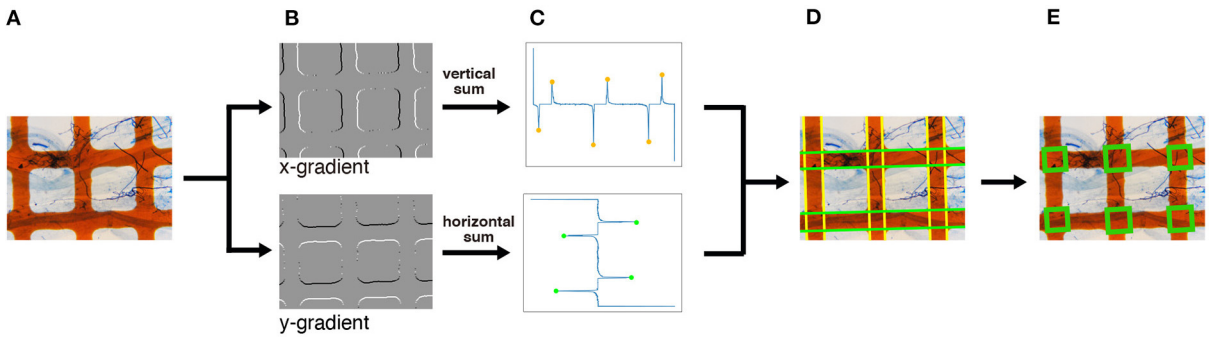

FIGURE 4 | An overview of the intersection detection process. **(A)** Input image. The normalized image generated in **Figure 3** is used as the input. **(B)** Edge detection. The *x*- and *y*-gradients are calculated by applying the Sobel filters horizontally and vertically, respectively. **(C)** Peak detection using projection profiles. The detected edges in **(B)** are projected horizontally and vertically, and the peaks are detected. **(D)** Grid line detection. Based on the peaks obtained in **(C)**, the horizontal and vertical grid lines, denoted in green and yellow, respectively, are detected. **(E)** Intersection detection. The intersections, denoted by green rectangles, are finally detected. The magnification of the slide images was 40x.

3.3.2.2. Categorization of the Sampling Areas

We categorize the sampling areas (i.e., the intersections of grid lines) according to the degree of colonization using a pattern recognition technique. An overview of the categorization process is shown in **Figure 5**. We extract a feature vector from the input image (i.e., sampling area) and categorize it into four classes. In the feature extraction, we use convolutional neural networks (CNNs) because classifiers using CNNs have previously performed well in image classification tasks (Russakovsky et al., 2015; Krizhevsky et al., 2017). As good classification accuracy is expected when the feature is extracted by CNNs, we employ CNNs for feature extraction. We used CNN models pretrained on ImageNet (Deng et al., 2009), which consisted of more than 10 million images of 1,000 categories. After connecting a fully connected (FC) layer to the end of the pretrained CNN model, we fine-tuned the model in the task of categorizing the training images into four classes.

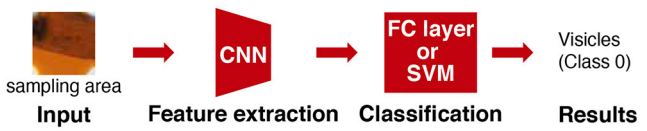

FIGURE 5 | An overview of the classification process of the TAIM method. The magnification of the slide images was 40x.

We used two kinds of classifiers in the categorization process: FC layer and support vector machine (SVM). In the former case, we used the FC layer that was used for pretraining. In the latter case, we used the SVM. To be more precise, we used the SVM for classification and the CNN model (without the FC layer) for feature extraction. In the training, the SVM was trained on the features extracted by the CNN model. Note that the SVM is a supervised learning model that shows good classification accuracy in biological image recognition (Noble, 2006). By using maximum-margin classifiers, the SVM achieves high recognition accuracy. Moreover, the SVM can cope with non-linear classification problems by introducing non-linear kernels.

The colonization degree is calculated as AC and VC in Equation (1) with at least 200 sampling areas.

3.3.3. Dataset

We constructed an original dataset to construct TAIM and conduct experiments. The dataset consisted of 896 microscopic slide images prepared for as described in Section 3.1 (**Figure 2A**). We reduced the images to $1,008 \times 756$ pixels for efficient detection and categorization of intersections. One of the authors manually classified the 5,002 intersection areas into four classes, which were mentioned in Section 3.2. We regarded the classification results as the ground truth (correct answers) of the data and used them to train and evaluate deep neural networks and SVM classifiers. Each intersection area was about 150×150 pixels.

3.3.4. Functions

In addition to calculating AMF colonization degree, TAIM has two other functions: modifying the classification results by users and adding new data to improve the classification accuracy. These two functions are implemented to improve the classification accuracy and the objectivity of AMF colonization.

When viewing the classification results, as shown in **Figure 2C**), the modification function allows users to correct erroneous classification results. In pattern recognition, classifiers sometimes make mistakes depending on the lighting and changes in appearance because of the limitations of the training data. It is also true for the classifiers of TAIM. Therefore, we implemented the modification function to fix incorrect classification results.

TAIM also has a function to register new data, which is expected to improve the classification accuracy. Currently, the classifiers of TAIM are trained on only our dataset, which consists of soybean roots grown in the field and labeled by us. Therefore, the classifiers are expected to perform well on our data and on data with similar properties, but are under-learned for those with different properties. For the classifiers to be robust, a diverse dataset is essential. This is because root data grown in diverse locations are expected to help the classifiers of TAIM to acquire a strongly robust recognition capability. Hence, we implemented the function of TAIM that allows users to register new data that are used for additional training. Adding new data through the functions of TAIM, which stores the data and modifies the categorization results, is also expected to improve the objectivity of the categorization of colonization degree by TAIM. The initial TAIM classifiers for the colonization categorization are trained with the data labeled by one of the authors. That is, the trained classifiers of TAIM reflect the criteria of a single observer. The modified categorization results can reflect the criteria of other observers. Therefore, if the number of users involved in the labeling process increases, the classifiers reflect the criteria of multiple observers, leading to the classifiers becoming more objective.

4. RESULTS

We conducted experiments to evaluate the detection and classification performance of TAIM using the dataset we created. This section presents details on the dataset as well as the detection and classification results.

4.1. Evaluation of Intersection Detection

We evaluated the intersection detection performance using the soybean root dataset. An overview of the proposed intersection detection method is presented in Section 3.3.2.1; here, we describe its implementation in more detail. We used the 3×3 Sobel filter as a derivative filter to calculate the gradient and direction of an image. From the image gradient direction, we estimated the rotation angle for normalization and normalized the image as described in Section 3.3.2.1. The projection profile used for line edge detection was calculated based on the gradient images. In the peak detection, we adopted a public domain code written in Python[1]. We set the distance parameter to 50 and used the default values for the other parameters to execute the code.

For evaluation of detection performance, we adopted the intersection over union (IoU) score. The IoU is a criterion of how accurately a method detects the areas of target objects. The IoU is calculated as the ratio of the overlapping area (intersection) between the ground truth and predicted area over their union (**Figure 6A**). Therefore, the larger the IoU score, the more accurately the sampling areas are detected. We used 896 images of the soybean root dataset for the experiment to calculate the IoU scores. The mean IoU score of TAIM was 0.86. If we considered successful detection in the IoU score as more than 0.75, the detection precision of TAIM was 0.95. Therefore, TAIM achieved a satisfactory detection performance. Based on the distribution of the IoU scores (**Figure 6B**), most sampling areas were detected correctly; the IoU score of most sampling areas was >0.75. However, detection of a few sampling areas failed, as indicated by an IoU score close to zero.

To clarify the reason for the failure in detection, we compared examples of successful and failed detection. **Supplementary Figure 1** shows examples of the detection experiments. The left column is an example of successful detection, and the central and right columns are examples of failed detection. In the detection results (the second row of **Supplementary Figure 1**), blue rectangles represent the ground truth and green rectangles the detection results. The IoU score of each detected area is shown in white text. In the peak detection results (the fifth and sixth rows of **Supplementary Figure 1**), detected peaks are indicated by red and green circles. In the left

[1]https://gist.github.com/endolith/250860

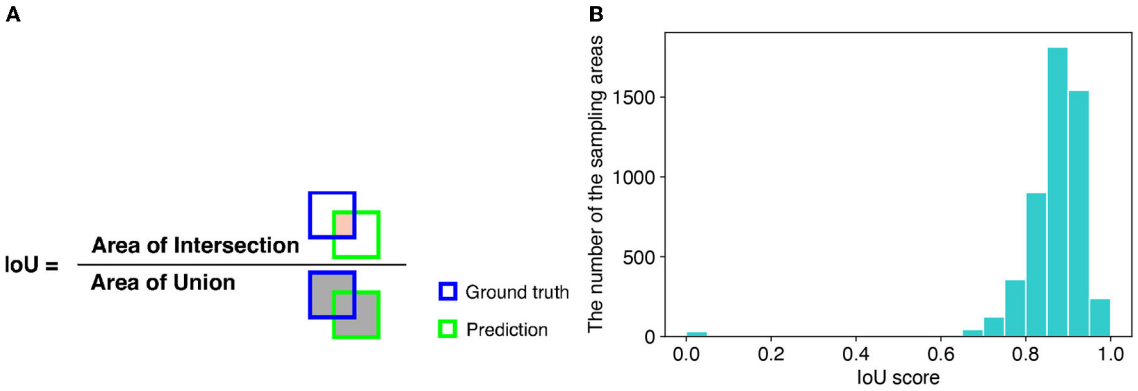

FIGURE 6 | (A) Definition of the IoU. The IoU is calculated as the ratio of the intersection between the ground truth and predicted area, denoted in orange, over their union, denoted in gray. **(B)** Distribution of IoU scores in intersection detection.

column, as the edges of the orange lines were clear, the edges were easily detected by peak detection. In contrast, in the central column, the edges of the orange lines were jagged. As a result, some sampling areas failed to be detected. In the right column, the input image contained bubbles, whereas the edges were clear. The bubble edges were incorrectly detected as a peak because the intensity of the gradient of the bubble edges was large.

4.2. Evaluation of Classification Accuracy

We conducted experiments to evaluate the classification accuracy of the proposed method. We used the cropped sampling areas from the soybean root dataset. We applied intersection detection, as described in Section 3.3.2.1, to the dataset and used the areas for which the IoU score was >0.5. The number of cropped sampling images was 5,002 and annotated manually. The images were cropped to be squares and normalized to 224 × 224 pixels using bilinear interpolation. The CNN models used for feature extraction were AlexNet (Krizhevsky et al., 2012), VGG-19 (Simonyan and Zisserman, 2015), and ResNet-18 (He et al., 2016). These models were pretrained on ImageNet and fine-tuned on the cropped sampling areas. The number of epochs, batch size, and initial learning coefficient were set to 20, 32, and 10e-4, respectively, and the learning rate was reduced by half every five epochs. For optimization, we used Adam with weight decay of 1e-5. For classification, we used the SVM with a radial basis function (RBF) kernel. The cost parameters of the SVM and RBF kernels were set to 1.0 and 0.25, respectively. The output from the network was compared with the annotation, and if they matched, the output was considered correct, and if they did not match, the output was considered incorrect. The percentage of correct outputs was considered to be the classification accuracy. We used five-fold cross-validation to evaluate the classification accuracy. We divided the cropped image samples into five subsamples. We fine-tuned the CNN models and trained classifiers with four subsamples and evaluated the remaining subsamples. We repeated the procedure five times so that all subsamples were evaluated, and the overall accuracy was averaged. Regardless of the combination of feature extractor and classifier, the classification accuracy was >84% (**Table 2**). The hightest classification accuracy (87.7%) was achieved when using VGG-19 as the feature extractor and FC as the classifier.

TABLE 2 | Results of the classification experiment.

Feature extractor (CNN)	Classifier	Accuracy (%)
AlexNet	FC	84.1
VGG-19	FC	87.7
ResNet-18	FC	84.6
AlexNet	SVM	84.0
VGG-19	SVM	86.9
ResNet-18	SVM	84.9

To clarify which class was misrecognized, a confusion matrix when VGG-19 and FC were used for feature extraction and classification was generated. TAIM tended to confuse class 0 (vesicles) with class 1 (arbuscules) and class 2 (negative) with class 1 (**Figure 7**). There are two possible reasons for misclassification. First, the appearance of the respective classes was similar. Classes 0 (vesicles) and 1 (arbuscules) were similar, and classes 2 (negative) and 1 were also similar (**Figure 1**). Therefore, such similarity in appearance may have caused misclassification. The second possible reason is the imbalance of the training data. The number of training data for the four classes was 423, 1,351, 628, and 2,600, respectively. As classes with fewer training data tend to be treated as less important, samples belonging to classes 0 and 2 were more frequently misclassified compared with the other classes.

We generated a class activation map (CAM) (Zhou et al., 2016) of the fine-tuned ResNet-18 to visualize how the CNN classified the sample. The CAM visualizes as a heat map the importance of regions for classification of the sample. In other words, important regions for classification of a class are considered to contain class-specific features for the class. **Figure 8** shows three original images and the corresponding CAM; blue regions are more important and red are less important. **Figure 8A** is an example

of an image that was classified as class 1 correctly. The CAM of this image showed that classification was based on the hyphae in the lower right corner. **Figures 8B,C** are examples of images that were misclassified; B was class 1 but classified as class 0, and C was class 1 but classified as class 2. The CAM of **Figure 8B** revealed that the only hyphae were located in the class-specific region. Therefore, the appearance of the original image in the region was similar to that of class 1. This appearance similarity led to the misclassification as the arbuscules class. In the original image of **Figure 8C**, hyphae were located at the top but only close to the edge of the image. Hence, this is a difficult sample to correctly classify. In the CAM, a class-specific area existed in the top right corner, which may exacerbate the misclassification.

As TAIM has a function that collects data from users, it is possible to increase the training data while TAIM is running. To clarify the effect of increasing the training data, we increased the number of images using augmentation techniques and observed the change in accuracy. We reflected images horizontally and vertically, cropped them randomly, and resized them to 224×224 pixels. The total dataset was increased to 300,012 images. The images were divided into training, validation, and test samples in the ratio of 3:1:1. We used the same feature extractors and classifiers as in **Figure 2**. We trained the networks while changing the training data from 1% of the total training data to 100%. We used the same hyperparameter setting for the networks as the previous classification experiment. We used validation data to evaluate the training accuracy of the networks and choose the parameter of the SVM. The training data were used for evaluation of the classification accuracy. **Figure 9** shows the relation between the number of training data and the classification accuracy. The figure shows that all combinations between the networks and classifiers tended to increase the accuracy. In addition, the accuracy is expected to be further improved using more training data because the accuracy still showed an increasing trend when 100% data were used for training. Therefore, it is expected that the classification accuracy of TAIM will improve with increase in the amount of data used for training.

5. DISCUSSION

In the experiments, we evaluated TAIM on soybean and one AMF. Further evaluation with other plants and AMFs should be conducted to demonstrate the usefulness of the proposed system.

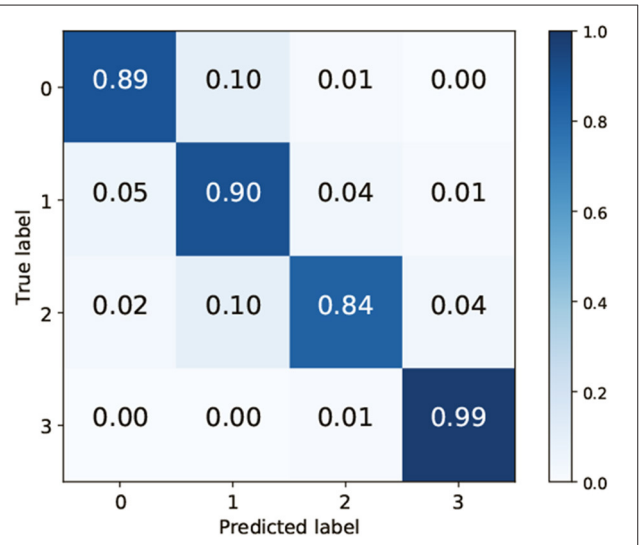

FIGURE 7 | Confusion matrix when using VGG-19 as the convolutional neural network and the fully connected layer as the classifier.

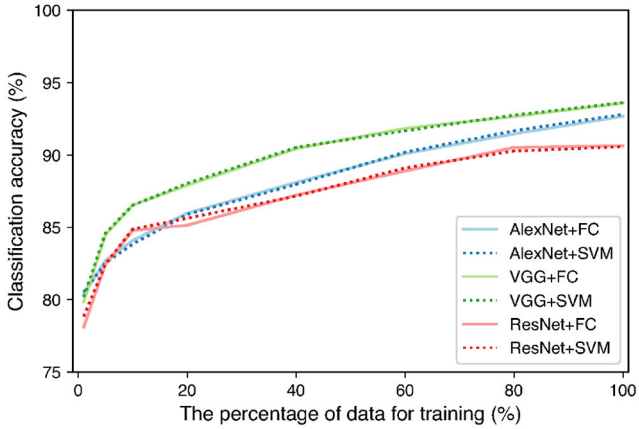

FIGURE 9 | Classification accuracy with increase in percentage of training data.

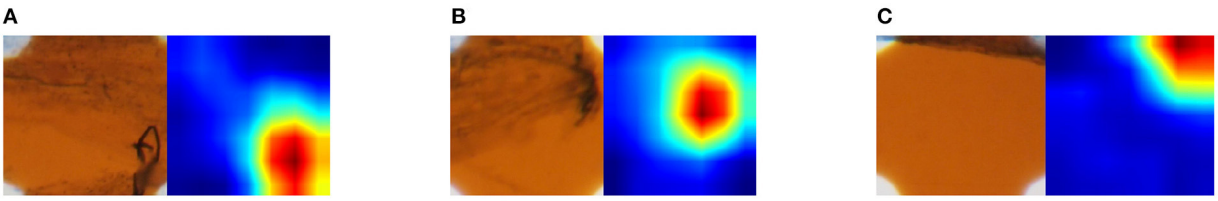

FIGURE 8 | Original sampling area (left) and importance of sampling areas indicated by CAM (right). CAM visualizes the importance for classifying images. The more red the pixel values are, the more important for classification, and the more blue, the less important. The magnification of the slide images was 40x. **(A)** Classified an image of class 1 correctly. **(B)** Misclassified an image of class 1 as class 0. **(C)** Misclassified an image of class 1 as class 2.

AMFinder (Evangelisti et al., 2021), introduced in Section 2, is a method that shares a similar motivation with TAIM. The most significant difference of AMFinder from TAIM is the presence or absence of grids in the input microscope images. TAIM used microscope slide images with the grids, whereas AMFinder used those without the grids. Regarding the difference, we mention two points from the technical perspective. The first is that the classification algorithm for TAM and AMFinder is not inseparable but can be plug in. It means that when a better algorithm is developed in the future, we can improve the classification performance by plugging in to the methods. The second is that it is even easier to use slide images without grids than with grids. The images with grids can be treated as follows. Training data can be created by randomly cropping original slide images from images without grids and annotating them. Using the training data, the network can be trained to classify the cropped images without grids into the categories of AMF infection. Moreover, it is possible to identify which part of the image is infected even without grids using a sliding window approach, which crops images by sliding a rectangle of a fixed size on an image and classifying each cropped image. In our future work, we would like to extend TAIM so that infection rates can be calculated regardless of the presence or absence of grids in slide images.

Although TAIM can potentially distinguish hyphae and arbuscles following the MI method, due to the annotation effort and data limitations, we were unable to perform an experiment that distinguishes hyphae and arbuscles. In the future, when we obtain the appropriate data, we would be able to perform such an experiment. Similarly, the difference in the number of classes classified in TAIM and AMFinder comes from the difference in the data used in the experiments. TAIM classified infected roots into two classes (Arbuscules and Vesicles) in our experiments, whereas AMFinder did into four classes (Arbuscules, Vesicles, Hyphopodia, and Intraradical hyphae). This difference does not mean superiority or inferiority of the classifiers themselves but the difference in the data used in the experiments. Therefore, if we can collect the appropriate training data, of which class labels are the same as those of AMFinder, TAIM would be able to identify infected roots in the same detail.

Since annotation is done manually, errors are inevitable, and the error affects the classification accuracy. For example, apart from plat science, there is a well-used handwritten digit image dataset in the computer vision field, called MNIST dataset[2]. The test data of the MNIST dataset, which consists of 10,000 handwritten digit images, has 0.15% of labels that are expected to be wrong (Northcutt et al., 2021). Our dataset consists of a smaller number of images and fewer classes than MNIST. However, the annotation task of our dataset is harder than that of the MNIST dataset. Hence, it is difficult to expect the number of annotation errors in our dataset. However, even if there are errors, it would not seriously affect the classification accuracy insofar as the errors occur randomly. Actually, there are two types of errors that should be considered. One is annotation errors that occur randomly due to human error, which is argued above. The other is a bias that occurs depending on annotators, which is caused by having different criteria. The effect of the latter is more critical when fewer annotators are involved. Since TAIM is currently trained on data annotated by one of the authors, it is expected that the dataset is biased. However, when the number of annotators increases, it is expected that the bias will decrease. TAIM proves the function that decreases bias because TAIM can be used by multiple users and the users can upload their own data, as described in Section 3.3.4. Therefore, when the number of users increases, TAIM is expected to provide better classification results than those manually annotated by a single person.

[2]http://yann.lecun.com/exdb/mnist/

6. CONCLUSION

This article describes a web-based application called TAIM, which calculates the colonization degree of AMF automatically from microscopic images. As AMF is now available for axenic culture, AMF is expected to be used a microbial fertilizer. To evaluate of the effectiveness of the AMF as a microbial fertilizer, colonization degree of AMF is required. One impediment to such research is that estimation of the colonization degree of AMF is still presently conducted manually. Therefore, we developed TAIM to automate calculation of the extent of AMF colonization. Because TAIM is a web-based application, it can be used *via* a web browser and does not require users to set up a calculation environment. TAIM also has a function to collect new training data from users and retrains the classifier of colonization. This function will contribute to reduction in variation of the decision criteria by observers by combining data annotated by multiple observers. We evaluated the detection and classification accuracy of TAIM with an experimental soybean root dataset comprising cropped 5,002 intersection areas. The experimental results showed that TAIM detected the intersection regions with a mean IoU score of 0.86. If an area with an IoU score of 0.75 is considered to represent successful detection, TAIM can detect the intersection regions with 95% accuracy. TAIM classified the detected regions into four classes with 87.7% accuracy. The classification accuracy improved with increase in number of training data. Therefore, the estimation accuracy of AMF colonization degree is predicted to improve by using the data collection function. TAIM is expected to contribute to an improved understanding of the effect of AMF as a microbial fertilizer.

DATA AVAILABILITY STATEMENT

The raw data supporting the conclusions of this article will be made available by the authors, without undue reservation.

AUTHOR CONTRIBUTIONS

YU conceptualized the research, managed the project, and sourced funding. KM, YU, and MI developed the methodology. KM and YU developed the software and wrote the original

draft of the manuscript. KM performed the validation, formal analysis, and investigation. AM and KK prepared the materials for the research. ST and KM were involved in data curation. MI and AM reviewed the manuscript. All authors have read and agreed to the final version of the manuscript.

FUNDING

This research was funded by the Osaka Prefecture University Female Researcher Support Project.

ACKNOWLEDGMENTS

We thank Robert McKenzie, Ph.D., from Liwen Bianji (Edanz) (www.liwenbianji.cn/) for editing the English text of a draft of this manuscript.

SUPPLEMENTARY MATERIAL

The Supplementary Material for this article can be found online at: https://www.frontiersin.org/articles/10.3389/fpls.2022.881382/full#supplementary-material

REFERENCES

Al-Kofahi, Y., Lassoued, W., Lee, W., and Roysam, B. (2010). Improved automatic detection and segmentation of cell nuclei in histopathology images. *IEEE Trans. Biomed. Eng.* 57, 841–852. doi: 10.1109/TBME.2009.2035102

Ave, M., Carpenter, A., and St, M. (2017). "Applying faster R-CNN for object detection on malaria images," in *Proceedings of the IEEE Conference on Computer Vision and Pattern Recognition (CVPR) Workshops* (Honolulu, HI), 56–61.

Battiato, S., Ortis, A., Trenta, F., Ascari, L., Politi, M., and Siniscalco, C. (2020). "Detection and classification of pollen grain microscope images," in *Proceedings of IEEE Computer Society Conference on Computer Vision and Pattern Recognition Workshops* (Virtual), 4220–4227. doi: 10.1109/CVPRW50498.2020.00498

Bourel, B., Marchant, R., de Garidel-Thoron, T., Tetard, M., Barboni, D., Gally, Y., et al. (2020). Automated recognition by multiple convolutional neural networks of modern, fossil, intact and damaged pollen grains. *Comput. Geosci.* 140:104498. doi: 10.1016/j.cageo.2020.104498

Buggenthin, F., Marr, C., Schwarzfischer, M., Hoppe, P. S., Hilsenbeck, O., Schroeder, T., et al. (2013). An automatic method for robust and fast cell detection in bright field images from high-throughput microscopy. *BMC Bioinformatics* 14:297. doi: 10.1186/1471-2105-14-297

Chen, X., Zhou, X., and Wong, S. T. (2006). Automated segmentation, classification, and tracking of cancer cell nuclei in time-lapse microscopy. *IEEE Trans. Biomed. Eng.* 53, 762–766. doi: 10.1109/TBME.2006.870201

Debeir, O., Van Ham, P., Kiss, R., and Decaestecker, C. (2005). Tracking of migrating cells under phase-contrast video microscopy with combined mean-shift processes. *IEEE Trans. Med. Imaging* 24, 697–711. doi: 10.1109/TMI.2005.846851

Deng, J., Dong, W., Socher, R., Li, L.-J., Kai Li, and Li Fei-Fei (2009). "ImageNet: a large-scale hierarchical image database," in *Proceedings of 2009 IEEE Conference on Computer Vision and Pattern Recognition* (Miami), 248–255. doi: 10.1109/CVPR.2009.5206848

Devan, K. S., Walther, P., von Einem, J., Ropinski, T., Kestler, H. A., and Read, C. (2019). Detection of herpesvirus capsids in transmission electron microscopy images using transfer learning. *Histochem. Cell Biol.* 151, 101–114. doi: 10.1007/s00418-018-1759-5

Dzyubachyk, O., Van Cappellen, W. A., Essers, J., Niessen, W. J., and Meijering, E. (2010). Advanced level-set-based cell tracking in time-lapse fluorescence microscopy. *IEEE Trans. Med. Imaging* 29, 852–867. doi: 10.1109/TMI.2009.2038693

Evangelisti, E., Turner, C., McDowell, A., Shenhav, L., Yunusov, T., Gavrin, A., et al. (2021). Deep learning-based quantification of arbuscular mycorrhizal fungi in plant roots. *New Phytol.* 232, 2207–2219. doi: 10.1111/nph.17697

Gallardo-Caballero, R., García-Orellana, C. J., García-Manso, A., González-Velasco, H. M., Tormo-Molina, R., and Macías-Macías, M. (2019). Precise pollen grain detection in bright field microscopy using deep learning techniques. *Sensors* 19, 1–19. doi: 10.3390/s19163583

Giovannetti, M., and Mosse, B. (1980). An evaluation of techniques for measuring vesicular arbuscular mycorrhizal infection in roots. *New Phytol.* 84, 489–500. doi: 10.1111/j.1469-8137.1980.tb04556.x

He, K., Zhang, X., Ren, S., and Sun, J. (2016). "Deep residual learning for image recognition," in *Proceedings of the IEEE Conference on Computer Vision and Pattern Recognition* (Las Vegas, NV), 770–778. doi: 10.1109/CVPR.2016.90

Huttunen, M. J., Hassan, A., McCloskey, C. W., Fasih, S., Upham, J., Vanderhyden, B. C., et al. (2018). Automated classification of multiphoton microscopy images of ovarian tissue using deep learning. *J. Biomed. Opt.* 23:1. doi: 10.1117/1.JBO.23.6.066002

Kameoka, H., Tsutsui, I., Saito, K., Kikuchi, Y., Handa, Y., Ezawa, T., et al. (2019). Stimulation of asymbiotic sporulation in arbuscular mycorrhizal fungi by fatty acids. *Nat. Microbiol.* 4, 1654–1660. doi: 10.1038/s41564-019-0485-7

Korfhage, N., Mühling, M., Ringshandl, S., Becker, A., Schmeck, B., and Freisleben, B. (2020). Detection and segmentation of morphologically complex eukaryotic cells in fluorescence microscopy images *via* feature pyramid fusion. *PLoS Comput. Biol.* 16:e1008179. doi: 10.1371/journal.pcbi.1008179

Krizhevsky, A., Sutskever, I., and Hinton, G. E. (2012). "Imagenet classification with deep convolutional neural networks," in *Proceedings of Advances in Neural Information Processing Systems* (Barcelona), 1097–1105.

Krizhevsky, A., Sutskever, I., and Hinton, G. E. (2017). Imagenet classification with deep convolutional neural networks. *Commun. ACM* 60, 84–90. doi: 10.1145/3065386

Kurmi, Y., Chaurasia, V., Ganesh, N., and Kesharwani, A. (2020). Microscopic images classification for cancer diagnosis. *Signal Image Video Process.* 14, 665–673. doi: 10.1007/s11760-019-01584-4

Kushwaha, A., Gupta, S., Bhanushali, A., and Dastidar, T. R. (2020). "Rapid training data creation by synthesizing medical images for classification and localization," in *Proceedings of IEEE Computer Society Conference on Computer Vision and Pattern Recognition Workshops* (Virtual), 4272–4279. doi: 10.1109/CVPRW50498.2020.00504

Landsmeer, S. H., Hendriks, E. A., De Weger, L., Reiber, J. H., and Stoel, B. C. (2009). Detection of pollen grains in multifocal optical microscopy images of air samples. *Microsc. Res. Techn.* 72, 424–430. doi: 10.1002/jemt.20688

Lempitsky, V., and Zisserman, A. (2010). "Learning to count objects in images," in *Proceedings of Advances in Neural Information Processing Systems* (Vancouver, BC), 1324–1332.

Liu, D., Zhang, D., Song, Y., Zhang, F., O'Donnell, L., Huang, H., et al. (2021). PDAM: a panoptic-level feature alignment framework for unsupervised domain adaptive instance segmentation in microscopy images. *IEEE Trans. Med. Imaging* 40, 154–165. doi: 10.1109/TMI.2020.3023466

McGonigle, T., Miller, M., Evans, D., Fairchild, G., and Swan, J. (1990). A new method which gives an objective measure of colonization of roots by vesicular arbuscular mycorrhizal fungi. *New Phytol.* 115, 495–501. doi: 10.1111/j.1469-8137.1990.tb00476.x

Muta, K., Takata, S., Utsumi, Y., Matsumura, A., Iwamura, M., and Kise, K. (2020). "Automatic calculation of infection rate of arbuscular mycorrhizal fungi using deep CNN," in *Proceedings of ECCV 2020 Workshop on Computer Vision Problems in Plant Phenotyping (CVPPP 2020)* (Virtual), 1.

Muthu, P., and Angeline Kirubha, S. P. (2020). Computational intelligence on image classification methods for microscopic image data. *J. Ambient Intell. Human. Comput*. doi: 10.1007/s12652-020-02406-z

Nishimura, K., Hayashida, J., Wang, C., Ker, D. F. E., and Bise, R. (2020). "Weakly-supervised cell tracking via backward-and-forward propagation," in *Proceedings of European Conference on Computer Vision* (Virtual), 104–121. doi: 10.1007/978-3-030-58610-2_7

Noble, W. S. (2006). What is a support vector machine? *Nat. Biotechnol*. 24, 1565–1567. doi: 10.1038/nbt1206-1565

Northcutt, C. G., Athalye, A., and Mueller, J. (2021). "Pervasive label errors in test sets destabilize machine learning benchmarks," in *Proceedings of the Neural Information Processing Systems* (New Orleans; Virtual).

Razzak, M. I., and Naz, S. (2017). "Microscopic blood smear segmentation and classification using deep contour aware cnn and extreme machine learning," in *Proceedings of 2017 IEEE Conference on Computer Vision and Pattern Recognition Workshops (CVPRW)* (Honolulu, HI), 801–807. doi: 10.1109/CVPRW.2017.111

Richardson, A. E., Lynch, J. P., Ryan, P. R., Delhaize, E., Smith, F. A., Smith, S. E., et al. (2011). Plant and microbial strategies to improve the phosphorus efficiency of agriculture. *Plant Soil* 349, 121–156. doi: 10.1007/s11104-011-0950-4

Rodríuez-Damián, M., Cernadas, E., Formella, A., Fernández-Delgado, M., and De Sá-Otero, P. (2006). Automatic detection and classification of grains of pollen based on shape and texture. *IEEE Trans. Syst. Man Cybern. Part C* 36, 531–542. doi: 10.1109/TSMCC.2005.855426

Romero, I. C., Kong, S., Fowlkes, C. C., Jaramillo, C., Urban, M. A., Oboh-Ikuenobe, F., et al. (2020). Improving the taxonomy of fossil pollen using convolutional neural networks and superresolution microscopy. *Proc. Natl. Acad. Sci. U.S.A*. 117, 28496–28505. doi: 10.1073/pnas.2007324117

Russakovsky, O., Deng, J., Su, H., Krause, J., Satheesh, S., Ma, S., et al. (2015). Imagenet large scale visual recognition challenge. *Int. J. Comput. Vis*. 115, 211–252. doi: 10.1007/s11263-015-0816-y

Schmidt, U., Weigert, M., Broaddus, C., and Myers, G. (2018). "Cell detection with star-convex polygons," in *Proceedings of 21st International Conference on Medical Image Computing and Computer Assisted Intervention 2018* (Granada), 265–273. doi: 10.1007/978-3-030-00934-2_30

Sharma, M., Saha, O., Sriraman, A., Hebbalaguppe, R., Vig, L., and Karande, S. (2017). "Crowdsourcing for Chromosome Segmentation and Deep Classification," in *Proceedings of 2017 IEEE Conference on Computer Vision and Pattern Recognition Workshops (CVPRW)*, *Vol. 2017* (Honolulu, HI), 786–793. doi: 10.1109/CVPRW.2017.109

Simonyan, K., and Zisserman, A. (2015). "Very deep convolutional networks for large-scale image recognition," in *Proceedings of International Conference on Learning Representations* (San Diego, CA), 1–14.

Smith, S. E., and Read, D. J. (2010). *Mycorrhizal SYMBIOSIS*. Academic press. Available online at: https://www.sciencedirect.com/book/9780123705266/mycorrhizal-symbiosis#book-info

Smith, S. E., Smith, F. A., and Jakobsen, I. (2004). Functional diversity in arbuscular mycorrhizal (AM) symbioses: the contribution of the mycorrhizal P uptake pathway is not correlated with mycorrhizal responses in growth or total P uptake. *New Phytol*. 162, 511–524. doi: 10.1111/j.1469-8137.2004.01039.x

Song, Y., Li, Q., Huang, H., Feng, D., Chen, M., and Cai, W. (2017). Low dimensional representation of fisher vectors for microscopy image classification. *IEEE Trans. Med. Imaging* 36, 1636–1649. doi: 10.1109/TMI.2017.2687466

Su, Y. T., Lu, Y., Chen, M., and Liu, A. A. (2017). Spatiotemporal joint mitosis detection using CNN-LSTM network in time-lapse phase contrast microscopy images. *IEEE Access* 5, 18033–18041. doi: 10.1109/ACCESS.2017.2745544

Sun, X. G., and Tang, M. (2012). Comparison of four routinely used methods for assessing root colonization by arbuscular mycorrhizal fungi. *Botany* 90, 1073–1083. doi: 10.1139/b2012-084

Treseder, K. K. (2013). The extent of mycorrhizal colonization of roots and its influence on plant growth and phosphorus content. *Plant Soil* 371, 1–13. doi: 10.1007/s11104-013-1681-5

Van Der Heijden, M. G., Klironomos, J. N., Ursic, M., Moutoglis, P., Streitwolf-Engel, R., Boller, T., et al. (1998). Mycorrhizal fungal diversity determines plant biodiversity, ecosystem variability and productivity. *Nature* 396, 69–72. doi: 10.1038/23932

Vu, Q. D., Graham, S., Kurc, T., To, M. N. N., Shaban, M., Qaiser, T., et al. (2019). Methods for segmentation and classification of digital microscopy tissue images. *Front. Bioeng. Biotechnol*. 7:53. doi: 10.3389/fbioe.2019.00053

Weigert, M., Schmidt, U., Haase, R., Sugawara, K., and Myers, G. (2020). "Star-convex polyhedra for 3D object detection and segmentation in microscopy," in *Proceedings of 2020 IEEE Winter Conference on Applications of Computer Vision (WACV)* (Snowmass Colorado), 3655–3662. doi: 10.1109/WACV45572.2020.9093435

Xiao, C., Chen, X., Xie, Q., Li, G., Xiao, H., Song, J., et al. (2021). Virus identification in electron microscopy images by residual mixed attention network. *Comput. Methods Prog. Biomed*. 198:105766. doi: 10.1016/j.cmpb.2020.105766

Xie, W., Noble, J. A., and Zisserman, A. (2018). Microscopy cell counting and detection with fully convolutional regression networks. *Comput. Methods Biomech. Biomed. Eng*. 6, 283–292. doi: 10.1080/21681163.2016.1149104

Xing, F., Xie, Y., Shi, X., Chen, P., Zhang, Z., and Yang, L. (2019). Towards pixel-to-pixel deep nucleus detection in microscopy images. *BMC Bioinformatics* 20:472. doi: 10.1186/s12859-019-3037-5

Yang, S. Y., Grønlund, M., Jakobsen, I., Grotemeyer, M. S., Rentsch, D., Miyao, A., et al. (2012). Nonredundant regulation of rice arbuscular mycorrhizal symbiosis by two members of the PHOSPHATE TRANSPORTER1 gene family. *Plant Cell* 24, 4236–4251. doi: 10.1105/tpc.112.104901

Yu, K. H., Zhang, C., Berry, G. J., Altman, R. B., Ré, C., Rubin, D. L., et al. (2016). Predicting non-small cell lung cancer prognosis by fully automated microscopic pathology image features. *Nat. Commun*. 7, 1–10. doi: 10.1038/ncomms12474

Zhou, B., Khosla, A., Lapedriza, A., Oliva, A., and Torralba, A. (2016). "Learning deep features for discriminative localization," in *Proceedings of the IEEE Conference on Computer Vision and Pattern Recognition* (Las Vegas, NV), 2921–2929. doi: 10.1109/CVPR.2016.319

Conflict of Interest: The authors declare that the research was conducted in the absence of any commercial or financial relationships that could be construed as a potential conflict of interest.

Publisher's Note: All claims expressed in this article are solely those of the authors and do not necessarily represent those of their affiliated organizations, or those of the publisher, the editors and the reviewers. Any product that may be evaluated in this article, or claim that may be made by its manufacturer, is not guaranteed or endorsed by the publisher.

frontiers | Frontiers in Plant Science

ORIGINAL RESEARCH
published: 11 May 2022
doi: 10.3389/fpls.2022.874819

Biocontrol Potential of Endophytic *Streptomyces malaysiensis* 8ZJF-21 From Medicinal Plant Against Banana Fusarium Wilt Caused by *Fusarium oxysporum* f. sp. *cubense* Tropical Race 4

*Lu Zhang[1], Ziyu Liu[1], Yong Wang[1], Jiaqi Zhang[1], Shujie Wan[1], Yating Huang[1], Tianyan Yun[2,3], Jianghui Xie[2] and Wei Wang[2]**

[1] Ministry of Education Key Laboratory for Ecology of Tropical Islands, Key Laboratory of Tropical Animal and Plant Ecology of Hainan Province, College of Life Sciences, Hainan Normal University, Haikou, China, [2] Key Laboratory of Biology and Genetic Resources of Tropical Crops, Institute of Tropical Bioscience and Biotechnology, Chinese Academy of Tropical Agricultural Sciences, Ministry of Agriculture, Haikou, China, [3] Haikou Experimental Station, Chinese Academy of Tropical Agricultural Sciences, Haikou, China

OPEN ACCESS

Edited by:
Sergio Saia,
University of Pisa, Italy

Reviewed by:
Sumera Yasmin,
National Institute for Biotechnology and Genetic Engineering, Pakistan
Guilhermina Marques,
University of Trás-os-Montes and Alto Douro, Portugal
Nutan Kaushik,
Amity University, India

***Correspondence:**
Wei Wang
wangweisys@ahau.edu.cn

Specialty section:
This article was submitted to Plant Symbiotic Interactions, a section of the journal Frontiers in Plant Science

Received: *13 February 2022*
Accepted: *11 April 2022*
Published: *11 May 2022*

Citation:
Zhang L, Liu Z, Wang Y, Zhang J, Wan S, Huang Y, Yun T, Xie J and Wang W (2022) Biocontrol Potential of Endophytic Streptomyces malaysiensis 8ZJF-21 From Medicinal Plant Against Banana Fusarium Wilt Caused by Fusarium oxysporum f. sp. cubense Tropical Race 4. Front. Plant Sci. 13:874819. doi: 10.3389/fpls.2022.874819

Banana (*Musa* spp.) is an important fruit crop cultivated in most tropical countries. Banana Fusarium wilt caused by *Fusarium oxysporum* f. sp. *cubense* tropical race 4 (*Foc* TR4) is the most destructive fungal disease. Biocontrol using endophytic microorganisms is considered as a safety and sustainable strategy. Actinomycetes have a potential for the production of diverse metabolites. Isolation of endophytic actinomycetes with high efficiency and broad-spectrum antagonism is key for exploring biocontrol agents. Our previous study showed that a total of 144 endophytic actinomycetes were isolated from different tissues of medicinal plants in Hainan, China. Especially, strain 8ZJF-21 exhibited a broad-spectrum antifungal activity. Its morphological, physiological, and biochemical characteristics were consistent with the genus *Streptomyces.* The phylogenetic tree demonstrated that strain 8ZJF-21 formed a distinct clade with *Streptomyces malaysiensis*. Average nucleotide identity (ANI) was 98.49% above the threshold of novel species. The pot experiment revealed that endophytic *Streptomyces malaysiensis* 8ZJF-21 could improve the plant resistance to *Foc* TR4 by enhancing the expression levels of defense-related and antioxidant enzyme genes. It also promoted the plant growth by producing several extracellular enzymes and metabolites. Antifungal mechanism assays showed that *S. malaysiensis* 8ZJF-21 extract inhibited mycelial growth and spore germination of *Foc* TR4 *in vitro.* Pathogenic cells occurred cytoplasmic heterogeneity, disappeared organelles, and ruptured ultrastructure. Sequencing and annotation of genome suggested that *S. malaysiensis* 8ZJF-21 had a potential of producing novel metabolites. Nineteen volatile organic compounds were obtained from the extract by Gas Chromatography-Mass Spectrometry (GC-MS). Hence, endophytic *Streptomyces* strains will become essential biocontrol agents of modern agricultural practice.

Keywords: endophytic *Streptomyces*, biocontrol, banana Fusarium wilt, genome sequencing, antifungal mechanism

INTRODUCTION

Bananas (including plantains and other cooking bananas) are the world's most important fruit with a global production of 113.9 million tons (Nansamba et al., 2020). They are also a staple food for millions of people throughout the developing world (Kema et al., 2020). In Africa, over 70 million people derive 25% of their dietary energy from bananas and plantains (Nansamba et al., 2020). Vegetative propagation of commercial cultivars results in a narrow genetic background, making plants susceptible to various pathogens, especially banana Fusarium wilt caused by *Fusarium oxysporum* f. sp. *cubense* (*Foc*) (Wang et al., 2012). The pathogen contains at least four races based on the pathogenicity to host cultivars. *Foc* tropical race 4 (*Foc* TR4) is the most destructive fungal disease. It can infect Cavendish banana and all cultivars that are sensitive to the other three races (Ploetz, 2015). Chemical control using fungicides is minimally effective (Jing et al., 2020; Wei et al., 2020). The intensive use results in the pathogenic resistance to fungicides and an increase in environmental contamination (Dita et al., 2018). No commercial varieties display an effective resistance against *Foc* TR4 until now (Dale et al., 2017; Wang et al., 2021). The presence of any resistant cultivars would not exclude the use of other disease control approaches that could contribute to maintaining the resistance to pathogens over time. Biological control is an eco-friendly strategy to manage soil-borne phytopathogens. Disease-suppressive soil provides the best example of microbe-associated defense against the invasion of *Foc* TR4 (Zhou et al., 2019). Therefore, the establishment of an effective way to stimulate the accumulation of beneficial microorganisms and decrease the abundances of pathogenic *Fusarium* is critical for the successful management of banana Fusarium wilt.

Beneficial microorganisms are an important source of agricultural biocontrol agents. Recently, endophytes have received considerable attention for their potential to control fungal phytopathogens (De Silva et al., 2019). They colonize mainly the root system and the xylem tissues of host plants, developing a mutualistic relationship to induce plant defense response toward various pathogens and promote plant growth. Among these endophytic microorganisms, the phylum Actinobacteria are reported as an important portion (Palaniyandi et al., 2013; Dinesh et al., 2017). Most endophytic actinomycetes isolated to date mainly belong to the genus *Streptomyces* (Golinska et al., 2015; Vurukonda et al., 2018). Previous studies reported the role of *Streptomyces* in the biocontrol of soil-borne phytopathogens such as *Foc* TR4 (Yun et al., 2021), *Glomerella cingulata* (Marian et al., 2020), *Sclerotium rolfsii* (Singh and Gaur, 2016), *Botrytis cinerea* (El-Shatoury et al., 2020), and *Alternaria brassicicola* (Hassan et al., 2017). The success of *Streptomyces* as a potential biocontrol agent encourages research into new microbial agents as alternatives to chemical fungicides (Dhanasekaran et al., 2005; Jing et al., 2020; Zhang et al., 2021).

Indeed, the antagonistic activity of *Streptomyces* spp. against phytopathogens is related to the production of antimicrobial compounds including antibiotics, enzymes, and alkaloids (Lacey and Rutledge, 2022). Among approximately 23,000 of the identified bioactive metabolites produced by microorganisms, about 7,600 compounds were found from the genus *Streptomyces* (Olanrewaju and Babalola, 2019). About 80% of the bioactive compounds for agricultural and medical use originate from the genus *Streptomyces* (Ferraiuolo et al., 2021). To discover novel biocontrol candidates, some researchers attempted to isolate endophytic actinomycetes from various medicinal plants (Passari et al., 2015; Ayswaria et al., 2020; Li et al., 2020; Musa et al., 2020; Yun et al., 2021). For example, 12 out of 68 endophytic actinomycetes isolated from six medicinal plants reduced the infection of collar rot caused by *Sclerotium rolfsii* in chickpea (Singh and Gaur, 2016). Five endophytic *Streptomyces* in the traditional medicinal plant *Arnica montana* produced a huge variety of bioactive secondary metabolites (Wardecki et al., 2015). Twenty-two endophytic actinomycetes recovered from medicinal plants exhibited inhibitory activity against at least one pathogen (Passari et al., 2015). Recent study showed that precious bioactive compounds produced by medicinal plants contribute to the natural regeneration of endophytes to cope with stressful conditions (Wu et al., 2021). The genomic evolution is beneficial for endophytes to produce novel bioactive compounds. Thus, endophytic *Streptomyces* from medicinal plants may have great potential as biocontrol agents.

In our previous study, 144 endophytic actinomycetes were isolated from different tissues of 23 medicinal plants. The antagonistic experiment showed that strain 8ZJF-21 had strong antifungal activity against *Foc* TR4. Here, our study's aim was to investigate the properties of the endophytic strain 8ZJF-2 from the roots of *Curculigo capitulata*. We first identified the species and genus of strain 8ZJF-2 and determined its broad-spectrum antifungal activity *in vitro*. Biocontrol efficiency and antifungal mechanism against *Foc* TR4 were further evaluated. To assay the potential ability to produce the antifungal metabolites, genomic sequencing and Gas Chromatography-Mass Spectrometry (GC-MS) were performed. Our results will provide a promising endophyte for controlling banana Fusarium wilt.

MATERIALS AND METHODS

Antifungal Bioassay of Endophytic Actinomycete Strain 8ZJF-2 Against *Foc* TR4

A total of 144 endophytic actinomycetes were isolated previously from different tissues of 23 medicinal plants in "Wuzhishan" Nature Reserve, Hainan, China the related data will be published in Phytopathology, but the publication period is a little long. Antagonistic activity was evaluated against *Foc* TR4 (ATCC 76255) *in vitro* as previously described (Jing et al., 2020). *Foc* TR4 was cultured on the potato dextrose agar (PDA) medium at 28°C for 7 days. An agar disc (5 mm in diameter) with *Foc* TR4 was placed on the center of Petri dishes 6 cm away from an endophytic actinomycete. Plates without endophytic actinomycetes were served as a control. After inoculation at 28°C for 10 days, the inhibition percentage was calculated as described by Wei et al. (2020). All experiments were performed

in triplicate. The endophytic strain 8ZJF-2 isolated from the roots of *C. capitulata* exhibited strong antifungal activity.

Assaying a Broad-Spectrum Antifungal Activity of Strain 8ZJF-2

To further analyze whether strain 8ZJF-2 owned a broad-spectrum antifungal activity, the antagonistic activities were investigated against ten phytopathogenic fungi, including *Curvularia lunata* (ATCC 42011) from banana, *Colletotrichum fragariae* (ATCC 58718) from strawberry, *Fusarium oxysporum* f. sp. *cucumerinum* (ATCC 36332) from cucumber, *Fusarium graminearum* Sehw (ATCC 11696) from wheat, *Fusarium oxysporum* f. sp. *cubense* race 1 (ACCC 31271) from banana, *Colletotrichum gloeosporioides* (Penz) Penz and Sacc 1884 (ACCC 36351) from mango, *Pyricularia oryzae* (ATCC 52083) from rice, *Alternaria tenuissima* (ATCC 58124) from cotton, *Colletotrichum acutatum* (ATCC 56815) from loquat, and *Colletotrichum gloeosporioides* (ATCC 16330) from mango. Antifungal activity of strain 8ZJF-2 was detected as the above-mentioned method. The inhibition zones were measured in millimeters (Zhang et al., 2021).

Morphological, Physiological, and Biochemical Characteristics of Strain 8ZJF-2

The strain 8ZJF-21 was inoculated in various types of growth media including PDA and different International *Streptomyces* Project media (ISP2, ISP3, ISP4, ISP5, ISP6, and ISP7) for 7 days at 28°C under dark conditions (Yun et al., 2021; Zhang et al., 2021). Cultural characteristics such as colonial morphology and diffusible pigment production were detected in the different media according to Shirling and Gottlieb (1966). Based on Bergey's manual of systematic bacteriology, strain 8ZJF-21 was classified by observing the color of aerial and substrate mycelia (Brinley-Morgan and McCullough, 1974). Phenotypic profile of strain 8ZJF-2 spore chain was observed by scanning electron microscopy (SEM, model S-4800, Hitachi Limited, Japan). Utilization of nitrogen and carbon sources was studied according to Qi et al. (2019). The capability of strain 8ZJF-21 to produce important enzymes (proteases, lipases, celluloses, nitrate reductases, pectinases, gelatinases, and ureases), indoleacetic acid (IAA), siderophores, and H_2S were determined (Jing et al., 2020; Wei et al., 2020; Zhang et al., 2021). Physiological tests were performed by inoculating strain 8ZJF-21 on the selected medium (ISP2) at different temperatures (20°C–50°C), pH (3.0–11.0), and NaCl (0–20% w/v).

Genomic Sequencing and Functional Annotation of Strain 8ZJF-21

Strain 8ZJF-21 was cultured in the ISP2 liquid medium at 200 rpm and 28°C for 4 days. Total genomic DNA was extracted using a Rapid Bacterial Genomic DNA Isolation Kit (Biotake corporation, Beijing, China). The sequencing libraries were generated using the Illumina TruSeq^{TM} RNA Sample Preparation Kit (Illumina, San Diego, CA, United States). The complete genome was sequenced in the Illumina Hiseq × Ten platform (Illumina, San Diego, CA, United States) by the Shanghai Majorbio Bio-pharm Technology Co. Ltd. Sequencing data were analyzed using an online platform of the Majorbio Cloud[1] and was deposited in GenBank with accession number JAJQWY000000000. The open reading frames (ORFs) were predicted by the Rapid Annotation using Subsystem Technology (Brettin et al., 2015). Functional annotation was performed using the Clusters of Orthologous Group (COG), the Gene Ontology (GO), and the Kyoto Encyclopedia of Genes and Genomes (KEGG) (Ogata et al., 1999; Tatusov et al., 2000). Biosynthetic gene clusters (BGCs) were identified by the online antiSMASH v4.0.2 software (Weber et al., 2015).

Construction of Phylogenetic Trees

The 16S rDNA sequence was extracted from the sequenced genome of strain 8ZJF-21. Sequence alignment was performed against the EzTaxon-e database.[2] The phylogenetic trees were constructed using a neighbor-joining (NJ) method of MEGA 7.0 (Kumar et al., 2016). Evolutionary distance was calculated using the maximum-parsimony algorithm. The confidence level was calculated using the bootstrap analysis on 1,000 replicates. Average nucleotide identity (ANI) was obtained by comparing genomes of the type strain and strain 8ZJF-21 using the online OrthoANI (Yoon et al., 2017). The closest homolog was considered as the type strain according to the phylogenetic tree. Its genome sequence was downloaded from the database of EzBioCloud.[3]

Extraction of Strain 8ZJF-21 Metabolites

Strain 8ZJF-21 was cultured in 100 ml of a soybean liquid medium (SLM, 15 g of corn flour, 10 g of glucose, 0.5 g of K_2HPO_4, 0.5 g of NaCl, 0.5 g of $MgSO_4$, 3 g of beef extract, 10 g of yeast extract, 10 g of soluble starch, 2g of $CaCO_3$, pH 7.2-7.4) with shaking at 180 rpm for 7 days at 28°C. The fermentation broth was filtered through a Whatman No.1 filter. After centrifugation at 10,000 rpm for 15 min, the supernatant was extracted twice in the ratio of 1:1 (culture supernatant: different gradient methanol). To remove the impurities, the suspension went through a silica-gel chromatography column (5.5 cm × 80 cm, inner diameter × length). The elution with gradient methanol solutions was filtered through a 0.22 μm sterile filter (Millipore, Bedford, MA, United States) (Li et al., 2021). The organic solvent was concentrated using a rotary vacuum evaporator (N-1300, EYELA, Ailang Instrument Co., Ltd., Shanghai, China). The obtained extract was redissolved in 10% (v/v) of dimethyl sulfoxide (DMSO) with a final concentration of 20 mg ml^{-1}.

Antifungal Activity of Extract Against *Foc* TR4

Sterilized PDA agar media containing final extract concentrations (1.563, 3.125, 6.25, 12.50, 25, 50, or 100 mg L^{-1}) were prepared by a serial dilution method (Yun et al., 2021). Ten percent (v/v) of DMSO was used as a control. A 5-mm-diameter disc of *Foc*

[1]www.majorbio.com

[2]http://www.ezbiocloud.net/eztaxon/identify

[3]https://www.ezbiocloud.net/search?tn=Nocardioides

TR4 was placed on the center of the plate. The growth diameter of *Foc* TR4 was recorded until the mycelia reaching the plate edge in the control group. The half-maximal effective concentration (EC_{50}) of the extract against *Foc* TR4 was calculated according to Hoekstra and Van Ewijk (1993). All experiments were repeated with three biological replicates.

Biocontrol Evaluation and Plant-Growth Promoting of Strain 8ZJF-21

To investigate the potentiality of strain 8ZJF-21 to control *Foc* TR4 and promote plant-growth traits, a pot experiment was carried out in a completely randomized design. *Foc* TR4-GFP strain overexpressing a green fluorescent protein (GFP) gene was selected to detect the infection in banana roots (Yun et al., 2021). *Foc* TR4-GFP was prepared by incubation in PDB (potato dextrose broth) in a rotary shaker (180 rpm) for 5 days at 28°C. The liquid culture was then filtered through four layers of sterile gauze. The spores were enumerated by hemocytometer under a light microscope (Axio Scope A1, Carl ZEISS, Germany) and were then diluted to 1.0×10^5 cfu/mL with sterile water. Strain 8ZJF-21 was inoculated in one liter of an Erlenmeyer flask containing 300 ml of sterilized SLM at 200 rpm and 28°C for 7 days. The suspension was diluted to the final concentration of 1×10^5 cfu/ml. Spore suspension of *Foc* TR4-GFP (100 ml) and strain 8ZJF-21 (100 ml) was completely mixed with 10 g of autoclaved soil. The banana seedlings (*Musa* AAA group, Cavendish cv. Brazil) with four to five leaves were transferred to the pots (12 cm in diameter). These banana seedlings were kept in a glasshouse under natural light at 28°C ± 2°C. Three experiment groups were set including sterilized SLM + *Foc* TR4-GFP (1×10^6 spores/g soil) (G1), fermentation broth of strain 8ZJF-21 (1×10^6 spores/g soil) + *Foc* TR4-GFP (1×10^6 spores/g soil) (G2), and sterilized SLM (G3). All experiments were performed in triplicates. Each group contained 60 pots with three replicates. After 0.5, 1, 2, 3, 4, and 5 days post inoculation (dpi), the root samples of banana seedlings were collected for determining the expression levels of defense-related and antioxidant enzyme genes. The chlorotic symptom of banana leaves was monitored at 30 dpi. The disease indexes were recorded according to Li et al. (2021). *Foc* TR4-GFP infection in banana roots was detected by a confocal microscope (FV1000-IX81, Olympus, Japan). The physiological parameters of banana seedlings were measured at 30 dpi, including stem diameter, chlorophyll content, leaf area, dry weight, fresh weight, plant height, and leaf thickness (Zhang et al., 2021).

Measurement of H_2O_2 and Malondialdehyde in Roots of Banana Seedlings

As above mentioned, roots treated with strain 8ZJF-21 and/or *Foc* TR4 were collected at 0.5, 1, 2, 3, 4, and 5 dpi. H_2O_2 was measured according to Ferguson et al. (1983). One gram of frozen sample was ground in 5 ml of pre-cooled acetone. After centrifugation at 10,000 rpm for 20 min at 4°C, the supernatant was mixed with 0.5 ml of $TiCl_4$ (20% v/v $TiCl_4$ in concentrated HCl). And then, 3.5 ml of NH_4OH was added dropwise with thorough mixing. Following centrifugation, the precipitates were redissolved in 25 ml of H_2SO_4 (2 mol/L). The absorbance was recorded at 415 nm. A blank without the addition of sample was made through the same procedure. The standards ranging from 0.15 to 0.75 mol L^{-1} H_2O_2 were also reacted with TiC14. Malondialdehyde (MDA) was determined using the reaction method of thiobarbituric acid. Four grams of frozen samples were ground in 15 ml of trichloroacetic acid (5%, w/v). After centrifugation at 6,000 rpm for 10 min, 1.5 ml of the supernatant were mixed with 2.5 ml of thiobarbituric acid (0.5%, w/v) in 15% of trichloroacetic acid. The mixture was incubated at 100°C for 20 min. Absorbance of the supernatant was recorded at 532 nm and corrected using non-specific turbidity by subtracting the absorbance at 600 nm. The content of MDA was calculated according to Pongprasert et al. (2011) and expressed as mol g^{-1} FW.

Expression Analysis of Defense-Related Genes by Quantitative Real-Time Polymerase Chain Reaction

The total RNA of banana roots was extracted using the method of Trizol (Wang et al., 2014). The quality and quantity of RNA were measured by Nanodrop (Thermo Scientific, United States). The first-strand cDNA was synthesized using the Prime Script™ RT Reagent Kit with gDNA Eraser (Takara, Dalian, China). Quantitative real-time polymerase chain reaction (qRT-PCR) was performed in a LightCycler® 480 System (Roche Diagnostics, Mannheim, Germany) with the SYBR Premix Ex Taq II kit (Takara, Dalian, Liaoning, China). Four defense-related marker genes such as β-1,3-glucanase (*Maβ-1,3-Glu*, GenBank ID: AF001523), mitogen-activated protein kinase 1 (*MaMAPK1*, GenBank ID: XM018826311), phenylalanine ammonia lyase (*MaPAL*, GenBank ID: XM009403673), and pathogen-related protein 1 (*MaPR-1*, GenBank ID: XM009388962) were selected. The primer sequences were listed in **Supplementary Table 1**. The reaction system of qRT-PCR was described in our previous study (Zhang et al., 2019). The house-keeping gene of 18S *rRNA* (GenBank ID: U42083) was used as a reference gene to normalize the expression levels of target genes using the $2^{-\Delta\Delta Ct}$ method (Wang et al., 2014). All experiments were repeated in triplicates with at least three biological replicates of each sample.

Effect of Extract on Spore Germination of *Foc* TR4

Foc TR4 was cultured in the potato dextrose broth (PBD) at 200 rpm for 7 days at 28°C. After filtration through six layers of gauze to remove hyphae, spores were collected at 1,000 rpm for 10 min and washed using sterile water four times. The spore suspension (1×10^6 spores/mL) of *Foc* TR4 was prepared using sterile water (Wang et al., 2012). The effect of the extract on spore germination of *Foc* TR4 was evaluated according to Wei et al. (2020). Briefly, different concentration extracts ($1 \times EC_{50}$, $2 \times EC_{50}$, $4 \times EC_{50}$ and $8 \times EC_{50}$) of strain 8ZJF-21 and *Foc* TR4 (1×10^6 spores/mL) were mixed completely and added to the concavity of slide. *Foc* TR4 spores treated with 10% (v/v) of DMSO were used as a control. After 16 h of incubation at

25°C, the spore germinated of *Foc* TR4 conidia were counted using a light microscope (Axio Scope A1, Carl ZEISS, Germany). Conidia were considered as germinated when germ tube began to appear. Five replicates were used in each treatment and at least 200 conidia were measured per replicate.

Effect of Extract on Mycelial Morphology and Ultrastructure of *Foc* TR4

Foc TR4 was grown on the PDA medium with 4 × EC_{50} of extract at 28°C for 5 days. The collected mycelia were fixed with 2.5% (v/v) of glutaraldehyde overnight at 4°C. DMSO (10%, v/v) treatment was used as a control. Agar plugs (5 mm in diameter) with *Foc* TR4 were cut from the edge of a 3-day-old fungal medium. The mycelial sections were prepared according to Jing et al. (2020). Morphological characteristics of *Foc* TR4 mycelia were detected using SEM. The effect of strain 8ZJF-21 extract on the cellular ultrastructure of *Foc* TR4 was observed by a transmission electron microscope (TEM, JEM-1400 Flash, Hitachi Limited, Tokyo, Japan) according to Wei et al. (2020). Four replicates were used per treatment and each experiment was repeated three times.

Component Identification of Strain 8Zjf-21 Extract by Gas Chromatography-Mass Spectrometry

The volatile organic compounds in strain 8ZJF-21 extract were identified using GC-MS as our previous description (Li et al., 2021). Extract of strain 8ZJF-21 was first dissolved in the chromatographic grade methanol and was filtered through a 0.2-μm filter. The solution was injected into a gas capillary column (DB-FFAP, 30 m × 0.25 mm × 0.25 μm) of a gas chromatograph (5973 Inert XL MSD, Agilent, United States). Helium was used as a carrier gas with a flow rate of 1 ml min^{-1}. The column temperatures were set as follows: initial column temperature at 70°C for 3 min, followed by an increment of 5°C/min up to 100°C and 10°C/min up to 250°C. The final temperature was kept at 300°C for 5 min. The mass spectrometer was operated in the electron ionization mode at 70 eV with a continuous scan from 50 to 800 m/z (Jing et al., 2020). The peaks were identified by matching the mass spectra with the National Institute of Standards and Technology (NIST, United States) library.

Statistical Analysis

All the experiments were implemented using a completely randomized design. Data were obtained from at least three biological replicates and were expressed as the mean ± standard deviation (SD). Data processing and statistical analysis were performed with the SPSS statistical software package (SPSS Inc., Cary, NC, United States, v.22). The significance was determined by Duncan's multiple range tests ($P < 0.05$).

RESULTS

Morphological, Biochemical, and Physiological Characteristics of Strain 8ZJF-21

Antifungal activity of the selected endophytic actinomycetes was further tested against *Foc* TR4. Strain 8ZJF-21 isolated from the roots of medicinal plant *C. capitulata* exhibited a strong antagonistic activity (**Figure 1A**). Strain 8ZJF-21 can

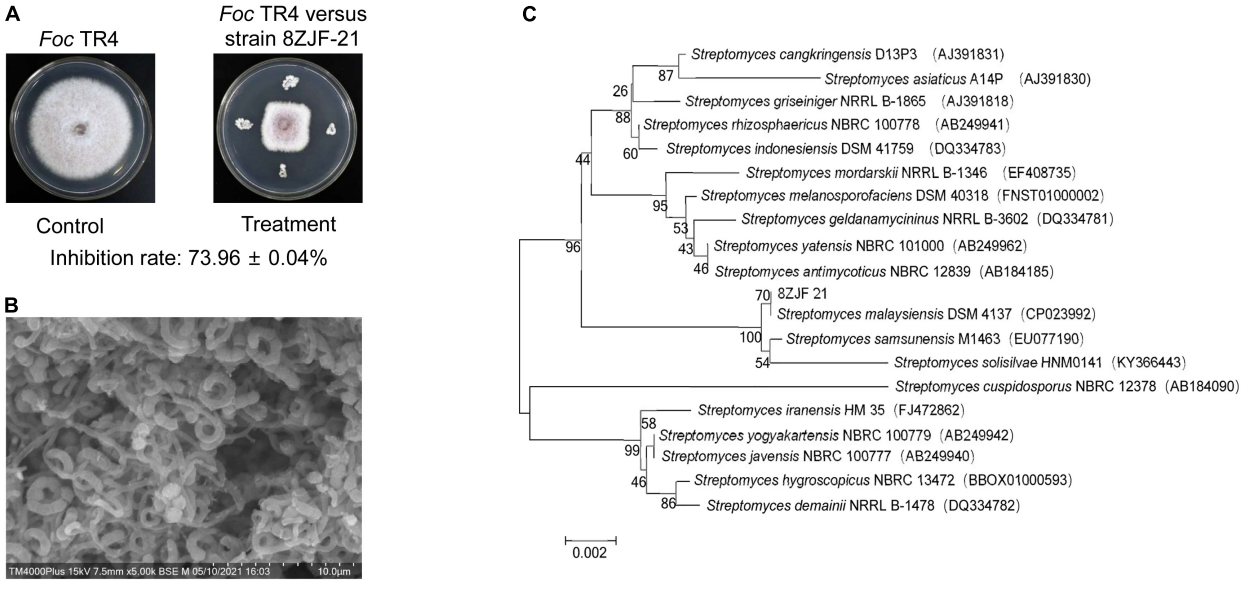

FIGURE 1 | Antifungal activity and identification of strain 8ZJF-21. **(A)** Antifungal activity of strain 8ZJF-21 on mycelial growth of *Foc* TR4. **(B)** Morphology of strain 8ZJF-21. **(C)** Phylogenetic tree of strain 8ZJF-21 using 16 rDNA sequences. The tree was constructed using the NJ method in the MEGA software. The level of bootstrap support (1,000 repetitions) was indicated at all nodes.

grow well on PDA and various ISP media (ISP2-ISP7). Different morphological characteristics of the colony were displayed in **Supplementary Table 2**. The strain can develop the branched substrate and aerial mycelia. Cream aerial mycelia and milky-white substrate hyphae were observed on all the selected ISP media. The grayish-white color of aerial and substrate mycelia was displayed on PDA. Diffusible pigment was not detected on the selected media except for ISP7, which was a typical profile of melanin pigment produced by *Streptomyces* (Shirling and Gottlieb, 1966). The spiral spore chains with rough surface were finally generated (**Figure 1B**).

In comparison with different culture conditions in the ISP2 medium, strain 8ZJF-21 can grow well at temperatures from 20 to 40°C (optimum at 30°C), NaCl up to 3% (w/v, optimal concentration 1%) and pH from 6.0 to 9.0 (optimum pH 7.0). It could produce extracellular enzymes such as amylase, cellulase, protease, and urease as well as reduce nitrate. It had no capacity to produce H_2S and respond to gelatin degradation. In addition, strain 8ZJF-21 was able to utilize all the tested sugars as sole carbon source and most of nitrogen source except for NH_4NO_3, arginine, and glutamic acid (**Table 1**). Compared with the reference *Streptomyces* strains (Qi et al., 2019; Jing et al., 2020; Wei et al., 2020), strain 8ZJF-21 was considered as a member of the genus *Streptomyces*.

TABLE 1 | Determination of physiological and biochemical properties of *S. malaysiensis* 8ZJF-21.

	Result	Characteristics	Result
Biochemical test		**Carbon source**	
Tween-20	−	Raffinose	+
Tween-40	−	D-Trehalose anhydrous	+
Tween-80	−	α-Lactose	+
Gelatin Liquefaction	−	Inositol	+
Starch hydrolysis	+	D(+)-Cellobiose	+
IAA production	+	D-Fructose	+
Cellulase	+	D-Melezitose	+
Urease	+	L-Arabinose	+
Protease	+	Ribose	+
Lipase	+	D-Galactose	+
H_2S production	−	D-Glucose	+
Nitrate reduction	+		
Siderophores	+		
pH tolerance test	6–9 (optimal pH 7.0)		
Temperature tolerance test	20°C–40°C (optimum at 30°C)		
NaCl tolerance test(%)	< 3 (optimal NaCl concentration 1%)		
Nitrogen source			
NH_4Cl	+	Histidine	+
$(NH_4)_2SO_4$	+	Tyrosine	+
NH_4NO_3	−	Methionine	+
Arginine	−	Glutamic acid	−
Glycine	+	Hydroxyproline	+
Phenylalanine	+		

"+" positive result; "−" negative result.

Identification of Strain 8ZJF-21

To further identify strain 8ZJF-21, the whole genome was sequenced. A 1,639 bp-length sequence of 16S rDNA was extracted from the genome sequences. One-hundred percent of nucleotide similarity was found with 16S rDNA of *S. malaysiensis* DSM 4137 (GenBank ID: NZ_CP023992). The phylogenetic tree showed that strain 8ZJF-21 was located in a well-delineated subclade with *S. malaysiensis* (**Figure 1C**). Compared with the genomes of strain 8ZJF-21 to the typal genome of *S. malaysiensis* DSM 4137 (**Supplementary Figure 1**), the calculated ANI value was 98.49 above the threshold value of 95-96% for species delineation (Richter and Rosselló-Móra, 2009). Therefore, strain 8ZJF-21 was identified as *S. malaysiensis*.

Detection of a Broad-Spectrum Antifungal Activity of *Streptomyces malaysiensis* 8ZJF-21 Against Phytopathogenic Fungi

The antifungal assay showed that *S. malaysiensis* 8ZJF-21 significantly inhibited the mycelial growth of all tested fungi (**Figure 2**). The inhibition rates ranged from 40.15 to 77.83%. The strongest antifungal activity was detected against the causal agent of strawberry anthracnose (*C. fragariae*, 77.83 ± 2.68), followed by *F. oxysporum* f. sp. *cucumerinum* (67.48 ± 1.32), *C. gloeosporioides* (63.96 ± 2.01), and *F. graminearum* Sehw (60.86 ± 1.32). In addition, strain 8ZJF-21 had also strong inhibition activities against *A. tenuissima* (59.73 ± 3.2), *C. lunata* (42.37 ± 2.31), *F. oxysporum* f. sp. *cubense* race 1 (42.88 ± 1.58), *C. gloeosporioides* (Penz) Penz and Sacc 1884 (43.33 ± 2.18), *P. oryzae* (48.51 ± 2.01), and *C. acutatum* (40.15 ± 1.32). It suggested that *S. malaysiensis* 8ZJF-21 had a broad-spectrum antifungal activity.

Biocontrol of *Foc* TR4 and Plant-Growth Promoting in the Pot Experiment

Streptomyces malaysiensis 8ZJF-21 inhibited the growth of different phytopathogenic fungi *in vitro*. It promoted us to evaluate its biocontrol efficiency against *Foc* TR4 using the pot experiment. The disease symptoms on banana seedlings were detected at 30 dpi. In the treatment group of *Foc* TR4 (G1), banana seedlings showed an obvious chlorotic symptom at the bottom of the leaves (**Figure 3A**). Compared with the control group, no obvious disease symptom was detected in the group of *S. malaysiensis* 8ZJF-21 + *Foc* TR4 (G2), suggesting that the protective treatment with *S. malaysiensis* 8ZJF-21 effectively prevented the infection of *Foc* TR4. The results were supported by the lack of obvious black symptoms in the split corms of banana seedlings treated with *S. malaysiensis* 8ZJF-21 (G2). We also evaluated *Foc* TR4-GFP infection in the roots of banana seedlings. The colony-forming units of *Foc* TR4-GFP in *S. malaysiensis* 8ZJF-21-treated roots were much lower than that in *Foc* TR4-GFP-treated roots (**Figure 3B**). The disease index was 65.37% in the G1 group, while only 18.07% were recorded in the G2 group (**Figure 3C**).

Compared to different agronomic traits of banana seedlings in different treatment groups (**Figures 3D–J**), *Foc* TR4 infection

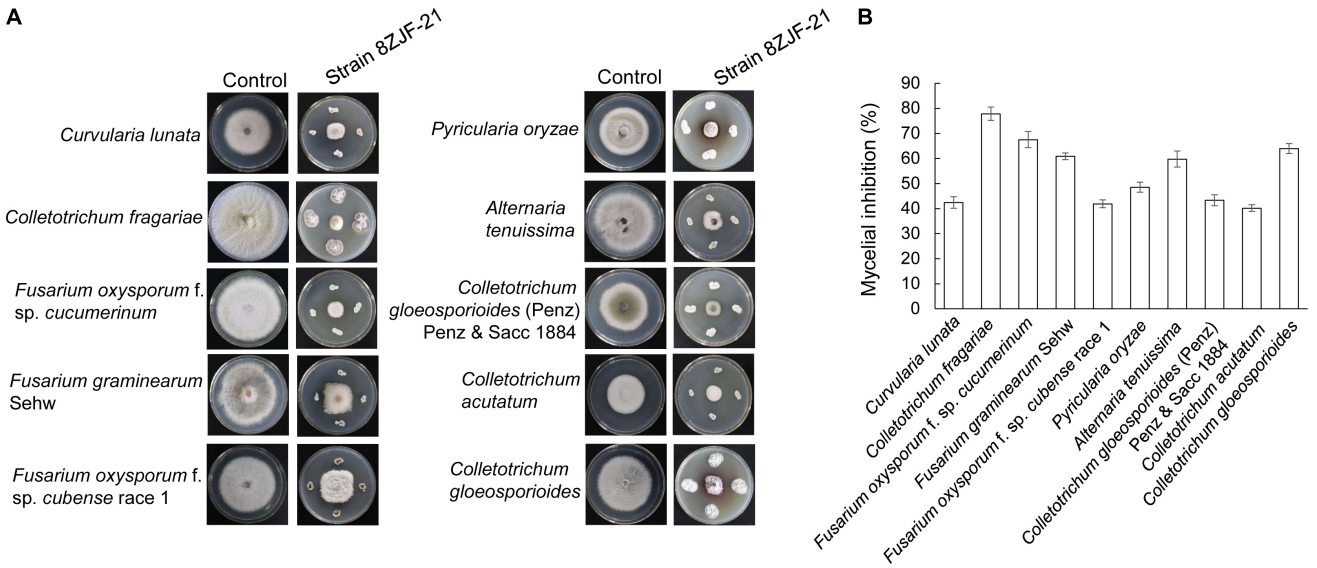

FIGURE 2 | Measurement of a broad-spectrum antifungal activity of *S. malaysiensis* 8ZJF-21 against the selected fungal phytopathogens. **(A)** Antagonistic assay of *S. malaysiensis* 8ZJF-21 against different phytopathogens. **(B)** Quantitative analysis of antifungal activity of *S. malaysiensis* 8ZJF-21 against different phytopathogens.

inhibited the growth of banana seedlings. Although no obvious difference of stem diameter was observed among the three treatment groups (**Figure 3D**), *S. malaysiensis* 8ZJF-21 significantly increased ($p = 0.0036$) the plant height and reached 46.73 ± 2.01 cm at 30 dpi (**Figure 3E**). Compared to the agronomic indicators in the G1 group, a significant increase was detected in the leaf area, leaf thickness, dry weight, and fresh weight in the G2 and G3 groups (**Figures 3F–I**). Chlorophyll content was sharply decreased in the *Foc* TR4-treated leaves due to chlorotic symptom (**Figure 3I**). Hence, *S. malaysiensis* 8ZJF-21 not only reduced the disease symptoms, but also promoted the growth of banana seedlings.

Effect of Extract on the Antioxidant System of Banana Seedlings

Biotic and abiotic stresses induce accumulation of reactive oxygen species in plant cells, thereby causing oxidative damage (Li et al., 2015). The oxidative damage expressed as the form of H_2O_2 was first determined in banana roots of different groups. *Foc* TR4 infection resulted in a rapid increase of H_2O_2 and reached a peak at 3 dpi (**Figure 4A**). *S. malaysiensis* 8ZJF-21 reduced the accumulation of H_2O_2 in *Foc* TR4-infected roots. It was supported by the changes of MDA contents in the G2 group, a marker for monitoring lipid peroxidation caused by oxidative damage (**Figure 4B**). The MDA contents in *Foc* TR4-inoculated roots dramatically increased from 0.5 dpi and reached the highest value at 4 dpi, which was four-fold higher than that in the G3 group. However, the increase of MDA contents in roots treated with *S. malaysiensis* 8ZJF-21 was obviously inhibited. The maximum was detected at 4dpi with the decrease of 69.04% in comparison with the G1 group.

To assay whether *S. malaysiensis* 8ZJF-21 could induce activities of antioxidant enzymes (such as CAT, SOD, PPO, and POD), the expression levels of these genes were investigated. The transcripts of *MaCAT* in banana roots treated with *S. malaysiensis* 8ZJF-21 increased gradually until 5 dpi (**Figure 4C**). In *Foc* TR4-treated roots, the expression peak was detected at 4 dpi. No obvious increase ($P < 0.01$) among different time points except for 2 dpi was detected in the G3 group. Similarly, *S. malaysiensis* 8ZJF-21 upregulated significantly ($P < 0.05$) the expression levels of *MaSOD* and *MaPOD*. Their transcripts reached the maximum at 4 dpi with two-fold higher than those in the G1 group (**Figures 4D,E**). Although *Foc* TR4 induced obviously the transcript accumulation of *MaPPO*, the expression levels were higher in the G2 group and increased by 21% at 3 dpi in comparison with *Foc* TR4-treated roots (**Figure 4F**).

Expression Levels of Defense-Related Genes in Banana Roots Treated With *Streptomyces malaysiensis* 8ZJF-21

To determine whether the defensive system was activated in response to *S. malaysiensis* 8ZJF-21 and/or *Foc* TR4, four defense-related genes (*Mab-1,3-Glu*, *MaPAL*, *MaMAPK1,* and *MaPR1*) were selected. By contrast, *S. malaysiensis* 8ZJF-21 and/or *Foc* TR4 significantly increased the transcripts of four defense-related genes with varying patterns (**Figure 5**). The transcript level of *MaPR1* in roots treated with *S. malaysiensis* 8ZJF-21 increased significantly at 0.5 dpi and reached the highest peak at 2 dpi, which was 1.3-fold and 7.0-fold higher than that in the G1 and G3 groups, respectively (**Figure 5A**). The transcript level of *MaPAL* was also upregulated by *S. malaysiensis* 8ZJF-21 and the expression peak was detected at 2 dpi with 1.6-fold higher

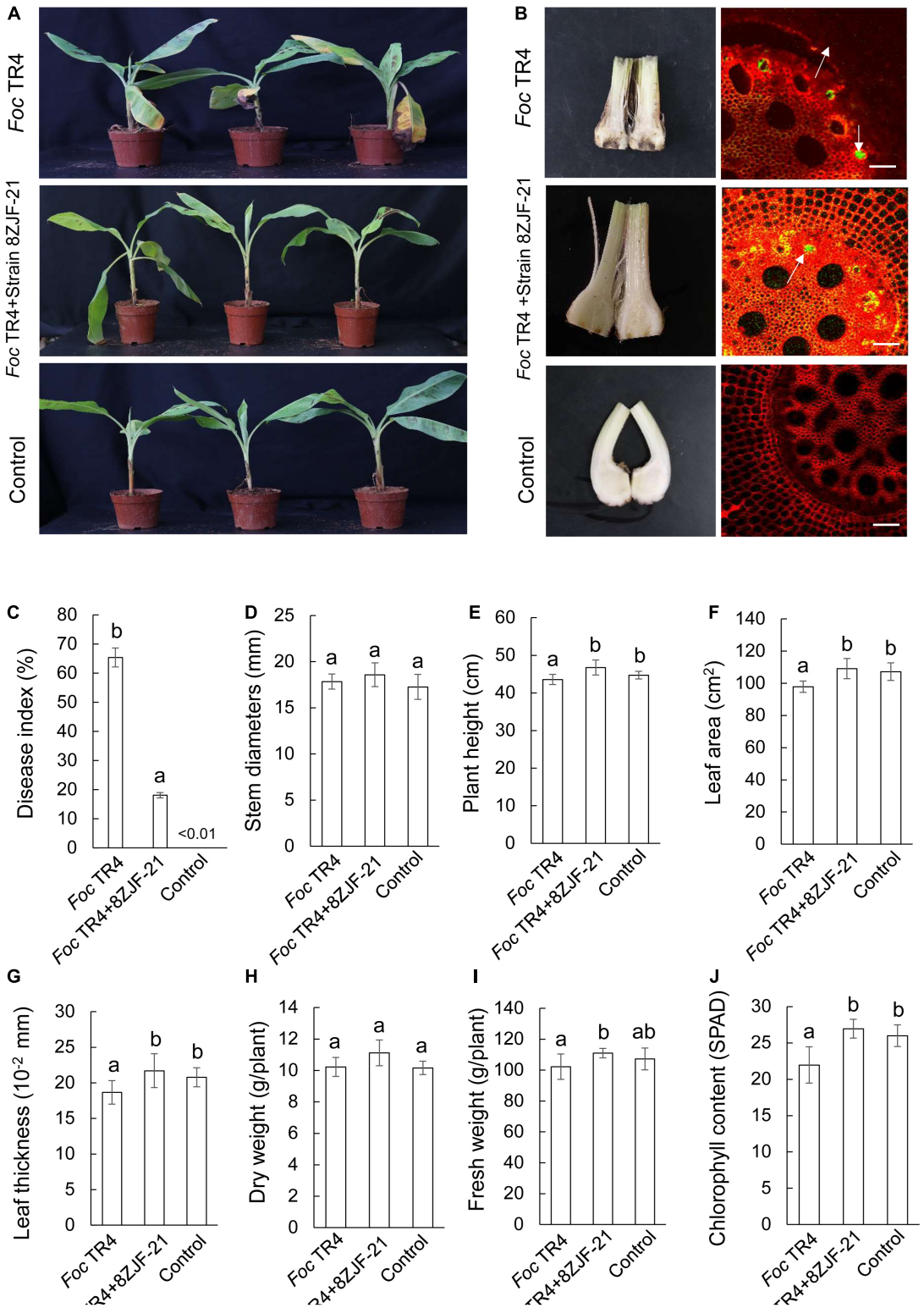

FIGURE 3 | Assay of Fusarium wilt disease control and plant-growth promoting after treatment with *S. malaysiensis* 8ZJF-21. **(A)** Chlorotic symptom of leaves in different treatment groups at 30 dpi. **(B)** Detection of Foc TR4 infection in the corm and root of banana seedlings at 30 dpi. **(C)** Quantitative analysis of disease index of banana seedlings at 30 dpi. Determination of physiological indicators including stem diameter **(D)**, plant height **(E)**, leaf area **(F)**, leaf thickness **(G)**, dry weight **(H)**, fresh weight **(I)**, and chlorophyll content **(J)** in different treatment groups at 30 dpi. Error bars indicate standard errors of the means from three repeated experiments. Different letters indicate a significant difference according to Duncan's multiple range test ($P < 0.05$).

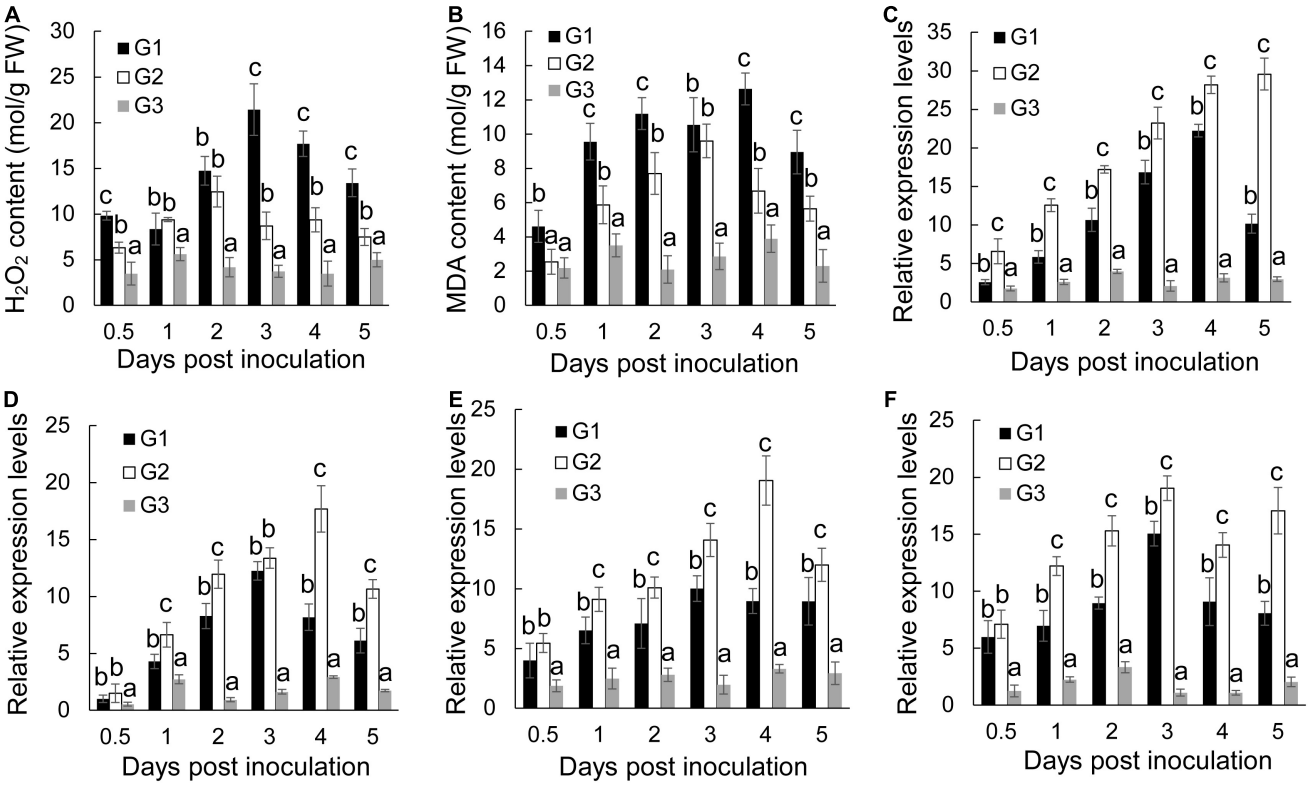

FIGURE 4 | Effects of *S. malaysiensis* 8ZJF-21 on the activation of antioxidant system. G1: *Foc* TR4-GFP treatment; G2: *S. malaysiensis* 8ZJF-21 + *Foc* TR4-GFP treatment; G3: medium treatment. **(A)** Measurement of H_2O_2 content in the roots of banana seedlings after treatment at different time points. **(B)** Measurement of MDA content in the roots of banana seedlings after treatment at different time points. The expression levels of antioxidant enzyme genes were determined by qRT-PCR, including *MaCAT* **(C)**, *MaSOD* **(D)**, *MaPOD* **(E)**, and *MaPPO* **(F)**. Error bars indicate standard errors of the means from three repeated experiments. Different letters indicate a significant difference according to Duncan's multiple range test ($P < 0.05$).

than that in the G1 group (**Figure 5B**). A similar expression pattern of *Ma*β-*1,3-Glu* was observed in the treated roots of *S. malaysiensis* 8ZJF-21. The transcripts of *Ma*β-*1,3-Glu* in the G2 group showed an increase of 1.64-fold at 1 dpi and 1.35-fold at 2 dpi in comparison with that in the G1 group (**Figure 5C**). The expression levels of *MaMAPK1* reached their maximum values at 2 dpi in the G1 group and at 1 dpi in the G2 group. High transcripts were maintained by *S. malaysiensis* 8ZJF-21 until 4 dpi (**Figure 5D**). It suggested that *S. malaysiensis* 8ZJF-21 could improve the plant resistance to *Foc* TR4 by activating the MAPK-mediated signaling pathway of defense response.

Effect of Extract on the Growth of *Foc* TR4

Foc TR4 was inoculated on the PDA plate containing different concentration extracts of *S. malaysiensis* 8ZJF-21. The inhibition of mycelial growth was measured, until hypha reached the edge of the plate in the control group (10% of DMSO treatment). The mycelial growth of *Foc* TR4 was inhibited dramatically along with the increase of extract concentration. More than 12.50 μg/ml of extract almost completely restricted the mycelial growth of *Foc* TR4 (**Figure 6A**). The EC_{50} value was 6.11 μg/ml (**Supplementary Figure 2**). Similarly, the extracts significantly reduced the germination rate of conidia and the length reduction of germ tubes (**Figures 6B,C**). All spore germination was almost completely inhibited by 4 × EC_{50} of extract. No obvious inhibition of *Foc* TR4 growth and spore germination was observed in the control group. In addition, the extract-treated hyphae became deformed, shrunk, ruptured, and swollen (**Figure 6D**). The normal hyphae with a smooth surface appeared to be uniform in thickness. For cellular ultrastructure of *Foc* TR4, 4 × EC_{50} of the extract caused vacuolization and organelle degradation. Mitochondria and cell nucleus gradually disappeared. High dense components were formed in treated cells (**Figure 6E**).

Genome Sequencing and Annotation of *Streptomyces malaysiensis* 8ZJF-21

After sequencing and assembly, the genome of *S. malaysiensis* 8ZJF-21 consisted of 11,434,537 bp and had 71.09% of GC content. The genome contained 8 rRNA genes, 63 tRNA genes, and 9,787 coding sequences (**Figure 7A**). By annotation, 34.24, 48.33, and 75.44% of genes were assigned to three categories of KEGG, GO, and COG, respectively. In KEGG annotation, 2,491 of genes participated into the regulation of cellular processes (193), metabolism (2,008), human diseases (142), genetic

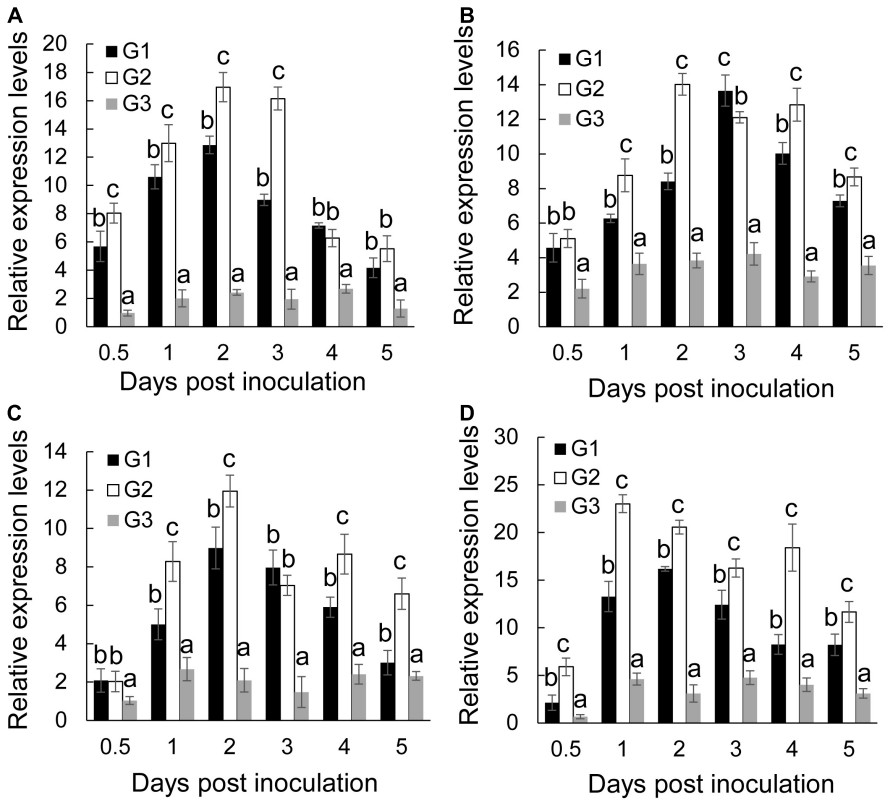

FIGURE 5 | Expression analysis of defense-related marker genes in banana roots. qRT-PCR determined the transcript levels of *MaPR1* **(A)**, *MaPAL* **(B)**, *Mab-1,3-Glu* **(C)**, and *MaMAPK1* **(D)** in banana roots after treatment with *S. malaysiensis* 8ZJF-21 at different time points. G1-G3 represented different treatment groups as described in **Figure 4**. Error bars indicate standard errors of the means from three repeated experiments. Different letters indicate a significant difference according to Duncan's multiple range test ($P < 0.05$).

information processing (216), environmental information processing (298), and organismal systems (44) (**Supplementary Figure 3**). For COG annotation, the top five categories contained transcription (833), nucleotide transport and metabolism (584), carbohydrate transport and metabolism (575), energy production and conversion (484) as well as inorganic ion transport and metabolism (400). Notably, 2,342 of genes were clustered into unknown function category (**Figure 7B**). A total of 4,730 genes were annotated into biological process (1,728), cellular component (1,657), and molecular function (3,950) using the GO database (**Supplementary Figure 4**).

Moreover, several BGCs in the genome of *S. malaysiensis* 8ZJF-21 were involved in secondary metabolism. By alignment with antiSMASH, the predicted 52 BGCs included NRPS (non-ribosomal peptide synthetase), PKS (polyketide synthase) type 1 and 2, siderophore, terpene, indole, butyrolactone, and betalactone (**Supplementary Table 3**). Fourteen BGCs exhibited more than 70% of similarity with the submitted BGCs in the database. Seven BGCs showed more than 100% of similarity with coelichelin, ectoine, nigericin B, ectoine, desferrioxamin B, echoside A/B, geosmin, and pristinol (**Figure 7C**). Six BGCs participated in the biosynthesis of antimicrobial compounds such as hopene, elaiophylin, coelichelin, ectoine, nigericin, and geldanamycin. Two BGCs probably regulated the biosynthesis of anticancer agent (hygrocin A/B and azalomycin F3a). Two siderophore molecules were encoded by cluster 21 and cluster 39. Gene clusters 67 and 78 were responsible for the biosynthesis of terpene. Clusters 66 and 71 were involved in the production of pigment. Notably, a high portion of unknown BGCs suggests that several novel secondary metabolites could be produced by *S. malaysiensis* 8ZJF-21.

Component Identification of Strain 8ZJF-21 Extract by Gas Chromatography-Mass Spectrometry

Gas Chromatography-Mass Spectrometry (GC-MS) was used to identify the bioactive compounds in *S. malaysiensis* 8ZJF-21 extract. Compared to mass spectra with the NIST library, 19 volatile organic compounds were obtained according to retention time and molecular weight (**Table 2**). They contained acetophenone (1), chloroacetic acid, 3-tetradecyl ester (2), 2,4-furandicarboxylic acid, dimethyl ester (3), formic acid, trans-4-methylcyclohexyl ester (4), 5-hydroxymethylfurfural (5), cyclohexane (6), pyrazoline (7), pentacosanoic acid, methyl ester (8), hexadecanoic acid, ethyl ester (9), borneol, dimethyl(pentafluorophenyl)silyl ether (10), pentacosanoic acid, methyl ester (11),

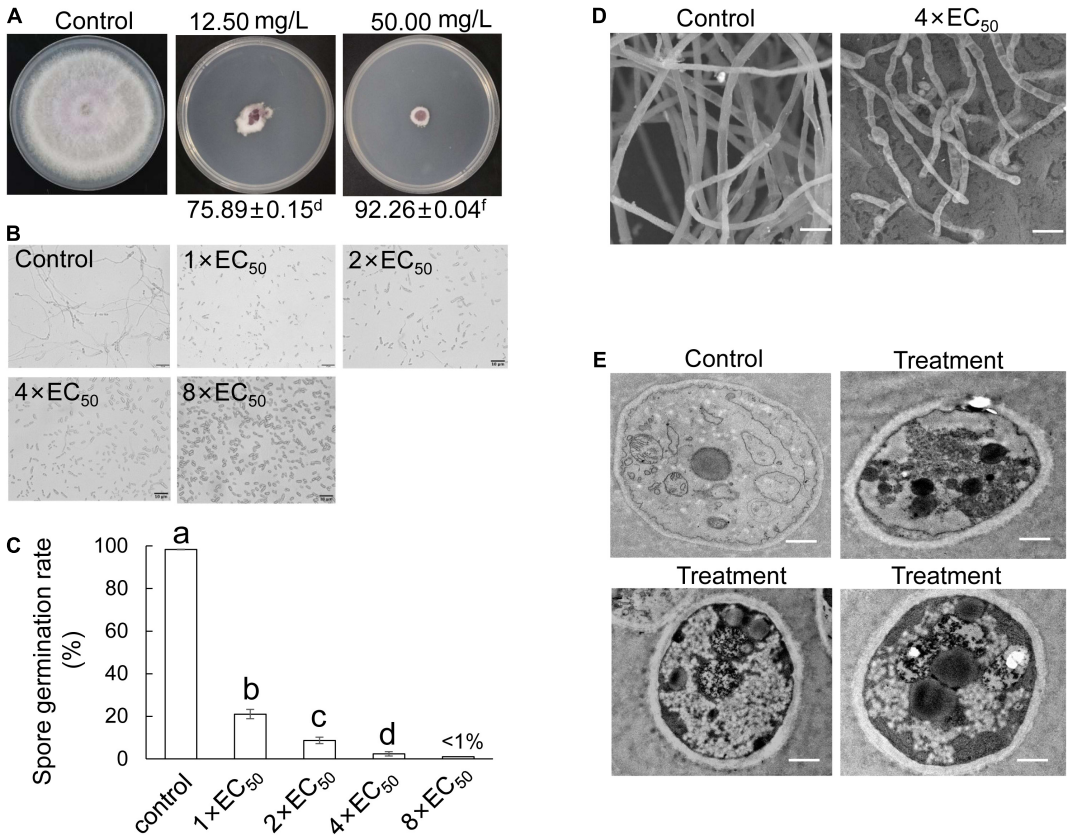

FIGURE 6 | Antifungal mechanism of *S. malaysiensis* 8ZJF-21 extract on *Foc* TR4 *in vitro*. **(A)** Inhibition ability assay of different dose extracts on the hyphal growth of Foc TR4. **(B)** Inhibition efficiency of different dose extracts on spore germination of *Foc* TR4. Bar = 10 μm. **(C)** Quantitative analysis of spore germination of *Foc* TR4 after treatment with different dose extracts. Different letters indicate a significant difference according to Duncan's multiple range test ($P < 0.05$). **(D)** Characteristics of hyphal morphology of *Foc* TR4 after treatment with 4 × EC_{50} extract. Bar = 1 μm. **(E)** Ultrastructural characteristics of *Foc* TR4 after treatment with 4 × EC_{50} extract. Bar = 0.5 μm.

1,2-benzenedicarboxylic acid, butyl 2-methylpropyl ester (12), 4-(3-methyl-2-butenyl)-1H-indole (13), 1,2-bis(p-(cis-styryl)phenyl)-trans-ethylene (14), colchiceinamide (15), 1,2-Bis(p-(cis-styryl)phenyl)-trans-ethylene (16), voaluteine (17), 4'-(3-(6-Methyl-3-pyridyl)-1-(p-tolyl)-2-pyrazolin-5-yl)acetanilide (18), and bufotalin (19). The peak area represented the relative proportion. Benzenedicarboxylic acid and 1H-Indole, 4-(3-methyl-2-butenyl) were two dominant components in *S. malaysiensis* 8ZJF-21 extract.

DISCUSSION

Actinobacteria are an important component of soil microbial communities, accounting for around 10% of the total soil microbiome (van Bergeijk et al., 2020). Some of them can enter directly into plant tissues and establish an endophytic lifestyle (Dinesh et al., 2017). Endophytic actinomycetes from medicinal plants were reported as major sources of antifungal agents (Golinska et al., 2015). However, there is still a lack of knowledge on their properties and application in the field. It prompted us to explore endophytic *Streptomyces* from medicinal plants as biocontrol agents. Our previous study demonstrated that 144 endophytic Actinomycete strains were isolated from different tissues of traditional medicinal plants. Especially, *Streptomyces* sp. strain 8ZJF-21 isolated from the roots of *C. capitulata* exhibited a strong antifungal activity against *Foc* TR4. Accumulated evidence indicated that secondary metabolites of medicinal plants promoted the development of microbial traits by mediating cross-talk between endophytes and their hosts (Granér et al., 2003). During the long-term interaction, endophytes gained some new genetic information and produced specific bioactive compounds (Chithra et al., 2014). Some rare actinomycetes isolated from the medicinal plant *Vochysia divergens* produced a wide diversity of antibacterial secondary metabolites (Gos et al., 2017). Our present results also showed that an endophytic *Streptomyces* sp. strain 8ZJF-21 exhibited strong antagonistic activities against *Fusarium* spp., *Curvularia* spp., *Alternaria* spp., and *Pyricularia* spp. (**Figure 2**). Similarly, 12 out of 65 endophytic actinomycetes isolated from medicinal plants *Artemisia argyi*, *Paeonia lactiflora*, *Radix platycodi,* and *Achyranthes bidentata* effectively suppressed penicillin-resistant *Staphylococcus aureus*, and majority of them belonged to *Streptomyces*

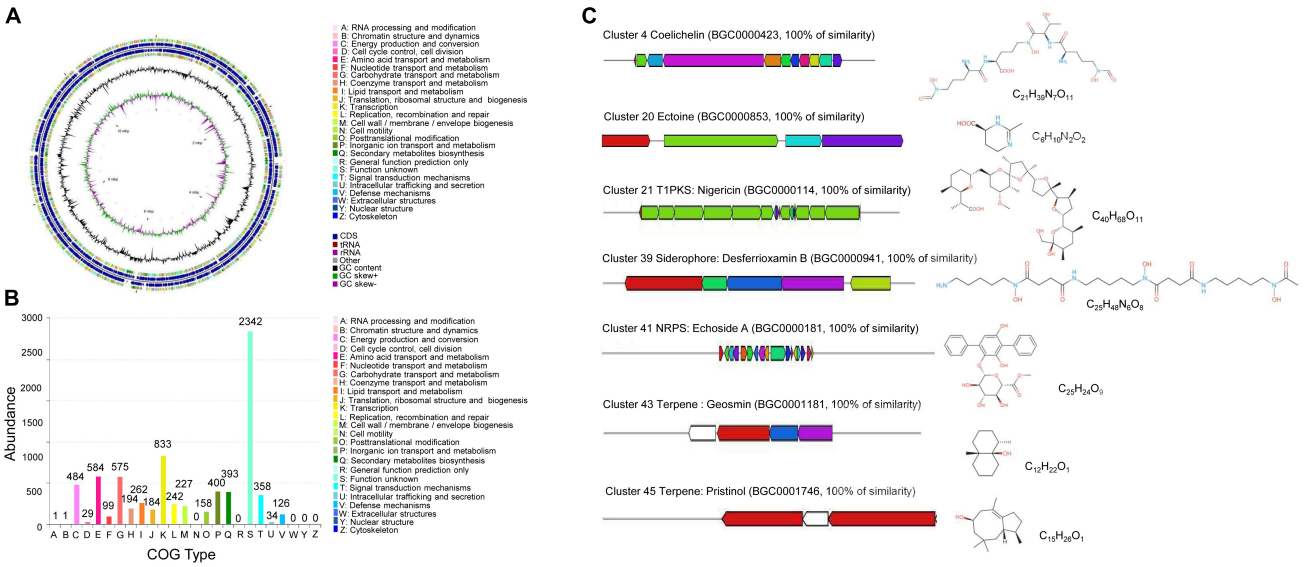

FIGURE 7 | Genome annotation of *S. malaysiensis* 8ZJF-21 and BGC prediction. **(A)** Circular map of strain 8ZJF-21 genome. From outside to center, ring 1 and ring 4 represented CDS in forward strand and reverse strand, respectively. Different colors indicate the functional category of COG. Rings 2 and 3 showed the CDS, tRNA, and rRNA in forward strand and reverse strand, respectively. Ring 5 and ring 6 show the G + C content and G + C skew, respectively. **(B)** COG functional annotation of *S. malaysiensis* 8ZJF-21 genome. **(C)** Genomic information and chemical structure of BGCs with 100% similarity with the known BGCs.

TABLE 2 | Identification of compound components in *S. malaysiensis* 8ZJF-21 extract by GC-MS.

No.	Retention time (min)	Peak area (Ab*s)	Baseline height (Ab)	Absolute height (Ab)	Peak width 50% (min)	Compounds	Molecular weight (amu)
1	13.12	70692	10852	19633	0.201	Acetophenone	120.058
2	14.294	18901	6915	14847	0.101	Chloroacetic acid	290.201
3	23.144	225670	46063	61558	0.268	2,4-Furandicarboxylic acid	184.037
4	24.679	249440	63347	86147	0.176	Formic acid	142.099
5	25.183	439371	113658	138820	0.159	5-Hydroxymethylfurfural	126.032
6	25.384	90802	21662	53877	0.159	Cyclohexane	112.125
7	25.594	1735455	503739	535781	0.201	Pyrazoline	112.100
8	26.802	88591	19037	55004	0.151	Pentacosanoic acid	396.397
9	28.085	152797	32432	77364	0.168	Hexadecanoic acid	284.272
10	29.377	83552	29050	90809	0.109	Dimethyl(pentafluorophenyl) silyl ether	378.144
11	30.971	342717	70703	162678	0.185	Hexadecanoic acid	284.272
12	37.782	2562283	756038	1177089	0.151	Benzenedicarboxylic acid	278.152
13	38.093	2371047	670528	1123216	0.185	4-(3-methyl-2-butenyl)-1H-indole	185.12
14	38.948	205896	48409	565497	0.143	1,2-Bis(p-(cis-styryl)phenyl)-trans-ethylene	384.188
15	40.551	474633	71382	760234	0.243	Colchiceinamide	384.169
16	40.836	524589	86333	811105	0.294	1,2-Bis(p-(cis-styryl)phenyl)-trans-ethylene	384.188
17	42.337	893803	104279	1086622	0.428	Voaluteine	384.205
18	43.31	901704	45557	1234395	0.738	4′-(3-(6-Methyl-3-pyridyl)-1-(p-tolyl)-2-pyrazolin-5-yl)acetanilide	384.195
19	43.956	542604	79901	1440011	0.252	Bufotalin	444.251

(Zhang et al., 2012). Therefore, endophytic actinomycetes from medicinal plants could be exploited as a novel source of biocontrol agents.

Until now, a number of endophytic *Streptomyces* species were isolated from different plant tissues, but many of which were poorly defined. In our study, the morphological, physiological,

and biochemical characteristics of strain 8ZJF-21 were consistent with the properties of the genus *Streptomyces*. The phylogenetic tree of 16S rDNA showed that the strain clustered into the same subgroup with *S. malaysiensis* DSM 4137. Sharma and Manhas (2020) reported that an obvious difference of morphological characteristics was found among the nearest phylogenetic relative strains. Hence, 16S rDNA did not provide a sufficient resolution for the species-level identification. Although the traditional method of DNA-DNA hybridization allowed the classification for prokaryote, serious shortcomings limited its application such as a time-consuming procedure, operational feasibility, and standard stain obtaining (Gevers et al., 2005). Based on the sequencing genomes, ANI provided an efficient method to identify the level of species (Gevers et al., 2005). It was supported by an ANI value of 98.49% that was calculated by the genomic alignment of strain 8ZJF-21 with the typal strain *S. malaysiensis* DSM 4137, which was above the threshold value of 95–96% for species delineation (Richter and Rosselló-Móra, 2009).

To further evaluate the biocontrol efficiency of *S. malaysiensis* 8ZJF-21, the pot experiment was carried out in this study. Strain 8ZJF-21 improved the system resistance of banana seedlings and inhibited the infection of *Foc* TR4. The previous reports also showed that the plant immune system could be triggered after the inoculation with pathogen or beneficial microbes (Zhang et al., 2019). In an early response, H_2O_2 is a key signaling molecule in early plant immune responses (Li et al., 2015). *Foc* TR4 induced H_2O_2 outbreak and MDA accumulation in banana roots. Lower levels of H_2O_2 were detected in roots treated with *S. malaysiensis* 8ZJF-21, suggesting that the strain alleviated the oxidative stress caused by *Foc* TR4. Moreover, *S. malaysiensis* 8ZJF-21 induced the higher and lasting expression levels of antioxidant enzyme genes (*MaPPO*, *MaPOD*, *MaCAT,* and *MaSOD*) and defense-related genes (*MaPAL*, *MaPR-1*, *MaMAPK1,* and *Maβ-1,3 glu*). PPO could oxidize phenol and transform phytoalexins to enhance plant resistance to pathogens (Richter et al., 2012). PAL degraded phenylalanine to trans-cinnamic acid, activating the biosynthesis of salicylic acid (SA) to induce the defense response (Shine et al., 2016). Hence, the SA-dependent signaling pathway might participate in the resistance activation of *S. malaysiensis* 8ZJF-21. Similarly, *Pseudomonas putida* and *Pseudomonas syringae* stimulated a systemic response against *Alternaria solani* by increasing the activities of PAL, POD, and PPO (Ahmed et al., 2011). *Streptomyces goshikiensis* triggered defense response against *Fusarium oxysporum* f. sp. *niveum* by enhancing activities of PPO, SOD, and β-1,3 glucanases (Faheem et al., 2015). Our previous studies also revealed that *Streptomyces* can activate defensive enzyme activities and inhibit the infection of *Foc* TR4 in banana roots (Zhang et al., 2021). Therefore, the expression of defense-related and defensive enzyme genes was associated with the priming of antagonistic microbes on host plants as an early and rapid response to pathogens.

Additionally, the metabolites of *S. malaysiensis* 8ZJF-21 exhibited strong antifungal activity against *Foc* TR4. The extract directly attacked fungal pathogens, resulting in abnormal morphology like sporulation inhibition, swollen and distorted mycelia, vacuolation, and organelle disappearance. Moreover, endophytic actinomycetes produced a large set of metabolic compounds to stimulate the expression of specific genes involved in resistance to pathogens (Taechowisan et al., 2005; Kenneth et al., 2019; van Bergeijk et al., 2020). These metabolites also had a strong influence on the rhizosphere colonization of endophytic actinomycetes (Zhang et al., 2021). Competition of nutrient availability and niche was an essential for biocontrol among pathogenic and non-pathogenic microbes (Heydari and Pessarakli, 2010). Our previous study reported that competitive colonization of *Streptomyces* sp. BITDG-11 reduced fungal population of *Foc* TR4 in banana roots (Zhang et al., 2021). The biocontrol agents depleted rapidly the limited nutrient making it unavailable to meet the growth of pathogens. It is noteworthy that *S. malaysiensis* 8ZJF-21 can also promote the growth of banana seedlings. Its production ability of siderophores, cellulose, and IAA supported the physiological characteristics of plant-growth promoting. Similar results were reported that endophytes promoted plant growth by producing siderophores, decomposing organic materials by cellulose or lignocellulose and also producing growth promoters such as IAA and gibberellic acid (Taechowisan et al., 2005). They formed a symbiotic relationship with the host plants, facilitating plant to uptake nutrients from the soil (Rosenblueth and Martínez-Romero, 2006). The nutrient cycling capacity made them ideal candidates for natural fertilizers. Therefore, the endophytic actinomycetes will be potential biocontrol agents against plant diseases caused by soil-borne pathogens and plant growth promoters.

To identify fully the biosynthetic potential of secondary metabolites, the genome of *S. malaysiensis* 8ZJF-21 was sequenced and annotated. Fifty-two BGCs were predicted for producing known or unknown secondary metabolites, including terpenes, PKS type I or type II, NRPS, siderophores, and ectoines. PKS and NRPS were mainly responsible for the synthesis of most biologically active polyketide and peptide compounds (Janso and Carter, 2010; Qi et al., 2019). Especially, BGCs of desferrioxamin B, coelichelin, ectoine, nigericin, echoside A, geosmin, and pristinal showed 100% similarity with known structures. Desferrioxamines B and coelichelin belonged to different types siderophores. Siderophore produced by *Streptomyces* spp. played a crucial role in suppressing *Fusarium* wilt disease by depleting iron (Vurukonda et al., 2018; Zeng et al., 2018; Zhang et al., 2021). Other siderophore-producing rhizobacteria were also reported as biocontrol agents including *Pseudomonas koreensis*, *Burkholderia cepacian*, *Rahnella aquatilis,* and *Bacillus subtilis* (Carmona-Hernandez et al., 2019; Ghazy and El-Nahrawy, 2021). Ectoine could interact with biomolecules such as lipids, proteins, and DNA to protect itself from environmental stresses (Fenizia et al., 2020; Wittmar et al., 2020). Nigericin produced by endophytic *S. endus* OsiSh-2 exhibited remarkable antagonistic activity against rice blast disease (Xu et al., 2017). Echoside A from *Streptomyces* sp. GMR22 had a high potential as an antiviral agent (Melinda et al., 2021). Pristinol was also identified as a sesquiterpene alcohol from *S. pristinaespiralis* (Klapschinski et al., 2016). In addition, the predicted cluster 11 containing 38 genes showed 96% of similarity with BGCs of hygrocin A/hygrocin B. Hygrocins belonging to a type of naphthoquinone ansamycins had antitumor and antimicrobial activities (Wang et al., 2018). Cluster 19 exhibited 95% of similarity with BGC of azalomycin

F3a. Azalomycin F and its analogs from different *Streptomyces* strains had broad-spectrum antimicrobial activities (Yuan et al., 2013). Notably, much more unknown BGCs were identified, suggesting that *S. malaysiensis* 8ZJF-21 had a great potential for producing novel secondary metabolites. It was supported that 33.9% of coding genes clustered into the unknown function category in the COG annotation (**Figure 7B**). How a number of PKS and NRPS gene clusters regulate the biosynthesis of bioactive metabolites still needs to be further investigated.

Gas chromatography-mass spectrometry was used to further identify the antifungal compounds of *S. malaysiensis* 8ZJF-21 extract in our study. A large number of acid compounds such as chloroacetic acid, furandicarboxylic acid, formic acid, pentacosanoic acid, hexadecanoic acid, and benzenedicarboxylic acid were a main type of antifungal production. Benzenedicarboxylic acid possessing high peak area is a main metabolite of *S. cuspidosporus* with high antagonistic activity against pathogenic bacteria, fungi, and nematode (Sholkamy et al., 2020). Chloroacetic acid and hexadecanoic acid had the potential for controlling *Colletotrichum gloeosporioides* (Rajaofera et al., 2019). In addition, 1H-Indole, 4-(3-methyl-2-butenyl) was the other main component in *S. malaysiensis* 8ZJF-21 extract. The compound produced by *Aeromonas hydrophila* was highly effective to suppress the growth of *Aspergillus flavus* (Mannaa and Kim, 2018). Thus, these compounds could altogether contribute to the broad-spectrum antifungal activity of *S. malaysiensis* 8ZJF-21. Interestingly, BGCs of these compounds were not found in its genome. It might be because of the different identification methods and alignment databases (Wei et al., 2020).

CONCLUSION

In the study, an endophytic strain 8ZJF-21 with strong antifungal activity was identified from the roots of a medicinal plant. Based on the morphological, physiological, and biochemical characteristics, the strain was defined as the genus *Streptomyces*. The phylogenetic tree and ANI calculation were further used to identify strain 8ZJF-21 as *S. malaysiensis*. The pot experiment demonstrated that *S. malaysiensis* 8ZJF-21 improved plant resistance against *Foc* TR4 and promoted the growth of banana seedlings. The antifungal mechanism showed that *S. malaysiensis* 8ZJF-21 extract could inhibit the spore germination and mycelial growth of *Foc* TR4, and damage the ultrastructure of pathogenic cells. Genome annotation and GC-MS analysis revealed that strain 8ZJF-21 has a great potential for producing bioactive metabolites, suggesting that it will become an essential biocontrol agent against *Foc* TR4.

DATA AVAILABILITY STATEMENT

The datasets presented in this study can be found in online repositories. The names of the repository/repositories and accession number(s) can be found in the article/ **Supplementary Material**.

AUTHOR CONTRIBUTIONS

LZ, ZL, and WW developed the ideas and designed the experimental plans. LZ and WW supervised the research, provided the fund support, and prepared the manuscript. LZ, YW, SW, and YH performed the experiments. YH, TY, and JX provided the materials. LZ, YW, JZ, TY, and WW analyzed the data. All authors contributed to the article and approved the submitted version.

FUNDING

This work was supported by the Hainan Provincial Natural Science Foundation of China (321RC543, 2019RC293, and 320CXTD441), the National Natural Science Foundation of China (32072504), and the China Agriculture Research System of MOF and MARA (CARS-31).

ACKNOWLEDGMENTS

We thank Zhufeng Gao for providing help with this work.

SUPPLEMENTARY MATERIAL

The Supplementary Material for this article can be found online at: https://www.frontiersin.org/articles/10.3389/fpls.2022.874819/full#supplementary-material

REFERENCES

Ahmed, H. E., Mohamed, Z. K., ElDean, M. E., and Farahat, M. G. (2011). Induced systemic protection against tomato leaf spot (early leaf blight) and bacterial speck by rhizobacterial isolates. *J. Exp. Biol.* 7, 49–57.

Ayswaria, R., Vasu, V., and Krishna, R. (2020). Diverse endophytic *Streptomyces* species with dynamic metabolites and their meritorious applications: a critical review. *Crit. Rev. Microbiol.* 46, 750–758. doi: 10.1080/1040841X.2020.1828816

Brettin, T., Davis, J. J., Disz, T., Edwards, R. A., Gerdes, S., Olsen, G. J., et al. (2015). RASTtk: a modular and extensible implementation of the RAST algorithm for building custom annotation pipelines and annotating batches of genomes. *Sci. Rep.* 5:8365. doi: 10.1038/srep08365

Brinley-Morgan, W. J., and McCullough N. B. (1974). "Genus Brucella Meyer and Shaw 1920", in *Bergey's Manual of Determinative Bacteriology* (ed.) Buchanan R. E. and Gibbons N. E., 8th Edn (Baltimore: The Williams and Wilkins Co). 742–842.

Carmona-Hernandez, S., Reyes-Pérez, J. J., Chiquito-Contreras, R. G., Rincon-Enriquez, G., Cerdan-Cabrera, C. R., and Hernandez-Montiel, L. G. (2019). Biocontrol of postharvest fruit fungal diseases by bacterial antagonists: a review. *Agronomy* 9:121. doi: 10.3390/agronomy9030121

Chithra, S., Jasim, B., Sachidanandan, P., Jyothis, M., and Radhakrishnan, E. K. (2014). Piperine production by endophytic fungus *Colletotrichum gloeosporioides* isolated from *Piper nigrum*. *Phytomedicine* 21, 534–540. doi: 10.1016/j.phymed.2013.10.020

Dale, J., James, A., Paul, J. Y., Khanna, H., Smith, M., Peraza-Echeverria, S., et al. (2017). Transgenic Cavendish bananas with resistance to Fusarium wilt tropical race 4. *Nat. Commun.* 8:1496. doi: 10.1038/s41467-017-01670-6

De Silva, N. I., Brooks, S., Lumyong, S., and Hyde, K. D. (2019). Use of endophytes as biocontrol agents. *Fungal Biol. Rev.* 33, 133–148. doi: 10.1016/j.fbr.2018.10.001

Dhanasekaran, D., Sivamani, P., Panneerselvam, A., Thajuddin, N., Rajakumar, G., and Selvamani, S. (2005). Biological control of tomato seedling damping off with *Streptomyces* sp. *Plant Pathol. J.* 4, 91–95. doi: 10.3923/ppj.2005.91.95

Dinesh, R., Srinivasan, V., Te, S., Anandaraj, M., and Srambikkal, H. (2017). Endophytic actinobacteria: diversity, secondary metabolism and mechanisms to unsilence biosynthetic gene clusters. *Crit. Rev. Microbiol.* 43, 546–566. doi: 10.1080/1040841X.2016.1270895

Dita, M., Barquero, M., Heck, D., Mizubuti, E. S., and Staver, C. P. (2018). Fusarium wilt of banana: current knowledge on epidemiology and research needs toward sustainable disease management. *Front. Plant Sci.* 9:1468. doi: 10.3389/fpls.2018.01468

El-Shatoury, S. A., Ameen, F., Moussa, H., Wahid, O. A., Dewedar, A., and AlNadhari, S. (2020). Biocontrol of chocolate spot disease (*Botrytis cinerea*) in faba bean using endophytic actinomycetes *Streptomyces*: a field study to compare application techniques. *PeerJ* 8:e8582. doi: 10.7717/peerj.8582

Faheem, M., Raza, W., Zhong, W., Nan, Z., Shen, Q., and Xu, Y. (2015). Evaluation of the biocontrol potential of *Streptomyces goshikiensis* YCXU against *Fusarium oxysporum* f. sp. *niveum*. *Biol. Control* 81, 101–110. doi: 10.1016/j.biocontrol.2014.11.012

Fenizia, S., Thume, K., Wirgenings, M., and Pohnert, G. (2020). Ectoine from bacterial and algal origin is a compatible solute in microalgae. *Mar. Drugs* 18:42. doi: 10.3390/md18010042

Ferguson, I. B., Watkins, C. B., and Harman, J. E. (1983). Inhibition by calcium of senescence of detached cucumber cotyledons: effect on ethylene and hydroperoxide production. *Plant Physiol.* 71, 182–186. doi: 10.1104/pp.71.1.182

Ferraiuolo, S. B., Cammarota, M., Schiraldi, C., and Restaino, O. F. (2021). *Streptomycetes* as platform for biotechnological production processes of drugs. *Appl. Microbiol. Biotechnol.* 105, 551–568. doi: 10.1007/s00253-020-11064-2

Gevers, D., Cohan, F. M., Lawrence, J. G., Spratt, B. G., Coenye, T., Feil, E. J., et al. (2005). Re-evaluating prokaryotic species. *Nat. Rev. Microbiol.* 3, 733–739. doi: 10.1038/nrmicro1236

Ghazy, N., and El-Nahrawy, S. (2021). Siderophore production by *Bacillus subtilis* MF497446 and *Pseudomonas koreensis* MG209738 and their efficacy in controlling *Cephalosporium maydis* in maize plant. *Arch. Microbiol.* 203, 1195–1209. doi: 10.1007/s00203-020-02113-5

Golinska, P., Wypij, M., Agarkar, G., Rathod, D., Dahm, H., and Rai, M. (2015). Endophytic actinobacteria of medicinal plants: diversity and bioactivity. *Anton. Leeuw.* 108, 267–289. doi: 10.1007/s10482-015-0502-7

Gos, F. M., Savi, D. C., Shaaban, K. A., Thorson, J. S., Aluizio, R., Possiede, Y. M., et al. (2017). Antibacterial activity of endophytic actinomycetes isolated from the medicinal plant *Vochysia divergens* (Pantanal, Brazil). *Front. Microbiol.* 8:1642. doi: 10.3389/fmicb.2017.01642

Granér, G., Persson, P., Meijer, J., and Alström, S. (2003). A study on microbial diversity in different cultivars of *Brassica napus* in relation to its wilt pathogen, *Verticillium longisporum*. *FEMS Microbiol. Lett.* 224, 269–276. doi: 10.1016/S0378-1097(03)00449-X

Hassan, N., Nakasuji, S., Elsharkawy, M. M., Naznin, H. A., Kubota, M., Ketta, H., et al. (2017). Biocontrol potential of an endophytic *Streptomyces* sp. strain MBCN152-1 against *Alternaria brassicicola* on cabbage plug seedlings. *Microbes Environ.* 32, 133–141. doi: 10.1264/jsme2.ME17014

Heydari, A., and Pessarakli, M. (2010). A review on biological control of fungal plant pathogens using microbial antagonists. *J. Biol. Sci.* 10, 273–290.

Hoekstra, J. A., and Van Ewijk, P. H. (1993). The bounded effect concentration as an alternative to the NOEC. *Sci. Total Environ.* 134, 705–711. doi: 10.1016/S0048-9697(05)80074-9

Janso, J. E., and Carter, G. T. (2010). Biosynthetic potential of phylogenetically unique endophytic actinomycetes from tropical plants. *Appl. Environ. Microb.* 76, 4377–4386. doi: 10.1128/AEM.02959-09

Jing, T., Zhou, D., Zhang, M., Yun, T., Qi, D., Wei, Y., et al. (2020). Newly isolated *Streptomyces* sp. JBS5-6 as a potential biocontrol agent to control banana fusarium wilt: genome sequencing and secondary metabolite cluster profiles. *Front. Microbiol.* 11:3036. doi: 10.3389/fmicb.2020.602591

Kema, G. H., Drenth, A., Dita, M., Jansen, K., Vellema, S., and Stoorvogel, J. J. (2020). Fusarium wilt of banana, a recurring threat to global banana production. *Front. Plant Sci.* 11:628888. doi: 10.3389/fpls.2020.628888

Kenneth, O. C., Nwadibe, E. C., Kalu, A. U., and Unah, U. V. (2019). Plant growth promoting rhizobacteria (PGPR): a novel agent for sustainable food production. *Am. J. Agric. Biol. Sci.* 14, 35–54. doi: 10.3844/ajabssp.2019.35.54

Klapschinski, T. A., Rabe, P., and Dickschat, J. S. (2016). Pristinol, a sesquiterpene alcohol with an unusual skeleton from *Streptomyces pristinaespiralis*. *Angew. Chem. Int. Edit.* 55, 10141–10144. doi: 10.1002/anie.201605425

Kumar, S., Stecher, G., and Tamura, K. (2016). MEGA7: molecular evolutionary genetics analysis version 7.0 for bigger datasets. *Mol. Biol. Evol.* 33, 1870–1874.

Lacey, H. J., and Rutledge, P. J. (2022). Recently discovered secondary metabolites from *Streptomyces* species. *Molecules* 27:887. doi: 10.3390/molecules27030887

Li, K., Guo, Y., Wang, J., Wang, Z., Zhao, J., and Gao, J. (2020). *Streptomyces aquilus* sp. nov., a novel actinomycete isolated from a Chinese medicinal plant. *Int. J. Syst. Evol. Microbiol.* 70, 1912–1917. doi: 10.1099/ijsem.0.003995

Li, X., Jing, T., Zhou, D., Zhang, M., Qi, D., Zang, X., et al. (2021). Biocontrol efficacy and possible mechanism of *Streptomyces* sp. H4 against postharvest anthracnose caused by *Colletotrichum fragariae* on strawberry fruit. *Postharvest Biol. Tec.* 175:111401. doi: 10.1016/j.postharvbio.2020.111401

Li, Z., Zhang, Y., Peng, D., Wang, X., Peng, Y., He, X., et al. (2015). Polyamine regulates tolerance to water stress in leaves of white clover associated with antioxidant defense and dehydrin genes via involvement in calcium messenger system and hydrogen peroxide signaling. *Front. Physiol.* 6:280. doi: 10.3389/fphys.2015.00280

Mannaa, M., and Kim, K. D. (2018). Biocontrol activity of volatile-producing *Bacillus megaterium* and *Pseudomonas protegens* against *Aspergillus* and *Penicillium* spp. predominant in stored rice grains: study II. *Mycobiology* 46, 52–63. doi: 10.1080/12298093.2018.1454015

Marian, M., Ohno, T., Suzuki, H., Kitamura, H., Kuroda, K., and Shimizu, M. (2020). A novel strain of endophytic *Streptomyces* for the biocontrol of strawberry anthracnose caused by *Glomerella cingulata*. *Microbiol. Res.* 234:126428. doi: 10.1016/j.micres.2020.126428

Melinda, Y. N., Widada, J., Wahyuningsih, T. D., Febriansah, R., Damayanti, E., and Mustofa, M. (2021). Metabologenomics approach to the discovery of novel compounds from *Streptomyces* sp. GMR22 as anti-SARS-CoV-2 drugs. *Heliyon* 7 e08308. doi: 10.1016/j.heliyon.2021.e08308

Musa, Z., Ma, J., Egamberdieva, D., Abdelshafy Mohamad, O. A., Abaydulla, G., Liu, Y., et al. (2020). Diversity and antimicrobial potential of cultivable endophytic actinobacteria associated with the medicinal plant thymus roseus. *Front. Microbiol.* 11:191. doi: 10.3389/fmicb.2020.00191

Nansamba, M., Sibiya, J., Tumuhimbise, R., Karamura, D., Kubiriba, J., and Karamura, E. (2020). Breeding banana (*Musa* spp.) for drought tolerance: a review. *Plant Breed.* 139, 685–696. doi: 10.1111/pbr.12812

Ogata, H., Goto, S., Sato, K., Fujibuchi, W., Bono, H., and Kanehisa, M. (1999). KEGG: kyoto encyclopedia of genes and genomes. *Nucleic Acids Res.* 27, 29–34. doi: 10.1093/nar/27.1.29

Olanrewaju, O. S., and Babalola, O. O. (2019). *Streptomyces*: implications and interactions in plant growth promotion. *Appl. Microbiol. Biotechnol.* 103, 1179–1188.

Palaniyandi, S. A., Yang, S. H., Zhang, L., and Suh, J. W. (2013). Effects of actinobacteria on plant disease suppression and growth promotion. *Appl. Microbiol. Biotechnol.* 97, 9621–9636. doi: 10.1007/s00253-013-5206-1

Passari, A. K., Mishra, V. K., Saikia, R., Gupta, V. K., and Singh, B. P. (2015). Isolation, abundance and phylogenetic affiliation of endophytic actinomycetes associated with medicinal plants and screening for their *in vitro* antimicrobial biosynthetic potential. *Front. Microbiol.* 6:273. doi: 10.3389/fmicb.2015.00273

Ploetz, R. C. (2015). Management of Fusarium wilt of banana: a review with special reference to tropical race 4. *Crop Prot.* 73, 7–15. doi: 10.1016/j.cropro.2015.01.007

Pongprasert, N., Sekozawa, Y., Sugaya, S., and Gemma, H. (2011). A novel postharvest UV-C treatment to reduce chilling injury (membrane damage, browning and chlorophyll degradation) in banana peel. *Sci. Hortic.* 130, 73–77. doi: 10.1016/j.scienta.2011.06.006

Qi, D., Zou, L., Zhou, D., Chen, Y., Gao, Z., Feng, R., et al. (2019). Taxonomy and broad-spectrum antifungal activity of *Streptomyces* sp. SCA3-4 isolated from rhizosphere soil of *Opuntia stricta*. *Front. Microbiol.* 10:1390. doi: 10.3389/fmicb.2019.01390

Rajaofera, M. J. N., Wang, Y., Dahar, G. Y., Jin, P., Fan, L., Xu, L., et al. (2019). Volatile organic compounds of *Bacillus atrophaeus* HAB-5 inhibit the growth of *Colletotrichum gloeosporioides*. *Pestic. Biochem. Phys*. 156, 170–176. doi: 10.1016/j.pestbp.2019.02.019

Richter, H., Lieberei, R., Strnad, M., Novák, O., Gruz, J., Rensing, S. A., et al. (2012). Polyphenol oxidases in *Physcomitrella*: functional PPO1 knockout modulates cytokinin-dependent developmentin the moss *Physcomitrella* patens. *J. Exp. Bot*. 63, 5121–5135. doi: 10.1093/jxb/ers169

Richter, M., and Rosselló-Móra, R. (2009). Shifting the genomic gold standard for the prokaryotic species definition. *Proc. Natl. Acad. Sci. U.S.A*. 106, 19126–19131. doi: 10.1073/pnas.0906412106

Rosenblueth, M., and Martínez-Romero, E. (2006). Bacterial endophytes and their interactions with hosts. *Mol. Plant Microbe Interact*. 19, 827–837. doi: 10.1094/MPMI-19-0827

Sharma, M., and Manhas, R. K. (2020). Purification and characterization of salvianolic acid B from *Streptomyces* sp. M4 possessing antifungal activity against fungal phytopathogens. *Microbiol. Res*. 237:126478. doi: 10.1016/j.micres.2020.126478

Shine, M. B., Yang, J. W., El-Habbak, M., Nagyabhyru, P., Fu, D. Q., Navarre, D., et al. (2016). Cooperative functioning between phenylalanine ammonia lyase and isochorismate synthase activities contributes to salicylic acid biosynthesis in soybean. *New Phytol*. 212, 627–636. doi: 10.1111/nph.14078

Shirling, E. T., and Gottlieb, D. (1966). Methods for characterization of *Streptomyces* species. *Int. J. Syst. Evol. Microbiol*. 16, 313–340. doi: 10.1099/00207713-16-3-313

Sholkamy, E. N., Muthukrishnan, P., Abdel-Raouf, N., Nandhini, X., Ibraheem, I. B., and Mostafa, A. A. (2020). Antimicrobial and antinematicidal metabolites from *Streptomyces cuspidosporus* strain SA4 against selected pathogenic bacteria, fungi and nematode. *Saudi J. Biol. Sci*. 27, 3208–3220. doi: 10.1016/j.sjbs.2020.08.043

Singh, S. P., and Gaur, R. (2016). Evaluation of antagonistic and plant growth promoting activities of chitinolytic endophytic actinomycetes associated with medicinal plants against *Sclerotium rolfsii* in chickpea. *J. Appl. Microbiol*. 121, 506–518. doi: 10.1111/jam.13176

Taechowisan, T., Lu, C., Shen, Y., and Lumyong, S. (2005). Secondary metabolites from endophytic *Streptomyces aureofaciens* CMUAc130 and their antifungal activity. *Microbiology* 151, 1691–1695. doi: 10.1099/mic.0.27758-0

Tatusov, R. L., Galperin, M. Y., Natale, D. A., and Koonin, E. V. (2000). The COG database: a tool for genome-scale analysis of protein functions and evolution. *Nucleic Acids Res*. 28, 33–36. doi: 10.1093/nar/28.1.33

van Bergeijk, D. A., Terlouw, B. R., Medema, M. H., and van Wezel, G. P. (2020). Ecology and genomics of Actinobacteria: new concepts for natural product discovery. *Nat. Rev. Microbiol*. 18, 546–558. doi: 10.1038/s41579-020-0379-y

Vurukonda, S. S. K. P., Giovanardi, D., and Stefani, E. (2018). Plant growth promoting and biocontrol activity of *Streptomyces* spp. as endophytes. *Int. J. Mol. Sci*. 19:952. doi: 10.3390/ijms19040952

Wang, J., Nong, X. H., Amin, M., and Qi, S. H. (2018). Hygrocin C from marine-derived *Streptomyces* sp. SCSGAA 0027 inhibits biofilm formation in *Bacillus amyloliquefaciens* SCSGAB0082 isolated from South China Sea gorgonian. *Appl. Microbiol. Biot*. 102, 1417–1427. doi: 10.1007/s00253-017-8672-z

Wang, W., Hu, Y., Sun, D., Staehelin, C., Xin, D., and Xie, J. (2012). Identification and evaluation of two diagnostic markers linked to Fusarium wilt resistance (race 4) in banana (*Musa* spp.). *Mol. Biol. Rep*. 39, 451–459. doi: 10.1007/s11033-011-0758-6

Wang, W., Xie, Z. P., and Staehelin, C. (2014). Functional analysis of chimeric lysin motif domain receptors mediating Nod factor-induced defense signaling in *Arabidopsis thaliana* and chitin-induced nodulation signaling in *Lotus japonicus*. *Plant J*. 78, 56–69. doi: 10.1111/tpj.12450

Wang, X., Yu, R., and Li, J. (2021). Using genetic engineering techniques to develop banana cultivars with fusarium wilt resistance and ideal plant architecture. *Front Plant Sci*. 11:2202. doi: 10.3389/fpls.2020.617528

Wardecki, T., Brötz, E., De Ford, C., von Loewenich, F. D., Rebets, Y., Tokovenko, B., et al. (2015). Endophytic *Streptomyces* in the traditional medicinal plant *Arnica montana* L.: secondary metabolites and biological activity. *Anton. Leeuw*. 108, 391–402. doi: 10.1007/s10482-015-0492-5

Weber, T., Blin, K., Duddela, S., Krug, D., Kim, H. U., Bruccoleri, R., et al. (2015). antiSMASH 3.0-a comprehensive resource for the genome mining of biosynthetic gene clusters. *Nucleic Acids Res*. 43, W237–W243. doi: 10.1093/nar/gkv437

Wei, Y., Zhao, Y., Zhou, D., Qi, D., Li, K., Tang, W., et al. (2020). A newly isolated Streptomyces sp. YYS-7 with a broad-spectrum antifungal activity improves the banana plant resistance to *Fusarium oxysporum* f. sp. *cubense* tropical race 4. *Front. Microbiol*. 11:1712. doi: 10.3389/fmicb.2020.01712

Wittmar, J., Meyer, S., Sieling, T., Kunte, J., Smiatek, J., and Brand, I. (2020). What does ectoine do to DNA? A molecular-scale picture of compatible solute-biopolymer interactions. *J. Phys. Chem. B* 124, 7999–8011. doi: 10.1021/acs.jpcb.0c05273

Wu, W., Chen, W., Liu, S., Wu, J., Zhu, Y., Qin, L., et al. (2021). Beneficial relationships between endophytic bacteria and medicinal plants. *Front. Plant Sci*. 12:646146. doi: 10.3389/fpls.2021.646146

Xu, T., Li, Y., Zeng, X., Yang, X., Yang, Y., Yuan, S., et al. (2017). Isolation and evaluation of endophytic *Streptomyces endus* OsiSh-2 with potential application for biocontrol of rice blast disease. *J. Sci. Food Agr*. 97, 1149–1157. doi: 10.1002/jsfa.7841

Yoon, S. H., Ha, S. M., Kwon, S., Lim, J., Kim, Y., Seo, H., et al. (2017). Introducing EzBioCloud: a taxonomically united database of 16S *rRNA* gene sequences and whole-genome assemblies. *Int. J. Syst. Evol. Microbiol*. 67, 1613–1617. doi: 10.1099/ijsem.0.001755

Yuan, G., Hong, K., Lin, H., She, Z., and Li, J. (2013). New azalomycin F analogs from mangrove *Streptomyces* sp. 211726 with activity against microbes and cancer cells. *Mar. Drugs* 11, 817–829. doi: 10.3390/md11030817

Yun, T., Zhang, M., Zhou, D., Jing, T., Zang, X., Qi, D., et al. (2021). Anti-Foc RT4 activity of a newly isolated *Streptomyces* sp. 5-10 from a medicinal plant (*Curculigo capitulata*). *Front. Microbiol*. 11:3544. doi: 10.3389/fmicb.2020.610698

Zeng, J., Xu, T., Cao, L., Tong, C., Zhang, X., Luo, D., et al. (2018). The role of iron competition in the antagonistic action of the rice endophyte *Streptomyces sporocinereus* OsiSh-2 against the pathogen *Magnaporthe oryzae*. *Microb. Ecol*. 76, 1021–1029. doi: 10.1007/s00248-018-1189-x

Zhang, L., Yuan, L., Staehelin, C., Li, Y., Ruan, J., Liang, Z., et al. (2019). The LYSIN MOTIF-CONTAINING RECEPTOR-LIKE KINASE 1 protein of banana is required for perception of pathogenic and symbiotic signals. *New Phytol*. 223, 1530–1546. doi: 10.1111/nph.15888

Zhang, L., Zhang, H., Huang, Y., Peng, J., Xie, J., and Wang, W. (2021). Isolation and evaluation of rhizosphere actinomycetes with potential application for biocontrolling fusarium wilt of banana caused by *Fusarium oxysporum* f. sp. *cubense* Tropical Race 4. *Front. Microbiol*. 12:763038. doi: 10.3389/fmicb.2021.763038

Zhang, X., Ren, K., and Zhang, L. (2012). Screening and preliminary identification of medicinal plants endophytic actinomycetes used for inhibiting penicillin-resistant *Staphylococcus aureus*. *Int. J. Biol*. 4, 119–124. doi: 10.5539/ijb.v4n2p119

Zhou, D., Jing, T., Chen, Y., Wang, F., Qi, D., Feng, R., et al. (2019). Deciphering microbial diversity associated with fusarium wilt-diseased and disease-free banana rhizosphere soil. *BMC Microbiol*. 19:161. doi: 10.1186/s12866-019-1531-6

Conflict of Interest: The authors declare that the research was conducted in the absence of any commercial or financial relationships that could be construed as a potential conflict of interest.

Publisher's Note: All claims expressed in this article are solely those of the authors and do not necessarily represent those of their affiliated organizations, or those of the publisher, the editors and the reviewers. Any product that may be evaluated in this article, or claim that may be made by its manufacturer, is not guaranteed or endorsed by the publisher.

frontiers | Frontiers in Plant Science

ORIGINAL RESEARCH
published: 27 May 2022
doi: 10.3389/fpls.2022.892826

Soil Inoculation With Beneficial Microbes Buffers Negative Drought Effects on Biomass, Nutrients, and Water Relations of Common Myrtle

Soghra Azizi[1,2], Masoud Tabari[1], Ali Reza Fallah Nosrat Abad[3], Christian Ammer[4], Lucia Guidi[5] and Martin K.-F. Bader[6]**

[1]Faculty of Natural Resources, Tarbiat Modares University, Tehran, Iran, [2]Department of Forestry, Faculty of Natural Resources and Marine Sciences, Tarbiat Modares University, Tehran, Iran, [3]Soil and Water Research Institute, Agricultural Research Education and Extension Organization (AREEO), Karaj, Iran, [4]Silviculture and Forest Ecology of the Temperate Zones, Georg-August-Universität Göttingen, Göttingen, Germany, [5]Department of Agriculture, Food and Environment, University of Pisa, Pisa, Italy, [6]Department of Forestry and Wood Technology, Linnaeus University, Växjö, Sweden

OPEN ACCESS

Edited by:
Ying Ma,
University of Coimbra, Portugal

Reviewed by:
Nieves Goicoechea,
University of Navarra, Spain
Roxana Vidican,
University of Agricultural Sciences and Veterinary Medicine of Cluj-Napoca, Romania

***Correspondence:**
Martin K.-F. Bader
martin.bader@lnu.se
Masoud Tabari
mtabari@modares.ac.ir

Specialty section:
This article was submitted to Plant Symbiotic Interactions, a section of the journal Frontiers in Plant Science

Received: *09 March 2022*
Accepted: *22 April 2022*
Published: *27 May 2022*

Citation:
Azizi S, Tabari M, Abad ARFN, Ammer C, Guidi L and Bader MK-F (2022) Soil Inoculation With Beneficial Microbes Buffers Negative Drought Effects on Biomass, Nutrients, and Water Relations of Common Myrtle. Front. Plant Sci. 13:892826. doi: 10.3389/fpls.2022.892826

Common myrtle (*Myrtus communis* L.) occurs in (semi-)arid areas of the Palearctic region where climate change, over-exploitation, and habitat destruction imperil its existence. The evergreen shrub is of great economic and ecological importance due to its pharmaceutical value, ornamental use, and its role in urban greening and habitat restoration initiatives. Under greenhouse conditions, we investigated the effect of soil inoculation with arbuscular mycorrhizal fungi (AMF) and plant growth-promoting rhizobacteria (PGPR) on biomass allocation, water relations, and nutritional status of drought-stressed myrtle seedlings. Single and dual AMF (*Funneliformis mosseae* and *Rhizophagus irregularis*) and PGPR (*Pseudomonas fluorescens* and *P. putida*) soil inoculations were applied to myrtle seedlings growing under different soil water regimes (100, 60, and 30% of field capacity) for 6 months using a full factorial, completely randomized design. AMF and PGPR treatments, especially dual inoculations, alleviated negative drought effects on biomass and morpho-physiological traits, except for water-use efficiency, which peaked under severe drought conditions. Under the greatest soil water deficit, dual inoculations promoted leaf biomass (104%–108%), root biomass (56%–73%), mesophyll conductance (58%), and relative water content (1.4-fold) compared to non-inoculated controls. Particularly, dual AMF and PGPR inoculations stimulated nutrient dynamics in roots (N: 138%–151%, P: 176%–181%, K: 112%–114%, Ca: 124%–136%, and Mg: 130%–140%) and leaves (N: 101%–107%, P: 143%–149%, K: 83%–84%, Ca: 98%–107%, and Mg: 102%–106%). Our findings highlight soil inoculations with beneficial microbes as a cost-effective way to produce highly drought resistant seedling stock which is vital for restoring natural myrtle habitats and for future-proofing myrtle crop systems.

Keywords: arbuscular mycorrhizal fungi, plant growth-promoting rhizobacteria, water deficit stress, *Myrtus communis*, drought

INTRODUCTION

Drought is one of the most important environmental stresses limiting growth and metabolic processes in plants (Trenberth et al., 2014). Plant responses to drought depend on the severity and duration of the drought period and on the stage of plant development. Severe drought stress impairs physiological processes, inhibits growth, and may eventually lead to plant death (Anjum et al., 2011). Drought-related reductions in root water uptake hamper tissue hydration thereby increasing osmotic stress (Aroca et al., 2008) and decreasing leaf water potential, foliage quantity, and dry mass so that at each developmental stage nutrient uptake and transfer are reduced (Anjum et al., 2011). As a result of the drought-induced deterioration of plant water status, membrane permeability and transport processes decline and the reduced mass flow of nutrients affects root uptake and nutrient allocation in turn (Sardans et al., 2008).

Soil inoculation with arbuscular mycorrhizal fungi (AMF) and plant growth-promoting rhizobacteria (PGPR) is currently being widely explored as a new approach to alleviate detrimental drought effects and to enhance crop drought resistance in agriculture and horticulture in arid and semi-arid regions. However, its potential for sustainable arboriculture and restoration remains virtually unexplored. As keystone soil engineers, AMF can partially offset the negative effects of drought stress on plants by increasing root water and nutrient uptake (especially recalcitrant nutrients, such as P, Zn, and Cu), photosynthetic activity, the production of antioxidant enzymes, and not least because of their beneficial effects on the rhizosphere environment including the rhizomicrobiome (Kung'u et al., 2008; Bárzana et al., 2015; Yin et al., 2016). In particular, AMF improve soil structural quality through the formation of stable soil aggregates supported by hyphal exudates and the enmeshment of particles in mycelial networks resulting in enhanced nutrient and water availability as well as reduced soil erosion (Curaqueo et al., 2010; Mardhiah et al., 2016). The widespread AMF species *Funneliformis mosseae* and *Rhizophagus irregularis* occur in various habitats and have a vast host range making them prime candidates for crop yield and quality improvements under drought (Ortiz et al., 2015; Zhang et al., 2019). The genus *Pseudomonas* contains the most important growth-promoting bacteria that regulate the amount of ethylene through production of siderophores, plant hormones, synthesis of antibiotics, phosphorus absorption, nitrogen fixation, and synthesis of enzymes (Henry et al., 2008).

Investigations on the drought mitigation potential of soil microorganisms often show improvements in growth, physiological, and biochemical traits along with a higher uptake of water and mineral elements in inoculated plants (e.g., Ortiz et al., 2015; Ullah et al., 2016). The literature is heavily crop-dominated but the few studies on woody plants (mainly horticultural species) also suggest better water supply evidenced by favourabale plant water relations, enhanced macro- and micronutrient uptake, greater growth, larger osmoregulant pools, and an upregulation of the antioxidant defence in AMF- and/or PGPR-inoculated individuals under drought (Abbaspour et al., 2012; Danielsen and Polle, 2014; Zarik et al., 2016; Zhang et al., 2019).

The medicinal plant *Myrtus communis* L. is an evergreen shrub (<3 m tall) of the Myrtaceae family. It is native to southern Europe and western Asia and grows well in sub-Mediterranean climates (Sumbul et al., 2011) including some provinces of Iran. *Myrtus communis* has many pharmacological properties and contains active components, including essential oils such as depantine or myrtenol, and is therefore of economic interest to the pharmaceutical industry (Moghrani and Maachi, 2008). Habitat destruction and over-exploitation have pushed *M. communis* to the brink of extinction in its natural habitats in Iran and other regions of the world, where it used to form dense, extensive stands in the past (Amiri et al., 2015; González-Varo et al., 2015). Besides its widespread cultivation for ornamental and medicinal reasons, myrtle is well-suited for the rehabilitation of degraded lands and the development of parks and (sub-)urban green spaces in arid areas (Azizi et al., 2021).

To better manage current and future shortages of water resources projected under climate change scenarios, research aimed at improving myrtle drought resistance is urgently needed.

The present study is part of a larger, overarching project on myrtle responses to drought. In a complementary trial, using the same experimental setup, we previously investigated mycorrhizal colonization, seedling survival, growth, and leaf gas-exchange along with oxidative damage and antioxidant defense (Azizi et al., 2021). AMF and PGPR soil inoculation treatments increased seedling survival under drought. Especially the dual AMF and PGPR inoculations had a positive impact on foliar physiology and led to a substantial decrease in oxidative damage as evidenced by reduced levels of oxidative stress markers, less electrolyte leakage, and fewer pigment losses in drought-exposed seedlings. Soil microbial-driven increases in the pool size of enzymatic and non-enzymatic antioxidants, including essential oils, indicated an upregulation of the antioxidant defense system of the seedlings subjected to drought (Azizi et al., 2021).

In the present study, we tested whether soil inoculation with beneficial microorganisms provides a viable option for adaptive management of myrtle propagation for cultivation and reforestation. We investigated the potential of single and dual AMF and PGPR inoculation for mitigating drought effects on biomass, leaf water relations as well as root and foliar nutrient content of common myrtle. We hypothesized that AMF and PGPR inoculation will improve biomass production, water relations and nutrient status in leaves and roots of *M. communis* seedlings under drought. We further anticipated a stronger efficacy of dual vs. single microbial inoculations in terms of mitigating the detrimental effects of drought on productivity and physiological functioning.

MATERIALS AND METHODS

Experimental Design

In early July 2017, 2-year-old potted seedlings (6 ± 1 mm in root collar diameter, 37 ± 3 cm in shoot length) of *M. communis* (originated from seed) raised in the greenhouse of Faculty of

Agriculture, Tarbiat Modares University, Iran (35°44′ N, 51°10′ E, and 1,215 m a. s. l.), were transferred to 5-L plastic pots containing a mixed soil (agricultural soil, green manure + sand + coco peat in a ratio of 1: 1: 1: 2) with physico-chemical properties indicated in **Table 1**. The green manure consisted of decomposed plant litter originating from various local forest trees, mainly oak and hawthorn species (*Quercus* spp., *Crataegus* spp.) and pistachio (*Pistacia vera*).

The experiment was carried out as a 3 × 7 factorial (water regime × microorganism inoculation) in a completely randomized design with three replicates each comprising four seedlings. The following microorganism inoculation treatments were applied: (1) control (no inoculation), (2) AMF-inoculation with *Funneliformis mosseae*, (3) AMF-inoculation with *Rhizophagus irregularis*, (4) combined inoculation of *F. mosseae* + *R. irregularis*, (5) PGPR-inoculation with *Pseudomonas fluorescens*, (6) PGPR-inoculation with *Pseudomonas putida*, and (7) combined inoculation of *P. fluorescens* + *P. putida*. For mycorrhizal fungi 40 g of inoculum (100 propagules g^{-1} of carrier material) and for *Pseudomonas* bacteria 15 ml of inoculum containing 10^7 ml^{-1} live bacterial cell were used. For the dual AMF inoculation, 40 g of each fungus was used and for the dual PGPR treatment, 15 ml of each bacterium were applied. Inocula were prepared from the Microbial Bank of the Microbiology Department of the Soil and Water Research Institute of Tehran, Iran. Water deficit stress included 100% field capacity (FC100, no stress), 60% FC (FC60, mild stress), and 30% FC (FC30, severe stress). Drought stress was applied *via* the watering regime following Zarik et al. (2016) for 180 days.

Root Mycorrhizal Colonization

The percentage of AMF-colonized roots was assessed in a complementary study (Azizi et al., 2021). Mycorrhizal colonization in control plants was highest in the FC100 treatment (9.4%) and dropped by nearly 80% under FC30 conditions. By contrast, mycorrhization in singly and dually inoculated plants ranged from 51 to 72.7% under FC100 conditions and only halved in response to increasing water limitation.

Biomass Allocation

For biomass determination, one seedling of each replicate was removed from the soil and after rinsing off the soil attached to the roots, seedlings were separated into their main organs and dried at 70°C for 48 h. Then, a digital scale with an accuracy of 0.0001 g, was used to measure leaf biomass (LB), stem biomass (SB), and root biomass (RB).

Water Relations and Gas Exchange Parameters

At the end of the experiment, the intracellular CO_2 concentration (C_i) was measured using a portable gas exchange device LI-6400 (LiCor Inc., Lincoln, NE, United States). For this purpose, four fully developed, healthy leaves were selected from the top of the crown from each of three seedlings per treatment. Measurements were taken between 9 and 12 am on a sunny day with a light intensity of 1,400 µmol m^{-2} s^{-1} (Dong et al., 2017). To measure the relative water content (RWC), three healthy, fully developed leaves from the top of the crown from each of three seedlings per treatment were sampled. After determination of fresh weight (FW), the leaf samples were placed in distilled water in the dark for 24 h to maximize absorption for turgor weight (TW) determination. Then turgid leaves were placed in an oven at 70°C for 48 h. Leaf weight was measured after drying (DW) and RWC was calculated according to Equation (1) (Yang et al., 2007).

$$\mathrm{RWC} = \left[\left(\mathrm{FW} - \mathrm{DW}\right) / \left(\mathrm{TW} - \mathrm{DW}\right)\right] \times 100 \quad (1)$$

Following the results of photosynthesis and transpiration in our previous study (Azizi et al., 2021), mesophyll conductance (g_m) and water use efficiency (WUE) were determined according to Equations (2, 3) (Moradi-ghahderijani et al., 2017; Biswas et al., 2019).

$$g_m = \frac{A}{C_i} \quad (2)$$

$$\mathrm{WUE} = \frac{A}{E} \quad (3)$$

where, A = photosynthesis, C_i = intracellular CO_2 concentration, and E = transpiration.

Root and Leaf Nutrients

At the end of the experiment, a representative seedling per replicate (average height and diameter) was chosen and its root and leaves were washed and placed in an oven (at 70°C) for 48 h until dry weight was reached. For root and foliar nitrogen determination by the Kjeldahl method, 0.5 g powdered sample was weighed and transferred to digestion tubes. One catalyst tablet was added with 10 ml of concentrated sulfuric

TABLE 1 | Physico-chemical properties of the soil used for growing *Myrtus communis* seedlings.

Texture	Sand (%)	Clay (%)	Silt (%)	Bulk density (g cm^{-3})	FC (m^3 m^{-3})	PWP (m^3 m^{-3})	EC (dS m^{-1})	pH
Clay-loam	33	29	38	1.59	0.34	0.13	1.61	7.9
N (%)	**P (mg kg^{-1})**	**K (mg kg^{-1})**	**OC (%)**	**OM (%)**	**Fe (mg kg^{-1})**	**Zn (mg kg^{-1})**	**Mn (mg kg^{-1})**	
0.18	5.6	458	1.77	3.06	9.7	3.36	10	

PWP, permanent wilting point; EC, electrical conductivity; OC, organic carbon content; and OM, organic matter content.

acid. The tubes were placed in a digestion furnace for 3–4 h at 40°C (until the color of the samples turned blue). After cooling, 10 ml of distilled water was added to each of the tubes prior to titration (Chapman and Pratt, 1962).

To measure phosphorus content a calorimetric method (yellow color of molybdate and vanadate) was utilized. After digestion of 1 g of powdered leaf and root sample, 5 ml of extract was poured into a 25 ml balloon and 5 ml of ammonium molybdate vanadate solution was added. Then, absorbance at 480 nm was read using a spectrophotometer (Lambda 45-UV/Visible, PerkinElmer, Waltham, MA, United States; Chapman and Pratt, 1962).

To measure the concentration of K, Ca, and Mg of roots and leaves, the samples were dried in an oven at 48°C for 48 h (Ribeiro et al., 2002). Then, 1 g of dried and powdered sample material was mixed with 10 ml of concentrated nitric acid and after staying under the hood for 12 h, it was exposed to 80°C for 2 h. The prepared solution after mixing with 3 ml of concentrated perchloric acid was kept at 160°C for 5 h. After cooling, the prepared samples were smoothed with filter paper and reached the 25 ml volume. Then, the content of the above elements was assessed using an atomic absorption spectrometer (Ribeiro et al., 2002).

Statistical Analysis

The data were analyzed using SPSS statistical software version 23 (SPSS Inc., Chicago, IL, United States), and graphs were drawn in Excel software version 2016 (Microsoft Office, 2016). Kolmogorov–Smirnov and Levene tests were used to evaluate the normality and variance homogeneity of the data, respectively. Two-way ANOVA was used to determine the overall significance of the treatments, and Duncan's new multiple range test was used as a *post hoc* test to compare differences between group means.

RESULTS

The two-way ANOVA revealed a significant water regime × microbial inoculation effect on organ-specific biomass, mesophyll conductance, relative water content, and root P and leaf Mg contents. All variables that remained unaffected by the two-way interaction were significantly influenced by the two main effects, apart from water use efficiency, which only showed a significant response to the water regime (**Table 2**).

Biomass Allocation

The detrimental effects of drought were evident in dry mass of all organs (**Table 2**). However, single AMF and PGPR inoculations (partly) compensated and dual inoculations sometimes even overcompensated the negative effects of drought stress compared to the well-watered, non-inoculated control (**Figures 1A–C**). For instance, in the FC60 treatment, dual inoculation almost always resulted in significantly larger biomass accrual than both the FC60 and the FC100 non-inoculated control. The strongest inoculation effects occurred in the FC30 treatment of leaf biomass, where dual AMF and PGPR more than doubled the values seen in the control (**Figure 1A**). The stimulation under severe drought was less pronounced in roots, where dual AMF inoculation produced 73% higher biomass than the control, but this was not statistically different from the magnitude seen in single AMF inoculations. Similarly, the dual PGPR inoculation stimulated root biomass significantly by 56%, but this was not significantly different from the increase related to single PGPR inoculations (**Figure 1B**). Under severe drought, only the single *R. irregularis* inoculation, the dual AMF and the dual PGPR inoculation caused significant increases in

TABLE 2 | Results of a two-way ANOVA testing the effect of microorganism inoculation on biomass allocation, water relations, and elemental concentration of *M. communis* seedlings under three different water regimes (100, 60, and 30% of field capacity).

	Water regime		Inoculation		Water regime × inoculation	
Traits	***df***	***F* value**	***df***	***F* value**	***df***	***F* value**
Leaf biomass	2	150.05***	6	19.87***	12	2.05*
Stem biomass	2	92.32***	6	10.73***	12	0.585^{ns}
Root biomass	2	365.78***	6	30.29***	12	3.33**
Intracellular CO_2 concentration	2	618.80***	6	18.21***	12	0.446^{ns}
Mesophyll conductance	2	815.02***	6	33.34***	12	6.44**
Water use efficiency	2	4.84*	6	0.316^{ns}	12	0.176^{ns}
Relative water content	2	456.07***	6	14.21***	12	2.19*
N root	2	733.15***	6	25.28***	12	0.189^{ns}
P root	2	1578.17***	6	35.15***	12	2.06*
K root	2	1403.53***	6	27.88***	12	0.837^{ns}
Ca root	2	409.95***	6	11.75***	12	0.655^{ns}
Mg root	2	698.02***	6	15.03***	12	0.823^{ns}
N leaf	2	671.28***	6	19.59***	12	1.39^{ns}
P leaf	2	2642.19***	6	51.48***	12	1.38^{ns}
K leaf	2	2126.72***	6	60.42***	12	1.47^{ns}
Ca leaf	2	597.77***	6	16.55***	12	0.26^{ns}
Mg leaf	2	504.173***	6	16.70***	12	2.34*

^{ns}*No significant difference.*
*$p \leq 0.05$; **$p \leq 0.01$; ***$p \leq 0.001$.*

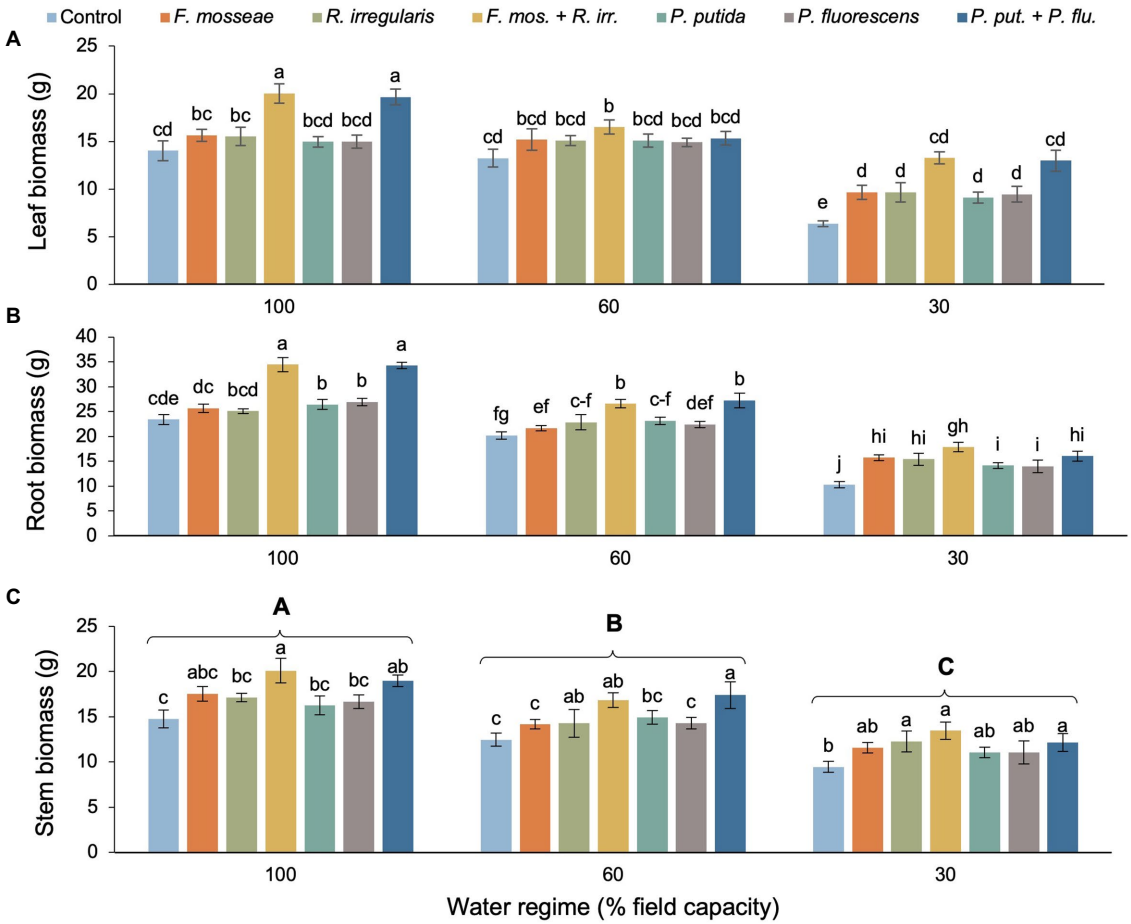

FIGURE 1 | Effect of water regime and soil microbial inoculation on the biomass allocation of *Myrtus communis* seedlings. For leaf biomass and root biomass there was a significant water regime × inoculation treatment interaction (**Table 2**), hence different lower-case letters indicate statistically significant differences across the 21 treatment combinations. For stem biomass, only the main effects of water regime and inoculation treatment were significant (**Table 2**), thus upper-case letters indicate a significant difference between different levels of drought stress and lower-case letters indicate a significant difference between different inoculation treatments within a water regime (Duncan's new multiple range test, $\alpha = 0.05$).

stem biomass compared to the control. The stem biomass values linked to the remaining inoculation treatments were in between the values of the control and the three effective inoculation treatments and therefore did not differ significantly from either (**Figure 1C**).

Water Relations

There was neither a statistically significant two-way interaction nor a microbial inoculation effect on seedling WUE (**Table 2**; **Figure 2A**). However, the severe drought treatment (FC30) produced significantly higher WUE compared to the remaining watering regimes, which showed similar values (**Figure 2A**). We did not detect a significant water regime × microbial inoculation interaction but both main effects were statistically significant (**Table 2**). Irrespective of the inoculation treatment, the intracellular CO_2 concentration (C_i) increased significantly with increasing drought stress (**Figure 2B**). Regardless of the water regime, the dual AMF inoculation induced significantly lower C_i values than the control and single inoculations (**Figure 2B**). In the FC30 treatment, the dual AMF treatment caused an 11% decrease in C_i compared to non-inoculated control seedlings (**Figure 2B**). A similar pattern was seen for the dual PGPR inoculation treatment across drought conditions, except for the FC30 group, where seedlings dually inoculated with PGPR showed C_i values that were significantly lower than the control but similar to all singly inoculated seedlings (**Figure 2B**).

Mesophyll conductance (g_m) declined with increasing soil water deficit, but this effect varied with inoculation treatment resulting in a significant two-way interaction (**Table 2**; **Figure 3A**). Dual AMF and PGPR inoculation caused the highest g_m values in well-irrigated (+86% relative to the control) and mildly drought-stressed seedlings (+63%–66% relative to the control; **Figure 3A**). Under severe water deficit, dual AMF and PGPR inoculation increased g_m by 64 and 57%, respectively, compared to the non-inoculated control (**Figure 3A**).

Water regime and microbial inoculation also had a significant interactive effect on RWC (**Table 2**). Dual AMF

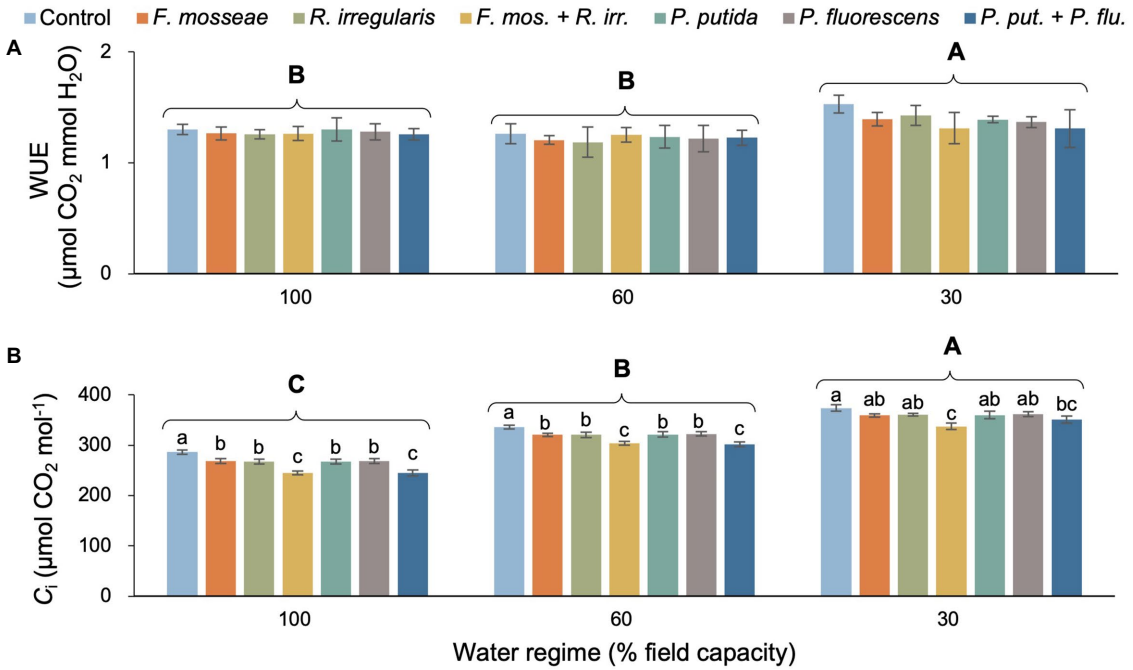

FIGURE 2 | Effect of water regime and soil microbial inoculation on the water use efficiency (WUE; **A**) and intracellular CO_2 concentration (C_i; **B**) of *M. communis* seedlings. For both variables, only the main effects of water regime and inoculation treatment were significant (**Table 2**). Different upper-case letters indicate significant differences between water regimes. Different lower-case letters indicate significant differences between microbial inoculation treatments within each water regime (Duncan's new multiple range test, $\alpha = 0.05$).

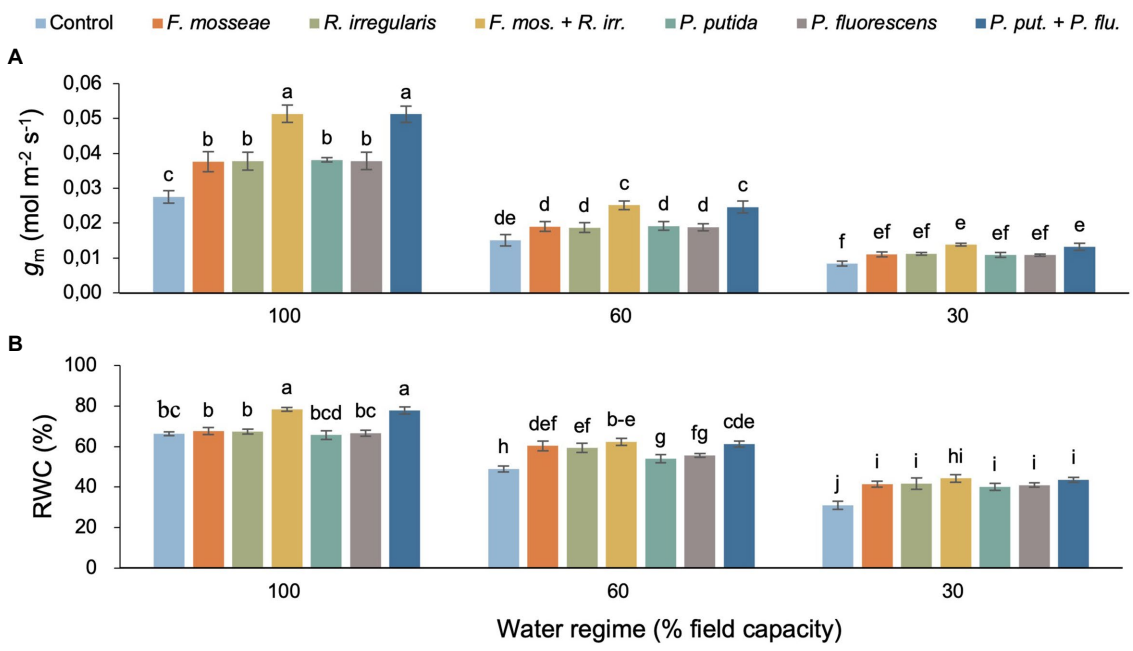

FIGURE 3 | The interaction effect of water regime and soil microbial inoculation on the mesophyll conductance (g_m; **A**) and relative water content (RWC; **B**) of *M. communis* seedlings. For both variables, there was a significant water regime × inoculation treatment interaction. Different lower-case letters thus indicate significant differences between microbial inoculation treatments across water regimes (Duncan's new multiple range test, $\alpha = 0.05$).

and PGPR inoculation significantly promoted leaf RWC in well-irrigated seedlings while single inoculations had no effect (**Figure 3B**). Under FC60 conditions, all AMF inoculations equally improved RWC relative to the control

(>20%) and a similar increase was seen in the dual PGPR treatment (**Figure 3B**). The effects of the single PGPR inoculations were slightly less pronounced but still represented a significant improvement compared to the control (**Figure 3B**). Under severe drought (FC30), all microbial inoculations significantly increased foliar RWC between 30 and 43% without significant differences among inoculation treatments (**Figure 3B**).

Root Nutrient Concentration

Except for P, there was no significant interaction between water regime and microbial inoculation for any of the tested root nutrients but both main effects were statistically significant (**Table 2**). With increasing drought stress, root N, P, K, Ca, and Mg content decreased, but the addition of AMF and PGPR, especially the dual inoculations, significantly improved the nutrient status of seedling roots (**Figures 4A–E**). Across

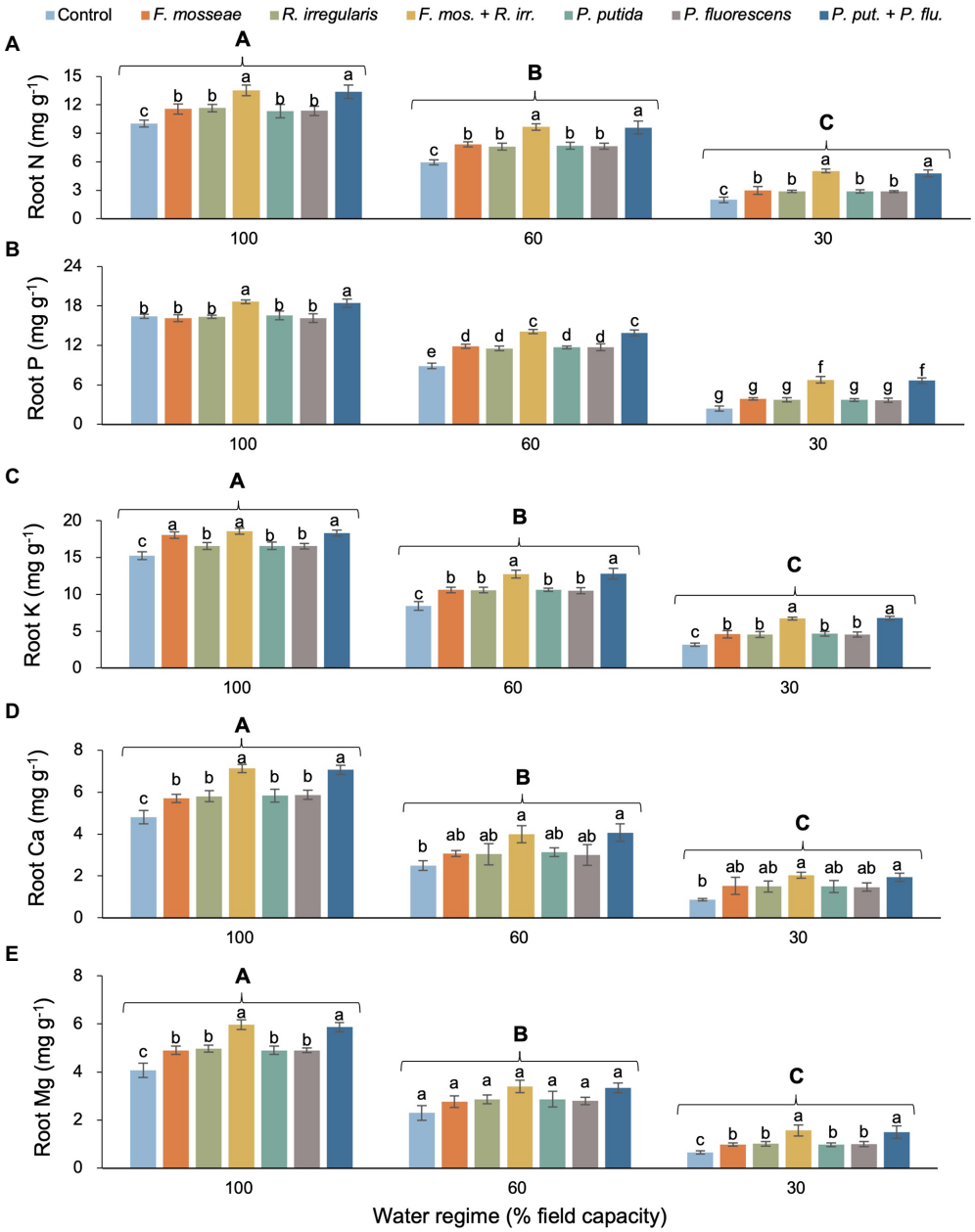

FIGURE 4 | Effect of water regime and soil microbial inoculation on the root N **(A)**, P **(B)**, K **(C)**, Ca **(D)**, and Mg **(E)** of *M. communis* seedlings (expressed on a dry weight basis). A significant water regime × inoculation treatment interaction only occurred for root P, while for all other root nutrients only the main effects were statistically significant. Accordingly, different lower-case letters indicate significant differences between microbial inoculation treatments across levels of water deficit for root P but only within water regimes in the remaining root nutrients (Duncan's new multiple range test, $\alpha = 0.05$). Different upper-case letters indicate significant differences between water regimes (Duncan's new multiple range test, $\alpha = 0.05$).

inoculation treatments, root N declined by 32% in mildly drought-stressed seedlings and by 72% under severe drought compared to well-watered control conditions (**Figure 4A**). Across water regimes, we observed the same inoculation-induced stimulatory pattern: all single AMF and PGPR inoculations caused similar increases in root N relative to the non-inoculated control (FC100: *ca.* 16%, FC60: *ca.* 30%, and FC30: *ca.* 45%), and the dual inoculations had even larger effects of equal magnitude among AMF and PGPR (FC100: *ca.* 34%, FC60: *ca.* 62%, and FC30: *ca.* 145%; **Figure 4A**).

Root P also showed a general decline with increasing drought intensity, but remarkably, single AMF and PGPR inoculations failed to improve root P status over the non-inoculated control in the FC100 and FC30 treatments (**Figure 4B**). Only under mild drought stress (FC60), single microbial inoculations significantly promoted root P uptake by a similar magnitude in comparison to the control. However, across water regimes, dual inoculations resulted in the largest increase in root P, significantly exceeding values seen in singly inoculated and control seedlings (**Figure 4B**). Root K, Ca, and Mg decreased by more than half with increasing drought intensity (**Figures 4C–E**). Within water regimes, single AMF and PGPR inoculations mostly stimulated K, Ca, and Mg content significantly, but the dual AMF and PGPR inoculations always had a far greater effect of equal magnitude (**Figures 4C–E**).

In the most severe drought regime (FC30), the dual AMF or PGPR inoculation increased root N by 151%–138%, P by 176%–181%, K by 114%–112%, Ca by 126%–136%, and Mg by 130%–140% compared to non-inoculated seedlings (**Figure 4**).

Foliar Nutrient Concentration

We found no evidence of a statistically significant interaction between water regime and microbial inoculation for any of the measured leaf nutrients apart from Mg (**Table 2**). However, as main effects, both water regime and microbial inoculation had a significant influence on foliar nutrient concentration. Regardless of the inoculation treatment, increasing water deficit reduced foliar N, P, K Ca, and Mg by at least about 50% (**Figures 5A–E**). In most cases, single AMF or PGPR inoculation caused a significant increase of similar magnitude in foliar nutrient status compared to non-inoculated controls (**Figures 5A–E**). However, peak foliar nutrient concentrations were invariably associated with dual AMF and PGPR inoculations (both with the same effect size) and the differences to singly inoculated seedlings and the non-inoculated control were almost always statistically significant (except for leaf N in the FC60 treatment and Mg in the FC100 treatment; **Figures 5A–E**). In the FC30 treatment, dual AMF and PGPR inoculations promoted N concentration by 102%–107%, P by 143%–149%, K by 83%–84%, Ca by 10%–98%, and Mg by 102%–106% compared to the non-inoculated control (**Figures 5A–E**).

DISCUSSION

Myrtus communis is an ecologically important species in its natural range and economically significant in (semi-)arid growing areas around the world. However, the rapidly changing climate complicates cultivation and, together with land use change and rampant illegal harvesting, imperils natural habitats (Amiri et al., 2015). In this study, we therefore tested whether AMF and PGPR inoculation may enhance the drought resistance of common myrtle to support habitat restoration programs in its native range and promote sustainable cultivation practices across the globe.

Biomass Allocation

Foliage, stem, and root biomass decreased with increasing drought stress, but the inoculation with microorganisms, especially the dual AMF and PGPR inoculations fully or at least partially compensated for the negative effects of drought stress when compared to the uninoculated, well-watered control (**Figure 1**). A reduction in leaf area and thus leaf biomass provides an effective means to curtail water use and is a common adaptation to drought in many plant species (Larcher, 2003). Our companion study showed drought-induced reductions in foliar gas-exchange of the myrtle seedlings that were fully or partially compensated by dual AMF or PGPR inoculation in the FC60 and FC30 treatments, respectively (Azizi et al., 2021). Growth processes have been shown to respond more sensitively to abiotic stresses (such as drought) than photosynthesis and it is therefore likely that the growth reductions seen in the stems and roots of our myrtle seedlings are due to carbon sink limitation rather than a limited supply of photo-assimilates (Palacio et al., 2013). Moreover, lack of soil water at any plant growth stage reduces the absorption, transport, and metabolization of nutrients, impairing carbon storage and dry matter (Hu and Schmidhalter, 2005). A disruption of the root-soil interface, which can already occur under mild drought stress, results in substantial losses in root conductivity triggering stomatal closure prior to the onset of cavitation (Kumar et al., 2010; Rodriguez-Dominguez and Brodribb, 2020). However, AMF-induced changes in root morphology and the vast hyphal-driven expansion of the root system strongly increase root uptake and nutrient transport (Orfanoudakis et al., 2010). PGPR also effectively improve seed germination, accelerate growth in the early stages, induce root formation, and increase the number of root hairs (Heinonsalo et al., 2004). Some rhizobacteria contain the enzyme 1-aminocyclopropane-1-carboxylate (ACC) deaminase that reduces the production of ethylene, which in turn regulates auxin synthesis and allocation, ultimately leading to stimulation of root growth (Xie et al., 1996; Růžička et al., 2007). Both *Pseudomonas* species used in our study have been shown to produce ACC (Saravanakumar and Samiyappan, 2007; Gamalero et al., 2008) suggesting that the increase in root growth observed in our myrtle seedlings is related to ACC activity. Increasing biomass and growth of various crops (e.g., rice, foxtail millet, and peppermint) resulting from AMF and PGPR soil inoculation during drought conditions have also been reported in agreement with our findings (Ruíz-Sánchez et al., 2011; Gong et al., 2015; Chiappero et al., 2019).

Water Relations

In line with the results reported for *Juglans regia* and *Eucaplytus camaldulensis*, WUE remained unaffected by soil microbial

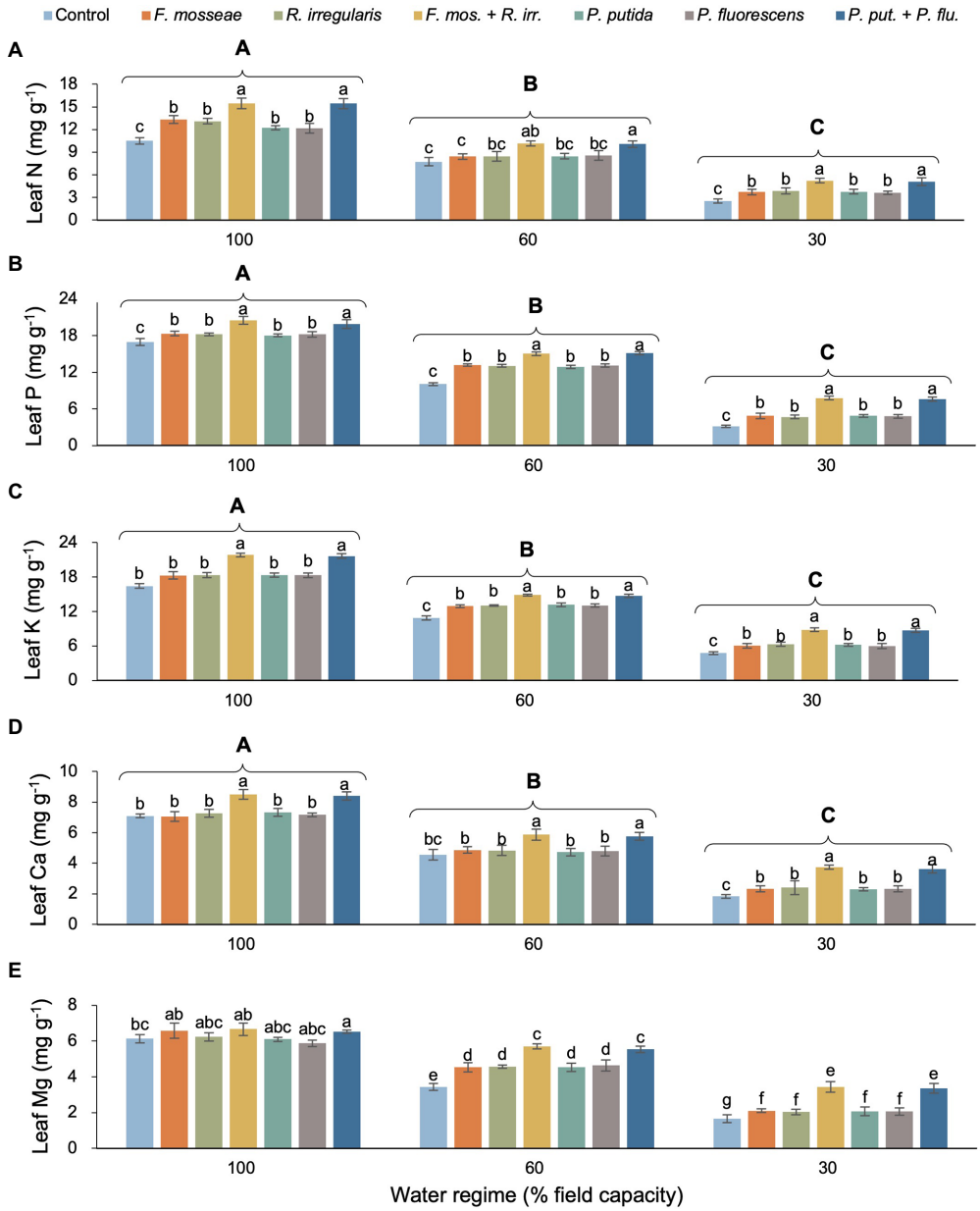

FIGURE 5 | Effect of water regime and soil microbial inoculation on leaf N **(A)**, P **(B)**, K **(C)**, Ca **(D)**, and Mg **(E)** of *M. communis* seedlings (expressed on a dry weight basis). Water regime and inoculation treatment had significant main effects on all shown leaf nutrients but a water regime × inoculation treatment interaction only occurred for leaf Mg (**Table 2**). Therefore, different lower-case letters indicate significant differences between microbial inoculation treatments across water regimes for leaf Mg but only within water regimes in the remaining root nutrients (Duncan's new multiple range test, $\alpha = 0.05$). Different upper-case letters indicate significant differences between water regimes (Duncan's new multiple range test, $\alpha = 0.05$).

inoculation (Liu et al., 2019; Mateus et al., 2021), but increased with increasing drought intensity in our myrtle seedlings (**Figure 2**). Water deficit affects photosynthesis and transpiration to different degrees, resulting in significant differences in WUE (El Hafid et al., 1998). WUE usually rises under drought stress, but this increase is not associated with enhanced production because the increase is driven by reduced transpiration rather than an increase in photosynthetic carbon assimilation (Blum, 2009). In the present study, g_m decreased with increasing water deficit stress, probably linked to reduced leaf water status and thus tissue hydration (Azizi et al., 2021; **Figure 3**). Lower rates of photosynthetic CO_2 assimilation in the presence of higher levels of C_i indicate low g_m and impaired carbon metabolism of mesophyll cells (Ratnayaka and Kincaid, 2005). Microbial soil inoculation, particularly dual AMF and PGPR applications, mitigated drought-related reductions in g_m, which was mirrored by lower C_i values indicating greater utilization of absorbed CO_2. Similar findings in terms of C_i and g_m were

obtained with *Azospirillum brasilense* and *Bacillus* sp. in seedlings of the tropical canopy tree *Cariniana estrellensis* (Tiepo et al., 2018), and with *Rhizophagus irregularis* in seedlings of *Robinia pseudoacacia* (He et al., 2016) under drought conditions.

The RWC of *M. communis* seedlings decreased with increasing drought stress, but soil inoculation with AMF or PGPR (especially the dual inoculations) largely or fully compensated for these declines in the FC60 treatment (also compared to the well-watered and uninoculated control) and still had a positive, albeit less pronounced, effect in the FC30 treatment (**Figure 3**). A similar pattern was observed for leaf water potential of these myrtle seedlings published recently as part of the overarching study (Azizi et al., 2021). *Cupressus atlantica* and tropical tree seedlings also showed increases in leaf RWC in response to AMF or PGPR treatments (Zarik et al., 2016; Tiepo et al., 2018). AMF hyphal networks greatly expand the root surface thus giving plants access to a larger soil volume and because of their small diameter they can grow into the smallest pores and crevices that fine roots could not reach. The symbiosis with AMF allows plants to take up more water and thus maintain favorable water relations over a wider range of environmental conditions and under drought, AMF have been shown to be able to increase hyphal moisture uptake (Augé et al., 2015). PGPR have been demonstrated to improve the water relations of seedlings by producing phytohormones that favorably affect plant water relations such as abscisic acid and auxin (Kothari et al., 1990; Boiero et al., 2007).

Root and Leaf Nutrient Concentration

Root and leaf N concentration decreased under water deficit conditions, but the soil inoculation treatments (especially dual AMF or PGPR inoculations) partially offset the negative drought effects on plant nutrient dynamics compared the non-inoculated control seedlings (**Figure 5**). These results are consistent with the studies of Abbaspour et al. (2012) on *Pistacia vera* seedlings and with those of Armada et al. (2015) on *Zea mays*. Rhizosphere bacteria increase the rate of nitrate translocation from root to shoot by increasing the amount of cytokinin in the host plant (Flores et al., 2005).

Mycorrhizal fungi also activate glutamine synthetase, arginase, and urease by affecting root physiology and thus increase the N uptake and utilization efficiency of host plants. Arginase and urease are key enzymes in the transfer of N from the mycelium to the roots of the host plant. Several ammonium and nitrate transporters have been identified in the mycelium of AMF (Tisserant et al., 2012) enabling mycelial N uptake in the form of nitrate or ammonium and subsequent conversion to organic compounds by glutamine synthetase (Bago et al., 2001).

In agreement with the findings of Zhang et al. (2019) and Ortiz et al. (2015), root and leaf P content in our myrtle seedlings decreased with increasing drought stress but AMF and PGPR inoculation mitigated this effect (**Figure 5**). While both single and dual inoculations produced significant positive effects in leaf P, root P responded more strongly to the dual inoculation treatments. This finding implies that multiple AMF or PGPR acting in concert are required to significantly increase P availability and subsequent root uptake while the activity of single AMF or PGPR species seems to be sufficient to steer allocation toward increased P supply to the leaves. Phosphorous plays an important role in many plant physiological processes linked to energy storage and transfer, photosynthesis, regulation of enzyme activity, and carbohydrate transport and it also affects plant water relations (Waraich et al., 2011). Numerous studies have shown that following AMF inoculation, P uptake in plants increases under stress conditions (Garg and Manchanda, 2008; Bowles et al., 2016), which has been attributed to the secretion of organic acids and phosphatase enzymes solubilizing inorganic P from soil minerals and mineralizing organic P sources (Subramanian et al., 2006).

Water deficit stress negatively affected root and leaf K of *M. communis* seedlings, but the inoculation treatments, especially the dual AMF and PGPR inoculations increased K uptake in both organs (**Figure 5**). Potassium is crucial for turgor control and thus for cell expansion during growth and guard cell osmoregulation (stomatal control), not to mention its key role in maintaining plasma membrane potential. The amount of plant-available K depends on the K content in the soil solution and the level of exchangeable K (Haby et al., 1990). Both K sources may increase in the presence of AMF and PGPR through organic acid-mediated silicate weathering and mineral dissolution causing the release of K thus allowing plants to increase their uptake (Campanelli et al., 2013).

Calcium plays a vital role in the regulation of many physiological processes in plants, thereby affecting growth processes and responses to environmental stresses. For example, the movement of water and dissolved mineral salts is affected by Ca through its influence on membrane structure and stomatal function, cell division, and cell wall construction (Hu and Schmidhalter, 2005). However, under water deficit stress, reduced water uptake and curtailed transpiration result in a decrease in leaf Ca content (Maksimović et al., 2003). In line with the findings of Dominguez-Nuñez et al. (2014) on *Pinus halepensis* and Meddich et al. (2015) on *Phoenix dactylifera*, we observed AMF- and PGPR-induced increases in root and foliar Ca contents of myrtle seedlings (**Figure 5**). Apart from increases in Ca availability resulting from the exploitation of a larger soil volume through AMF hyphae and accelerated mineral weathering linked to PGPR secretions, the positive inoculation effect on Ca levels in myrtle seedlings may in part be due to increases in stomatal conductance and transpiration given the role of xylem sap flow in Ca mobility (Ruiz-Lozano et al., 1995; Wu and Xia, 2006; Garg and Bhandari, 2016; Azizi et al., 2021).

A very similar pattern of drought-induced decrease was observed for Mg contents in roots and leaves of *Myrtus* seedlings exposed to drought (**Figure 5**). Under water deficit stress, single and dual inoculations with AMF or PGPR increased the Mg content in seedling roots and foliage which is consistent with the results of Danielsen and Polle (2014) on *Populus* × *canescens* and Armada et al. (2015) on *Zea mays*. The increase in Mg uptake is probably due to the hyphal expansion of the root system and consequently enhanced uptake of this element by the plant in the case of AMF and likely results from microbial solubilization of Mg-bearing carbonates and minerals in the PGPR treatments (Smith and Read, 2008; Evelin et al., 2012).

Our study revealed that, depending on drought intensity, AMF or PGPR inoculation can largely or at least partially offset the detrimental effects of drought on biomass production,

water relations, and nutrient dynamics of *M. communis* seedlings. Especially the dual inoculations proved to be very potent suggesting even greater benefits from inoculations including multiple AMF and PGPR species. These findings motivate further research testing the effects of combined AMF and PGPR inoculations and linked to this, determining the composition of the microbial consortium that optimally supports myrtle health and performance. Most importantly though, our results highlight soil inoculations with beneficial microorganisms as a cost-effective, easy-to-use tool to promote drought resistance of myrtle. Such readily applicable approaches are urgently needed in support of conservation initiatives geared toward restoring natural myrtle populations and habitats. At the same time, such methods can be used to refine operational nursery practices to help future-proof myrtle cultivation.

Resource Identification Initiative

https://scicrunch.org/resolver/RRID:SCR_016479

DATA AVAILABILITY STATEMENT

The raw data supporting the conclusions of this article will be made available by the authors, without undue reservation.

AUTHOR CONTRIBUTIONS

SA conducted the experiments, helped devise the study design, and wrote the first draft with help of MT. MT, main supervisor of SA, devised the idea and study design and co-wrote the first draft. AA provided technical input and assistance. CA and LG provided editorial input. MB guided the analysis and writing process of earlier versions and wrote the final version of the manuscript. All authors contributed to the article and approved the submitted version.

FUNDING

This study was fully funded by the Tarbiat Modares University, Iran.

ACKNOWLEDGMENTS

We thank Tarbiat Modares University for providing the research facilities and its Departments of Agriculture and Forest Science and Engineering for providing laboratory space and equipment.

REFERENCES

Abbaspour, H., Saeidi-Sar, S., Afshari, H., and Abdel-Wahhab, M. A. (2012). Tolerance of mycorrhiza infected pistachio (*Pistacia vera* L.) seedling to drought stress under glasshouse conditions. *J. Plant Physiol.* 169, 704–709. doi: 10.1016/j.jplph.2012.01.014

Amiri, N., Emadian, S. F., Fallah, A., Adeli, K., and Amirnejad, H. (2015). Estimation of conservation value of myrtle (*Myrtus communis*) using a contingent valuation method: a case study in a Dooreh forest area, Lorestan Province, Iran. *For. Ecosyst.* 2, 1–11. doi: 10.1186/s40663-015-0051-6

Anjum, S. A., Xie, X., Wang, L., Saleem, M. F., Man, C., Lei, W., et al. (2011). Morphological, physiological and biochemical responses of plants to drought stress. *Afr. J. Agric. Res.* 6, 2026–2032. doi: 10.5897/AJAR10.027

Armada, E., Azcón, R., López-Castillo, O. M., Calvo-Polanco, M., and Ruiz-Lozano, J. M. (2015). Autochthonous arbuscular mycorrhizal fungi and *Bacillus thuringiensis* from a degraded Mediterranean area can be used to improve physiological traits and performance of a plant of agronomic interest under drought conditions. *Plant Physiol. Biochem.* 90, 64–74. doi: 10.1016/j.plaphy.2015.03.004

Aroca, R., Del Mar Alguacil, M., Vernieri, P., and Ruiz-Lozano, J. M. (2008). Plant responses to drought stress and exogenous ABA application are modulated differently by mycorrhization in tomato and an ABA-deficient mutant (Sitiens). *Microb. Ecol.* 56, 704–719. doi: 10.1007/s00248-008-9390-y

Augé, R. M., Toler, H. D., and Saxton, A. M. (2015). Arbuscular mycorrhizal symbiosis alters stomatal conductance of host plants more under drought than under amply watered conditions: a meta-analysis. *Mycorrhiza* 25, 13–24. doi: 10.1007/s00572-014-0585-4

Azizi, S., Tabari Kouchaksaraei, M., Hadian, J., Fallah Nosrat Abad, A. R., Modarres Sanavi, S. A. M., Ammer, C., et al. (2021). Dual inoculations of arbuscular mycorrhizal fungi and plant growth-promoting rhizobacteria boost drought resistance and essential oil yield of common myrtle. *For. Ecol. Manag.* 497:119478. doi: 10.1016/j.foreco.2021.119478

Bago, B., Pfeffer, P., and Shachar-Hill, Y. (2001). Could the urea cycle be translocating nitrogen in the arbuscular mycorrhizal symbiosis? *New Phytol.* 149, 4–8. doi: 10.1046/j.1469-8137.2001.00016.x

Bárzana, G., Aroca, R., and Ruiz-Lozano, J. M. (2015). Localized and non-localized effects of arbuscular mycorrhizal symbiosis on accumulation of osmolytes and aquaporins and on antioxidant systems in maize plants subjected to total or partial root drying. *Plant Cell Environ.* 38, 1613–1627. doi: 10.1111/pce.12507

Biswas, D. K., Ma, B. L., and Morrison, M. J. (2019). Changes in leaf nitrogen and phosphorus content, photosynthesis, respiration, growth, and resource use efficiency of a rapeseed cultivar as affected by drought and high temperatures. *Can. J. Plant Sci.* 99, 488–498. doi: 10.1139/cjps-2018-0023

Blum, A. (2009). Effective use of water (EUW) and not water-use efficiency (WUE) is the target of crop yield improvement under drought stress. *Field Crop Res.* 112, 119–123. doi: 10.1016/j.fcr.2009.03.009

Boiero, L., Perrig, D., Masciarelli, O., Penna, C., Cassán, F., and Luna, V. (2007). Phytohormone production by three strains of *Bradyrhizobium japonicum* and possible physiological and technological implications. *Appl. Microbiol. Biotechnol.* 74, 874–880. doi: 10.1007/s00253-006-0731-9

Bowles, T. M., Barrios-Masias, F. H., Carlisle, E. A., Cavagnaro, T. R., and Jackson, L. E. (2016). Effects of arbuscular mycorrhizae on tomato yield, nutrient uptake, water relations, and soil carbon dynamics under deficit irrigation in field conditions. *Sci. Total Environ.* 566-567, 1223–1234. doi: 10.1016/j.scitotenv.2016.05.178

Campanelli, A., Ruta, C., De Mastro, G., and Morone-Fortunato, I. (2013). The role of arbuscular mycorrhizal fungi in alleviating salt stress in *Medicago sativa* L. var. icon. *Symbiosis* 59, 65–76. doi: 10.1007/s13199-012-0191-1

Chapman, H. D., and Pratt, P. F. (1962). Methods of analysis for soils, plants and waters. *Soil Sci.* 93:68. doi: 10.1097/00010694-196201000-00015

Chiappero, J., Cappellari, L. D. R., Sosa Alderete, L. G., Palermo, T. B., and Banchio, E. (2019). Plant growth promoting rhizobacteria improve the antioxidant status in *Mentha piperita* grown under drought stress leading to an enhancement of plant growth and total phenolic content. *Ind. Crop. Prod.* 139:111553. doi: 10.1016/j.indcrop.2019.111553

Curaqueo, G., Acevedo, E., Cornejo, P., Seguel, A., Rubio, R., and Borie, F. (2010). Tillage effect on soil organic matter, mycorrhizal hyphae and aggregates in a mediterranean agroecosystem. *Rev. Cienc. Suelo Nutr. Veg.* 10, 12–21. doi: 10.4067/S0718-27912010000100002

Danielsen, L., and Polle, A. (2014). Poplar nutrition under drought as affected by ectomycorrhizal colonization. *Environ. Exp. Bot.* 108, 89–98. doi: 10.1016/j.envexpbot.2014.01.006

Dominguez-Nuñez, J. A., Delgado-Alvez, D., Berrocal-Lobo, M., Anriquez, A., and Albanesi, A. (2014). Controlled-release fertilizers combined with *Pseudomonas fluorescens* rhizobacteria inoculum improve growth in *Pinus halepensis* seedlings. *IForest* 8, 12–18. doi: 10.3832/ifor1110-007

Dong, J., Li, X., Chu, W., Duan, Z., Dong, J., Li, X., et al. (2017). High nitrate supply promotes nitrate assimilation and alleviates photosynthetic acclimation of cucumber plants under elevated CO_2. *Sci. Hortic.* 218, 275–283. doi: 10.1016/j.scienta.2016.11.026

El Hafid, R., Smith, D. H., Karrou, M., and Samir, K. (1998). Physiological responses of spring durum wheat cultivars to early-season drought in a Mediterranean environment. *Ann. Bot.* 81, 363–370. doi: 10.1006/anbo.1997.0567

Evelin, H., Giri, B., and Kapoor, R. (2012). Contribution of *Glomus intraradices* inoculation to nutrient acquisition and mitigation of ionic imbalance in NaCl-stressed *Trigonella foenum-graecum*. *Mycorrhiza* 22, 203–217. doi: 10.1007/s00572-011-0392-0

Flores, E., Frías, J. E., Rubio, L. M., and Herrero, A. (2005). Photosynthetic nitrate assimilation in cyanobacteria. *Photosynth. Res.* 83, 117–133. doi: 10.1007/s11120-004-5830-9

Gamalero, E., Berta, G., Massa, N., Glick, B. R., and Lingua, G. (2008). Synergistic interactions between the ACC deaminase-producing bacterium *pseudomonas putida* UW4 and the AM fungus Gigaspora rosea positively affect cucumber plant growth. *FEMS Microbiol. Ecol.* 64, 459–467. doi: 10.1111/j.1574-6941.2008.00485.x

Garg, N., and Bhandari, P. (2016). Silicon nutrition and mycorrhizal inoculations improve growth, nutrient status, K+/Na+ ratio and yield of *Cicer arietinum* L. genotypes under salinity stress. *Plant Growth Regul.* 78, 371–387. doi: 10.1007/s10725-015-0099-x

Garg, N., and Manchanda, G. (2008). Effect of arbuscular mycorrhizal inoculation on salt-induced nodule senescence in *Cajanus cajan* (pigeonpea). *Plant Growth Regul.* 27, 115–124. doi: 10.1007/s00344-007-9038-z

Gong, M., You, X., and Zhang, Q. (2015). Effects of *Glomus intraradices* on the growth and reactive oxygen metabolism of *foxtail millet* under drought. *Ann. Microbiol.* 65, 595–602. doi: 10.1007/s13213-014-0895-y

González-Varo, J. P., Albaladejo, R. G., Aizen, M. A., Arroyo, J., and Aparicio, A. (2015). Extinction debt of a common shrub in a fragmented landscape. *J. Appl. Ecol.* 52, 580–589. doi: 10.1111/1365-2664.12424

Haby, V. A., Rosselle, M. P., and Skogley, E. O. (1990). Testing soils for potassium, calcium, and magnesium. *Soil Test. Plant Analy.* 3, 181–227. doi: 10.2136/sssabookser3.3ed.c8

He, F., Zhang, H., and Tang, M. (2016). Aquaporin gene expression and physiological responses of *Robinia pseudoacacia* L. to the mycorrhizal fungus *Rhizophagus irregularis* and drought stress. *Mycorrhiza* 26, 311–323. doi: 10.1007/s00572-015-0670-3

Heinonsalo, J., Frey-Klett, P., Pierrat, J.-C., Churin, J.-L., Vairelles, D., and Garbaye, J. (2004). Fate, tree growth effect and potential impact on soil microbial communities of mycorrhizal and bacterial inoculation in a forest plantation. *Soil Biol. Biochem.* 36, 211–216. doi: 10.1016/j.soilbio.2003.09.007

Henry, S., Texier, S., Hallet, S., Bru, D., Dambreville, C., Chèneby, D., et al. (2008). Disentangling the rhizosphere effect on nitrate reducers and denitrifiers: insight into the role of root exudates. *Environ. Microbiol.* 10, 3082–3092. doi: 10.1111/j.1462-2920.2008.01599.x

Hu, Y., and Schmidhalter, U. (2005). Drought and salinity: a comparison of their effects on mineral nutrition of plants. *J. Soil Sci. Plant Nutr.* 168, 541–549. doi: 10.1002/jpln.200420516

Kothari, S. K., Marschner, H., and George, E. (1990). Effect of VA mycorrhizal fungi and rhizosphere microorganisms on root and shoot morphology, growth and water relations in maize. *New Phytol.* 116, 303–311. doi: 10.1111/j.1469-8137.1990.tb04718.x

Kumar, A., Sharma, S., and Mishra, S. (2010). Influence of arbuscular mycorrhizal (AM) fungi and salinity on seedling growth, solute accumulation, and mycorrhizal dependency of *Jatropha curcas* L. *J. Plant Growth Regul.* 29, 297–306. doi: 10.1007/s00344-009-9136-1

Kung'u, J. B., Lasco, R. D., LUD, C., RED, C., and Husain, T. (2008). Effect of vesicular arbuscular mycorrhiza (VAM) fungi inoculation on coppicing ability and drought resistance of *Senna spectabilis*. *Pak. J. Bot.* 40, 2217–2224.

Larcher, W. (2003). *Physiological Plant Ecology: Ecophysiology and Stress Physiology of Functional Groups. 4th Edn*. Heidelberg: Springer Science & Business Media.

Liu, B., Liang, J., Tang, G., Wang, X., Liu, F., and Zhao, D. (2019). Drought stress affects on growth, water use efficiency, gas exchange and chlorophyll fluorescence of *Juglans* rootstocks. *Sci. Hortic.* 250, 230–235. doi: 10.1016/j.scienta.2019.02.056

Maksimović, I. V., Kastori, R. R., Petrović, N. M., Kovačev, L. M., and Sklenar, P. S. (2003). The effect of water potential on accumulation of some essential elements in sugarbeet leaves, *Beta vulgaris* ssp. *vulgaris*. *Zb. Matice Srp. Prir. Nauke* 104, 39–50. doi: 10.2298/ZMSPN0304039M

Mardhiah, U., Caruso, T., Gurnell, A., and Rillig, M. C. (2016). Arbuscular mycorrhizal fungal hyphae reduce soil erosion by surface water flow in a greenhouse experiment. *Appl. Soil Ecol.* 99, 137–140. doi: 10.1016/j.apsoil.2015.11.027

Mateus, N. D. S., Leite, A. F., Santos, E. F., Ferraz, A. D. V., Goncalves, J. L. D. M., and Lavres, J. (2021). Partial substitution of K by Na alleviates drought stress and increases water use efficiency in *Eucalyptus* species seedlings. *Front. Plant Sci.* 12:632342. doi: 10.3389/fpls.2021.632342

Meddich, A., Jaiti, F., Bourzik, W., Asli, A. E., and Hafidi, M. (2015). Use of mycorrhizal fungi as a strategy for improving the drought tolerance in date palm (*Phoenix dactylifera*). *Sci. Hortic.* 192, 468–474. doi: 10.1016/j.scienta.2015.06.024

Moghrani, H., and Maachi, R. (2008). Valorization of *Myrtus communis* essential oil obtained by steam driving distillation. *Asian J. Sci. Res.* 1, 518–524. doi: 10.3923/ajsr.2008.518.524

Moradi-ghahderijani, M., Jafarian, S., and Keshavarz, H. (2017). Alleviation of water stress effects and improved oil yield in sunflower by application of soil and foliar amendments. *Rhizosphere* 4, 54–61. doi: 10.1016/j.rhisph.2017.06.002

Orfanoudakis, M., Wheeler, C. T., and Hooker, J. E. (2010). Both the arbuscular mycorrhizal fungus Gigaspora rosea and Frankia increase root system branching and reduce root hair frequency in *Alnus glutinosa*. *Mycorrhiza* 20, 117–126. doi: 10.1007/s00572-009-0271-0

Ortiz, N., Armada, E., Duque, E., Roldán, A., and Azcón, R. (2015). Contribution of arbuscular mycorrhizal fungi and/or bacteria to enhancing plant drought tolerance under natural soil conditions: effectiveness of autochthonous or allochthonous strains. *J. Plant Physiol.* 174, 87–96. doi: 10.1016/j.jplph.2014.08.019

Palacio, S., Hoch, G., Sala, A., Körner, C., and Millard, P. (2013). Does carbon storage limit tree growth? *New Phytol.* 201, 1096–1100. doi: 10.1111/nph.12602

Ratnayaka, H. H., and Kincaid, D. (2005). Gas exchange and leaf ultrastructure of Tinnevelly senna, *Cassia angustifolia*, under drought and nitrogen stress. *Crop Sci.* 45, 840–847. doi: 10.2135/cropsci2003.737

Ribeiro, M. M., LeProvost, G., Gerber, S., Vendramin, G. G., Anzidei, M., Decroocq, S., et al. (2002). Origin identification of maritime pine stands in France using chloroplast simple-sequence repeats. *Ann. For. Sci.* 59, 53–62. doi: 10.1051/forest

Rodriguez-Dominguez, C. M., and Brodribb, T. J. (2020). Declining root water transport drives stomatal closure in olive under moderate water stress. *New Phytol.* 225, 126–134. doi: 10.1111/nph.16177

Ruiz-Lozano, J. M., Azcon, R., and Gomez, M. (1995). Effects of arbuscular-mycorrhizal Glomus species on drought tolerance: physiological and nutritional plant responses. *Appl. Environ. Microbiol.* 61, 456–460. doi: 10.1128/aem.61.2.456-460.1995

Ruíz-Sánchez, M., Armada, E., Muñoz, Y., García de Salamone, I. E., Aroca, R., Ruíz-Lozano, J. M., et al. (2011). Azospirillum and arbuscular mycorrhizal colonization enhance rice growth and physiological traits under well-watered and drought conditions. *J. Plant Physiol.* 168, 1031–1037. doi: 10.1016/j.jplph.2010.12.019

Růžička, K., Ljung, K., Vanneste, S., Podhorská, R., Beeckman, T., Friml, J., et al. (2007). Ethylene regulates root growth through effects on auxin biosynthesis and transport-dependent auxin distribution. *Plant Cell* 19, 2197–2212. doi: 10.1105/tpc.107.052126

Saravanakumar, D., and Samiyappan, R. (2007). ACC deaminase from *Pseudomonas fluorescens* mediated saline resistance in groundnut (*Arachis hypogea*) plants. *J. Appl. Microbiol.* 102, 1283–1292. doi: 10.1111/j.1365-2672.2006.03179.x

Sardans, J., Peñuelas, J., and Ogaya, R. (2008). Drought's impact on Ca, Fe, Mg, Mo, and S concentration and accumulation patterns in the plants and soil of a Mediterranean evergreen *Quercus ilex* forest. *Biogeochemistry* 87, 49–69. doi: 10.1007/s10533-007-9167-2

Smith, S. E., and Read, D. J. (2008). *Mycorrhizal Symbiosis*. London: Cambridge, UK, Academic Press.

Subramanian, K. S., Santhanakrishnan, P., and Balasubramanian, P. (2006). Responses of field grown tomato plants to arbuscular mycorrhizal fungal colonization under varying intensities of drought stress. *Sci. Hortic.* 107, 245–253. doi: 10.1016/j.scienta.2005.07.006

Sumbul, S., Aftab Ahmad, M., Asif, M., and Akhtar, M. (2011). *Myrtus communis* Linn—A review. *Indian J. Nat. Prod. Resour.* 2, 395–402.

Tiepo, A. N., Hertel, M. F., Rocha, S. S., Calzavara, A. K., De Oliveira, A. L. M., Pimenta, J. A., et al. (2018). Enhanced drought tolerance in seedlings of Neotropical tree species inoculated with plant growth-promoting bacteria. *Plant Physiol. Biochem.* 130, 277–288. doi: 10.1016/j.plaphy.2018.07.021

Tisserant, E., Kohler, A., Dozolme-Seddas, P., Balestrini, R., Benabdellah, K., Colard, A., et al. (2012). The transcriptome of the arbuscular mycorrhizal fungus *Glomus intraradices* (DAOM 197198) reveals functional tradeoffs in an obligate symbiont. *New Phytol.* 193, 755–769. doi: 10.1111/j.1469-8137.2011.03948.x

Trenberth, K. E., Dai, A., Van Der Schrier, G., Jones, P. D., Barichivich, J., Briffa, K. R., et al. (2014). Global warming and changes in drought. *Nat. Clim. Chang.* 4, 17–22. doi: 10.1038/nclimate2067

Ullah, U., Ashraf, M., Shahzad, S. M., Siddiqui, A. R., Piracha, M. A., and Suleman, M. (2016). Growth behavior of tomato (*Solanum lycopersicum* L.) under drought stress in the presence of silicon and plant growth promoting rhizobacteria. *Soil Environ.* 35, 65–75.

Waraich, E. A., Ahmad, R., Ashraf, M. Y., and Saifullah, A. M. (2011). Improving agricultural water use efficiency by nutrient management in crop plants. *Acta Agric. Scand. Sect. B Soil Plant Sci.* 61, 291–304. doi: 10.1080/09064710.2010.491954

Wu, Q. S., and Xia, R. X. (2006). Arbuscular mycorrhizal fungi influence growth, osmotic adjustment and photosynthesis of citrus under well-watered and water stress conditions. *J. Plant Physiol.* 163, 417–425. doi: 10.1016/j.jplph.2005.04.024

Xie, H., Pasternak, J. J., and Glick, B. R. (1996). Isolation and characterization of mutants of the plant growth-promoting rhizobacterium *Pseudomonas putida* GR12-2 that overproduce indoleacetic acid. *Curr. Microbiol.* 32, 67–71. doi: 10.1007/s002849900012

Yang, Y., Liu, Q., Han, C., Qiao, Y. Z., Yao, X. Q., and Yin, H. J. (2007). Influence of water stress and low irradiance on morphological and physiological characteristics of *Picea asperata* seedlings. *Photosynthetica* 45, 613–619. doi: 10.1007/s11099-007-0106-1

Yin, N., Zhang, Z., Wang, L., and Qian, K. (2016). Variations in organic carbon, aggregation, and enzyme activities of gangue-fly ash-reconstructed soils with sludge and arbuscular mycorrhizal fungi during 6-year reclamation. *Environ. Sci. Pollut. Res.* 23, 17840–17849. doi: 10.1007/s11356-016-6941-5

Zarik, L., Meddich, A., Hijri, M., Hafidi, M., Ouhammou, A., Ouahmane, L., et al. (2016). Use of arbuscular mycorrhizal fungi to improve the drought tolerance of *Cupressus atlantica* G. *C. R. Biol.* 339, 185–196. doi: 10.1016/j.crvi.2016.04.009

Zhang, Z., Zhang, J., Xu, G., Zhou, L., and Li, Y. (2019). Arbuscular mycorrhizal fungi improve the growth and drought tolerance of *Zenia insignis* seedlings under drought stress. *New For.* 50, 593–604. doi: 10.1007/s11056-018-9681-1

Conflict of Interest: The authors declare that the research was conducted in the absence of any commercial or financial relationships that could be construed as a potential conflict of interest.

Publisher's Note: All claims expressed in this article are solely those of the authors and do not necessarily represent those of their affiliated organizations, or those of the publisher, the editors and the reviewers. Any product that may be evaluated in this article, or claim that may be made by its manufacturer, is not guaranteed or endorsed by the publisher.

frontiers | Frontiers in Plant Science

MINI REVIEW
published: 23 June 2022
doi: 10.3389/fpls.2022.922982

Molecular Mechanisms of Intercellular Rhizobial Infection: Novel Findings of an Ancient Process

Johan Quilbé[1], Jesús Montiel[1,2], Jean-François Arrighi[3] and Jens Stougaard[1]**

[1]Department of Molecular Biology and Genetics, Aarhus University, Aarhus, Denmark, [2]Centre for Genomic Sciences, National Autonomous University of Mexico (UNAM), Cuernavaca, Mexico, [3]IRD, Plant Health Institute of Montpellier (PHIM), UMR IRD/SupAgro/INRAE/UM/CIRAD, Montpellier, France

Establishment of the root-nodule symbiosis in legumes involves rhizobial infection of nodule primordia in the root cortex that is dependent on rhizobia crossing the root epidermal barrier. Two mechanisms have been described: either through root hair infection threads or through the intercellular passage of bacteria. Among the legume genera investigated, around 75% use root hair entry and around 25% the intercellular entry mode. Root-hair infection thread-mediated infection has been extensively studied in the model legumes *Medicago truncatula* and *Lotus japonicus*. In contrast, the molecular circuit recruited during intercellular infection, which is presumably an ancient and simpler pathway, remains poorly known. In recent years, important discoveries have been made to better understand the transcriptome response and the genetic components involved in legumes with obligate (*Aeschynomene* and *Arachis* spp.) and conditional (*Lotus* and *Sesbania* spp.) intercellular rhizobial infections. This review addresses these novel findings and briefly considers possible future research to shed light on the molecular players that orchestrate intercellular infection in legumes.

Keywords: intercellular symbiosis, legumes, nodule, *Lotus*, *Aeschynomene*, *Arachis*, *Sesbania*

OPEN ACCESS

Edited by:
Katharina Pawlowski, Stockholm University, Sweden

Reviewed by:
Euan James, The James Hutton Institute, United Kingdom
Senjuti Sinharoy, National Institute of Plant Genome Research (NIPGR), India

****Correspondence:***
Jesús Montiel
jmontiel@ccg.unam.mx
Jens Stougaard
stougaard@mbg.au.dk

Specialty section:
This article was submitted to Plant Symbiotic Interactions, a section of the journal Frontiers in Plant Science

Received: *18 April 2022*
Accepted: *16 May 2022*
Published: *23 June 2022*

Citation:
Quilbé J, Montiel J, Arrighi J-F and Stougaard J (2022) Molecular Mechanisms of Intercellular Rhizobial Infection: Novel Findings of an Ancient Process. Front. Plant Sci. 13:922982. doi: 10.3389/fpls.2022.922982

INTRODUCTION

The root nodule symbiosis (RNS) has been widely studied in the model legumes *Lotus japonicus* and *Medicago truncatula*. In these species, rhizobia infect the roots *via* a root-hair infection thread (IT), after a chemical recognition that occurs in the rhizosphere. The molecular dialog involves the secretion of flavonoid root exudates that are perceived by the rhizobial partner. In response, the microsymbiont synthesizes and releases lipochito-oligosaccharides known as nodulation factors (NF), which are recognized by the NF receptors located at the root hair plasma membrane. This complex signal exchange leads to the formation of the nodule primordia by reactivation of cortical cell division. This structure gives rise to the root nodule, where the bacteria are released from the ITs into the nodule cells to become bacteroids, carrying out the conversion of atmospheric nitrogen into ammonia (Roy et al., 2020). Among the six subfamilies of the Fabaceae (Koenen et al., 2020), only the Caesalpinioideae (+Mimosoid clade) and Papilionoideae are considered to harbor nodulating genera and it is estimated that about one quarter of all legume genera employ a rhizobial invasion programme called intercellular infection (Sprent et al., 2017). This infection process is presumed to be a simpler mechanism

than root-hair IT-mediated infection that involves many biological functions (Roy et al., 2020). Furthermore, since intercellular infection is found in different legume subfamilies (Sprent et al., 2017; Koenen et al., 2020), and beyond the legume family in the Parasponia-Bradyrhizobium symbiosis and in certain actinorhizal plants (**Figure 1A**), it is likely to be an ancient and fundamental mechanism (Huisman and Geurts, 2020). Intercellular infection comprises different modalities that have been described through histological analyses in several species (James et al., 1992; Subba-Rao et al., 1995; Ibañez et al., 2017). These modalities need to be characterized at a molecular level. Here, we review emerging knowledge of the molecular genetics of nodulation by intercellular infection, and discuss why exploring these mechanisms in legumes, where this process is either obligate or conditional, is complementary.

CONDITIONAL INTERCELLULAR INFECTION

Certain legume species are remarkable because although they usually employ root hair ITs infection they can in certain conditions switch to the intercellular infection process. Such plasticity in the infection mode has repeatedly (although not exclusively) been observed within the robinoid subclade, in *Sesbania* spp. and *Lotus* spp. (**Figure 1A**; Ndoye et al., 1994; Cummings et al., 2009; Acosta-Jurado et al., 2016; Mitra et al., 2016; Liang et al., 2019). In these species, intercellular colonization either takes place under specific growth conditions or is observed with specific rhizobial partners (Ranga Rao, 1977; Karas et al., 2005). In the semi-aquatic legume *Sesbania rostrata*, root hair ITs are readily observed in aeroponic conditions, while lateral root base (LRB) nodulation is observed under flooded conditions, *via* a crack-entry mechanism in which *Azorhizobium caulinodans* enters through epidermal fissures of emerging adventitious roots (Capoen et al., 2010b). Similarly to *S. rostrata*, under flooded conditions the robinoid *Lotus uliginosus* is intercellularly colonized by *M. loti*, culminating in the formation of nitrogen-fixing nodules (James and Sprent, 1999). Another *Lotus* species, *L. burttii*, is an interesting model for studying rhizobial infection, since it can be nodulated by a large diversity of rhizobial species (Zarrabian et al., 2021). The evidence collected indicates that some of these associations occur intercellularly; for instance, the interactions with *Sinorhizobium fredii* HH103 (Acosta-Jurado et al., 2016) and *Rhizobium leguminosarum* biovar Norway (Liang et al., 2019), the latter leading to ineffective nodules. In the model legume *L. japonicus*, infection takes place *via* root hair ITs with its cognate symbiont *M. loti*, but plasticity in the infection mode was first revealed in different plant mutants: the *root-hair less 1* and NF-receptor mutants, where intercellular infection was detected at a low frequency (Karas et al., 2005; Madsen et al., 2010). More recently, functional nodules were found to be induced by IRBG74 invading *L. japonicus*, intercellularly. The IRBG74 strain has been isolated from *Sesbania cannabina* nodules and after sequencing assigned as an *Agrobacterium pusense* strain that possesses a symbiotic plasmid. It can infect *Sesbania* spp. either under flooded or non-flooded conditions (Cummings et al., 2009; Mitra et al., 2016). In *L. japonicus* inoculated with IRBG74, the cortical cells are invaded *via* peg-mediated entry from the apoplast into the symbiosome of the infected cells (**Figure 1C**; Montiel et al., 2021). All these cases of conditional intercellular infection are valuable because they provide the opportunity for direct comparison of the two invasion routes in the same host plants, thus identifying mechanistic commonalities and differences (Goormachtig et al., 2004). Despite this advantage, the molecular components of this mechanism have only been investigated in *S. rostrata* and *L. japonicus*, as described below.

During the *S. rostrata-A. caulinodans* symbiosis, axillary root-hairs are induced by the presence of the bacteria at the emergence of lateral roots and the intercellular infection process take place at the LRB. The progression of bacteria in the root is followed by a cell death programme in cortical cells that give rise to the formation of an infection pocket (IP; Capoen et al., 2010a). From these structures, rhizobia migrate into inner root cell layers through transcellular ITs or intercellularly. This symbiotic association served as precursor to understanding the molecular components involved in intercellular infection in legumes. One of the first discoveries was to demonstrate that IP formation is a NF-dependent process, since the *A. caulinodans nodA* mutant, disrupted in NF production, is unable to colonize the legume roots (D'haeze et al., 1998). Likewise, in this initial stage, gibberellins, reactive oxygen species and ethylene are produced, playing a positive role (D'haeze et al., 2003; Lievens et al., 2005). Interestingly, intercellular cortical infection was not affected in *S. rostrata* transgenic roots downregulated in the leucine-rich repeat (LRR) receptor-like kinase (SymRK) by RNAi (Capoen et al., 2005). Similarly, RNAi-mediated silencing of the calcium- and calmodulin-dependent protein kinase (CCaMK) did not interfere with the intercellular infection (Capoen et al., 2009). These two players (*SrSymRK* and *SrCCaMK*), crucial for root-hair IT colonization. However, based on the RNAi results they seem not to be necessary for intercellular infection, although they are still required in subsequent stages of the nodulation process (**Figure 2**). A transcriptomic study on *S. rostrata* roots evidenced 627 differentially-expressed gene tags that are induced during root hair curling and crack-entry rhizobial infection. However, the number of tags was considerably lower during intercellular infection (Capoen et al., 2007). The milder transcriptomic response during intercellular infection indicates that a reduced gene machinery is required in this mechanism. This notion is supported by the less stringent NF recognition in the intercellular symbiotic program compared to the root-hair infection process (Goormachtig et al., 2004).

Similarly, in the *L. japonicus*-IRBG74 association, an IP is formed in the cortical cells after intercellular infection, which follows an inter/intracellular pathway towards the nodule cells (**Figure 1C**). With the abundant genetic resources in *L. japonicus*, a robust compendium of symbiotic mutants was tested in the interaction with the IRBG74 strain. This approach allowed a core of symbiotic genes involved in the nodulation program to be delimited by the type of rhizobial infection and grouped as preferentially recruited for the intracellular or intercellular

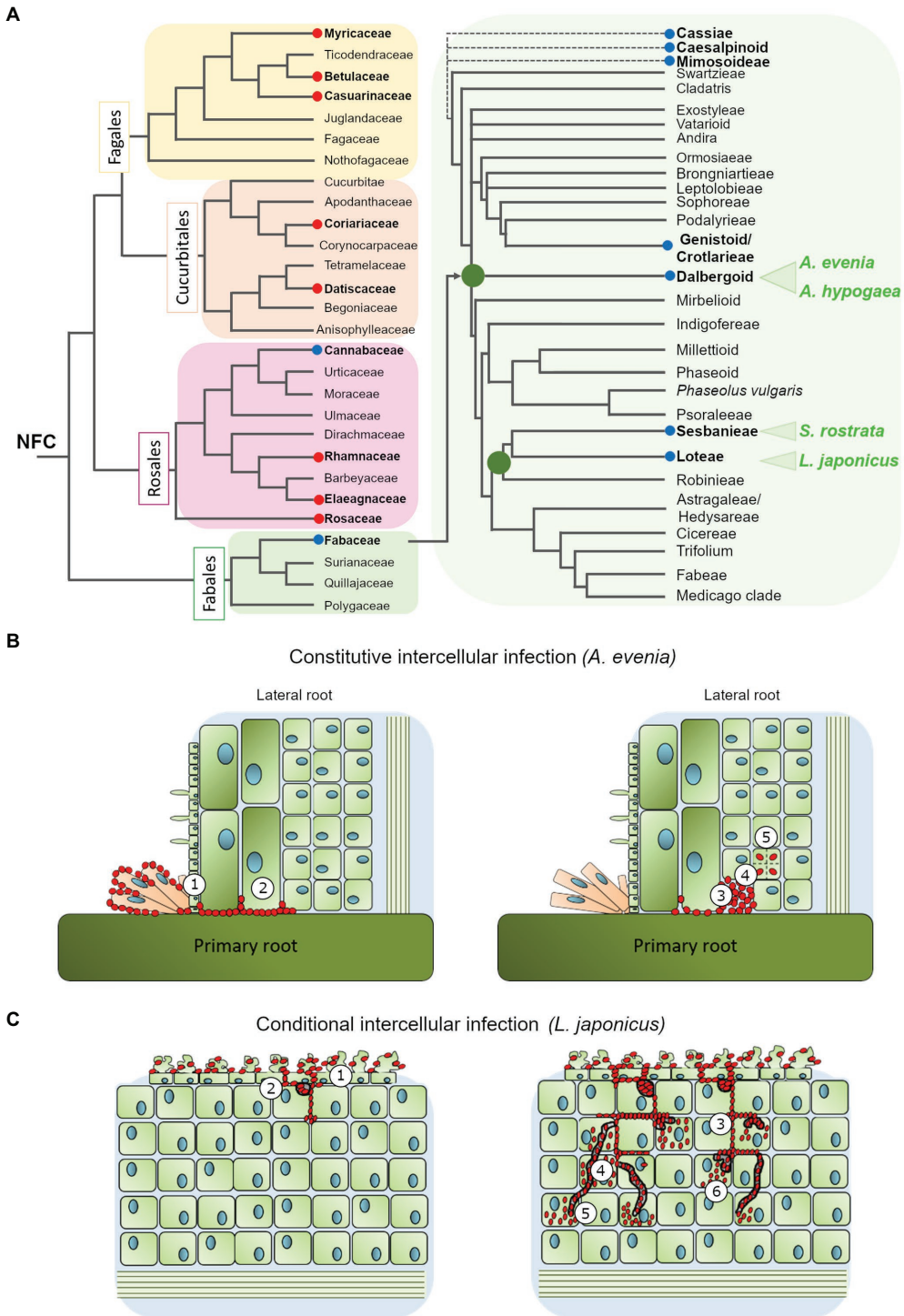

FIGURE 1 | (A) Phylogenetic relationship of the nitrogen-fixing clade (based on Sun et al., 2016; Shen and Bisseling, 2020) with special emphasis in the Fabaceae family (modified from Sprent et al., 2017). The red and blue circles highlight the genera where intercellular colonization by Frankia or Rhizobia occurs, respectively. The four species discussed in this review are marked in green **(B)**. Intercellular infection mechanism in *Aeschynomene evenia*: the bradyrhizobium ORS278 intensively colonizes the axillary root hairs at the lateral root base and progresses between cells (1) to reach the cortex (2) where they could induce cell-collapse (3), before bacteria are finally internalized (4) and induce cell division (5). **(C)** Intercellular infection mechanism in *Lotus japonicus*: IRBG74 induce massive root hair curling and twisting, followed by intercellular infection of the root epidermis (1). In the cortical cells, IRBG74 is accumulated in infection pockets (2) and from these structures migrates to the nodule cells intercellularly (3) or through transcellular infection threads (4). The bacteria are released into the nodule cells from transcellular infection threads (5) or intercellular infection peg structures (6).

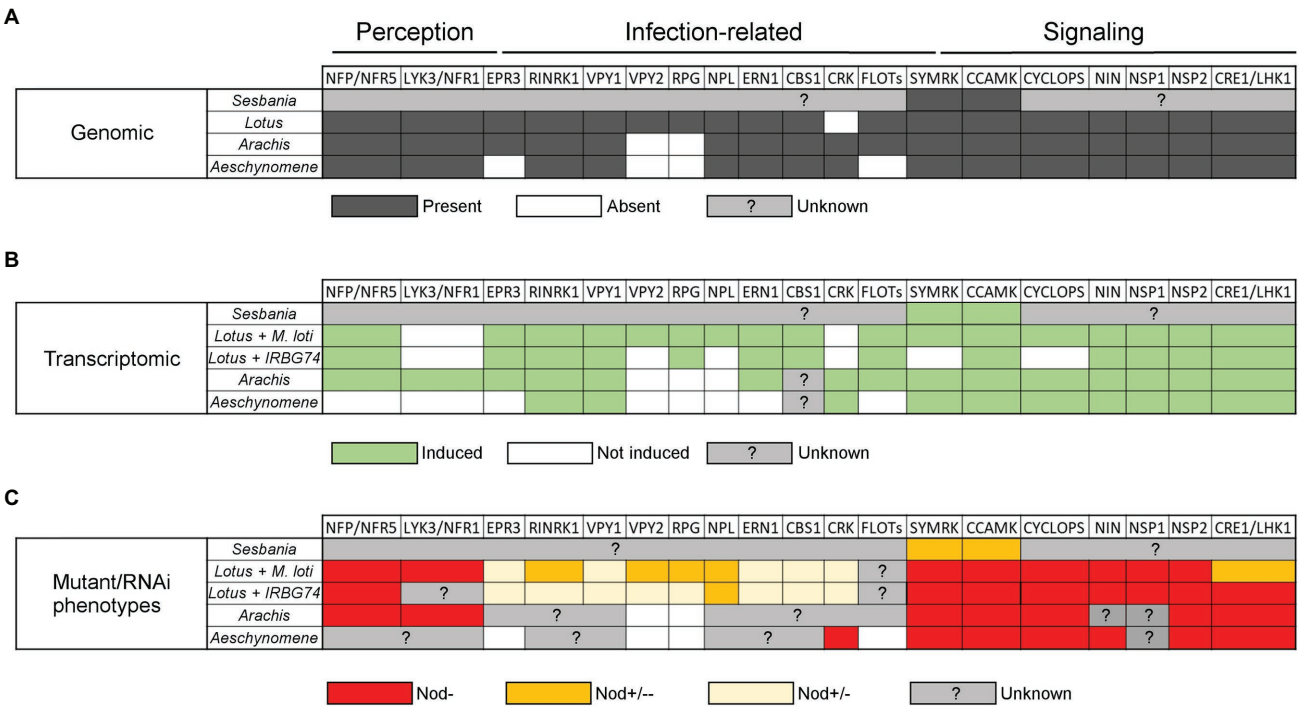

FIGURE 2 | Table comparing data on symbiotic genes involved in different nodulation steps in *Arachis hypogaea*, *Aeschynomene evenia*, *Lotus japonicus*, and *Sesbania rostrata* according to their symbionts. **(A)** Comparison of the presence (dark grey), absence (white), or unknown status (light grey) of symbiotic genes in the genome of *A. hypogaea*, *A. evenia*, *L. japonicus*, and *S. rostrata*. **(B)** Comparison of symbiotic genes that are induced (green), not induced (white) or of unknown status (grey) during nodulation in the four species. For *L. japonicus* this comparison includes the symbiont making intercellular infection (IRBG74) and intracellular infection (*M. loti*). **(C)** Comparison of the phenotypes with different genetic approaches (mutant or RNAi) in the four species and *L. japonicus* with the two symbionts. Red indicates absence of nodules (Nod-), orange indicates an intermediate strong phenotype (Nod+/−−), yellow indicates an intermediate weak phenotype (Nod+/−), and grey indicates the absence of data. For the *Lotus*-IRBG74 interaction, only transcriptome data of early time points is available (3, 5, and 10 dpi).

colonization in *L. japonicus* (**Figure 2**). For instance, *nfr5*, *symrk*, *ccamk*, *nin-2*, *nsp1*, and *nsp2* mutants altered in NF perception and the Nod signaling pathway, were unable to induce nodule development in *L. japonicus* after IRBG74 inoculation. Although these findings are relevant, it is still unclear whether intercellular infection occurs in the roots of these mutants, considering the evidence recorded in *S. rostrata*, where intercellular cortical colonization was not prevented in the *SymRK*-RNAi and *CCaMK*-RNAi lines (Capoen et al., 2005, 2009). Unexpectedly, mutants affected in cytokinin-related genes such as *lhk1*, *cyp753a*, and *ipt4* had a more severe negative impact in the intercellular symbiosis with IRBG74. The most prominent difference was the performance of the *lhk1* mutant, since it was unable to form any nodule structure with IRBG74 (Montiel et al., 2021). On the other hand, mutants affected in the infection genes *CYCLOPS*, *CBS*, *EPR3*, or *VPY1* showed comparable symbiotic phenotypes during intra–intercellular interactions (Montiel et al., 2021). However, a milder symbiotic perturbance was observed in the *rbohE*, *rbohG*, *RPG*, *RPG-Like*, *RINRK1*, *ERN1*, and *VPY2* infection gene mutants in the intercellular interaction with IRBG74, compared to the phenotype observed with *M. loti* as the inoculum. These results suggest that an intercellular symbiotic process employs a different, and apparently reduced, repertoire of molecular players compared to intracellular colonization *via* root-hair ITs (**Figure 2**). This hypothesis is further supported by the remarkable contrast in number of differentially expressed genes (DEGs) in the susceptible zone of roots exposed to *M. loti* or IRBG74; 473 vs. 250, respectively. Interestingly, a large proportion (67%) of the DEGs by *M. loti* were not differentially expressed with IRBG74. Nonetheless, a core of relevant symbiotic genes was upregulated to comparable levels with both symbionts (Montiel et al., 2021).

CONSTITUTIVE INTERCELLULAR INFECTION PROCESS

The constitutive intercellular infection process has been reported in certain species of the Mimosoidae-Caesalpinea-Cassieae clade but it is best described in two Papilionoid subclades using different modalities: Genistoids (Direct Entry) and Dalbergioids (Crack Entry; Ibañez et al., 2017). Recently, two legume species from the Dalbergioid subclade, *Arachis hypogaea* (peanut) and *Aeschynomene evenia*, emerged for the study of nodulation (**Figure 1A**). Since they are phylogenetically related, their comparative analysis is predicted to facilitate the finding of

common features related to crack entry. However, *A. evenia* uses a Nod-independent process by interacting with *Bradyrhizobia* lacking the Nod-factors' nodulation (*nod*) genes. Therefore, studying this singular genetic system is also expected to reveal the minimal set of genes that are required for intercellular infection without the additional components linked to the classic perception of rhizobia. In these two legume species, tufts of multicellular axillary root hairs are present at the base of lateral roots that represent the infection sites. In *A. hypogaea*, the bradyrhizobia pass through the middle lamella between two root-hair cells at the LRB and spread into the cortex *via* the middle lamella. Uptake into the susceptible cell occurs through a structurally-altered cell wall. The Nod factors are not required for colonization of the peanut root surface but are required for the induction of cortical cell division of the first infected cell that will form the nodule primordia, when interacting with its natural symbionts (Ibañez and Fabra, 2011). However, very recent occurrences of Nod-independent nodulation have been reported in *Arachis* when inoculated with non-cognate symbionts, but the underlying mechanisms are not yet documented (Guha et al., 2022). Within the *Aeschynomene* genus, some species nodulate in a NF-dependent fashion and their root infection by bradyrhizobia occurs in a way that is comparable to *A. hypogaea* (Giraud et al., 2007). In contrast, other species such as *A. evenia* nodulate in a Nod-independent way and their root infection is distinctive in that the bradyrhizobia first intensely colonize the axillary root-hairs and then penetrate into the root between axillary root-hair cells or *via* a crack at the lateral root basis (**Figure 1B**). Another notable feature is that when bacteria progress into the root in the intercellular space, they induce cell collapse among the first-invaded cortical cells, after which they are internalized in an inner susceptible cortical cell by invagination of the cell wall, and the infected cell initiates successive divisions that give birth to the nodule primordia (Bonaldi et al., 2011).

Recent genome sequencing projects and transcriptomic studies have enabled investigation into the presence and expression of symbiotic genes in *A. hypogeae* and *A. evenia*. Almost all the determinants characterized in the model legumes *M. truncatula* and *L. japonicus* are also present in their genome, notably the Nod-factor perception genes *NFP/NFR5* and *LYK3/NFR1*, symbiotic signaling genes *SYMRK*, *POLLUX*, *CCAMK*, *CYCLOPS*, *NIN*, *NSP2*, and *CRE1/LHK1*, and infection-related genes *RINRK1*, *VPY*, *NPL*, *ERN1*, and *CBS1* (Roy et al., 2020; Krönuer and Radutoiu, 2021; **Figure 2**). In contrast, the *RPG* gene, coding for a coiled-coil protein and linked to infection in *M. truncatula* (Arrighi et al., 2008), is absent from the genome in both of these species (Chaintreuil et al., 2016; Peng et al., 2017; Gully et al., 2018; Karmakar et al., 2019). This suggests that *RPG* is specific to IT-mediated infection and is not involved in intercellular infection. In *A. evenia*, some specificities are also observed with the non-expression of LYK3 and the absence of the infection-related genes *EPR3* and *FLOT*s in the genome (Quilbe et al., 2021). In *A. hypogeae*, known symbiotic genes acting in the common IT mediated nodulation (125 peanut orthologs) are also expressed during symbiosis (**Figure 2**). The majority of DEGs are observed during nodule functioning, then nodule organogenesis and finally infection (Raul et al., 2022). Transcriptomic analyses of a time-course experiment in *A. evenia* allowed the identification of DEGs at early and late stages of the symbiotic interaction. A small number of DEGs at early stages, corresponding to the colonization of the roots by bradyrhizobia, are linked to responses to stress and abiotic stimuli. In general, the number of DEGs decrease as the nodulation process progresses (Chaintreuil et al., 2016; Peng et al., 2017; Gully et al., 2018; Karmakar et al., 2019). Other gene expression analyses in *A. evenia* have revealed that determinants such as *VPY*, *LIN*, and *EXO70H4*, required for polar growth of infection threads and subsequent intracellular accommodation of symbionts in *M. truncatula,* show a symbiotic expression pattern. However, it is not yet known whether they are involved in intercellular infection and/or only in the latter stages of the symbiotic process (Quilbe et al., 2021).

Genetic analyses have been conducted on these two Dalbergioid species to determine which genes are important for nodulation by intercellular infection (**Figure 2**). In *A. hypogeae*, a reverse genetic approach based on CRISPR/Cas9 in hairy roots showed that the mutants edited in *AhNFR5* are unable to produce nodules (Shu et al., 2020). In addition, the silencing of three symbiotic genes with RNAi experiments led to the discovery that CCaMK, CYCLOPS and LHK1 are involved in the nodulation process (Sinharoy and DasGupta, 2009; Kundu and DasGupta, 2018; Das et al., 2019). More recently, thanks to map-based cloning and QTL-seq approaches, Peng et al. have shown that the two homoeologs of the *NSP2* gene control nodulation in *A. hypogeae* (Peng et al., 2021). Similarly, in *A. evenia*, some RNAi studies have shown that *SYMRK*, *CCAMK*, and *LHK1* are required for nodulation, although the role of these genes in intercellular infection has not been investigated (Fabre et al., 2015). More recently, in *A. evenia*, a forward genetic approach led to the selection of hundreds of EMS nodulation mutants, among which some Nod$^-$ mutants allowed for the identification of *AePOLLUX*, *AeCCAMK*, *AeCYCLOPS*, *AeNIN*, and *AeNSP2* as essential determinants for the establishment of Nod-independent symbiosis. Among all the mutants screened, none of them showed mutations in any LysM-RLK genes, to which NF receptor genes belong. Furthermore, this screen led to the discovery of a novel symbiotic gene, *AeCRK*, coding a Cystein-rich Receptor Kinase that is required to trigger nodulation. The nodule-less phenotype of the *crk* mutants and the expression profile of *AeCRK* suggest a function in both early and later stages of symbiosis. In plants, CRK functions are not clearly established but they are often linked to immunity and the authors suggested that in *A. evenia* this receptor could be involved in ROS signaling during Nod-independent symbiosis (Quilbe et al., 2021). Interestingly, this particular gene is also found in other Papilionoid legumes using intercellular infection, like *Lupin* and *Arachis* spp., but not in those using an IT-mediated infection process, such as *M. truncatula* or *L. japonicus*. Therefore, investigating the role of AeCRK could reveal a novel important function for intercellular infection.

CONCLUSION AND FUTURE DIRECTIONS

The evolution of nodulation in legumes and their infection processes has been recently reviewed and explored (Fonseca et al., 2012; Sprent et al., 2017; De Faria et al., 2022), however, since intracellular and intercellular infection occurs in nodulating legume subfamilies that originated nearly simultaneously in evolution (Koenen et al., 2020), it is complicated to determine the ancestral colonization mechanism. Consequently, a more complete understanding of the molecular mechanisms underlying intercellular rhizobial infection in legumes becomes more relevant. Getting a general view is difficult because there are different patterns of intercellular infection and the available molecular data are still fragmented. However, one clear outcome from these studies, the most extensive in *L. japonicus*, is that NF perception and symbiotic signaling are important for intercellular infection (Montiel et al., 2021). *A. evenia* is likely an exception, since there are no indications of any NF receptor involvement in the Nod-independent symbiosis (Quilbe et al., 2021). The next main challenge will be to understand the molecular mechanisms that underpin the passage through the epidermis, the accommodation of bacteria within the apoplast, cell collapse or peg formation, and the entry by cell wall invagination during intercellular infection (**Figure 1**). They remain largely unknown since they have not been identified with the studies based on knowledge from the IT-mediated infection process.

These mechanisms could be elucidated by screening plant mutants and performing careful microscopic phenotyping for alterations in infection. To perform such an investigation, *L. japonicus* and *A. evenia* appear to be appropriate study models because genetic resources are available for both legumes. The Lotus collection of LORE1 insertion mutants has been mined for genes important for IT-mediated nodulation (Montiel et al., 2021). It can also serve to directly screen mutants involved in intercellular infection. Similarly, the genetic work initiated in *A. evenia*, and that enabled the recent identification of *AeCRK*, can be extended to available infection mutants (Quilbe et al., 2021). Since *L. japonicus* and *A. evenia* belong to distant Papilionoid lineages and make use of different intercellular infection programs, we anticipate that their concomitant study will be complementary to identify novel infection genes. Extending these studies with comparative phylogenomics and transcriptomics studies comparing root-hair IT and intercellular infected legume species would also help define the genetic specificities of intercellular infection. Such knowledge will enrich our understanding of rhizobial infection in legumes. It may also offer new engineering strategies to achieve biological nitrogen fixation in non-legume crops such as cereals.

AUTHOR CONTRIBUTIONS

JQ and JM drafted the article and figures. JM, JQ, and JS contributed to conception and design of the work. J-FA and JS contributed to critical revision of the article. All authors contributed to the article and approved the submitted version.

FUNDING

This work was supported by the grant Engineering the Nitrogen Symbiosis for Africa made to the University of Cambridge by the Bill & Melinda Gates Foundation (ENSA; OPP11772165), the European Research Council (ERC) under the European Union's Horizon 2020 research and innovation programme (grant agreement no. 834221), and the project Molecular Mechanisms and Dynamics of Plant-microbe interactions at the Root-Soil Interface (InRoot), supported by the Novo Nordisk Foundation grant no. NNF19SA0059362.

REFERENCES

Acosta-Jurado, S., Rodriguez-Navarro, D. N., Kawaharada, Y., Perea, J. F., Gil-Serrano, A., Jin, H., et al. (2016). *Sinorhizobium fredii* HH103 invades Lotus burttii by crack entry in a nod factor-and surface polysaccharide-dependent manner. *Mol. Plant Microbe Interact.* 29, 925–937. doi: 10.1094/MPMI-09-16-0195-R

Arrighi, J. F., Godfroy, O., De Billy, F., Saurat, O., Jauneau, A., and Gough, C. (2008). The RPG gene of *Medicago truncatula* controls Rhizobium-directed polar growth during infection. *Proc. Natl. Acad. Sci. U. S. A.* 105, 9817–9822. doi: 10.1073/pnas.0710273105

Bonaldi, K., Gargani, D., Prin, Y., Fardoux, J., Gully, D., Nouwen, N., et al. (2011). Nodulation of Aeschynomene afraspera and *A. indica* by photosynthetic Bradyrhizobium Sp. strain ORS285: the nod-dependent versus the nod-independent symbiotic interaction. *Mol. Plant Microbe Interact.* 24, 1359–1371. doi: 10.1094/MPMI-04-11-0093

Capoen, W., Den Herder, J., Rombauts, S., De Gussem, J., De Keyser, A., Holsters, M., et al. (2007). Comparative transcriptome analysis reveals common and specific tags for root hair and crack-entry invasion in *Sesbania rostrata*. *Plant Physiol.* 144, 1878–1889. doi: 10.1104/pp.107.102178

Capoen, W., Den Herder, J., Sun, J., Verplancke, C., De Keyser, A., De Rycke, R., et al. (2009). Calcium spiking patterns and the role of the calcium/calmodulin-dependent kinase CCaMK in lateral root base nodulation of *Sesbania rostrata*. *Plant Cell* 21, 1526–1540. doi: 10.1105/tpc.109.066233

Capoen, W., Goormachtig, S., De Rycke, R., Schroeyers, K., and Holsters, M. (2005). SrSymRK, a plant receptor essential for symbiosome formation. *Proc. Natl. Acad. Sci. U. S. A.* 102, 10369–10374. doi: 10.1073/pnas.0504250102

Capoen, W., Goormachtig, S., and Holsters, M. (2010a). Water-tolerant legume nodulation. *J. Exp. Bot.* 61, 1251–1255. doi: 10.1093/jxb/erp326

Capoen, W., Oldroyd, G., Goormachtig, S., and Holsters, M. (2010b). *Sesbania rostrata*: a case study of natural variation in legume nodulation. *New Phytol.* 186, 340–345. doi: 10.1111/j.1469-8137.2009.03124.x

Chaintreuil, C., Rivallan, R., Bertioli, D. J., Klopp, C., Gouzy, J., Courtois, B., et al. (2016). A gene-based map of the nod factor-independent *Aeschynomene evenia* sheds new light on the evolution of nodulation and legume genomes. *DNA Res.* 23, 365–376. doi: 10.1093/dnares/dsw020

Cummings, S. P., Gyaneshwar, P., Vinuesa, P., Farruggia, F. T., Andrews, M., Humphry, D., et al. (2009). Nodulation of Sesbania species by Rhizobium (Agrobacterium) strain IRBG74 and other rhizobia. *Environ. Microbiol.* 11, 2510–2525. doi: 10.1111/j.1462-2920.2009.01975.x

Das, D. R., Horvath, B., Kundu, A., Kalo, P., and Dasgupta, M. (2019). Functional conservation of CYCLOPS in crack entry legume *Arachis hypogaea*. *Plant Sci.* 281, 232–241. doi: 10.1016/j.plantsci.2018.12.003

De Faria, S., Ringelberg, J. J., Gross, E., Koenen, E. J. M., Cardoso, D., Ametsisi, G. K. D., et al. (2022). The innovation of the symbiosome has

enhanced the evolutionary stability of nitrogen fixation in legumes. bioRxiv [Preprint].

D'haeze, W., De Rycke, R., Mathis, R., Goormachtig, S., Pagnotta, S., Verplancke, C., et al. (2003). Reactive oxygen species and ethylene play a positive role in lateral root base nodulation of a semiaquatic legume. *Proc. Natl. Acad. Sci. U. S. A.* 100, 11789–11794. doi: 10.1073/pnas.1333899100

D'haeze, W., Gao, M. S., De Rycke, R., Van Montagu, M., Engler, G., and Holsters, M. (1998). Roles for azorhizobial nod factors and surface polysaccharides in intercellular invasion and nodule penetration, respectively. *Mol. Plant Microbe Interact.* 11, 999–1008. doi: 10.1094/MPMI.1998.11.10.999

Fabre, S., Gully, D., Poitout, A., Patrel, D., Arrighi, J. F., Giraud, E., et al. (2015). Nod factor-independent nodulation in *Aeschynomene evenia* required the common plant-microbe symbiotic toolkit. *Plant Physiol.* 169, 2654–2664. doi: 10.1104/pp.15.01134

Fonseca, M. B., Peix, A., De Faria, S. M., Mateos, P. F., Rivera, L. P., Simoes-Araujo, J. L., et al. (2012). Nodulation in Dimorphandra wilsonii Rizz. (Caesalpinioideae), a threatened species native to the *Brazilian Cerrado*. *PLoS One* 7:e49520. doi: 10.1371/journal.pone.0049520

Giraud, E., Moulin, L., Vallenet, D., Barbe, V., Cytryn, E., Avarre, J. C., et al. (2007). Legumes symbioses: absence of nod genes in photosynthetic bradyrhizobia. *Science* 316, 1307–1312. doi: 10.1126/science.1139548

Goormachtig, S., Capoen, W., James, E. K., and Holsters, M. (2004). Switch from intracellular to intercellular invasion during water stress-tolerant legume nodulation. *Proc. Natl. Acad. Sci. U. S. A.* 101, 6303–6308. doi: 10.1073/pnas.0401540101

Guha, S., Molla, F., Sarkar, M., Ibanez, F., Fabra, A., and Dasgupta, M. (2022). Nod factor-independent 'crack-entry' symbiosis in dalbergoid legume *Arachis hypogaea*. *Environ. Microbiol.* 1462–2912. doi: 10.1111/1462-2920.15888

Gully, D., Czernic, P., Cruveiller, S., Mahe, F., Longin, C., Vallenet, D., et al. (2018). Transcriptome profiles of nod factor-independent Symbiosis in the tropical legume *Aeschynomene evenia*. *Sci. Rep.* 8:10934. doi: 10.1038/s41598-018-29301-0

Huisman, R., and Geurts, R. (2020). A roadmap toward engineered nitrogen-fixing nodule Symbiosis. *Plant Commun.* 1:100019. doi: 10.1016/j.xplc.2019.100019

Ibañez, F., and Fabra, A. (2011). Rhizobial nod factors are required for cortical cell division in the nodule morphogenetic programme of the Aeschynomeneae legume Arachis. *Plant Biol. (Stuttg.)* 13, 794–800. doi: 10.1111/j.1438-8677.2010.00439.x

Ibañez, F., Wall, L., and Fabra, A. (2017). Starting points in plant-bacteria nitrogen-fixing symbioses: intercellular invasion of the roots. *J. Exp. Bot.* 68, 1905–1918. doi: 10.1093/jxb/erw387

James, E. K., and Sprent, J. I. (1999). Development of N2-fixing nodules on the wetland legume *Lotus uliginosus* exposed to conditions of flooding. *New Phytol.* 142, 219–231. doi: 10.1046/j.1469-8137.1999.00394.x

James, E. K., Sprent, J. I., Sutherland, J. M., Mcinroy, S. G., and Minchin, F. R. (1992). The structure of nitrogen fixing root nodules on the aquatic Mimosoid legume *Neptunia plena*. *Ann. Bot.* 69, 173–180. doi: 10.1093/oxfordjournals.aob.a088323

Karas, B., Murray, J., Gorzelak, M., Smith, A., Sato, S., Tabata, S., et al. (2005). Invasion of Lotus japonicus root hairless 1 by *Mesorhizobium loti* involves the nodulation factor-dependent induction of root hairs. *Plant Physiol.* 137, 1331–1344. doi: 10.1104/pp.104.057513

Karmakar, K., Kundu, A., Rizvi, A. Z., Dubois, E., Severac, D., Czernic, P., et al. (2019). Transcriptomic analysis With the Progress of Symbiosis in 'Crack-Entry' legume *Arachis hypogaea* highlights its contrast With 'Infection Thread' adapted legumes. *Mol. Plant Microbe Interact.* 32, 271–285. doi: 10.1094/MPMI-06-18-0174-R

Koenen, E. J. M., Ojeda, D. I., Steeves, R., Migliore, J., Bakker, F. T., Wieringa, J. J., et al. (2020). Large-scale genomic sequence data resolve the deepest divergences in the legume phylogeny and support a near-simultaneous evolutionary origin of all six subfamilies. *New Phytol.* 225, 1355–1369. doi: 10.1111/nph.16290

Krönuer, C., and Radutoiu, S. (2021). Understanding nod factor signalling paves the way for targeted engineering in legumes and non-legumes. *Curr. Opin. Plant Biol.* 62:102026. doi: 10.1016/j.pbi.2021.102026

Kundu, A., and Dasgupta, M. (2018). Silencing of putative cytokinin receptor Histidine Kinase1 inhibits Both inception and differentiation of root nodules in *Arachis hypogaea*. *Mol. Plant Microbe Interact.* 31, 187–199. doi: 10.1094/MPMI-06-17-0144-R

Liang, J., Klingl, A., Lin, Y. Y., Boul, E., Thomas-Oates, J., and Marin, M. (2019). A subcompatible rhizobium strain reveals infection duality in Lotus. *J. Exp. Bot.* 70, 1903–1913. doi: 10.1093/jxb/erz057

Lievens, S., Goormachtig, S., Den Herder, J., Capoen, W., Mathis, R., Hedden, P., et al. (2005). Gibberellins are involved in nodulation of Sesbania rostrata. *Plant Physiol.* 139, 1366–1379. doi: 10.1104/pp.105.066944

Madsen, L. H., Tirichine, L., Jurkiewicz, A., Sullivan, J. T., Heckmann, A. B., Bek, A. S., et al. (2010). The molecular network governing nodule organogenesis and infection in the model legume Lotus japonicus. *Nat. Commun.* 1:10. doi: 10.1038/ncomms1009

Mitra, S., Mukherjee, A., Wiley-Kalil, A., Das, S., Owen, H., Reddy, P. M., et al. (2016). A rhamnose-deficient lipopolysaccharide mutant of Rhizobium sp. IRBG74 is defective in root colonization and beneficial interactions with its flooding-tolerant hosts *Sesbania cannabina* and wetland rice. *J. Exp. Bot.* 67, 5869–5884. doi: 10.1093/jxb/erw354

Montiel, J., Reid, D., Gronbaek, T. H., Benfeldt, C. M., James, E. K., Ott, T., et al. (2021). Distinct signaling routes mediate intercellular and intracellular rhizobial infection in Lotus japonicus. *Plant Physiol.* 185, 1131–1147. doi: 10.1093/plphys/kiaa049

Ndoye, I., De Billy, F., Vasse, J., Dreyfus, B., and Truchet, G. (1994). Root nodulation of *Sesbania rostrata*. *J. Bacteriol.* 176, 1060–1068. doi: 10.1128/jb.176.4.1060-1068.1994

Peng, Z., Chen, H. Q., Tan, L. B., Shu, H. M., Varshney, R. K., Zhou, Z. K., et al. (2021). Natural polymorphisms in a pair of NSP2 homoeologs can cause loss of nodulation in peanut. *J. Exp. Bot.* 72, 1104–1118. doi: 10.1093/jxb/eraa505

Peng, Z., Liu, F., Wang, L., Zhou, H., Paudel, D., Tan, L., et al. (2017). Transcriptome profiles reveal gene regulation of peanut (*Arachis hypogaea* L.) nodulation. *Sci. Rep.* 7:40066. doi: 10.1038/srep40066

Quilbe, J., Lamy, L., Brottier, L., Leleux, P., Fardoux, J., Rivallan, R., et al. (2021). Genetics of nodulation in *Aeschynomene evenia* uncovers mechanisms of the rhizobium-legume symbiosis. *Nat. Commun.* 12:829. doi: 10.1038/s41467-021-21094-7

Ranga Rao, V. (1977). Effect of root temperature on the infection processes and nodulation in Lotus and Stylosanthes. *J. Exp. Bot.* 28, 241–259. doi: 10.1093/jxb/28.2.241

Raul, B., Bhattacharjee, O., Ghosh, A., Upadhyay, P., Tembhare, K., Singh, A., et al. (2022). Microscopic and transcriptomic analyses of Dalbergoid legume peanut reveal a divergent evolution leading to nod-factor-dependent epidermal crack-entry and terminal bacteroid differentiation. *Mol. Plant Microbe Interact.* 35, 131–145. doi: 10.1094/MPMI-05-21-0122-R

Roy, S., Liu, W., Nandety, R. S., Crook, A., Mysore, K. S., Pislariu, C. I., et al. (2020). Celebrating 20 years of genetic discoveries in legume nodulation and symbiotic nitrogen fixation([OPEN]). *Plant Cell* 32, 15–41. doi: 10.1105/tpc.19.00279

Shen, D., and Bisseling, T. (2020). The evolutionary aspects of legume nitrogen-fixing nodule Symbiosis. *Results Probl. Cell Differ.* 69, 387–408. doi: 10.1007/978-3-030-51849-3_14

Shu, H., Luo, Z., Peng, Z., and Wang, J. (2020). The application of CRISPR/Cas9 in hairy roots to explore the functions of AhNFR1 and AhNFR5 genes during peanut nodulation. *BMC Plant Biol.* 20:417. doi: 10.1186/s12870-020-02614-x

Sinharoy, S., and Dasgupta, M. (2009). RNA interference highlights the role of CCaMK in dissemination of Endosymbionts in the Aeschynomeneae legume Arachis. *Mol. Plant Microbe Interact.* 22, 1466–1475. doi: 10.1094/MPMI-22-11-1466

Sprent, J. I., Ardley, J., and James, E. K. (2017). Biogeography of nodulated legumes and their nitrogen-fixing symbionts. *New Phytol.* 215, 40–56. doi: 10.1111/nph.14474

Subba-Rao, N. S., Mateos, P. F., Baker, D., Pankratz, H. S., Palma, J., Dazzo, B., et al. (1995). The unique root-nodule symbiosis between Rhizobium and the aquatic legume, *Neptunia natans* (L. f.) Druce. *Planta* 196, 311–320. doi: 10.1007/BF00201390

Sun, M., Naeem, R., Su, J. X., Cao, Z. Y., Burleigh, J. G., Soltis, P. S., et al. (2016). Phylogeny of the Rosidae: A dense taxon sampling analysis. *J. Syst. Evol.* 54, 363–391. doi: 10.1111/jse.12211

Zarrabian, M., Montiel, J., Sandal, N., Jin, H., Lin, Y.Y., Klingl, V., et al. (2021). A promiscuity locus confers Lotus burttii nodulation with rhizobia from five different genera. bioRxiv [Preprint].

Conflict of Interest: The authors declare that the research was conducted in the absence of any commercial or financial relationships that could be construed as a potential conflict of interest.

Publisher's Note: All claims expressed in this article are solely those of the authors and do not necessarily represent those of their affiliated organizations, or those of the publisher, the editors and the reviewers. Any product that may be evaluated in this article, or claim that may be made by its manufacturer, is not guaranteed or endorsed by the publisher.

frontiers | Frontiers in Plant Science

REVIEW
published: 30 June 2022
doi: 10.3389/fpls.2022.900231

Ectomycorrhizal Networks in the Anthropocene: From Natural Ecosystems to Urban Planning

Louise Authier[1,2], *Cyrille Violle*[1] *and Franck Richard*[1]*

[1]CEFE, Univ Montpellier - CNRS - EPHE - IRD, Montpellier, France, [2]Ilex Paysage + Urbanisme, Lyon, France

Trees acquire hydric and mineral soil resources through root mutualistic associations. In most boreal, temperate and Mediterranean forests, these functions are realized by a chimeric structure called ectomycorrhizae. Ectomycorrhizal (ECM) fungi are highly diversified and vary widely in their specificity toward plant hosts. Reciprocally, association patterns of ECM plants range from highly specialist to generalist. As a consequence, ECM symbiosis creates interaction networks, which also mediate plant–plant nutrient interactions among different individuals and drive plant community dynamics. Our knowledge of ECM networks essentially relies on a corpus acquired in temperate ecosystems, whereas the below-ground facets of both anthropogenic ECM forests and inter-tropical forests remain poorly investigated. Here, we successively (1) review the current knowledge of ECM networks, (2) examine the content of early literature produced in ECM cultivated forests, (3) analyze the recent progress that has been made in understanding the place of ECM networks in urban soils, and (4) provide directions for future research based on the identification of knowledge gaps. From the examined corpus of knowledge, we reach three main conclusions. First, the emergence of metabarcoding tools has propelled a resurgence of interest in applying network theory to ECM symbiosis. These methods revealed an unexpected interconnection between mutualistic plants with arbuscular mycorrhizal (AM) herbaceous plants, embedding ECM mycelia through root-endophytic interactions. This affinity of ECM fungi to bind VA and ECM plants, raises questions on the nature of the associated functions. Second, despite the central place of ECM trees in cultivated forests, little attention has been paid to these man-made landscapes and in-depth research on this topic is lacking. Third, we report a lag in applying the ECM network theory to urban soils, despite management initiatives striving to interconnect motile organisms through ecological corridors, and the highly challenging task of interconnecting fixed organisms in urban greenspaces is discussed. In particular, we observe a pauperized nature of resident ECM inoculum and a spatial conflict between belowground human pipelines and ECM networks. Finally, we identify the main directions of future research to make the needed link between the current picture of plant functioning and the understanding of belowground ECM networks.

Keywords: plant-fungal interactions, ectomycorrhizal symbiosis, endophytic fungi, anthropogenic soils, forest soils, ecological succession, sylvigenetic cycle

OPEN ACCESS

Edited by:
Sabine Dagmar Zimmermann, Délégation Languedoc Roussillon (CNRS), France

Reviewed by:
Joske Ruytinx, Vrije University Brussel, Belgium
Raffaella Balestrini, Institute for Sustainable Plant Protection (CNR), Italy
Roland Mrmeisse, UMR7205 Institut de Systématique, Evolution, Biodiversité (ISYEB), France

***Correspondence:**
Franck Richard
franck.richard@cefe.cnrs.fr

Specialty section:
This article was submitted to Plant Symbiotic Interactions, a section of the journal Frontiers in Plant Science

Received: *20 March 2022*
Accepted: *30 May 2022*
Published: *30 June 2022*

Citation:
Authier L, Violle C and Richard F (2022) Ectomycorrhizal Networks in the Anthropocene: From Natural Ecosystems to Urban Planning. Front. Plant Sci. 13:900231. doi: 10.3389/fpls.2022.900231

INTRODUCTION

In most boreal, temperate and Mediterranean ecosystems, as in a part of tropical and sub-tropical forests, the canopies of few ectomycorrhizal (ECM) tree species dominate multi-layered communities of arbuscular mycorrhizal (AM) plants (Smith and Read, 2010; Tedersoo and Nara, 2010; Liang et al., 2020). ECM symbiosis shapes a wide variety of landscapes worldwide, from highly-preserved old-growth forests of the northern hemisphere (Smith et al., 2002; Spake et al., 2016), to emblematic oak savannas in Mediterranean biodiversity hotspots (Kennedy et al., 2012; Baptista et al., 2015), to highly artificialized tree plantations (Giachini et al., 2000) and orchards (Belfiori et al., 2012).

Belowground, ECM assist plant mineral nutrition by hydrolyzing natural polymeric compounds contained in litter and forest organic debris (Pritsch et al., 2011; Martin et al., 2016), and mobilizing soil water through absorptive hyphae (Lehto and Zwiazek, 2011). Based on their ability to densely colonize tree root systems, ECM mycelia establish hundreds of thousands of connections per square meter through short roots (Dahlberg et al., 1997; Taylor, 2002), from which thousands of kilometers of extrametrical mycelia are annually produced exploring soil for water, nutrients and new apices to colonize (Leake et al., 2004; Hagenbo et al., 2016), or provide physical support to plant–plant interactions in the soil.

Taxonomically, ECM mutualism is highly asymmetric, with a high diversity of some 20,000 species of Ascomycetes and Basidiomycetes linking only 6,000 species of Angiosperms and Gymnosperms within very few families (van der Heijden et al., 2015). In the ECM symbiosis, both the host and symbiotic species highly vary in their degree of specificity with their partners, from highly specialized (e.g., species in the Basidiomycete genera *Alnicola* and *Alpova* are strict associates of *Alnus* spp), to broad-host range species (e.g., the Ascomycete *Cenoccocum geophilum* associated with a wide range of Angiosperms and Gymnosperms; Bruns et al., 2002; Barham et al., 2014). These patterns underly the ability of ECM fungal diversity to interconnect ECM hosts through compatible dispersed inoculum across landscapes (Taudiere et al., 2015).

In multi-layered forests, the co-occurrence of plants from various mycorrhizal guilds constitutes the support for the establishment of common mycorrhizal networks (CMNs) linking canopies to the undergrowth through belowground mycelia. While AM networks interconnect roots from similar or different AM species of trees to shrubs and herbaceous plants (Wipf et al., 2019), fully autotrophs ECM trees exchange nutrients among each other (Klein et al., 2016) and with mixotrophic and mycoheterotrophic orchids (e.g., Li et al., 2021 for orchids) and ericaceous forest plants (Suetsugu et al., 2021).

Based on its ability to establish dense networks of hyphal connections among roots, ECM symbiosis strongly influences plant community composition and dynamics (Richard et al., 2009; van der Heijden et al., 2015; Nagati et al., 2019). Broad-host range species of fungi drive interspecific plant–plant interactions through shared mycelia (Beiler et al., 2010), which are then interconnected into CMNs. Reciprocally, hub species of ECM plants typically accumulate hyper-diverse communities of ECM fungi that co-occur on the local scale by their root systems (Tedersoo et al., 2012; Courty et al., 2016). In forest soils, these mycelial-mediated physical links among roots are involved in an underground carbon trade among co-occurring plant individuals (Simard et al., 2003; Klein et al., 2016). They constitute the below-ground facet of mycohetero- and mixotrophic plant evolutionary lineages, whose species become established and survive along with ECM trees (Bidartondo, 2005; Selosse et al., 2006). From a phytocentric perspective, these interaction networks mediate positive soil feedbacks among co-occurring plants and drive ecological successions (Bever, 2002; Kennedy et al., 2012).

One of the best markers of the Anthropocene lies on the dramatic degradation of physical, chemical, and biological signatures of the pedosphere, and the rapid extension of human-made soil profiles in most parts of the world (e.g., *Anthrosols* and *Technosols*; Certini and Scalenghe, 2011). As organisms are highly dependent on soil physico-chemical conditions, ECM fungal communities are critical components of soil history by responding to short-term as well as long-term human impacts (Dupouey et al., 2002). Inevitably, the composition and dynamics of ECM community are profoundly influenced by forest management (Tomao et al., 2020) and anthropic disturbance derived from agronomic practices in man-made ecosystems (Olivera et al., 2014; Taschen et al., 2015), with cascading effects on the underlying interaction networks (Correia et al., 2021).

Since the early 2000s and the first evidence of the pivotal role of ECM CMNs in the dynamics of temperate plant communities during both primary (Nara, 2006a) and secondary successions (Simard et al., 1997), the ecological significance of ECM fungal-mediated interactions among plants has been a matter of ongoing debate (Bever et al., 2010; Birch et al., 2020). As a consequence, our understanding of the physical nature, functional boundaries, and trophic influence of ECM CMNs has considerably increased for the last decade, propelled by both the emergence of powerful metabarcoding tools and the deployment of a variety of experimental approaches in order to decipher underground ECM-based processes.

In this review, we provide an overview of major advances of our understanding of the ECM CMNs, focusing on the spatial extent, associated functions and effects of anthropic practices on mycelium sharing among plants. We evaluate the published literature and identify research gaps to determine promising research avenues along a gradient of anthropic footprint, extending from forests driven by spontaneous processes on one hand, to cultivated forests (see **Glossary**) and highly artificial urban ecosystems on the other. First, we provide a diachronic perspective on the role of ECM CMNs in natural ecosystems along ecological successions, with a focus on the sylvigenetic cycle (i.e., the ontogenetic cycle of the forest *sensu* Oldeman, 2012). Second, we mobilize the state-of-the-art concerning ECM network-based research in cultivated forests, including agroforests, to discuss the unexpected diversity of ecological guilds involved in ECM networks, and the consequences of our understanding of forest functioning. Third,

we assemble current knowledge concerning ECM diversity patterns in urban soils, and discuss the challenge of conciliating ECM network-based services in cities and the development of human networks. Last, we propose a framework for future research across the gradient of ecosystems explored in the first three sections of the review.

ECTOMYCORRHIZAL NETWORKS DRIVE PLANT COMMUNITY DYNAMICS ALONG ECOLOGICAL SUCCESSION

During ecological successions in temperate, Mediterranean, and boreal ecosystems, two dependent processes concomitantly unfold after disturbance. While aboveground communities of pioneer herbs and shrubs are progressively enriched by tree species, a microbiological switchover occurs belowground, from primarily arbuscular mycorrhizae associations (AM) on roots of early vegetation stages to their replacement by ectomycorrhizal association patterns on tree root systems (van der Heijden et al., 2015). In these ecosystems, the main tree families (i.e., Fagaceae, Betulaceae, Pinaceae, and Salicaceae; Taudiere et al., 2015) have the ability to associate with ECM fungi. Contrastingly, only two families of shrubs (i.e., Cistaceae and Ericaceae *pro parte*; Comandini et al., 2006; Richard et al., 2009) are ectomycorrhizal. In this section, we successively discuss (1) the networking role of these ecologically pivotal shrub species that endure the transition between VA and ECM plant communities and (2) our knowledge of the role of ECM CMNs during the sylvigenetic cycle, from seedling establishment to the senescence of forest trees.

ECM Networks Mediate Plant–Plant Interactions in Early Successional Stages

Our knowledge of the ecological significance of ECM networks along succession almost entirely relies on data accumulated in boreal and temperate ecosystems of the Nearctic and palearctic regions (but see Ramanankierana et al., 2007 for a tropical perspective). In this documented area, and using a combination of *in situ* measurements, soil bioassays, and seedling transplantation, a consistent pattern of CMN-mediated nurse effect by shrubs on ECM late successional tree species has been reported in northern America (*Arbutus menziesii* vs. *Pseudotsuga menziesii*; Molina et al., 1997; Horton et al., 1999; Kennedy et al., 2012); *Helianthemum bicknellii* vs. *Quercus spp*; (Dickie et al., 2004), southern Europe (*Arbutus unedo* vs. *Quercus ilex*; Richard et al., 2009) and eastern Asia (*Salix reinii* vs. *Betula ermanii* and *Larix kaempferi*; Nara and Hogetsu, 2004; Nara, 2006b).

In the different investigated case studies, the highlighted CMNs-based facilitation process similarly lies on two complementary characteristics regarding the ecology of the nurse shrub species. First, ECM nurses have the ability to hold a prominent place in early stages of ecological succession, by either surviving after disturbance (Nara and Hogetsu, 2004) or establishing as a pioneer ECM species in a plant matrix exclusively composed of VA species (Dickie et al., 2004; Richard et al., 2009; Kennedy et al., 2012). Second, beyond this role of ecological hinge, ECM nurses act as inoculum relays for late successional tree species by accumulating diversified communities of ECM fungal partners on their roots, including generalist species which increase the potential for connection into common mycorrhizal networks. In previous research, the efficiency of CMNs in early vegetation stages has been evaluated by measuring the ability of these hub species to sustain the mycorrhization of the benefactor species (e.g., Kennedy et al., 2012) and by evaluating the subsequent gain on their growth, nutrient uptake and survival (e.g., Nara and Hogetsu, 2004).

Understanding the drivers of tree seedling establishment and survival is a central question in forest ecology, and a major challenge for forest and land managers. As a consequence, most research has been focused on the understanding of the role of ECM CMNs at the end of a shrub-dominated stage, when ECM tree species spontaneously establish in matrices of ECM nurse shrubs. These works overlook the major part of the chronological sequence since disturbance (**Figure 1A**). In particular, we still know little about the early ecological bases of early ECM networks, i.e., upon ECM shrub establishment in VA plant communities (**Figure 1A**). Interconnections among roots of VA and ECM plants through ECM-based mycelia may occur, as suggested by recent studies showing a possible dual [ECM + endophytic; see **Glossary**] niche for species of various lineages of ECM fungi in both asco- (e.g., *Tuber melanosporum* and *Tuber aestivum*; Schneider-Maunoury et al., 2018, 2020) and basidiomycetes (e.g., *Rhizopogon* spp.; Toju et al., 2018). The functional role of such plant–plant interactions is not clearly understood, and may include nutrient transfer from VA to ECM plants (see Taschen et al., 2020 for *Tuber melanosporum*), with possible consequences on the establishment and survival of ECM shrubs in stressful environments. Identifying both ECM fungal and VA plant hubs involved in these tripartite interaction networks may provide insights into the biotic dimension of both ECM plant and fungal fundamental niches, and offer promising perspective on restoration ecology, similarly to nurse-based processes of restoration developed on post-mining degraded ecosystems (Demenois et al., 2017).

Furthermore, the belowground facet of the functioning of highly resilient shrub populations is still poorly known in the later succession stages (**Figure 1A**). In particular, the role of mycelium sharing among conspecific ECM shrubs, as a possible mechanism underlying the drought tolerance and adaptation of these communities to disturbance remains poorly addressed. This is the case for Cistaceae, an emblematic family of evergreen shrubs dominating Mediterranean-type landscapes at low elevation (Guzmán and Vargas, 2009). Based on fruitbody surveys, there is evidence to suggest that Cistaceae host highly diversified and species-rich ECM fungal communities (Comandini et al., 2006; Loizides, 2016; Leonardi et al., 2020), yet little is known of their belowground patterns and functioning. Exploring the topology (see **Glossary**) of the corresponding CMNs, and their response to drought and disturbance in widely distributed monospecific stands, may contribute to a systemic understanding of the belowground adaptation processes of Mediterranean plants.

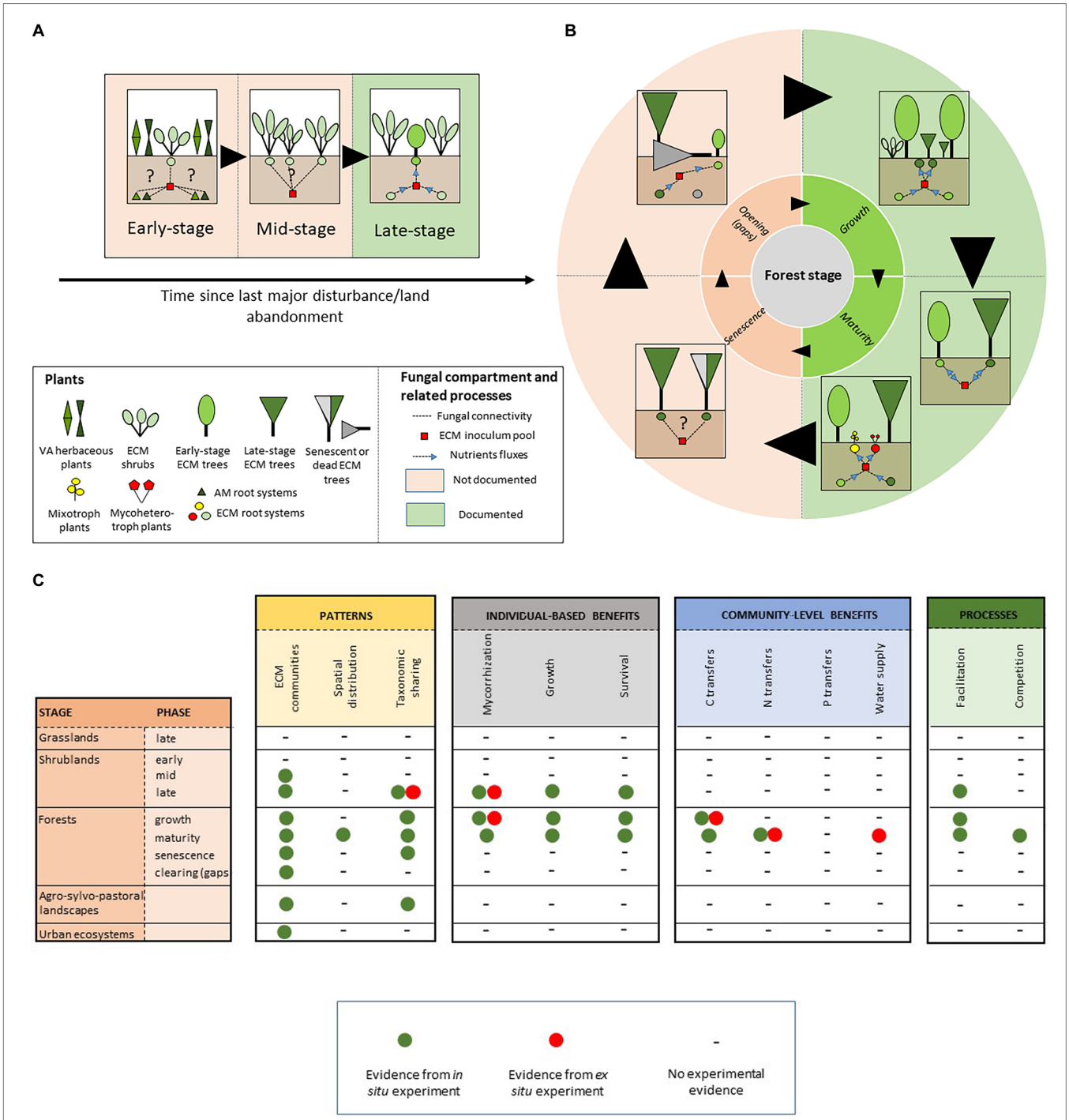

FIGURE 1 | Schematic representation of ectomycorrhizal-based networks **(A)** across early ecological succession and **(B)** during sylvigenetic cycle. Dashed lines indicate plant–plant interactions through ECM CMNs. Blue arrows indicate nutrient transfers through ECM CMNs. **(C)** Summary of ECM network-related effects documented along the chronosequence.

ECM Networks Sustain Nutrient Exchange Among Trees Along the Sylvigenetic Cycle

As forests age, two highly dependent community dynamics concomitantly occur. Thus, the progressive replacement of short-lived early-stage ECM trees (e.g., Betulaceae, Salicaceae, and Pinaceae pro parte) by long-lived shade-tolerant dryads aboveground (e.g., Fagaceae and Pinaceae *pro parte*) is accompanied by a marked shift in the composition of associated belowground communities (Bruns et al., 2002; Taudiere et al., 2015). On tree roots, while early-stage trees host poor ECM

fungal communities, dryads associate with multiple fungal species, and progressively accumulate species on their roots (e.g., Smith et al., 2002; Richard et al., 2005), with specialization degree of fungal partners increasing with tree aging (Bruns et al., 2002; Barham et al., 2014; Taudiere et al., 2015). Meanwhile, the underground composition of early-stage ECM fungal communities reciprocally drives the recruitment of late-stage plants. On roots of pioneer trees, broad host range fungal hubs transfer nutrients to late-stage trees through CMNs (Teste and Simard, 2008; Nagati et al., 2019), increasing their establishment success through soil feedbacks (Liang et al., 2020), most notably in arid environments (Bingham and Simard, 2012; Montesinos-Navarro et al., 2019).

Simard's pioneer work (Simard et al., 1997) propelled intensive research on the understanding of the role of ECM CMNs along forest sylvigenetic cycle. In particular, the ability of CMNs to mediate the recruitment of late-stage tree seedlings under the canopies of pioneer species has been largely explored. Interplant nutrient transferring through ECM CMNs is now considered as one of the most fascinating mechanisms involved in shade tolerance of late-stage tree species, which establish during forest ontogeny (**Figure 1B**; Teste and Simard, 2008; Simard et al., 2012), and partially and fully heterotrophic plant lineages living in the undergrowth (**Figure 1B**; Li et al., 2021). However, we still know little about the ecological significance of these trophic interactions among neighboring trees at the forest ecosystem level. Consistent evidence suggests that plant–plant interactions through shared ECM mycelia may play a central role in the performance of tree seedlings in mature forests in boreal (Nagati et al., 2019), temperate (Teste and Simard, 2008), Mediterranean (Egerton-Warburton et al., 2007), and tropical climates (Liang et al., 2020). The consequences of these interactions on the long-term ecosystem dynamics still need to be tested. For instance, community patterns and dynamics suggest that CMNs may drive soil-mediated positive feedback loops (Bever et al., 2010), which in turn may shape directional succession induced by climate change in boreal ecosystems (Deslippe and Simard, 2011; Nagati et al., 2019). In natural forests, the role of CMNs-based, long-term process in forest dynamics still need to be evaluated. For instance, in Mediterranean old-growth forests, shade-tolerant *Q. ilex* seedlings survive in light-restricted conditions for decades, until the senescent phase and the advent of canopy openings (Panaiotis et al., 1997). In gaps, these pre-established individuals avail of these conditions to emerge from the shrubby matrix and renew tree populations (Panaïotis et al., 1998). In the soil of senescent *Q. ilex* forest patches, seedlings and old *Q. ilex* individuals share high diversity of ECM symbionts on their roots (Richard et al., 2005). Along this well-described sylvigenetic cycle, quantifying nutrient transfers among conspecific individuals during mature and senescent phases, may advance our knowledge of the efficiency of CMNs-based interaction in forest regeneration.

The mechanisms underlying CMNs effect on forest dynamics are not fully understood. In particular, our knowledge of the nature and the ecological importance of transferred resource among co-occurring hosts remains partial. However, CMNs undoubtedly drive carbon transfer along reversible source-sink avenues at the local scale (Teste et al., 2009; Song et al., 2015; Cahanovitc et al., 2022). One of the most spectacular demonstration of this mechanism consists of carbon transfers among adult trees in temperate mixed conifer-hardwood forests (Klein et al., 2016). This finding is the first to reveal bidirectional nutrient exchanges among co-occurring ECM mature trees, with a significant amount of the carbon accumulated on roots of adult trees being transferred from neighboring donors. These transfers may be mainly based on fungal genera which typically dominate in mature forest stands (i.e., *Russula*, *Cortinarius*, *Lactarius*, and *Tricholoma*; Courty et al., 2005; Richard et al., 2005). Contrastingly, the influence of ECM CMNs on nitrogen and phosphorus sharing among co-occurring individuals remains less obvious (**Figure 1C**). However, ECM network-mediated nitrogen fluxes have been evidenced between co-occurring ECM tree species with contrasted nitrogen-acquisition strategies (He et al., 2006; Teste et al., 2015). The importance of these nutrient transfers on forest functioning is still under debate. Nevertheless, recent data suggest that they may drive feedback loops which promote tree population dynamics in monospecific tropical forests (Corrales et al., 2016). More generally, nutrient transfers through ECM CMNs are highly suspected to shape soil feedbacks and drive either cyclic or directional succession in the corresponding plant communities, from the tropics to arctic ecosystems (Deslippe and Simard, 2011; Kadowaki et al., 2018; Montesinos-Navarro et al., 2019; Liang et al., 2020). The knowledge accumulated during the last decade revealed an unexpectedly large biogeographical range and functional significance of ECM network-based ecosystem processes along forest ontogeny. However, research gaps still persist on both descriptive and functional facets of ECM networks in forest ecosystems. In particular, the role of ECM CMNs at the end of the sylvigenetic cycle, and particularly in natural canopy gaps, still need to explored (**Figure 1C**).

The belowground architecture of root systems of ECM trees, and the spatial distribution of the associated ECM fungal symbionts are poorly predicted by the vertical projection of the corresponding canopies (Lian et al., 2006; Taschen et al., 2015). Likewise, documenting the spatial patterns of plant–plant physical links through CMNs provide apparently counter-intuitive connections among highly spatially-distant individuals and determine unexpected hub individuals among populations (Teste et al., 2009), with consequences on forest management when tree individuals sustain production of associated resources (e.g., Lian et al., 2006 for Matsutake forests). At the local scale, we still know little about the distribution of links between plant and fungal individuals. However, first evidence from temperate *P. menziesii* uneven forests strikingly revealed the ability of ECM CMN to interconnect most co-occurring plant individuals with each-other (Beiler et al., 2010). In those ecosystems, and based on the use of multi-locus, microsatellite DNA markers, Beiler et al. (2015) revealed the nested topology of *Rhizopogon* ssp.-based ECM networks, suggesting a potential role in the resilience of tree population through the prevention of cascading

effect following tree death. To the best of our knowledge, most ECM ecosystems still await for similar systemic (i.e., network-based) assessments of their belowground functioning, despite the promising potential of networks-derived metrics for forest management and conservation (Taudiere et al., 2015).

IN CULTIVATED ECOSYSTEMS, ANTHROPIC PRACTICES AFFECT ECTOMYCORRHIZAL NETWORKS

Only 2% of vascular plant species are ectomycorrhizal (van der Heijden et al., 2015; Brundrett and Tedersoo, 2020). The majority of timber, softwood lumber and construction wood traded worldwide derives from this low percentage of vascular plants (Smith and Read, 2010). Most emblematic agro-sylvo-pastoral landscapes in the northern hemisphere are shaped by these plant species (e.g., Conedera et al., 2016 for an illustration with the domesticated ECM tree *Castanea sativa*). As a consequence, the effect of sylvicultural practices on ECM fungal communities, and the nature of adapted forest management practices to maintain diverse ECM communities has been intensively debated (see Tomao et al., 2020 for a review). Here, we successively discuss the current knowledge of the effect of human practices on ECM fungal networks in two main contexts. We first consider cultivated ecosystems as a wide variety of ECM forest types cultivated for timber production (see **Glossary**). Second, we review the state of the art in agroforests, i.e., in ECM socio-ecosystems where timber production is associated with a wide variety of human services, including crop and fruit productions (e.g., Dehesas, Montados, and planted orchards; Grove and Rackham, 2001).

Anthropic Disturbances Shape ECM Communities and Networks in Cultivated Forests

In cultivated ECM forests, sylvicultural practices generally consist of interrupting the sylvigenetic cycle at the maturity phase, truncating the end of both aboveground and belowground ecological successions. In most documented ecosystems dominated by either angiosperms or gymnosperms, both selective tree logging and clearcutting have been reported to induce marked compositional change in ECM fungal communities. The higher the intensity of practices, the higher are the deleterious effects on ECM diversity (Sterkenburg et al., 2019). Specifically, it has been shown that ECM community diversity positively responds to tree diversity, basal area and canopy cover in cultivated forest systems (Tomao et al., 2020; but see Craig et al., 2016; Spake et al., 2016 for case study-dependant contrasted responses). As a practical consequence, the retention of forest patches (Kranabetter et al., 2013; Varenius, 2017), green trees (Sterkenburg et al., 2019), and to a lesser extent coarse woody debris (Walker et al., 2012) at harvest time have been reported as efficient compensatory measures to maintain ECM fungal diversity in cultivated ecosystems. If direct effect of tree removal are widely documented, indirect effect deleterious of forest logging have been also reported, including environmental change (Varenius, 2017), soil compaction (Hartmann et al., 2014), and soil amendment (Olivera et al., 2014; Almeida et al., 2018).

The effect of forest management practices on ECM CMNs have been poorly investigated so far. However, the accumulated knowledge during the last decade in forest ecosystems gives a theoretical framework to analyze the response of plant-fungi bipartite networks to forest practices. From a plant-centered perspective, the reported pauperization effect of forest exploitation on ECM communities may alter the topology of ECM networks. Early evidence of age influence on network topology already exists: using high-throughput sequencing of soils, Correia et al. (2021) reported contrasted ECM network topologies along a chronosequence of *Fagus sylvatica* forest establishment, plant nodes in long-established forests presenting higher numbers of connection links than in recent patches. From a fungal perspective, silvicultural practices tend to reduce the number and diversity of available plant nodes for fungal genets. As a consequence, tree logging may decrease the linkage density of ECM CMNs in cultivated stands. When considering the highly saturated and nested nature of ECM CMNs (Beiler et al., 2010; Taudiere et al., 2015), one may suggest consequences of tree logging on ECM network-mediated processes in forest ecosystems, including affected tree regeneration dynamics (Pec et al., 2020). On the basis of scarce preliminary works, further research is needed to illuminate the relationships between the complexity and the stability of ECM CMNs. Cultivated forests are also ideal candidate systems to study the links between the stability of ECM CMNs and the resilience of forest ecosystems.

ECM Fungi Shape Complex Interaction Networks in Tree Savannas

Ectomycorrhizal trees dominate millions of hectares of anthropogenic landscapes in temperate and Mediterranean ecoregions, where trees, pastures, and croplands amalgamate in complex and species-rich mosaics called tree savannas (Grove and Rackham, 2001; Moreno and Pulido, 2009; see **Glossary**). Most ECM tree species contribute to the current highly diversified physiognomy of these systems, but the most emblematic ones are dominated by various species of oaks (e.g., from *Quercus velutina* dominating north America oak openings and typical *Quercus suber* dehesas, which cover one-eighth of Spain), sweet chestnut (e.g., *C. sativa* montados currently covering one-sixth of the area of Portugal), or larches and pines, which dominate multifunctional transitional landscapes between subalpine forests and alpine shrublands across Europe.

Because tree savannas play important ecological, social, and economic roles for societies (e.g., Conedera et al., 2016), understanding their functioning and analyzing their biodiversity patterns has been subject of much attention (Bugalho et al., 2011). Within their soils, these ecosystems concentrate some of the richest ECM communities described so far (Tedersoo et al., 2006; Morris et al., 2008; Baptista et al., 2015; Reis et al., 2018) and harbor highly specific fungal assemblies dominated by ascomycetes, in response to a unique combination of environmental and anthropic drivers (Dickie et al., 2009).

Despite the primary importance of tree savannas for conservation, very little is known about their belowground functioning, and ECM-mediated plant–plant interactions remain poorly explored in most of them.

Within this panorama, spontaneous oak savannas and planted orchards for the production of the emblematic black truffle (*Tuber melanosporum*) are an exception. Indeed, during the last decade, very few ECM communities received as much attention as *T. melanosporum* truffle grounds. In these transient ecosystems, a set of practices by truffle growers shape species-rich ECM communities, typically dominated by lineages of ascomycetes (e.g., Pyrenomataceae, Tuberaceae, and Helvellaceae) and early-stage lineages of basidiomycetes (e.g., Thelephoraceae) in both spontaneous and planted truffle grounds (e.g., Belfiori et al., 2012; Taschen et al., 2015). In these communities, *T. melanosporum* and few species in the early-stage lineages of basidio- (i.e., Thelephoraceae, Sebacinaceae, *Inocybe* spp., and *Scleroderma* spp.) and ascomycetes (i.e., *Cenoccocum geophilum* and Pyronemataceae), simultaneously associate as mutualists with their host through ECM root tips, and interact as fungal endophytes on the roots of most VA plant species established under host canopies (Schneider-Maunoury et al., 2018, 2020; **Figure 2A**). In these systems, the topology of the below-ground fungal interaction networks remains undescribed (**Figure 2A**). Similarly, the ecological consequences of the "beyond forest edge" spatial extent of ECM CMNs remains poorly addressed (Taschen et al., 2020). In particular, the ability of ECM fungi to transcend their host range and to establish as endophytes in the tissues of AM plants (Taschen et al., 2020) still need to be examined under a functional perspective. These remarkable findings pave the way for pursuing the exploration of ECM-VA plant interaction mediated by shared ECM fungal hubs (**Figure 2B**), to provide systemic views of forest functioning.

ECM COMMON MYCORRHIZAL NETWORKS IN URBAN SOILS: HEADACHE IN A SATURATED BELOW-GROUND

In anthropogenic urban ecosystems, a few ECM trees and shrubs (e.g., *Tilia*, *Pinus*, *Quercus*, and *Cistus*) hold a prominent place among a wide range of plant species adapted to the environmental conditions and physical constraints of cities (Bainard et al., 2011; Williams et al., 2015; Jenerette et al., 2016). In urban green spaces, the selection of plant species by urban land managers is in priority driven by socioeconomic constrains (Hope et al., 2003). In particular, a panel of aesthetical traits, including blooming intensity, flower size and color, shape patterns of urban tree diversity in cities (Kendal et al., 2012; Conway and Vander Vecht, 2015; Jenerette et al., 2016; Goodness, 2018). To a lesser extent, ecophysiological traits of species also matter, in particular plant tolerance to drought or freeze (Jenerette et al., 2016; McPherson et al., 2018). On the other hand, plant-related extended phenotype functions (Dawkins, 2016), such as fungal-mediated adaptation to drought through mycorrhizal symbionts, or nutrient uptake based on connection with neighboring individuals through ECM CMNs, still struggle to be included in selection processes among plant candidates.

Urban Soils Host Pauperized ECM Fungal Communities

The composition of soil fungal communities in urban soils remains largely unexplored (Delgado-Baquerizo et al., 2021). Published research consistently shows eroded patterns of ECM diversity in cities, as compared to forest ecosystems (Bainard et al., 2011; Karpati et al., 2011; Martinová et al., 2016). In particular, a low

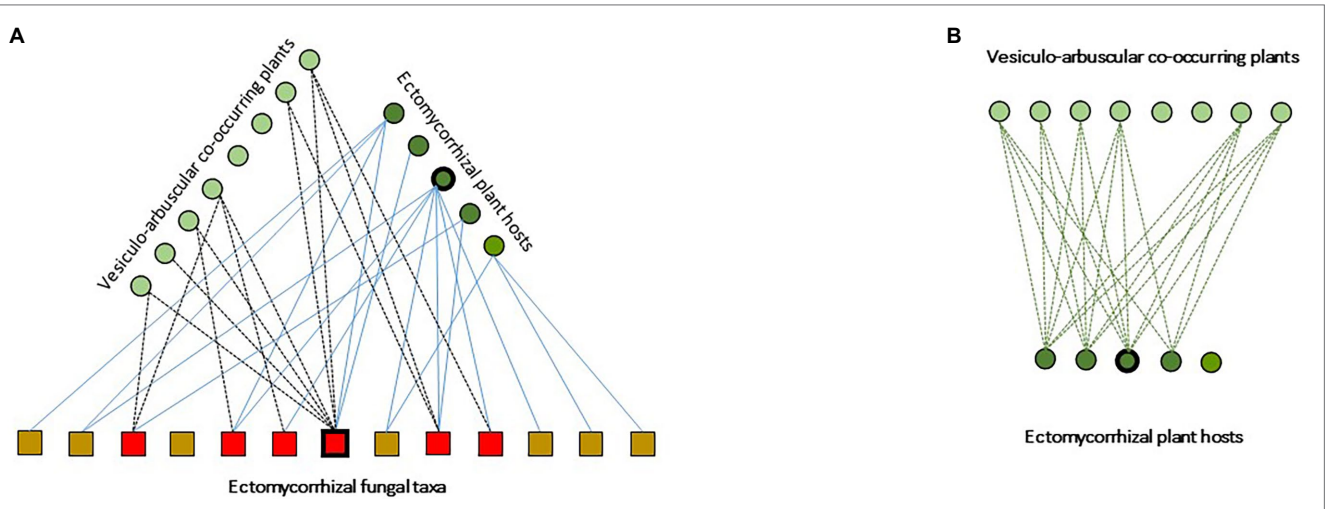

FIGURE 2 | Schematic representation of ectomycorrhizal-based multipartite networks in *Tuber ssp.* temperate agroforests, from Schneider-Maunoury et al. (2018) modified. **(A)** Species of co-occurring ectomycorrhizal and arbuscular mycorrhizal plants are represented by dark and clear green dots, respectively. The different taxa of ECM fungi are represented by squares. Interaction hubs are indicated by thickened outlines (here, *Quercus ilex* and *Tuber melanosposrum*). Solid lines indicate plant-fungi ECM interaction links. Dotted lines indicate interaction links between ECM fungal tava and VA plants. **(B)** Schematic representation of the corresponding projected VA-ECM plant network.

ECM species richness has been observed at the local scale, on roots of planted trees in city parks (Bainard et al., 2011; Karpati et al., 2011), streetscapes (Bainard et al., 2011), and private residential properties (Bainard et al., 2011), with an unusual dominance of hypogeous fungi (e.g., species in the Tuberaceae) and an underrepresentation of ECM families which typically dominate in forest soils (i.e., *Russulaceae*, *Inocybaceae*, and *Cortinariaceae*; Martinová et al., 2016; Hui et al., 2017; Van Geel et al., 2018). Interestingly, these pauperized communities show a high ability to colonize root systems, with similar ECM colonization rates on roots in urban soils as comparted to forests (Timonen and Kauppinen, 2008; Bainard et al., 2011; Tonn and Ibáñez, 2017). This pauperized nature of ECM communities in urban soils and subsequent homogenization of ECM fungal communities among cities on a continental scale (Schmidt et al., 2017; Delgado-Baquerizo et al., 2021), question about the mechanisms driving the observed compositional change and the consequences of species shift on urban ecosystem functioning. Three main mechanisms may concomitantly drive the observed patterns.

First, a deleterious effect of urban environment on both the dispersion (by physical barriers among poorly connected and highly fragmented habitats) and establishment (by unsuitable physico-chemical conditions in anthrosols; **Figure 3A**) are likely to act as filters on the potential communities of airborne and biotically dispersed ECM inoculum (Kasprzyk and Worek, 2006; Koide et al., 2011). In particular, sealing of urban soil surface may impact ECM dispersion from adjacent forests to city streets, with negative effects on ECM richness and diversity in urban soils (Martinová et al., 2016; **Figure 3A**).

Moreover, the low alpha diversity of ECM communities in cities may reflect the specific physicochemical properties of urban soils (Newbound et al., 2012; Lüttge and Buckeridge, 2020). Thus, the role of soil chemical signature as one of the main drivers of the composition, diversity, temporal dynamics and spatial patterns of ECM fungal communities has been widely documented in forest ecosystems (e.g., Lilleskov et al., 2011 for a review; Courty et al., 2016 for a functional perspective). Unsurprinsingly, in urban as in forest soils, the vegetative development (Olchowik et al., 2021), and the species richness (Newbound et al., 2012; Martinová et al., 2016; Van Geel et al., 2018) of ECM communities are negatively affected by soil alkalinity, and positively respond to organic matter and moisture content (Van Geel et al., 2018). The consistent pattern of ECM richness decrease and the composition drift observed in urban soils have then to be considered in light of (1) currently widespread practices along city roads, including deicing salts contributing to the alkalization of urban soils (Czerniawska-Kusza et al., 2004) and (2) the critically low organic matter content in city soils, in particular in sealed contexts (Scharenbroch et al., 2005; Alzetta et al., 2012), and its deleterious consequences on the establishment of species with affinities for organic soils (e.g., Genney et al., 2006; Kranabetter et al., 2009).

Last, the simplification of ECM communities in urbanized contexts may be a consequence of anthrosol assembling process in urban green spaces. This highly artificial growth matrix generally consists of a unique soil horizon intercalated between a deeper layer of mineral anthropogenic substrate, and a cover of impermeable materials (Rodríguez-Espinosa et al., 2021; **Figure 3A**). The specific physical soil properties of anthrosols (Lorenz and Lal, 2009) combined with surface sealing, drastically affects biological processes (Lu and Weng, 2006; Martinová et al., 2016; Salvati et al., 2016; Hui et al., 2017) limiting the differentiation of soil profile into distinct horizons during pedogenesis (Hui et al., 2017; **Figures 3A,B**). As a consequence, anthrosols remain unsuitable habitats for the vertical stratification of ECM diversity from organic surface to the underlying mineral horizons (Rosling et al., 2003; Genney et al., 2006), by penalizing hyper diverse ECM sub-communities with affinities for surface organic layers (Richard et al., 2011).

Traffic Jam in Urban Soils

During the last decade, restoring ecological networks in urban areas (Ignatieva et al., 2011) has become a priority for urban landscape planners, in order to provide suitable habitats for organisms and re-establish connectivity among fragmented meta-populations (Peng et al., 2017). The development of urban green corridors connecting habitat patches has been successfully developed in cities worldwide, as an efficient strategy to maintain high levels of alpha diversity (see **Glossary**), in particular for motile organisms (Beninde et al., 2015).

Contrastingly, fixed organisms such as plants and their fungal root associates still await to benefit from an adequate declination of network-based strategy for the conservation of dedicated belowground mutualistic interactions and their underlying functions. In particular, the topology of pauperized ECM CMNs in urban soils remains poorly described, the network-based signature of plant adaptation to urban environment still need to be explored, and the role of ECM CMNs for plant species coexistence in cities still need to be understood.

Yet, in urban areas as in natural ecosystems, there is strong evidence for a pivotal role of ECM colonization and diversity for promoting nutrient uptake (Newbound et al., 2010), acclimatation to hydric stress (Fini et al., 2011), tolerance to salt exposition (Zwiazek et al., 2019), and survival of ECM plants (Tonn and Ibáñez, 2017). Despite this pivotal role of ECM symbiosis, planning practices fail at integrating plant–plant ECM interconnexion through CMNs in urban design. At the individual level first, urbanization imposes to belowground counterparts of trees undersized dedicated soil volumes in compartmentalized planting pits (Day et al., 2010; **Figure 3A**). At the plant population/community level, the organization of cities constrains root development patterns along green linearities bordering transport networks (Levinson, 2012), anthropic pipelines (e.g., electrical, water, internet; Galle et al., 2019), and carriageway stabilizing materials (Randrup et al., 2001). Moreover, from a temporal perspective, high turnover of land-use of volatile urban landscapes hampers belowground mycelial dynamics by inducing severe soil disturbance regime (Moore, 2008; Lüttge and Buckeridge, 2020).

All in all, and further considering the temptation to consider urban underground space as an opportunity to compact city development (Cui et al., 2021), there is clear evidence that the establishment of functional ECM CMNs in cities may collide with the current geographical conceptualization of urban underground in the cities of the Anthropocene (Qihu, 2016; Connor and McNeill, 2022).

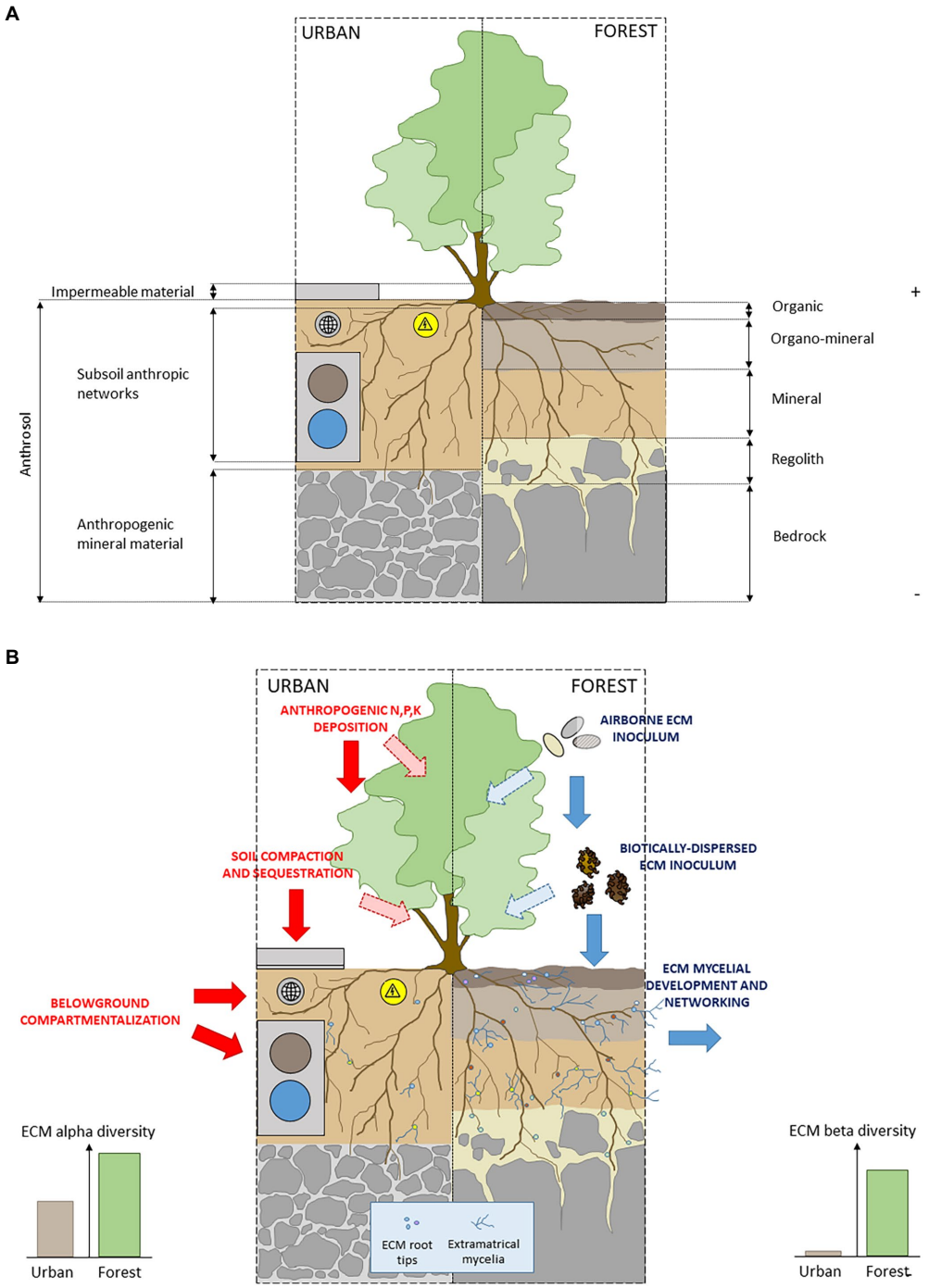

FIGURE 3 | (A) Schematic representation of pedogenic conditions for the development of ectomycorrhizal plants in urban and forest soil conditions and **(B)** schematic representation of ECM network-based mechanisms and anthropic filters in urban and forest soils conditions.

PERSPECTIVES AND CONCLUSIONS

The understanding of ectomycorrhizal interaction networks is a growing body of research. Their deterioration by human impacts is an overlooked marker of the anthropogenic footprint on terrestrial ecosystems. The pedosphere is particularly impacted by the rise to dominance of anthropic disturbances (Certini and Scalenghe, 2011). Here, we aimed at providing a comprehensive overview of the recent advances on our understanding of ECM CMNs in a wide range of ecosystems differing in the intensity of anthropic influence, in order to draw up a framework of

timely research avenues. From this analysis, three issues should be primarily addressed.

Knowledge Gaps in Natural Gaps

During the last decade, the development of metabarcoding tools propelled an unprecedented level of knowledge of belowground fungal patterns in forest soils, and enlarge perspectives on fungal assembly at both local (e.g., Baptista et al., 2015) and global (Tedersoo et al., 2014, 2020) scales. Despite significant progress been made, several gray areas persist. First, the topology of CMNs at the establishment time of pivotal ECM shrubs (**Figure 1A**) and the affinity of ECM fungi toward AM plant hosts, remain fascinating and poorly documented issues in ecology. Second, studies investigating network-based dynamics in soils of natural canopy gaps are surprisingly lacking. Yet, understanding the remobilization of late-stage trees inoculum heritage in soil by pioneer species to initiate a new sylvigenetic cycle (**Figure 1B**) is a central question for forest ecologists and managers. Last, there is urgent need to assess the effect of forest management practices on the topology of ECM networks since forest ecosystems face dramatic change through the combined effects of local impactful disturbance and global change.

Taxonomic Limits and Spatial Patterns of ECM CMNs

One major recent advance in our knowledge of ECM symbiosis is the ability of various ECM fungal lineages to interconnect between their hosts and VA plants, in both forests (Toju et al., 2018) and tree savannas (Schneider-Maunoury et al., 2020). This unexpected porosity among ecological guilds of plants raises the questions of (1) the spatial limits of ECM CMNs through physical links among involved plant individuals and (2) the taxonomic basis of these interactions in multi-layered plant communities. Moreover, the role of these mixed (ectomycorrhizal-endophytic) connections by polyvalent fungal species for forest community dynamics necessitates more effort to be fully understood (Taschen et al., 2020). This finding suggests to re-examine, from a biotic and below-ground perspective, the mechanisms involved in the particularly widespread nursing effect of VA plants for ECM trees.

Toward Soil Corridors for Underground Cities

Our synthesis reveals that patterns and functions of ECM CMNs in urban soils are poorly understood. However, given the rate of soil artificialization in cities worldwide (Scalenghe and Ajmone-Marsan, 2009; Just et al., 2018), there is crucial need to consider urban soils and their living organisms as a valuable resource for citizens in the Anthropocene. From a landscape management perspective, cities may be ideal candidates for the establishment of ECM network-based plant synergies in artificial green spaces, by designing interconnected planted pits along soil continuums, to maintain functional and multi-scaled ECM CMNs within *beige* corridors.

In such corridors, mimicking ECM networks established in natural ecosystems may be a promising avenue for urban planners to design functionally efficient artificial green spaces. First, in the cities of the Anthropocene, the composition of plant communities may (1) favor species with high number of associated ECM fungal species (i.e., interaction hub species such as Fagaceae; Taudiere et al., 2015) to increase the alpha diversity of ECM fungal inoculum, (2) associate nurse plants and late-stage benefactor species in multi-layered designs (**Figure 1**), and (3) promote synergies between AM and ECM plant guilds through endophytic interaction (see **Glossary**; **Figure 2**). In these artificial ecosystems, tree populations may be uneven-aged, to increase the complexity of ECM networks by promoting the emergence of interaction-hub tree individuals (i.e., aged individuals with high number of linked fungal individuals; Beiler et al., 2010), and subsequently favor the ecological stability within nested network patterns (Montoya et al., 2006).

Second, from a belowground perspective, the conception of anthrosols within *beige* corridors may be rethought to reach suitable soil properties (i.e., biotic and abiotic conditions, including chemical and physical properties) for the establishment and the expansion of physical ECM links among plants. Accommodations may encompass a reduction of soil sealing area, the use of permeable sealing materials, the edification of stratified and organic-enriched pedological profiles, and controlled ECM inoculation by native fungi (**Figure 3**). Ultimately, combining above- and belowground facets of *beige* corridors may be in line with the rewilding projects that gain popularity in landscape planning.

AUTHOR CONTRIBUTIONS

FR, LA, and CV wrote the manuscript and designed the figures. All authors contributed to the article and approved the submitted version.

FUNDING

This research was funded by the French Agency for Research and Technology (ANRT; contract CIFRE n°2020/0269).

ACKNOWLEDGMENTS

The authors thank Guerric Péré, Isabelle Vignolle, and Maël Camus from Ilex Paysages Inc., and Brice Chandon from EPA Euroméditerranée, who provided financial and technical support to LA. The authors also particularly grateful to Jean-Claude Durual from Pure Inc., who came up with the idea of LA's PhD, and who offered the support of its company for its realization. The authors sincerely thank Michael Loizides for his careful proofreading of the manuscript.

REFERENCES

Almeida, J. P., Rosenstock, N. P., Forsmark, B., Bergh, J., and Wallander, H. (2018). Ectomycorrhizal community composition and function in a spruce forest transitioning between nitrogen and phosphorus limitation. *Fungal Ecol.* 40, 20–31. doi: 10.1016/j.funeco.2018.05.008

Alzetta, C., Scattolin, L., Scopel, C., and Mutto Accordi, S. (2012). The ectomycorrhizal community in urban linden trees and its relationship with soil properties. *Trees* 26, 751–767. doi: 10.1007/s00468-011-0641-z

Bainard, L. D., Klironomos, J. N., and Gordon, A. M. (2011). The mycorrhizal status and colonization of 26 tree species growing in urban and rural environments. *Mycorrhiza* 21, 91–96. doi: 10.1007/s00572-010-0314-6

Baptista, P., Reis, F., Pereira, E., Tavares, R. M., Santos, P. M., Richard, F., et al. (2015). Soil DNA pyrosequencing and fruitbody surveys reveal contrasting diversity for various fungal ecological guilds in chestnut orchards. *Environ. Microbiol. Rep.* 7, 946–954. doi: 10.1111/1758-2229.12336

Barham, M., Harend, H., and Tedersoo, L. (2014). Network perspectives of ectomycorrhizal associations. *Fungal Ecol.* 7, 70–77. doi: 10.1016/j.funeco.2013.10.003

Beiler, K. J., Durall, D. M., Simard, S. W., Maxwell, S. A., and Kretzer, A. M. (2010). Architecture of the wood-wide web: Rhizopogon spp. genets link multiple Douglas-fir cohorts. *New Phytol.* 185, 543–553. doi: 10.1111/j.1469-8137.2009.03069.x

Beiler, K. J., Simard, S. W., and Durall, D. M. (2015). Topology of tree-mycorrhizal fungus interaction networks in xeric and Mesic Douglas-fir forests. *J. Ecol.* 103, 616–628. doi: 10.1111/1365-2745.12387

Belfiori, B., Riccioni, C., Tempesta, S., Pasqualetti, M., Paolocci, F., and Rubini, A. (2012). Comparison of ectomycorrhizal communities in natural and cultivated tuber melanosporum truffle grounds. *FEMS Microbiol. Ecol.* 81, 547–561. doi: 10.1111/j.1574-6941.2012.01379.x

Beninde, J., Veith, M., and Hochkirch, A. (2015). Biodiversity in cities needs space: a meta-analysis of factors determining intra-urban biodiversity variation. *Ecol. Lett.* 18, 581–592. doi: 10.1111/ele.12427

Bever, J. D. (2002). Negative feedback within a mutualism: Host-specific growth of mycorrhizal fungi reduces plant benefit. *Proc. R. Soc. Lond. B.* 269, 2595–2601. doi: 10.1098/rspb.2002.2162

Bever, J. D., Dickie, I. A., Facelli, E., Facelli, J. M., Klironomos, J., Moora, M., et al. (2010). Rooting theories of plant community ecology in microbial interactions. *Trends Ecol. Evol.* 25, 468–478. doi: 10.1016/j.tree.2010.05.004

Bidartondo, M. I. (2005). The evolutionary ecology of myco-heterotrophy. *New Phytol.* 167, 335–352. doi: 10.1111/j.1469-8137.2005.01429.x

Bingham, M. A., and Simard, S. (2012). Ectomycorrhizal networks of *Pseudotsuga menziesii var. glauca* trees facilitate establishment of conspecific seedlings under drought. *Ecosystems* 15, 188–199. doi: 10.1007/s10021-011-9502-2

Birch, J. D., Simard, S. W., Beiler, K. J., and Karst, J. (2020). Beyond seedlings: Ectomycorrhizal fungal networks and growth of mature *Pseudotsuga menziesii*. *J. Ecol.* 109, 806–818. doi: 10.1111/1365-2745.13507

Brundrett, M. C., and Tedersoo, L. (2020). Resolving the mycorrhizal status of important northern hemisphere trees. *Plant Soil* 454, 3–34. doi: 10.1007/s11104-020-04627-9

Bruns, T. D., Bidartondo, M. I., and Taylor, L. D. (2002). Host specificity in ectomycorrhizal communities: what do the exceptions tell us? *Integr. Comp. Biol.* 42, 352–359. doi: 10.1093/icb/42.2.352

Bugalho, M. N., Caldeira, M. C., Pereira, J. S., Aronson, J., and Pausas, J. G. (2011). Mediterranean cork oak savannas require human use to sustain biodiversity and ecosystem services. *Front. Ecol. Environ.* 9, 278–286. doi: 10.1890/100084

Cahanovitc, R., Livne-Luzon, S., Angel, R., and Klein, T. (2022). Ectomycorrhizal fungi mediate belowground carbon transfer between pines and oaks. *ISME J.* 16, 1420–1429. doi: 10.1038/s41396-022-01193-z

Certini, G., and Scalenghe, R. (2011). Anthropogenic soils are the golden spikes for the Anthropocene. *Holocene* 21, 1269–1274. doi: 10.1177/0959683611408454

Comandini, O., Contu, M., and Rinaldi, A. C. (2006). An overview of Cistus ectomycorrhizal fungi. *Mycorrhiza* 16, 381–395. doi: 10.1007/s00572-006-0047-8

Conedera, M., Tinner, W., Krebs, P., de Rigo, D., and Caudullo, G. (2016). "*Castanea sativa* in Europe: distribution, habitat, usage and threats," in *European Atlas of Forest Tree Species*. eds. J. San-Miguel-Ayanz, D. de Rigo, G. Caudullo, T. Houston Durrant and A. Mauri, 78–79.

Connor, A., and McNeill, D. (2022). Geographies of the urban underground. *Geogr. Compass* 16, 1–9. doi: 10.1111/gec3.12601

Conway, T. M., and Vander Vecht, J. (2015). Growing a diverse urban forest: species selection decisions by practitioners planting and supplying trees. *Landsc. Urban Plan.* 138, 1–10. doi: 10.1016/j.landurbplan.2015.01.007

Corrales, A., Arnold, A. E., Ferrer, A., Turner, B. L., and Dalling, J. W. (2016). Variation in ectomycorrhizal fungal communities associated with *Oreomunnea mexicana* (Juglandaceae) in a Neotropical montane forest. *Mycorrhiza* 26, 1–17. doi: 10.1007/s00572-015-0641-8

Correia, M., Espelta, J. M., Morillo, J. A., Pino, J., and Rodríguez-Echeverría, S. (2021). Land-use history alters the diversity, community composition and interaction networks of ectomycorrhizal fungi in beech forests. *J. Ecol.* 109, 2856–2870. doi: 10.1111/1365-2745.13674

Courty, P.-E., Pritsch, K., Schloter, M., Hartmann, A., and Garbaye, J. (2005). Activity profiling of ectomycorrhiza communities in two forest soils using multiple enzymatic tests. *New Phytol.* 167, 309–319. doi: 10.1111/j.1469-8137.2005.01401.x

Courty, P.-E., et al. (2016). Into the functional ecology of ectomycorrhizal communities: environmental filtering of enzymatic activities. *J. Ecol.* 104, 1585–1598. doi: 10.1111/1365-2745.12633

Craig, A. J., Woods, S., and Hoeksema, J. D. (2016). Influences of host plant identity and disturbance on spatial structure and community composition of ectomycorrhizal fungi in a northern Mississippi uplands ecosystem. *Fungal Ecol.* 24, 7–14. doi: 10.1016/j.funeco.2016.08.007

Cui, J., Broere, W., and Lin, D. (2021). Underground space utilisation for urban renewal. *Tunn. Undergr. Space Technol.* 108:103726. doi: 10.1016/j.tust.2020.103726

Czerniawska-Kusza, I., Kusza, G., and Duzyński, M. (2004). Effect of deicing salts on urban soils and health status of roadside trees in the Opole region. *Environ. Toxicol.* 19, 296–301. doi: 10.1002/tox.20037

Dahlberg, A., Jonsson, L., and Nylund, J.-E. (1997). Species diversity and distribution of biomass above and below ground among ectomycorrhizal fungi in an old-growth Norway spruce forest in South Sweden. *Can. J. Bot.* 75, 1323–1335. doi: 10.1139/b97-844

Dawkins, R. (2016). *The Extended Phenotype: The Long Reach of the Gene*. United Kingdom: Oxford University Press.

Day, S. D., et al. (2010). Tree root ecology in the urban environment and implications for a sustainable Rhizosphere. *Arboricult. Urban For.* 36, 193–205. doi: 10.48044/jauf.2010.026

Delgado-Baquerizo, M., Eldridge, D. J., Liu, Y. R., Sokoya, B., Wang, J. T., Hu, H. W., et al. (2021). Global homogenization of the structure and function in the soil microbiome of urban greenspaces. *Sci. Adv.* 7:eabg5809. doi: 10.1126/sciadv.abg5809

Demenois, J., Rey, F., Stokes, A., and Carriconde, F. (2017). Does arbuscular and ectomycorrhizal fungal inoculation improve soil aggregate stability? A case study on three tropical species growing in ultramafic Ferralsols. *Pedobiologia* 64, 8–14. doi: 10.1016/j.pedobi.2017.08.003

Deslippe, J. R., and Simard, S. W. (2011). Below-ground carbon transfer among *Betula nana* may increase with warming in Arctic tundra. *New Phytol.* 192, 689–698. doi: 10.1111/j.1469-8137.2011.03835.x

Dickie, I. A., Dentinger, B. T. M., Avis, P. G., McLaughlin, D. J., and Reich, P. B. (2009). Ectomycorrhizal fungal communities of oak savanna are distinct from forest communities. *Mycologia* 101, 473–483. doi: 10.3852/08-178

Dickie, I. A., Guza, R. C., Krazewski, S. E., and Reich, P. B. (2004). Shared ectomycorrhizal fungi between a herbaceous perennial (*Helianthemum bicknellii*) and oak (*Quercus*) seedlings. *New Phytol.* 164, 375–382. doi: 10.1111/j.1469-8137.2004.01177.x

Dupouey, J. L., Dambrine, E., Laffite, J. D., and Moares, C. (2002). Irreversible impact of past land use on forest soils and biodiversity. *Ecology* 83, 2978–2984. doi: 10.1890/0012-9658

Egerton-Warburton, L. M., Querejeta, J. I., and Allen, M. F. (2007). Common mycorrhizal networks provide a potential pathway for the transfer of hydraulically lifted water between plants. *J. Exp. Bot.* 58, 1473–1483. doi: 10.1093/jxb/erm009

Fini, A., Frangi, P., Amoroso, G., Piatti, R., Faoro, M., Bellasio, C., et al. (2011). Effect of controlled inoculation with specific mycorrhizal fungi from the urban environment on growth and physiology of containerized shade tree species growing under different water regimes. *Mycorrhiza* 21, 703–719. doi: 10.1007/s00572-011-0370-6

Galle, N. J., Nitoslawski, S. A., and Pilla, F. (2019). The internet of nature: how taking nature online can shape urban ecosystems. *Anthr. Rev.* 6, 279–287. doi: 10.1177/2053019619877103

Genney, D. R., Anderson, I. C., and Alexander, I. J. (2006). Fine-scale distribution of pine ectomycorrhizas and their extramatrical mycelium. *New Phytol.* 170, 381–390. doi: 10.1111/j.1469-8137.2006.01669.x

Giachini, A. J., Oliveira, V. L., Castellano, M. A., and Trappe, J. M. (2000). Ectomycorrhizal fungi in Eucalyptus and Pinus plantations in southern Brazil. *Mycologia* 92, 1166–1177. doi: 10.1080/00275514.2000.12061264

Goodness, J. (2018). Urban landscaping choices and people's selection of plant traits in Cape Town, South Africa. *Environ. Sci. Policy* 85, 182–192. doi: 10.1016/j.envsci.2018.02.010

Grove, and Rackham. (2001). *The Nature of Mediterranean Europe: an Ecological History*. New Haven and London: Yale University Press.

Guzmán, B., and Vargas, P. (2009). Historical biogeography and character evolution of Cistaceae (Malvales) based on analysis of plastid rbcL and trnL-trnF sequences. *Org. Divers. Evol.* 9, 83–99. doi: 10.1007/s11104-019-04340-2

Hagenbo, A., Clemmensen, K. E., Finlay, R. D., Kyaschenko, J., Lindahl, B. D., Fransson, P., et al. (2016). Changes in turnover rather than production regulate biomass of ectomycorrhizal fungal mycelium across a *Pinus sylvestris* chronosequence. *New Phytol.* 214, 424–431. doi: 10.1111/nph.14379

Hartmann, M., Niklaus, P. A., Zimmermann, S., Schmutz, S., Kremer, J., Abarenkov, K., et al. (2014). Resistance and resilience of the forest soil microbiome to logging-associated compaction. *ISME J.* 8, 226–244. doi: 10.1038/ismej.2013.141

He, X., Bledsoe, C. S., Zasoski, R. J., Southworth, D., and Horwath, W. R. (2006). Rapid nitrogen transfer from ectomycorrhizal pines to adjacent ectomycorrhizal and arbuscular mycorrhizal plants in a California oak woodland. *New Phytol.* 170, 143–151. doi: 10.1111/j.1469-8137.2006.01648.x

Hope, D., Gries, C., Zhu, W., Fagan, W. F., Redman, C. L., Grimm, N. B., et al. (2003). Socioeconomics drive urban plant diversity. *PNAS* 100, 8788–8792. doi: 10.1007/978-0-387-73412-5_21

Horton, T. R., Bruns, T. D., and Parker, V. T. (1999). Ectomycorrhizal fungi associated with Arctostaphylos contribute to *Pseudotsuga menziesii* establishment. *Can. J. Bot.* 77, 93–102. doi: 10.1139/b98-208

Hui, N., Liu, X., Kotze, D. J., Jumpponen, A., Francini, G., and Setälä, H. (2017). Ectomycorrhizal fungal communities in urban parks are similar to those in natural forest but shaped by vegetation and park age. *Appl. Environ. Microbiol.* 83, 1–12. doi: 10.1128/AEM.01797-17

Ignatieva, M., Stewart, G. H., and Meurk, C. (2011). Planning and design of ecological networks in urban areas. *Landsc. Ecol. Eng.* 7, 17–25. doi: 10.1007/s11355-010-0143-y

Jenerette, G. D., Clarke, L. W., Avolio, M. L., Pataki, D. E., Gillespie, T. W., Pincetl, S., et al. (2016). Climate tolerances and trait choices shape continental patterns of urban tree biodiversity. *Glob. Ecol. Biogeogr.* 25, 1367–1376. doi: 10.1111/geb.12499

Just, M. G., Frank, S. D., and Dale, A. G. (2018). Impervious surface thresholds for urban tree site selection. *Urban For. Urban Green.* 34, 141–146. doi: 10.1016/j.ufug.2018.06.008

Kadowaki, K., Yamamoto, S., Sato, H., Tanabe, A. S., Hidaka, A., and Toju, H. (2018). Mycorrhizal fungi mediate the direction and strength of plant–soil feedbacks differently between arbuscular mycorrhizal and ectomycorrhizal communities. *Commun. Biol.* 1, 196–195. doi: 10.1038/s42003-018-0201-9

Karpati, A. S., Handel, S. N., Dighton, J., and Horton, T. R. (2011). *Quercus rubra*-associated ectomycorrhizal fungal communities of disturbed urban sites and mature forests. *Mycorrhiza* 21, 537–547. doi: 10.1007/s00572-011-0362-6

Kasprzyk, I., and Worek, M. (2006). Airborne fungal spores in urban and rural environments in Poland. *Aerobiologia* 22, 169–176. doi: 10.1007/s10453-006-9029-8

Kendal, D., Williams, K. J. H., and Williams, N. S. G. (2012). Plant traits link people's plant preferences to the composition of their gardens. *Landsc. Urban Plan.* 105, 34–42. doi: 10.1016/j.landurbplan.2011.11.023

Kennedy, P. G., Smith, D. P., Horton, T. R., and Molina, R. J. (2012). *Arbutus menziesii* (Ericaceae) facilitates regeneration dynamics in mixed evergreen forests by promoting mycorrhizal fungal diversity and host connectivity. *Am. J. Bot.* 99, 1691–1701. doi: 10.3732/ajb.1200277

Klein, T., Siegwolf, R. T. W., and Körner, C. (2016). Belowground carbon trade among tall trees in a temperate forest. *Science* 352, 342–344. doi: 10.1126/science.aad6188

Koide, R. T., Fernandez, C., and Petprakob, K. (2011). General principles in the community ecology of ectomycorrhizal fungi. *Ann. For. Sci.* 68, 45–55. doi: 10.1007/s13595-010-0006-6

Kranabetter, J. M., de Montigny, L., and Ross, G. (2013). Effectiveness of green-tree retention in the conservation of ectomycorrhizal fungi. *Fungal Ecol.* 6, 430–438. doi: 10.1016/j.funeco.2013.05.001

Kranabetter, J. M., Durall, D. M., and MacKenzie, W. H. (2009). Diversity and species distribution of ectomycorrhizal fungi along productivity gradients of a southern boreal forest. *Mycorrhiza* 19, 99–111. doi: 10.1007/s00572-008-0208-z

Leake, J., Johnson, D., Donnelly, D., Muckle, G., Boddy, L., and Read, D. (2004). Networks of power and influence: The role of mycorrhizal mycelium in controlling plant communities and agroecosystem functioning. *Can. J. Bot.* 82, 1016–1045. doi: 10.1139/B04-060

Lehto, T., and Zwiazek, J. J. (2011). Ectomycorrhizas and water relations of trees: A review. *Mycorrhiza* 21, 71–90. doi: 10.1007/s00572-010-0348-9

Leonardi, M., Furtado, A. N. M., Comandini, O., Geml, J., and Rinaldi, A. C. (2020). Halimium as an ectomycorrhizal symbiont: new records and an appreciation of known fungal diversity. *Mycol. Prog.* 19, 1495–1509. doi: 10.1007/s11557-020-01641-0

Levinson, D. (2012). Network structure and city size. *PLoS One* 7:e29721. doi: 10.1371/journal.pone.0029721

Li, Y. Y., Boeraeve, M., Cho, Y. H., Jacquemyn, H., and Lee, Y. I. (2021). Mycorrhizal switching and the role of fungal abundance in seed germination in a fully Mycoheterotrophic orchid, Gastrodia confusoides. *Front. Plant Sci.* 12:775290. doi: 10.3389/fpls.2021.775290

Lian, C., Narimatsu, M., Nara, K., and Hogetsu, T. (2006). Tricholoma matsutake in a natural *Pinus densiflora* forest: correspondence between above- and below-ground genets, association with multiple host trees and alteration of existing ectomycorrhizal communities. *New Phytol.* 171, 825–836. doi: 10.1111/j.1469-8137.2006.01801.x

Liang, M., Johnson, D., Burslem, D. F. R. P., Yu, S., Fang, M., Taylor, J. D., et al. (2020). Soil fungal networks maintain local dominance of ectomycorrhizal trees. *Nat. Commun.* 11, 2636–2637. doi: 10.1038/s41467-020-16507-y

Lilleskov, E. A., Hobbie, E. A., and Horton, T. R. (2011). Conservation of ectomycorrhizal fungi: exploring the linkages between functional and taxonomic responses to anthropogenic N deposition. *Fungal Ecol.* 4, 174–183. doi: 10.1016/j.funeco.2010.09.008

Loizides, M. (2016). Macromycetes within Cistaceae-dominated ecosystems in Cyprus. *Mycotaxon* 131, 255–256. doi: 10.5248/131.255

Lorenz, K., and Lal, R. (2009). Biogeochemical C and N cycles in urban soils. *Environ. Int.* 35, 1–8. doi: 10.1016/j.envint.2008.05.006

Lu, D., and Weng, Q. (2006). Use of impervious surface in urban land-use classification. *Remote Sens. Environ.* 102, 146–160. doi: 10.1016/j.rse.2006.02.010

Lüttge, U., and Buckeridge, M. (2020). Trees: structure and function and the challenges of urbanization. *Trees* 26:251. doi: 10.1007/s00468-020-01964-1

Martin, F., Kohler, A., Murat, C., Veneault-Fourrey, C., and Hibbett, D. S. (2016). Unearthing the roots of ectomycorrhizal symbioses. *Nat. Rev. Microbiol.* 14, 760–773. doi: 10.1038/nrmicro.2016.149

Martinová, V., van Geel, M., Lievens, B., and Honnay, O. (2016). Strong differences in *Quercus robur*-associated ectomycorrhizal fungal communities along a forest-city soil sealing gradient. *Fungal Ecol.* 20, 88–96. doi: 10.1016/j.funeco.2015.12.002

McPherson, E. G., Berry, A. M., and van Doorn, N. S. (2018). Performance testing to identify climate-ready trees. *Urban For. Urban Green.* 29, 28–39. doi: 10.1016/j.ufug.2017.09.003

Molina, R., Smith, J., McKay, D., and Melville, L. (1997). Biology of the ectomycorrhizal genus, *Rhizopogon* III. Influence of co-cultured conifer species on mycorrhizal specificity with the arbutoid hosts *Arctostaphylos uvaursi* and *Arbutus menziesii*. *New Phytol.* 137, 519–528. doi: 10.1046/j.1469-8137.1997.00836.x

Montesinos-Navarro, A., Valiente-Banuet, A., and Verdú, M. (2019). Processes underlying the effect of mycorrhizal symbiosis on plant-plant interactions. *Fungal Ecol.* 40, 98–106. doi: 10.1016/j.funeco.2018.05.003

Montoya, J. M., Pimm, S. L., and Solé, R. V. (2006). Ecological networks and their fragility. *Nature* 442, 259–264. doi: 10.1038/nature04927

Moore, G. M. (2008). "Managing urban tree root systems." in *TREENET Proceedings of the 9th National Street Tree Symposium 4th and 5th September*.

Moreno, G., and Pulido, F. J. (2009). "The functioning, management and persistence of Dehesas," in *Agroforestry in Europe* (Dordrecht: Springer), 127–160.

Morris, M. H., Smith, M. E., Rizzo, D. M., Rejmánek, M., and Bledsoe, C. S. (2008). Contrasting ectomycorrhizal fungal communities on the roots of co-occurring oaks (*Quercus* spp.) in a California woodland. *New Phytol.* 178, 167–176. doi: 10.1111/j.1469-8137.2007.02348.x

Nagati, M., Roy, M., Desrochers, A., Manzi, S., Bergeron, Y., and Gardes, M. (2019). Facilitation of balsam fir by trembling aspen in the boreal forest: do ectomycorrhizal communities matter? *Front. Plant Sci.* 10, 1–12. doi: 10.3389/fpls.2019.00932

Nara, K. (2006a). Ectomycorrhizal networks and seedling establishment during early primary succession. *New Phytol.* 169, 169–178. doi: 10.1111/j.1469-8137.2005.01545.x

Nara, K. (2006b). Pioneer dwarf willow may facilitate tree succession by providing late colonizers with compatible ectomycorrhizal fungi in a primary successional volcanic desert. *New Phytol.* 171, 187–198. doi: 10.1111/j.1469-8137.2006.01744.x

Nara, K., and Hogetsu, T. (2004). Ectomycorrhizal fungi on established shrubs facilitate subsequent seedling establishment of successional plant species. *Ecology* 85, 1700–1707. doi: 10.1890/03-0373

Newbound, M., Mccarthy, M. A., and Lebel, T. (2010). Fungi and the urban environment: A review. *Landsc. Urban Plan.* 96, 138–145. doi: 10.1016/j.landurbplan.2010.04.005

Newbound, M., et al. (2012). Soil chemical properties, rather than landscape context, influence woodland fungal communities along an urban-rural gradient. *Austral Ecol.* 37, 236–247. doi: 10.1111/j.1442-9993.2011.02269.x

Olchowik, J., Suchocka, M., Jankowski, P., Malewski, T., and Hilszczańska, D. (2021). The ectomycorrhizal community of urban linden trees in Gdańsk, Poland. *PLoS ONE* 16, 1–15. doi: 10.1371/journal.pone.0237551

Oldeman, R. A. (2012). *Forests: Elements of Silvology*. Berlin: Springer Science & Business Media.

Olivera, A., Bonet, J. A., and Oliach, D. (2014). Time and dose of irrigation impact tuber melanosporum ectomycorrhiza proliferation and growth of *Quercus ilex* seedling hosts in young black truffle orchards. *Mycorrhiza* 24, 73–78. doi: 10.1007/s00572-013-0545-4

Panaiotis, C., Carcaillet, C., and M'Hamedi, M. (1997). Determination of the natural mortality age of an holm oak (*Quercus ilex* L.) stand in Corsica (Mediterranean Island). *Acta Oecol.* 18, 519–530. doi: 10.1016/S1146-609X(97)80038-0

Panaïotis, C., Loisel, R., and Roux, M. (1998). Analyse de la réponse de la végétation aux trouées naturelles dans une futaie âgée de Quercus ilex L. en Corse (île Méditerranéenne). *Can. J. For. Res.* 28, 1125–1134. doi: 10.1139/x98-070

Pec, G. J., Simard, S. W., Cahill, J. F. Jr., and Karst, J. (2020). The effects of ectomycorrhizal fungal networks on seedling establishment are contingent on species and severity of overstorey mortality. *Mycorrhiza* 30, 173–183. doi: 10.1007/s00572-020-00940-4

Peng, J., Zhao, H., and Liu, Y. (2017). Urban ecological corridors construction: A review. *Acta Ecol. Sin.* 37, 23–30. doi: 10.1016/j.chnaes.2016.12.002

Pritsch, K., Courty, P. E., Churin, J. L., Cloutier-Hurteau, B., Ali, M. A., Damon, C., et al. (2011). Optimized assay and storage conditions for enzyme activity profiling of ectomycorrhizae. *Mycorrhiza* 21, 589–600. doi: 10.1007/s00572-011-0364-4

Qihu, Q. (2016). Present state, problems and development trends of urban underground space in China. *Tunn. Undergr. Space Technol.* 55, 280–289. doi: 10.1016/j.tust.2015.11.007

Ramanankierana, N., Ducousso, M., Rakotoarimanga, N., Prin, Y., Thioulouse, J., Randrianjohany, E., et al. (2007). Arbuscular mycorrhizas and ectomycorrhizas of Uapaca bojeri L. (Euphorbiaceae): Sporophore diversity, patterns of root colonization, and effects on seedling growth and soil microbial catabolic diversity. *Mycorrhiza* 17, 195–208. doi: 10.1007/s00572-006-0095-0

Randrup, T. B., McPherson, E. G., and Costello, L. R. (2001). A review of tree root conflicts with sidewalks, curbs, and roads. *Urban Ecosyst.* 5, 209–225. doi: 10.1023/A:1024046004731

Reis, F., Valdiviesso, T., Varela, C., Tavares, R. M., Baptista, P., and Lino-Neto, T. (2018). Ectomycorrhizal fungal diversity and community structure associated with cork oak in different landscapes. *Mycorrhiza* 28, 357–368. doi: 10.1007/s00572-018-0832-1

Richard, F., Gardes, M., and Selosse, M.-A. (2009). Facilitated establishment of *Quercus ilex* in shrub-dominated communities within a Mediterranean ecosystem: do mycorrhizal partners matter? *FEMS Microbiol. Ecol.* 68, 14–24. doi: 10.1111/j.1574-6941.2009.00646.x

Richard, F., Millot, S., Gardes, M., and Selosse, M. A. (2005). Diversity and specificity of ectomycorrhizal fungi retrieved from an old-growth Mediterranean forest dominated by *Quercus ilex*. *New Phytol.* 166, 1011–1023. doi: 10.1111/j.1469-8137.2005.01382.x

Richard, F., Roy, M., Shahin, O., Sthultz, C., Duchemin, M., Joffre, R., et al. (2011). Ectomycorrhizal communities in a Mediterranean forest ecosystem dominated by *Quercus ilex*: seasonal dynamics and response to drought in the surface organic horizon. *Ann. For. Sci.* 68, 57–68. doi: 10.1007/s13595-010-0007-5

Rodríguez-Espinosa, T., Navarro-Pedreño, J., Gómez-Lucas, I., Jordán-Vidal, M. M., Bech-Borras, J., and Zorpas, A. A. (2021). Urban areas, human health and technosols for the green deal. *Environ. Geochem. Health* 43, 5065–5086. doi: 10.1007/s10653-021-00953-8

Rosling, A., Landeweert, R., Lindahl, B. D., Larsson, K. H., Kuyper, T. W., Taylor, A. F. S., et al. (2003). Vertical distribution of ectomycorrhizal fungal taxa in a podzol soil profile. *New Phytol.* 159, 775–783. doi: 10.1046/j.1469-8137.2003.00829.x

Salvati, L., Quatrini, V., Barbati, A., Tomao, A., Mavrakis, A., Serra, P., et al. (2016). Soil occupation efficiency and landscape conservation in four mediaterranean urban regions. *Urban For. Urban Green.* 20, 419–427. doi: 10.1016/j.ufug.2016.10.006

Scalenghe, R., and Ajmone-Marsan, F. (2009). The anthropogenic sealing of soils in urban areas. *Landsc. Urban Plan.* 90, 1–10. doi: 10.1016/j.landurbplan.2008.10.011

Scharenbroch, B. C., Lloyd, J. E., and Johnson-Maynard, J. L. (2005). Distinguishing urban soils with physical, chemical, and biological properties. *Pedobiologia* 49, 283–296. doi: 10.1016/j.pedobi.2004.12.002

Schmidt, D. J. E., et al. (2017). Urbanization erodes ectomycorrhizal diversity and may cause microbial communities to converge. *Nat. Ecol. Evol.* 1, 1–9. doi: 10.1038/s41559-017-0123

Schneider-Maunoury, L., Deveau, A., Moreno, M., Todesco, F., Belmondo, S., Murat, C., et al. (2020). Two ectomycorrhizal truffles, tuber melanosporum and *T. aestivum*, endophytically colonise roots of non-ectomycorrhizal plants in natural environments. *New Phytol.* 225, 2542–2556. doi: 10.1111/nph.16321

Schneider-Maunoury, L., Leclercq, S., Clément, C., Covès, H., Lambourdière, J., Sauve, M., et al. (2018). Is tuber melanosporum colonizing the roots of herbaceous, non-ectomycorrhizal plants? *Fungal Ecol.* 31, 59–68. doi: 10.1016/j.funeco.2017.10.004

Selosse, M. A., Richard, F., He, X., and Simard, S. W. (2006). Mycorrhizal networks: des liaisons dangereuses? *Trends Ecol. Evol.* 21, 621–628. doi: 10.1016/j.tree.2006.07.003

Simard, S. W., Beiler, K. J., Bingham, M. A., Deslippe, J. R., Philip, L. J., and Teste, F. P. (2012). Mycorrhizal networks: mechanisms, ecology and modelling. *Fungal Biol. Rev.* 26, 39–60. doi: 10.1016/j.fbr.2012.01.001

Simard, S. W., Jones, M. D., and Durall, D. M. (2003). Carbon and nutrient fluxes within and between mycorrhizal plants. *Ecol. Stud.* 157, 32–72. doi: 10.1007/978-3-540-38364-2_2

Simard, S. W., Perry, D. A., Jones, M. D., Myrold, D. D., Durall, D. M., and Molina, R. (1997). Net transfer of carbon between ectomycorrhizal tree species in the field. *Nature* 388, 579–582. doi: 10.1038/41557

Smith, J. E., Molina, R., Huso, M. M. P., Luoma, D. L., McKay, D., Castellano, M. A., et al. (2002). Species richness, abundance, and composition of hypogeous and epigeous ectomycorrhizal fungal sporocarps in young, rotation-age, and old-growth stands of Douglas-fir (*Pseudotsuga menziesii*) in the Cascade Range of Oregon, U.S.A. *Can. J. Bot.* 80, 186–204. doi: 10.1139/b02-003

Smith, S. E., and Read, D. J. (2010). *Mycorrhizal Symbiosis* Harcourt Brace & Company, Publishers: Academic Press.

Song, Y. Y., Simard, S. W., Carroll, A., Mohn, W. W., and Zeng, R. S. (2015). Defoliation of interior Douglas-fir elicits carbon transfer and stress signalling to ponderosa pine neighbors through ectomycorrhizal networks. *Sci. Rep.* 5, 1–9. doi: 10.1038/srep08495

Spake, R., van der Linde, S., Newton, A. C., Suz, L. M., Bidartondo, M. I., and Doncaster, C. P. (2016). Similar biodiversity of ectomycorrhizal fungi in set-aside plantations and ancient old-growth broadleaved forests. *Biol. Conserv.* 194, 71–79. doi: 10.1016/j.biocon.2015.12.003

Sterkenburg, E., Clemmensen, K. E., Lindahl, B. D., and Dahlberg, A. (2019). The significance of retention trees for survival of ectomycorrhizal fungi in clear-cut scots pine forests. *J. Appl. Ecol.* 56, 1367–1378. doi: 10.1111/1365-2664.13363

Suetsugu, K., Matsuoka, S., Shutoh, K., Okada, H., Taketomi, S., Onimaru, K., et al. (2021). Mycorrhizal communities of two closely related species, Pyrola subaphylla and *P. japonica*, with contrasting degrees of mycoheterotrophy in a sympatric habitat. *Mycorrhiza* 31, 219–229. doi: 10.1007/s00572-020-01002-5

Taschen, E., Sauve, M., Taudiere, A., Parlade, J., Selosse, M. A., and Richard, F. (2015). Whose truffle is this? Distribution patterns of ectomycorrhizal fungal diversity in Tuber melanosporum brûlés developed in multi-host Mediterranean plant communities. *Environ. Microbiol.* 17, 2747–2761. doi: 10.1111/1462-2920.12741

Taschen, E., Sauve, M., Vincent, B., Parladé, J., van Tuinen, D., Aumeeruddy-Thomas, Y., et al. (2020). Insight into the truffle brûlé: tripartite interactions between the black truffle (tuber melanosporum), holm oak (*Quercus ilex*) and arbuscular mycorrhizal plants. *Plant Soil* 446, 577–594. doi: 10.1007/s11104-019-04340-2

Taudiere, A., Munoz, F., Lesne, A., Monnet, A. C., Bellanger, J. M., Selosse, M. A., et al. (2015). Beyond ectomycorrhizal bipartite networks: projected networks demonstrate contrasted patterns between early- and late-successional plants in Corsica. *Front. Plant Sci.* 6, 1–14. doi: 10.3389/fpls.2015.00881

Taylor, A. F. S. (2002). "Fungal diversity in ectomycorrhizal communities: sampling effort and species detection," in *Diversity and Integration in Mycorrhizas* (Dordretch: Springer), 19–28.

Tedersoo, L., Bahram, M., and Zobel, M. (2020). How mycorrhizal associations drive plant population and community biology. *Science* 367. doi: 10.1126/science.aba1223

Tedersoo, L., Hansen, K., Perry, B. A., and Kjøller, R. (2006). Molecular and morphological diversity of pezizalean ectomycorrhiza. *New Phytol.* 170, 581–596. doi: 10.1111/j.1469-8137.2006.01678.x

Tedersoo, L., and Nara, K. (2010). General latitudinal gradient of biodiversity is reversed in ectomycorrhizal fungi. *New Phytol.* 185, 351–354. doi: 10.1111/j.1469-8137.2009.03134.x

Tedersoo, L., et al. (2012). Towards global patterns in the diversity and community structure of ectomycorrhizal fungi. *Mol. Ecol.* 21, 4160–4170. doi: 10.1111/j.1365-294X.2012.05602.x

Tedersoo, L., et al. (2014). Global diversity and geography of soil fungi. *Science* 346, 1052–1053. doi: 10.1126/science.aaa1185

Teste, F. P., and Simard, S. W. (2008). Mycorrhizal networks and distance from mature trees alter patterns of competition and facilitation in dry Douglas-fir forests. *Oecologia* 158, 193–203. doi: 10.1007/s00442-008-1136-5

Teste, F. P., Simard, S. W., and Durall, D. M. (2009). Role of mycorrhizal networks and tree proximity in ectomycorrhizal colonization of planted seedlings. *Fungal Ecol.* 2, 21–30. doi: 10.1016/j.funeco.2008.11.003

Teste, F. P., et al. (2015). Is nitrogen transfer among plants enhanced by contrasting nutrient-acquisition strategies? *Plant Cell Environ.* 38, 50–60. doi: 10.1111/pce.12367

Timonen, S., and Kauppinen, P. (2008). Mycorrhizal colonisation patterns of Tilia trees in street, nursery and forest habitats in southern Finland. *Urban For. Urban Green.* 7, 265–276. doi: 10.1016/j.ufug.2008.08.001

Toju, H., Sato, H., Yamamoto, S., and Tanabe, A. S. (2018). Structural diversity across arbuscular mycorrhizal, ectomycorrhizal, and endophytic plant-fungus networks. *BMC Plant Biol.* 18, 1–12. doi: 10.1186/s12870-018-1500-5

Tomao, A., Antonio Bonet, J., Castaño, C., and de-Miguel, S. (2020). How does forest management affect fungal diversity and community composition?, Current knowledge and future perspectives for the conservation of forest fungi. *For. Ecol. Manag.* 457:117678. doi: 10.1016/j.foreco.2019.117678

Tonn, N., and Ibáñez, I. (2017). Plant-mycorrhizal fungi associations along an urbanization gradient: implications for tree seedling survival. *Urban Ecosyst.* 20, 823–837. doi: 10.1007/s11252-016-0630-5

van der Heijden, M. G. A., et al. (2015). Mycorrhizal ecology and evolution: The past, the present, and the future. *New Phytol.* 205, 1406–1423. doi: 10.1111/nph.13288

Van Geel, M., et al. (2018). Variation in ectomycorrhizal fungal communities associated with silver linden (*Tilia tomentosa*) within and across urban areas. *FEMS Microbiol. Ecol.* 94, 1–11. doi: 10.1093/femsec/fiy207

Varenius, K. (2017). Interactions between fungi, forest management, and ecosystem services. Available at: https://pub.epsilon.slu.se/14629/ (Accessed February 24, 2022).

Walker, J. K. M., Ward, V., Paterson, C., and Jones, M. D. (2012). Coarse woody debris retention in subalpine clearcuts affects ectomycorrhizal root tip community structure within fifteen years of harvest. *Appl. Soil Ecol.* 60, 5–15. doi: 10.1016/j.apsoil.2012.02.017

Williams, N. S. G., Hahs, A. K., and Vesk, P. A. (2015). Urbanisation, plant traits and the composition of urban floras. *Perspect. Plant Ecol. Evol.* 17, 78–86. doi: 10.1016/j.ppees.2014.10.002

Wipf, D., Krajinski, F., Tuinen, D., Recorbet, G., and Courty, P. E. (2019). Trading on the arbuscular mycorrhiza market: from arbuscules to common mycorrhizal networks. *New Phytol.* 223, 1127–1142. doi: 10.1111/nph.15775

Zwiazek, J. J., Equiza, M. A., Karst, J., Senorans, J., Wartenbe, M., and Calvo-Polanco, M. (2019). Role of urban ectomycorrhizal fungi in improving the tolerance of lodgepole pine (*Pinus contorta*) seedlings to salt stress. *Mycorrhiza* 29, 303–312. doi: 10.1007/s00572-019-00893-3

Conflict of Interest: The authors declare that the research was conducted in the absence of any commercial or financial relationships that could be construed as a potential conflict of interest.

Publisher's Note: All claims expressed in this article are solely those of the authors and do not necessarily represent those of their affiliated organizations, or those of the publisher, the editors and the reviewers. Any product that may be evaluated in this article, or claim that may be made by its manufacturer, is not guaranteed or endorsed by the publisher.

GLOSSARY

Alpha-diversity	Diversity of co-occurring organisms at local scale. Species richness is a widely used measurement of alpha diversity as a taxonomical facet of biodiversity. Contrastingly, the beta-diversity of metacommunities characterizes the level of composition differences between communities.
Anthropogenic	Refers to processes, assemblies and ecosystem compartments driven by, or resulting from human activity. Anthropogenic landscapes typically consist of vegetation mosaics induced by long-term human activity (forestry, pastoralism, fire regime, etc.). Anthropogenic soils include pedological profiles that are physico-chemically altered by long-term anthropic pressures as well as matrices of artificial materials from urban/industrial origin (Anthrosols).
Cultivated forest	Consists of highly diversified physiognomies of vegetation dominated by trees, originated from either natural process (spontaneous establishment of seedlings) of plantations, where human practices drive the structure, the composition and the dynamics of tree populations. Cultivated forests encompass forestry-based managed forests and agroforests, including planted orchards and multifunctional tree savannas.
Endophytic lifeforms	Micro-organisms, including bacteria and filamentous fungi, leaving inside plant tissues (roots, seeds, leaves, bark, etc.) where they accomplish a part or their entire biological cycle. Recent research shows the ability of ectomycorrhizal fungi (e.g., Tuber melanosporum) to colonize root tissues of AM host as endophytes.
Network topology	Set of properties characterizing an interaction network, used to infer ecological/evolutionary hypotheses, and based on the analysis of the distribution of links between the objects (nodes) constituting the network.
Sealed soils	Soils that have sequestered in the mid-term by a cover of impermeable materials (e.g., tar) hindering pedogenesis.

frontiers | Frontiers in Plant Science

TYPE Original Research
PUBLISHED 14 September 2022
DOI 10.3389/fpls.2022.884726

OPEN ACCESS

EDITED BY
Katharina Pawlowski,
Stockholm University, Sweden

REVIEWED BY
Attila Kereszt,
Institute of Plant Biology, Hungary
Dong Wang,
University of Massachusetts Amherst, United States

*CORRESPONDENCE
Vladimir A. Zhukov
vladimir.zhukoff@gmail.com;
vzhukov@arriam.ru

SPECIALTY SECTION
This article was submitted to Plant Symbiotic Interactions, a section of the journal Frontiers in Plant Science

RECEIVED 26 February 2022
ACCEPTED 08 August 2022
PUBLISHED 14 September 2022

CITATION
Zorin EA, Kliukova MS, Afonin AM, Gribchenko ES, Gordon ML, Sulima AS, Zhernakov AI, Kulaeva OA, Romanyuk DA, Kusakin PG, Tsyganova AV, Tsyganov VE, Tikhonovich IA and Zhukov VA (2022) A variable gene family encoding nodule-specific cysteine-rich peptides in pea (*Pisum sativum* L.). *Front. Plant Sci.* 13:884726. doi: 10.3389/fpls.2022.884726

A variable gene family encoding nodule-specific cysteine-rich peptides in pea (*Pisum sativum* L.)

Evgeny A. Zorin[1], Marina S. Kliukova[1], Alexey M. Afonin[1], Emma S. Gribchenko[1], Mikhail L. Gordon[1], Anton S. Sulima[1], Aleksandr I. Zhernakov[1], Olga A. Kulaeva[1], Daria A. Romanyuk[1], Pyotr G. Kusakin[1], Anna V. Tsyganova[1], Viktor E. Tsyganov[1], Igor A. Tikhonovich[1,2] and Vladimir A. Zhukov[1]*

[1]All-Russia Research Institute for Agricultural Microbiology, Saint Petersburg, Russia, [2]Department of Genetics and Biotechnology, Faculty of Biology, Saint Petersburg State University, Saint Petersburg, Russia

Various legume plants form root nodules in which symbiotic bacteria (rhizobia) fix atmospheric nitrogen after differentiation into a symbiotic form named bacteroids. In some legume species, bacteroid differentiation is promoted by defensin-like nodule-specific cysteine-rich (NCR) peptides. NCR peptides have best been studied in the model legume *Medicago truncatula* Gaertn., while in many other legumes relevant information is still fragmentary. Here, we characterize the NCR gene family in pea (*Pisum sativum* L.) using genomic and transcriptomic data. We found 360 genes encoding NCR peptides that are expressed in nodules. The sequences of pea NCR genes and putative peptides are highly variable and differ significantly from NCR sequences of *M. truncatula*. Indeed, only one pair of orthologs (*PsNCR47–MtNCR312*) has been identified. The NCR genes in the pea genome are located in clusters, and the expression patterns of NCR genes from one cluster tend to be similar. These data support the idea of independent evolution of NCR genes by duplication and diversification in related legume species. We also described spatiotemporal expression profiles of NCRs and identified specific transcription factor (TF) binding sites in promoters of "early" and "late" NCR genes. Further, we studied the expression of NCR genes in nodules of Fix$^-$ mutants and predicted potential regulators of

NCR gene expression, one among them being the TF ERN1 involved in the early steps of nodule organogenesis. In general, this study contributes to understanding the functions of NCRs in legume nodules and contributes to understanding the diversity and potential antibiotic properties of pea nodule-specific antimicrobial molecules.

KEYWORDS

Pisum sativum **L., nitrogen-fixing symbiosis, root nodules, NCR peptides, transcriptomics, spatiotemporal expression pattern, prediction of antimicrobial properties**

Introduction

Legumes (family Fabaceae) form a unique group among plants owing to their ability to fix atmospheric nitrogen in symbiosis with nodule bacteria (rhizobia). Most legume plants develop specialized root organs, called root nodules, where rhizobia perform biological nitrogen fixation while hosted within plant cells in special compartments (symbiosomes) (Sprent, 2001; Tsyganova et al., 2018). In legumes belonging to the inverted repeat-lacking clade (IRLC) and Dalbergoids, rhizobia undergo terminal (i.e., irreversible) differentiation into symbiotic forms called bacteroids. This process prompts an increase in cell size, endoreduplication of the genome, and nitrogen-fixing capabilities (Mergaert et al., 2006; Alunni and Gourion, 2016). In other legumes, the differentiation of bacteroids is reversible and their changes from the free-living state are not so pronounced (Sprent et al., 1987; Denison, 2000; Kereszt et al., 2011). It is considered that terminal bacteroid differentiation (TBD) is more beneficial for the macrosymbiont (i.e., the host plant) since it is associated with better nitrogen fixation efficiency and higher plant-to-nodule mass ratio (Oono and Denison, 2010). It should be noted that the process of TBD is gradual, as was shown using a series of pea mutants blocked at various stages of nodule development (Tsyganov et al., 2003).

The TBD is governed by short defensin-like peptide molecules named nodule-specific cysteine-rich (NCR) peptides that are produced in nodule cells and stimulate rhizobia to terminal differentiation (Mergaert et al., 2003; Pan and Wang, 2017). NCR peptides are transported to symbiosomes and (at least several of them) are able to permeate into bacterial cells, thus promoting TBD (Durgo et al., 2015; Durán et al., 2021). The signal peptidase DNF1 guides the NCR peptides to symbiosomes, while a lack in its activity leads to the complete absence of NCRs in symbiosomes and, consequently, to the absence of TBD. This, in turn, results in undifferentiated bacteroids in the *dnf1* mutant (Van de Velde et al., 2010; Wang et al., 2010). The crucial role of NCR peptides for TBD is also supported by the fact that no gene coding for protein/peptide similar to NCRs could be found in nodule EST and genomic sequences of *Glycine max* (L.) Merr. and *Lotus japonicus* (Regel) K. Larsen that form nodules in which the bacteroids have unmodified morphotype (Mergaert et al., 2003; Graham et al., 2004; Downie and Kondorosi, 2021), nor were NCR genes found in the genome of *L. japonicus* (Alunni et al., 2007).

The NCR peptide family is best studied in the genome of the model legume *Medicago truncatula* Gaertn. where more than 700 NCR genes were predicted and over 600 were found expressed in nodules (Mergaert et al., 2003; Montiel et al., 2017). In general, NCR peptides are small (20–50 amino acids long) molecules having highly variable sequences containing four or six cysteines in conserved positions. These potentially form two or three disulfide bridges, whereas other amino acids can vary between different members of this protein family (recently reviewed in Roy et al., 2020). Like evolutionarily related defensins, NCR genes are translated into non-functional pro-peptides from which signal peptides are cut off, resulting in the production of mature NCR peptides. The mechanism by which NCR peptides switch the bacterial lifecycle to the terminal state is still not completely understood; however, it is suggested that this involves the interaction of NCRs with bacterial membranes and intracellular targets (much like the antibiotic effects of defensins) (Mikuláss et al., 2016). However, a detailed analysis of the structure and antimicrobial activity was performed only for some NCR peptides of *M. truncatula*—*MtNCR247*, *MtNCR335,* and *MtNCR169* (hereinafter Mt and Ps refers to *M. truncatula* and *P. sativum* gene and/or protein, respectively) (Tiricz et al., 2013; Farkas et al., 2014, 2017; Mikuláss et al., 2016; Isozumi et al., 2021). Based on the isoelectric point of the mature peptide, NCRs can be divided into groups of cationic, anionic, and neutral peptides, of which cationic NCRs usually have strong antimicrobial activity *in vitro*, whereas anionic and neutral NCR peptides are soft antibiotics and, at least against rhizobia, do not exhibit high toxicity (Lima et al., 2020; Downie and Kondorosi, 2021). This fact indicates that anionic and neutral NCRs in nodules may not serve to kill bacterial cells, as do cationic NCRs,

but perform some other purpose. One hypothesis is that anionic and neutral NCRs may bind to cationic NCRs to attenuate their antibacterial effect (Montiel et al., 2017; Roy et al., 2020). This might explain the interesting and somewhat paradoxical situation where mutations in two NCR-encoding genes (*DNF4* = *MtNCR211* and *DNF7* = *MtNCR169*) lead to preliminary senescence of nodules and death of bacteria inside nodules (Horváth et al., 2015; Kim et al., 2015). NCR peptides are also predicted to be able to bind to proteins and be ranked according to the so-called Boman index that reflects their protein-binding potential [for instance, MtNCR247 with the highest Boman index, 1.7 kcal/mol, can bind to multiple proteins in bacteroids. This is associated with inhibiting transcription, translation, and cell division (Farkas et al., 2014)].

Rhizobia can resist the NCR peptide attack with the help of specific proteins. One of them, BacA in *Sinorhizobium meliloti* or BclA in *Bradyrhizobium* spp., is a membrane transporter critical for symbiosis because it can import NCR peptides into the cytosol, thus removing them from the cell surface (Haag et al., 2013; Guefrachi et al., 2015). Another example is an M16A family zinc metallopeptidase (host range restriction peptidase, hrrP) that can degrade NCRs. This protein contributes to an increase in bacterial proliferation inside the nodules and participates in the control of host–symbiont specificity since its presence can lead to the formation of non-functional nodules without differentiated bacteroids dependent on the *M. truncatula* genotype (Price et al., 2015).

NCR genes are expressed almost exclusively in nodules in successive waves (with maximum expression either in younger or older nodules), which also may be indicative of their different functions and roles in TBD (Maunoury et al., 2010; Nallu et al., 2013; Guefrachi et al., 2014). Also, more detailed studies of gene expression with the use of microdissection showed that the expression level of NCR genes reaches the maximum in different zones of nodules (predominantly, in the interzone where TBD is taking place), but there is still a diversity in expression patterns (Roux et al., 2014). Apparently, specific transcription factors (TFs) control NCR gene expression, and some of them were computationally predicted for *M. truncatula* (Nallu et al., 2013). The detailed information on NCR gene expression patterns is lacking for other legumes.

Although NCRs have a single origin, their evolution has followed different routes in individual legume lineages (Montiel et al., 2017). This is confirmed by the fact that no orthologs of the essential *MtNCR169* of *M. truncatula* were recognized in the genomic and/or transcriptomic data of other legumes, including pea (Horváth et al., 2015). Hence, the study of members of this gene family in different lineages of different legumes should enrich the knowledge of the evolution of plant antimicrobial peptides and their particular features in particular legume species.

Garden pea is an important legume plant, often classified as an orphan crop due to poor knowledge of its genomics and transcriptomics (Smýkal et al., 2012; Pandey et al., 2021). However, the pea has seen considerable progress of late, enabling the characterization of the genes and gene families over the whole-genomic level (Kreplak et al., 2019). Also, a large collection of well-characterized mutants that are defective in nodule development has been made available for the pea, a development facilitating studies of nodule-related genes (Tsyganov and Tsyganova, 2020). The aim of the present study was to describe the NCR gene family in the pea based on a new genome assembly (NCBI accession number: JANEYU000000000) and study its spatiotemporal expression profiles along with other features. Here, we also confirm the fact of clustering the NCR genes in the pea genome and prove that the expression patterns of closely located NCR genes are more similar than those of the remote ones. Finally, we built the co-expression modules that contain sets of NCR genes together with other symbiotic genes and predicated the TFs that may regulate the expression of pea NCR genes.

Materials and methods

Plant material, bacterial strain, and growth conditions

Pea (*Pisum sativum* L.) wild-type line SGE (Kosterin and Rozov, 1993) and the corresponding symbiotically ineffective mutant lines SGEFix$^-$-1 (*sym40-1*) and SGEFix$^-$-2 (*sym33-3*) (Tsyganov et al., 1998) were used.

Seeds were surface-sterilized in concentrated sulfuric acid for 10 min, rinsed in distilled water five times, and germinated on Petri dishes with humidified sterile vermiculite (3 days at 28°C). Five seedlings of each sample were planted into 2-L metal pots filled with sieved and heat-sterilized (200°C, 2 h) quartz sand.

Rhizobium leguminosarum bv. *viciae* strain RCAM1026 (Afonin et al., 2017) grown on solid TY medium for 3 days at 28°C was used for inoculation [resuspended in distilled water to a concentration of 10^7 colony-forming units (CFUs) per liter]. Inoculation was carried out with 250 ml of *Rhizobium* suspension per pot. At the same time, a mineral nutrition solution without ammonium nitrate (250 ml per pot) was added to trigger the symbiotic phenotype under conditions of nitrogen starvation (Sulima et al., 2019). The plants were cultivated in a VB 1014 (Vötsch Industrietechnik, Germany) growth chamber under the following climatic conditions: day/night: 16/8 h, the temperature of 21 ± 1°C, relative humidity of 75%, illumination 600 μmol photons m^{-2} s^{-1}. The plants were watered with distilled H_2O as needed.

Microscopy

Three-week-old nodules were fixed and processed using the low-temperature embedding procedure as previously described (Tsyganova et al., 2009). For light microscopy, 0.5-μm-thick, resin-embedded sections were cut with a glass knife and collected on slides. Specimens were stained in 5% Toluidine blue in 0.1 mM sodium borate. Sections were examined on a Nikon Eclipse 800 with a Nikon Coolpix 995 digital camera (Nikon Corp., Tokyo, Japan). For transmission electron microscopy, 90–100-nm-thick ultrathin sections were collected on copper grids with 4% pyroxylin and carbon. The grids with sections were counterstained in 2% aqueous uranyl acetate for 1 h followed by lead citrate for 1 min. The sections of nodules were examined and photographed in a JEM-1200 EM (JEOL Corp., Tokyo, Japan) transmission electron microscope at 80 kV.

Identification of genes encoding nodule-specific cysteine-rich peptides and computational prediction of physicochemical properties of the peptides

The genes encoding NCR peptides were identified in the new assembly of pea cv. Frisson (NCBI accession number: JANEYU000000000; Afonin et al., unpublished) using the searching algorithm Small Peptide Alignment Discovery Application (SPADA) for the discovery of short peptides (Zhou et al., 2013). Peptide sequences shorter than 30 amino acids in length and peptides not containing cysteine were removed by a custom python script.[1] The sequences of NCR peptides were analyzed using the Antimicrobial Peptide Database with APD3 algorithm: Antimicrobial Peptide Calculator and Predictor (Wang et al., 2016) to predict its physicochemical properties. The IPC 2.0 (Kozlowski, 2021) tool was used to calculate the isoelectric point (pI) for mature NCR peptides (without a signal peptide). A peptide was recognized as cationic at a value of pI above 8.5 and anionic at a value below 6.5; peptides with an intermediate pI value were defined as neutral. The boundary of the signal and mature part of the peptides was predicted using SignalP 6.0 (Teufel et al., 2022).

Nodulation experiment and sequencing library preparation

At 12, 21, 28, and 42 days postinoculation, the plants of the SGE line were extracted from pots, root systems were rinsed with cold tap water, and the visually pink mature nodules were separated from roots with sterile forceps and snap-frozen in liquid nitrogen. The mutants SGEFix$^-$-1 (*sym40-1*) and SGEFix$^-$-2 (*sym33-3*) forming white nodules were analyzed at 21 dpi only. Five plants from each pot constituted one biological replicate; three biological replicates were used for subsequent procedures. Total RNA from each replicate was isolated using TRIzol (Thermo Fisher Scientific, Waltham, MA, United States) according to the manufacturer's instruction, RNA quality was evaluated using gel electrophoresis in 1.5% agarose gel, and the concentration of RNA was measured on a Shimadzu UV mini-1240 spectrophotometer (Shimadzu, Japan). The 3′ MACE sequencing libraries were prepared from RNA samples using a 3′ MACE kit (GenXPro GmbH, Frankfurt am Main, Germany) and sequenced on Illumina HiSeq 2500 at GenXPro GmbH (Frankfurt am Main, Germany). The raw data are deposited in the NCBI SRA database under accession number PRJNA812957.

Gene expression analysis

For each library, all reads were processed to filter out adaptor sequences and low-quality sequences. Then, all of the clean reads were mapped to the reference *P. sativum* cv. Frisson genome assembly (NCBI accession number: JANEYU000000000) using STAR (ver. 2.7.6a). 1) (Dobin and Gingeras, 2015). In total, from 4 to 13 million clean reads per sample were mapped to the genome. Using the principal component method, it was shown that all samples have a high degree of grouping according to replicates (**Supplementary Figure 1**).

Differential expression analysis was conducted using DESeq2 (ver. 1.34.0) package (Michael Love, 2017) in R programming environment (ver. 4.1.2). The differentially expressed genes were considered to be significant at the level of the adjusted p-value of < 0.05.

The heatmap showing gene expression patterns was based on a 1-Pearson correlation matrix calculated on normalized per million and logarithmic (log2) expression values transformed into a z-score (which gives the number of standard deviations that a value is away from the mean of all the values in the same gene) using edgeR (ver. 3.20.9) (Robinson et al., 2010) and pheatmap function in R. The expression values of the three biological replicates for a particular stage of symbiosis were averaged. All genes with very low expression (less than 10 reads per sample) were discarded.

In order to identify gene expression clusters, Pearson correlation values were calculated. The final dendrogram for analysis by heatmap was built on the basis of the correlation matrix by the complete linkage method.

1 https://github.com/kjokkjok/NCRs_filter/

Phylogenetic tree construction

All the phylogenetic trees were built using phangorn (ver. 2.4.0) (Schliep, 2011) and ggtree (ver. 1.10.5) (Yu et al., 2017) packages in R on the basis of the alignment of mature peptides of NCR genes obtained by MAFFT program (ver. 37.90) (Katoh, 2002) with G-INS-i option. The maximum likelihood method was used to construct all phylogenetic trees. The phylogenetic trees were evaluated using bootstrap analysis with 1,000 replicates. Each terminal node was colored according to one of the physicochemical properties, namely, the total net charge and the Boman index.

dN/dS substitution analysis

To evaluate the rates of dS and dnS substitutions, the coding sequences of NCR genes were split into the signal peptide and the mature peptide section. The total set of sequences was divided into clusters according to the percent of identity: each cluster consists of a group of NCR genes with identity from 65 to 95% (all sequences with < 65 and $> 95\%$ identity were discarded). The sequences were aligned using ClustalW. The dS and dnS substitution values were calculated in the PAML software package (ver. 4.9j) (Yang, 2007) by the Nei-Gojobori method (Jukes-Cantor correction), which, by counting the number of dN and dnS substitutions, takes into account multiple potential substitutions at the same site. Gaps were removed in pal2nal (Suyama et al., 2006).

Single nucleotide polymorphism analysis

An analysis of single nucleotide polymorphism (SNP) sites was conducted with the following procedure. First, nodule transcriptome sequencing raw reads of SGE (Zhukov et al., 2015) and cv. Caméor (Alves-Carvalho et al., 2015; Kreplak et al., 2019) pea lines were obtained from NCBI (NCBI SRA accession number: PRJNA267198). Removing low-quality reads and adapter trimming was performed using the BBDuk tool from the BBMap toolkit.[2] Clean reads were then mapped to the reference genome of cv. Frisson with bowtie2 (ver. 2.3.4.1) (Langmead and Salzberg, 2012). For the analysis of the obtained SNPs, BCFtools (Danecek et al., 2021) and VCFtools (Danecek et al., 2011) were used. SNPs specific to NCR genes were obtained using bedtools (Quinlan and Hall, 2010).

2 https://sourceforge.net/projects/bbmap/

Localization of nodule-specific cysteine-rich (NCR) genes in the genome and their similarity within and between clusters

Genome-wide localization of NCR genes was visualized in chromoMap (ver. 0.3) (Anand and Rodriguez Lopez, 2022). The percentage of average similarity for the alignment of NCR genes within and between genomic clusters was obtained using the EMBOSS Needle tool (Madeira et al., 2019).

Construction of co-expression modules, transcription factor prediction, and promoter sequence detection

The co-expression modules of differentially expressed genes were built using CEMiTool (ver. 4.1) (Russo et al., 2018). TFs and their potential targets were identified in co-expression modules using the GENIE3 tool (ver. 4.1) (Huynh-Thu et al., 2010). Potential promoter sequences were searched for in regions with a length of 200 and 1,000 nucleotides at 5′ end of NCR genes by the MEME program (Bailey et al., 2009). The relationships between TF and NCR genes were analyzed and visualized in Cytoscape (ver. 3.9.1) (Shannon et al., 2003).

Results

Nodule-specific cysteine-rich (NCR) genes discovery in pea cv. Frisson genome assembly

The search for NCR genes in the pea genome (NCBI accession number: JANEYU000000000) was performed using the SPADA—a specific algorithm for the discovery of short peptides. The known NCR peptides of *M. truncatula* and, in the following iterations, *P. sativum* were loaded in SPADA as a training dataset. A total of 653 sequences were identified after three iterations, and sequences less than 30 aa were filtered out along with sequences that contain less than four or six conservative cysteines and/or lack signal peptides. This left 360 remaining sequences. Of them, 206 were also found in the dataset of Montiel et al. (2017) (sequences with an identity of $> 95\%$ at the putative protein level were considered alleles of the same NCR genes), and 154 sequences were novel. For a number of peptides of sufficient length and with four or six cysteines in their sequence, the SignalP algorithms did not predict the cleavage sites of a signal peptide. These peptides were labeled in the dataset as NCR-like peptides (**Supplementary Table 1**) and were not included in further analysis. As for the

nomenclature of the NCR genes and peptides, we kept the names of PsNCR1-PsNCR353 for the sequences from Montiel et al. (2017) and continued numeration for our novel sequences up to PsNCR507.

All 360 NCR genes were found to be expressed in nodules in our experiment (see below); thus, we consider them the core members of the NCR gene family in *P. sativum* cv. Frisson. Similar to *M. truncatula*, NCR peptides encoded by the identified genes of pea can be divided into two groups: group A (97 sequences) and group B (263 sequences), having four and six cysteines in conservative positions, respectively (**Supplementary Table 1**).

Most of the identified NCR genes, such as that of *M. truncatula*, were composed of two exons separated by an intron (**Figure 1A**). The first exon, in most cases, encodes the signal peptide, and the second encodes the mature peptide. The length of the first exon varies from 45 to 138 bp, the second exon from 63 to 396 bp, and the intron from 29 to 4,672 bp. Seven percent of NCR genes contain an additional (second) intron with the third exon encoding the last few amino acids of the peptide. The shortest gene was 141 bp, and the longest was 4,880 bp.

The putative NCR peptides deduced from the gene sequences were 46–156 amino acids in length. Some NCRs differ from others by only one amino acid change. In the list of the discovered NCRs, we found peptides translated from previously known genes of *P. sativum* such as *PsENOD3* (Scheres et al., 1990) (*PsNCR34*, according to our naming scheme), *PsENOD14* (Scheres et al., 1990) (*PsNCR66*), and *PsN466* (*PsNCR110*) (Kato et al., 2002).

Extreme variability of pea nodule-specific cysteine-rich (NCR) genes

The NCR gene sequences from the pea genome were found to be highly variable and greatly different from the corresponding sequences of *M. truncatula*. Pairwise comparison of putative amino acid sequences of NCR peptides showed a low similarity between the sequence sets from *P. sativum* and *M. truncatula* (**Table 1** and **Figure 1B**), as well as within *P. sativum* set (**Supplementary Figure 2**). Alignment of all sequences of NCR peptides of *P. sativum* against that of *M. truncatula* using a blastp allowed us to establish that the maximal identity on protein level recorded for pea—*M. truncatula* sequence pairs (*PsNCR47–MtNCR312*) was 70.9% (**Table 1**). Only this pair of NCR genes can be considered orthologs since they are located in syntenic regions of *P. sativum* and *M. truncatula* genomes, a fact which is not the case for the other sequences which are the most similar (**Table 1**). However, no sequences similar to *PsNCR47–MtNCR312* were found in genomes of *Cicer arietinum* L., *Trifolium pratense* L., and *Vicia faba* L. Moreover, in the genomic and transcriptomic data of *C. arietinum, T. pratense,* and *V. faba*, we did not find orthologs for any NCR genes of pea. Likewise, no orthologs were found in the pea genome for the well-studied *M. truncatula* NCR genes such as *MtNCR169* (Isozumi et al., 2021) and *MtNCR211* (Kim et al., 2015) (which are indispensable for symbiosis), *MtNFS1* and *MtNFS2* (which encode peptides that eliminate some rhizobial strains such as Rm41 and A145 from nodules of cv. Jemalong) (Wang et al., 2017, 2018; Yang et al., 2017), or *MtNCR335* and *MtNCR247* (encoding peptides with unique physicochemical properties) (Tiricz et al., 2013). This observation confirms that members of the NCR gene family in related legume species underwent independent evolution (Montiel et al., 2017; Downie and Kondorosi, 2021).

The putative amino acid sequences of the signal peptide were, in general, better conserved than those of the mature peptide, as has been recorded for *M. truncatula* (Alunni et al., 2007). In order to compare the selection pressure on signal and mature peptide parts, we calculated their dN/dS statistics separately. Analysis indicated that the number of synonymous and non-synonymous substitutions is comparable within the mature peptide section. This means that the mature NCR peptides are evolving according to a neutral evolutionary model (**Figure 2A**). In contrast, within the region encoding the signal peptide, synonymous substitutions prevail against the non-synonymous ones, indicating that this part of NCR genes is undergoing stabilizing selection (**Figure 2B**).

In order to estimate the allelic polymorphism of NCR genes, cleaned paired-end reads from the pea nodule transcriptome sequencing projects [cv. SGE (NCBI SRA accession number: PRJNA773870) and cv. Caméor (NCBI SRA accession number: PRJNA267198)] were mapped to the genome of cv. Frisson. The single nucleotide variant (SNV) analysis revealed a large number of allelic variants in NCR genes, and NCR genes of SGE line had a greater number of SNVs in the gene coding sequence (**Table 2**) in comparison to that of cv. Caméor. Thus, NCR genes of the SGE line were more distinct from those of cv. Frisson and cv. Caméor. The pattern of distribution of SNVs by gene region exhibits no significant differences between genotypes (**Supplementary Figure 3**).

Physicochemical properties of pea nodule-specific cysteine-rich peptides

The physicochemical properties of pea NCR peptides such as the Boman index and the total net charge were inferred from the putative protein sequences. We noticed that the ratio of cationic, anionic, and neutral peptides in our data differed from that described in Montiel et al. (2017), probably because we used a later-version IPC-2.0 tool built on machine learning algorithms. For adequate comparison, we also recalculated the values of isoelectric points for NCR peptides of *M. truncatula*

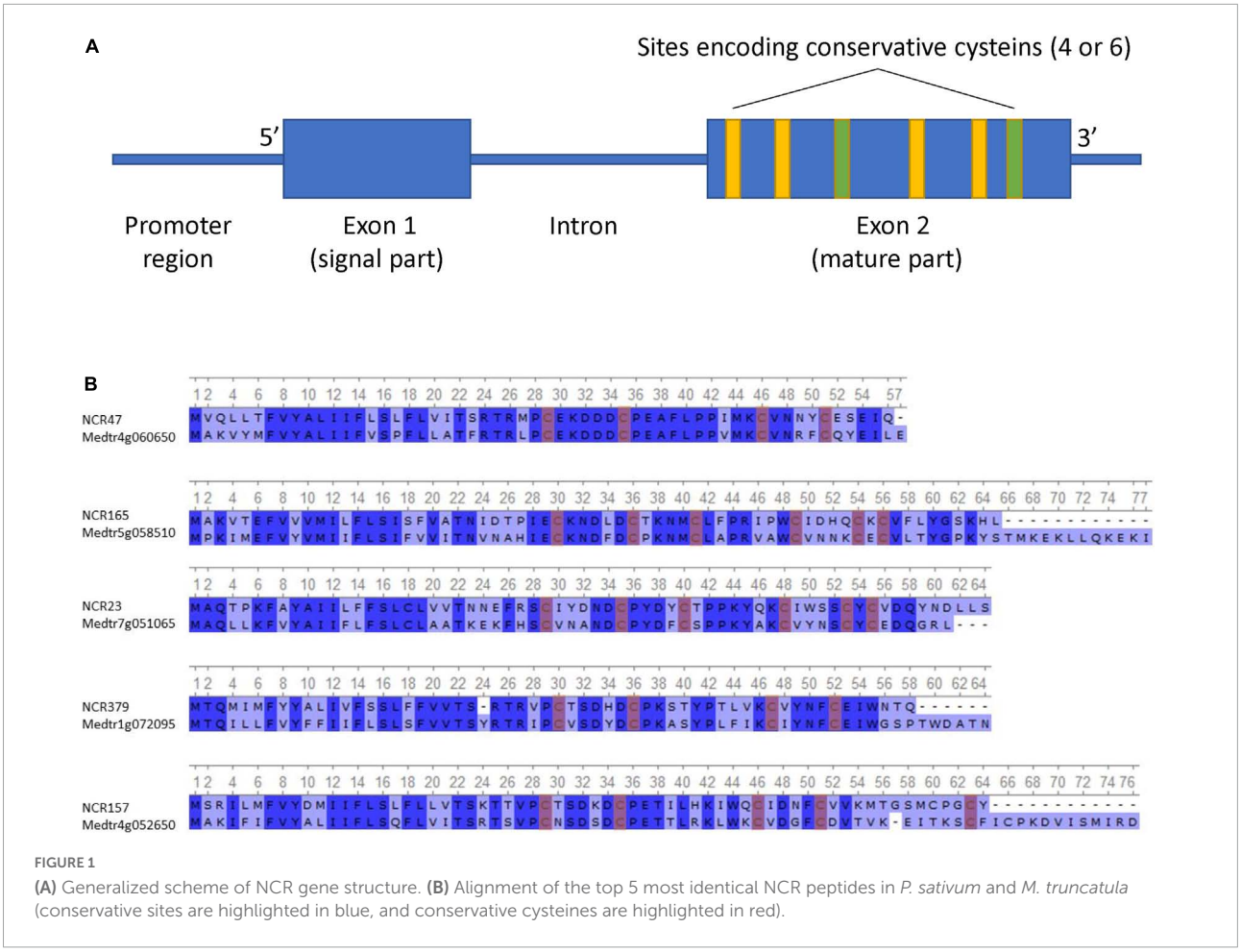

FIGURE 1
(A) Generalized scheme of NCR gene structure. **(B)** Alignment of the top 5 most identical NCR peptides in *P. sativum* and *M. truncatula* (conservative sites are highlighted in blue, and conservative cysteines are highlighted in red).

TABLE 1 List of five *P. sativum* NCRs that are most similar to *M. truncatula* peptides.

P. sativum ID	*P. sativum* chromosome location	*M. truncatula* ID	*M. truncatula* chromosome location	% identity	Length alignment	*E*-value score
PsNCR47	chr7LG7	Medtr4g060650	chr4	70.909	55	1.35e-27
PsNCR165	chr6LG2	Medtr5g058510	chr5	59.375	64	2.9e-27
PsNCR23	chr5LG3	Medtr7g051065	chr7	63.793	58	2.49e-26
PsNCR379	chr1LG6	Medtr1g072095	chr1	63.158	57	1.22e-25
PsNCR157	chr6LG2	Medtr4g052650	chr4	62.264	53	1.8e-23

and *P. sativum* cv. Caméor. Similar to the *M. truncatula* NCRs, anionic peptides prevail among NCR peptides of *P. sativum* cv. Frisson: 126 cationic (34%), 156 anionic (43%), and 83 neutral (23%) (Table 3). The isoelectric pI of pea NCRs ranged from 2.8 to 10.2, and the Boman index varied between −1.09 and 3.88. The distribution of pI and Boman index within the NCR family in all three pea genotypes analyzed was similar to that in *M. truncatula*. Probably due to a large number of amino acid substitutions, the distribution of isoelectric points of mature NCR peptides exhibits slight differences in SGE and Caméor in comparison with Frisson (Table 3).

The physicochemical parameters of pea NCR peptides were represented on phylogenetic trees constructed separately for peptides of group A (four cysteines) and group B (six cysteines). Each terminal node was colored according to either the total net charge or Boman index (Figure 3). As expected, NCRs with similar physicochemical parameter values were grouped within clades (branches) of phylogenetic trees (i.e., they possibly originate from a relatively recent duplication event); however, many remote clades were characterized with nearly the same physicochemical parameter values (Figure 3), that may indicate convergent evolution of diverse clades of NCR peptides, or may simply be a consequence of the extreme variability of

10.3389/fpls.2022.884726

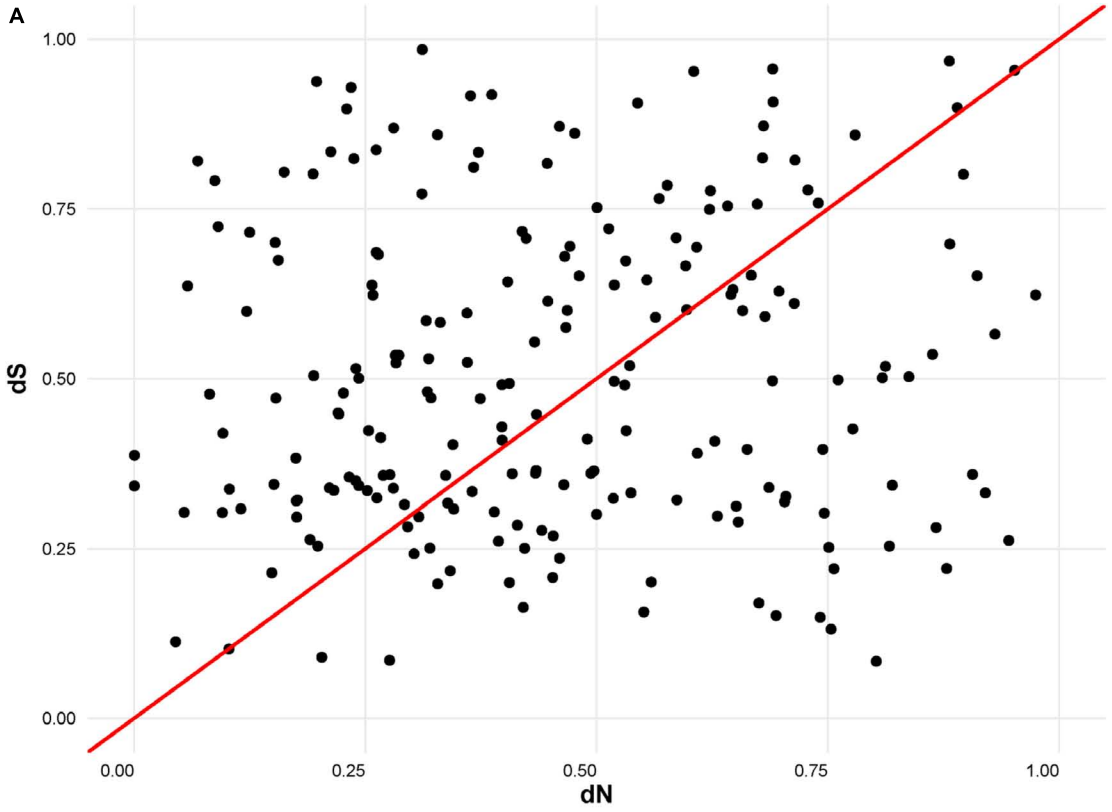

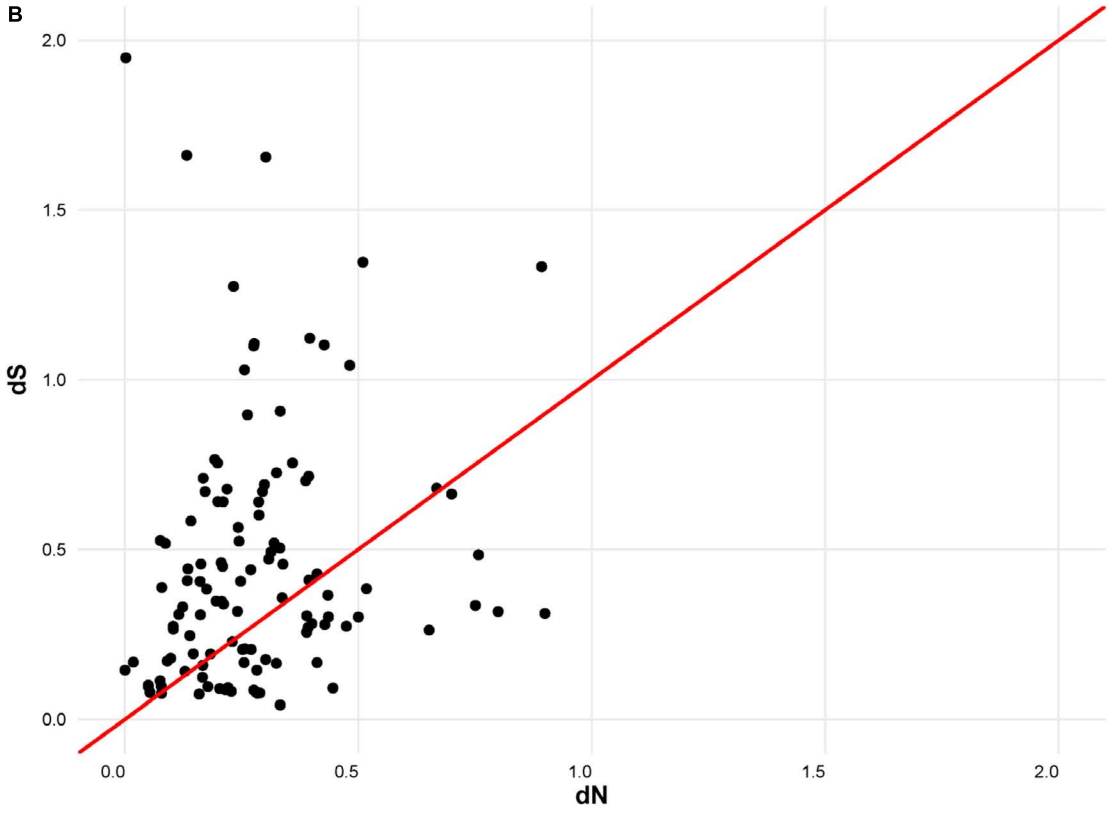

FIGURE 2
(A) dN/dS ratios for mature part of NCR peptides. **(B)** dN/dS ratios for signal part of NCR peptides.

TABLE 2 Analysis of SNVs in SGE and Caméor NCR genes as compared to Frisson.

	Total SNV in genes	Total genes with SNVs	No synonymous SNVs	No non-synonymous SNVs
SGE	1,435	247	440	995
Caméor	963	158	251	712

NCR peptide sequences and the high degree of dependence of physicochemical properties on the amino acid composition.

Localization of pea nodule-specific cysteine-rich (NCR) genes in the genome

Mapping NCR gene sequences to the genome allowed us to reveal a cluster pattern of genomic organization in this gene family in *P. sativum* (**Figure 4A**). The maximum number of NCR genes (129) is localized on LG1chr2. In order to confirm that the evolution of NCR genes was based on duplication events, we calculated the average percentage of sequence similarity between and within genomic clusters. The boxplots (**Figure 4B**) clearly demonstrate that the similarity of sequences within clusters on the genome is higher than between clusters. In addition, by analyzing the gene expression data (that is described in detail below) we observed that NCR genes within genomic clusters have a similar level of expression, which supports the hypothesis that a set of genes in a genomic cluster is regulated uniformly (**Figure 4C**). The expression level in some clusters has a high level of variance, which may be an artifactual result of combining some small clusters of NCR genes into one because of their proximity to each other. Together, these data support the idea that recent duplication events leading to the emerging number of NCR genes played an important role in the evolution of the NCR gene family in pea.

Expression profiles of the nodule-specific cysteine-rich (NCR) genes

For all identified NCR genes, the analysis of spatiotemporal expression profiles was carried out using data of 3′ MACE sequencing of *P. sativum* wild-type nodules (SGE line) at 12, 21, 28, and 42 dpi and data of RNAseq obtained from microdissected nodules (early zone II, late zone II, and zone III) of the same SGE line at 11 dpi (for a description of methods, see Kusakin et al., 2021).

NCR genes were divided into five clusters in accordance with their temporal expression pattern (**Figure 5A**). The most numerous cluster includes NCR genes, for which the expression level reached its maximum at 12 dpi and gradually decreased to 28 dpi. Large clusters of genes with maximal expression levels at 21 and 28 dpi were also identified. Clusterization data show that the majority of NCR genes are activated prior to 12 dpi. Thus, NCR genes begin to express at various stages of symbiosis. The three main clusters were identified with a maximal expression level at 12, 21, and 28 dpi (corresponding to bacteroid differentiation, nodule maintenance/nitrogen fixation, and initiation of senescence, respectively). Two of them were referred to as "early" and "late" NCR genes with the maximum at 12 and 28 dpi, respectively (**Figure 5A**). Such a coordinated expression of NCR genes implies that they are regulated by a limited number of TFs.

For analysis of the spatial expression patterns of NCR genes, RNA sequencing data from the nodule microdissection experiment were used (Kusakin et al., 2021). Based on NCR gene expression levels in the early infection zone (zone early II), late infection zone (zone late II), and nitrogen fixation zone (zone III) of the nodule, two main clusters were revealed—a maximum of expression in late II zone and a maximum in zone III (**Figure 5B**). A small group of NCR genes were also identified whose expression was induced in early II zone, reached a maximum in late II zone, and then was repressed in zone III (**Figure 5B**).

Data from the two experiments match since NCR genes with maximal expression at 12 dpi are expressed in late II and III zones (**Figure 6A**), while the vast majority of genes with a maximum of expression at 28 dpi are expressed only in nodules' zone III (**Figure 6B**). As expected, the "late" NCR genes are active mainly in the nitrogen fixation zone (zone III), while the "early" ones are expressed mostly in the late II zone.

NCR genes encoding anionic, neutral, and cationic peptides are expressed relatively uniformly at all studied time points, with maximal number of expressed sequences at 28 dpi (**Figure 7A**). Cationic peptides were active mainly in the early II zone of the nodule (**Figure 7B**). Interestingly, two groups of anionic peptides can be distinguished: with pI 4.9–5.4 (the maximal number of which stands at 28 dpi) and with pI 5.4–5.9 (the maximal number of which stands at 12 dpi).

Expression of nodule-specific cysteine-rich (NCR) genes in nodules of SGEFix$^-$-1 (*sym40-1*) and SGEFix$^-$-2 (*sym33-3*) mutants

Pea symbiotic mutants SGEFix$^-$-1 and SGEFix$^-$-2 carry mutations in TF genes *Sym40* = *PsEFD* and *Sym33* = *PsIPD3*,

TABLE 3 Distribution of isoelectric points of NCR peptides in *M. truncatula* and *P. sativum*.

	Percent of NCR peptides in *M. truncatula* (cv. A17)	Percent of NCR peptides in *P. sativum* (cv. Frisson)	Percent of NCR peptides in *P. sativum* (cv. SGE)	Percent of NCR peptides in *P. sativum* (cv. Caméor)
Cationic	38%	34%	32%	38%
Anionic	41%	43%	47%	36%
Neutral	21%	23%	21%	26%

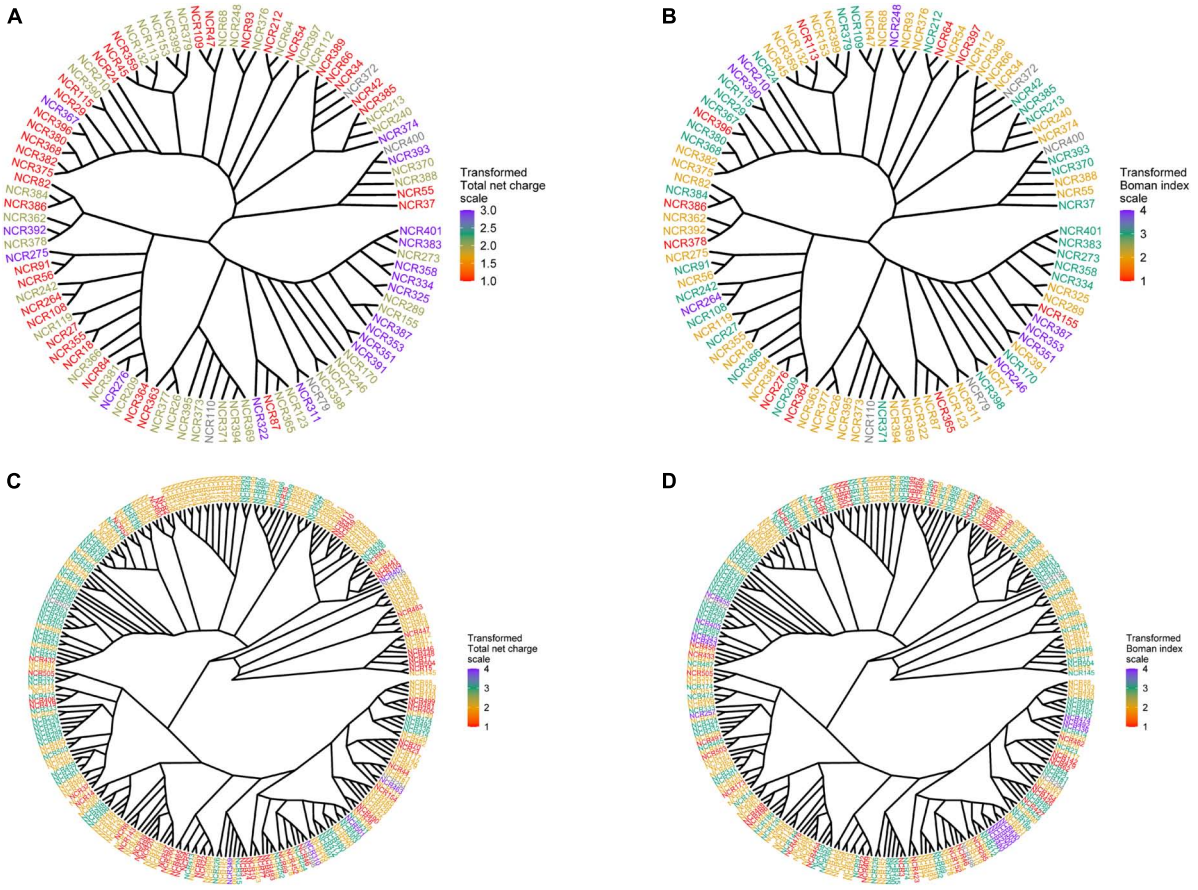

FIGURE 3
Phylogenetic trees built for groups A and B of NCR genes. Each terminal node was colored according to one of the physicochemical properties. **(A)** Phylogenetic tree for group A colored according to the total net charge values. **(B)** Phylogenetic tree for group A colored according to the Boman index values. **(C)** Phylogenetic tree for group B colored according to the total net charge values. **(D)** Phylogenetic tree for group B colored according to the Boman index values.

respectively (Tsyganov et al., 1998; Ovchinnikova et al., 2011). Thus, these lines are suitable models for studying the potential link between the activity of TFs EFD and IPD3 and the expression of NCR genes in pea. The mutant SGEFix$^-$-1 (*sym40-1*) forms numerous white nodules that, in contrast to wild-type pleomorphic bacteroids (**Figure 8A**), contain abnormal bacteroids (**Figure 8B**) and multibacteroid symbiosomes (**Figure 8C**; Tsyganov et al., 1998). Occasionally, pink nodules with a normal ultrastructural organization are formed. The mutant SGEFix$^-$-2 is able to form two types of nodules: white with "locked" infection threads (**Figure 8D**) and pinkish with rod-shaped bacteroids surrounded by the common symbiosome membrane (Tsyganov et al., 1998). However, the white nodules of some cells form infection droplets prompting the release of bacteria (**Figure 8E**) that leads to the formation of multibacteroid symbiosomes (**Figure 8F**; Tsyganov et al., 1998, 2011). In this study, both mutants formed only white nodules.

Transcriptomic analysis was performed for mutant and wild-type nodules harvested at 21 dpi. In nodules of SGEFix$^-$-2 (*sym33-3*) with no signs of TBD, severe suppression of almost all NCR genes (323 out of 360) was detected, which is in agreement with the phenotype (**Figures 9B,D**). In nodules of SGEFix$^-$-1

10.3389/fpls.2022.884726

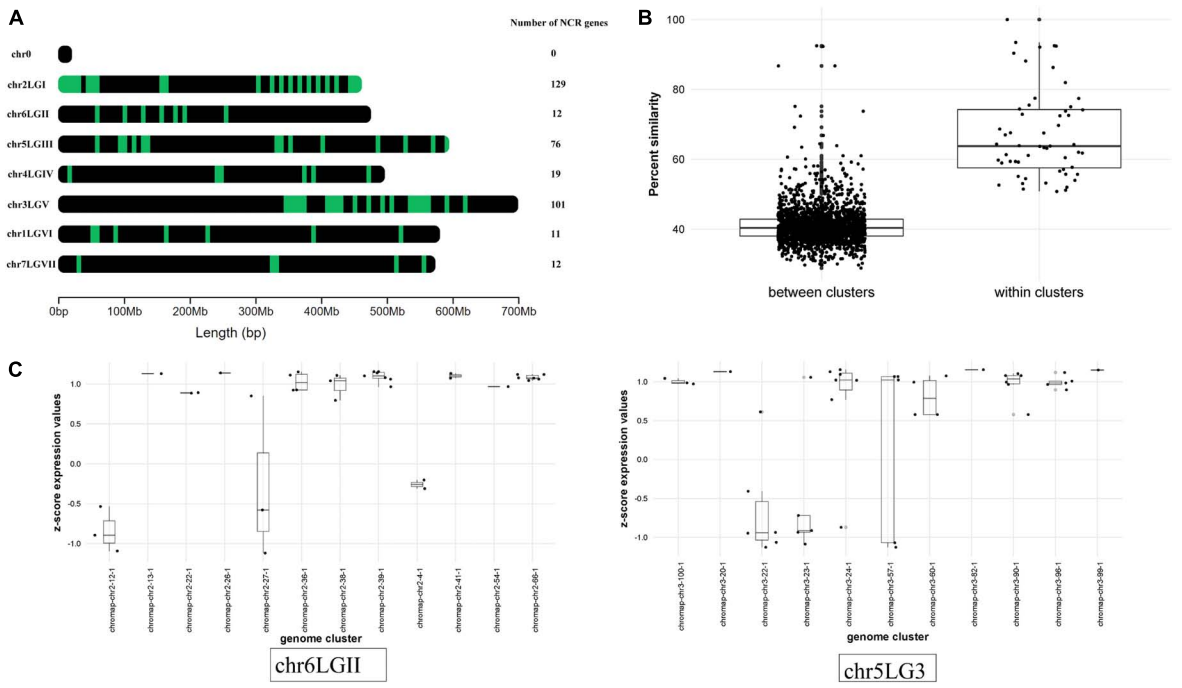

FIGURE 4
(A) Localization of NCR genes in *P. sativum* genome. Green dashes indicate NCR genes. **(B)** Comparison of the average percentage similarity of NCR genes within and between clusters in the genome using boxplots. Each comparison group contains the results of a pairwise alignment of NCR peptides with each other in the form of % similarity of their sequences. The group "within clusters" contains the results of the alignment of peptides among themselves within the same cluster in the genome. The "between clusters" group contains the results of the alignment of peptides belonging to different clusters with each other. **(C)** Evaluation of the NCR gene expression at 12 dpi within and between clusters in the genome. The level of NCR gene expression in clusters is represented by the transformation of log2(CPM) into a *z*-score. Chromosomes with a more pronounced effect are selected for visualization.

(sym40-1), in turn, 150 NCRs genes were differentially expressed (downregulated), as compared to SGE nodules. Most of the downregulated NCR genes in SGEFix$^-$-1 nodules are assigned to the "late" group (maximal expression at 28 dpi in wild-type nodules), whereas all the genes with no differential expression are from the "early" group (maximal expression at 12 dpi in wild-type nodules) (Figure 9A). At the same time, among the differentially expressed genes in SGEFix$^-$-1, the genes encoding cationic, anionic, and neutral peptides are distributed almost equally (Figure 9C).

Co-expression analysis

In order to get an insight into the potential mechanisms behind the regulation of the NCR gene expression, we conducted a search for gene co-expression modules in MACE sequencing data for time series 12, 21, and 28 dpi. Using CEMiTool, three modules of genes with a high degree of co-expression were detected (Figure 9A). Modules M1 and M3 were enriched with NCR genes with maximal expression at 12 dpi ("early"), while module M2 was enriched with NCR genes with maximal expression at 28 dpi ("late"). The gene ontology analysis showed that modules 1 and 3 were characterized by early activation of biological processes associated with resistance reactions, response to biotic stimuli, ethanol, cytokinins, and response to fungi (Figure 10A). The last two groups may include various symbiotic genes common to both mycorrhizal and nodule symbioses. Module 2 is characterized by overexpression of genes at late stages of symbiosis and is associated with the response to abscisic acid, phosphate starvation, response to chitin, and stimulation of root growth (Figure 10A).

The list of genes co-expressed with NCR genes in these modules was scanned for the presence of TFs genes using the GENIE3 tool. Five TFs potentially regulating the expression of NCR genes were identified: WRKY40, NAC969, RITF1, PTI5, and ERF053 (Figure 10B). Interestingly, NAC969 was found to regulate the expression of "early" NCR genes, while other TFs tended to regulate mainly "late" genes (Figure 9B).

The data of misexpression of NCR genes in the nodules of mutants SGEFix$^-$-1 and SGEFix$^-$-2 were also subjected to co-expression analysis. With respect to these, the putative TFs that can regulate the expression of NCR genes and thus influence the manifestation of the mutant phenotype in SGEFix$^-$-1 and SGEFix$^-$-2 were predicted. The list of the TFs identified in our data as potential regulators of NCR gene expression includes

10.3389/fpls.2022.884726

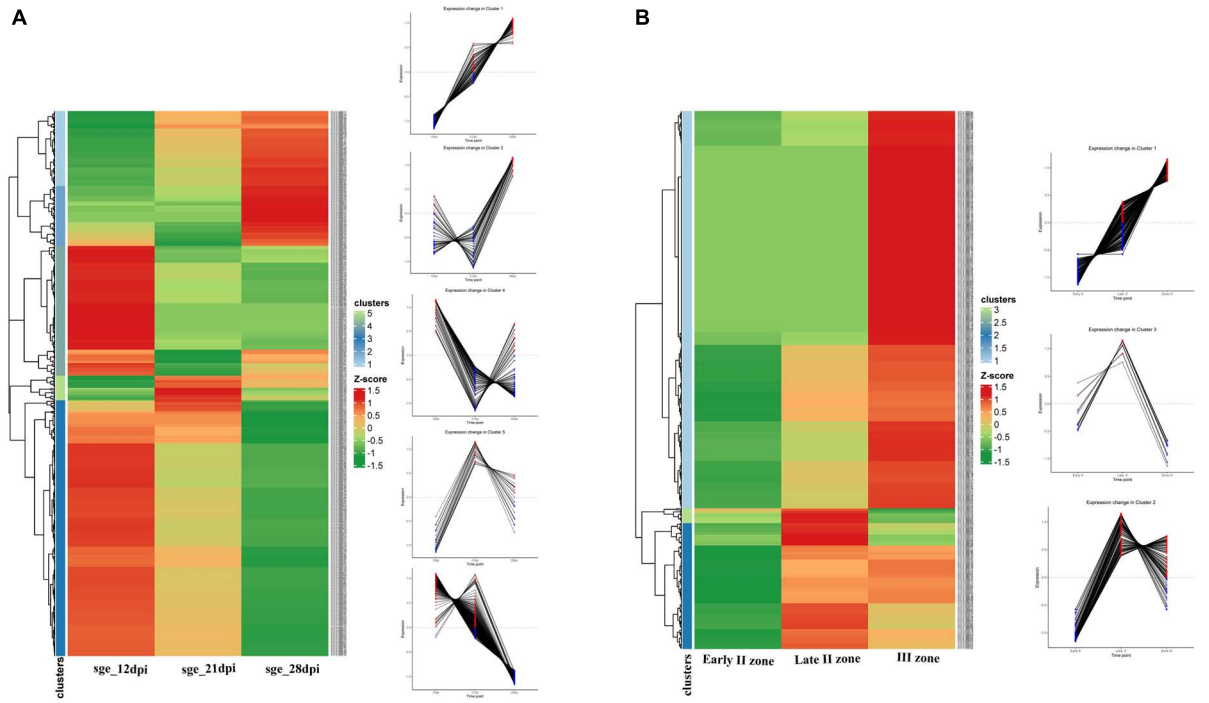

FIGURE 5
(A) Cluster analysis of *P. sativum* NCR genes on the basis of the expression pattern change at the different stages of symbiosis. MACE sequencing data of wild-type line SGE at 12, 21, and 28 dpi. **(B)** Cluster analysis of *P. sativum* NCR genes on the basis of the expression pattern change at the different stages of nodule development. RNA sequencing data of wild-type line SGE in early II nodule zone and late II and III nodule zones. All log2(CPM) expression values were transformed into *z*-score to build heatmaps.

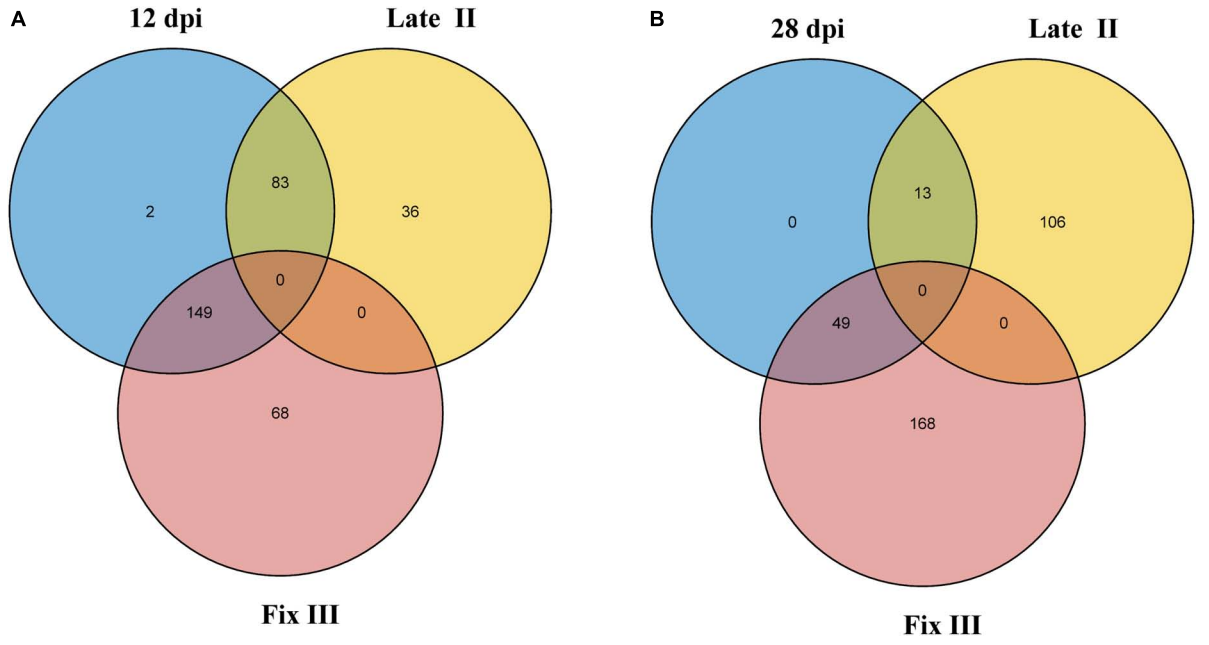

FIGURE 6
Intersection of NCR genes with expression maximum at different dpi and different nodule zones. **(A)** Intersection of NCRs with maximum expression at 12 dpi and with maximum expression in late II and III zones. **(B)** Intersection of NCRs with maximum expression at 28 dpi and with maximum expression in late II and III zones.

10.3389/fpls.2022.884726

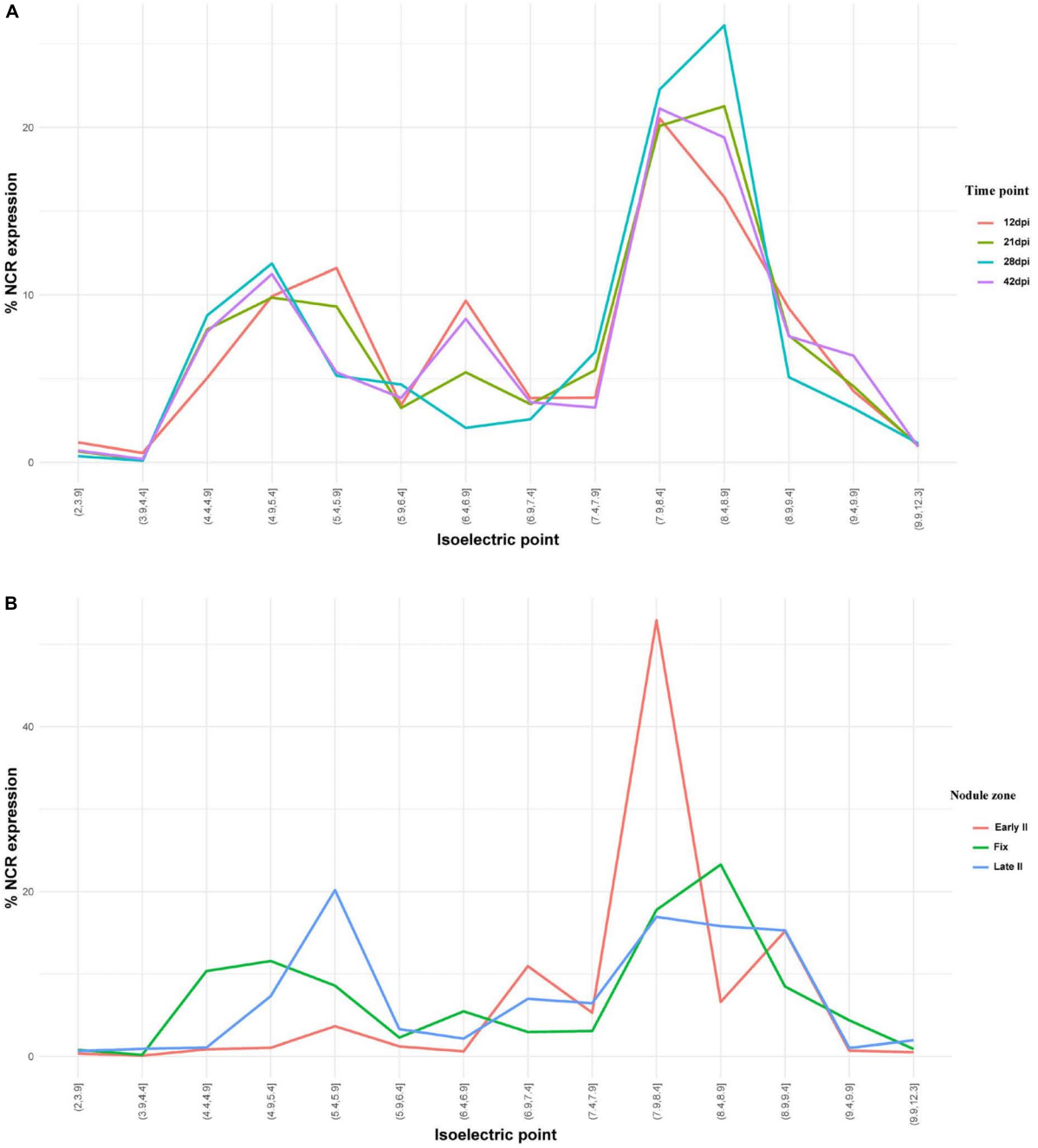

FIGURE 7
(A) Isoelectric point profiles of NCR peptides and the relative expression of NCRs with different PI across days after inoculation (dpi).
(B) Isoelectric point profiles of NCR peptides and the relative expression of NCRs with different PI in different zones of *P. sativum* nodules.
% NCR expression is % CPM normalized values of different isoelectric point categories to whole-nodule NCR expression.

ERN1 involved in the early steps of nodule organogenesis and other TFs related to nodule development and functioning, namely ERF.C.3, ERF34, and BBM1 (Figure 9E).

Co-expression modules containing NCR genes were also analyzed for enrichment by biological processes in GO terms. Thus, such biological processes as cellular response to phosphate starvation, response to external biotic stimuli, auxin-activated signaling pathway, reaction to ethanol, and regulation of auxin polar transport are suppressed in the nodules of mutants SGEFix^{-}-1 and SGEFix^{-}-2. It is worth noting that such biological processes as the defense response to bacteria, the regulation of defense reactions, the response to wounding,

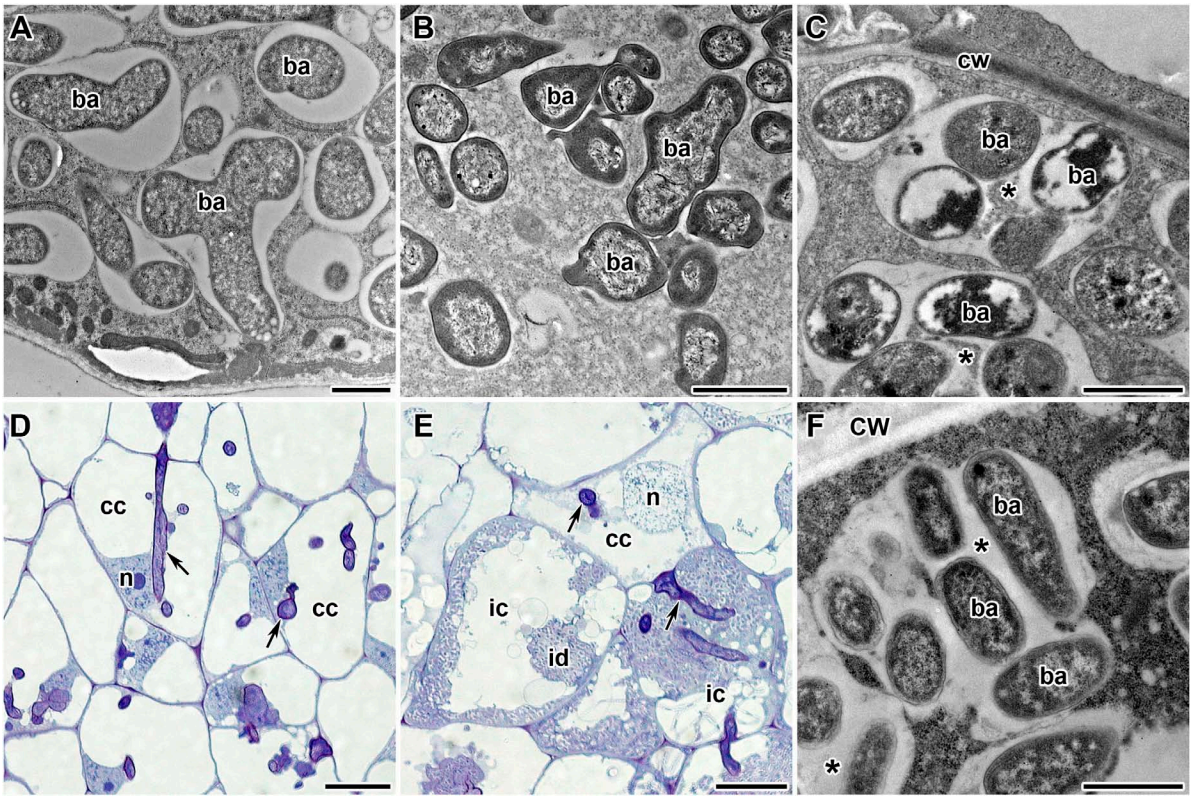

FIGURE 8
Phenotypes of pea (*Pisum sativum* L.) nodules. **(A)** Wild-type bacteroids. **(B,C)** Bacteroids of mutant SGEFix$^-$-1 (*sym40-1*): **(B)** abnormal bacteroids; **(C)** multibacteroid symbiosomes. **(D–F)** Phenotype of nodules of mutant SGEFix$^-$-2 (*sym33-3*): **(D)** nodule with "locked" infection threads and no release of bacteria; **(E)** nodule with occasionally released bacteria; **(F)** multibacteroid symbiosomes in the nodule with released bacteria. ic, infected cell; cc, colonized cell; id, infection droplet; n, nucleus; cw, cell wall; ba, bacteroid; *multibacteroid symbiosome. Arrows indicate infection threads. Scale bars = 1 μm **(A–C,F)** and = 20 μm **(D,E)**.

and the response to karrikins are increased in mutants compared to the wild type. At the same time, the nodules of SGEFix$^-$-1 converge with nodules of SGE by such biological processes as those involved in symbiotic interaction, cellular response to auxin stimuli, cellular response to oxidative stress, starch metabolism, and plant-type hypersensitive response (**Supplementary Figure 4**).

Additionally, to search for conserved motifs present in promoters of "early" and "late" NCR genes, the 1,000 bp upstream from the translational start site were scanned using the MEME tool. The analysis revealed nine conservative motifs in promoters of NCR genes (**Table 4**). To identify putative TF binding sites in the promoter regions of NCR genes, we scanned these regions using the SEA program and found different putative TF binding sites for "early" and "late" NCR genes (**Table 5**). Interestingly, we identified the same conservative motifs in promoter regions of some genes co-expressed with NCR genes [namely, the genes encoding nodulin-13, subunit NF-YB1, gibberellin signaling DELLA protein LA, nodulin-26-like intrinsic protein (NIP), Early nodulin-5, and receptor-like protein CLAVATA2].

Discussion

Recent success in the development of high-throughput sequencing technologies enables the construction of high-quality genome assemblies for several plant species with large and complex genomes, such as garden pea (Kreplak et al., 2019). These genome assemblies become an invaluable source for deep analysis of gene families encoding small peptides that have usually been overlooked during the analysis of the previous genome and transcriptome assemblies. Indeed, the analysis of Montiel et al. (2017), identified only 353 expressed genes encoding NCR peptides in pea (and 469 in *Medicago sativa* L. and 639 in *M. truncatula*). In our work, the number of detected NCR genes in pea turned out to be essentially the same (360 genes), but among them, we found 154 novel genes. The incomplete intersection of the NCR gene/peptide datasets identified by Montiel et al. (2017) and us can be due to consideration of the allelic variations characteristic for cv. Caméor and cv. Frisson as different genes at our threshold of > 95% protein identity [i.e., many of our novel sequences could be

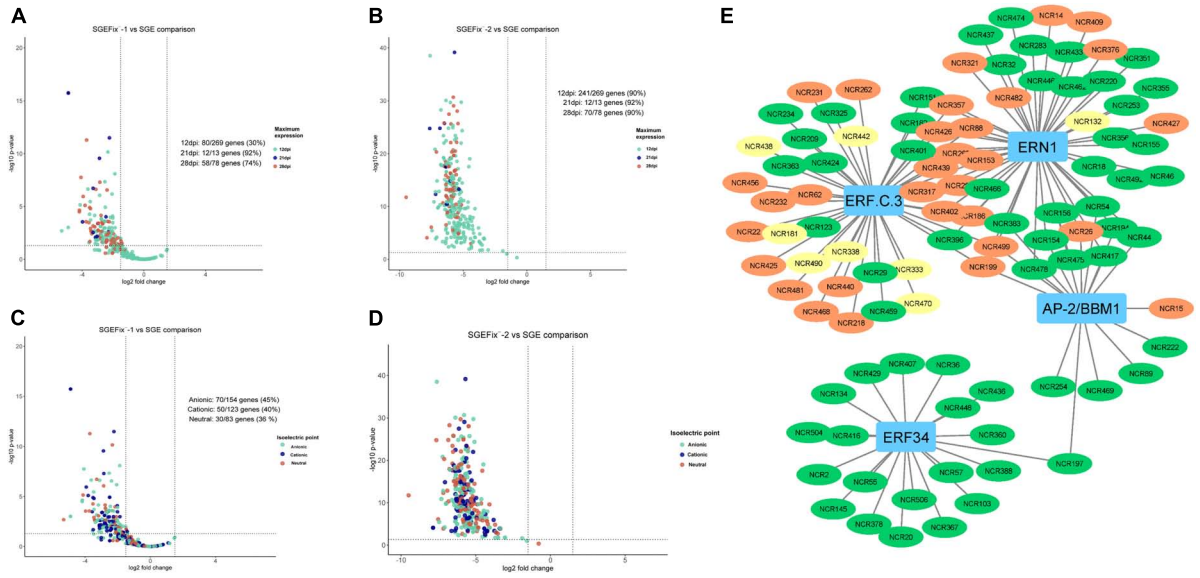

FIGURE 9
(A) Volcano plot showing the distribution of "early" and "late" NCRs among differentially expressed NCR genes in mutant SGEFix$^-$-1 (*sym40-1*). **(B)** Volcano plot showing the distribution of "early" and "late" NCRs among differentially expressed NCR genes in mutant SGEFix$^-$-2 (*sym33-3*). **(C)** Volcano plot showing the distribution of cationic/anionic/neutral NCR peptides among differentially expressed NCR genes in mutant SGEFix$^-$-1 (*sym40-1*). **(D)** Volcano plot showing the distribution of cationic/anionic/neutral NCR peptides among differentially expressed NCR genes in mutant SGEFix$^-$-2 (*sym33-3*). **(E)** NCR gene regulatory network based on gene expression data of wild-type and mutants SGEFix$^-$-1 and SGEFix$^-$-2. NCR genes with a maximum expression at 12 dpi are colored green. NCR genes with a maximum expression at 21 dpi are colored yellow. NCR genes with a maximum expression at 28 and 42 dpi are colored red.

alleles of genes previously described by Montiel et al. (2017)]. Alternatively, the sets of expressed and non-expressed NCR genes could also be different in different pea genotypes and cultivars.

It is also possible that the number of NCR genes in pea and other legume genomes is underestimated [this, however, gives no reason to doubt the conclusion of Montiel et al. (2017) that the degree of TBD correlated with the number of NCR genes]. Moreover, the search algorithms used in our work did not permit us to identify several genes encoding cysteine-rich nodule proteins (namely, *PsN1*, *PsN6*, *PsN314*, and *PsN335*) that were previously described for pea cv. Sparkle (Kato et al., 2002). Therefore, the actual number of NCR genes in the genome of cv. Frisson may be even higher. Apparently, analysis of genomes of other pea accessions and cultivars, including the wild ones such as cv. Afghanistan and *Pisum fulvum* Sm. forms, may result in the discovery of other members of the NCR gene family that will lead to a better understanding of its variability and evolution.

The NCR genes in pea are extremely polymorphic, which is true for comparisons of its sequences either within the one genotype or between unrelated genotypes (however, *PsNCR47*, for which the orthologous gene was identified in *M. truncatula*, is not polymorphic at the peptide level in Frisson/Caméor/SGE genotypes). The presence of polymorphism enables estimation of selection pressure using the dN/dS method, and it is clearly seen that the parts of NCR genes undergo different modes of selection pressure [which is also the case for *M. truncatula* nodule-specific NCR and GRP genes (Alunni et al., 2007)]. The parts that encode signal peptides undergo stabilizing (purifying) selection, which is logical given that the peptides must be correctly targeted to specific cell compartments. In turn, the parts encoding mature peptides in pea are evolving neutrally, which, probably, reflects the superposition of some acts of stabilizing selection with respect to some crucial NCR genes and crucial amino acids, i.e., the cysteines, and acts of diversifying selection that leads to an increase in the diversity of NCRs (a factor which is believed to be beneficial for plants). Diversifying (or disruptive) selection is also clearly observed when comparing NCR gene sequences between pea cultivars where the number of non-synonimic changes is much higher than that of the synonymic. In general, this fact, together with the extremely low percentage of similarity between NCR peptides of *P. sativum* and *M. truncatula* (and the absence of orthologous sequences apart for the *PsNCR47–MtNCR312* pair) confirms that the evolutionary trajectories of this family are independent in each of the IRLC species. The lack of orthology, which is unusual for symbiotic genes (that are often quite conservative in different legumes), is, however, consistent with the concept that defense proteins of any organism evolve at faster rates than structural or regulatory ones where a minor change in sequence may lead to the serious disturbance of cell function or that of the whole organism.

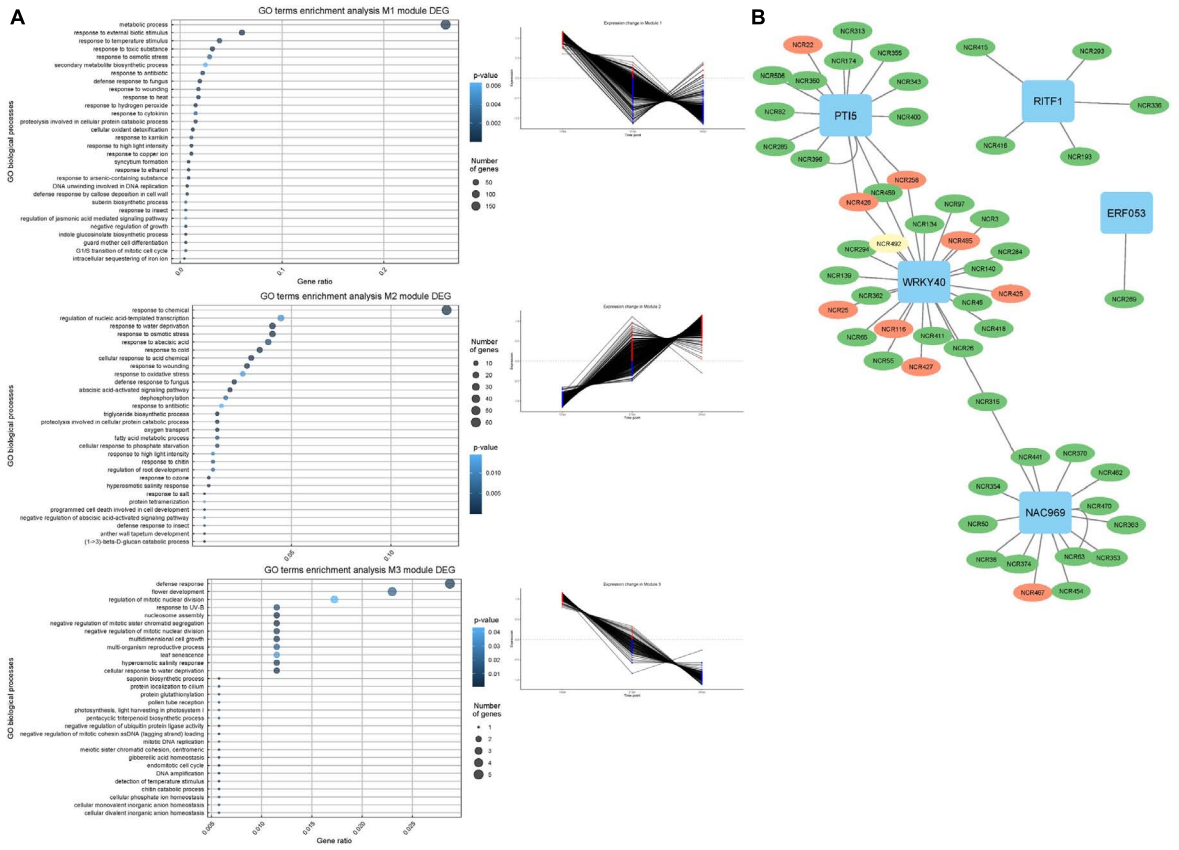

FIGURE 10
(A) Co-expression gene modules and their expression pattern identified using CEMiTool at 12, 21, and 28 dpi and biological process GO enrichment of the differentially expressed genes in detected co-expression modules. **(B)** NCR gene regulatory network based on gene expression data. NCR genes with a maximum expression at 12 dpi are colored green. NCR genes with a maximum expression at 21 dpi are colored yellow. NCR genes with a maximum expression at 28 and 42 dpi are colored red.

Like those of *M. truncatula*, pea NCR genes are located in clusters, a fact consistent with the accepted mode of their evolution by duplication and diversification, and they have an uneven distribution between chromosomes: 101 and 129 NCR genes in chromosomes LG5chr3 and LG1chr2, respectively, with fewer on other chromosomes. The NCR gene clusters contain many repetitive sequences and transposons, and many of the surrounding genes in the current pea genome annotation encode short peptides with unknown functions. Apparently, the presence of repeats facilitates unequal recombination events that lead to duplications of NCR genes.

In general, the closer the NCR genes are located to each other the more similar their expression patterns are. This is also a consequence of the recent duplication events that involve promoter sequences along with coding parts of NCR genes. However, diversification and specialization are characteristics not only for coding parts of NCR genes but also for its promoters. The detection of expression waves of NCR genes indicates that some features in promoter regions of different NCR genes have independently evolved for matching different TFs. Indeed, we found different motifs in promoters of late and early NCR genes and identified some TFs that are co-expressed with early or late NCR genes. Although other methods like ChIP-Seq are needed to detect the direct interaction of particular TFs with NCR gene promoters, the TFs identified in our analysis seem relevant in light of the nature of the data. The TF WRKY40 regulates the expression of genes related to response to bacteria and refers to such GO biological processes as “defense response to bacteria” and as “defense response to fungus” (Chakraborty et al., 2018). Similarly, PTI5 is a TF regulating the expression of pathogen resistance genes (He et al., 2001; Gu et al., 2002). NAC969 is a negative transcriptional regulator of nodule senescence and regulates nodule premature senescence and abiotic stress tolerance in *M. truncatula*. Experiments using RNAi have shown that suppression of NAC969 expression leads to premature nodule senescence, which may be directly connected with the absence of early NCR gene expression (de Zélicourt et al., 2012).

TABLE 4 (A) The conserved motifs found in the upstream regions of "early" NCR genes using the MEME tool. (B) The conserved motifs found in the upstream regions of "late" NCR genes using the MEME tool.

(A)

Motif consensus	*E*-value	Sites	Length
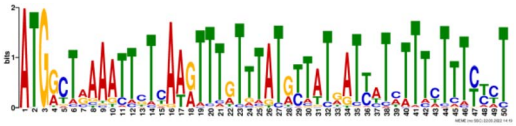	1.2e−302	108	50
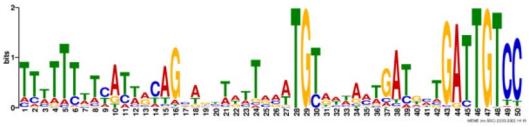	2.0e−179	85	50
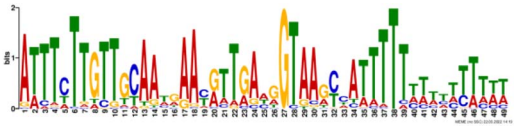	9.4e−105	44	49
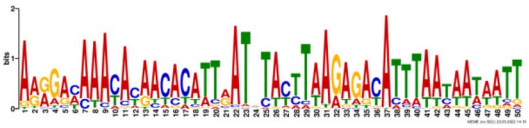	1.4e−102	60	50
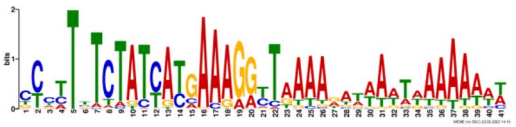	1.2e−070	52	41

(B)

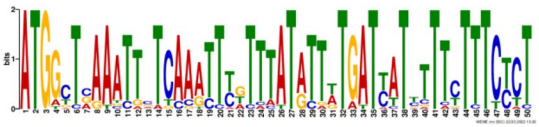	6.2e−140	18	50
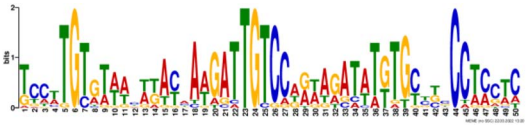	4.6e−088	16	50
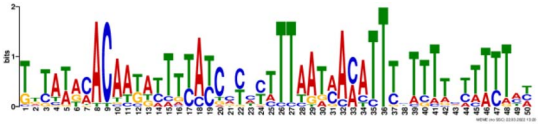	6.5e−053	20	50
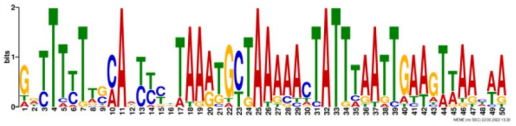	1.1e−050	14	50
	4.5e−039	6	50

The promoters of NCR genes in pea have putative binding sites for the TF NLP7, a member of the NIN-like protein family, which is accumulated in the nucleus in response to nitrate and directly regulates the production of CLE-RS2, a root-derived mobile peptide that acts as a negative regulator of nodule number (Nishida et al., 2018). The results obtained in our work suggest that NLP7 may also regulate the expression of "early" NCR genes. Other binding sites in promoters of

TABLE 5 (A) Putative TF binding sites in "early" NCR promoter regions predicted by the SEA tool. (B) Putative TF binding sites in "late" NCR promoter regions predicted by the SEA tool.

(A)

ID	ALT_ID	Consensus
RWPRK_tnt.NLP7_col_a_m1	NLP7	WWWTGVCYYTTSRDD
AP2EREBP_tnt.AT1G71450_col_a_m1	AT1G71450	CDCCRCCRCCDCCRCCGYCR
LOBAS2_tnt.AS2_col_a_m1	AS2	YCDCCGCCGYHDYYKCCGCCG
BBRBPC_tnt.BPC6_col_a_m1	BPC6	CTCTCTCTCTCTCTCTCTC
ARF_tnt.ARF2_col_v31_m1	ARF2	WDSMGACAWR
C2C2gata_tnt.ZML1_col_a_m1	ZML1	TCATCATCATCATCA

(B)

C2H2_tnt.STZ_col_m1	STZ	CACTNHCACTN
C2C2gata_tnt.GATA20_colamp_a_m1	GATA20	TNGATCNGATYND
Orphan_tnt.BBX31_col_a_m1	BBX31	AAAAAGTAAAAARDW
C2H2_tnt.TF3A_col_a_m1	TF3A	CYTCCTCCTCCTCCTCCTC
ND_tnt.FRS9_col_a_m1	FRS9	CTCTCTCTCTCTCTCTCTC
MYB_tnt.MYB55_colamp_a_m1	MYB55	WGGTWGGTRRRNNDD

NCR genes can be targets of auxin-response TF ARF2. It is known that ARF2 (together with ARF3 and ARF4) is involved in nodule organogenesis and rhizobia infection during nitrogen-fixing symbiosis in *M. truncatula*, regulating auxin-mediated developmental programs. Nallu et al. (2013) also identified ARF elements in the upstream region of NCR genes. Still, the question of whether ARF2 is the key regulator of NCR gene expression needs further investigation with the use of direct methods. Interestingly, promoters of genes that are co-expressed with NCR genes contain the same conservative motifs as promoters of NCR genes (**Table 4**). Since some of these co-expressed genes are related to hormonal signaling (nodulin-13 and gibberellin signaling DELLA protein LA) and autoregulation of nodulation (AON) (receptor-like protein CLAVATA2), this similarity of promoter regions may be the molecular genetic base of the possible link between long-distance signaling during nodulation and the expression of NCR genes.

The majority of NCR genes are expressed at 12 and 21 dpi, which coincides with the time of differentiation of free-living bacteria into bacteroids. However, a significant part of NCR genes has higher expression at 28 dpi and, especially, at 42 dpi (when the bacteroid differentiation is already completed). Obviously, the roles played by these late NCRs are different from those of early NCRs; for example, they could be involved in stricter control over the metabolic exchange between symbionts, or in the processes of senescence of symbiosomes. Interestingly, the spatial expression profiles indicate that the NCRs with pI 7.9–8.4 constitute the majority of NCR genes expressed in the early II zone (**Figure 7B**). A similar pattern was detected for NCR genes in *M. trunacatula* nodule microdissection as well (Montiel et al., 2017). Regarding the temporal expression profiles, at 28 dpi all groups of peptides (anionic, neutral, and cationic) are expressed at a high level, while for anionic peptides (pI < 6.5) two subgroups can be distinguished: those with (i) pI 4.4–5.4, with a maximal expression at 28 dpi and (ii) pI 5.4–5.9, with a maximal expression at 12 dpi. The specific roles of anionic NCR peptides pI 5.4–5.9 were at an early stage of nodule development and could be connected with its possible ability to neutralize the activity of cationic peptides for the precise tuning of TBD.

White nodules of SGEFix$^-$-1 are characterized by abnormal morphological differentiation of bacteroids and premature degradation of nodule symbiotic structures (Tsyganov et al., 1998). Some of the "early" genes encoding NCR peptides whose expression in SGEFix$^-$-1 does not differ from the wild type may be associated with the initiation of the terminal differentiation of bacteroids, while the "late" genes, whose expression is downregulated in SGEFix$^-$-1, may be involved in completion of the TBD process, in nitrogen fixation, and in initiation (and/or suppression) of senescence of nodules.

The *sym33-3* allele is a weak allele that leads to the synthesis of truncated protein (Ovchinnikova et al., 2011). As a result, the SGEFix$^-$-2 mutant is characterized by a leaky phenotype. In white nodules, most nodule cells are colonized cells containing infection threads without bacterial release. However, in some white nodules, bacterial release may occur and such cells become infected. Nonetheless, the bacteroids remain undifferentiated rod-shaped and gather in multibacteroid symbiosomes. This means that IPD3/CYCLOPS TF is a prerequisite for NCR peptide synthesis since its disruption leads to total downregulation of the expression

of genes encoding NCR peptides in SGEFix$^-$-2 nodules. Interestingly, the nodule phenotype of the *M. truncatula* mutant in the *ERN1* gene (Cerri et al., 2016) resembles, to an extent, the mutant phenotype of the SGEFix$^-$-2 mutant. The co-expression and regulatory relationships identified between the *ERN1* gene and the genes encoding NCR peptides may indicate that *sym33-3* helps determine the expression of NCR genes through a change in *ERN1* gene expression.

The gene expression analysis demonstrated that in mutants, in comparison with wild-type nodules, the upregulated biological process terms comprised the defense response to bacteria and the regulation of defense reactions. Previously, an activation of strong defense responses in SGEFix$^-$-1 and SGEFix$^-$-2 mutant nodules was observed (Ivanova et al., 2015; Tsyganova et al., 2019). These responses included activation of defense response genes, suberinization, increased unesterified pectin deposition in infection threads walls, and enhanced cell wall material deposition around the vacuole. Further studies are needed to clarify the potential link between NCR gene expression and suppression of defense reactions in nodules.

A co-expression analysis using the data of wild-type and mutant nodule transcriptomes revealed several potential regulators of the NCR gene expression. However, the set of the identified TFs does not overlap with the set of TFs obtained on the data of gene expression in the wild-type SGE nodules at different time points. This can be explained by the fact that, in the wild-type nodules, the change in gene expression over time (from 12 to 28 dpi) is less pronounced as compared to the difference between wild-type and mutant nodules where the development of symbiotic structures is aborted. Possibly, transcriptomic studies involving other pea Fix$^-$ mutants and younger wild-type nodules will contribute to identifying more potential regulators of NCR gene expression.

The number of known pea accessions in germplasm collections exceeds 70,000 (Smýkal et al., 2013). Apparently, further analysis of the NCR gene expression and polymorphism in a large set of pea accessions is needed to fully describe the role of this gene family in symbiosis, as single amino acid changes in some cultivars and genotypes may significantly change the physicochemical properties of NCR peptides and its effect on TBD and their viability in nodules.

Conclusion

The gene family encoding NCR peptides in the pea, as in other IRLC legumes, is highly variable, and this variability leads to the production of a strong cocktail of defensin-like molecules in nodule cells. Although the antibiotic activity of a single NCR peptide may be minor, the toxicity of a peptide cocktail including molecules with different properties and modes of action against bacteria is much higher so that only compatible nodule bacteria could resist treatment with NCR peptides within nodules (Lima et al., 2020). The study of this antibiotic activity may help advance the formulation of new generations of antibiotics, an important effort in the light of increased pathogenic antibiotic-resistant bacteria. As it is known that NCR peptides penetrate bacterial cells and interfere with their vital functions, an antibiotic cocktail made of several NCR peptides may be formulated on the basis of calculated predictions related to the functions of relevant NCR peptides. Moreover, modification of the NCR gene and peptide sequences may result in stronger antibiotics, which may be useful in medicine and agricultural practices as well.

From the fundamental point of view, it is still not known whether mutations in NCR genes of pea might result in the Fix$^-$ phenotype. Although no mutations in NCR genes in pea are known to date, the number of described and not sequenced genes still exceeds 10 (Tsyganov and Tsyganova, 2020). The mapping-based approach, which has recently demonstrated its feasibility (Zhernakov et al., 2019), may likely help identify such mutations in the near future and thus contribute to a more complete description of the NCR gene family in the pea.

Data availability statement

The data presented in this study are deposited in the NCBI repository, accession numbers: PRJNA812957 and PRJNA853105.

Author contributions

EZ, MK, IT, and VZ contributed to the conception and design of the study. EZ, MK, AA, MG, OK, and AZ searched for NCR genes, conducted polymorphism analysis, and computationally predicted properties of putative NCR peptides. EZ, MK, AA, EG, AS, AZ, OK, DR, and VZ carried out nodulation experiments and MACE RNAseq analysis. EZ and AA executed co-expression and promoter sequence analysis. PK and VT performed microdissection following RNAseq analysis. AT performed microscopy. VZ, EZ, and MK wrote the first draft of the manuscript. All authors contributed to the manuscript revision, read, and approved the submitted version.

Funding

This research was funded by the Ministry of Science and Higher Education of the Russian Federation in accordance with agreement no. 075-15-2020-920 date 16 November 2020 on providing a grant in the form of subsidies from the Federal budget of the Russian Federation. The grant was provided for state support for the creation and development of a World-class Scientific Center "Agrotechnologies for the Future."

Acknowledgments

We thank Ekaterina Vasileva, Natalia Kichigina, Lyudmila Dvoryaninova, Gulnar Akhtemova, and Oksana Shtark for their assistance in nodulation experiments. This article was dedicated to the memory of our colleague Peter Winter.

Conflict of interest

The authors declare that the research was conducted in the absence of any commercial or financial relationships that could be construed as a potential conflict of interest.

Publisher's note

Supplementary material

The Supplementary Material for this article can be found online at: https://www.frontiersin.org/articles/10.3389/fpls.2022.884726/full#supplementary-material

References

Afonin, A., Sulima, A., Zhernakov, A., and Zhukov, V. (2017). Draft genome of the strain RCAM1026 *Rhizobium leguminosarum* bv. *viciae*. *Genomics Data* 11, 85–86. doi: 10.1016/j.gdata.2016.12.003

Alunni, B., and Gourion, B. (2016). Terminal bacteroid differentiation in the legume-rhizobium symbiosis: nodule-specific cysteine-rich peptides and beyond. *New Phytol.* 211, 411–417. doi: 10.1111/nph.14025

Alunni, B., Kevei, Z., Redondo-Nieto, M., Kondorosi, A., Mergaert, P., and Kondorosi, E. (2007). Genomic organization and evolutionary insights on *GRP* and *NCR* genes, two large nodule-specific gene families in *Medicago truncatula*. *Mol. Plant Microbe Interact.* 20, 1138–1148. doi: 10.1094/MPMI-20-9-1138

Alves-Carvalho, S., Aubert, G., Carrère, S., Cruaud, C., Brochot, A. L., Jacquin, F., et al. (2015). Full-length *de novo* assembly of RNA-seq data in pea (*Pisum sativum* L.) provides a gene expression atlas and gives insights into root nodulation in this species. *Plant J.* 84, 1–19. doi: 10.1111/tpj.12967

Anand, L., and Rodriguez Lopez, C. M. (2022). Chromomap: an R package for interactive visualization of multi-omics data and annotation of chromosomes. *BMC Bioinformatics* 23:33. doi: 10.1186/s12859-021-04556-z

Bailey, T. L., Boden, M., Buske, F. A., Frith, M., Grant, C. E., Clementi, L., et al. (2009). MEME SUITE: tools for motif discovery and searching. *Nucleic Acids Res.* 37, W202–W208. doi: 10.1093/nar/gkp335

Cerri, M. R., Frances, L., Kelner, A., Fournier, J., Middleton, P. H., Auriac, M. C., et al. (2016). The symbiosis-related ERN transcription factors act in concert to coordinate rhizobial host root infection. *Plant Physiol.* 171, 1037–1054. doi: 10.1104/pp.16.00230

Chakraborty, J., Ghosh, P., Sen, S., and Das, S. (2018). Epigenetic and transcriptional control of chickpea WRKY40 promoter activity under *Fusarium* stress and its heterologous expression in *Arabidopsis* leads to enhanced resistance against bacterial pathogen. *Plant Sci.* 276, 250–267. doi: 10.1016/j.plantsci.2018.07.014

Danecek, P., Auton, A., Abecasis, G., Albers, C. A., Banks, E., DePristo, M. A., et al. (2011). The variant call format and VCFtools. *Bioinformatics* 27, 2156–2158. doi: 10.1093/bioinformatics/btr330

Danecek, P., Bonfield, J. K., Liddle, J., Marshall, J., Ohan, V., Pollard, M. O., et al. (2021). Twelve years of SAMtools and BCFtools. *GigaScience* 10:giab008. doi: 10.1093/gigascience/giab008

de Zélicourt, A., Diet, A., Marion, J., Laffont, C., Ariel, F., Moison, M., et al. (2012). Dual involvement of a *Medicago truncatula* NAC transcription factor in root abiotic stress response and symbiotic nodule senescence: root stress response and nodule senescence. *Plant J.* 70, 220–230. doi: 10.1111/j.1365-313X.2011.04859.x

Denison, R. F. (2000). Legume sanctions and the evolution of symbiotic cooperation by rhizobia. *Am. Nat.* 156, 567–576. doi: 10.1086/316994

Dobin, A., and Gingeras, T. R. (2015). Mapping RNA-seq reads with STAR. *Curr. Protoc. Bioinfor.* 51, 1–11. doi: 10.1002/0471250953.bi1114s51

Downie, J. A., and Kondorosi, E. (2021). Why should Nodule Cysteine-Rich (NCR) peptides be absent from nodules of some groups of legumes but essential for symbiotic N-Fixation in others? *Front. Agron.* 3:654576. doi: 10.3389/fagro.2021.654576

Durán, D., Albareda, M., García, C., Marina, A. I., Ruiz-Argüeso, T., and Palacios, J. M. (2021). Proteome analysis reveals a significant host-specific response in *Rhizobium leguminosarum* bv. *viciae* endosymbiotic cells. *Mol. Cell. Prot.* 20:100009. doi: 10.1074/mcp.RA120.002276

Durgo, H., Klement, E., Hunyadi-Gulyas, E., Szucs, A., Kereszt, A., Medzihradszky, K. F., et al. (2015). Identification of nodule-specific cysteine-rich plant peptides in endosymbiotic bacteria. *Proteomics* 15, 2291–2295. doi: 10.1002/pmic.201400385

Farkas, A., Maroti, G., Durg, H., Gyorgypal, Z., Lima, R. M., Medzihradszky, K. F., et al. (2014). *Medicago truncatula* symbiotic peptide NCR247 contributes to bacteroid differentiation through multiple mechanisms. *Proc. Natl. Acad. Sci. U.S.A.* 111, 5183–5188. doi: 10.1073/pnas.1404169111

Farkas, A., Maróti, G., Kereszt, A., and Kondorosi, É (2017). Comparative analysis of the bacterial membrane disruption effect of two natural plant antimicrobial peptides. *Front. Microbiol.* 8:51. doi: 10.3389/fmicb.2017.00051

Graham, M. A., Silverstein, K. A. T., Cannon, S. B., and VandenBosch, K. A. (2004). Computational identification and characterization of novel genes from legumes. *Plant Physiol.* 135, 1179–1197. doi: 10.1104/pp.104.037531

Gu, Y. Q., Wildermuth, M. C., Chakravarthy, S., Loh, Y. T., Yang, C., He, X., et al. (2002). Tomato transcription factors Pti4, Pti5, and Pti6 activate defense responses when expressed in Arabidopsis. *Plant Cell* 14, 817–831. doi: 10.1105/tpc.000794

Guefrachi, I., Nagymihaly, M., Pislariu, C. I., Van de Velde, W., Ratet, P., Mars, M., et al. (2014). Extreme specificity of NCR gene expression in *Medicago truncatula*. *BMC Genomics* 15:712. doi: 10.1186/1471-2164-15-712

Guefrachi, I., Pierre, O., Timchenko, T., Alunni, B., Barrière, Q., Czernic, P., et al. (2015). *Bradyrhizobium* BclA is a peptide transporter required for bacterial differentiation in symbiosis with *Aeschynomene* legumes. *Mol. Plant Microbe Interact.* 28, 1155–1166. doi: 10.1094/MPMI-04-15-0094-R

Haag, A. F., Arnold, M. F. F., Myka, K. K., Kerscher, B., Dall'Angelo, S., Zanda, M., et al. (2013). Molecular insights into bacteroid development during *Rhizobium*– legume symbiosis. *FEMS Microbiol. Rev.* 37, 364–383. doi: 10.1111/1574-6976.12003

He, P., Warren, R. F., Zhao, T., Shan, L., Zhu, L., Tang, X., et al. (2001). Overexpression of *Pti5* in tomato potentiates pathogen-induced defense gene expression and enhances disease resistance to *Pseudomonas syringae* pv. *tomato*. *Mol. Plant Microbe Interact.* 14, 1453–1457. doi: 10.1094/MPMI.2001.14.12.1453

Horváth, B., Domonkos, Á, Kereszt, A., Szűcs, A., Ábrahám, E., and Ayaydin, F. (2015). Loss of the nodule-specific cysteine rich peptide, NCR169, abolishes symbiotic nitrogen fixation in the *Medicago truncatula dnf7* mutant. *Proc. Natl. Acad. Sci. U.S.A.* 112, 15232–15237. doi: 10.1073/pnas.1500777112

Huynh-Thu, V. A., Irrthum, A., Wehenkel, L., and Geurts, P. (2010). Inferring regulatory networks from expression data using tree-based methods. *PLoS One* 5:e12776. doi: 10.1371/journal.pone.0012776

Isozumi, N., Masubuchi, Y., Imamura, T., Mori, M., Koga, H., and Ohki, S. (2021). Structure and antimicrobial activity of NCR169, a nodule-specific cysteine-rich peptide of *Medicago truncatula*. *Sci. Rep.* 11:9923. doi: 10.1038/s41598-021-89485-w

Ivanova, K. A., Tsyganova, A. V., Brewin, N. J., Tikhonovich, I. A., and Tsyganov, V. E. (2015). Induction of host defences by *Rhizobium* during ineffective nodulation of pea (*Pisum sativum* L.) carrying symbiotically defective mutations *sym40* (*PsEFD*), *sym33 (PsIPD3/PsCYCLOPS)* and *sym42*. *Protoplasma* 252:6, 1505–1517. doi: 10.1007/s00709-015-0780-y

Kato, T., Kawashima, K., Miwa, M., Mimura, Y., Tamaoki, M., Kouchi, H., et al. (2002). Expression of genes encoding late nodulins characterized by a putative signal peptide and conserved cysteine residues is reduced in ineffective pea nodules. *Mol. Plant Microbe Interact.* 15, 129–137. doi: 10.1094/MPMI.2002.15.2.129

Katoh, K. (2002). MAFFT: a novel method for rapid multiple sequence alignment based on fast Fourier transform. *Nucleic Acids Res.* 30, 3059–3066. doi: 10.1093/nar/gkf436

Kereszt, A., Mergaert, P., and Kondorosi, E. (2011). Bacteroid development in legume nodules: evolution of mutual benefit or of sacrificial victims? *Mol. Plant Microbe Interact.* 24, 1300–1309. doi: 10.1094/MPMI-06-11-0152

Kim, M., Chen, Y., Xi, J., Waters, C., Chen, R., and Wang, D. (2015). An antimicrobial peptide essential for bacterial survival in the nitrogen-fixing symbiosis. *Proc. Natl. Acad. Sci. U.S.A.* 112, 15238–15243. doi: 10.1073/pnas.1500123112

Kosterin, O. E., and Rozov, S. M. (1993). Mapping of the new mutation *blb* and the problem of integrity of linkage group I. *Pisum Genet.* 25, 27–31.

Kozlowski, L. P. (2021). IPC 2.0: prediction of isoelectric point and p *K* a dissociation constants. *Nucleic Acids Res.* 49, W285–W292. doi: 10.1093/nar/gkab295

Kreplak, J., Madoui, M. A., Cápal, P., Novák, P., Labadie, K., Aubert, G., et al. (2019). A reference genome for pea provides insight into legume genome evolution. *Nat. Genet.* 51, 1411–1422. doi: 10.1038/s41588-019-0480-1

Kusakin, P. G., Serova, T. A., Gogoleva, N. E., Gogolev, Y. V., and Tsyganov, V. E. (2021). Laser microdissection of *Pisum sativum* L. nodules followed by RNA-seq analysis revealed crucial transcriptomic changes during infected cell differentiation. *Agronomy* 11:2504. doi: 10.3390/agronomy11122504

Langmead, B., and Salzberg, S. L. (2012). Fast gapped-read alignment with Bowtie 2. *Nat. Methods* 9, 357–359. doi: 10.1038/nmeth.1923

Lima, R. M., Kylarová, S., Mergaert, P., and Kondorosi, É (2020). Unexplored arsenals of legume peptides with potential for their applications in medicine and agriculture. *Front. Microbiol.* 11:1307. doi: 10.3389/fmicb.2020.01307

Madeira, F., Park, Y. M., Lee, J., Buso, N., Gur, T., and Madhusoodanan, N. (2019). The EMBL-EBI search and sequence analysis tools APIs in 2019. *Nucleic Acids Res.* 47, W636–W641. doi: 10.1093/nar/gkz268

Maunoury, N., Redondo-Nieto, M., Bourcy, M., Van de Velde, W., Alunni, B., Laporte, P., et al. (2010). Differentiation of symbiotic cells and endosymbionts in *Medicago truncatula* nodulation are coupled to two transcriptome-switches. *PLoS One* 5:e9519. doi: 10.1371/journal.pone.0009519

Mergaert, P., Nikovics, K., Kelemen, Z., Maunoury, N., Vaubert, D., Kondorosi, A., et al. (2003). A novel family in *Medicago truncatula* consisting of more than 300 nodule-specific genes coding for small, secreted polypeptides with conserved cysteine motifs. *Plant Physiol.* 132, 161–173. doi: 10.1104/pp.102.018192

Mergaert, P., Uchiumi, T., Alunni, B., Evanno, G., Cheron, A., Catrice, O., et al. (2006). Eukaryotic control on bacterial cell cycle and differentiation in the *Rhizobium*-legume symbiosis. *Proc. Natl. Acad. Sci. U.S.A.* 103, 5230–5235. doi: 10.1073/pnas.0600912103

Michael Love, S. A. (2017). *DESeq2*. Heidelberg: European Bioconductor. doi: 10.18129/B9.BIOC.DESEQ2

Mikuláss, K. R., Nagy, K., Bogos, B., Szegletes, Z., Kovács, E., Farkas, A., et al. (2016). Antimicrobial nodule-specific cysteine-rich peptides disturb the integrity of bacterial outer and inner membranes and cause loss of membrane potential. *Ann. Clin. Microbiol. Antimicrob.* 15:43. doi: 10.1186/s12941-016-0159-8

Montiel, J., Downie, J. A., Farkas, A., Bihari, P., Herczeg, R., Bálint, B., et al. (2017). Morphotype of bacteroids in different legumes correlates with the number and type of symbiotic NCR peptides. *Proc. Natl. Acad. Sci. U.S.A.* 114, 5041–5046. doi: 10.1073/pnas.1704217114

Nallu, S., Silverstein, K. A. T., Samac, D. A., Bucciarelli, B., Vance, C. P., and VandenBosch, K. A. (2013). Regulatory patterns of a large family of defensin-like genes expressed in nodules of *Medicago truncatula*. *PLoS One* 8:e60355. doi: 10.1371/journal.pone.0060355

Nishida, H., Tanaka, S., Handa, Y., Ito, M., Sakamoto, Y., Matsunaga, S., et al. (2018). A NIN-LIKE PROTEIN mediates nitrate-induced control of root nodule symbiosis in *Lotus japonicus*. *Nat. Commun.* 9:499. doi: 10.1038/s41467-018-02831-x

Oono, R., and Denison, R. F. (2010). Comparing symbiotic efficiency between swollen versus nonswollen rhizobial bacteroids. *Plant Physiol.* 154, 1541–1548. doi: 10.1104/pp.110.163436

Ovchinnikova, E., Journet, E.-P., Chabaud, M., Cosson, V., Ratet, P., Duc, G., et al. (2011). IPD3 controls the formation of nitrogen-fixing symbiosomes in pea and *Medicago* Spp. *Mol. Plant Microbe Interact.* 24, 1333–1344. doi: 10.1094/MPMI-01-11-0013

Pan, H., and Wang, D. (2017). Nodule cysteine-rich peptides maintain a working balance during nitrogen-fixing symbiosis. *Nat. Plants* 3:17048. doi: 10.1038/nplants.2017.48

Pandey, A. K., Rubiales, D., Wang, Y., Fang, P., Sun, T., Liu, N., et al. (2021). Omics resources and omics-enabled approaches for achieving high productivity and improved quality in pea (*Pisum sativum* L.). *Theor. Appl. Genet.* 134, 755–776. doi: 10.1007/s00122-020-03751-5

Price, P. A., Tanner, H. R., Dillon, B. A., Shabab, M., Walker, G. C., and Griffitts, J. S. (2015). Rhizobial peptidase HrrP cleaves host-encoded signaling peptides and mediates symbiotic compatibility. *Proc. Natl. Acad. Sci. U.S.A.* 112, 15244–15249. doi: 10.1073/pnas.1417797112

Quinlan, A. R., and Hall, I. M. (2010). BEDTools: a flexible suite of utilities for comparing genomic features. *Bioinformatics* 26, 841–842. doi: 10.1093/bioinformatics/btq033

Robinson, M. D., McCarthy, D. J., and Smyth, G. K. (2010). edgeR: a Bioconductor package for differential expression analysis of digital gene expression data. *Bioinformatics* 26, 139–140. doi: 10.1093/bioinformatics/btp616

Roux, B., Rodde, N., Jardinaud, M. F., Timmers, T., Sauviac, L., Cottret, L., et al. (2014). An integrated analysis of plant and bacterial gene expression in symbiotic root nodules using laser-capture microdissection coupled to RNA sequencing. *Plant J.* 77, 817–837. doi: 10.1111/tpj.12442

Roy, P., Achom, M., Wilkinson, H., Lagunas, B., and Gifford, M. L. (2020). Symbiotic outcome modified by the diversification from 7 to over 700 nodule-specific cysteine-rich peptides. *Genes* 11:348. doi: 10.3390/genes11040348

Russo, P. S. T., Ferreira, G. R., Cardozo, L. E., Bürger, M. C., Arias-Carrasco, R., Maruyama, S. R., et al. (2018). CEMiTool: a Bioconductor package for performing comprehensive modular co-expression analyses. *BMC Bioinformatics* 19:56. doi: 10.1186/s12859-018-2053-1

Scheres, B., van Engelen, F., van der Knaap, E., van de Wiel, C., van Kammen, A., and Bisseling, T. (1990). Sequential induction of nodulin gene expression in the developing pea nodule. *Plant Cell* 2, 687–700. doi: 10.1105/tpc.2.8.687

Schliep, K. P. (2011). phangorn: phylogenetic analysis in R. *Bioinformatics* 27, 592–593. doi: 10.1093/bioinformatics/btq706

Shannon, P., Markiel, A., Ozier, O., Baliga, N. S., Wang, J. T., Ramage, D., et al. (2003). Cytoscape: a software environment for integrated models of biomolecular interaction networks. *Genome Res.* 13, 2498–2504. doi: 10.1101/gr.1239303

Smýkal, P., Aubert, G., Burstin, J., Coyne, C. J., Ellis, N. T. H., Flavell, A. J., et al. (2012). Pea (*Pisum sativum* L.) in the genomic era. *Agronomy* 2, 74–115. doi: 10.3390/agronomy2020074

Smýkal, P., Coyne, C., and Redden, R. (2013). Smýkal, P., Coyne, C., Redden, R., and Maxted, N. (2013). "3 – Peas", in *Genetic and Genomic Resources of Grain Legume Improvement*, eds M. Singh, H. D. Upadhyaya, and I. S. Bisht (Oxford: Elsevier), 41–80. doi: 10.1016/C2012-0-00217-7

Sprent, J. I. (2001). *Nodulation in Legumes*. Kew: Royal Botanic Gardens.

Sprent, J. I., Sutherland, J., De Faria, S., Dilworth, M., Corby, H., Becking, J., et al. (1987). Some aspects of the biology of nitrogen-fixing organisms. *Phil. Trans. R. Soc. Lond. B* 317, 111–129. doi: 10.1098/rstb.1987.0051

Sulima, A. S., Zhukov, V. A., Kulaeva, O. A., Vasileva, E. N., Borisov, A. Y., and Tikhonovich, I. A. (2019). New sources of *Sym2* ^{A} allele in the pea (*Pisum sativum* L.) carry the unique variant of candidate LysM-RLK gene *LykX*. *PeerJ* 7:e8070. doi: 10.7717/peerj.8070

Suyama, M., Torrents, D., and Bork, P. (2006). PAL2NAL: robust conversion of protein sequence alignments into the corresponding codon alignments. *Nucleic Acids Res.* 34, W609–W612. doi: 10.1093/nar/gkl315

Teufel, F., Almagro Armenteros, J. J., Johansen, A. R., Gíslason, M. H., Pihl, S. I., Tsirigos, K. D., et al. (2022). SignalP 6.0 predicts all five types of signal peptides using protein language models. *Nat. Biotechnol.* 40, 1023–1025. doi: 10.1038/s41587-021-01156-3

Tiricz, H., Szűcs, A., Farkas, A., Pap, B., Lima, R. M., Maróti, G., et al. (2013). Antimicrobial nodule-specific cysteine-rich peptides induce membrane depolarization-associated changes in the transcriptome of *Sinorhizobium meliloti*. *Appl. Environ. Microbiol.* 79, 6737–6746. doi: 10.1128/AEM.01791-13

Tsyganov, V. E., Morzhina, E. V., Stefanov, S. Y., Borisov, A. Y., Lebsky, V. K., and Tikhonovich, I. A. (1998). The pea (*Pisum sativum* L.) genes *sym33* and *sym40* control infection thread formation and root nodule function. *Mol. Gen. Genet.* 259, 491–503. doi: 10.1007/s004380050840

Tsyganov, V. E., Seliverstova, E., Voroshilova, V., Tsyganova, A., Pavlova, Z., Lebskii, V., et al. (2011). Double mutant analysis of sequential functioning of pea (*Pisum sativum* L.) genes *Sym13*, *Sym33*, and *Sym40* during symbiotic nodule development. *Russ. J. Genet. Appl. Res.* 1:343. doi: 10.1134/S2079059711050145

Tsyganov, V. E., and Tsyganova, A. V. (2020). Symbiotic regulatory genes controlling nodule development in *Pisum sativum* L. *Plants* 9:1741. doi: 10.3390/plants9121741

Tsyganov, V. E., Voroshilova, V. A., Herrera-Cervera, J. A., Sanjuan-Pinilla, J. M., Borisov, A. Y., Tikhonovich, I. A., et al. (2003). Developmental downregulation of rhizobial genes as a function of symbiosome differentiation in symbiotic root nodules of *Pisum sativum*. *New Phytol.* 159, 521–530. doi: 10.1046/j.1469-8137.2003.00823.x

Tsyganova, A. V., Kitaeva, A. B., and Tsyganov, V. E. (2018). Cell differentiation in nitrogen-fixing nodules hosting symbiosomes. *Func. Plant Biol.* 45:47. doi: 10.1071/FP16377

Tsyganova, A. V., Seliverstova, E. V., Brewin, N. J., and Tsyganov, V. E. (2019). Bacterial release is accompanied by ectopic accumulation of cell wall material around the vacuole in nodules of *Pisum sativum sym33*-3 allele encoding transcription factor *PsCYCLOPS/PsIPD3*. *Protoplasma* 256, 1449–1453. doi: 10.1007/s00709-019-01383-1

Tsyganova, A. V., Tsyganov, V. E., Findlay, K. C., Borisov, A. Y., Tikhonovich, I. A., and Brewin, N. J. (2009). Distribution of legume arabinogalactan protein-extensin (AGPE) glycoproteins in symbiotically defective pea mutants with abnormal infection threads. *Cell Tissue Biol.* 3, 93–102. doi: 10.1134/s1990519x09010131

Van de Velde, W., Zehirov, G., Szatmari, A., Debreczeny, M., Ishihara, H., Kevei, Z., et al. (2010). Plant peptides govern terminal differentiation of bacteria in symbiosis. *Science* 327, 1122–1126. doi: 10.1126/science.1184057

Wang, D., Griffitts, J., Starker, C., Fedorova, E., Limpens, E., Ivanov, S., et al. (2010). A nodule-specific protein secretory pathway required for nitrogen-fixing symbiosis. *Science* 327, 1126–1129. doi: 10.1126/science.1184096

Wang, G., Li, X., and Wang, Z. (2016). APD3: the antimicrobial peptide database as a tool for research and education. *Nucleic Acids Res* 44, D1087–D1093. doi: 10.1093/nar/gkv1278

Wang, Q., Liu, J., Li, H., Yang, S., Körmöczi, P., Kereszt, A., et al. (2018). Nodule-specific cysteine-rich peptides negatively regulate nitrogen-fixing symbiosis in a strain-specific manner in *Medicago truncatula*. *Mol. Plant Microbe Interact.* 31, 240–248. doi: 10.1094/mpmi-08-17-0207-r

Wang, Q., Yang, S., Liu, J., Terecskei, K., Ábrahám, E., Gombár, A., et al. (2017). Host-secreted antimicrobial peptide enforces symbiotic selectivity in *Medicago truncatula*. *Proc. Natl. Acad. Sci. USA.* 114, 6854–6859. doi: 10.1073/pnas.1700715114

Yang, S., Wang, Q., Fedorova, E., Liu, J., Qin, Q., Zheng, Q., et al. (2017). Microsymbiont discrimination mediated by a host-secreted peptide in *Medicago truncatula*. *Proc. Natl. Acad. Sci. U.S.A.* 114, 6848–6853. doi: 10.1073/pnas.1700460114

Yang, Z. (2007). PAML 4: phylogenetic analysis by maximum likelihood. *Mol. Biol. Evol.* 24, 1586–1591. doi: 10.1093/molbev/msm088

Yu, G., Smith, D. K., Zhu, H., Guan, Y., and Lam, T. T. (2017). ggtree?: an r package for visualization and annotation of phylogenetic trees with their covariates and other associated data. *Methods Ecol. Evol.* 8, 28–36. doi: 10.1111/2041-210X.12628

Zhernakov, A. I., Shtark, O. Y., Kulaeva, O. A., Fedorina, J. V., Afonin, A. M., Kitaeva, A. B., et al. (2019). Mapping-by-sequencing using NGS-based 3'-MACE-Seq reveals a new mutant allele of the essential nodulation gene *Sym33* (*IPD3*) in pea (*Pisum sativum* L.). *PeerJ* 7:e6662. doi: 10.7717/peerj.6662

Zhou, P., Silverstein, K. A., Gao, L., Walton, J. D., Nallu, S., Guhlin, J., et al. (2013). Detecting small plant peptides using SPADA (Small Peptide Alignment Discovery Application). *BMC Bioinformatics* 14:335. doi: 10.1186/1471-2105-14-335

Zhukov, V. A., Zhernakov, A. I., Kulaeva, O. A., Ershov, N. I., Borisov, A. Y., and Tikhonovich, I. A. (2015). *De novo* assembly of the pea (*Pisum sativum* L.) nodule transcriptome. *Int. J. Genomics* 2015:695947. doi: 10.1155/2015/695947

Frontiers in Plant Science

Cultivates the science of plant biology and its applications

The most cited plant science journal, which advances our understanding of plant biology for sustainable food security, functional ecosystems and human health.

Discover the latest Research Topics

See more →

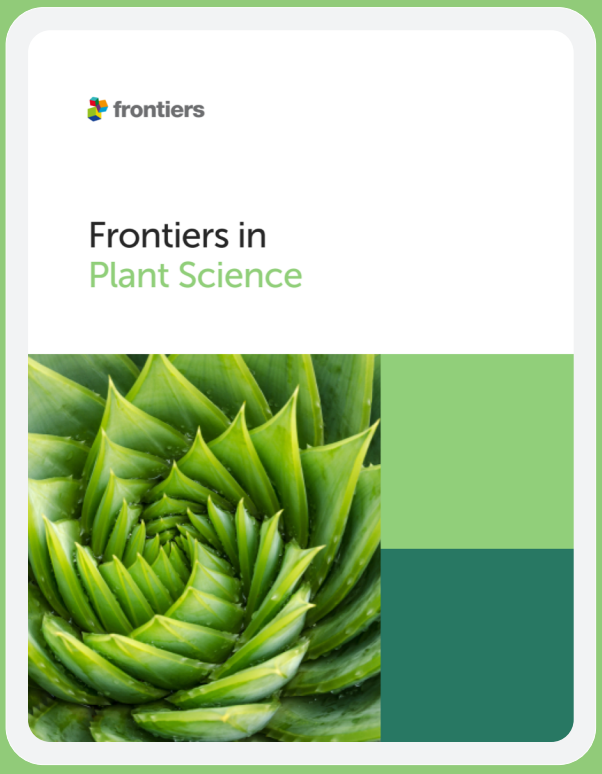

Frontiers

Avenue du Tribunal-Fédéral 34
1005 Lausanne, Switzerland
frontiersin.org

Contact us

+41 (0)21 510 17 00
frontiersin.org/about/contact